Project: B-USEFUL, EC HEU Grant No. 101059823

This project has received funding from the European Union's Horizon Europe research and innovation programme under Grant Agreement No. 101059823 (B-USEFUL)

European Commission

User-oriented Solutions for Improved Monitoring and Management of Biodiversity and Ecosystem services in vulnerable European Seas

Deliverable 3.2 Report on biodiversity status, state-pressure relationships and cumulative impacts across European waters.

Deliverable Title: **Report on biodiversity status, state-pressure relationships and cumulative impacts across European waters**

Work package: **3 – Biodiversity status and cumulative impacts**

Deliverable no: **D3.2**

Lead beneficiary: **Agencia Estatal Consejo Superior de Investigaciones Científicas (CSIC)**

Lead responsible for the report: Manuel Hidalgo (CSIC)
jm.hidalgo@ieo.csic.es

Submission date: 31st January 2026

Authors and citation:

Manuel Hidalgo, Nicolas Barrier, Stratos Batziakas, Marion Billy, Silvia Blum, Corina Chaves, Antonella Consiglio, Keith Cooper, Elena Couce, Georg Engelhard, Heino O. Fock, Alicia Gran, Lily Greig, Pierre Hélaouët, Sofia Henriques, Alexandros Kaninas, Stefanos Kavadas, Eva Maire, André Martins, Bastien Mérigot, Marcel Montanyes, Fabien Moullec, Federico Maioli, Teresa Moura, Maria L. D. Palomares, Myron A. Peck, Panagiota Peristeraki, Laurene Pecuchet, John K. Pinnegar, Patricia Puerta, Marcel Rozemeijer, Fernanda Silva, Marcel Sole, Camilla Sguotti, Maria Teresa Spedicato, Murray Thompson, Justin Tiano, George Tserpes, Daniel van Denderen, Rita Vasconcelos, Laure Velez, Antoni Vivó-Pons, Walter Zupa and Martin Lindegren (2026) – B-USEFUL. Report on biodiversity status, state-pressure relationships and cumulative impacts across European waters. Technical University of Denmark.

Dissemination Level: **PU**

PU: Public

PP: Restricted to other programme participants (including the Commission Services)

RE: Restricted to a group specified by the consortium (including the Commission Services)

CO: Confidential, only for partners of the consortium (including the Commission Services)

Version History

HISTORY OF CHANGES		
Version	**Date**	**Changes**
1	14/10/2025	Report structure and core text by Manuel Hidalgo.
2	20/12/2025	Individual chapter contributions by various co-authors.
3	12/01/2026	Reviewing overall structure and approach by Manuel Hidalgo
4	19/01/2026	Generating content finished, reviews and suggestions to be terminated, start final editing.
5	23/01/2026	Final concept to be submitted to project leader for final review by project leader Martin Lindegren.
6	29/01/2026	Final version updated based on comments and edits of project leader Martin Lindegren.

Contributors

Manuel Hidalgo, Centro Oceanográfico de Baleares, Instituto Español de Oceanografía (IEO-CSIC), Palma, Spain

Nicolas Barrier, MARBEC, Univ Montpellier, Ifremer, CNRS, IRD, Sète, France

Stratos Batziakas, Hellenic Centre for Marine Research (HCMR), Institute of Marine Biological Resources and Inland Waters, Thalassokosmos, 71500 Heraklion, Greece

Marion Billy, Centro Oceanográfico de Baleares, Instituto Español de Oceanografía (IEO-CSIC), Palma, Spain

Silvia Blum, Centro Oceanográfico de Baleares, Instituto Español de Oceanografía (IEO-CSIC), Palma, Spain

Corina Chaves, Instituto Português do Mar e da Atmosfera (IPMA), Avenida Alfredo Magalhães Ramalho 6, 1495-165 Algés, Portugal

Antonella Consiglio, Fondazione COISPA ETS, Via dei Trulli 18-20, 70126 Bari, Italy

Keith M. Cooper, Centre for Environment, Fisheries and Aquaculture Science (Cefas), Pakefield Road, Lowestoft NR33 0HT, UK; and University of East Anglia (UEA), Norwich, NR4 7TJ, UK

Elena Couce, Centre for Environment, Fisheries and Aquaculture Science (Cefas), Pakefield Road, Lowestoft NR33 0HT, UK; and University of East Anglia (UEA), Norwich, NR4 7TJ, UK

Georg H. Engelhard, Centre for Environment, Fisheries and Aquaculture Science (Cefas), Pakefield Road, Lowestoft NR33 0HT, UK; and University of East Anglia (UEA), Norwich, NR4 7TJ, UK

Heino O. Fock, Institute of Sea Fisheries, Bremerhaven, Germany

Alicia Gran, Centro Oceanográfico de Baleares, Instituto Español de Oceanografía (IEO-CSIC), Palma de Mallorca, Spain

Lilly Greig, Centre for Environment, Fisheries and Aquaculture Science (Cefas), Pakefield Road, Lowestoft NR33 0HT, UK; and University of East Anglia (UEA), Norwich, NR4 7TJ, UK

Pierre Hélaouët, The Marine Biological Association (MBA), The Laboratory, Citadel Hill Plymouth, Devon, PL1 2PB, UK

Sofia Henriques, Instituto Português do Mar e da Atmosfera (IPMA), Avenida Alfredo Magalhães Ramalho 6, 1495-165 Algés, Portugal

Alexandros Kaninas, MARBEC, Univ Montpellier, Ifremer, CNRS, IRD, Montpellier, France

Stefanos Kavadas, Hellenic Centre for Marine Research (HCMR), Institute of Marine Biological Resources and Inland Waters, Anavyssos, Attiki, Greece.

Federico Maioli, National Institute of Aquatic Resources, Technical University of Denmark, Kemitorvet Bygning 202 2800 Kgs. Lyngby, Denmark

Irida Maina, Hellenic Centre for Marine Research (HCMR), Institute of Marine Biological Resources and Inland Waters, Anavyssos, Attiki, Greece.

Eva Maire, MARBEC, Univ Montpellier, Ifremer, CNRS, IRD, Montpellier, France

André Martins, Instituto Português do Mar e da Atmosfera (IPMA), Avenida Alfredo Magalhães Ramalho 6, 1495-165 Algés, Portugal

Bastien Mérigot, MARBEC, Univ Montpellier, Ifremer, CNRS, IRD, Sète, France

Marcel Montanyès, National Institute of Aquatic Resources, Technical University of Denmark, Kemitorvet Bygning 202 2800 Kgs. Lyngby, Denmark

Fabien Moullec, MARBEC, Univ Montpellier, Ifremer, CNRS, IRD, Montpellier, France

Teresa Moura, Instituto Português do Mar e da Atmosfera (IPMA), Avenida Alfredo Magalhães Ramalho 6, 1495-165 Algés, Portugal

Maria L. D. Palomares, Sea Around Us, Institute for the Oceans and Fisheries, The University of British Columbia, Vancouver, British Columbia, Canada

Myron A. Peck, Netherlands Institute for Sea Research (NIOZ), Landsdiep 4, 1797 SZ 't Horntje (Texel), The Netherlands.

Panagiota Peristeraki, Hellenic Centre for Marine Research (HCMR), Institute of Marine Biological Resources and Inland Waters, Thalassokosmos, 71500 Heraklion, Greece

Laurene Pecuchet, Norwegian College of Fishery Science, The Arctic University of Norway (UiT), Tromsø, Norway

John K. Pinnegar, Centre for Environment, Fisheries and Aquaculture Science (Cefas), Pakefield Road, Lowestoft NR33 0HT, UK; and University of East Anglia (UEA), Norwich, NR4 7TJ, UK

Patricia Puerta, Centro Oceanográfico de Baleares, Instituto Español de Oceanografía (IEO-CSIC), Palma, Spain

Marcel J.C. Rozemeijer, Wageningen Marine Research, Haringkade 1, 1976 CP IJmuiden, The Netherlands

Fernanda Silva, National Institute of Aquatic Resources, Technical University of Denmark, Kemitorvet Bygning 202 2800 Kgs. Lyngby, Denmark

Marcel Sole, National Institute of Aquatic Resources, Technical University of Denmark, Kemitorvet Bygning 202 2800 Kgs. Lyngby, Denmark

Camilla Sguotti, University of Padova, Italy

Maria Teresa Spedicato, Fondazione COISPA ETS, via dei Trulli 18-20, 70126 Bari, Italy

Murray Thompson, Centre for Environment, Fisheries and Aquaculture Science (Cefas), Pakefield Road, Lowestoft NR33 0HT, UK; and University of East Anglia (UEA), Norwich, NR4 7TJ, UK

Justin Tiano, Wageningen Marine Research, Haringkade 1, 1976 CP IJmuiden, The Netherlands

George Tserpes, Hellenic Centre for Marine Research (HCMR), Institute of Marine Biological Resources and Inland Waters, Thalassokosmos, 71500 Heraklion, Greece

Daniel van Denderen, National Institute of Aquatic Resources, Technical University of Denmark, Kemitorvet Bygning 202 2800 Kgs. Lyngby, Denmark

Rita Vasconcelos, , Instituto Português do Mar e da Atmosfera (IPMA), Avenida Alfredo Magalhães Ramalho 6, 1495-165 Algés, Portugal

Laure Velez, MARBEC, Univ Montpellier, Ifremer, CNRS, IRD, Sète, France

Antoni Vivó-Pons, National Institute of Aquatic Resources, Technical University of Denmark, Kemitorvet Bygning 202 2800 Kgs. Lyngby, Denmark

Walter Zupa, Fondazione COISPA ETS, via dei Trulli 18-20, 70126 Bari, Italy

Martin Lindegren, National Institute of Aquatic Resources, Technical University of Denmark, Kemitorvet Bygning 202 2800 Kgs. Lyngby, Denmark

Executive summary

The goal the B-USEFUL project is to contribute to achieve policy goals of the EU Green Deal and the Biodiversity Strategy 2030 by developing user-oriented tools and solutions to conserve and protect marine biodiversity, while effectively building and improving upon existing European data infrastructures and governance frameworks. The role of this Deliverable is to *report on how drivers and stressors impact biodiversity and how their independent and cumulative impacts are mediated shaping biodiversity trends and patterns*, which has been undertaken by partners under Task 3.2. To do that, the B-USEFUL team has applied a variety of analytical techniques over a broad range of marine ecosystems and organisms sampled along European shelf seas from the Eastern Mediterranean Sea to Greenland and the Barents Sea. All these areas are exposed to different regional environmental gradients in terms of climate and hydrography, but also local pressures mainly associated to anthropogenic activities. This Deliverable focuses on three main aspects: *i)* the combination of environmental gradients with local drivers spatially shaping the baselines for biodiversity patterns, *ii)* the context dependence and cross-scale approaches needed to explain global to local biodiversity variations, and *iii)* the cumulative pressures influence on the spatial heterogeneity of biodiversity-pressure relationships.

Our main findings indicate that environmental gradients like depth and sea-bottom variables (mainly bottom temperature) are the primary drivers of community composition and the different biodiversity facets. This highlights the crucial role of environmental filtering structuring marine communities by selecting species with traits capable of thriving in a particular range of environmental conditions of any given area. Local processes linked to natural environmental variability can also influence local biodiversity, but often play a secondary role to that of fishing pressure, especially for the nektobenthic and epibenthic communities analyzed here. Functional and life history traits explained a substantial fraction of among-species variation in biodiversity responses to pressures, particularly to temperature and anthropogenic drivers. In particular, several studies show that fish communities are strongly structured by ontogenetic variation in responses to environmental gradients and anthropogenic pressures, demonstrating that life stages should be treated as distinct ecological entities with potentially divergent niches, sensitivities, and vulnerabilities to global change. In the Northeast Atlantic, studies analyzing responses across the food web are able to reveal divergent responses to climate change across the different trophic levels, which are amplified under future scenarios. All these studies together evidence how biodiversity baselines are shifting, impacting biodiversity protection and conservation.

Cumulative effects and complex interactions in the biodiversity responses has been shown in different areas, evidencing that fishing, local environment and climate do not act independently in modifying biodiversity. For instance, in many Mediterranean areas, impacts on sea-bottom are amplified in shallow, thermally stressed areas where communities are near physiological tolerance limits or dominated by long-living and slow-recovering species. Some studies have paid particular attention to the three general types of cumulative interacting effects (additive, synergistic and antagonistic) with dominant interactions displayed a clear spatial structure in terms of temperature, primary production and fishing pressure. Context dependence and cross-scale biodiversity responses have been transversally considered in all the studies, albeit through different methods, including a set of potential environmental and local drivers to describe, in an integrative way, the mechanisms of biodiversity variation from local to regional scales. The co-occurrence of strong climatic and anthropogenic stressors along productive shelves and coastal areas has trigger an observed erosion of local biodiversity in the Mediterranean Sea, with a biotic homogenization over regional scales driven by the preferential loss of sensitive species and expansion of more tolerant taxa. Many studies stress the limitations of uniform, basin-wide measures for biodiversity

protection, and thus, the diversity of cumulative impacts should be tailored to the environmental and ecological context of each region. This was expected in high heterogenous ecosystems such as in the Mediterranean Sea, but also reported in the North Sea epibenthic communities with a clear spatial heterogeneity in the biodiversity-pressure relationships, and over the large climate-driven redistribution of fish species at a biogeographic scale over the whole Northeast Atlantic. Such results report a combination of context-dependent and species-specific responses all over the European Seas.

Taking the results of this Deliverable together, there is clear evidence of the need to develop region-specific management approaches under the Marine Strategy Framework Directive's Good Environmental Status (GES) objectives. A careful assessment of where conservation interventions are likely to be the most effective, together with the implementation of dynamic and adaptive measures as part of the Marine Spatial Planning (MSP) are also urgently required. Considering regional environmental and ecological context in the biodiversity responses enables a more holistic identification of the candidate areas for protection under realistic scenarios of change.

Index

1 The role of this deliverable

This deliverable (D3.2) is the second of three reports in the WP3 of the EU project "*user-oriented solutions for improved monitoring and management of biodiversity and ecosystem services in vulnerable European Seas*" (B-USEFUL) that together comprise "biodiversity status and cumulative impacts". Identifying and Understanding the key drivers and stressors that impact biodiversity and how their independent and cumulative impacts are mediated are crucial to ultimately understand the responses of biodiversity in terms of spatial and temporal variation. This knowledge is therefore central to support the overarching aim of B-USEFUL to develop tools and solutions to manage marine biodiversity, and ultimately national and international policies.

WP3 is structured in three main elements to establish the links from the status, trends, and cumulative impacts of pressures acting on multiple biodiversity indicators, to the links to ecosystem functions and services. These elements are: **(i)** estimate a set of multiple biodiversity indicators at different spatial and temporal scales (Deliverable 3.1, Lindegren et al. 2025), **(ii)** assess the status and cumulative impacts of multiple stressors acting on biodiversity (present Deliverable 3.2), and **(iii)** assess the effect and relative importance of various biodiversity indicators on overall measures of ecosystem functions and services (Deliverable 3.3).

In the present deliverable we report a diversity of impacts and biodiversity responses in marine communities of nektobenthic fish, crustaceans and cephalopods, as well as in marine benthic communities. The different sections provide evidence across European waters (Mediterranean, North Sea, Northeast Atlantic, Greenland and Barents Sea), and also over the northwest Atlantic and Pacific communities, with particular attention to:

(1) Identify the main natural drivers and human stressors driving the spatial patterns and temporal trends in biodiversity indicators and Essential Biodiversity Variables (EBV) of marine communities.

(2) Assess the spatial patterns and temporal trends of biodiversity responses to univariate or cumulative stressors, including complex interactions and cross-scale effects.

(3) Describe state-pressure relationships and quantify thresholds of different degrees of impact across spatial (from local to regional) and temporal scales.

The deliverable is structured to first provide a brief background of the field and the main aspects addressed in it (i.e., cumulative impacts, responses of diversity, state-pressure relationships, among others), followed by a series of sections describing how these aspects have been assessed in different regions and type of communities. The methods used and implemented are described in each section, ranging across a variety of methodologies including Joint-Species Distribution Models (JSDM), other statistical data-driven approaches, or specific state-pressure methods. All sections represent primarily manuscripts in preparation, or in review, with no single contribution published prior to submission of this report.

Acronyms and abbreviations

EBVs: Essential Biodiversity Variables

ESM: Environmental Safety Margins

MSP: Marine Spatial Planning

MPAs: Marine Protected Areas

SDM: Species Distribution Modelling

JSDM: Joint Species Distribution Modelling

HMSC: Hierarchical Modelling of Species Communities

BTS: Beam Trawl Surveys

BPR: Biodiversity-Pressure Relationships

DATRAS: online database of trawl surveys at ICES

DOI: Digital Identifier of an Object

EMODnet: European Marine Observation and Data Network

EFH: Essential Fish Habitats

GFCM: General Fisheries Commission for the Mediterranean

GFW: Global Fishing Watch

GSA: GFCM Geographical Sub Area

IBTS: International Bottom Trawl Surveys

ICES: International Council for the Exploration of the Sea

IPCC: Intergovernmental Panel on Climate Change

IUCN: International Union for the Conservation of Nature

LSM: Lower safety margins (ESM)

MEDITS: Mediterranean International Bottom Trawl Survey

MSFD: Marine Strategy Framework Directive

OSPAR: Convention for the Protection of the Marine Environment of the North-East Atlantic

PT-IBTS: International Bottom Trawl Survey in Portugal

SP-NORTH: Spanish North Coast Bottom Trawl Survey

SST: Sea Surface Temperature

USM: Upper safety margins (ESM)

VMS: Vessel Monitoring Systems

2 General introduction

2.1 Aim and background

Natural systems are evolutionarily adapted to cope with environmental variability and thus, the rapid and accelerating loss of worldwide biodiversity is primarily attributed to a combination of impacts of anthropogenic origin, often referred in general terms to 'global change' (Pim et al. 2014, IPBES 2019). This includes, but not restricted to, climate change, pollution, overexploitation of resources, exotic species or land use. In the marine realm, the impact on marine biodiversity is mainly attributed to the variety of impacts of the climate change (e.g. warming, extreme events, seasonal shifts), resources overexploitation, habitat loss, pollution and the arrival of non-indigenous species (Boyce et al., 2022, Halpern et al., 2008, 2025). For some of these drivers, such as warming, the mechanisms driving distributional shifts and rates of extinctions over large geographic scales are better understood (Pinsky et al., 2013; Freeman et al., 2018), as well as how they are profoundly altering the community assemblages, the structure and functioning of ecosystems (McGill *et al.*, 2006; Mouillot *et al.*, 2013). However, the mechanisms of impact and how biodiversity responds under the combination of different impacts (natural and anthropogenic) are poorly known, and tools to monitor and assess these complex impacts across regions are still lacking. Thus, it is urgent to resolve how biodiversity change occurs at multiple temporal and spatial scales in response to climate warming, species introductions and habitat degradation (Snelgrove et al. 2014, Chase et al. 2019), to anticipate the effects of the rapidly changing environment on biodiversity and ecosystem functioning (e.g. Harley et al. 2006; Mouillot *et al.*, 2013). This combination of accumulation of impacts has a higher relevance at lower scales (regional to local) where the spatial management measures such as Marine Protected Areas (MPAs) become more operational (Murray et al. 2025).

The relative contribution of the main drivers impacting biodiversity varies across ecological and geographic gradients and contributes to the multi-faceted nature of biodiversity (González et al. 2020). Additionally, how the combination of cumulative impacts interacts affects the response of biodiversity changes in different ecosystems (Low et al. 2022). Biodiversity indicators derived from Essential Biodiversity Variables (EBV) helps to synthesize the different facets of biodiversity variation (Lindegren et al. 2025: Deliverable 3.1), and they will, therefore, respond in a different way to cumulative impacts. Existing policy goals and reference levels denoting an unfavourable or favourable status (such as "Good Environmental Status" (GES) according to Marine Strategy Framework Directive, MSFD, Descriptor 1 on biodiversity) are commonly based in univariate state-pressure relationships. Making use of large spatiotemporal standardized databases of the benthic and nektobenthic communities across the European Seas, the task 3.2 of the B-USEFUL project has assessed the status of a series of biodiversity indicators, as well as investigated state-pressure relationships and cumulative impacts on biodiversity arising from multiple natural and human stressors, and compared across organism groups and European and non-European Seas. To do that, this deliverable builds on WP2, by using various catalogues of datasets containing biological traits, as well as of epibenthic and necktobenthic species abundances and distributions as informed by survey datasets from the Mediterranean and North-east Atlantic (Spedicato et al. 2024, Deliverable 2.2). In addition, the present Deliverable represents a continuation from the recent report of the Deliverable 3.1 (Lindegren et al. 2025) where the trends and spatial patterns of a set of biodiversity indicators and generated EBVs have been reported across organism groups and regions.

2.2 Cumulative impacts: natural drivers and human stressors interactions

Biodiversity conservation cannot be dissociated to the ecosystem-based management (EBM) (Ellis et al. 2025), which aims to balance human activities with environmental stewardships in order to maintain ecosystem properties, functions and services. That requires an understanding of how and to what extent human activities and natural events interact and affect ecosystem components and their functioning. It also requires the identification of solutions to prevent and mitigate the pressures being caused by such interactions (e.g. Halpern et al, 2008; Levin et al., 2009). Those interactions are known as '*cumulative impacts*' or '*cumulative effects*', and represent the interaction of natural environmental variability with a number of pressures, many of which are derived from human activities ultimately resulting in biodiversity loss such as: climate change, the extraction of resources, pollution, invasive species, habitat damage and fragmentation, and disease. While the terms '*cumulative impacts*' or '*cumulative effects*' are often used interchangeably to describe how pressures affect ecosystems, it is recommended the term '*cumulative effects*', noting that impacts are hypothesized and have been either not directly observed or attributed (Murray et al. 2015).

There are three general types of cumulative effects: additive, synergistic and antagonistic (Crain et al. 2008). Additive effects are incremental additions to the pressures caused by an activity, with each increment adding to previous increments over time. This effect represents the commonly assumed in research and most management tools for biodiversity conservation. Synergistic effects, also referred to as amplifying or exponential effects, magnify the consequences of individual pressures to produce a joint consequence that is greater than the additive effect (e.g. Hidalgo et al. 2011). Antagonistic or compensatory effects trigger a joint consequence lower than the additive (e.g. Lange and Marshall 2017). The identification and quantification of these effects on biodiversity explaining its spatiotemporal variation represent an urgent challenge to avoid mismanagement and to more efficiently anticipate the effects of the changing environment on biodiversity and ecosystem functioning, or considering more realistic scenarios of impact in biodiversity projections.

2.3 From impacts to responses in marine biodiversity under a cross-scale framework

Environmental variability and anthropogenic pressures do not act synoptically over large regions because of the spatial heterogeneity in the impacts and the environmental gradients, but also due to spatial variability in the sensitivity of the species and their response (Thorson, 2019). However, there is still certain lack of knowledge to understand how activities and stressors are spatially propagated triggering system responses (Low et al. 2023). The biodiversity responses to different pressures are often context-dependent and therefore, detecting signals of change will depend on the way the system is defined or delimited (Heim et al. 2021). Ecological theory has long emphasized that ecosystems are hierarchically structured and that many ecological processes are inher-

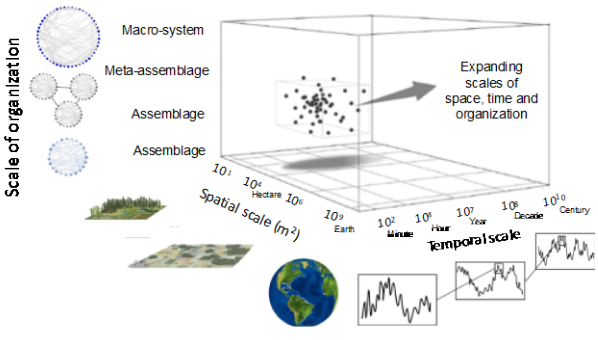

Figure 2.1. Cross-scale perspective of the biodiversity-ecosystem functioning (Gonzalez et al. 2020).

ently scale-dependent (Levin, 1992, Gonzalez et al. 2020, Figure. 2.1), while environmental and anthropogenic pressures also act at different spatial-scales. For instance, fishing pressure shows strong impacts on biodiversity at local scales, where direct extraction and habitat disturbance alter community structure and functional composition (Hidalgo et al. 2022, Shin et al., 2018), while water temperature has a stronger influence on biodiversity patterns on large spatial scale (e.g., latitudinal pattern) (Worm & Lotze, 2021). Indeed, activity and stressor imprint can generate a variety of systems response footprints because seascapes can have varying levels of physical and biological variation and connectivity (Low et al. 2023) (Fig. 2.2).

Broader scales may mask or dilute locally important effects and show an apparent temporal stability, partly due to statistical averaging, species–area relationships and compensatory dynamics among species (Flensborg et al., 2025). Therefore, larger-scales may potentially obscure early warnings of biodiversity change and conceal substantial local variability and localized declines. Thus, biodiversity indicators as well as stressors´ effects can be contrasted and even opposed when progressively moving from larger to smaller spatial units of analyses. This scale dependence is further complicated when multiple stressors interact, since drivers and responses operating at different spatial or temporal scales, often produce nonlinear and emergent dynamics that cannot be inferred from single-scale analyses (Peters et al., 2007; Soranno et al., 2014). Despite this context dependency, most studies still focus on a single spatial scale, neglecting the need to explicitly consider scale when interpreting biodiversity trends, assessing state–pressure relationships and identifying ecological thresholds.

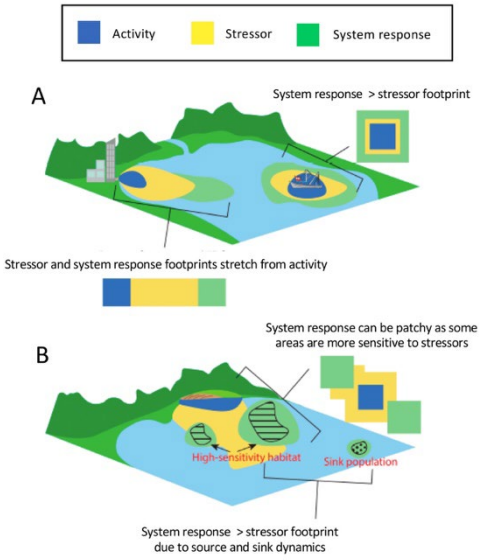

Figure 2.2. Conceptual diagram showing how the scale of the response (A) might or (B) might not agree with the scale of the impact (adapted from Low et al. 2023).

Cross-scale perspective is essential to achieve a holistic understanding of spatio-temporal changes in marine biodiversity, having profound implications for ecosystem resilience, recovery and management effectiveness, particularly under cumulative and interacting stressors. This deliverable shows how B-USEFUL has done that across the European Seas.

2.4 State-pressure relationships

The quantification of marine biodiversity is strongly linked with the concept of state-pressure relationships, which relate variations in the biodiversity indicators with gradients of natural or anthropogenic pressures. Existing EU policies, and particularly MSFD, uses this concept to define thresholds for unfavorable or favorable states (e.g., Good Environmental Status, GES) to operationalize the policy objectives into real context management decisions when risk of degraded biodiversity is detected, enabling preventive or responsive actions.

The biodiversity states are divided by ecological thresholds that represent points along a pressure gradient at which relatively small increases in a stressor lead to disproportionately large changes in the biodiversity state (Kenny et al. 2025). However, as aforementioned, pressures and biodiversity responses vary across-scales with cumulative and interacting effects occurring from local to regional and basin-wide ecosystems. This heterogeneity makes single,

system-wide thresholds difficult to generalize (Osland et al. 2025) and poses great methodological challenges in the identification of meaningful ecological thresholds that encompass such context complexity (Tam et al. 2017).

Nevertheless, incorporating cumulative effects, interacting pressures and meaningful spatial scales is key to understanding the variability in state–pressure relationships (commonly non-linear) and identifying ecological thresholds that support effective spatially explicit management measures aimed at maintaining ecological resilience. This B-USEFUL deliverable goes one step beyond common univariate state-pressure relationships towards multi-faceted ecological thresholds, and considering a cross-scale vision on biodiversity dynamics over the European Seas.

2.5 References

Boyce, D. G., Tittensor, D. P., Garilao, C., Henson, S., Kaschner, K., Kesner-Reyes, K., ... & Worm, B. (2022). A climate risk index for marine life. Nature Climate Change, 12(9), 854-862.

Crain, C. M., Kroeker, K., & Halpern, B. S. (2008). Interactive and cumulative effects of multiple human stressors in marine systems. Ecology letters, 11(12), 1304-1315.

Ellis, J., Macpherson, E., Thrush, S., Fisher, K., Pilditch, C., Jorgensen, E., ... & Hewitt, J. (2025). Scale and ecosystem-based management: Navigating mismatches between socio-ecological systems. Biological Conservation, 302, 111000.

Flensborg, L. C., Montanyès, M., Vivó Pons, A., Carolina Da Silva, F. and Lindegren, M. 2025. Scale-dependent effects of biodiversity and stability on marine ecosystem dynamics. - Ecography 2025: 1–10.

Gonzalez, A., Germain, R. M., Srivastava, D. S., Filotas, E., Dee, L. E., Gravel, D., ... & Loreau, M. (2020). Scaling-up biodiversity-ecosystem functioning research. Ecology Letters, 23(4), 757-776.

Heim, K. C., Thorne, L. H., Warren, J. D., Link, J. S. and Nye, J. A. 2021. Marine ecosystem indicators are sensitive to ecosystem boundaries and spatial scale. - Ecological Indicators 125: 107522.

Hidalgo, M., Vasilakopoulos, P., García-Ruiz, C., Esteban, A., López-López, L., & García-Gorriz, E. (2022). Resilience dynamics and productivity-driven shifts in the marine communities of the Western Mediterranean Sea. Journal of Animal Ecology, 91(2), 470-483.

Hidalgo, M., Rouyer, T., Molinero, J. C., Massutí, E., Moranta, J., Guijarro, B., & Stenseth, N. C. (2011). Synergistic effects of fishing-induced demographic changes and climate variation on fish population dynamics. Marine Ecology Progress Series, 426, 1-12.

Halpern, Benjamin S., and others (2008). A global map of human impact on marine ecosystems. Science, vol. 319, No. 5865, pp. 948–952.

Halpern, B. S., Frazier, M., O'Hara, C. C., Vargas-Fonseca, O. A., & Lombard, A. T. (2025). Cumulative impacts to global marine ecosystems projected to more than double by mid-century. Science, 389(6766), 1216-1219.

Harley, C. D., Randall Hughes, A., Hultgren, K. M., Miner, B. G., Sorte, C. J., Thornber, C. S., ... & Williams, S. L. (2006). The impacts of climate change in coastal marine systems. Ecology letters, 9(2), 228-241.

IPBES. (2019). The global assessment report on Biodiversity and Ecosystem services.

Kenny, A. J., Pepin, P., Bell, J., Downie, A., Kenchington, E., Koen-Alonso, M., Lirette, C., Froján, C. B., Ollerhead, N., Javier Murillo, F., Sacau, M., Fuller, S. and Diz, D. 2025. Reference points for assessing significant adverse impacts on deep sea vulnerable marine ecosystems. - Ecological Indicators in press.

Lange, R., & Marshall, D. (2017). Ecologically relevant levels of multiple, common marine stressors suggest antagonistic effects. Scientific Reports, 7(1), 6281.

Levin, S. A. 1992. The Problem of Pattern and Scale in Ecology: The Robert H. MacArthur Award Lecture. - Ecology 73: 1943–1967.

Levin, P. S., Fogarty, M. J., Murawski, S. A., & Fluharty, D. (2009). Integrated ecosystem assessments: developing the scientific basis for ecosystem-based management of the ocean. PLoS biology, 7(1), e1000014.

Lindegren, M., Hidalgo, M., Montanyes, M., Mioli, F., et al. (2025) Deliverable 3.1 Report on temporal trends and spatial patterns of multiple biodiversity indicators. B-USEFUL project. 133 pp.

Low, J. M., Gladstone-Gallagher, R. V., Hewitt, J. E., Pilditch, C. A., Ellis, J. I., & Thrush, S. F. (2023). Using ecosystem response footprints to guide environmental management priorities. Ecosystem Health and Sustainability, 9, 0115.

McGill, B. J., Enquist, B. J., Weiher, E., & Westoby, M. (2006). Rebuilding community ecology from functional traits. Trends in Ecology and Evolution, 21, 178–185.

Murray, C. C., Agbayani, S., Alidina, H. M., & Ban, N. C. (2015). Advancing marine cumulative effects mapping: An update in Canada's Pacific waters. Marine Policy, 58, 71-77.

Murray, C. C., Dunham, A., Rubidge, E., Francis, F. T., Hunter, K. L., & Hannah, L. C. (2025). Safeguarding marine protected areas from cumulative effects: a review of methods, best practices, and applications. Environmental Management, 1-15.

Mouillot, D., Graham, N. A. J., Villéger, S., Mason, N. W. H., & Bellwood, D. R. (2013). A functional approach reveals community responses to disturbances. Trends in Ecology and Evolution, 28, 167–177.

Osland, M. J., Bradford, J. B., Toth, L. T., Germino, M. J., Grace, J. B., Drexler, J. Z., Stagg, C. L., Grossman, E. R., Thorne, K. M., Romañach, S. S., Passeri, D. L., Noe, G. B., Lacy, J. R., Krauss, K. W., Kowalski, K. P., Guntenspergen, G. R., Ganju, N. K., Enwright, N. M., Carr, J. A., Byrd, K. B. and Buffington, K. J. 2025. Ecological thresholds and transformations due to climate change: The role of abiotic stress. - Ecosphere 16: e70229.

Peters, D. P. C., Bestelmeyer, B. T. and Turner, M. G. 2007. Cross–Scale Interactions and Changing Pattern–Process Relationships: Consequences for System Dynamics. - Ecosystems 10: 790–796.

Pimm, S. L., Jenkins, C. N., Abell, R., Brooks, T. M., Gittleman, J. L., Joppa, L. N., … Sexton, J. O. (2014). The biodiversity of species and their rates of extinction, distribution, and protection. Science, 344.

Shin, Y.-J., Houle, J. E., Akoglu, E., Blanchard, J. L., Bundy, A., Coll, M., Demarcq, H., Fu, C., Fulton, E. A., Heymans, J. J., Salihoglu, B., Shannon, L., Sporcic, M. and Velez, L. 2018. The specificity of marine ecological indicators to fishing in the face of environmental change: A multi-model evaluation. - Ecological Indicators 89: 317–326.

Soranno, P. A., Cheruvelil, K. S., Bissell, E. G., Bremigan, M. T., Downing, J. A., Fergus, C. E., Filstrup, C. T., Henry, E. N., Lottig, N. R., Stanley, E. H., Stow, C. A., Tan, P.-N., Wagner, T. and Webster, K. E. 2014. Cross-scale interactions: quantifying multi-scaled cause–effect relationships in macrosystems. - Frontiers in Ecol & Environ 12: 65–73.

Spedicato, M.T., Zupa, W., Villamor, A., Soni, V., et al. (2024) Deliverable 2.2 Report of available meta data and data gaps across case studies. B-USEFUL project. 133 pp.

Tam, J. C., Link, J. S., Large, S. I., Andrews, K., Friedland, K. D., Gove, J., Hazen, E., Holsman, K., Karnauskas, M., Samhouri, J. F., Shuford, R., Tomilieri, N. and Zador, S. 2017. Comparing Apples to Oranges: Common Trends and Thresholds in Anthropogenic and Environmental Pressures across Multiple Marine Ecosystems. Frontiers in Marine Science, 4, 282.

Thorson, J. T. (2019). Measuring the impact of oceanographic indices on species distribution shifts: the spatially varying effect of cold-pool extent in the eastern Bering Sea. Limnology and Oceanography, 64(6), 2632-2645.

Worm, B. and Lotze, H. K. 2021. Marine biodiversity and climate change. - In: Letcher, T. M. (ed), Climate Change (Third Edition). Elsevier, pp. 445–464.

3 Alpha and Beta diversity and cumulative impacts in the Mediterranean Sea

Authors: Wupa W., Puerta P., Consiglio A., Batziakas S., Moullec F., Peristeraki P., Mérigot B., Spedicato M.T., Hidalgo M.

3.1. Introduction

The Mediterranean Sea is a semi-enclosed basin connected to the Atlantic Ocean and, since 1869, to the Red Sea via the Suez Canal. The Strait of Sicily separates the western from the central-eastern sub-regions with substantial environmental, ecological and impacts differences. The present-day structure and environmental conditions of the basin are the legacy of past geological events that shaped its actual climate and physical features (Agiadi et al., 2025), and over a more contemporary temporal scale of decades of intense exploitation and degradation. Evaporation in the basin increases eastwards, raising salinity and driving an inflow of cooler, less saline Atlantic waters (AW) through the Strait of Gibraltar (Coll et al., 2010). These waters gradually warm and become saltier as they move eastwards, then sink in the Levantine basin before returning westwards as Levantine Intermediate Waters (LEW) beneath AW (100-500m of depth) and ultimately reaching the Channel of Sicily and the Strait of Gibraltar (Millot and Taupier-Letage, 2005). Overall, the Mediterranean basin is oligotrophic, mostly in its eastern part, and productivity generally declines from north to south and from west to east, inversely related to temperature and salinity (Danovaro et al., 1999). All this together makes the Mediterranean a complex combination of large-scale gradients and local/regional oceanographic features that generate a highly heterogeneous seascape (Boudouresque C., 2004), where temperate and subtropical biota coexist and a large proportion of endemic species persists (Bianchi et al., 2012).

Mediterranean diversity is increasingly affected by multiple, interacting pressures (Lejeusne et al., 2010; Bianchi et al., 2012; Anastasopoulou and Fortibuoni, 2019; Spedicato et al., 2019a; Lam et al., 2020; Soto-Navarro et al., 2021), including both those of natural and of anthropogenic origin. Climate change is causing rapid warming and shifts in hydrographic conditions (Mannino et al., 2017; Hidalgo M. et al., 2018), with cascading consequences on life cycle processes such as growth, survival, reproduction (Crozier and Hutchings, 2014) and physiology (Alter et al., 2024) of marine organisms, ultimately impacting their spatial distribution. These responses can drive range shifts, reorganisation of community composition (Pita et al., 2021; Rubino et al., 2024) or changes in ecosystem functioning (Moullec et al., 2019; Hidalgo et al., 2022) Additionally, alterations in biodiversity (Milazzo et al., 2013), are compounded by biological invasions and emerging fish diseases (Goren and Galil, 2005; Carella et al., 2020). In parallel, the Mediterranean has long been a hotspot of intensive fishing (Colloca et al., 2017), and many stocks remain exploited beyond sustainable levels despite recent management efforts and local improvements of stock status (FAO, 2025).

In this context, describing biodiversity patterns is essential to understand ecosystem responses, both local and regional, to ongoing pressures and to support ecosystem-based management. Biodiversity is usually quantified through indicators of species richness and relative abundance (Magurran, 2013). Alpha-diversity metrics, such as species richness, Shannon diver-

sity (Shannon, 1948) and Pielou's evenness (Pielou, 1966), describe local diversity and the abundance distribution of species within communities, while gamma-diversity describes the total diversity observed at the regional scale, integrating the contribution of multiple local assemblages across the broader area (Whittaker, 1972). Beta-diversity represents the ratio between regional and local species diversity and is often measured as the compositional dissimilarity among sites (Whittaker, 1972). Beta-diversity can be further partitioned into components related to species replacement (turnover) and nestedness (Baselga, 2010). Here we use an integrated analytical workflow that combines HMSC joint species distribution modelling, estimation of spatial and temporal patterns in the α- and β-diversity, together with constrained ordination (redundancy analysis, RDA) (Oksanen et al., 2020) and generalised dissimilarity modelling (GDM) (Ferrier et al., 2007) to relate spatial and temporal turnover to climatic, environmental and fishing gradients. This framework allows to assess both the cumulative and interactive effects of these pressures to be explicitly explored on demersal community structure across spatial scales and sub-basins.

3.2. Materials and methods

An integrated analytical workflow was developed to describe spatial and temporal patterns of demersal biodiversity in the Central-Eastern Mediterranean Sea and to assess the cumulative effects of climatic, environmental and anthropogenic drivers. The workflow combined joint species distribution modelling, multi-scale biodiversity indices, spatial and temporal β-diversity, generalised dissimilarity modelling and constrained ordination. First, information of species abundance and distribution were obtained from the posterior predictions of the joint species distribution model, specifically, we used hierarchical models of species communities (HMSC) framework (Tikhonov et al., 2020). In HMSC multiple species are modelled jointly as a function of shared environmental covariates and explicitly structured random effects. Using the hurdle approach (i.e., combining predictions of independent occurrence and abundance sub-models), two different models were fitted for each sub-basins, Western (WMS) and Central-Eastern Mediterranean Sea (CEMS), comprising 18 GFCM GSAs (Resolution GFCM/33/2009/2) (WMS: GSAs 1, 2, 5-11; CEMS: GSAs 15-20, 22, 23, 25) (Figure 3.1). The models' inputs used a 23-year time series (1999–2021) of MEDITS trawl-survey (Spedicato et al., 2019b) data Taxa were retained when their frequency of occurrence exceeded 1% across all hauls and trait information was available. Species traits were compiled following Beukhof et al. (2019a, 2019b) from FishBase for fish and from SeaLifeBase and WoRMS for cephalopods and decapod crustaceans. Traits included maximum body length, life span, larval and juvenile development, vertical zone, depth range, temperature preferences, diet and trophic level. In total, 191 taxa (146 fish, 21 crustaceans, 24 cephalopods) were modelled in the WMS and 158 taxa (120 fish, 18 crustaceans, 20 cephalopods) in the CEMS. The two sub-basin models were parametrised separatly to reflect regional conditions, using alternative combinations of environmental and anthropogenic drivers selected according to model fit. Predictors included depth (Schmitt et al., 2025), bottom and surface temperature, bottom and surface salinity (Escudier et al., 2021), chlorophyll-a (Cossarini et al., 2021), fishing effort (Kavadas et al., 2015; Kroodsma et al., 2018; STECF, 2023) and substrate type (Vasquez et al., 2021). These variables were specified as fixed effects in both occurrence and abundance sub-models, whereas spatial and temporal variability was modelled via random effects. For each sub-model, four MCMC chains were run with 250 posterior samples per chain; thinning intervals were adjusted to optimise convergence diagnostics and computational efficiency (100 for the WMS, 2000 for the CEMS). Further details on parametrization are reported in B-Useful deliverable 3.1 (Lindegren et al., 2025).

All HMSC predictions were performed on a regular 0.1° grid covering the two sub-basins, over 18 GSAs in four broader sub-regions: Western Mediterranean Sea (WMS), Adriatic Sea (AS), Central Mediterranean Sea (CMS) and Eastern Mediterranean Sea (EMS). Predicted probabilities of occurrence were converted into presence–absence using species-specific thresholds that maximised the percentage correctly classified (PCC) from confusion matrices (Cantor et al., 1999; Manel et al., 2001; Freeman and Moisen, 2008).

All the subsequent analyses were based on the posterior predictions of abundance conditioned on presence derived from the HMSC framework. Three α-diversity metrics were computed (R package vegan): species richness (number of species with predicted abundance > 0), Shannon diversity (Oksanen et al., 2020) and Pielou's evenness (Shannon, 1948; Pielou, 1966). Temporal trends in α-diversity were evaluated using Spearman rank correlations with time over multiple spatial scales. Spatial patterns and their persistence through time were examined by applying the Getis–Ord Gi* statistic (Getis and Ord, 1992) by year. Thus, cell with values higher than the 90th percentile and lower than the 10th percentile were classified as hotspot or cold-spot respectively, and the number of years classified as such, were used to derive the temporal persistence of high and low biodiversity. β-diversity was used to characterise compositional differentiation among sites and to relate community turnover to geographic distance. For each year, occurrence matrices were used to compute pairwise Jaccard dissimilarity (Jaccard, 1908; Legendre and Legendre, 2012) among grid cells. Total β-diversity, estimated with the betapart R package (Baselga, 2010; Baselga et al., 2018). Distance–dissimilarity relationships were analysed by combining annual Jaccard matrices with projected Euclidean distances among grid-cell centroids and fitting a power model (Bevilacqua et al., 2023). The intercept (a) and slope (b) of this model described short-distance similarity and its rate of decline with distance, allowing comparisons among years and spatial scales. Temporal β-diversity, including turnover and nestedness components, was mapped at the grid-cell scale. Spearman correlations were then used to relate these indices to longitude and latitude, thereby describing large-scale spatial gradients in temporal compositional change at different spatial scales.

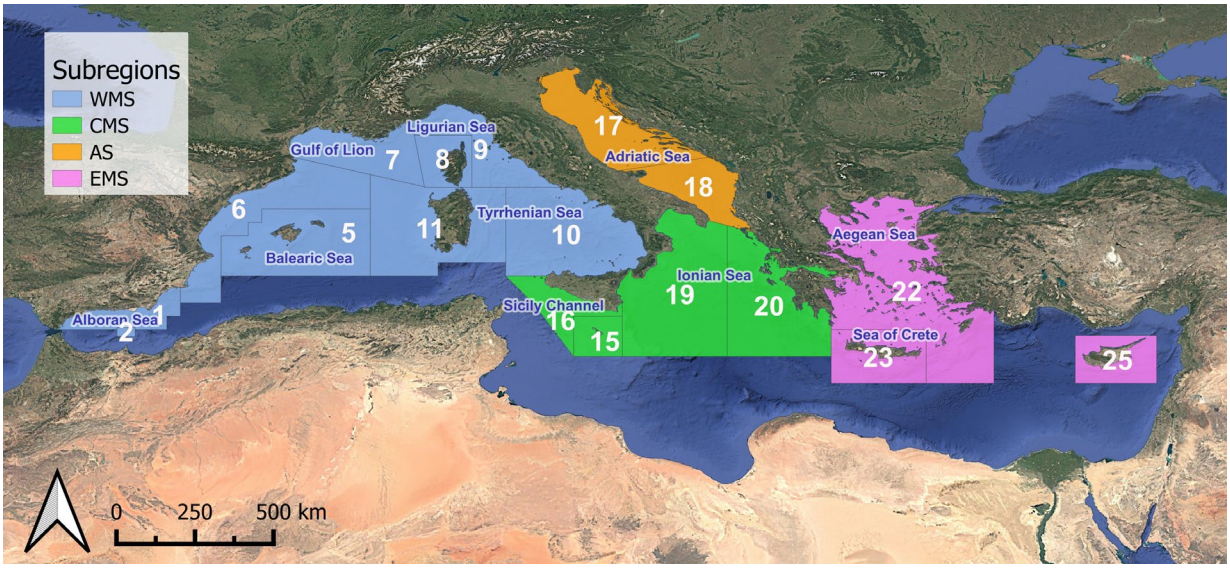

Figure 3.1. Map of the study area divided by subregion and relative GSAs. WMS: Western Mediterranean Sea, CMS: Central Mediterranean Sea; AS: Adriatic Sea; EMS: Eastern Mediterranean Sea.

Partial redundancy analysis (RDA) (Oksanen et al., 2020) was applied to Hellinger-transformed community abundances (Legendre and Gallagher, 2001) to partition variation among four predictor sets: climate (bottom and sea-surface temperature), local environment (surface and bottom salinity, chlorophyll-a, depth), fishing pressure (FDI data spatially disaggregated using the Global Fishing Watch footprint) and space–time structure. The latter was included as a conditional covariate to control for spatial and temporal autocorrelation. Fishing pressure was based on the demersal trawling fishery gears covering the vessels with length greather than 15m (not including the small scale fishery, for which the use of AIS is not mandatory). Since the FDI data do not cover the Albania and Montenegro, the fishing effort is limited to the EU countries, underestimating the coverage in the southern-estern Adriatic Sea. Variation partitioning was quantified as unique and shared fractions of Hellinger-based compositional variation attributable to each predictor set (Borcard et al., 1992; Peres-Neto et al., 2006; Legendre and Legendre, 2012). An extended RDA including interaction terms between fishing effort and key climatic variables (e.g. bottom temperature, sea-surface temperature) was used to test potential synergistic or antagonistic effects (Crain et al., 2008; Legendre and Legendre, 2012). Significance of predictor sets was assessed in order to evaluate the relative contributions of climate, environment and fishing after accounting for space–time structure, including both additive and interactive effects.

Compositional dissimilarity was further related to environmental and anthropogenic drivers using generalised dissimilarity modelling (GDM) (Ferrier et al., 2007), as implemented in the gdm R package (Fitzpatrick et al., 2022). GDMs were applied to Bray–Curtis dissimilarities in predicted species abundances conditioned on occurrence between all pairs of grid cells and years for a subset of time points (2012, 2021). Models were fitted with depth, surface and bottom temperature, surface and bottom salinity, log-transformed chlorophyll-a, log-transformed trawling effort and year as predictors, using I-spline basis functions to model non-linear turnover along each gradient. Predictor importance was quantified by permutation, and model performance was assessed by cross-validation in terms of deviance explained and predictive accuracy.

3.3. Results

α-diversity

In the WMS, the highest species richness values occurred along the Iberian coasts (GSA 6) and the western coast of Sardinia (GSA 11), whereas in the CEMS high richness was detected in the northern Aegean (GSA 22) and eastern Ionian Seas (GSA 20). In contrast, consistently lower richness characterised the Ligurian and Tyrrhenian Seas (GSAs 9 and 10) in the WMS, the Northern AS (GSA 17), and the southern part of the CEMS (GSAs 23, 25 and southern part of GSA 22). Getis–Ord Gi* maps highlighted these areas as persistent hot- and coldspots over time. The temporal analysis (Table S3.1, Figure 3.2) indicated a pervasive long-term decline in species richness at multiple spatial scales. At the sub-region level, richness decreased significantly, with the most widespread trends in the WMS (up to -6.5% in the time series), where all GSAs displayed consistent reductions, reaching the highest reduction rate of -13.4% in GSA 8 (Corsica Island) and -10.8% in GSA 7 (Gulf of Lion). CEMS sub-regions also tended to show declining richness (especially in Malta Island, -3.6%; Northern AS -4.9%; Aegean Sea -3.6%; respectively GSAs 15, 17 and 22) (Table S3.1), but with greater heterogeneity at the GSA scale. Spatial patterns of Shannon diversity broadly mirrored those of richness. Stable hotspots of Shannon index (Figure S3.1) occurred along the Iberian and Sardinian coasts (GSAs 7, 8 and 11), in the

southern Adriatic (GSA 18), the eastern Ionian (GSA 20) and the central Aegean Sea (GSA 22), whereas the Ligurian and Tyrrhenian Seas (GSAs 9 and 10), the western part of the Northern Adriatic (GSA 17), the Thermaic Gulf (northern-western part of Aegean Sea) and the southern Aegean Sea (GSA 22) showed the lowest values. Through time, Shannon diversity declined significantly at the scale of the whole study area, with pronounced and consistent decreases in the WMS (-2.1%) and generally weaker, but still negative, trends in most central and eastern subregions (from -0.7% to -1.3% in the CEMS). Pielou's evenness displayed similar large-scale spatial contrasts, with persistent hotspots and coldspots largely overlapping the Shannon patterns. A general tendency towards decreasing evenness emerged across most of the study area, particularly in the WMS (-1.5%) and in parts of the AS and EMS (-1.0% both), aligned with an increase in dominance of some species within assemblages and communities, whereas the CMS displayed comparatively stable trajectories (-0.4%), without significant long-term trends at GSA level. Globally, the Western basin shows higher values in all the indices, even though those differences could be likely biased by the different parametrization of the two models in terms of number of species covered. On the other side, the indices estimated for the CEMS show that the highest average values of species richness are reported for the CMS, followed by EMS and finally AS, with the lowest richness values. Notwithstanding, this trend is partially inverted in Shannon and evenness indexes in which the AS shows higher values of both indexes in comparison to the CMS.

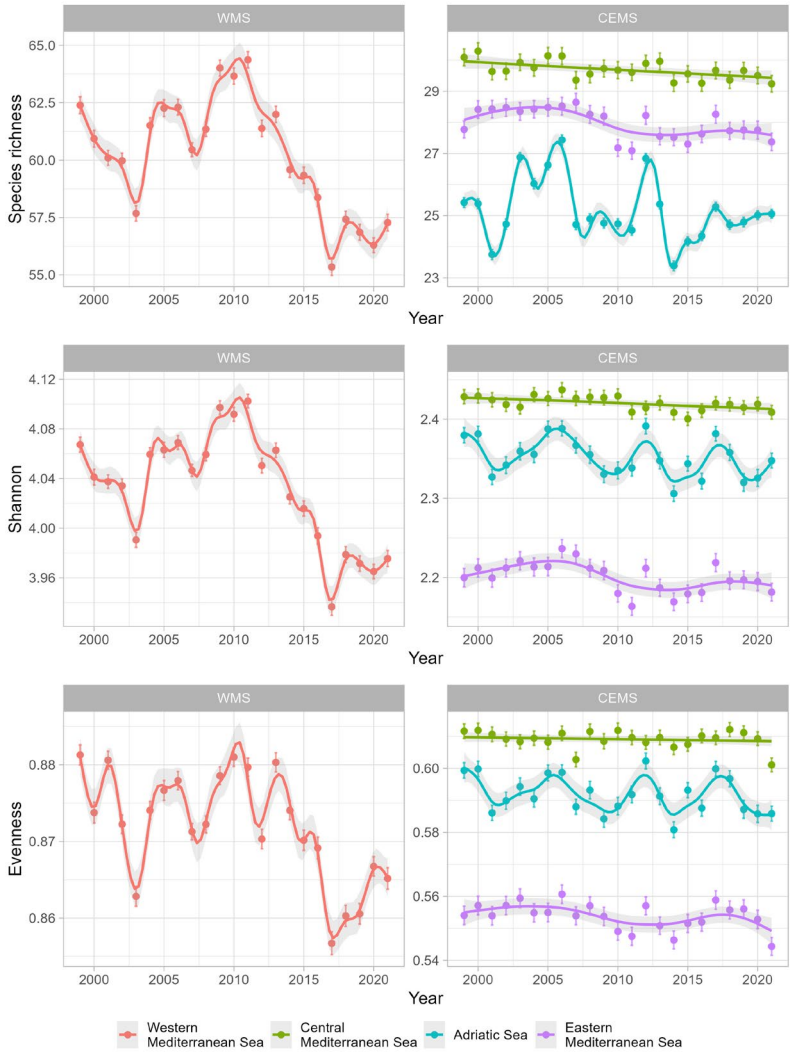

Figure 3.1. Temporal pattern of the alpha-diversity metrics (species richness, Shannon and evenness indices) at sub-region spatial scale (WMS: Western Mediterranean Sea, CEMS: Central-Eastern Mediterranean Sea).

β-diversity

Patterns of β-diversity revealed a temporally variable distance–dissimilarity structure across Mediterranean sub-areas (Table S3.2). At the basin scale, the a (intercept, representing changes in baseline compositional contrast) and b (slope, describing the rate at which assemblages diverge with distance) parameters of the power relationships between Jaccard index and inter-cell distance remained generally stable, with one notable exception: in the EMS, the b coefficient increased significantly over time, indicating stronger spatial structuring of community dissimilarity, while a parameter remained stable. The WMS, CMS and AS did not show significant basin-scale trends in either parameter. At the GSA scale, temporal changes in distance–dissimilarity parameters were more heterogeneous. In the WMS, GSAs 9 and 10 exhibited significant negative trends in both a and b, consistent with a gradual weakening of spatial turnover and increasing homogenisation of assemblages. In the CMS, GSAs 15 and 20 showed the opposite pattern, with strong positive trends in both parameters. In the EMS, GSA 23 also displayed significant positive trends in a and b, mirroring the basin-scale strengthening of distance–dissimilarity in this region. No significant temporal changes were detected in the Adriatic GSAs 17 and 18, or in the remaining GSAs of the CEMS, where β-diversity patterns appeared largely stationary through time.

Temporal β-diversity between 1999 and 2021 showed marked and spatially structured patterns (Figure 3.3). The strongest compositional reorganisation occurred in the WMS around Sardinia and in parts of the Ligurian and Tyrrhenian Seas, mainly due to the nestedness high values. The Gulf of Lion and the Balearic Islands also exhibited high species turnover, while a more patched and heterogenous pattern over the WMED is observed compared to the clear gradient in nestedness. In the CEMS, elevated temporal turnover was mainly concentrated in the northern Adriatic and along the northern and western Ionian shelves. There, nestedness contributed more modestly and displayed a heterogeneous and spatially fragmented pattern, with higher values mostly in the western AS and the central-southern Aegean Sea. Overall, absolute levels of temporal diversity were higher in the WMS than in the CEMS. Analysis of temporal trends along longitude and latitude further clarified these patterns (Table S3.3). In the WMS, temporal β-diversity shows the higher local variations along the time series in the northern-eastern quadrant, following a significant trend along the west-east and south-north geographic gradients. These positive gradients were particularly pronounced in Balearic Sea and along the Iberian coasts (GSAs 5 and 6), whereas negative gradients in the Gulf of Lion and Sardinia Island (GSAs 7 and 11) highlighted contrasting patterns between the Alboran–Balearic region and the Ligurian–northern Tyrrhenian sector. In the CMS, longitudinal gradients were generally weak, but Sicily Channel and the Western Ionian Sea (GSAs 15, 16 and 19) showed clear increases in temporal β-diversity, especially in nestedness, towards their north-eastern areas, while Eastern Ionian Sea (GSA 20) exhibited a stronger latitudinal signal with higher turnover at higher latitudes. In the Adriatic Sea, temporal β-diversity decreased eastwards and increased northwards, mainly driven by turnover, pointing to stronger community reorganisation in the western and northern Adriatic. In the EMS, both total β-diversity and its turnover component declined sharply from west to east but increased towards higher latitudes.

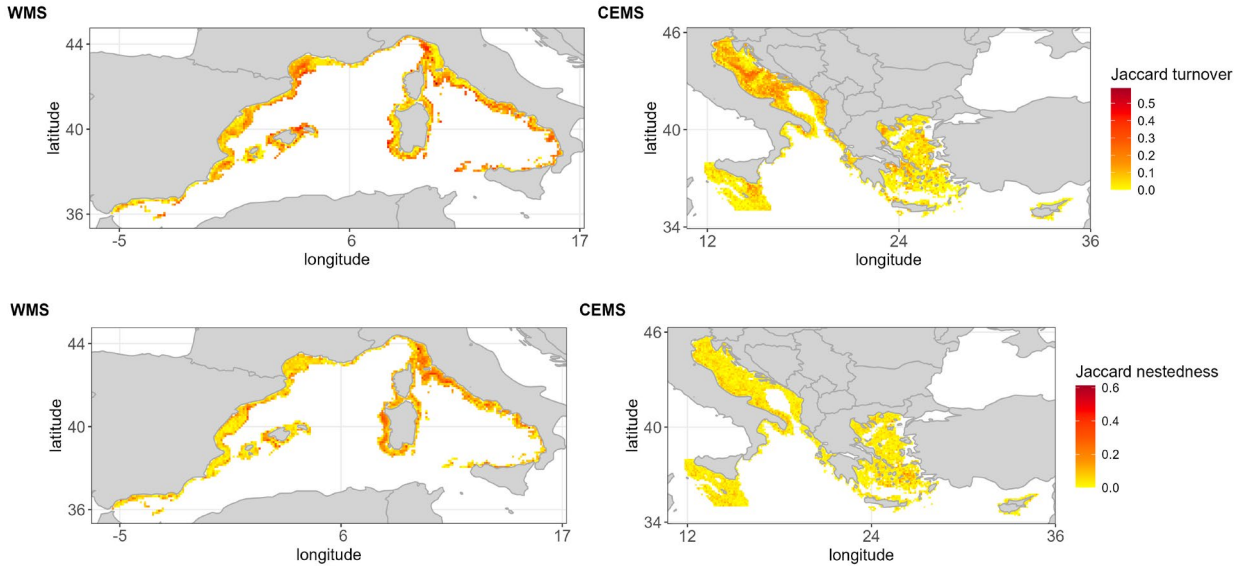

Figure 3.2. Maps of the estimated temporal β-diversity split into turnover and nestedness components in the WMS (left) and CEMS (right) sub-basins.

Effects of Cumulative drivers

The partial redundancy analysis (RDA) on Hellinger-transformed HMSC outputs for the WMS showed that explicit environmental and fishing covariates explained an adjusted R^2 of about 0.39 of community variation ($F = 1857.8$, $p = 0.002$), after conditioning on broad-scale space–time structure. The first canonical axis (RDA1) accounted for 76% of the constrained variance, and all canonical axes were highly significant. Sequential and marginal tests consistently highlighted bottom properties and depth as the main drivers, with bottom salinity (bso), depth and bottom temperature (btemp) clearly dominating over surface salinity (so), chlorophyll-a concentration (chl), fishing effort (fe) and sea-surface temperature (sst). Variation partitioning across climate, environment, fishing and space–time indicated that the full model explained 53% of total community variation, with unique fractions of 3.9% for climate, 22.0% for local environmental gradients, 0.4% for fishing and 3.7% for space–time. Although the unique fishing fraction was small, adding interaction terms between fishing and environmental covariates (btemp×fe, fe×sst, depth×fe) significantly improved model fit ($F = 68.7$, $p = 0.002$), indicating non-additive effects of fishing along thermal and bathymetric gradients (Figure 3.4). In the EMS, the RDA showed a lower adjusted R^2 (R^2_adj ≈ 0.25; $F = 2784.3$, $p = 0.002$), but with a very strong overall significance. As in the WMS, RDA1 concentrated most of the constrained variance (about 71%), and all axes were highly significant. Depth emerged as the dominant predictor, followed by btemp, while fe, chl, so, bso and sst contributed to a smaller but still significant fraction. The full model reached 56% of explained deviance, with unique contributions of 3.6% for climate, 16.2% for environmental gradients, 0.7% for fishing and 13.4% for space–time. Thus, in the CEMS, space–time accounted for a much larger unique fraction than in the WMS, and fishing also showed a marginal fraction. Interactions between fishing and environmental variables had an even stronger effect than in the WMS due to the higher regional and spatial heterogeneity, with depth×fe explaining the largest marginal fraction among interactions (Figure 3.4). The RDA biplots with interaction terms (Figure 3.5) visualise how climate and fishing jointly shape community composition. In the WMS (left panel), the fishing effort vector (fe) points roughly opposite to depth, while btemp is nearly orthogonal to depth, suggesting that the fishing gradient tends to counteract depth-related community segregation. The depth×fe interaction is almost collinear with fe and clearly inverse to depth, behaving synergistically with

fishing and antagonistically with depth. This reflected the strong covariance between fishing effort and bathymetry, indicating that the compositional signal associated with effort was mainly expressed on shallower grounds and progressively weakened with increasing depth. By contrast, btemp×fe and fe×sst point towards the same quadrant as btemp, sst and chl, and away from the pure fe vector, suggesting that the observed fishing-related turnover was context-dependent and co-occurred with the same physical drivers structuring assemblage composition, indicating that these interactions act synergistically with the main environmental gradient and antagonistically with the pure fishing effect. In the CEMS (right panel), the structure of main effects is similar, with depth and btemp showing the strongest environmental axes and fe oriented roughly opposite to depth. The depth×fe vector is closely aligned with fe and opposed to depth and is about 2.7 times longer than the fe vector itself, indicating that most depth-related changes in communities under high fishing pressure are captured by the interaction rather than by the main fe term. Interactions with temperature (btemp×fe and fe×sst) also show a stronger cumulative signal than in the WMS: both fall between depth and chl along the sst axis and are longer than the fe main effect (≈1.2× for btemp×fe and ≈0.7× for fe×sst). Overall, these patterns support a non-uniform fishing imprint across the study area, with the apparent effect of effort being modulated by depth and temperature regimes, rather than acting as a spatially constant additive pressure. In turn, the effect of fishing, if considered alone, is likely underestimated in comparison to the total amount of variance accounted for fishing, included the shared portion with the other components considered in the RDA analysis (environment, climate and space-time) that is almost 8%.

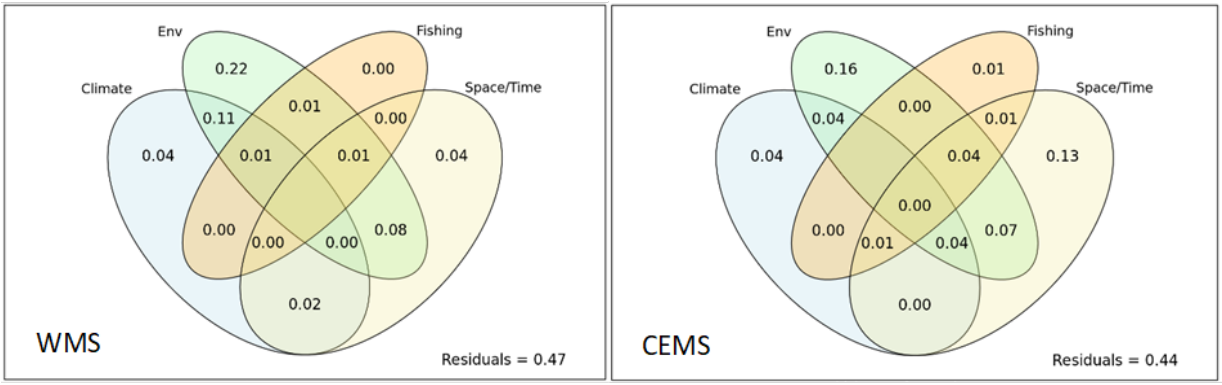

Figure 3.3. Variance partitioning of the redundancy analyses (RDA) conducted for the Western Mediterranean Sea (WMS, left) and Central–Eastern Mediterranean Sea (CEMS, right), accounting for 4 different groups of variables: Climate (bottom and sea-surface temperature); Env (surface and bottom salinity, chlorophyll-a, depth); Fishing (fishing effort); Space/Time (Year, Latitude, Longitude).

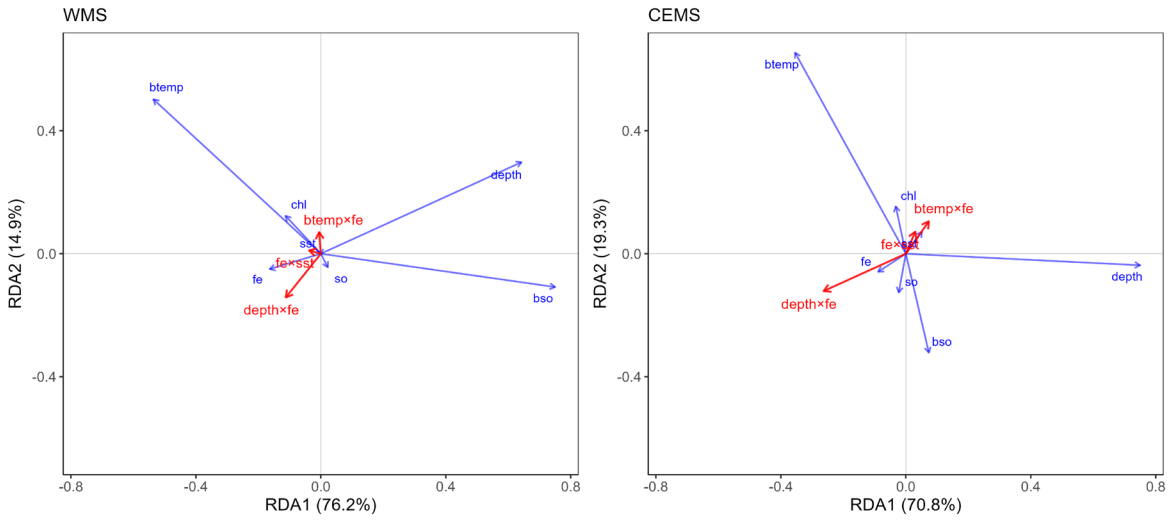

Figure 3.4. Partial RDA biplots of demersal community composition for the WMS (left) and CEMS (right) including main effects (blue arrows) and fishing–environment interactions (red arrows). sst: sea surface temperature; btemp: bottom temperature, so: surface salinity; bso: bottom salinity; chl: chlorophyll a; depth: bathymetrical depth;fe: fishing effort; btemp:fe, fe:sst, depth:fe represent the interaction components of fishing effort with bottom temperature, sea surface temperature and depth, respectively.

Generalised dissimilarity modelling

Generalised dissimilarity models (GDMs) provided a robust description of temporal β-diversity in both basins, with full models explaining 69.1–85.0% and 77.3–93.8% of deviance in the WMS and CEMS, respectively, and cross-validation yielding similarly high predictive performances (68.3–85.1% and 77.5–93.7%). These diagnostics indicate that the models captured most of the temporal variation in Bray–Curtis dissimilarity and that this explanatory power was not restricted to calibration data but remained stable under cross-validation.

In the western basin, the relative importance of predictors (Table S3.5) was biased towards bottom level variables: bottom salinity and temperature emerged as the main drivers, as also reported by HMSC model, with depth remaining a secondary yet important factor, while chlorophyll, surface salinity and sea-surface temperature had comparatively smaller effects. In the eastern basin, depth was by far the dominant predictor, followed by bottom temperature and, with lower but consistent contributions, bottom salinity, chlorophyll a, surface salinity and sea-surface temperature. Across both basins, fishing effort showed a lower yet still significant contribution in shaping biodiversity patterns.

Spatial predictions of Bray–Curtis dissimilarity derived from these models showed coherent patterns between basins. In both western and eastern regions, moderate to very high temporal turnover was concentrated along continental shelves and coastal margins, whereas deeper slope and offshore areas exhibited more moderate changes.

3.4. Discussion

The complementary analysis of α- and β-diversity combining local and regional scales indicates that Mediterranean demersal biodiversity is undergoing a pervasive but spatially heterogeneous reorganisation facilitated by strong environmental gradients (Lacoue-Labarthe et al., 2016; Tuel and Eltahir, 2020), where productivity, hydrodynamics and topographic complexity shape contrasts in community structure (Coll et al., 2010; Micheli et al., 2013). Diversity hotspots lo-

calised along continental shelves and upper slopes in both basins are consistent with previous MEDITS-based evidence of higher diversity in western and central areas and in frontal or upwelling zones (Farriols et al., 2020; Veloy et al., 2022). Long-term declines in species richness, Shannon diversity and evenness, especially in the WMS and in parts of the CEMS subbasin, suggest progressive erosion of local diversity and redistribution of relative abundances (Coll Marta et al., 2010). These trends are consistent with the Mediterranean being one of the fastest-warming ocean regions, already exposed to frequent and intense marine heatwaves and temperature extremes with widespread biological impacts (Marbà et al., 2015; Darmaraki et al., 2019; Garrabou et al., 2022), particularly in the Alboran and western Mediterranean Seas, where many species sensitive to climate change occur (Chatzimentor et al., 2023). Meridionalisation processes favour thermophilic species (including invasive species from Indo-Pacific Ocean) over temperate ones that are approaching their upper thermal limits (Bensoussan et al., 2010; Calvo et al., 2011), while warming-induced reductions in chlorophyll-a and enhanced water column stratification likely reduce food supply (Kim et al., 2019). At the same time, cumulative human impacts and fishing pressure remain concentrated along productive shelves and coastal areas (Coll et al., 2012; Micheli et al., 2013; Piroddi et al., 2020a), so the observed erosion of α-diversity in these regions is consistent with the co-occurrence of strong climatic and anthropogenic stressors. β-diversity results show that these changes are not a simple uniform loss of species richness, but involve marked spatial restructuring of assemblages (Pennino et al., 2024): distance–dissimilarity parameters derived from Jaccard dissimilarities reveal contrasting trajectories among sub-regions and GSAs, with some areas showing declining of dissimilarity al local and wider scale (both a and b parameters of power function), consistent with biotic homogenisation driven by the preferential loss of sensitive species and expansion of more tolerant taxa (Soininen et al., 2007; Bevilacqua et al., 2023). Other areas show increasing in these two components, indicating stronger distance-structured turnover under spatially heterogeneous climatic forcing, fishing induced fishing erosion and decreasing ecological similarity (Hidalgo et al., 2017; Bevilacqua et al., 2023), even at local scale. Maps of temporal Jaccard components between 1999 and 2021 confirm that high turnover clusters along continental shelves, particularly in the CEMS, the northern AS and the northern and western Ionian (Giani et al., 2012), while offshore areas of the WMS show more pronounced changes, in line with increasing β-diversity trends reported for the North Catalan Sea and Gulf of Lion (Veloy et al., 2022). Temporal β-diversity generally increases towards higher latitudes in both basins, with stronger turnover likely driven by meridionalisation processes (Coll et al., 2010; Lloret et al., 2015), especially in the northern Adriatic, Gulf of Lion and Ligurian Sea, where shallow hydrography, eutrophication and long-term exploitation are known to produce highly dynamic assemblages (Giani et al., 2012; Veloy et al., 2022).

Constrained ordination provides a mechanistic interpretation of these patterns, highlighting depth and bottom level variables (bottom temperature and salinity) as primary drivers of community composition and fishing effort as a smaller but still significant additional factor, consistent with previous Mediterranean studies emphasizing bathymetry and water-mass controls on demersal assemblages and productivity (Farré et al., 2016; Peristeraki et al., 2017; Carlucci et al., 2018; Quattrocchi et al., 2026). RDA and variance partitioning show that fishing, local environment and climate do not act independently. Interaction terms between fishing effort and thermal or bathymetric gradients improve model fit, and most of the fishing signal emerges through joint, non-additive associations with depth and temperature, especially in the CEMS basin. This supports the view that climate and fishing operate as cumulative but interacting drivers of community change, with trawling effects amplified in shallow, thermally stressed areas where communities are near physiological limits or dominated by long-living, slow-

recovering species (Micheli et al., 2013; Marbà et al., 2015; Colloca et al., 2017). The small unique fraction attributed to fishing reflects its tight coupling with environmental gradients rather than a negligible role. GDMs corroborate this interpretation, showing that a limited set of predictors (primarily depth and bottom climate) explain a large proportion of temporal Bray–Curtis dissimilarity. These results are in accordance with observations and projections reported for several demersal species indicating northward and downslope range shifts, contraction of suitable habitat for cold-affinity taxa and potential local reductions in shallow, warm sectors, particularly in the EMS (Ben Lamine et al., 2022; Panzeri et al., 2024) but also in the WMED (Sanz-Martín et al., 2024), and consistent with the stronger turnover and distance–dissimilarity signals observed there. Overall, our findings indicate that Mediterranean demersal fauna are simultaneously exposed to progressive climatic change and to the legacy of historically intense, spatially structured fishing, so that biodiversity responses still reflect combined influences of climate and both past and present exploitation. Because fishing acts synergistically with warming and related environmental change, even modest direct effects of trawling can be amplified under more climatic exposed areas, and thus biodiversity changes cannot be attributed to climate alone. Trait-based and risk-assessment studies show that many long-living, slow-growing demersal species, including commercially important taxa, are highly vulnerable to warming, deoxygenation and recurrent marine heatwaves, as well as to chronic exploitation (Marbà et al., 2015; Chatzimentor et al., 2023; Polo et al., 2025; Zupa et al., 2025). On the other way around, fishing can also likely amplify or modulate climate-driven changes by selectively removing large, late-maturing individuals and altering size structure and mean trophic levels (Colloca et al., 2017; Pecuchet et al., 2017; Beukhof et al., 2019a; Piroddi et al., 2020b; Polo et al., 2025), even though a complete consensus on the latter point is not still achieved even though a complete consensus on the latter point is not still achieved (Peristeraki et al., 2019). The stronger role of space–time structure and fishing–environment interactions, especially in the CEMS basin, determined by the semi-enclosed nature of the basin together with steep west-to-east trophic gradients and complex circulation, points to emerging hotspots where climatic anomalies and intense trawling coincide, potentially accelerating turnover and eroding resilience. From a management perspective, the spatially explicit patterns described identify priority areas for climate-aware conservation and fisheries regulation. Regions characterized by high β-diversity along continental shelves, and in the northern Adriatic, Ionian and parts of the Aegean, correspond to rapidly reorganising communities under strong cumulative bottom warming and fishing. Those areas may require reinforced control of trawling effort, protection of climatically resilient habitats and strengthened networks of closed areas that preserve connectivity along depth and temperature gradients. Scenario-based evaluations of spatial restrictions across EU waters indicate that biodiversity and habitat gains may be undermined when effort is displaced rather than reduced, and that outcomes depend strongly on closure placement and on their combination with other areas with complementary fisheries controls (Bastardie et al., 2025). Additionally, within such networks, species-targeted removals may be needed to effectively control invasive fish populations, particularly in the EMS (Giakoumi et al., 2019). By contrast, sectors with lower turnover and relatively stable β-diversity may function as refugia under future climate scenarios and provide long-term protection. This information will be thus critical to properly assess the trade-off between biodiversity conservation and fisheries management in future decision making and marine spatial planning.

3.5. References

Agiadi, K., Hohmann, N., Gliozzi, E., Thivaiou, D., Bosellini, F. R., Taviani, M., Bianucci, G., et al. 2025. Late Miocene transformation of Mediterranean Sea biodiversity. Science Advances, 10: eadp1134. American Association for the Advancement of Science. https://doi.org/10.1126/sciadv.adp1134.

Alter, K., Jacquemont, J., Claudet, J., Lattuca, M. E., Barrantes, M. E., Marras, S., Manríquez, P. H., et al. 2024.

Hidden impacts of ocean warming and acidification on biological responses of marine animals revealed through meta-analysis. Nature Communications, 15(1), 2885.

Anastasopoulou, A., and Fortibuoni, T. 2019. Impact of Plastic Pollution on Marine Life in the Mediterranean Sea. Handbook of Environmental Chemistry, 111: 135–196. Springer, Cham.

Baselga, A. 2010. Partitioning the turnover and nestedness components of beta diversity. Global ecology and biogeography, 19: 134–143. Wiley Online Library.

Baselga, A., Orme, D., Villeger, S., De Bortoli, J., Leprieur, F., Logez, M., and Martinez-Santalla, S. 2018. betapart: Partitioning beta diversity into turnover and nestedness components. R package version, 1.

Bastardie, F., Astarloa, A., Binch, L., Bitetto, I., Damalas, D., Depestele, J., Hernvann, P. Y., et al. 2025. Anticipating how spatial fishing restrictions in EU waters perform to protect marine species, habitats, and dependent fisheries. Frontiers in Marine Science, 12. Frontiers Media SA.

Ben Lamine, E., Schickele, A., Goberville, E., Beaugrand, G., Allemand, D., and Raybaud, V. 2022. Expected contraction in the distribution ranges of demersal fish of high economic value in the Mediterranean and European Seas. Scientific Reports, 12: 10150. Nature Publishing Group UK London.

Bensoussan, N., Romano, J.-C., Harmelin, J.-G., and Garrabou, J. 2010. High resolution characterization of northwest Mediterranean coastal waters thermal regimes: to better understand responses of benthic communities to climate change. Estuarine, Coastal and Shelf Science, 87: 431–441. Elsevier.

Beukhof, E., Frelat, R., Pecuchet, L., Maureaud, A., Dencker, T. S., Sólmundsson, J., Punzón, A., et al. 2019a. Marine fish traits follow fast-slow continuum across oceans. Scientific reports, 9: 17878. Nature Publishing Group UK London.

Beukhof, E., Dencker, T. S., Palomares, M. L. D., and Maureaud, A. 2019b. A trait collection of marine fish species from North Atlantic and Northeast Pacific continental shelf seas. Pangaea, 1: 12.

Bevilacqua, S., Boero, F., De Leo, F., Guarnieri, G., Mačić, V., Benedetti-Cecchi, L., Terlizzi, A., et al. 2023. β-diversity reveals ecological connectivity patterns underlying marine community recovery: Implications for conservation. Ecological Applications, 33: e2867. Wiley Online Library.

Bianchi, C. N., Morri, C., Chiantore, M., Montefalcone, M., Parravavicini, V., and Rovere, A. 2012. Mediterranean Sea biodiversity between the legacy from the past and a future of change. Life in the Mediterranean Sea: a look at habitat changes, 1, 55.

Borcard, D., Legendre, P., and Drapeau, P. 1992. Partialling out the spatial component of ecological variation. Ecology, 73: 1045–1055. Wiley Online Library.

Boudouresque C. 2004. Marine biodiversity in the Mediterranean: status of species, populations and communities.

Calvo, E., Simó, R., Coma, R., Ribes, M., Pascual, J., Sabatés, A., Gili, J. M., et al. 2011. Effects of climate change on Mediterranean marine ecosystems: the case of the Catalan Sea. Climate Research, 50: 1–29.

Cantor, S. B., Sun, C. C., Tortolero-Luna, G., Richards-Kortum, R., and Follen, M. 1999. A comparison of C/B ratios from studies using receiver operating characteristic curve analysis. Journal of clinical epidemiology, 52: 885–892. Elsevier.

Carella, F., Elisabetta, A., Simone, F., Fulvio, S., Daniela, M., Prado, P., Rossella, P., et al. 2020. In the Wake of the Ongoing Mass Mortality Events: Co-occurrence of Mycobacterium, Haplosporidium and Other Pathogens in Pinna nobilis Collected in Italy and Spain (Mediterranean Sea). Frontiers in Marine Science, 7: 510441. Frontiers Media S.A.

Carlucci, R., Bandelj, V., Ricci, P., Capezzuto, F., Sion, L., Maiorano, P., Tursi, A., et al. 2018. Exploring spatio-temporal changes in the demersal and benthopelagic assemblages of the north-western Ionian Sea (central Mediterranean Sea). Marine Ecology Progress Series, 598: 1–19.

Chatzimentor, A., Doxa, A., Katsanevakis, S., and Mazaris, A. D. 2023. Are Mediterranean marine threatened species at high risk by climate change? Global Change Biology, 29: 1809–1821. Wiley Online Library.

Coll, M., Piroddi, C., Albouy, C., Ben Rais Lasram, F., Cheung, W. W. L., Christensen, V., Karpouzi, V. S., et al. 2012. The Mediterranean Sea under siege: Spatial overlap between marine biodiversity, cumulative threats and marine reserves. Global Ecology and Biogeography, 21: 465–480. John Wiley & Sons, Ltd. doi: 10.1111/j.1466-8238.2011.00697.x

Coll Marta, Piroddi Chiara, Steenbeek Jeroen, Kaschner Kristin, Lasram Frida Ben Rais, Aguzzi Jacopo, Ballesteros, E., et al. 2010. The Biodiversity of the Mediterranean Sea: Estimates, Patterns, and Threats. PLOS ONE, 5: e11842. Public Library of Science. Doi:10.1371/journal.pone.0011842

Colloca, F., Scarcella, G., and Libralato, S. 2017. Recent trends and impacts of fisheries exploitation on Mediterranean stocks and ecosystems. Frontiers in Marine Science, 4: 244. Frontiers Media SA.

Cossarini, G., Feudale, L., Teruzzi, A., Bolzon, G., Coidessa, G., Solidoro, C., Di Biagio, V., et al. 2021. High-resolution reanalysis of the Mediterranean Sea biogeochemistry (1999–2019). Frontiers in Marine Science, 8: 741486. Frontiers Media SA.

Crain, C. M., Kroeker, K., and Halpern, B. S. 2008. Interactive and cumulative effects of multiple human stressors in marine systems. Ecology letters, 11: 1304–1315. Wiley Online Library.

Crozier, L. G., and Hutchings, J. A. 2014. Plastic and evolutionary responses to climate change in fish. Evolutionary Applications, 7: 68–87. John Wiley & Sons, Ltd. Doi:10.1111/eva.12135

Danovaro, R., Dinet, A., Duineveld, G., and Tselepides, A. 1999. Benthic response to particulate fluxes in different trophic environments: a comparison between the Gulf of Lions–Catalan Sea (western-Mediterranean) and the Cretan Sea (eastern-Mediterranean). Progress in Oceanography, 44: 287–312. Pergamon.

Darmaraki, S., Somot, S., Sevault, F., and Nabat, P. 2019. Past variability of Mediterranean Sea marine heatwaves. Geophysical Research Letters, 46: 9813–9823. Wiley Online Library.

Escudier, R., Clementi, E., Cipollone, A., Pistoia, J., Drudi, M., Grandi, A., Lyubartsev, V., et al. 2021. A High Resolution Reanalysis for the Mediterranean Sea. Frontiers in Earth Science, 9. Frontiers Media SA.

FAO. 2025. The State of Mediterranean and Black Sea Fisheries 2025. FAO. https://openknowledge.fao.org/handle/20.500.14283/cd7701en.

Farré, M., Tuset, V. M., Cartes, J. E., Massutí, E., and Lombarte, A. 2016. Depth-related trends in morphological and functional diversity of demersal fish assemblages in the western Mediterranean Sea. Progress in Oceanography, 147: 22–37. Elsevier.

Farriols, M. T., Ordines, F., Carbonara, P., Casciaro, L., Di Lorenzo, M., Esteban, A., Follesa, C., et al. 2020. Spatio-temporal trends in diversity of demersal fish assemblages in the Mediterranean. SCIENTIA MARINA, 83: 189–206. CSIC Consejo Superior de Investigaciones Cientificas. https://iris.unica.it/handle/11584/283399.

Ferrier, S., Manion, G., Elith, J., and Richardson, K. 2007. Using generalized dissimilarity modelling to analyse and predict patterns of beta diversity in regional biodiversity assessment. Diversity and distributions, 13: 252–264. Wiley Online Library.

Fitzpatrick, M., Mokany, K., Manion, G., Nieto-Lugilde, D., and Ferrier, S. 2022. gdm: Generalized dissimilarity modeling. R package version 1.5. 0-1. R Foundation.

Freeman, E. A., and Moisen, G. 2008. PresenceAbsence: An R package for presence absence analysis. Journal of Statistical Software, 23: 1–31.

Garrabou, J., Gómez-Gras, D., Medrano, A., Cerrano, C., Ponti, M., Schlegel, R., Bensoussan, N., et al. 2022. Marine heatwaves drive recurrent mass mortalities in the Mediterranean Sea. Global Change Biology, 28: 5708–5725. Wiley Online Library.

Getis, A., and Ord, J. K. 1992. The analysis of spatial association by use of distance statistics. Geographical analysis, 24: 189–206. Wiley Online Library.

Giakoumi, S., Pey, A., Di Franco, A., Francour, P., Kizilkaya, Z., Arda, Y., Raybaud, V., et al. 2019. Exploring the relationships between marine protected areas and invasive fish in the world's most invaded sea. Ecological Applications, 29: e01809. John Wiley & Sons, Ltd. doi: 10.1002/eap.1809.

Giani, M., Djakovac, T., Degobbis, D., Cozzi, S., Solidoro, C., and Umani, S. F. 2012. Recent changes in the marine ecosystems of the northern Adriatic Sea. Estuarine, Coastal and Shelf Science, 115: 1–13. Elsevier.

Goren, M., and Galil, B. S. 2005. A review of changes in the fish assemblages of Levantine inland and marine ecosystems following the introduction of non-native fishes. Journal of Applied Ichthyology, 21: 364–370. John Wiley & Sons, Ltd. doi: 10.1111/j.1439-0426.2005.00674.x

Hidalgo, M., Quetglas, A., Ordines, F., ıa Rueda, L., Punz on, A., Delgado, M., Gil de Sola, L., et al. 2017. Size-spectra across geographical and bathymetric gradients reveal contrasting resilient mechanisms of recovery between Atlantic and Mediterranean fish communities.

Hidalgo M., Mihneva V., Vasconcellos M., and Bernal M. 2018. Impacts of climate change on fisheries and aquaculture Synthesis of current knowledge, adaptation and mitigation options.

Hidalgo, M., Bartolino, V., Coll, M., Hunsicker, M. E., Travers-Trolet, M., and Browman, H. I. 2022. 'Adaptation science' is needed to inform the sustainable management of the world's oceans in the face of climate change. ICES Journal of Marine Science, 79: 457–462. Oxford Academic. doi: 10.1093/icesjms/fsac014

Jaccard, P. 1908. Nouvelles recherches sur la distribution florale. Bull. Soc. Vaud. Sci. Nat., 44: 223–270.

Kavadas, S., Maina, I., Damalas, D., Dokos, I., Pantazi, M., and Vassilopoulou, V. 2015. Multi-criteria decision analysis as a tool to extract fishing footprints: Application to small scale fisheries and implications for management in the context of the maritime spatial planning directive. Mar. Sci, 16: 294–304.

Kim, G.-U., Seo, K.-H., and Chen, D. 2019. Climate change over the Mediterranean and current destruction of marine ecosystem. Scientific Reports, 9: 18813. Nature Publishing Group UK London.

Kroodsma, D. A., Mayorga, J., Hochberg, T., Miller, N. A., Boerder, K., Ferretti, F., Wilson, A., et al. 2018. Tracking the global footprint of fisheries. Science, 359: 904–908. American Association for the Advancement of Science. doi: 10.1126/science.aao5646?download=true

Lacoue-Labarthe, T., Nunes, P. A. L. D., Ziveri, P., Cinar, M., Gazeau, F., Hall-Spencer, J. M., Hilmi, N., et al. 2016. Impacts of ocean acidification in a warming Mediterranean Sea: An overview. Regional Studies in Marine Science, 5: 1–11. Elsevier.

Lam, V. W. Y., Allison, E. H., Bell, J. D., Blythe, J., Cheung, W. W. L., Frölicher, T. L., Gasalla, M. A., et al. 2020. Climate change, tropical fisheries and prospects for sustainable development. Nature Reviews Earth & Environment 2020 1:9, 1: 440–454. Nature Publishing Group.

Legendre, P., and Gallagher, E. D. 2001. Ecologically meaningful transformations for ordination of species data. Oecologia, 129: 271–280. doi: 10.1007/s004420100716.

Legendre, P., and Legendre, L. 2012. Interpretation of Ecological Structures. Numerical ecology 3rd English edn. Elsevier Science BV, Amsterdam.

Lejeusne, C., Chevaldonné, P., Pergent-Martini, C., Boudouresque, C. F., and Pérez, T. 2010. Climate change effects on a miniature ocean: the highly diverse, highly impacted Mediterranean Sea. Trends in Ecology and Evolution, 25: 250–260. Elsevier.

Lindegren, M., Hidalgo, M., Montanyes, M., Maioli, F., Weigel, B., van Denderen, D., Tikhnov, G., et al. 2025. B-USEFUL. Report on temporal trends and spatial patterns of multiple biodiversity indicators.

Lloret, J., Sabatés, A., Muñoz, M., Demestre, M., Solé, I., Font, T., Casadevall, M., et al. 2015. How a multidisciplinary approach involving ethnoecology, biology and fisheries can help explain the spatio-temporal changes in marine fish abundance resulting from climate change. Global Ecology and Biogeography, 24: 448–461. John Wiley & Sons, Ltd. doi: 10.1111/geb.12276.

Magurran, A. E. (2013). Ecological diversity and its measurement. Springer Science & Business Media.

Manel, S., Williams, H. C., and Ormerod, S. J. 2001. Evaluating presence–absence models in ecology: the need to account for prevalence. Journal of applied Ecology, 38: 921–931. Wiley Online Library.

Mannino, A. M., Balistreri, P., Deidun, A., Mannino, A. M., Balistreri, P., and Deidun, A. 2017. The Marine Biodiversity of the Mediterranean Sea in a Changing Climate: The Impact of Biological Invasions. Mediterranean Identities - Environment, Society, Culture. IntechOpen.

Marbà, N., Jorda, G., Agusti, S., Girard, C., and Duarte, C. M. 2015. Footprints of climate change on Mediterranean Sea biota. Frontiers in Marine Science, Volume 2-2015. doi: 10.3389/fmars.2015.00056.

Micheli, F., Halpern, B. S., Walbridge, S., Ciriaco, S., Ferretti, F., Fraschetti, S., Lewison, R., et al. 2013. Cumulative Human Impacts on Mediterranean and Black Sea Marine Ecosystems: Assessing Current Pressures and Opportunities. PLOS ONE, 8: e79889. Public Library of Science. doi: 10.1371/journal.pone.0079889

Milazzo, M., Mirto, S., Domenici, P., and Gristina, M. 2013. Climate change exacerbates interspecific interactions in sympatric coastal fishes. Journal of Animal Ecology, 82: 468–477. John Wiley & Sons, Ltd. doi: 10.1111/j.1365-2656.2012.02034.x

Millot, C., and Taupier-Letage, I. 2005. Circulation in the Mediterranean sea. In The Mediterranean Sea, pp. 29–66. Springer.

Moullec, F., Barrier, N., Drira, S., Guilhaumon, F., Marsaleix, P., Somot, S., Ulses, C., et al. 2019. An end-to-end model reveals losers and winners in a warming Mediterranean Sea. Frontiers in Marine Science, 6: 345. Frontiers Media SA.

Oksanen, J., Blanchet, F. G., Friendly, M., Kindt, R., Legendre, P., McGlinn, D., Minchin, P. R., et al. 2020. vegan: Community Ecology Package. https://CRAN.R-project.org/package=vegan.

Panzeri, D., Reale, M., Cossarini, G., Salon, S., Carlucci, R., Spedicato, M. T., Zupa, W., et al. 2024. Future distribution of demersal species in a warming Mediterranean sub-basin. Frontiers in Marine Science, 11: 1308325. Frontiers Media SA.

Pecuchet, L., Lindegren, M., Hidalgo, M., Delgado, M., Esteban, A., Fock, H. O., Gil de Sola, L., et al. 2017. From traits to life-history strategies: Deconstructing fish community composition across European seas. Global Ecology and Biogeography, 26: 812–822. Wiley Online Library.

Pennino, M. G., Zurano, J. P., Hidalgo, M., Esteban, A., Veloy, C., Bellido, J. M., and Coll, M. 2024. Spatial patterns of β-diversity under cumulative pressures in the Western Mediterranean Sea. Marine Environmental Research, 195: 106347. Elsevier.

Peres-Neto, P. R., Legendre, P., Dray, S., and Borcard, D. 2006. Variation partitioning of species data matrices: estimation and comparison of fractions. Ecology, 87: 2614–2625. Wiley Online Library.

Peristeraki, P., Tserpes, G., Lampadariou, N., and Stergiou, K. I. 2017. Comparing demersal megafaunal species diversity along the depth gradient within the South Aegean and Cretan Seas (Eastern Mediterranean). PLoS One, 12: e0184241. Public Library of Science San Francisco, CA USA.

Peristeraki, P., Bitetto, I., Carbonara, P., Carlucci, R., Certain, G., De Carlo, F., Gristina, M., et al. 2019. Investigation of spatiotemporal patterns in mean temperature and mean trophic level of MEDITS survey catches in the Mediterranean Sea. Scientia Marina, 83: 165–174. Consejo Superior de Investigaciones Científicas.

Pielou, E. C. 1966. Species-diversity and pattern-diversity in the study of ecological succession. Journal of theoretical biology, 10: 370–383. Elsevier.

Piroddi, C., Colloca, F., and Tsikliras, A. C. 2020a. The living marine resources in the Mediterranean Sea Large Marine Ecosystem. Environmental Development, 36: 100555.

Piroddi, C., Colloca, F., and Tsikliras, A. C. 2020b. The living marine resources in the Mediterranean Sea large marine ecosystem. Environmental Development, 36: 100555. Elsevier.

Pita, I., Mouillot, D., Moullec, F., and Shin, Y. J. 2021. Contrasted patterns in climate change risk for Mediterranean fisheries. Global Change Biology, 27: 5920–5933. John Wiley and Sons Inc. doi: 10.1111/gcb.15814

Polo, J., López López, L., Engelhard, G. H., Punzón, A., Hidalgo, M., Rutterford, L. A., Bariáin, M. S., et al. 2025. Trait-Based Indicators of Marine Communities' Sensitivity to Climate Change and Fishing. Diversity and Distributions, 31: e13959. Wiley Online Library.

Quattrocchi, F., Bono, G., Cattano, C., Fiorentino, F., Lauria, V., Calò, A., Milazzo, M., et al. 2026. Warming-driven biotic differentiation of demersal fish across depths in the central mediterranean sea. Marine Environmental Research, 213: 107627.

Rubino, C., Adelfio, G., Abbruzzo, A., Bosch-Belmar, M., Lorenzo, M. Di, Fiorentino, F., Gancitano, V., et al. 2024. Exploring the effects of temperature on demersal fish communities in the Central Mediterranean Sea using INLA-SPDE modeling approach. Environmental and Ecological Statistics, 31: 629–647. Springer.

Sanz-Martín, M., Hidalgo, M., Puerta, P., Molinos, J. G., Zamanillo, M., Brito-Morales, I., González-Irusta, J. M., et al. 2024. Climate velocity drives unexpected southward patterns of species shifts in the Western Mediterranean Sea. Ecological Indicators, 160: 111741. Elsevier.

Schmitt, T., Schaap, D., Spoelstra, G., Loubrieu, B., and Poncelet, C. 2025. EMODnet (European Marine Observation and Data network) Bathymetry: A New Digital Bathymetric Model Compilation (2024). In OCEANS 2025 Brest, pp. 1–7. IEEE.

Shannon, C. E. 1948. A mathematical theory of communication. The Bell system technical journal, 27: 379–423. Nokia Bell Labs.

Soininen, J., McDonald, R., and Hillebrand, H. 2007. The distance decay of similarity in ecological communities. Ecography, 30: 3–12. Wiley Online Library.

Soto-Navarro, J., Jordá, G., Compa, M., Alomar, C., Fossi, M. C., and Deudero, S. 2021. Impact of the marine litter pollution on the Mediterranean biodiversity: A risk assessment study with focus on the marine protected areas. Marine Pollution Bulletin, 165: 112169. Pergamon.

Spedicato, M. T., Zupa, W., Carbonara, P., Fiorentino, F., Follesa, M. C., Galgani, F., García-Ruiz, C., et al. 2019a. Spatial distribution of marine macro-litter on the seafloor in the northern Mediterranean Sea: the MEDITS initiative. Scientia Marina, 83: 257–270.

Spedicato, M. T., Massutí, E., Mérigot, B., Tserpes, G., Jadaud, A., and Relini, G. 2019b. The MEDITS trawl survey specifications in an ecosystem approach to fishery management. Scientia Marina, 83: 9–20. CSIC Consejo Superior de Investigaciones Cientificas.

STECF. 2023. Scientific, Technical and Economic Committee for Fisheries (STECF) – Fisheries Dependent Information FDI (STECF-22-10). Publications Office of the European Union.

Tikhonov, G., Opedal, Ø. H., Abrego, N., Lehikoinen, A., de Jonge, M. M. J., Oksanen, J., and Ovaskainen, O. 2020. Joint species distribution modelling with the r-package Hmsc. Methods in Ecology and Evolution, 11: 442–447. John Wiley & Sons, Ltd. doi: 10.1111/2041-210X.13345.

Tuel, A., and Eltahir, E. A. B. 2020. Why is the Mediterranean a climate change hot spot? Journal of Climate, 33: 5829–5843.

Vasquez, M., Allen, H., Manca, E., Castle, L., Lillis, H., Agnesi, S., Al Hamdani, Z., et al. 2021. EUSeaMap 2021. A European broad-scale seabed habitat map.

Veloy, C., Hidalgo, M., Pennino, M. G., Garcia, E., Esteban, A., García-Ruiz, C., Certain, G., et al. 2022. Spatial-temporal variation of the Western Mediterranean Sea biodiversity along a latitudinal gradient. Ecological Indicators, 136: 108674. doi: 10.1016/j.ecolind.2022.108674

Whittaker, R. H. 1972. Evolution and measurement of species diversity. Taxon, 21: 213–251. John Wiley & Sons, Ltd.

Zupa, W., Carbonara, P., Bitetto, I., Casini, M., Maiorano, P., D'Onghia, G., Isajlovic, I., et al. 2025. Relative benthic status guides sustainable trawl management in the Adriatic–Ionian Seas. ICES Journal of Marine Science, 82: fsaf148. doi: 10.1093/icesjms/fsaf148.

4 Life stages matter: community-based Essential Fish Habitats reveal conservation priorities in the Mediterranean Sea

Authors: Fabien Moullec, Stratos Batziakas, Walter Zupa, Patricia Puerta, Nicolas Barrier, Laure Velez, Manuel Hidalgo, Stephanos Kavadas, Irida Maina, Eva Maire, Maria L. D. Palomares, Panagiota Peristeraki, Maria-Teresa Spedicato, Bastien Mérigot

4.1. Introduction

Across terrestrial, freshwater and marine ecosystems, habitat degradation, pollutions, overexploitation, invasive species and intensifying climate extremes are driving rapid population declines, community reorganization and erosion of ecosystem functions (Halpern et al., 2025; Newbold et al., 2015; A. J. Reid et al., 2019; Seebens et al., 2018). Pervasive losses in the abundance and diversity of species and growing risks to nature's contributions to people are reported across the globe, with compounding effects where pressures co-occur (Ceballos et al., 2017; IPBES, 2019; Isbell et al., 2017). To be efficient, management and conservation measures must combine area-based protection with effective threat reduction across land and sea (Allan et al., 2022; Watson et al., 2018). With the accelerating expansion of the blue economy, marine ecosystems are particularly impacted by cumulative human activities and rapid environmental change, leading to widespread declines in biodiversity and ecosystem functioning (Ceballos et al., 2020; Halpern et al., 2025; Herbert-Read et al., 2022; IPBES, 2019; Lotze, 2021). In response, international and regional frameworks have committed to protecting at least 30% of the global ocean by 2030 - the "30 × 30" target (CBD, 2022). Achieving this ambition requires conservation strategies that explicitly consider the ecological complexity of marine systems and ensure that management and protection measures remain effective under ongoing and future changes (Davies et al., 2017; Grorud-Colvert et al., 2021; Sala et al., 2021). Well-designed, area-based management measures can simultaneously address biodiversity loss and climate risks (Mackelworth et al., 2024; Pörtner et al., 2021), but their success rests on identifying locations where protection will generate the greatest ecological benefit.

Within this policy context, the concept of biodiversity hotspots provides remains central to spatial and conservation prioritization (Jefferson & Costello, 2020; Marchese, 2015). Initially defined as zones characterized by exceptional species richness, endemism, rarity and/or exposure to severe threats (Costello et al., 2022; Myers, 1988), hotspot are now recognized as multi-dimensional entities and as a cornerstone of conservation planning. They are also commonly based on high levels of abundance and threatened taxa (Ge et al., 2022; W. V. Reid, 1998) as well as more recently integrate phylogenetic and functional diversities (Albouy et al., 2017; Granger et al., 2015; Stuart-Smith et al., 2013). Yet hotspot delineation remains heterogeneous across studies and typically performed on a case-by-case basis, with thresholds and criteria varying according to ecological and methodological context, which complicates transferability and decision making (Sussman et al., 2019).

Despite substantial global advances in conservation planning and biodiversity indicators, marine hotspot identification remains incomplete (Chaplin-Kramer et al., 2023; Neugarten et al., 2024; Vasileiadou et al., 2024), particularly regarding the integration of life-stage specific habitats, such as nurseries and spawning grounds (Kuismanen et al., 2023), even though these habitats are fundamental to population dynamics and ecosystem resilience (Champagnat et al.,

2021). Species generally concentrate on areas that offer the resources needed to maximize survival and reproduction. As a result, habitat suitability and distribution patterns emerged from interacting biotic factors including prey availability and predation risk, and abiotic conditions, including physical and environmental variables (Aarts et al., 2013; Guisan et al., 2017; Planque et al., 2011). Ontogenetic shifts in habitat use—driven by size-dependent changes in foraging, reproduction, and predator avoidance—commonly yield distinct habitats for juveniles and adults (Giakoumi & Pey, 2017; Grüss et al., 2019; Le Pape et al., 2014; Stamp et al., 2025).

In marine ecosystems, Essential Fish Habitats (EFHs) are used in an explicitly ecological and spatial sense (Le Pape et al., 2014; Tugores et al., 2019). EFHs are life-stage specific areas that make a disproportionate contribution to individual performance and population persistence through enhanced survival, growth and reproduction. Operationally, EFHs are spatially explicit zones where demographic processus, or their empirical proxies such as density, biomass, or the occurrence of spawning adults and juveniles, recur under particular environmental regimes and seascape structure. These zones may be persistent core areas, seasonally recurrent features, or mobile habitats shaped by circulation, temperature, productivity, substrate, and biotic interactions. This framing links EFHs to ontogenetic niche dynamics and metapopulation connectivity, rather than to a purely sectoral view of fisheries management. However, limitations in standardized data, spatial coverage, and analytical constraints under data scarcity and observation bias have contributed to the under representation of EFHs in conservation frameworks (Lukyanova et al., 2025), even though the concept is recognized in initiatives such as Ecologically or Biologically Significant Areas (EBSAs; Dunn et al., 2025). A further challenge is the lack of comprehensive, long-term, spatially explicit information on fish distributions across life stages, which constrains robust habitat mapping and the identification of the environmental and anthropogenic drivers of habitat persistence (Lahellec et al., 2025). Yet, these aspects are critical for delineating population structure, informing spatial management (e.g., Marine Protected Areas, MPAs), and advancing ecosystem-based fisheries management (EBFM) (NOAA, 2025). Although numerous studies have identified nurseries or spawning habitats for individual benthic, demersal, or pelagic species (Colloca et al., 2015; Giannoulaki et al., 2013; Izquierdo et al., 2021; MediSeH, 2013; Milisenda et al., 2021; Pennino et al., 2020), most are limited by local scale, short time series, or single/subset species focus. No study has yet integrated, at the community scale, life stages and ecological traits while jointly accounting for environmental drivers, anthropogenic pressures, and interspecific interactions at large spatio-temporal scale. This limits our capacity to design spatial measures robust to environmental variability and to anticipate community-level responses to anthropogenic pressures (Katsanevakis et al., 2011), particularly in the Mediterranean Sea, where management needs are most pressing (Aminian-Biquet, Gorjanc, et al., 2024).

The Mediterranean is one of the most socio-ecologically distinctive Large Marine Ecosystems on Earth (Aurelle et al., 2022; Piroddi et al., 2020) where these challenges converge. Despite covering only 0.82% of the global ocean surface, it hosts over 17,000 species—more than 20% of which are endemic due to its unique position at the interface of temperate and subtropical regimes and its complex mosaic of habitats shaped by oceanographic processes (Bianchi & Morri, 2000; Coll et al., 2010; D'Ortenzio & Ribera d'Alcalà, 2009). This semi-enclosed basin, bordered by 22 countries and home to over 520 million people (~7% of the global population) is a hotspot of global change (Coll et al., 2012; Micheli, Halpern, et al., 2013) and among the regions projected to experience the fastest warming and most intense cumulative anthropogenic pressures (Cramer et al., 2018; Halpern et al., 2025; Marbà et al., 2015; Micheli, Halpern, et al., 2013). Intensive fishing, pollution, habitat modification,

biological invasions and climate change have collectively reshaped species distributions and community structures (Albouy et al., 2014; Azzurro et al., 2019; Bensebaini et al., 2022; Moullec et al., 2023), accelerated biodiversity loss (Coll et al., 2012; MedECC, 2020; UNEP, 2024), and reduced ecosystem productivity (Hassoun et al., 2025; Piroddi et al., 2017; Reale et al., 2022). Among these stressors, fishing is one of the primary drivers of ecological change (Colloca et al., 2017; IPBES, 2018; Vasilakopoulos et al., 2014). Ecosystem modelling reveals significant biomass declines since 1950, particularly among demersals and small pelagics (Piroddi et al., 2015, 2017, 2022), while demersal communities support culturally and economically important fisheries. Despite recent reductions in fishing pressure, exploitation remains more than twice sustainable thresholds (FAO, 2023). In addition, unselective bottom trawl fisheries, often capturing undersized individuals (i.e., catch at size below Minimum Conservation Reference Size (MCRS)), undermine recovery and hinder progress toward the targets of the European Common Fisheries Policy (CFP 1380/2013), the Marine Strategy Framework Directive (MSFD 2008/56/EC), and the EU Biodiversity Strategy for 2030 (COM (2020) 380) (Bahamon et al., 2024; Colloca et al., 2017).

In response, the European Union and the General Fisheries Commission for the Mediterranean (GFCM) have promoted spatially explicit measures—such as Marine Protected Areas (MPAs) and Fisheries Restricted Areas (FRAs)—to protect juveniles and spawning habitats. The GFCM 2030 Strategy and the MedFish4Ever Declaration advocate a regional network of EFHs and expanded area-based fisheries management measures (FAO, 2021). However, despite these commitments, protection remains limited in extent and strength, with only about 15% of the basin currently protected and less than 2% are under strong protection (Aminian-Biquet, Gorjanc, et al., 2024). Moreover, the spatial congruence between EFH hotspots and existing MPAs remains poorly assessed at large scale (Ortega et al., 2023), highlighting the need for integrated analyses that link biodiversity, environmental pressures, and fisheries management.

In this context, to what extent does integrating life-stage-specific habitat use into community distribution modelling improve our ability to identify persistent biodiversity hotspots and inform spatial conservation planning? In other words, how do environmental and anthropogenic drivers, life-history traits, and interspecific associations jointly shape the spatial distribution and persistence of juvenile and adult habitats across fish communities, and to what extent do current conservation measures encompass these community-based, life-stage-specific essential fish habitats in the Mediterranean Sea? To address this research question, we cover the four following objectives and steps. First, we quantify the relative influence of environmental and anthropogenic drivers, ecological traits, phylogenetic relatedness, and interspecific associations on juvenile and adult distributions. Second, we characterize long term spatio-temporal abundance patterns across life stages. Third, we identify persistent and non-persistent juvenile and adult habitats on a regional scale. Fourth, we evaluate the spatial congruence between community-basef EFHs and the Marine Protected Area network currently implemented in the western Mediterranean Sea. We test three related hypotheses: (i) juvenile and adult EFHs exhibit distinct spatial patterns that are structured by life history traits and environmental gradients (Galaiduk et al., 2017; Planque et al., 2011), (ii) persistent EFHs are more likely to occur in areas with comparatively lower anthropogenic pressure (Edgar et al., 2014; Halpern et al., 2015), (iii) the current protection network insufficiently encompasses multispecies EFHs (Aminian-Biquet, Gorjanc, et al., 2024; Claudet et al., 2020), particularly those critical to early life stages (Ortega et al., 2023).

To our knowledge, this study represents the first sub-basin-scale, community-based, life-stage-integrated assessment of Essential Fish Habitats in the Mediterranean Sea. Using over two

decades (1999-2021) of standardized trawl data from the scientific Mediterranean International Trawl Survey (MEDITS, Bertrand et al., 2002; Spedicato et al., 2019)), encompassing over 60 demersal and pelagic species and more than 12 000 hauls in the western Mediterranean Sea, we combined a joint Species distribution Modelling (jSDM, Ovaskainen, Tikhonov, Norberg, et al., 2017) framework with spatio-temporal hotspot analyses to define Essential Fish Habitats at the community level, explicitly accounting for life-stage differences and temporal variability. By integrating life-stage-specific patterns into conservation planning, this study advances the incorporation of ontogenetic habitat niches into biodiversity distributions and marine spatial planning to align fisheries management with ecological processes, supporting both stock recovery and biodiversity conservation in the Mediterranean Sea. Although developed in the western Mediterranean, the approach is transferable to other regions and taxa, thereby linking community ecology, spatial demography, and conservation design.

4.2. Materials and Methods

Study area and survey data

The western Mediterranean Sea extends from 34.3° N to 45.7° N and from 5.2° W to 34.1° E and comprises 12 Geographical Sub-Areas (GSAs) as defined by the GFCM. For computational and ecological reasons, our analysis focused on a subset of European western GSAs (1, 2, 5, 6, 7, 8, 9, 10, 11.1 and 11.2). This subset ensured relatively greater homogeneity in environmental conditions and fish assemblages, which improve model calibration and predictive accuracy. Biogeographically, the western basin has stronger affinities with the Atlantic Ocean and support a higher proportion of cold-temperate species, whereas the eastern basin is more closely related to the Indo-Pacific region and supports a greater number of subtropical taxa (Coll et al., 2010).

Fish data were obtained from annual standardized bottom trawl surveys conducted within the Mediterranean International Trawl Survey program (MEDITS; Bertrand et al., 2002; Spedicato et al., 2019). Surveys were carried out each year from 1999 to 2021 during late spring to early summer (May–July) and covered continental shelves (10–200 m) and upper slopes (200–800 m) of the western Mediterranean. MEDITS applies an harmonized sampling protocols across participating countries to ensure spatial and temporal comparability (Spedicato et al., 2019). A standardized experimental bottom trawl of GOC-73 type with a stretched-mesh codend of 20 mm was used at all stations (Bertrand et al., 2002; MEDITS, 2017; Spedicato et al., 2019). Sampling stations were selected according to a stratified random design, with depth strata defined at 10–50, 51–100, 101–200, 201–500, and 501–800 m. The GOC-73 gear has an average vertical opening of about 2 m and a horizontal spread of about 18 m. These specifications allow efficient sampling of both juvenile and adult demersal species and facilitates the estimation of recruitment indices (Abella et al., 1999; Spedicato et al., 2019). The protocol also records abundance for small pelagic species, such as sardine (*Sardina pilchardus*) and anchovy (*Engraulis encrasicolus*), that are routinely caught at shelf stations (Fiorentino et al., 2013). Consequently, MEDITS data provide valuable information on the population dynamics of both demersal and small pelagic stocks in the Mediterranean Sea (Fiorentino et al., 2013; Pennino et al., 2020; Sbrana et al., 2010).

All hauls were conducted during daylight at a standard towing speed of approximately 3 knots, with a duration of 30 minutes on the continental shelf and 60 minutes on the slope. Trawl performance (e.g., swept area, towing time) and gear geometry (horizontal and vertical openings) were continuously monitored using a SCANMAR acoustic system to ensure high-quality and consistent data acquisition. Data validation was performed using the “RoMEBS” R

package which performs multiple cross-checks across MEDITS survey datasets, including haul metadata, aggregated abundance and biomass by species, and length–frequency distributions by sex and maturity stage (Bitetto et al., 2023). All identified errors and warnings were corrected. Only hauls with validated gear performance and complete metadata were retained for analysis, corresponding to about 550 hauls per year at the subregional scale and about 66 hauls per GSA per year. In total, 12,654 validated hauls collected between 1999 and 2021 were included in the analyses.

Fish community data

More than 1,470 taxa have been recorded in MEDITS surveys, including about 385 bony fishes and 54 elasmobranchs. For the present analyses, we restricted the dataset to fish taxa and retained only individuals identified to the species level within the classes Actinopterygii and Elasmobranchii. Because our primary interest was to assess relative rather than absolute changes in species abundances across space and time, and given that MEDITS data samples both benthodemersal and small pelagic assemblages (Angelini et al., 2021; Fiorentini et al., 1999; Fiorentino et al., 2013), we retained all species from these ecological groups.

Individuals of each species were classified as juveniles or adults according to their length at first maturity (see Section 2.3). To limit bias from extremely rare taxa and life-stage combinations, we excluded those recorded in fewer than 1% of hauls within the western Mediterranean subregion during the 1999–2021 period. This threshold retained species–life stage combinations that together represented about 95% of total fish abundance.

For each retained species, haul, and life stage, standardized abundance (number of individuals per km²) was computed by dividing raw catch by the area swept of the tow. The final dataset comprised 73 fish species represented by 51 juvenile and 65 adult species-life stage combinations.

Species traits and phylogeny

To account for traits in species responses to environmental and anthropogenic covariates, we compiled data on eight continuous and categorical traits related to life history, habitat use and trophic ecology for each species. These traits included offspring size, length at maturity, maximum body length, von Bertalanffy growth coefficient (K), body shape, trophic guild, trophic level and water column position (table sup mat). Trait data for Mediterranean species were primarily obtained from Fishbase (Boettiger et al., 2012; Froese & Pauly, 2025), following the methodology of Beukhof et al. (2019), and complemented with information from additional open-access trait databases (Beukhof et al., 2019; Coulon et al., 2023; Koutsidi et al., 2020).

Missing trait values were estimated using a phylogenetic structural-equation mixed-trait imputation approach (Thorson et al., 2023), implemented in the R package phylosem (Thorson & van der Bijl, 2023). This method leverages both trait correlations and phylogenetic dependencies to provide statistically robust imputed values, for both continuous and categorical traits, while maintaining ecological coherence.

To represent phylogenetic relationships among the study species, we constructed a taxonomic tree using the ape R package (Paradis & Schliep, 2019), including hierarchical taxonomic levels from phylum to species (phylum, class, order, family, genus, species) retrieved from the taxize R package (Chamberlain & Szöcs, 2013). Given the lack of a comprehensive molecular phylogeny encompassing all species included in this analysis (spanning Actinopterygii and Elasmobranchii), we assumed equal branch lengths of one unit between taxonomic nodes, consistent with previous studies applying HMSC to diverse fish assemblages (Gordó-Vilaseca et al.,

2024; Maioli et al., 2023; Montanyès et al., 2023; Ovaskainen & Abrego, 2020). For the purpose of modeling life-stage-dependent distributions and abundances, juvenile and adult stages were added as terminal branches to each species, with a short branch length of 0.1 to represent intraspecific differences between stages.

To capture life-stage-specific variation in body size, we derived two composite size-related traits—minimum size and maximum size—from offspring size, size at maturity, and maximum body length. For juveniles, minimum and maximum sizes corresponded respectively to offspring size and length at maturity, while for adults they corresponded to length at maturity and maximum body length. All other traits were assumed to remain constant between life stages due to limited empirical data on life-stage variation across the studied species (Dimarchopoulou et al., 2017).

Environmental and anthropogenic covariates

We selected a set of environmental (physical and biogeochemical) and anthropogenic predictors known to influence the spatial-temporal distribution and abundance of marine fish communities (IPBES, 2019; Last et al., 2011; Mérigot et al., 2019; Navarro et al., 2015). Environmental covariates included bathymetry (depth, m), sea surface and bottom temperature (SST, SBT, °C), sea surface salinity (SSS, psu) and chlorophyll-a concentration (chl-a, $mg.m^{-3}$) as a proxy for primary production and resource availability. Environmental data were obtained from the Marine Copernicus platform (https://marine.copernicus.eu/) using the Mediterranean Sea Physics Reanalysis and Mediterranean Sea Biogeochemistry Reanalysis products, both available at 1/24° spatial resolution (ca. 4-5km) (Cossarini et al., 2021; Escudier et al., 2021). Bathymetric information was extracted from the European Marine Observation Data Network (EMODnet) Digital Bathymetry (DTM)-2022 (1/16° resolution). For each sampling location (i.e., hauls), environmental values corresponded to the mean June-July conditions for each year along the temporal window from 1999 to 2021 of the MEDITS surveys.

Because human activities strongly affect the distribution and abundance of marine organisms (IPBES, 2019; Last et al., 2011; Navarro et al., 2015), we included two anthropogenic covariates: fishing pressure and the human gravity indices. Yearly fishing pressure was quantified using a Fishing Pressure Index (FPI) derived through a Multi-Criteria Decision Analysis (MCDA) framework (Hidalgo et al., 2019; Kavadas et al., 2015; Mérigot et al., 2019). The FPI ranges from 0 to 1 and notably integrates data from the EU fishing fleet register for bottom trawl, purse seine, and small-scale fisheries. It is computed as the fuzzy product of a fishery suitability index (Sc) and an activity index (Ac), such that FPI = Sc × Ac (Kavadas et al., 2015). Criteria for Sc included bathymetry, distance from coast, chlorophyll-a concentration, fisheries restricted areas, and no-take zones. Each factor was normalized on a 0–1 fuzzy scale and weighted using the Analytic Hierarchy Process (AHP). The Ac was estimated from vessel length and tonnage data through spatial interpolation and fuzzy normalization. The final product provides a spatially explicit footprint of relative fishing pressure at a 1/24° grid resolution (see Mérigot et al. (2019) for more details about the computation of the FPI at the spatio-temporal scale of the MEDITS).

As a proxy for global human pressure on marine ecosystems (e.g., pollution, including eutrophication, and habitat degradation), we included the human gravity index (Cinner et al., 2018). This spatial index was calculated as the ratio between the population size of the nearest settlement (within 500 km) and the squared travel time between that settlement and the marine grid cell. Higher values indicate stronger human influence. Previous studies have demonstrated that this index is a reliable predictor of fish biomass and community structure (Cinner et al., 2016, 2018; Mahaut et al., 2025; Maire et al., 2024).

Finally, to minimize multicollinearity among predictors, we examined pairwise correlations and calculated Variance Inflation Factors (VIF) (Dormann et al., 2013). Covariates showing high collinearity (Pearson's correlation coefficient| > 0.7 or VIF > 3) were excluded. In particular, sea bottom salinity and seabed substrate (not described here) were removed due to their strong correlation with bathymetry. The remaining predictors all met the independence criteria ($|r| \leq 0.7$; VIF < 3), ensuring robust model estimation.

Joint Species Distribution modelling

We applied the Hierarchical Modelling Species Communities (HMSC) framework to jointly model the juvenile and adult life stages of fish species across the western Mediterranean Sea. This approach allows to quantify how environmental and anthropogenic drivers, species traits and phylogenetic relationships shape life-stage-specific distributions while accounting for spatial and temporal autocorrelation (Ovaskainen et al., 2017; Ovaskainen & Abrego, 2020; Tikhonov, Opedal, et al., 2020). HMSC is a multi-variate Bayesian generalized linear mixed-effect model framework within the class of joint Species Distribution Models (jSDMs) (Warton et al., 2015). It integrates community data with environmental and anthropogenic covariates, species traits, phylogenetic relationships, and the spatio-temporal structure of the study, providing predictive insights into community assembly processes from non-manipulative observational data (Ovaskainen et al., 2017; Ovaskainen & Abrego, 2020; Tikhonov, Opedal, et al., 2020).

Given the zero-inflated nature of the data and heterogeneous abundance patterns, we implemented a two-part hurdle modelling approach to model species-life stage abundance distributions (Maioli et al., 2023; Stephenson et al., 2024; Weigel et al., 2021). In this approach, a binomial model with a probit link was first used to estimate the probability of species-life stage occurrence (presence–absence model). Then, a separate Gaussian model was fitted to predict the log-transformed abundances at locations where presence was predicted (abundance conditional on presence). The two model outputs were subsequently multiplied (i.e., hurdled) to obtain an overall expected abundance conditional on presence at a 0.05° spatial grid resolution (ca. 4-5km). Both sub-models shared identical parameterization and default prior distributions, as recommended by Ovaskainen & Abrego (2020), and they incorporated the same set of environmental and anthropogenic predictors: bathymetry, sea surface and bottom temperature, sea surface salinity, chlorophyll-a concentration, fishing pressure and gravity indices.

As fixed effects, we included all predictors listed above, estimating second-order polynomial terms for environmental covariates to capture potential unimodal niche responses, while linear terms were retained for fishing pressure and gravity indices. Quadratic terms encode the assumption that observed conditions may include optimal levels of these covariates (Maioli et al., 2023; Montanyès et al., 2023; Stephenson et al., 2024; Weigel et al., 2021). To account for variation in other (unmeasured) environmental or anthropogenic factors, interannual fluctuations, and residual co-occurrence among species-life stage combinations, we included temporal (year) and spatial (using 0.05° grid cells) random effects. These latent random effects may also capture unobserved biotic interactions - such as competition, predation, or facilitation - though their ecological interpretation remains uncertain (Ovaskainen & Abrego, 2020). Spatially structured latent variables were modelled using the Nearest Neighbour Gaussian Process (NNGP) implementation, which provides a computationally efficient approximation for large spatial datasets (Tikhonov, Duan, et al., 2020).

To model species-specific variation in environmental and anthropogenic responses, we included species traits (minimum and maximum length, growth coefficient, trophic level and

guild, body shape and position in the water column) and taxonomic relationships as hierarchical levels (see above).

Both the presence-absence and abundance conditional-on-presence models were fitted using a high-performance computing (HPC) accelerated version (Rahman et al., 2024) of the Hmsc R package (Tikhonov, Opedal, et al., 2020). Computations were performed on the Jean Zay French supercomputer, using a single GPU node with four Tesla V100 SXM2 32 GB GPUs. The posterior distributions were sampled with four Markov chain Monte Carlo (MCMC) chains of 1,500,000 iterations each, of which 500,000 were omitted as burn-in. Chains were thinned by 4,000 to yield 250 posterior samples per chain, resulting in 1,000 posterior samples per model.

Convergence and model performance were evaluated for both components of the hurdle model. MCMC convergence was assessed using the Gelman-Rubin Potential Scale Reduction Factor (PSRF) for both β (species-environment/anthropogenic relationship) and γ (trait-environment/anthropogenic relationship) parameters, with PSRF values below 1.1-1.2 indicating satisfactory convergence (Gelman & Rubin, 1992; Ovaskainen et al., 2017; Tikhonov, Opedal, et al., 2020). Model explanatory power was quantified by computing the area under the curve of the receiver operating characteristic metric (AUC), the coefficient of discrimination Tjur's R^2 (Tjur, 2009) for the presence-absence model (Pearce & Ferrier, 2000), and the coefficient of determination (R^2) for the abundance model, for each species-life stage combination. AUC values (ranging 0-1) indicate the probability that a randomly chosen occupied sampling unit has a higher predicted occurrence probability than an unoccupied one, while Tjur's R^2 measures the difference in mean predicted occupancy between presences and absences (Abrego & Ovaskainen, 2023; Tjur, 2009).

After model fitting, variance partitioning was applied to quantify the relative contributions of environmental, anthropogenic, trait-based and phylogenetic factors to species-life stage distributions. Explained variation was partitioned between fixed and random effects, and the relative weights of individual covariates were summarized separately for the presence-absence and abundance conditional-on-presence components. Specifically, we estimated the proportion of variance attributable to environmental and anthropogenic predictors (β-parameters), species traits (γ-parameters), and phylogenetic structure (ρ-parameter). The ρ parameter, ranging from 0 to 1, represents the degree of phylogenetic signal in species responses, with higher values indicating stronger similarity among closely related taxa (Ovaskainen & Abrego, 2020). Finally, spatio-temporal predictions for each species–life stage combination were generated for the 1999-2021 period using the "constructGradient" and "predict" functions in the Hmsc R package (Ovaskainen & Abrego, 2020; Tikhonov, Opedal, et al., 2020).

Spatio-temporal patterns of life stage distributions and abundances

To quantify and map long-term spatio-temporal changes in the abundance of both juvenile and adult stages from 1999 to 2021, we applied a combined approach by using the Mann-Kendall (MK) trend test and Sen's slope estimator implemented in the trend R package (Pohlert, 2023). This non-parametric approach, robust to outliers, is widely used to identify monotonic directional trends in ecological time-series data. For each grid cell, the MK test evaluated whether a significant trend was present ($p < 0.05$), while Sen's slope provided an estimate of the trend magnitude.

To further explore spatio-temporal clustering in juvenile and adult fish abundances, representing potential EFHs, we applied Emerging Hotspot Analysis (EHSA) using the sfdep R package (Parry & Locke, 2024). EHSA integrates spatial and temporal dimensions by combining the Getis-Ord Gi* statistic (Getis & Ord, 1992; Ord & Getis, 1995) with a Mann-Kendall trend test,

enabling the identification of statistically significant spatio-temporal patterns such as new, intensifying, persistent, or diminishing hotspots (i.e., areas of high abundance) and coldspots (i.e., areas of low abundance) (ESRI, 2025).

Predicted abundances (individuals per km²) from HMSC were aggregated on a regular 0.05° spatial grid and organized as a space time cube of locations by years, covering the 1999–2021 period. Each grid cell defined a spatial unit with a total annual abundance estimate for either the juvenile or adult stage. Spatial dependence among grid cells was modelled using Queen's contiguity adjacency, including self-neighbors so that each cell contributed to its own Gi* statistic, which improves sensitivity to local clustering.

For each year, the local Getis-Ord Gi* statistic quantified whether abundances in a given cell and its spatial neighborhood were significantly higher (hotspots) or lower (coldspots) than expected under a random spatial distribution. The resulting time series of Gi* values were then analyzed using the Mann-Kendall test to detect monotonic temporal trends in clustering intensity. Results from the Gi* and MK tests were combined to assign each location to one of 17 hotspot or coldspot categories, such as new, intensifying, persistent, diminishing, or historical, following the ESRI (2025) classification scheme (Table 4.1).

EHSA results were summarized as spatial maps for both life stages, highlighting where hotspots of high abundance are emerging, stable, or declining through time.

Table 4.1. Definitions of the classification scheme of Emerging Hot and Cold Spot analysis (ESRI, 2025)

Pattern name	Definition
No Pattern Detected	Does not fall into any of the hot or cold spot patterns defined below.
New Cold/Hot Spot	A location that is a statistically significant Cold/Hot spot for the final time step (i.e., 2021) and has never been a statistically significant Cold/Hot spot before.
Consecutive Cold/Hot Spot	A location with a single uninterrupted run of at least two statistically significant Cold/Hot spot bins in the final time-step intervals (i.e., 2020-2021). The location has never been a statistically significant Cold/Hot spot prior to the final Cold/Hot spot run and less than 90 percent of all bins (i.e., 20 years) are statistically significant Cold/Hot spots.
Intensifying Cold/Hot Spot	A location that has been a statistically significant Cold/Hot spot for 90 percent of the time-step intervals (i.e., 21 years), including the final time step (i.e., 2021). In addition, the intensity of clustering of low/high counts in each time step is increasing overall and that increase is statistically significant.
Persistent Cold/Hot Spot	A location that has been a statistically significant Cold/Hot spot for 90 percent of the time-step intervals (i.e., 21 years) with no discernible trend in the intensity of clustering over time.
Diminishing Cold/Hot Spot	A location that has been a statistically significant Cold/Hot spot for 90 percent of the time-step intervals (i.e., 21 years), including the final time step (i.e., 2021). In addition, the intensity of clustering in each time step is decreasing overall and that decrease is statistically significant.
Sporadic Cold/Hot Spot	A statistically significant Cold/Hot spot for the final time-step interval with a history of also being an on-again and off-again Cold/Hot spot. Less than 90 percent of the time-step intervals have been statistically significant Cold/Hot spots and none of the time-step intervals have been statistically significant Hot/Cold spots.
Oscillating Hot Spot	A statistically significant Cold/Hot spot for the final time-step interval (i.e., 2021) that has a history of also being a statistically significant Hot/Cold spot during a prior time step. Less than 90 percent of the time-step intervals have been statistically significant Cold/Hot spots.
Historical Hot Spot	The most recent time period is not Cold/Hot, but at least 90 percent of the time-step intervals (i.e., 21 years) have been statistically significant Cold/Hot spots.

Spatial congruence between hotspots and Marine Protected Areas

We further evaluated the spatial congruence between community-based EFHs (i.e., abundance hotspots of key life stages) and the existing network of Marine Protected Areas (MPAs) in the western Mediterranean Sea. Spatial overlap was quantified between congruent hotspots, i.e., cells identified as hotspots for both juvenile and adult stages, and MPA polygons. These congruent hotspots were considered the most critical areas for conservation.

MPA data were sourced from the comprehensive EU-wide database compiled by Aminian-Biquet, Colegrove, et al. (2024), integrating multiple sources including the European Environment Agency (EEA), ProtectedSeas Navigator, MAPAMED, and the World Database on Protected Areas (WDPA) (Aminian-Biquet, Colegrove, et al., 2024; Aminian-Biquet, Gorjanc, et al., 2024). In this dataset, MPAs were classified into four protection levels based on human-use intensity and frequency following Grorud-Colvert et al. (2021): minimally protected (high-impact activities), lightly protected (moderate-impact activities), highly protected (low-impact activities), or fully protected (no extractive activities). Areas classified as "incompatible" with biodiversity conservation (i.e., where high-impact or industrial activities are allowed) were considered unprotected.

Following the MPA Guide framework (Grorud-Colvert et al., 2021), we focused exclusively on MPAs with explicit conservation objectives, excluding other area-based management tools such as Locally Managed Marine Areas or Fisheries Management Areas, which fall under the category of Other Effective Area-Based Conservation Measures (OECMs). To avoid double-counting overlapping MPAs and to best reflect de facto protection levels, we dissolved overlapping polygons and retained the highest protection level per spatial unit (Aminian-Biquet, Gorjanc, et al., 2024; Pike et al., 2024).

All analyses were conducted in R v4.2.2 (R Core Team, 2022) in RStudio v2025.05.0+496 (Posit team, 2025).

4.3. Results

Model convergence and fit

The Markov Chain Monte Carlo (MCMC) convergence diagnostics for both the presence-absence (PA) and abundance conditional on presence (ABU) models indicated satisfactory convergence across all parameters. Potential scale reduction factors (psrf) were consistently below 1.1-1.2 for both β-parameters (species responses to environmental and anthropogenic covariates) and γ-parameters (trait effects). Specifically, psrf point estimates for the β-parameters averaged 1.04 ± 0.08 and 1.11 ± 0.22 for the PA and ABU models, respectively, while the γ-parameters averaged 1.01 ± 0.01 and 1.02 ± 0.03 for the same models. For both PA and ABU models, effective sample sizes were close to the total number of posterior samples, suggesting minimal autocorrelation. The overall explanatory power of the PA model was high, with mean Tjur's R^2 = 0.42 ± 0.19 and mean AUC = 0.94 ± 0.05, indicating strong discriminatory power in distinguishing presences from absences. The explanatory power of the ABU model (R^2 = 0.37 ± 0.13) further supported its ability to capture key environmental and anthropogenic gradients shaping community composition. Finally, there were no significant differences in model fit between juvenile and adult life stages for either the PA or ABU models (Wilcoxon tests, $p > 0.05$).

Explained variation in species-life stage occurrence and abundance

We identified pronounced spatio-temporal structuring in fish assemblages at both the species–life stage and community levels. Spatial random effects associated with grid cells accounted for a substantial share of the explained variance in both modelling frameworks (Figure 4.1). In the PA model, grid-cell effects explained nearly half of the variation for juveniles (50%) and adults (47%), whereas in the ABU model they accounted for 33% and 30% of the variation for juveniles and adults, respectively. Temporal random effects capturing interannual variability contributed to a smaller, yet meaningful, proportion of the variance, explaining 19% in the PA model (16%

for juveniles and 22% for adults) and 7% for both life-stage in the ABU model. Among fixed effects, depth emerged as the dominant predictor, explaining on average 28% and 43% of the variance across species–life stages in the PA and ABU models, respectively, followed by temperature (2% and 10%, respectively). The other environmental and anthropogenic covariates (salinity, chlorophyll-a concentration and human pressures) each accounted for less than 5% of the explained variance in species occurrences and abundances. Nevertheless, human pressures, including fishing intensity and the gravity index, contributed approximately four times more explained variation in the ABU model than in the PA model, indicating a stronger influence on population abundance than on species occurrence. Across both models, variance partitioning revealed pronounced heterogeneity among species–life stage combinations, reflected by large standard deviations. For some species–life stage combinations, most of the explained variance was attributable to fixed effects (e.g., in the PA model, depth explained 75% and 77% of the variance in the occurrence of juvenile and adult *Solea solea*, respectively), whereas for others it was largely driven by spatial and temporal random effects (e.g., in the PA model, spatial random effects accounted for 91% of the explained variance in the occurrence of both juvenile and adult *Eutrigla gurnardus*).

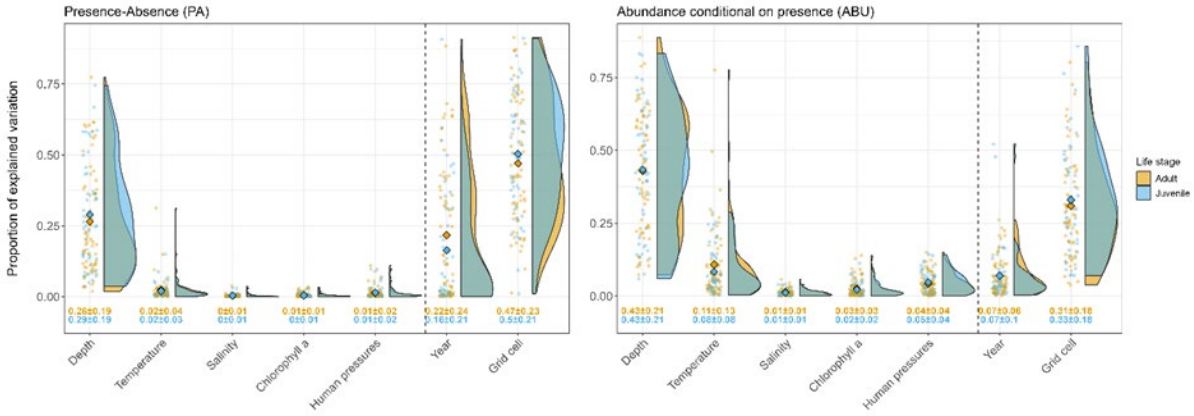

Figure 4.1. Total explained variations of species occurrences (PA model, Tjur R^2) and abundance conditional on presence (ABU model, R^2) partitioned into responses to fixed (depth, temperature, salinity, chlorophyll-a concentration and human pressures; to the left of the dashed line) and random effects (year and grid cell; to the right of the dashed line). Each point represents a species–life stage combination (orange for species-adult life stage and blue for species-juvenile life stage). The mean variance proportions averaged over the species and life stages are reported for each covariate and denoted by diamonds.

A moderate proportion of the variation in species–life stage responses to environmental and anthropogenic drivers (fixed effects) was explained by the trait sets included in the models (γ-R^2 = 0.17 and 0.33 for the PA and ABU models, respectively). Overall, traits accounted for approximately twice as much among–species–life stage variation in occurrence (PA model) as in abundance (ABU model). In the PA model, trait-mediated variation in species–life stage responses ranged from 1% for depth to 16% for the gravity index, with the strongest effects associated with responses to the gravity index, fishing pressure, and temperature (SST and SBT), explaining 16.2%, 12.4%, and an average of 11.7% of the variance, respectively. In contrast, in the ABU model, the proportion of variance explained by traits ranged from 5.6% for the gravity index to 36% for temperature (SST), with the strongest trait effects linked to responses to temperature (SST), salinity, and chlorophyll-a (34.2%, 32%, and 21.5%, respectively).

Environmental and anthropogenic niches of species-life stages

The linear effect of fishing pressure significantly influenced the occurrence of most species–life stage combinations, with 16% showing negative and 43% showing positive responses supported by ≥95% posterior probability. Similarly, the linear effect of gravity significantly affected the occurrence of a large proportion of species–life stage combinations, with 50% exhibiting negative and 29% positive responses. In contrast, fishing pressure had no significant linear effect on the abundance of most species–life stage combinations (68%) at ≥95% posterior probability. Gravity, however, significantly influenced abundance for more than half of the species–life stage combinations (55%), with predominantly negative effects (52%). For all covariates considered, we did not detect pronounced differences between juvenile and adult responses.

Depth significantly affected almost all species and life stages occurrences (94%), mostly with a positive linear response and a negative quadratic response (43% of species-life stage combinations), indicating a hum-shaped response of the species-life stage occurrences to this covariate. More than half of species-life stage occurrences were affected by temperature (SST and SBT), salinity and chlorophyll-a concentration, with a balanced mix of a positive linear response associated with a negative quadratic response or a negative linear response associated with a positive quadratic response.

Evidence for phylogenetic signal in species-life stage responses to environmental and anthropogenic covariates

Species responses exhibited a strong phylogenetic structure, with the posterior mean of the phylogenetic correlation parameter ρ reaching 0.96 in both the PA (95% confidence interval from 0.94 to 0.97) and ABU (95% confidence interval from 0.93 to 0.97) models, indicating a high degree of similarity in environmental and anthropogenic responses among closely related species. These results suggest that closely related species share similar combinations of traits that mediate their responses to environmental and anthropogenic gradients, and that additional phylogenetically structured traits, beyond those explicitly included in the models, likely contribute to shaping species' ecological niches.

Species-life stage co-occurrence patterns at spatial random effect level

Residual species co-occurrence patterns were examined at the spatial random-effect level of the PA model. We identified numerous positive and negative associations among species–life stage combinations with posterior support ≥95%. At the grid cell scale, 4,527 significant associations were detected (out of 6,786 possible), of which approximately 71% were positive co-occurrences and 29% were negative. For both types of associations, links involving both juvenile and adult life stages accounted for roughly half of the significant interactions (48% for positive and 50% for negative co-occurrences). Among positive co-occurrences, approximately 20% occurred exclusively between juveniles and 32% exclusively between adults. Similarly, among negative co-occurrences, about 23% involved juveniles only and 27% involved adults only.

Spatio-temporal trends in species–life stage abundance

To assess large-scale temporal trends in juvenile and adult abundances, we applied Sen's slope analyses to spatio-temporal abundance predictions across the western Mediterranean Sea (Figure 4.2). This non-parametric approach allowed us to quantify monotonic trends while accounting for interannual variability in model-based abundance estimates. Spatial predictions revealed contrasting patterns across the study area. Juvenile abundance trends were highly heterogene-

ous at the western Mediterranean scale, with increasing trends observed in the Ligurian and Tyrrhenian Seas, between Corsica and Italy, and along the western Italian coast on the upper continental slope. These areas were, however, characterized by low abundance of juveniles. In contrast, decreasing trends in juvenile abundance were detected along the outer continental slope of the Gulf of Lion, off northern Spain, and around the Balearic Islands. Across half of the study area (ca. 52%), Sen's slopes were not significant, indicating relatively stable juvenile abundances on the study period. By contrast, adult abundances displayed a more homogeneous and consistently negative pattern. Between 1999 and 2021, negative Sen's slope values dominated across much of the western Mediterranean, indicating widespread declines in adult abundance through time. These declines were particularly pronounced along the continental shelf and slope in several sub-areas (e.g., gulf of Lion, Balearic Islands, Sardinia), pointing to a basin-wide signal that contrasts with the more spatially heterogeneous and locally variable trends observed for juveniles.

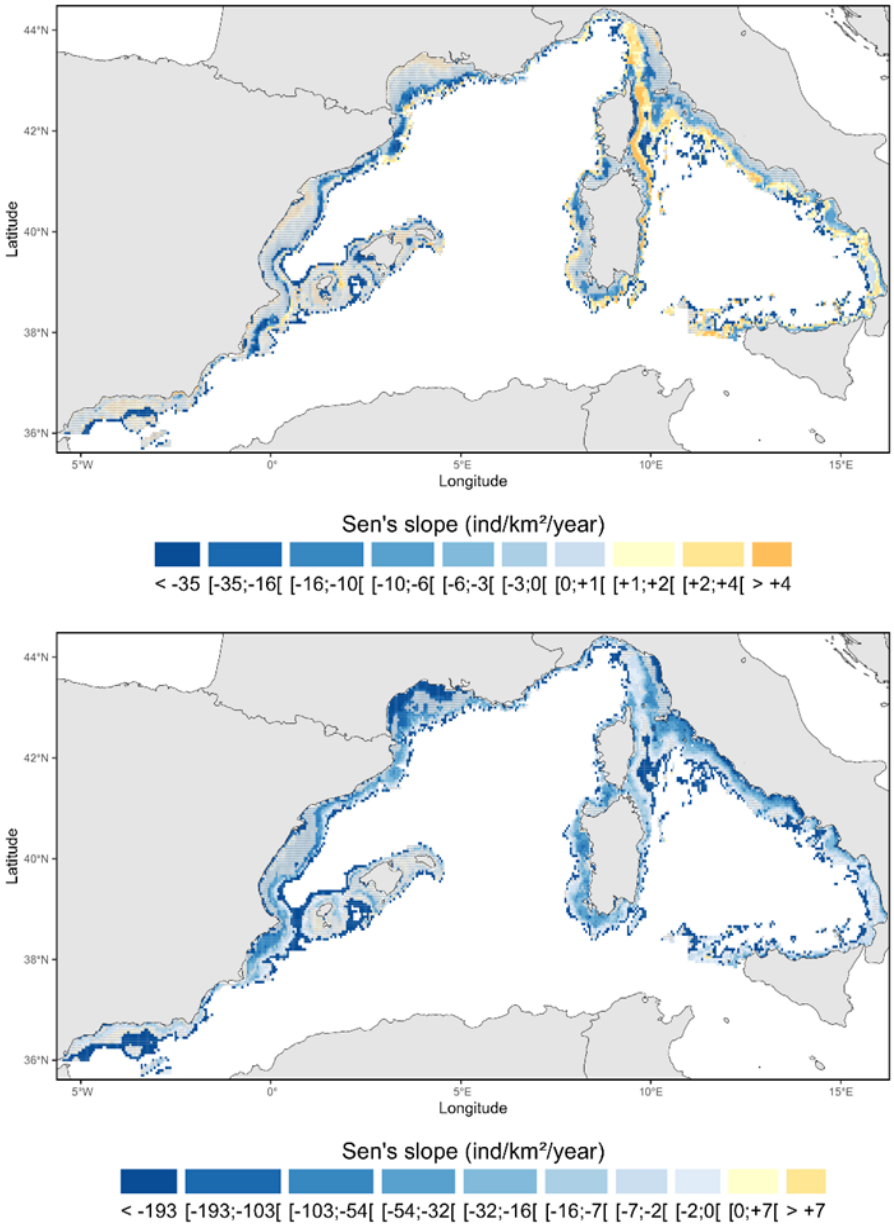

Figure 4.2. Spatial patterns of Sen's slope estimates (ind·km^{-2}·year^{-1}) derived from HMSC-predicted abundances across the western Mediterranean Sea for juvenile (top) and adult (bottom) life stages. Positive and negative values indicate increasing and decreasing abundance trends, respectively. Dots denote grid cells where Sen's slope was not significant based on the Mann–Kendall trend test ($p \geq 0.05$).

Identification of essential fish habitats

The Emerging Hotspot Analysis (EHSA) revealed marked differences in the spatial distribution of hotspots and coldspots between juvenile and adult life stages (Figure 4.3). On the continental shelf of the Gulf of Lion, no consistent spatial pattern was detected for juveniles, except near the Rhône River mouth, where a mosaic of sporadic, persistent, and intensifying hotspots emerged. In contrast, most of the Gulf of Lion continental shelf was identified as a combination of persistent and sporadic hotspots for adults. A similar life-stage contrast was observed around the Balearic Islands, which emerged as a major hotspot area for juveniles, dominated by intensifying and persistent hotspots, whereas adult patterns were largely absent or characterized by persistent coldspots.

At the scale of the western Mediterranean, juvenile hotspots (including sporadic, persistent, and intensifying hotspots) accounted for approximately 33.5% of the study area, while adult hotspots covered about 38.4% (Figure 4.4). Conversely, juvenile coldspots represented 40.7% of the study area, compared to 48.6% for adults, indicating a broader spatial extent of low-abundance areas for adult life stages.

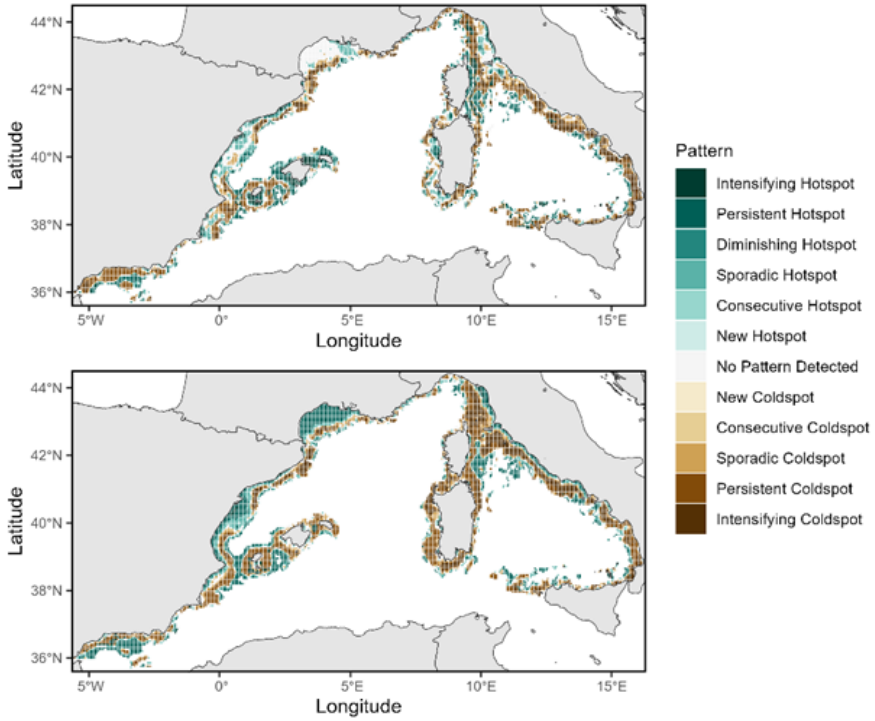

Figure 4.3. Emerging hotspot patterns of juvenile (top panel) and adult (bottom panel) life-stage abundances across the western Mediterranean Sea. See Table 1 for definitions of the different hotspot and coldspot categories.

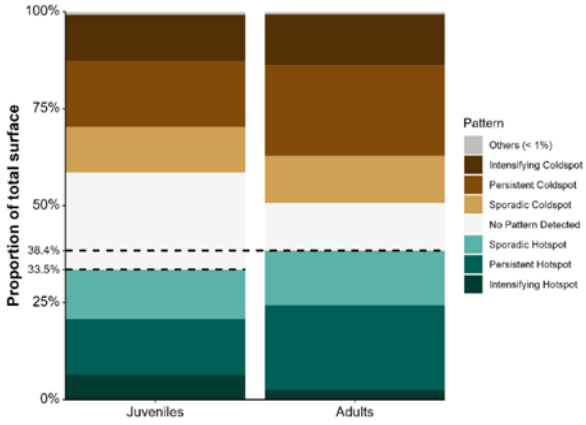

Figure 4.4. Proportion of the total study area covered by hotspot and coldspot patterns identified using emerging hotspot analysis. Spatial patterns representing less than 1% of the study area are grouped into the category "Others".

By overlapping hotspot and coldspot patterns between juvenile and adult life stages, we identified spatially congruent areas of high and low abundance (Figure 4.5). At the scale of the western Mediterranean Sea, approximately half of all hotspot and coldspot areas (ca. 50.7%) were congruent between juveniles and adults (Figure 4.6), highlighting strong life-stage specificity in the remaining patterns. Congruent hotspots were spatially concentrated in the western sub-basins, particularly in the Alboran Sea, the Catalan Sea along the Spanish coast, and around the Balearic Islands. These areas accounted for about 20.2% of the study area, with persistent hotspots representing the dominant congruent juvenile-adult hotspot type (ca. 8.5%). In contrast, congruent coldspots were more extensive and spatially segregated, occurring primarily in the eastern part of the western Mediterranean, notably along the upper continental slope of the Tyrrhenian Sea. Congruent coldspots covered approximately 30.6% of the study area, exceeding the extent of congruent hotspots, and were dominated by persistent coldspot patterns shared by juveniles and adults (ca. 7.6%).

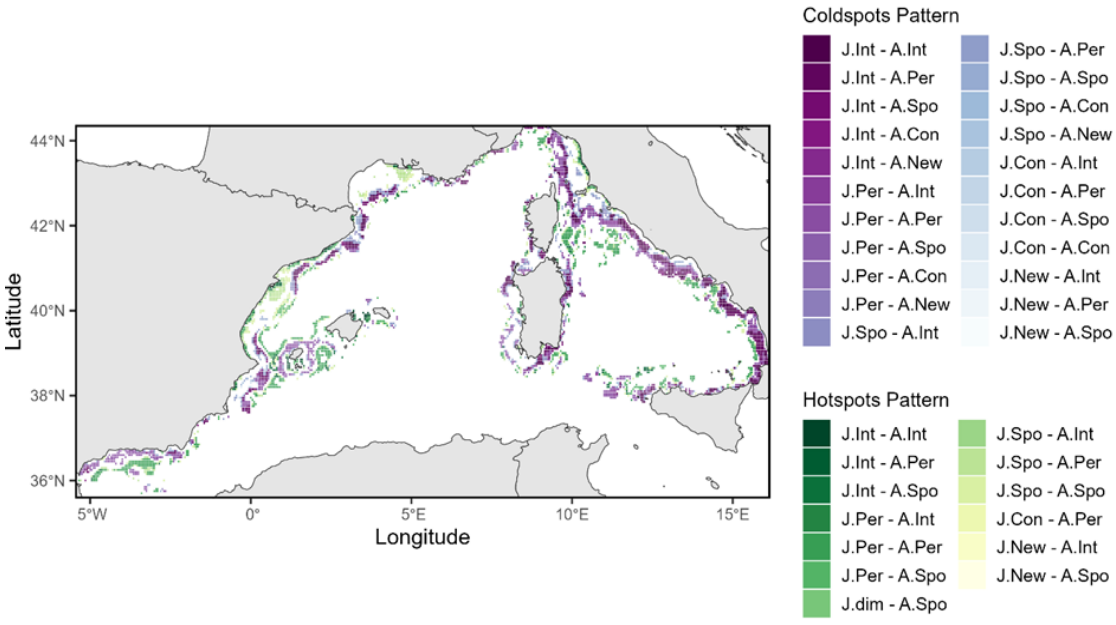

Figure 4.5. Spatial distribution of congruent hotspot and coldspot patterns between juvenile and adult life stages identified using emerging hotspot analysis across the western Mediterranean Sea. Congruent areas correspond to grid cells where juveniles and adults share the same hotspot or coldspot classification. In the legend, "J" denotes

juveniles and “A” denotes adults; “Int” indicates intensifying, “Per” persistent, “Spo” sporadic, and “Con” consecutive hotspot or coldspot patterns.

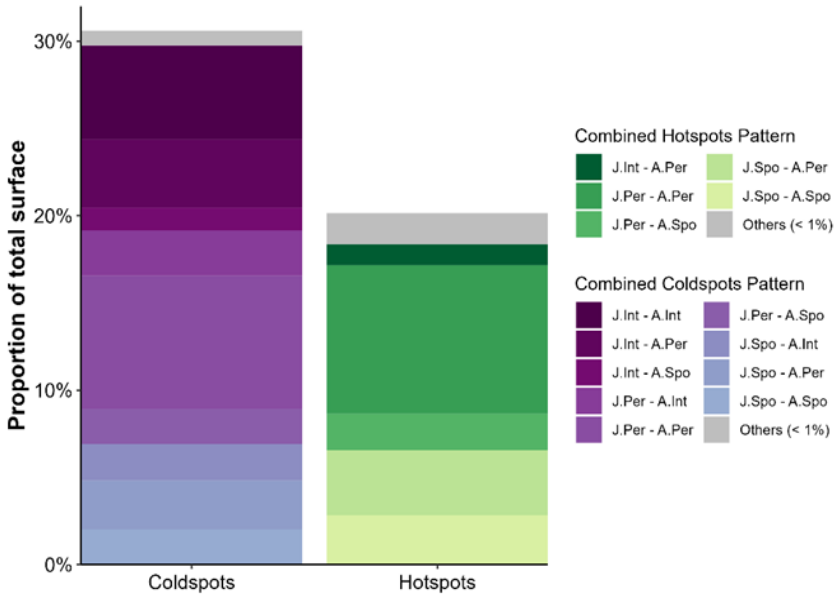

Figure 4.6. Proportion of the total study area covered by congruent hotspot and coldspot patterns identified using emerging hotspot analysis. Congruent spatial patterns representing less than 1% of the study area are grouped into the category “Others”.

Spatial congruence between essential fish habitats and marine protected areas

In the following section, spatially congruent hotspot patterns between juvenile and adult life stages were considered as essential fish habitats (EFHs), and thus as priority areas for conservation. Overall, approximately 76% of the total area of congruent hotspots identified as EFHs was not covered by Marine Protected Areas (MPAs), indicating that only 24% of these priority habitats currently benefit from some level of protection (Figure 4.7). Among the protected congruent hotspots, about 21% fell under minimal protection, primarily within the Pelagos Sanctuary (France–Monaco–Italy) and around the Balearic Islands, while approximately 3% were subject to light protection. Highly protected and fully protected areas accounted for only a negligible fraction of EFHs (ca. 0.05% and 0.02%, respectively). A similar pattern was observed for spatially congruent coldspots. Approximately 21% of congruent coldspot areas were under minimal protection, 4% under light protection, and 1.4% under high protection, nearly three times the proportion observed for congruent hotspots, while fully protected areas represented only 0.01% of the total congruent coldspot surface.

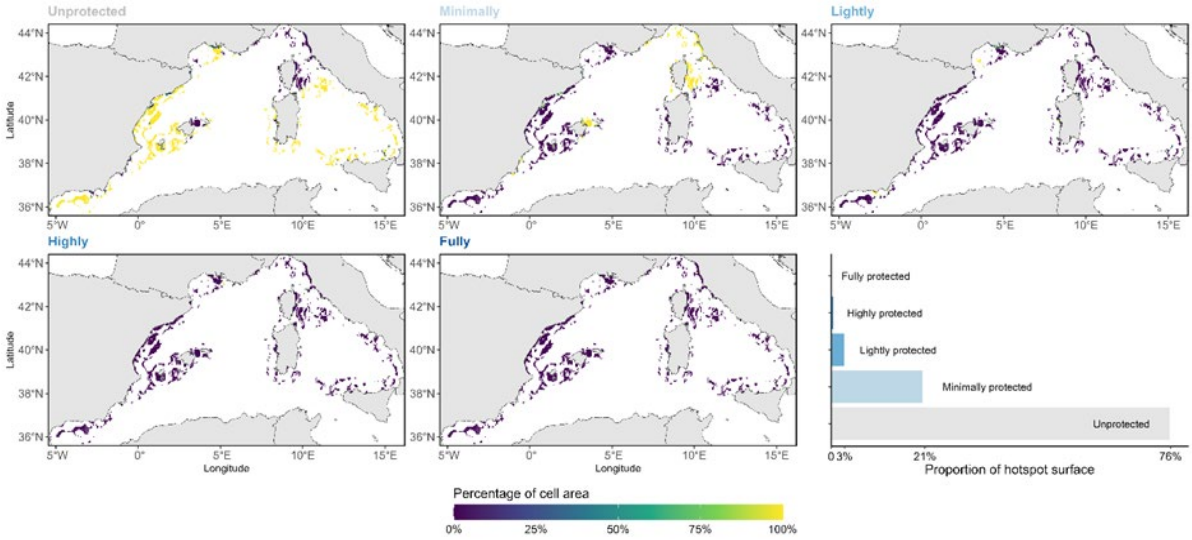

Figure 4.7. Spatial overlap between congruent hotspots of juvenile and adult life stages and the protection levels of existing Marine Protected Areas (MPAs) in the western Mediterranean Sea. The bar plot in the bottom-right panel shows the proportion of the congruent hotspot surface under different protection levels.

4.4. Discussion

By linking life-stage-specific species distributions, phylogenetic structure and spatio-temporal abundance dynamics, this study provides a macroecological basis for redefining EFHs as dynamic, community-based conservation priorities. Our results demonstrate that Mediterranean fish communities are strongly structured by ontogenetic variation in responses to environmental gradients and anthropogenic pressures, consistent with previous local, sub-regional and basin-scale assessments (Bellisario et al., 2025; Druon et al., 2015, 2016; MediSeH, 2013). By explicitly modelling juvenile and adult life stages within a joint species distribution framework, we show that life stage constitutes a major axis of ecological differentiation, comparable in magnitude to interspecific variation. This supports a growing body of macroecological evidence suggesting that life stages should be treated as distinct ecological entities with potentially divergent niches, sensitivities, and vulnerabilities to global change (Dahlke et al., 2020; Gherardi, 2025; Marshall & Morgan, 2011; Nagelkerken et al., 2015; Sánchez-Hernández, 2025).

Depth and temperature emerged as dominant drivers of both juvenile and adult distributions, reflecting the high vertical structuring and rapid warming of Mediterranean ecosystems (Albouy et al., 2013; Bartolino et al., 2008; Ben Lamine et al., 2022; Coll et al., 2010; Rozanski et al., 2024; Schickele et al., 2021). However, their relative importance varied markedly among species and life stages, highlighting the heterogeneous nature of thermal and bathymetric niches within Mediterranean fish assemblages. At the same time, the use of gridded environmental and human pressure datasets capturing broad-scale gradients inevitably overlooks fine-scale habitat features, such as sediment type, seabed complexity, localized hydrodynamics, and small-scale anthropogenic impacts, that are known to strongly influence demersal fish distributions (Cheminée et al., 2017; Cuadros et al., 2019; Druon et al., 2015; Garcia et al., 2022; MediSeH, 2013). These limitations likely contribute to the substantial spatial structure captured by random effects in our models.

Species responses to environmental and anthropogenic covariates exhibited a strong phylogenetic signal, indicating that vulnerability to global change is structured by evolutionary history. Closely related species tended to share similar response profiles, suggesting that conserved trait syndromes shape ecological niches and sensitivities to warming, fishing pressure,

and human accessibility (Comte et al., 2014; Comte & Olden, 2017; MacNeil et al., 2025; Maioli et al., 2023). Functional and life history traits explained a substantial fraction of among-species variation in responses, particularly to temperature and anthropogenic drivers, highlighting the mechanistic role of functional traits in mediating species-environment relationships. However, the persistence of a strong phylogenetic signal beyond the traits included in the model suggests that additional, unmeasured traits (e.g., behavioural strategies, fine-scale habitat specialization, physiological tolerances) contribute to shaping species niches. This pattern is consistent with recent macroecological studies showing that phylogeny often captures latent ecological dimensions not fully described by available trait data (Maioli et al., 2023; Montanyès et al., 2023; Weigel et al., 2021, 2023). This also suggests that entire phylogenetic lineages may be more vulnerable to ongoing environmental change and exploitation, potentially leading to non-random biodiversity loss and erosion of ecosystem functioning (Olden et al., 2004; Pinsky et al., 2011; Purvis et al., 2000; Sunday et al., 2015). Collecting and integrating trait information at the life-stage scale (i.e., for juveniles (adult-like form, immature) and adults (sexually mature, reproductive)) therefore appears crucial to improve mechanistic understanding of species–life stage niches and community assembly, and to strengthen trait-based links between environmental and anthropogenic gradients and fish diversity (Daskalaki et al., 2022; Di Stefano et al., 2024).

Several limitations of this study are related to the characteristics of the underlying survey data. The MEDITS bottom trawl survey is not designed to capture the full spatial distribution of all target species and life stages, particularly early juveniles whose nursery habitats often occur in shallow coastal areas that are poorly or not sampled by the survey (Cheminée et al., 2021; Colloca et al., 2015; Garcia et al., 2022; Giannoulaki et al., 2017; MediSeH, 2013). In addition, MEDITS is conducted almost exclusively during the spring-summer period, which may lead to temporal mismatches between survey timing and key biological processes such as spawning or early recruitment for some species (Fiorentini et al., 1999; Spedicato et al., 2019). These limitations likely contribute to the large proportion of the variance explained by the random effects (especially the spatial random effect) and residual co-occurrence patterns observed in our models.

The large number of significant residual co-occurrences indicates that species–life stage assemblages are structured by processes not fully captured by the measured environmental and anthropogenic covariates (Ovaskainen & Abrego, 2020). The predominance of positive residual associations suggests that shared habitat preferences, unmeasured environmental or anthropogenic drivers, facilitative processes and/or biotic interaction such as predation could play a major role in shaping local assemblage composition at the spatial scale considered (D'Amen et al., 2018; Montanyès et al., 2023). Such positive residual co-occurrences are also consistent with habitat filtering acting on fine-scale environmental features not explicitly included in the model, such as seabed complexity, microhabitat heterogeneity or localized hydrodynamic conditions, which are known to structure Mediterranean fish assemblages (Druon et al., 2015; Ordines et al., 2011; Ospina-Alvarez et al., 2012). Negative residual co-occurrences, although less frequent, likely reflect spatial segregation driven by competition (for food and/or habitat), predation avoidance or contrasting responses to unconsidered physico-chemical gradients (Ovaskainen & Abrego, 2020). The comparable contribution of juvenile and adult life stages to both positive and negative associations suggests that these structuring processes operate across ontogenetic stages, rather than being restricted to a particular phase of the life cycle. However, the higher proportion of adult–adult positive associations may reflect stronger habitat specialization or aggregation of mature individuals, whereas juvenile-only negative associations may indicate nursery habitat partitioning or density-dependent interactions during early

life stages, a consistent spatial pattern in the Mediterranean Sea (Cuadros et al., 2019; D'Iglio et al., 2021; Gouraguine et al., 2011; Haak et al., 2020; Mytilineou et al., 2013; Panzeri et al., 2025; Sion et al., 2019). Overall, these residual co-occurrence patterns point to the importance of biotic interactions, both inter- and intra-specific, and fine-scale habitat structure in shaping community assembly, complementing the effects of broad-scale environmental gradients and anthropogenic pressures captured by the fixed effects. While residual associations cannot be interpreted as direct interactions (Blanchet et al., 2020; Ovaskainen & Abrego, 2020), they provide valuable insight into latent processes influencing species coexistence and spatial organization.

Spatio-temporal trend analyses revealed a pronounced contrast between juvenile and adult life stages. Juvenile abundance trends were spatially heterogeneous, with localized increases, stability or declines, whereas adult abundances showed a more spatially homogenous and widespread decrease across much of the western Mediterranean Sea. This pattern suggests that recruitment limitation is not the primary driver of population decline for many species and that post-recruitment processes, especially fishing mortality, play a key role in shaping adult population dynamics through time (Quinzán et al., 2020; Vasilakopoulos et al., 2014). This is consistent with basin-wide assessments showing chronic overexploitation of Mediterranean stocks (FAO, 2025; Fiorentino & Vitale, 2021). These results underscore the importance of explicitly incorporating demographic structure into analyses of species distributions and temporal dynamics.

Essential Fish Habitats (EFHs) are widely recognized as a cornerstone of fisheries sustainability and marine ecosystem functioning, as they support key life-history processes such as spawning, nursery development, feeding and refuge from predation (Le Pape et al., 2014; Moore et al., 2016; Stamp et al., 2025; Sundblad et al., 2014). By sustaining recruitment, biomass production and trophic interactions, EFHs underpin critical ecosystem services, including food provision, biodiversity maintenance and ecosystem resilience (Liquete et al., 2016). In the Mediterranean Sea, however, EFHs are increasingly threatened by cumulative pressures from fishing, sea-use change, pollution, biological invasions and rapid climate warming (Bevilacqua et al., 2020; Coll et al., 2010; Halpern et al., 2025; Micheli, Halpern, et al., 2013). The degradation or loss of EFHs can propagate through populations and food webs, reducing recruitment success, truncating age structures, and diminishing ecosystem resilience (Barrientos et al., 2024; Fonseca et al., 2025; Peterson & Lowe, 2009; Tao et al., 2021).

Traditionally, EFHs have been identified at the species level, often focusing on a limited number of commercially important stocks and specific life stages (Colloca et al., 2009; Crec'hriou et al., 2008; Lauria et al., 2015; MediSeH, 2013; Ortega et al., 2023; Panzeri et al., 2025). Such approaches typically rely on static distribution maps, expert judgement (e.g., Bousquet et al., 2024) or coarse habitat classifications and rarely account for spatio-temporal variability, multispecies interactions, or climate-driven distribution shifts. In dynamic and species-rich systems such as the Mediterranean, this species-centric perspective is increasingly inadequate, as rapid warming, biological invasions, and changing exploitation patterns are reshaping species distributions and community composition (Azzurro et al., 2019; Chust et al., 2024; Damalas et al., 2021; Moullec et al., 2019; Sanz-Martín et al., 2024).

Here, we move beyond these limitations by adopting a community-based, life-stage-explicit and spatio-temporally dynamic framework. By combining joint species distribution modelling (Ovaskainen et al., 2017) with Emerging Hotspot Analysis (ESRI, 2025), we identified dynamic hotspots and coldspots of abundance across multiple species and life stages. Only about half of these areas were spatially congruent between life stages, indicating that high or

low abundance areas are strongly life-stage-specific. Spatial congruence between juvenile and adult hotspots (i.e., areas supporting high abundances of both juveniles and adults) delineates areas where multiple demographic processes co-occur (e.g., recruitment, growth, natural mortality) and can be interpreted as community-based EFHs. These areas can be considered as ecologically significant and priority conservation areas at the community level and provide an operational basis for ecosystem-based fisheries management.

Despite their ecological importance, most of these community-based EFHs remain outside the current Mediterranean MPA network. Approximately 76% of their surface fall outside MPAs, and the majority of protected EFHs are subject only to minimal or light protection. This spatial mismatch reflects the fragmented development of Mediterranean MPAs, which have largely emerged from national or subnational initiatives driven by socioeconomic and historical factors rather than basin-scale ecological evidence (Aminian-Biquet, Gorjanc, et al., 2024; Claudet et al., 2020; Francour et al., 2001). It also mirrors broader patterns observed across the Mediterranean Sea, where MPAs often fail to encompass ecologically critical areas or to provide adequate protection levels (Abello et al., 2025; Claudet et al., 2020; Giakoumi et al., 2017; Guilhaumon et al., 2015; Mouillot et al., 2011), thereby undermining progress toward the objectives of the EU Marine Strategy Framework Directive, the Common Fisheries Policy, and the EU Biodiversity Strategy for 2030. Our results suggest that MPA designed to encompass areas used by both juvenile and adult life stages could deliver greater long-term biodiversity and fisheries benefits than approaches focusing on a single demographic component (Beck et al., 2001; Dahlgren et al., 2006; Gaines et al., 2010; Grüss et al., 2019; Olds et al., 2016; White, 2015). Indeed, protecting areas that simultaneously support recruitment and spawning has been shown to enhance population replenishment, stabilize biomass, and increase fisheries yields through spillover and larval export (Baskett & Barnett, 2015; Edgar et al., 2014; Gaines et al., 2010; Goñi et al., 2008). Notably, congruent persistent juvenile–adult hotspots represent approximately 8.5% of the study area, close to the EU target of strictly protecting 10% of marine waters under the EU Biodiversity Strategy for 2030. While illustrative rather than prescriptive, this proximity highlights the potential of such areas as scientifically grounded references for improving the ecological coherence and effectiveness of MPA networks. These priority areas could be integrated with complementary biodiversity metrics and conservation initiatives to support the design of interconnected, climate-resilient MPA networks accounting for population connectivity and cumulative pressures (Abello et al., 2025; Mazor et al., 2014; Micheli, Levin, et al., 2013).

Taken together, our results highlight the urgent need to integrate dynamic, community-based EFHs into marine spatial planning, fisheries management and MPA network design. Protecting EFHs is not only a biodiversity conservation objective but a prerequisite for maintaining ecosystem services and long-term fisheries productivity. Incorporating life-stage dynamics and spatio-temporal variability into EFH identification offers a practical pathway to operationalize ecosystem-based fisheries management under European and regional policy frameworks. Extending this approach to project EFH shifts under climate change scenarios and cumulative human pressures will be critical to support adaptive, forward-looking conservation strategies in the Mediterranean Sea.

4.5. Conclusion

Our results show that conservation strategies based on static, species-centric representations of habitat use are likely to underestimate both the spatial extent and ecological importance of key marine habitats in rapidly changing systems. By explicitly accounting for life-stage-specific responses, phylogenetic structure and spatio-temporal dynamics, we demonstrate that areas of

high ecological importance can differ markedly among demographic stages and through time, particularly under strong environmental gradients and anthropogenic pressures. Spatially congruent hotspots between juvenile and adult life stages provide a dynamic, community-level representation of Essential Fish Habitats, identifying locations where recruitment, growth, and adult persistence can co-occur across multiple species. These habitats are therefore likely to contribute disproportionately to population connectivity, biomass production and ecosystem resilience, yet only a limited fraction currently overlaps with existing protected areas in the western Mediterranean Sea. The strong phylogenetic structuring of species responses further suggests that protecting community-based habitats may help safeguard phylogenetic and functional diversity, thereby buffering ecosystems against climate-driven range shifts and reorganization. More broadly, integrating joint species distribution models with spatio-temporal hotspot analyses offers a transferable macroecological framework to identify dynamic conservation priorities and improve the ecological representativeness and long-term effectiveness of marine protected area networks under ongoing global change.

4.6. References

Aarts, G., Fieberg, J., Brasseur, S., & Matthiopoulos, J. (2013). Quantifying the effect of habitat availability on species distributions. Journal of Animal Ecology, 82(6), 1135–1145. https://doi.org/10.1111/1365-2656.12061

Abella, A., Belluscio, A., Bertrand, J., Carbonara, P. L., Giordano, D., Sbrana, M., & Zamboni, A. (1999). Use of MEDITS trawl survey data and commercial fleet information for the assessment of some Mediterranean demersal resources. Aquatic Living Resources, 12(3), 155–166. https://doi.org/10.1016/S0990-7440(00)88467-3

Abello, C., Ernande, B., Moullec, F., Barrier, N., Pita-Vaca, I., & Shin, Y.-J. (2025). Beyond the 30x30 target: Science-informed marine protected area networks outperform random and opportunistic designs. Research Square. https://doi.org/10.21203/rs.3.rs-5653319/v2

Abrego, N., & Ovaskainen, O. (2023). Evaluating the predictive performance of presence–absence models: Why can the same model appear excellent or poor? Ecology and Evolution, 13(12), e10784. https://doi.org/10.1002/ece3.10784

Albouy, C., Delattre, V. L., Mérigot, B., Meynard, C. N., & Leprieur, F. (2017). Multifaceted biodiversity hotspots of marine mammals for conservation priorities. Diversity and Distributions, 23(6), 615–626. https://doi.org/10.1111/ddi.12556

Albouy, C., Guilhaumon, F., Leprieur, F., Lasram, F. B. R., Somot, S., Aznar, R., Velez, L., Le Loc'h, F., & Mouillot, D. (2013). Projected climate change and the changing biogeography of coastal Mediterranean fishes. Journal of Biogeography, 40(3), 534–547. https://doi.org/10.1111/jbi.12013

Albouy, C., Velez, L., Coll, M., Colloca, F., Le Loc'h, F., Mouillot, D., & Gravel, D. (2014). From projected species distribution to food-web structure under climate change. Global Change Biology, 20(3), 730–741. https://doi.org/10.1111/gcb.12467

Allan, J. R., Possingham, H. P., Atkinson, S. C., Waldron, A., Di Marco, M., Butchart, S. H. M., Adams, V. M., Kissling, W. D., Worsdell, T., Sandbrook, C., Gibbon, G., Kumar, K., Mehta, P., Maron, M., Williams, B. A., Jones, K. R., Wintle, B. A., Reside, A. E., & Watson, J. E. M. (2022). The minimum land area requiring conservation attention to safeguard biodiversity. Science, 376(6597), 1094–1101. https://doi.org/10.1126/science.abl9127

Aminian-Biquet, J., Colegrove, C., Driedger, A., Raudsepp, N., Sletten, J., Vincent, T., Zetterlind, V., Roessger, J., Laznya, A., Vaidianu, N., Claudet, J., Young, J., & Horta e Costa, B. (2024). Regulations of activities and protection levels in marine protected areas of the European Union: A dataset

compiled from multiple data sources. Data in Brief, 57, 111177. https://doi.org/10.1016/j.dib.2024.111177

Aminian-Biquet, J., Gorjanc, S., Sletten, J., Vincent, T., Laznya, A., Vaidianu, N., Claudet, J., Young, J., & Horta e Costa, B. (2024). Over 80% of the European Union's marine protected area only marginally regulates human activities. One Earth, 7(9), 1614–1629. https://doi.org/10.1016/j.oneear.2024.07.010

Angelini, S., Armelloni, E. N., Costantini, I., De Felice, A., Isajlović, I., Leonori, I., Manfredi, C., Masnadi, F., Scarcella, G., Tičina, V., & Santojanni, A. (2021). Understanding the Dynamics of Ancillary Pelagic Species in the Adriatic Sea. Frontiers in Marine Science, 8. https://doi.org/10.3389/fmars.2021.728948

Aurelle, D., Thomas, S., Albert, C., Bally, M., Bondeau, A., Boudouresque, C.-F., Cahill, A. E., Carlotti, F., Chenuil, A., Cramer, W., Davi, H., De Jode, A., Ereskovsky, A., Farnet, A.-M., Fernandez, C., Gauquelin, T., Mirleau, P., Monnet, A.-C., Prévosto, B., … Fady, B. (2022). Biodiversity, climate change, and adaptation in the Mediterranean. Ecosphere, 13(4), e3915. https://doi.org/10.1002/ecs2.3915

Azzurro, E., Sbragaglia, V., Cerri, J., Bariche, M., Bolognini, L., Ben Souissi, J., Busoni, G., Coco, S., Chryssanthi, A., Fanelli, E., Ghanem, R., Garrabou, J., Gianni, F., Grati, F., Kolitari, J., Letterio, G., Lipej, L., Mazzoldi, C., Milone, N., … Moschella, P. (2019). Climate change, biological invasions, and the shifting distribution of Mediterranean fishes: A large-scale survey based on local ecological knowledge. Global Change Biology, 25(8), 2779–2792. https://doi.org/10.1111/gcb.14670

Bahamon, N., Recasens, L., Sala-Coromina, J., Calero, B., Garcia, J. A., Rotllant, G., Maurer, A., Rojas, A., Muth, L., Quevedo, J., Vigo, M., Ribera-Altimir, J., & Company, J. B. (2024). Selectivity-based management for reversing overexploitation of demersal fisheries in North-western Mediterranean Sea. Marine Policy, 165, 106185. https://doi.org/10.1016/j.marpol.2024.106185

Barrientos, S., Piñeiro-Corbeira, C., Díaz-Tapia, P., García, M. E., & Barreiro, R. (2024). Recruitment as a possible indicator of declining resilience in degraded kelp forests. Ecological Indicators, 160, 111917. https://doi.org/10.1016/j.ecolind.2024.111917

Bartolino, V., Ottavi, A., Colloca, F., Ardizzone, G. D., & Stefánsson, G. (2008). Bathymetric preferences of juvenile European hake (Merluccius merluccius). ICES Journal of Marine Science, 65(6), 963–969. https://doi.org/10.1093/icesjms/fsn079

Baskett, M. L., & Barnett, L. A. K. (2015). The Ecological and Evolutionary Consequences of Marine Reserves. Annual Review of Ecology, Evolution, and Systematics, 46(Volume 46, 2015), 49–73. https://doi.org/10.1146/annurev-ecolsys-112414-054424

Beck, M. W., Heck, K. L., Able, K. W., Childers, D. L., Eggleston, D. B., Gillanders, B. M., Halpern, B., Hays, C. G., Hoshino, K., Minello, T. J., Orth, R. J., Sheridan, P. F., & Weinstein, M. P. (2001). The Identification, Conservation, and Management of Estuarine and Marine Nurseries for Fish and Invertebrates: A better understanding of the habitats that serve as nurseries for marine species and the factors that create site-specific variability in nursery quality will improve conservation and management of these areas. BioScience, 51(8), 633–641. https://doi.org/10.1641/0006-3568(2001)051%255B0633:TICAMO%255D2.0.CO;2

Bellisario, B., Lattanzi, A., & Cimmaruta, R. (2025). The fingerprint of functional strategies in Mediterranean seagrass fish assemblages. Functional Ecology, 39(7), 1665–1677. https://doi.org/10.1111/1365-2435.70070

Ben Lamine, E., Schickele, A., Goberville, E., Beaugrand, G., Allemand, D., & Raybaud, V. (2022). Expected contraction in the distribution ranges of demersal fish of high economic value in the Mediterranean and European Seas. Scientific Reports, 12(1), 10150. https://doi.org/10.1038/s41598-022-14151-8

Bensebaini, C. M., Certain, G., Billet, N., Jadaud, A., Gourguet, S., Hattab, T., & Fromentin, J. M. (2022). Interactions between demersal fish body condition and density during the regime shift of the Gulf of Lions. ICES Journal of Marine Science, 79(6), 1765–1776. https://doi.org/10.1093/icesjms/fsac106

Bertrand, J. A., Sola, L. G. de, Papaconstantinou, C., Relini, G., & Souplet, A. (2002). The general specifications of the MEDITS surveys. Scientia Marina, 66(S2), Article S2. https://doi.org/10.3989/scimar.2002.66s29

Beukhof, E., Dencker, T. S., Palomares, M. L. D., & Maureaud, A. (2019). A trait collection of marine fish species from North Atlantic and Northeast Pacific continental shelf seas [Dataset]. PANGAEA. https://doi.org/10.1594/PANGAEA.900866

Bevilacqua, S., Katsanevakis, S., Micheli, F., Sala, E., Rilov, G., Sarà, G., Malak, D. A., Abdulla, A., Gerovasileiou, V., Gissi, E., Mazaris, A. D., Pipitone, C., Sini, M., Stelzenmüller, V., Terlizzi, A., Todorova, V., & Fraschetti, S. (2020). The Status of Coastal Benthic Ecosystems in the Mediterranean Sea: Evidence From Ecological Indicators. Frontiers in Marine Science, 7. https://doi.org/10.3389/fmars.2020.00475

Bianchi, C. N., & Morri, C. (2000). Marine Biodiversity of the Mediterranean Sea: Situation, Problems and Prospects for Future Research. Marine Pollution Bulletin, 40(5), 367–376. https://doi.org/10.1016/S0025-326X(00)00027-8

Bitetto, I., Zupa, W., & Spedicato, M. T. (2023). R Code to Perform Multiple Checks on MEDITS Survey Data. R package version 0.3.0. [Computer software].

Blanchet, F. G., Cazelles, K., & Gravel, D. (2020). Co-occurrence is not evidence of ecological interactions. Ecology Letters, 23(7), 1050–1063. https://doi.org/10.1111/ele.13525

Boettiger, C., Lang, D. T., & Wainwright, P. C. (2012). rfishbase: Exploring, manipulating and visualizing FishBase data from R. Journal of Fish Biology, 81(6), 2030–2039. https://doi.org/10.1111/j.1095-8649.2012.03464.x

Bousquet, C., Mourier, J., Giovos, I., Meyers, E. K., Dijoux, J., & Durieux, E. D. H. (2024). Local Ecological Knowledge and Fishery Data Provides Important Information on the Distribution and Seasonal Dynamic of Critically Endangered Angel Sharks in Corsica (Mediterranean Sea, France) (SSRN Scholarly Paper No. 4872813). Social Science Research Network. https://doi.org/10.2139/ssrn.4872813

CBD. (2022). Kunming-Montreal Global Biodiversity Framework (Decision 15/4). Secretariat of the Convention on Biological Diversity. 〈https://www.cbd.int/doc/decisions/cop-15/cop-15-dec-04-en.pdf〉 .

Ceballos, G., Ehrlich, P. R., & Dirzo, R. (2017). Biological annihilation via the ongoing sixth mass extinction signaled by vertebrate population losses and declines. Proceedings of the National Academy of Sciences, 114(30), E6089–E6096. https://doi.org/10.1073/pnas.1704949114

Ceballos, G., Ehrlich, P. R., & Raven, P. H. (2020). Vertebrates on the brink as indicators of biological annihilation and the sixth mass extinction. Proceedings of the National Academy of Sciences, 117(24), 13596–13602. https://doi.org/10.1073/pnas.1922686117

Chamberlain, S. A., & Szöcs, E. (2013). taxize: Taxonomic search and retrieval in R. F1000Research, 2, 191. https://doi.org/10.12688/f1000research.2-191.v2

Champagnat, J., Lecomte, J. B., Rivot, E., Douchet, L., Martin, N., Grasso, F., Mounier, F., Labadie, P., Loizeau, V., Bacq, N., & Pape, O. L. (2021). Multidisciplinary assessment of nearshore nursery habitat restoration for an exploited population of marine fish. Marine Ecology Progress Series, 680, 97–109. https://doi.org/10.3354/meps13881

Chaplin-Kramer, R., Neugarten, R. A., Sharp, R. P., Collins, P. M., Polasky, S., Hole, D., Schuster, R., Strimas-Mackey, M., Mulligan, M., Brandon, C., Diaz, S., Fluet-Chouinard, E., Gorenflo, L. J.,

Johnson, J. A., Kennedy, C. M., Keys, P. W., Longley-Wood, K., McIntyre, P. B., Noon, M., … Watson, R. A. (2023). Mapping the planet's critical natural assets. Nature Ecology & Evolution, 7(1), 51–61. https://doi.org/10.1038/s41559-022-01934-5

Cheminée, A., Le Direach, L., Rouanet, E., Astruch, P., Goujard, A., Blanfuné, A., Bonhomme, D., Chassaing, L., Jouvenel, J.-Y., Ruitton, S., Thibaut, T., & Harmelin-Vivien, M. (2021). All shallow coastal habitats matter as nurseries for Mediterranean juvenile fish. Scientific Reports, 11(1), 14631. https://doi.org/10.1038/s41598-021-93557-2

Cheminée, A., Pastor, J., Bianchimani, O., Thiriet, P., Sala, E., Cottalorda, J.-M., Dominici, J.-M., Lejeune, P., & Francour, P. (2017). Juvenile fish assemblages in temperate rocky reefs are shaped by the presence of macro-algae canopy and its three-dimensional structure. Scientific Reports, 7(1), 14638. https://doi.org/10.1038/s41598-017-15291-y

Chust, G., Villarino, E., McLean, M., Mieszkowska, N., Benedetti-Cecchi, L., Bulleri, F., Ravaglioli, C., Borja, A., Muxika, I., Fernandes-Salvador, J. A., Ibaibarriaga, L., Uriarte, A., Revilla, M., Villate, F., Iriarte, A., Uriarte, I., Zervoudaki, S., Carstensen, J., Somerfield, P. J., … Lindegren, M. (2024). Cross-basin and cross-taxa patterns of marine community tropicalization and deborealization in warming European seas. Nature Communications, 15(1), 2126. https://doi.org/10.1038/s41467-024-46526-y

Cinner, J. E., Huchery, C., MacNeil, M. A., Graham, N. A. J., McClanahan, T. R., Maina, J., Maire, E., Kittinger, J. N., Hicks, C. C., Mora, C., Allison, E. H., D'Agata, S., Hoey, A., Feary, D. A., Crowder, L., Williams, I. D., Kulbicki, M., Vigliola, L., Wantiez, L., … Mouillot, D. (2016). Bright spots among the world's coral reefs. Nature, 535(7612), 416–419. https://doi.org/10.1038/nature18607

Cinner, J. E., Maire, E., Huchery, C., MacNeil, M. A., Graham, N. A. J., Mora, C., McClanahan, T. R., Barnes, M. L., Kittinger, J. N., Hicks, C. C., D'Agata, S., Hoey, A. S., Gurney, G. G., Feary, D. A., Williams, I. D., Kulbicki, M., Vigliola, L., Wantiez, L., Edgar, G. J., … Mouillot, D. (2018). Gravity of human impacts mediates coral reef conservation gains. Proceedings of the National Academy of Sciences, 115(27), E6116–E6125. https://doi.org/10.1073/pnas.1708001115

Claudet, J., Loiseau, C., Sostres, M., & Zupan, M. (2020). Underprotected Marine Protected Areas in a Global Biodiversity Hotspot. One Earth, 2(4), 380–384. https://doi.org/10.1016/j.oneear.2020.03.008

Coll, M., Piroddi, C., Albouy, C., Ben Rais Lasram, F., Cheung, W. W. L., Christensen, V., Karpouzi, V. S., Guilhaumon, F., Mouillot, D., Paleczny, M., Palomares, M. L., Steenbeek, J., Trujillo, P., Watson, R., & Pauly, D. (2012). The Mediterranean Sea under siege: Spatial overlap between marine biodiversity, cumulative threats and marine reserves. Global Ecology and Biogeography, 21(4), 465–480. https://doi.org/10.1111/j.1466-8238.2011.00697.x

Coll, M., Piroddi, C., Steenbeek, J., Kaschner, K., Ben Rais Lasram, F., Aguzzi, J., Ballesteros, E., Bianchi, C. N., Corbera, J., Dailianis, T., Danovaro, R., Estrada, M., Froglia, C., Galil, B., Gasol, J., Gertwagen, R., Gil, J., Guilhaumon, F., Kesner-Reyes, K., … Voultsiadou, E. (2010). The Biodiversity of the Mediterranean Sea: Estimates, Patterns, and Threats. PLoS ONE, 5(8), e11842. https://doi.org/10.1371/journal.pone.0011842

Colloca, F., Bartolino, V., Lasinio, G. J., Maiorano, L., Sartor, P., & Ardizzone, G. (2009). Identifying fish nurseries using density and persistence measures. Marine Ecology Progress Series, 381, 287–296. https://doi.org/10.3354/meps07942

Colloca, F., Garofalo, G., Bitetto, I., Facchini, M. T., Grati, F., Martiradonna, A., Mastrantonio, G., Nikolioudakis, N., Ordinas, F., Scarcella, G., Tserpes, G., Tugores, M. P., Valavanis, V., Carlucci, R., Fiorentino, F., Follesa, M. C., Iglesias, M., Knittweis, L., Lefkaditou, E., … Spedicato, M. T. (2015). The Seascape of Demersal Fish Nursery Areas in the North Mediterranean Sea, a First Step Towards the Implementation of Spatial Planning for Trawl Fisheries. PLOS ONE, 10(3), e0119590. https://doi.org/10.1371/journal.pone.0119590

Colloca, F., Scarcella, G., & Libralato, S. (2017). Recent Trends and Impacts of Fisheries Exploitation on Mediterranean Stocks and Ecosystems. Frontiers in Marine Science, 4. https://doi.org/10.3389/fmars.2017.00244

Comte, L., Murienne, J., & Grenouillet, G. (2014). Species traits and phylogenetic conservatism of climate-induced range shifts in stream fishes. Nature Communications, 5(1), 5053. https://doi.org/10.1038/ncomms6053

Comte, L., & Olden, J. D. (2017). Climatic vulnerability of the world's freshwater and marine fishes. Nature Climate Change, 7(10), 718–722. https://doi.org/10.1038/nclimate3382

Cossarini, G., Feudale, L., Teruzzi, A., Bolzon, G., Coidessa, G., Solidoro, C., Di Biagio, V., Amadio, C., Lazzari, P., Brosich, A., & Salon, S. (2021). High-Resolution Reanalysis of the Mediterranean Sea Biogeochemistry (1999–2019). Frontiers in Marine Science, 8. https://doi.org/10.3389/fmars.2021.741486

Costello, M. J., Vale, M. M., Kiessling, W., Maharaj, S., Price, J., & Talukdar, G. H. (2022). Cross-Chapter Paper 1: Biodiversity Hotspots. In: Climate Change 2022: Impacts, Adaptation and Vulnerability. Contribution of Working Group II to the Sixth Assessment Report of the Intergovernmental Panel on Climate Change [H.-O. Pörtner, D.C. Roberts, M. Tignor, E.S. Poloczanska, K. Mintenbeck, A. Alegría, M. Craig, S. Langsdorf, S. Löschke, V. Möller, A. Okem, B. Rama (eds.)]. Cambridge University Press, Cambridge, UK and New York, NY, USA, pp. 2123–2161, doi:10.1017/9781009325844.018. (1st ed.). https://www.cambridge.org/core/product/identifier/9781009325844/type/book

Coulon, N., Lindegren, M., Goberville, E., Toussaint, A., Receveur, A., & Auber, A. (2023). Threatened fish species in the Northeast Atlantic are functionally rare. Global Ecology and Biogeography, 32(10), 1827–1845. https://doi.org/10.1111/geb.13731

Cramer, W., Guiot, J., Fader, M., Garrabou, J., Gattuso, J.-P., Iglesias, A., Lange, M. A., Lionello, P., Llasat, M. C., Paz, S., Peñuelas, J., Snoussi, M., Toreti, A., Tsimplis, M. N., & Xoplaki, E. (2018). Climate change and interconnected risks to sustainable development in the Mediterranean. Nature Climate Change, 8(11), 972–980. https://doi.org/10.1038/s41558-018-0299-2

Crec'hriou, R., Bonhomme, P., Criquet, G., Cadiou, G., Lenfant, P., Bernard, G., Roussel, E., Le Diréach, L., & Planes, S. (2008). Spatial patterns and GIS habitat modelling of fish in two French Mediterranean coastal areas. Hydrobiologia, 612(1), 135–153. https://doi.org/10.1007/s10750-008-9483-0

Cuadros, A., Moranta, J., Cardona, L., Thiriet, P., Francour, P., Vidal, E., Sintes, J., & Cheminee, A. (2019). Juvenile fish in Cystoseira forests: Influence of habitat complexity and depth on fish behaviour and assemblage composition. Mediterranean Marine Science, 20(2), 380–392. https://doi.org/10.12681/mms.18857

Dahlgren, C. P., Kellison, G. T., Adams, A. J., Gillanders, B. M., Kendall, M. S., Layman, C. A., Ley, J. A., Nagelkerken, I., & Serafy, J. E. (2006). Marine nurseries and effective juvenile habitats: Concepts and applications. Marine Ecology Progress Series, 312, 291–295. https://doi.org/10.3354/meps312291

Dahlke, F. T., Wohlrab, S., Butzin, M., & Pörtner, H.-O. (2020). Thermal bottlenecks in the life cycle define climate vulnerability of fish. Science, 369(6499), 65–70. https://doi.org/10.1126/science.aaz3658

Damalas, D., Sgardeli, V., Vasilakopoulos, P., Tserpes, G., & Maravelias, C. (2021). Evidence of climate-driven regime shifts in the Aegean Sea's demersal resources: A study spanning six decades. Ecology and Evolution, 11(23), 16951–16971. https://doi.org/10.1002/ece3.8330

D'Amen, M., Mod, H. K., Gotelli, N. J., & Guisan, A. (2018). Disentangling biotic interactions, environmental filters, and dispersal limitation as drivers of species co-occurrence. Ecography, 41(8), 1233–1244. https://doi.org/10.1111/ecog.03148

Daskalaki, E., Koufalis, E., Dimarchopoulou, D., & Tsikliras, A. C. (2022). Scientific progress made towards bridging the knowledge gap in the biology of Mediterranean marine fishes. PLOS ONE, 17(11), e0277383. https://doi.org/10.1371/journal.pone.0277383

Davies, T. E., Maxwell, S. M., Kaschner, K., Garilao, C., & Ban, N. C. (2017). Large marine protected areas represent biodiversity now and under climate change. Scientific Reports, 7(1), 9569. https://doi.org/10.1038/s41598-017-08758-5

Di Stefano, M., Nerini, D., Alvarez, I., Ardizzone, G., Astruch, P., Basterretxea, G., Blanfuné, A., Bonhomme, D., Calò, A., Catalan, I., Cattano, C., Cheminée, A., Crec'hriou, R., Cuadros, A., Di Franco, A., Diaz-Gil, C., Estaque, T., Faillettaz, R., Félix-Hackradt, F. C., … Rossi, V. (2024). Early-life dispersal traits of coastal fishes: An extensive database combining observations and growth models. Earth System Science Data, 16(8), 3851–3871. https://doi.org/10.5194/essd-16-3851-2024

D'Iglio, C., Albano, M., Famulari, S., Savoca, S., Panarello, G., Di Paola, D., Perdichizzi, A., Rinelli, P., Lanteri, G., Spanò, N., & Capillo, G. (2021). Intra- and interspecific variability among congeneric Pagellus otoliths. Scientific Reports, 11(1), 16315. https://doi.org/10.1038/s41598-021-95814-w

Dimarchopoulou, D., Stergiou, K. I., & Tsikliras, A. C. (2017). Gap analysis on the biology of Mediterranean marine fishes. PLOS ONE, 12(4), e0175949. https://doi.org/10.1371/journal.pone.0175949

Dormann, C. F., Elith, J., Bacher, S., Buchmann, C., Carl, G., Carré, G., Marquéz, J. R. G., Gruber, B., Lafourcade, B., Leitão, P. J., Münkemüller, T., McClean, C., Osborne, P. E., Reineking, B., Schröder, B., Skidmore, A. K., Zurell, D., & Lautenbach, S. (2013). Collinearity: A review of methods to deal with it and a simulation study evaluating their performance. Ecography, 36(1), 27–46. https://doi.org/10.1111/j.1600-0587.2012.07348.x

D'Ortenzio, F., & Ribera d'Alcalà, M. (2009). On the trophic regimes of the Mediterranean Sea: A satellite analysis. Biogeosciences, 6(2), 139–148. https://doi.org/10.5194/bg-6-139-2009

Druon, J.-N., Fiorentino, F., Murenu, M., Knittweis, L., Colloca, F., Osio, C., Mérigot, B., Garofalo, G., Mannini, A., Jadaud, A., Sbrana, M., Scarcella, G., Tserpes, G., Peristeraki, P., Carlucci, R., & Heikkonen, J. (2015). Modelling of European hake nurseries in the Mediterranean Sea: An ecological niche approach. Progress in Oceanography, 130, 188–204. https://doi.org/10.1016/j.pocean.2014.11.005

Druon, J.-N., Fromentin, J.-M., Hanke, A. R., Arrizabalaga, H., Damalas, D., Tičina, V., Quílez-Badia, G., Ramirez, K., Arregui, I., Tserpes, G., Reglero, P., Deflorio, M., Oray, I., Saadet Karakulak, F., Megalofonou, P., Ceyhan, T., Grubišić, L., MacKenzie, B. R., Lamkin, J., … Addis, P. (2016). Habitat suitability of the Atlantic bluefin tuna by size class: An ecological niche approach. Progress in Oceanography, 142, 30–46. https://doi.org/10.1016/j.pocean.2016.01.002

Dunn, D. C., Cleary, J., DeLand, S., Bax, N., Bentley, L. K., Curtice, C., Donnelly, B., Dunstan, P. K., Froján, C. B., Gjerde, K. M., Gunn, V., Johnson, D. E., Klein, E., Kot, C. Y., Nisthar, D., Crespo, G. O., & Halpin, P. N. (2025). What is an ecologically or biologically significant area? Npj Ocean Sustainability, 4(1), 28. https://doi.org/10.1038/s44183-025-00126-5

Edgar, G. J., Stuart-Smith, R. D., Willis, T. J., Kininmonth, S., Baker, S. C., Banks, S., Barrett, N. S., Becerro, M. A., Bernard, A. T. F., Berkhout, J., Buxton, C. D., Campbell, S. J., Cooper, A. T., Davey, M., Edgar, S. C., Försterra, G., Galván, D. E., Irigoyen, A. J., Kushner, D. J., … Thomson, R. J. (2014). Global conservation outcomes depend on marine protected areas with five key features. Nature, 506(7487), 216–220. https://doi.org/10.1038/nature13022

Escudier, R., Clementi, E., Cipollone, A., Pistoia, J., Drudi, M., Grandi, A., Lyubartsev, V., Lecci, R., Aydogdu, A., Delrosso, D., Omar, M., Masina, S., Coppini, G., & Pinardi, N. (2021). A High Resolution Reanalysis for the Mediterranean Sea. Frontiers in Earth Science, 9. https://doi.org/10.3389/feart.2021.702285

ESRI. (2025). How Emerging Hot Spot Analysis works—ArcGIS Pro | Documentation. https://pro.arcgis.com/en/pro-app/latest/tool-reference/space-time-pattern-mining/learnmoreemerging.htm

FAO. (2021). GFCM 2030 Strategy for sustainable fisheries and aquaculture in the Mediterranean and the Black Sea. Rome. Https://doi.org/10.4060/cb7562en.

FAO. (2023). The State of Mediterranean and Black Sea Fisheries 2023. FAO. https://doi.org/10.4060/cc8888en

FAO. (2025). The State of Mediterranean and Black Sea Fisheries 2025. General Fisheries Commission for the Mediterranean (GFCM), Rome, Italy. FAO. https://doi.org/10.4060/cd7701en

Fiorentini, L., Dremière, P.-Y., Leonori, I., Sala, A., & Palumbo, V. (1999). Efficiency of the bottom trawl used for the Mediterranean international trawl survey (MEDITS). Aquatic Living Resources, 12(3), 187–205. https://doi.org/10.1016/S0990-7440(00)88470-3

Fiorentino, F., Patti, B., Colloca, F., Bonanno, A., Basilone, G., Gancitano, V., Garofalo, G., Goncharov, S., Gristina, M., Sinacori, G., & Mazzola, S. (2013). A comparison between acoustic and bottom trawl estimates to reconstruct the biomass trends of sardine and anchovy in the Strait of Sicily (Central Mediterranean). Fisheries Research, 147, 290–295. https://doi.org/10.1016/j.fishres.2013.06.001

Fiorentino, F., & Vitale, S. (2021). How Can We Reduce the Overexploitation of the Mediterranean Resources? Frontiers in Marine Science, 8. https://doi.org/10.3389/fmars.2021.674633

Fonseca, V. F., Bertucci, F., Solé, M., Human, L. R. D., Le Pape, O., & Brown, E. J. (2025). Habitat degradation impacts on marine fish. In Ecology of Marine Fish (pp. 325–342). Elsevier. https://doi.org/10.1016/B978-0-323-99036-3.00016-7

Francour, P., Harmelin, J.-G., Pollard, D., & Sartoretto, S. (2001). A review of marine protected areas in the northwestern Mediterranean region: Siting, usage, zonation and management. Aquatic Conservation: Marine and Freshwater Ecosystems, 11(3), 155–188. https://doi.org/10.1002/aqc.442

Froese, R., & Pauly, D. (2025). Editors. 2025. FishBase. World Wide Web electronic publication. Www.fishbase.org, (04/2025) [Computer software].

Gaines, S. D., White, C., Carr, M. H., & Palumbi, S. R. (2010). Designing marine reserve networks for both conservation and fisheries management. Proceedings of the National Academy of Sciences, 107(43), 18286–18293. https://doi.org/10.1073/pnas.0906473107

Galaiduk, R., Radford, B. T., Saunders, B. J., Newman, S. J., & Harvey, E. S. (2017). Characterizing ontogenetic habitat shifts in marine fishes: Advancing nascent methods for marine spatial management. Ecological Applications, 27(6), 1776–1788. https://doi.org/10.1002/eap.1565

Garcia, J., Pasqualini, V., Vanalderweireldt, L., Bisgambiglia, P. A., Marengo, M., Lejeune, P., Aiello, A., & Durieux, E. D. H. (2022). Global patterns and environmental drivers of suitable habitat for Dentex dentex and Sciaena umbra along the Corsican coast. ICES Journal of Marine Science, 79(9), 2461–2472. https://doi.org/10.1093/icesjms/fsac184

Ge, D., Qu, Y., Deng, T., Thuiller, W., Fišer, C., Ericson, P. G. P., Guo, B., de la Sancha, N. U., von der Heyden, S., Hou, Z., Li, J., Abramov, A., Vogler, A. P., Jønsson, K. A., & Mittermeier, R. (2022). New progress in exploring the mechanisms underlying extraordinarily high biodiversity in global hotspots and their implications for conservation. Diversity and Distributions, 28(12), 2448–2458. https://doi.org/10.1111/ddi.13657

Gelman, A., & Rubin, D. B. (1992). Inference from Iterative Simulation Using Multiple Sequences. Statistical Science, 7(4), 457–472. https://doi.org/10.1214/ss/1177011136

Getis, A., & Ord, J. K. (1992). The Analysis of Spatial Association by Use of Distance Statistics. Geographical Analysis, 24(3), 189–206. https://doi.org/10.1111/j.1538-4632.1992.tb00261.x

Gherardi, D. F. M. (2025). Niche and neutral processes shape the response of marine communities to ocean warming. Marine Biology, 173(1), 9. https://doi.org/10.1007/s00227-025-04740-2

Giakoumi, S., & Pey, A. (2017). Assessing the Effects of Marine Protected Areas on Biological Invasions: A Global Review. Frontiers in Marine Science, 4. https://doi.org/10.3389/fmars.2017.00049

Giakoumi, S., Scianna, C., Plass-Johnson, J., Micheli, F., Grorud-Colvert, K., Thiriet, P., Claudet, J., Di Carlo, G., Di Franco, A., Gaines, S. D., García-Charton, J. A., Lubchenco, J., Reimer, J., Sala, E., & Guidetti, P. (2017). Ecological effects of full and partial protection in the crowded Mediterranean Sea: A regional meta-analysis. Scientific Reports, 7(1), 8940. https://doi.org/10.1038/s41598-017-08850-w

Giannoulaki, M., Iglesias, M., Tugores, M. P., Bonanno, A., Patti, B., De Felice, A., Leonori, I., Bigot, J. L., Tičina, V., Pyrounaki, M. M., Tsagarakis, K., Machias, A., Somarakis, S., Schismenou, E., Quinci, E., Basilone, G., Cuttitta, A., Campanella, F., Miquel, J., … Valavanis, V. (2013). Characterizing the potential habitat of European anchovy Engraulis encrasicolus in the Mediterranean Sea, at different life stages. Fisheries Oceanography, 22(2), 69–89. https://doi.org/10.1111/fog.12005

Giannoulaki, M., Pyrounaki, M. M., Bourdeix, J.-H., Ben Abdallah, L., Bonanno, A., Basilone, G., Iglesias, M., Ventero, A., De Felice, A., Leonori, I., Valavanis, V. D., Machias, A., & Saraux, C. (2017). Habitat Suitability Modeling to Identify the Potential Nursery Grounds of the Atlantic Mackerel and Its Relation to Oceanographic Conditions in the Mediterranean Sea. Frontiers in Marine Science, 4. https://doi.org/10.3389/fmars.2017.00230

Goñi, R., Adlerstein, S., Alvarez-Berastegui, D., Forcada, A., Reñones, O., Criquet, G., Polti, S., Cadiou, G., Valle, C., Lenfant, P., Bonhomme, P., Pérez-Ruzafa, A., Sánchez-Lizaso, J., García-Charton, J., Bernard, G., Stelzenmüller, V., & Planes, S. (2008). Spillover from six western Mediterranean marine protected areas: Evidence from artisanal fisheries. Marine Ecology Progress Series, 366, 159–174. https://doi.org/10.3354/meps07532

Gordó-Vilaseca, C., Costello, M. J., Coll, M., Jüterbock, A., Reiss, H., & Stephenson, F. (2024). Future trends of marine fish biomass distributions from the North Sea to the Barents Sea. Nature Communications, 15(1), 5637. https://doi.org/10.1038/s41467-024-49911-9

Gouraguine, A., Hidalgo, M., Moranta, J., Bailey, D. M., Ordines, F., Guijarro, B., Valls, M., Barberá, C., & Mesa, A. D. (2011). Elasmobranch spatial segregation in the western Mediterranean. Scientia Marina, 75(4), 653–664. https://doi.org/10.3989/scimar.2011.75n4653

Granger, V., Fromentin, J.-M., Bez, N., Relini, G., Meynard, C. N., Gaertner, J.-C., Maiorano, P., Garcia Ruiz, C., Follesa, C., Gristina, M., Peristeraki, P., Brind'Amour, A., Carbonara, P., Charilaou, C., Esteban, A., Jadaud, A., Joksimovic, A., Kallianiotis, A., Kolitari, J., … Mérigot, B. (2015). Large-scale spatio-temporal monitoring highlights hotspots of demersal fish diversity in the Mediterranean Sea. Progress in Oceanography, 130, 65–74. https://doi.org/10.1016/j.pocean.2014.10.002

Grorud-Colvert, K., Sullivan-Stack, J., Roberts, C., Constant, V., Horta e Costa, B., Pike, E. P., Kingston, N., Laffoley, D., Sala, E., Claudet, J., Friedlander, A. M., Gill, D. A., Lester, S. E., Day, J. C., Gonçalves, E. J., Ahmadia, G. N., Rand, M., Villagomez, A., Ban, N. C., … Lubchenco, J. (2021). The MPA Guide: A framework to achieve global goals for the ocean. Science, 373(6560), eabf0861. https://doi.org/10.1126/science.abf0861

Grüss, A., Biggs, C. R., Heyman, W. D., & Erisman, B. (2019). Protecting juveniles, spawners or both: A practical statistical modelling approach for the design of marine protected areas. Journal of Applied Ecology, 56(10), 2328–2339. https://doi.org/10.1111/1365-2664.13468

Guilhaumon, F., Albouy, C., Claudet, J., Velez, L., Ben Rais Lasram, F., Tomasini, J.-A., Douzery, E. J. P., Meynard, C. N., Mouquet, N., Troussellier, M., Araújo, M. B., & Mouillot, D. (2015). Representing taxonomic, phylogenetic and functional diversity: New challenges for Mediterranean marine-protected areas. Diversity and Distributions, 21(2), 175–187. https://doi.org/10.1111/ddi.12280

Guisan, A., Zimmermann, N. E., & Thuiller, W. (Eds.). (2017). What Drives Species Distributions? In Habitat Suitability and Distribution Models: With Applications in R (pp. 21–40). Cambridge University Press. https://doi.org/10.1017/9781139028271.007

Haak, C. R., Hui, F. K. C., Cowles, G. W., & Danylchuk, A. J. (2020). Positive interspecific associations consistent with social information use shape juvenile fish assemblages. Ecology, 101(2), e02920. https://doi.org/10.1002/ecy.2920

Halpern, B. S., Frazier, M., O'Hara, C. C., Vargas-Fonseca, O. A., & Lombard, A. T. (2025). Cumulative impacts to global marine ecosystems projected to more than double by mid-century. Science, 389(6766), 1216–1219. https://doi.org/10.1126/science.adv2906

Halpern, B. S., Frazier, M., Potapenko, J., Casey, K. S., Koenig, K., Longo, C., Lowndes, J. S., Rockwood, R. C., Selig, E. R., Selkoe, K. A., & Walbridge, S. (2015). Spatial and temporal changes in cumulative human impacts on the world's ocean. Nature Communications, 6(1), 7615. https://doi.org/10.1038/ncomms8615

Hassoun, A. E. R., Mojtahid, M., Merheb, M., Lionello, P., Gattuso, J.-P., & Cramer, W. (2025). Climate change risks on key open marine and coastal mediterranean ecosystems. Scientific Reports, 15(1), 24907. https://doi.org/10.1038/s41598-025-07858-x

Herbert-Read, J. E., Thornton, A., Amon, D. J., Birchenough, S. N. R., Côté, I. M., Dias, M. P., Godley, B. J., Keith, S. A., McKinley, E., Peck, L. S., Calado, R., Defeo, O., Degraer, S., Johnston, E. L., Kaartokallio, H., Macreadie, P. I., Metaxas, A., Muthumbi, A. W. N., Obura, D. O., … Sutherland, W. J. (2022). A global horizon scan of issues impacting marine and coastal biodiversity conservation. Nature Ecology & Evolution, 6(9), 1262–1270. https://doi.org/10.1038/s41559-022-01812-0

Hidalgo, M., Ligas, A., Bellido, J. M., Bitetto, I., Carbonara, P., Carlucci, R., Guijarro, B., Jadaud, A., Lembo, G., Manfredi, C., Esteban, A., Garofalo, G., Ikica, Z., García, C., Sola, L. G. de, Kavadas, S., Maina, I., Sion, L., Vittori, S., & Vrgoc, N. (2019). Size-dependent survival of European hake juveniles in the Mediterranean Sea. Scientia Marina, 83(S1), 207–221. https://doi.org/10.3989/scimar.04857.16A

IPBES. (2018). The IPBES regional assessment report on biodiversity and ecosystem services for Europe and Central Asia. Rounsevell, M., Fischer, M., Torre-Marin Rando, A. and Mader, A. (eds.). Secretariat of the Intergovernmental Science-Policy Platform on Biodiversity and Ecosystem Services, Bonn, Germany. 892 pages. Intergovernmental Science-Policy Platform on Biodiversity and Ecosystem Services (IPBES).

IPBES. (2019). Global assessment report on biodiversity and ecosystem services of the Intergovernmental Science-Policy Platform on Biodiversity and Ecosystem Services. Zenodo. https://doi.org/10.5281/zenodo.6417333.

Isbell, F., Gonzalez, A., Loreau, M., Cowles, J., Díaz, S., Hector, A., Mace, G. M., Wardle, D. A., O'Connor, M. I., Duffy, J. E., Turnbull, L. A., Thompson, P. L., & Larigauderie, A. (2017). Linking the influence and dependence of people on biodiversity across scales. Nature, 546(7656), 65–72. https://doi.org/10.1038/nature22899

Izquierdo, F., Paradinas, I., Cerviño, S., Conesa, D., Alonso-Fernández, A., Velasco, F., Preciado, I., Punzón, A., Saborido-Rey, F., & Pennino, M. G. (2021). Spatio-Temporal Assessment of the European Hake (Merluccius merluccius) Recruits in the Northern Iberian Peninsula. Frontiers in Marine Science, 8. https://doi.org/10.3389/fmars.2021.614675

Jefferson, T., & Costello, M. J. (2020). Hotspots of Marine Biodiversity. In Encyclopedia of the World's Biomes (pp. 586–596). Elsevier. https://doi.org/10.1016/B978-0-12-409548-9.11952-9

Katsanevakis, S., Stelzenmüller, V., South, A., Sørensen, T. K., Jones, P. J. S., Kerr, S., Badalamenti, F., Anagnostou, C., Breen, P., Chust, G., D'Anna, G., Duijn, M., Filatova, T., Fiorentino, F., Hulsman, H., Johnson, K., Karageorgis, A. P., Kröncke, I., Mirto, S., … Hofstede, R. T. (2011). Ecosystem-based marine spatial management: Review of concepts, policies, tools, and critical issues. Ocean & Coastal Management, 54(11), 807–820. https://doi.org/10.1016/j.ocecoaman.2011.09.002

Kavadas, S., Maina, I., Damalas, D., Dokos, I., Pantazi, M., & Vassilopoulou, V. (2015). Multi-Criteria Decision Analysis as a tool to extract fishing footprints and estimate fishing pressure: Application to small scale coastal fisheries and implications for management in the context of the Maritime Spatial Planning Directive. Mediterranean Marine Science, 16(2), 294–304. https://doi.org/10.12681/mms.1087

Koutsidi, M., Moukas, C., & Tzanatos, E. (2020). Trait-based life strategies, ecological niches, and niche overlap in the nekton of the data-poor Mediterranean Sea. Ecology and Evolution, 10(14), 7129–7144. https://doi.org/10.1002/ece3.6414

Kuismanen, L. M. J., Virtanen, E. A., Lappalainen, J., Kurvinen, L., Blankett, P., & Viitasalo, M. (2023). Identifying ecologically valuable marine areas to support conservation and spatial planning at scales relevant for decision making. Marine Policy, 158, 105890. https://doi.org/10.1016/j.marpol.2023.105890

Lahellec, G., Vermard, Y., & Pape, O. L. (2025). Mapping essential juvenile habitats of exploited marine fish: Complementary insights from a scientific survey-based model, fishers' knowledge and fisheries-dependent data. Fisheries Research, 281, 107217. https://doi.org/10.1016/j.fishres.2024.107217

Last, P. R., White, W. T., Gledhill, D. C., Hobday, A. J., Brown, R., Edgar, G. J., & Pecl, G. (2011). Long-term shifts in abundance and distribution of a temperate fish fauna: A response to climate change and fishing practices. Global Ecology and Biogeography, 20(1), 58–72. https://doi.org/10.1111/j.1466-8238.2010.00575.x

Lauria, V., Gristina, M., Attrill, M. J., Fiorentino, F., & Garofalo, G. (2015). Predictive habitat suitability models to aid conservation of elasmobranch diversity in the central Mediterranean Sea. Scientific Reports, 5(1), 13245. https://doi.org/10.1038/srep13245

Le Pape, O., Delavenne, J., & Vaz, S. (2014). Quantitative mapping of fish habitat: A useful tool to design spatialised management measures and marine protected area with fishery objectives. Ocean & Coastal Management, 87, 8–19. https://doi.org/10.1016/j.ocecoaman.2013.10.018

Liquete, C., Piroddi, C., Macías, D., Druon, J.-N., & Zulian, G. (2016). Ecosystem services sustainability in the Mediterranean Sea: Assessment of status and trends using multiple modelling approaches. Scientific Reports, 6(1), 34162. https://doi.org/10.1038/srep34162

Lotze, H. K. (2021). Marine biodiversity conservation. Current Biology, 31(19), R1190–R1195. https://doi.org/10.1016/j.cub.2021.06.084

Lukyanova, O., Pouso, S., García-Barón, I., Borja, A., Bas, M., Cormier, R., Katsanevakis, S., Neuenfeldt, S., Stelzenmüller, V., & Galparsoro, I. (2025). Operationalising Ecologically or Biologically Significant Marine Areas criteria for ecosystem-based conservation and management: The Bay of Biscay case. Biological Conservation, 308, 111156. https://doi.org/10.1016/j.biocon.2025.111156

Mackelworth, P., Fortuna, C. M., Antoninić, M., Holcer, D., Abdul Malak, D., Attia, K., Bricelj, M., Guerquin, F., Marković, M., Nunes, E., Perez-Valverde, C., Ramieri, E., Stojanović, I., Tunesi, L., & McGowan, J. (2024). Ecologically and Biologically Significant Areas (EBSAs) as an enabling mechanism for transboundary marine spatial planning. Marine Policy, 166, 106231. https://doi.org/10.1016/j.marpol.2024.106231

MacNeil, L., McLean, M., Tittensor, D. P., Bayer, T., Reusch, T. B. H., & Scotti, M. (2025). Environmental Filtering Drives Widespread Trait Convergence in Marine Demersal Ray-Finned Fishes. Global Ecology and Biogeography, 34(11), e70150. https://doi.org/10.1111/geb.70150

Mahaut, L., Loiseau, N., Villéger, S., Auber, A., Hautecoeur, C., Maire, A., Mellin, C., Mouquet, N., Stuart-Smith, R., Violle, C., & Mouillot, D. (2025). Functional diversity shapes the stability of reef fish biomass under global change. Proceedings of the Royal Society B: Biological Sciences, 292(2046), 20250252. https://doi.org/10.1098/rspb.2025.0252

Maioli, F., Weigel, B., Chiarabelli, E., Manfredi, C., Anibaldi, A., Isailović, I., Vrgoč, N., & Casini, M. (2023). Influence of ecological traits on spatio-temporal dynamics of an elasmobranch community in a heavily exploited basin. Scientific Reports, 13(1), 9596. https://doi.org/10.1038/s41598-023-36038-y

Maire, E., Robinson, J. P. W., McLean, M., Arif, S., Zamborain-Mason, J., Cinner, J. E., Ferse, S. C. A., Graham, N. A. J., Hoey, A. S., MacNeil, M. A., Mouillot, D., & Hicks, C. C. (2024). Managing nutrition-biodiversity trade-offs on coral reefs. Current Biology, 34(20), 4612-4622.e5. https://doi.org/10.1016/j.cub.2024.08.031

Marbà, N., Jorda, G., Agusti, S., Girard, C., & Duarte, C. M. (2015). Footprints of climate change on Mediterranean Sea biota. Frontiers in Marine Science, 2. https://doi.org/10.3389/fmars.2015.00056

Marchese, C. (2015). Biodiversity hotspots: A shortcut for a more complicated concept. Global Ecology and Conservation, 3, 297–309. https://doi.org/10.1016/j.gecco.2014.12.008

Marshall, D. J., & Morgan, S. G. (2011). Ecological and Evolutionary Consequences of Linked Life-History Stages in the Sea. Current Biology, 21(18), R718–R725. https://doi.org/10.1016/j.cub.2011.08.022

Mazor, T., Giakoumi, S., Kark, S., & Possingham, H. P. (2014). Large-scale conservation planning in a multinational marine environment: Cost matters. Ecological Applications, 24(5), 1115–1130. https://doi.org/10.1890/13-1249.1

MedECC. (2020). Summary for Policymakers. In: Climate and Environmental Change in the Mediterranean Basin – Current Situation and Risks for the Future. First Mediterranean Assessment Report [Cramer W, Guiot J, Marini K (eds.)] Union for the Mediterranean, Plan Bleu, UNEP/MAP, Marseille, France, pp 11-40, doi:10.5281/zenodo.5513887. https://zenodo.org/doi/10.5281/zenodo.5513887

MediSeH. (2013). Edited by Giannoulaki M., A. Belluscio, F. Colloca, S. Fraschetti, M. Scardi, C. Smith, P. Panayotidis, V. Valavanis M.T. Spedicato. DG MARE Specific Contract SI2.600741, Final Report, 557 p.

MEDITS. (2017). MEDITS-Handbook. Version n. 9, 2017, MEDITS Working Group: 106 pp. Http://www.sibm.it/MEDITS%202011/principaledownload.htm.

Mérigot, B., Gaertner, J. C., Brind'Amour, A., Carbonara, P., Esteban, A., Garcia-Ruiz, C., Gristina, M., Imzilen, T., Jadaud, A., Joksimovic, A., Kavadas, S., Kolitari, J., Maina, I., Maiorano, P., Manfredi, C., Micallef, R., Peristeraki, P., Relini, G., Sbrana, M., … Vrgoc, N. (2019). Stability of the relationships among demersal fish assemblages and environmental-trawling drivers at large spatio-temporal scales in the northern Mediterranean Sea. Scientia Marina, 83(S1), 153–163. https://doi.org/10.3989/scimar.04954.30A

Micheli, F., Halpern, B. S., Walbridge, S., Ciriaco, S., Ferretti, F., Fraschetti, S., Lewison, R., Nykjaer, L., & Rosenberg, A. A. (2013). Cumulative Human Impacts on Mediterranean and Black Sea Marine Ecosystems: Assessing Current Pressures and Opportunities. PLOS ONE, 8(12), e79889. https://doi.org/10.1371/journal.pone.0079889

Micheli, F., Levin, N., Giakoumi, S., Katsanevakis, S., Abdulla, A., Coll, M., Fraschetti, S., Kark, S., Koutsoubas, D., Mackelworth, P., Maiorano, L., & Possingham, H. P. (2013). Setting Priorities for Regional Conservation Planning in the Mediterranean Sea. PLOS ONE, 8(4), e59038. https://doi.org/10.1371/journal.pone.0059038

Milisenda, G., Garofalo, G., Fiorentino, F., Colloca, F., Maynou, F., Ligas, A., Musumeci, C., Bentes, L., Gonçalves, J. M. S., Erzini, K., Russo, T., D'Andrea, L., & Vitale, S. (2021). Identifying Persistent Hot Spot Areas of Undersized Fish and Crustaceans in Southern European Waters: Implication for Fishery Management Under the Discard Ban Regulation. Frontiers in Marine Science, 8. https://doi.org/10.3389/fmars.2021.610241

Montanyès, M., Weigel, B., & Lindegren, M. (2023). Community assembly processes and drivers shaping marine fish community structure in the North Sea. Ecography, 2023(10), e06642. https://doi.org/10.1111/ecog.06642

Moore, C., Drazen, J. C., Radford, B. T., Kelley, C., & Newman, S. J. (2016). Improving essential fish habitat designation to support sustainable ecosystem-based fisheries management. Marine Policy, 69, 32–41. https://doi.org/10.1016/j.marpol.2016.03.021

Mouillot, D., Albouy, C., Guilhaumon, F., Ben Rais Lasram, F., Coll, M., Devictor, V., Meynard, C. N., Pauly, D., Tomasini, J. A., Troussellier, M., Velez, L., Watson, R., Douzery, E. J. P., & Mouquet, N. (2011). Protected and Threatened Components of Fish Biodiversity in the Mediterranean Sea. Current Biology, 21(12), 1044–1050. https://doi.org/10.1016/j.cub.2011.05.005

Moullec, F., Barrier, N., Drira, S., Guilhaumon, F., Marsaleix, P., Somot, S., Ulses, C., Velez, L., & Shin, Y.-J. (2019). An End-to-End Model Reveals Losers and Winners in a Warming Mediterranean Sea. Frontiers in Marine Science, 6. https://www.frontiersin.org/articles/10.3389/fmars.2019.00345

Moullec, F., Barrier, N., Guilhaumon, F., Peck, M. A., Ulses, C., & Shin, Y.-J. (2023). Rebuilding Mediterranean marine resources under climate change. Marine Ecology Progress Series, 708, 1–20. https://doi.org/10.3354/meps14269

Myers, N. (1988). Threatened biotas: “Hot spots” in tropical forests. Environmentalist, 8(3), 187–208. https://doi.org/10.1007/BF02240252

Mytilineou, Ch., Tsagarakis, K., Bekas, P., Anastasopoulou, A., Kavadas, S., Machias, A., Haralabous, J., Smith, C. J., Petrakis, G., Dokos, J., & Kapandagakis, A. (2013). Spatial distribution and life-history aspects of blackspot seabream Pagellus bogaraveo (Osteichthyes: Sparidae). Journal of Fish Biology, 83(6), 1551–1575. https://doi.org/10.1111/jfb.12271

Nagelkerken, I., Sheaves, M., Baker, R., & Connolly, R. M. (2015). The seascape nursery: A novel spatial approach to identify and manage nurseries for coastal marine fauna. Fish and Fisheries, 16(2), 362–371. https://doi.org/10.1111/faf.12057

Navarro, J., Coll, M., Cardador, L., Fernández, Á. M., & Bellido, J. M. (2015). The relative roles of the environment, human activities and spatial factors in the spatial distribution of marine biodiversity in the Western Mediterranean Sea. Progress in Oceanography, 131, 126–137. https://doi.org/10.1016/j.pocean.2014.12.004

Neugarten, R. A., Chaplin-Kramer, R., Sharp, R. P., Schuster, R., Strimas-Mackey, M., Roehrdanz, P. R., Mulligan, M., van Soesbergen, A., Hole, D., Kennedy, C. M., Oakleaf, J. R., Johnson, J. A., Kiesecker, J., Polasky, S., Hanson, J. O., & Rodewald, A. D. (2024). Mapping the planet’s critical areas for biodiversity and nature’s contributions to people. Nature Communications, 15(1), 261. https://doi.org/10.1038/s41467-023-43832-9

Newbold, T., Hudson, L. N., Hill, S. L. L., Contu, S., Lysenko, I., Senior, R. A., Börger, L., Bennett, D. J., Choimes, A., Collen, B., Day, J., De Palma, A., Díaz, S., Echeverria-Londoño, S., Edgar, M. J., Feldman, A., Garon, M., Harrison, M. L. K., Alhusseini, T., … Purvis, A. (2015). Global effects of land use on local terrestrial biodiversity. Nature, 520(7545), 45–50. https://doi.org/10.1038/nature14324

NOAA. (2025). Ecosystem-Based Fisheries Management | NOAA Fisheries. https://www.fisheries.noaa.gov/national/ecosystems/ecosystem-based-fisheries-management

Olden, J. D., LeRoy Poff, N., Douglas, M. R., Douglas, M. E., & Fausch, K. D. (2004). Ecological and evolutionary consequences of biotic homogenization. Trends in Ecology & Evolution, 19(1), 18–24. https://doi.org/10.1016/j.tree.2003.09.010

Olds, A. D., Connolly, R. M., Pitt, K. A., Pittman, S. J., Maxwell, P. S., Huijbers, C. M., Moore, B. R., Albert, S., Rissik, D., Babcock, R. C., & Schlacher, T. A. (2016). Quantifying the conservation value of seascape connectivity: A global synthesis. Global Ecology and Biogeography, 25(1), 3–15. https://doi.org/10.1111/geb.12388

Ord, J. K., & Getis, A. (1995). Local Spatial Autocorrelation Statistics: Distributional Issues and an Application. Geographical Analysis, 27(4), 286–306. https://doi.org/10.1111/j.1538-4632.1995.tb00912.x

Ordines, F., Jordà, G., Quetglas, A., Flexas, M., Moranta, J., & Massutí, E. (2011). Connections between hydrodynamics, benthic landscape and associated fauna in the Balearic Islands, western Mediterranean. Continental Shelf Research, 31(17), 1835–1844. https://doi.org/10.1016/j.csr.2011.08.007

Ortega, M., Castro-Cadenas, M. D., Steenbeek, J., & Coll, M. (2023). Identifying and prioritizing demersal fisheries restricted areas based on combined ecological and fisheries criteria: The western Mediterranean. Marine Policy, 157, 105850. https://doi.org/10.1016/j.marpol.2023.105850

Ospina-Alvarez, A., Parada, C., & Palomera, I. (2012). Vertical migration effects on the dispersion and recruitment of European anchovy larvae: From spawning to nursery areas. Ecological Modelling, 231, 65–79. https://doi.org/10.1016/j.ecolmodel.2012.02.001

Ovaskainen, O., & Abrego, N. (2020). Joint Species Distribution Modelling: With Applications in R. Cambridge University Press. https://doi.org/10.1017/9781108591720

Ovaskainen, O., Tikhonov, G., Norberg, A., Guillaume Blanchet, F., Duan, L., Dunson, D., Roslin, T., & Abrego, N. (2017). How to make more out of community data? A conceptual framework and its implementation as models and software. Ecology Letters, 20(5), 561–576. https://doi.org/10.1111/ele.12757

Panzeri, D., Gil Herrera, J., García-Ruíz, C., Rueda, L., Benziane, M., Malouli, M. I., Hernández, P., & Libralato, S. (2025). Integration of fisheries and ecological data to support spatial management: The case of blackspot seabream (Pagellus bogaraveo) in the western Mediterranean Sea. Fisheries Research, 291, 107549. https://doi.org/10.1016/j.fishres.2025.107549

Paradis, E., & Schliep, K. (2019). ape 5.0: An environment for modern phylogenetics and evolutionary analyses in R. Bioinformatics, 35(3), 526–528. https://doi.org/10.1093/bioinformatics/bty633

Parry, J., & Locke, D. H. (2024). Sfdep: Spatial Dependence for Simple Features. R package version 0.2.4, https://github.com/josiahparry/sfdep. https://sfdep.josiahparry.com

Pearce, J., & Ferrier, S. (2000). Evaluating the predictive performance of habitat models developed using logistic regression. Ecological Modelling, 133(3), 225–245. https://doi.org/10.1016/S0304-3800(00)00322-7

Pennino, M. G., Coll, M., Albo-Puigserver, M., Fernández-Corredor, E., Steenbeek, J., Giráldez, A., González, M., Esteban, A., & Bellido, J. M. (2020). Current and Future Influence of Environmental Factors on Small Pelagic Fish Distributions in the Northwestern Mediterranean Sea. Frontiers in Marine Science, 7. https://doi.org/10.3389/fmars.2020.00622

Peterson, M. S., & Lowe, M. R. (2009). Implications of Cumulative Impacts to Estuarine and Marine Habitat Quality for Fish and Invertebrate Resources. Reviews in Fisheries Science, 17(4), 505–523. https://doi.org/10.1080/10641260903171803

Pike, E. P., MacCarthy, J. M. C., Hameed, S. O., Harasta, N., Grorud-Colvert, K., Sullivan-Stack, J., Claudet, J., Horta e Costa, B., Gonçalves, E. J., Villagomez, A., & Morgan, L. (2024). Ocean protection quality is lagging behind quantity: Applying a scientific framework to assess real marine protected area progress against the 30 by 30 target. Conservation Letters, 17(3), e13020. https://doi.org/10.1111/conl.13020

Pinsky, M. L., Jensen, O. P., Ricard, D., & Palumbi, S. R. (2011). Unexpected patterns of fisheries collapse in the world's oceans. Proceedings of the National Academy of Sciences, 108(20), 8317–8322. https://doi.org/10.1073/pnas.1015313108

Piroddi, C., Coll, M., Liquete, C., Macias, D., Greer, K., Buszowski, J., Steenbeek, J., Danovaro, R., & Christensen, V. (2017). Historical changes of the Mediterranean Sea ecosystem: Modelling the role

and impact of primary productivity and fisheries changes over time. Scientific Reports, 7(1), 44491. https://doi.org/10.1038/srep44491

Piroddi, C., Coll, M., Macias, D., Steenbeek, J., Garcia-Gorriz, E., Mannini, A., Vilas, D., & Christensen, V. (2022). Modelling the Mediterranean Sea ecosystem at high spatial resolution to inform the ecosystem-based management in the region. Scientific Reports, 12(1), 19680. https://doi.org/10.1038/s41598-022-18017-x

Piroddi, C., Coll, M., Steenbeek, J., Moy, D. M., & Christensen, V. (2015). Modelling the Mediterranean marine ecosystem as a whole: Addressing the challenge of complexity. Marine Ecology Progress Series, 533, 47–65. https://doi.org/10.3354/meps11387

Piroddi, C., Colloca, F., & Tsikliras, A. C. (2020). The living marine resources in the Mediterranean Sea Large Marine Ecosystem. Environmental Development, 36, 100555. https://doi.org/10.1016/j.envdev.2020.100555

Planque, B., Loots, C., Petitgas, P., LINDSTRøM, U., & Vaz, S. (2011). Understanding what controls the spatial distribution of fish populations using a multi-model approach. Fisheries Oceanography, 20(1), 1–17. https://doi.org/10.1111/j.1365-2419.2010.00546.x

Pohlert, T. (2023). Trend: Non-Parametric Trend Tests and Change-Point Detection. R package version 1.1.6. [Computer software]. https://CRAN.R-project.org/package=trend

Pörtner, H.-O., Scholes, R. J., Agard, J., Archer, E., Bai, X., Barnes, D., Burrows, M., Chan, L., Cheung, W. L. (William), Diamond, S., Donatti, C., Duarte, C., Eisenhauer, N., Foden, W., Gasalla, M. A., Handa, C., Hickler, T., Hoegh-Guldberg, O., Ichii, K., … Ngo, H. (2021). IPBES-IPCC co-sponsored workshop report on biodiversity and climate change (Version 2). Zenodo. https://doi.org/10.5281/ZENODO.4782538

Posit team. (2025). RStudio: Integrated Development Environment for R. Posit Software, PBC, Boston, MA. URL http://www.posit.co/. [Computer software].

Purvis, A., Agapow, P.-M., Gittleman, J. L., & Mace, G. M. (2000). Nonrandom Extinction and the Loss of Evolutionary History. Science, 288(5464), 328–330. https://doi.org/10.1126/science.288.5464.328

Quinzán, M., Castro, J., Massutí, E., Rueda, L., & Hidalgo, M. (2020). Disentangling the influence of fishing, demography, and environment on population dynamics of Iberian Peninsula waters fish stocks. ICES Journal of Marine Science, 77(1), 1–11. https://doi.org/10.1093/icesjms/fsz190

R Core Team. (2022). R: A language and environment for statistical computing. R Foundation for Statistical Computing, Vienna, Austria. URL https://www.R-project.org/. [Computer software].

Rahman, A. U., Tikhonov, G., Oksanen, J., Rossi, T., & Ovaskainen, O. (2024). Accelerating joint species distribution modelling with Hmsc-HPC by GPU porting. PLOS Computational Biology, 20(9), e1011914. https://doi.org/10.1371/journal.pcbi.1011914

Reale, M., Cossarini, G., Lazzari, P., Lovato, T., Bolzon, G., Masina, S., Solidoro, C., & Salon, S. (2022). Acidification, deoxygenation, and nutrient and biomass declines in a warming Mediterranean Sea. Biogeosciences, 19(17), 4035–4065. https://doi.org/10.5194/bg-19-4035-2022

Reid, A. J., Carlson, A. K., Creed, I. F., Eliason, E. J., Gell, P. A., Johnson, P. T. J., Kidd, K. A., MacCormack, T. J., Olden, J. D., Ormerod, S. J., Smol, J. P., Taylor, W. W., Tockner, K., Vermaire, J. C., Dudgeon, D., & Cooke, S. J. (2019). Emerging threats and persistent conservation challenges for freshwater biodiversity. Biological Reviews, 94(3), 849–873. https://doi.org/10.1111/brv.12480

Reid, W. V. (1998). Biodiversity hotspots. Trends in Ecology & Evolution, 13(7), 275–280. https://doi.org/10.1016/S0169-5347(98)01363-9

Rozanski, R., Velez, L., Hocdé, R., Duhamet, A., Waldock, C., Mouillot, D., Pellissier, L., & Albouy, C. (2024). Seasonal dynamics of Mediterranean fish communities revealed by eDNA: Contrasting compositions across depths and Marine Fully Protected Area boundaries. Ecological Indicators, 166, 112290. https://doi.org/10.1016/j.ecolind.2024.112290

Sala, E., Mayorga, J., Bradley, D., Cabral, R. B., Atwood, T. B., Auber, A., Cheung, W., Costello, C., Ferretti, F., Friedlander, A. M., Gaines, S. D., Garilao, C., Goodell, W., Halpern, B. S., Hinson, A., Kaschner, K., Kesner-Reyes, K., Leprieur, F., McGowan, J., … Lubchenco, J. (2021). Protecting the global ocean for biodiversity, food and climate. Nature, 592(7854), 397–402. https://doi.org/10.1038/s41586-021-03371-z

Sánchez-Hernández, J. (2025). Climate-induced shifts in ontogenetic niches threaten ecosystem coupling. Trends in Ecology & Evolution, 40(3), 224–227. https://doi.org/10.1016/j.tree.2024.11.018

Sanz-Martín, M., Hidalgo, M., Puerta, P., Molinos, J. G., Zamanillo, M., Brito-Morales, I., González-Irusta, J. M., Esteban, A., Punzón, A., García-Rodríguez, E., Vivas, M., & López-López, L. (2024). Climate velocity drives unexpected southward patterns of species shifts in the Western Mediterranean Sea. Ecological Indicators, 160, 111741. https://doi.org/10.1016/j.ecolind.2024.111741

Sbrana, M., Ranieri, S. D., Ligas, A., Reale, B., Rossetti, I., & Sartor, P. (2010). Comparison of trawl survey and commercial data on small pelagic from the FAO geographical sub-area 9 (Western Mediterranean). Available online at: Http://www.ciesm.org/online/archives/abstracts/pdf/39/PG_0658.pdf.

Schickele, A., Goberville, E., Leroy, B., Beaugrand, G., Hattab, T., Francour, P., & Raybaud, V. (2021). European small pelagic fish distribution under global change scenarios. Fish and Fisheries, 22(1), 212–225. https://doi.org/10.1111/faf.12515

Seebens, H., Blackburn, T. M., Dyer, E. E., Genovesi, P., Hulme, P. E., Jeschke, J. M., Pagad, S., Pyšek, P., van Kleunen, M., Winter, M., Ansong, M., Arianoutsou, M., Bacher, S., Blasius, B., Brockerhoff, E. G., Brundu, G., Capinha, C., Causton, C. E., Celesti-Grapow, L., … Essl, F. (2018). Global rise in emerging alien species results from increased accessibility of new source pools. Proceedings of the National Academy of Sciences, 115(10), E2264–E2273. https://doi.org/10.1073/pnas.1719429115

Sion, L., Calculli, C., Capezzuto, F., Carlucci, R., Carluccio, A., Cornacchia, L., Maiorano, P., Pollice, A., Ricci, P., Tursi, A., & D'Onghia, G. (2019). Does the Bari Canyon (Central Mediterranean) influence the fish distribution and abundance? Progress in Oceanography, 170, 81–92. https://doi.org/10.1016/j.pocean.2018.10.015

Spedicato, M. T., Massutí, E., Mérigot, B., Tserpes, G., Jadaud, A., & Relini, G. (2019). The MEDITS trawl survey specifications in an ecosystem approach to fishery management. Scientia Marina, 83(S1), Article S1. https://doi.org/10.3989/scimar.04915.11X

Stamp, T., West, E., Stewart, J. E., Plenty, S., Robbins, T., & Sheehan, E. (2025). Effective protection of essential fish habitat requires understanding fish spatial ecology—Lessons learnt from protected European bass nursery areas. ICES Journal of Marine Science, 82(4), fsaf035. https://doi.org/10.1093/icesjms/fsaf035

Stephenson, F., Bowden, D. A., Rowden, A. A., Anderson, O. F., Clark, M. R., Bennion, M., Finucci, B., Pinkerton, M. H., Goode, S., Chin, C., Davey, N., Hart, A., & Stewart, R. (2024). Using joint species distribution modelling to predict distributions of seafloor taxa and identify vulnerable marine ecosystems in New Zealand waters. Biodiversity and Conservation, 33(11), 3103–3127. https://doi.org/10.1007/s10531-024-02904-y

Stuart-Smith, R. D., Bates, A. E., Lefcheck, J. S., Duffy, J. E., Baker, S. C., Thomson, R. J., Stuart-Smith, J. F., Hill, N. A., Kininmonth, S. J., Airoldi, L., Becerro, M. A., Campbell, S. J., Dawson, T. P., Navarrete, S. A., Soler, G. A., Strain, E. M. A., Willis, T. J., & Edgar, G. J. (2013). Integrating abundance and functional traits reveals new global hotspots of fish diversity. Nature, 501(7468), 539–542. https://doi.org/10.1038/nature12529

Sunday, J. M., Pecl, G. T., Frusher, S., Hobday, A. J., Hill, N., Holbrook, N. J., Edgar, G. J., Stuart-Smith, R., Barrett, N., Wernberg, T., Watson, R. A., Smale, D. A., Fulton, E. A., Slawinski, D., Feng, M., Radford, B. T., Thompson, P. A., & Bates, A. E. (2015). Species traits and climate velocity explain geographic

range shifts in an ocean-warming hotspot. Ecology Letters, 18(9), 944–953. https://doi.org/10.1111/ele.12474

Sundblad, G., Bergström, U., Sandström, A., & Eklöv, P. (2014). Nursery habitat availability limits adult stock sizes of predatory coastal fish. ICES Journal of Marine Science, 71(3), 672–680. https://doi.org/10.1093/icesjms/fst056

Sussman, A. L., Gardner, B., Adams, E. M., Salas, L., Kenow, K. P., Luukkonen, D. R., Monfils, M. J., Mueller, W. P., Williams, K. A., Leduc-Lapierre, M., & Zipkin, E. F. (2019). A comparative analysis of common methods to identify waterbird hotspots. Methods in Ecology and Evolution, 10(9), 1454–1468. https://doi.org/10.1111/2041-210X.13209

Tao, H.-H., Dur, G., Ke, P.-J., Souissi, S., & Hsieh, C. (2021). Age-specific habitat preference, carrying capacity, and landscape structure determine the response of population spatial variability to fishing-driven age truncation. Ecology and Evolution, 11(11), 6358–6370. https://doi.org/10.1002/ece3.7486

Thorson, J. T., Maureaud, A. A., Frelat, R., Mérigot, B., Bigman, J. S., Friedman, S. T., Palomares, M. L. D., Pinsky, M. L., Price, S. A., & Wainwright, P. (2023). Identifying direct and indirect associations among traits by merging phylogenetic comparative methods and structural equation models. Methods in Ecology and Evolution, 14(5), 1259–1275. https://doi.org/10.1111/2041-210X.14076

Thorson, J. T., & van der Bijl, W. (2023). phylosem: A fast and simple R package for phylogenetic inference and trait imputation using phylogenetic structural equation models. Journal of Evolutionary Biology, 36(10), 1357–1364. https://doi.org/10.1111/jeb.14234

Tikhonov, G., Duan, L., Abrego, N., Newell, G., White, M., Dunson, D., & Ovaskainen, O. (2020). Computationally efficient joint species distribution modeling of big spatial data. Ecology, 101(2), e02929. https://doi.org/10.1002/ecy.2929

Tikhonov, G., Opedal, Ø. H., Abrego, N., Lehikoinen, A., de Jonge, M. M. J., Oksanen, J., & Ovaskainen, O. (2020). Joint species distribution modelling with the r-package Hmsc. Methods in Ecology and Evolution, 11(3), 442–447. https://doi.org/10.1111/2041-210X.13345

Tjur, T. (2009). Coefficients of Determination in Logistic Regression Models—A New Proposal: The Coefficient of Discrimination. The American Statistician, 63(4), 366–372. https://doi.org/10.1198/tast.2009.08210

Tugores, M. P., Ordines, F., Guijarro, B., García-Ruíz, C., Esteban, A., & Massutí, E. (2019). Essential fish habitats and hotspots of nekto-benthic diversity and density in the western Mediterranean. Aquatic Conservation: Marine and Freshwater Ecosystems, 29(3), 461–471. https://doi.org/10.1002/aqc.3031

UNEP. (2024). Mediterranean Quality Status Report: The State of the Mediterranean Sea and Coast from 2018-2023. United Nations Environment Programme. https://wedocs.unep.org/xmlui/handle/20.500.11822/46733

Vasilakopoulos, P., Maravelias, C. D., & Tserpes, G. (2014). The Alarming Decline of Mediterranean Fish Stocks. Current Biology, 24(14), 1643–1648. https://doi.org/10.1016/j.cub.2014.05.070

Vasileiadou, K., Chatzinikolaou, E., Klayn, S., Pavloudi, C., & Reizopoulou, S. (2024). Editorial: Marine biodiversity hotspots – challenges and resilience. Frontiers in Marine Science, 11. https://doi.org/10.3389/fmars.2024.1338242

Warton, D. I., Blanchet, F. G., O'Hara, R. B., Ovaskainen, O., Taskinen, S., Walker, S. C., & Hui, F. K. C. (2015). So Many Variables: Joint Modeling in Community Ecology. Trends in Ecology & Evolution, 30(12), 766–779. https://doi.org/10.1016/j.tree.2015.09.007

Watson, J. E. M., Venter, O., Lee, J., Jones, K. R., Robinson, J. G., Possingham, H. P., & Allan, J. R. (2018). Protect the last of the wild. Nature, 563(7729), 27–30. https://doi.org/10.1038/d41586-018-07183-6

Weigel, B., Graco-Roza, C., Hultman, J., Pajunen, V., Teittinen, A., Kuzmina, M., Zakharov, E. V., Soininen, J., & Ovaskainen, O. (2023). Local eukaryotic and bacterial stream community assembly is shaped by regional land use effects. ISME Communications, 3(1), 65. https://doi.org/10.1038/s43705-023-00272-2

Weigel, B., Mäkinen, J., Kallasvuo, M., & Vanhatalo, J. (2021). Exposing changing phenology of fish larvae by modeling climate effects on temporal early life-stage shifts. Marine Ecology Progress Series, 666, 135–148. https://doi.org/10.3354/meps13676

White, J. W. (2015). Marine reserve design theory for species with ontogenetic migration. Biology Letters, 11(1), 20140511. https://doi.org/10.1098/rsbl.2014.0511

5 Biodiversity status and drivers of fish juvenile life-stages in the Central-Eastern Mediterranean Sea

Authors: Stratos Batziakas, Fabien Moullec, Walter Zupa, Patricia Puerta, George Tserpes, Nota Peristeraki, Stephanos Kavadas, Irida Maina, Martin Lindegren, Manuel Hidalgo

5.1. Introduction

The Mediterranean Sea is a highly complex marine environment that hosts a plethora of species, with a high level of endemism (D'Ortenzio & D'Alcalà 2009, Bianchi et al. 2012, Coll et al. 2015). Several nursery habitats have been reported in the basin, notably *Posidonia oceanica* (Lattanzi et al., 2024) and other seagrass meadows (Cuadros et al., 2017), algal forests (Cheminée et al., 2013) and biogenic reefs (Boudouresque et al., 2016). These, mostly shallow, coastal habitats form a mosaic of habitats important for early fish life-stages (Cheminée et al., 2021).

Juvenile fish community distribution and diversity information in the Mediterranean, and especially on the eastern part of the basin, is sparse. Few studies refer on the matter, and only for specific habitat types (Lattanzi et al., 2024), for a small area (Ntouni et al., 2023) or for a single species (Druon et al., 2015). Similarly, areas with large aggregations of multiple juvenile fish species (hot spots) have not yet been identified.

In the present study we aimed to identify the environmental and anthropogenic drivers that shape the juvenile fish community of the Central-Eastern (CE) Mediterranean. We used joint species distribution modelling in order to be able to predict the species distributions across the spatial and environmental gradient, and subsequently assess the status and trends of juvenile fish alpha biodiversity. By combining the model results with a spatial statistical analysis framework, we aimed to map the essential for early fish life-stages habitats.

5.2. Material and Methods

In order to assess the biodiversity status (spatial and temporal patterns) and drivers (environmental and anthropogenic variables) of juvenile fish in the CE Mediterranean, we utilised a joint species distribution modelling approach, and specifically the *Hierarchical Modelling for Species Communities* (HMSC) framework. HMSC is "a multivariate hierarchical generalised linear mixed model fitted with Bayesian inference" that can combine species' occurrence or abundance data (response matrix) with environmental data (explanatory variables), species' traits data and phylogenetic/taxonomic information to infer community assembly processes (Ovaskainen & Abrego, 2020).

To start building our models we used fish occurrence, abundance and length frequency data (abundance per length class) from the Mediterranean International Trawl Surveys (MEDITS) (Anonymous, 2017), along with the hauls' coordinate, depth, distance and gear information, from 1999 to 2021. Before the analyses, potential errors in the MEDITS data were identified and corrected (where needed) with the help of the 'RoME' R package (Bitetto & Zupa, 2025). To allot the fish data to the different life-stages, we used the abundance per length class data included in the TC files and the length at first maturity (L_{mat}) of each species from the traits database (see below) to split the abundances between juveniles (length class ≤ L_{mat}) and adults

(length class > L_{mat}). Afterwards, the abundance data were standardised to units of surface ($N \cdot km^{-2}$) by dividing with the corresponding haul's swept area (Anonymous, 2017). Species' data were filtered further to include only the life-stages that occurred in at least 1% of the total hauls in the final dataset. In total, 104 species/life-stages were included (60 juvenile and 44 adult life-stages, from 61 unique species) and 12924 unique hauls (sampling points) (Figure 5.1).

To construct the covariate matrix, we used monthly modelled data from the Copernicus CMEMS Mediterranean Sea Physics Reanalysis (Escudier et al. 2021) and the Mediterranean Sea Biochemistry Reanalysis (Teruzzi et al. 2021) products. To minimise computation time and avoid overfitting, we first checked for significant collinearities between the covariates and successively removed those with variance inflation factors > 3 (Zurr, 2014). We then performed a distance-based redundancy analysis on the log(x+1) Bray-Curtis transformed abundance dissimilarity matrix, using the remaining covariates (Legendre & Anderson, 1999). The environmental variables with the largest scores in the first three RDA axes were then selected to perform the first few HMSC test runs. The variables that displayed an insignificant contribution on the overall explained variance were eliminated. Additionally, to model the effect of human pressures on the juvenile fish community, we elected to include fishing pressure as the *a priori* dominant stressor on Mediterranean marine habitats. Three fishing pressure indices were computed annually for the area, for small-scale fisheries, trawlers and purseiners, by using a Multi-Criteria Decision Analysis (MCDA) that takes into account the various interactions between the fishing fleet's characteristics, human activities (e.g. marine traffic, fishing effort, legislation) and environmental factors (e.g. bathymetry, temperature, winds), as described in Kavadas et al. (2015, 2025). These indices were subsequently summed and then rescaled back to *(0, 1)* to produce a single fishing pressure index (FPI). All in all, the covariates that were used to fit the HMSC models were bottom depth, bottom temperature (botT), bottom salinity (botS), log-transformed surface chl*a* concentrations (chl) and fishing pressure index (FPI).

To construct the species traits matrix, we used information from the Mediterranean fish traits database developed and presented in Deliverable 2.2 (Spedicato et al., 2024), and selected five traits (two categorical and three continuous), the trophic guild (categorical), the caudal shape (categorical), the trophic level (continuous), the log-transformed growth coefficient (continuous) (all shared between the two life-stages), and the maximum size (continuous) that was set equal to the length at first maturity for juveniles and the maximum observed length for adults. Finally, using the 'ape' R package, we generated a taxonomic tree from phylum (root) to life-stages (tips), with branches of length 1 between nodes, except for the life-stages tips that were set at a length of 0.1 in order to simulate a pseudo-differentiation between the juveniles and the adults of the same species.

Finally, to construct the spatial random factor, we generated a 1^{o} hexagonal grid covering the entire area and used the id number and the centroids of the grid cells to construct the first random factor (89 levels), and set the maximum number of latent factors to 5 (Figure 5.1). We avoided using a finer resolution grid because most of the explained variance was absorbed by the spatial random factor during test trials. For the temporal random factor, we used the sampling year as factor (23 levels), with a maximum of 2 latent factors.

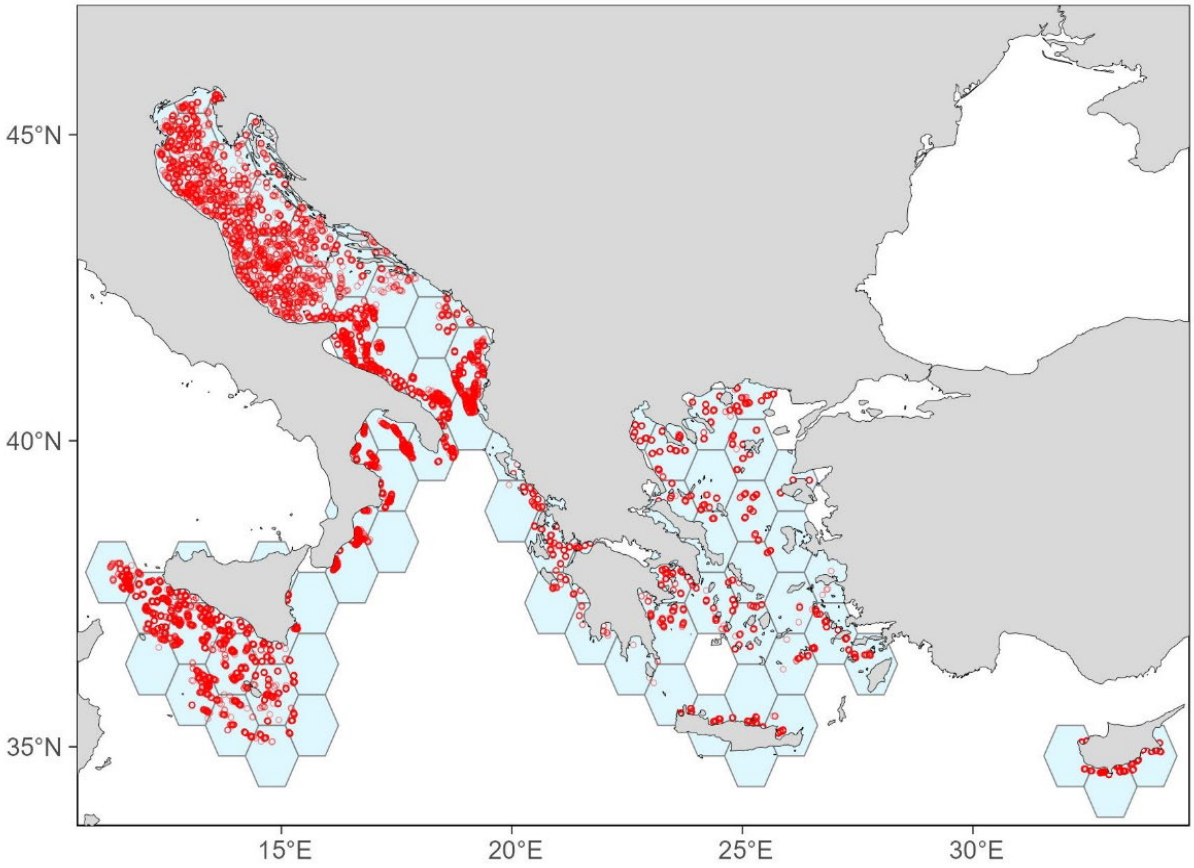

Figure 5.1. Distribution of the 12924 sampling points (MEDITS hauls), from 1999 to 2021, in the Central-Eastern Mediterranean. The 1° hexagonal grid used for the models' spatial random factor is also denoted.

To fit our model, we used a hurdle approach, which requires the fitting of two separate models, a Presence/Absence (PA) and an Abundance Conditional on Presence (ACP) model, that are then combined to produce a single model. The PA model was fitted by applying a probit regression on the species/life-stages presence/absence binary matrix, and the ACP model by applying linear regression on the log-transformed abundance matrix. For the covariates, depth, boT and botS were added as quadratic terms, in order to better model the species'/life-stages' depth, temperature and salinity niches, while log(chl) and FPI were added as linear terms. Each model was sampled four times with Markov Chains Monte Carlo (MCMC) simulations, run for $1.35 \cdot 10^6$ iterations, with the first 1/3 of the iterations being discarded as burn-in. Each of the four chains was thinned by 3000 and sampled 300 times, resulting in a total of 1200 posterior samples per model.

After fitting the models, the MCMC convergence was checked by examining the effective sizes and the potential scale reduction factors (PSRFs) of the beta, gamma and omega model parameters. The overall performance of the models was gauged by calculating the mean Tjur's R^2 and Area Under the Curve (AUC) (for the PA model) and the mean R^2 (for the ACP model). The variance partitioning was calculated to check the variance explained by each covariate, overall and by species/life-stage, for both models. The posterior distributions were then used to predict the effect of the covariates on the overall juvenile species richness and abundance along each covariate's gradient.

Afterwards, we aggregated annually the monthly modelled CMEMS environmental data for the covariates included in the models into a 0.1° hexagonal grid, and calculated their mean

per grid cell between May and August (which corresponds to the period 86.3% of the sampling took place). From these data we constructed a spatial environmental gradient that was then used to predict the probability of occurrence (using the PA model) and the abundance (using the ACP model) of species/life-stages across the entire area and up to 1000 m in depth, for every year. For a subset of species/life-stages that displayed erroneous probabilities outside their expected depth niche, the probability predictions were subsequently refined by manually setting them to zero for depths larger than their maximum recorded depth in the CE Mediterranean dataset. The hurdle model predictions were then calculated by multiplying the probability and the ACP abundance matrices for each year. The hurdle predictions were also subsequently refined to curtail some extreme values (typically no more than five for a small minority of species/life-stages) to manually set them equal to the 99.9 percentile. Finally, abundances < 0.012 km^{-2} (which corresponds to <1 individual per grid cell) were set to zero.

The annual hurdle model predictions were then used to calculate the juveniles' Shannon Diversity, species richness and Pielou's Evenness indices. To check for significant temporal trends, we performed a Mann-Kendall trend test (Mann, 1945) for each grid cell and for each index. The delta of each index per grid cell was calculated and then summarised to get their overall change. The summarised deltas of the grid cells that demonstrated significant temporal trends were then plotted to identify areas that have undergone significant alpha diversity changes from the past to the present.

Finally, in order to identify significant juvenile hot spots in the CE Mediterranean, we performed an Emerging Hot Spot Analysis (EHSA) (Baeza-González & Kamakura, 2025; Esri, 2026). In brief, EHSA is an analysis that uses the Getis-Ord Gi* statistic (Getis & Ord, 1992; Ord & Getis 1995) and the Mann-Kendall trend test to identify significant clusters of high (hot spots) or low (cold spots) values, and then classify them under an easy-to-follow convention. First, the annual hurdle model predictions were normalised to unit variance, by dividing each value with the annual standard deviation of each species, to reduce the scale of difference between species' abundance, but preserve their temporal and spatial variability. The normalised juvenile abundances were then summarised to produce a single juvenile abundance index that is not heavily influenced by the most abundant species. Hence, large values of this index will indicate areas where both juvenile abundance *and* richness is high. We then performed the EHSA using the aforementioned index, Queen's contiguity spatially weighted neighbors, a time lag of 3 years, a significance threshold of 0.01, and run for 100 simulations.

All analyses were performed in R ver. 4.4.x to 4.5.x. The HMSC models were fit using the 'Hmsc' R package (ver. 3.2 to 3.3-7) and the 'Hmsc-HPC' python module (Rahman et al., 2024). Distance-based RDA and alpha diversity indices were calculated using the 'vegan' R package (ver. 2.7-2). The Mann-Kendall trend tests were done with the 'Kendall' R package (ver. 2.2.1). The EHSA was done with the 'sfdep' R package (ver. 0.2.5).

5.3. Results

The MCMC convergence of the beta, gamma and omega parameters of both PA and ACP models were deemed satisfactory, with mean effective sample sizes very close to 1200 (i.e., the number of posterior samples), and PSRF point estimates and upper confidence intervals very close to 1 (Figure S5.1). The performance of PA model was fairly good, with mean Tjur's R^2 = 0.313 and mean AUC = 0.914. The ACP model's performance was, expectedly, worse by comparison, with mean R^2 = 0.250.

The dominant variable affecting the juvenile species distributions was depth, which explained 55.6% and 51.9% of the total variance for the PA and the ACP model, respectively (Figure 5.2). Bottom temperature was the next most influential variable, explaining 4.9% and 5.7% of the total variance (for the PA and the ACP model, respectively), followed by bottom salinity (1.9% and 3.8%), chl*a* concentrations (1.6% and 2%), and fishing pressure (1% and 1.8%). The spatial random factor absorbed 30.8% of the variance from the PA model and 31.3% from the ACP model, hinting there was much spatially-structured residual variance that was not covered by the covariates. The temporal random factor also hinted at the existence of temporally-structured residual variance, albeit weaker than the spatial one (4.3% and 3.6% of the total variance for the PA and the ACP model, respectively).

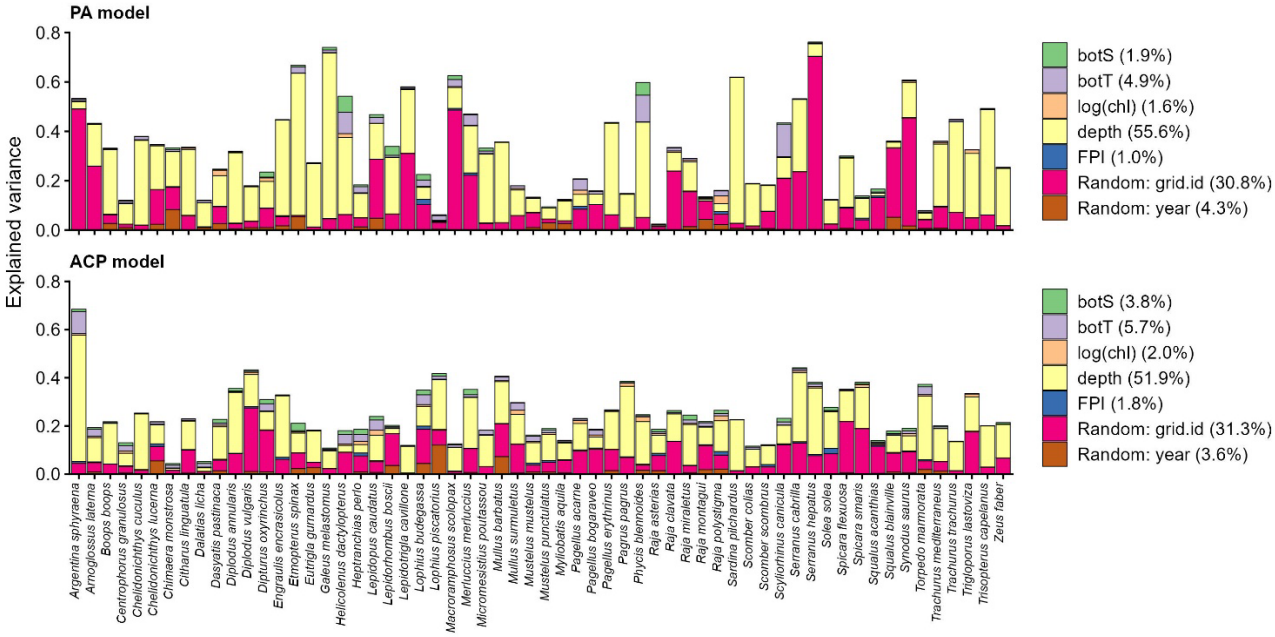

Figure 5.2. Variance explained per species for the 60 juvenile life-stages included in the HMSC models, partitioned between the model covariates and random factors. Top: Presence/Absence (PA) model, Bottom: Abundance Conditional on Presence (ACP) model. botS: bottom salinity, botT: bottom temperature, log(chl): log-transformed surface chl*a* concentrations, FPI: fishing pressure index, grid.id: Spatial random factor, year: temporal random factor.

The overall influence of traits on the species'/life-stages' occurrence was 13.5%, while on abundance 22%. The species responses to the covariates attributable to traits showed different patterns between the models, with depth, botS and FPI being the most important in the case of the PA model, and depth, botT and log(chl) in the case of the ACP model (Figure S5.2). By contrast, the mean taxonomic signal was very strong in both models (87.65% and 78.18%, for the PA and the ACP model, respectively), hinting that the residual variation in species niches was influenced by the species life-stage.

Regarding the influence of covariates on the juvenile richness and abundance, overall, both showed the same trends, albeit non-linear in the case of richness (Figure 5.3). Bottom temperature, chl*a* concentrations and fishing pressure correlated positively with both richness and abundance, while depth and bottom salinity displayed a negative correlation.

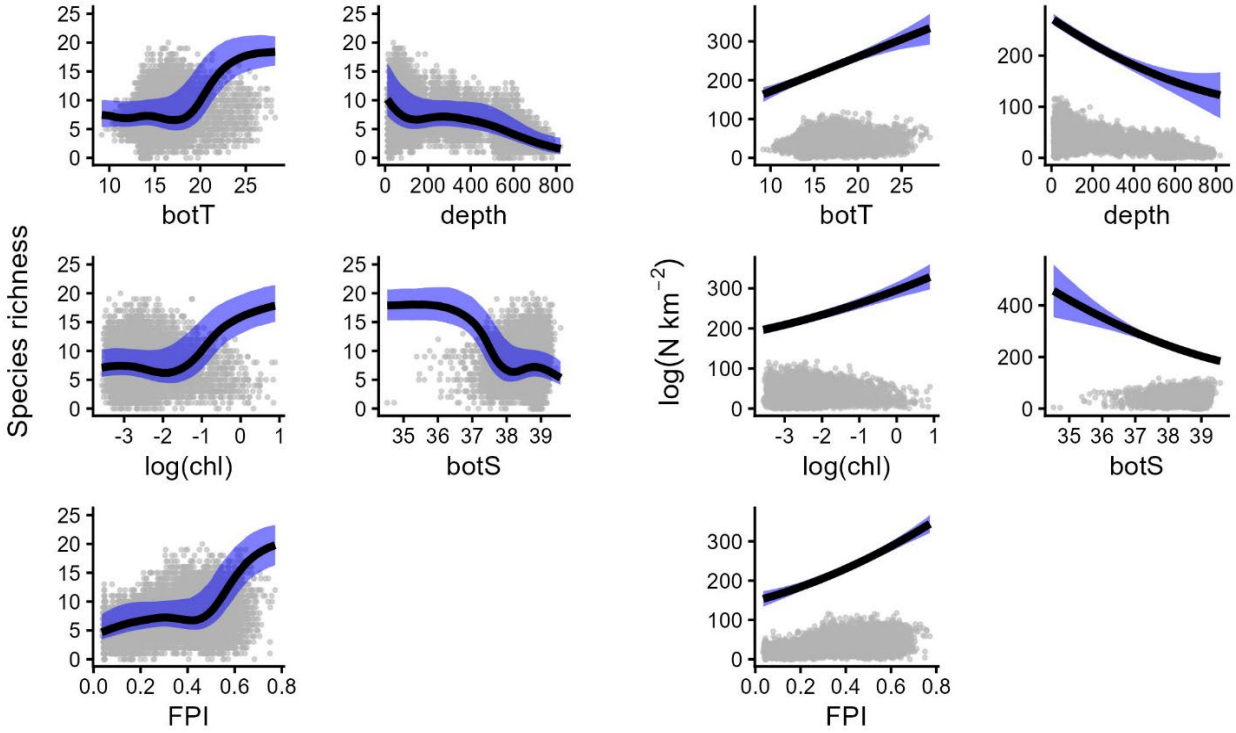

Figure 5.3. Effect of the covariates on juvenile species richness (left) and abundance (right). The black line denotes the mean trend along the covariate's gradient and the blue shade the 95% confidence intervals. The grey points represent the sampling points. N: number of individuals, botT: bottom temperature, log(chl): log-transformed surface chl*a* concentrations, botS: bottom salinity, FPI: fishing pressure index.

The juvenile alpha diversity patterns in the CE Mediterranean revealed high spatial heterogeneity both at the area and at the subarea level (Figure 5.4). In general, deeper waters showed lower Shannon diversity and species richness, and average or high evenness. A weak north-south species richness gradient could also be observed. The areas that displayed the highest Shannon diversity were the C Cyclades and the C Dodecanese in the C Aegean Sea, and the N Ionian Islands in the Ionian Sea. For species richness, the C Aegean Sea, the C Ionian Sea, the N Adriatic and the shelf area along the strait of Sicily showed the highest values. Regarding Pielou's evenness, the Aegean Sea and the Ionian Sea generally displayed high evenness (except for Thermaikos Gulf in the N Aegean), while the opposite was true for the Sicilian shelf waters and for most of the Adriatic. The Sicilian slope waters, though, and the open waters in the N Adriatic Sea, were characterised by relatively high evenness scores.

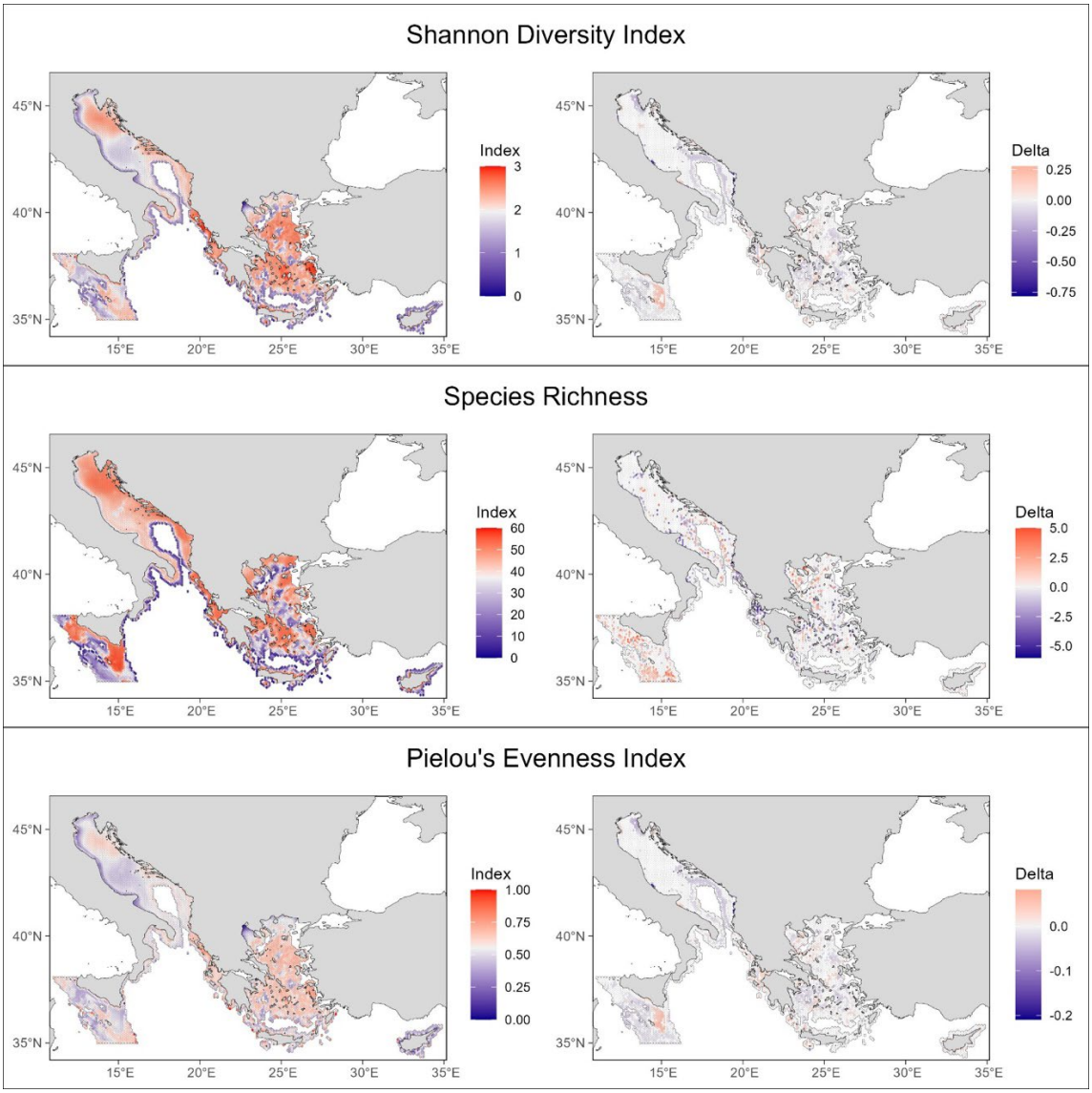

Figure 5.4. Juvenile fish alpha diversity patterns (mean Shannon's Diversity, Species Richness and Pielou's Evenness indices between 1999 – 2021) (left) and significant temporal trends (Delta) (right). Delta represents the overall change of the index from 1999 to 2021. Only deltas in grid cells that displayed significant Mann-Kendall trends are shown. The colour switch for indices is set at their mean, and for deltas at zero. Grid cells represent the predicted space.

Looking more closely at the subarea level, several noteworthy patterns arise. In the N Aegean, Thermaikos Gulf, although it presented average species richness, had very low diversity and evenness scores. In the Adriatic two contrasting patterns were observed, along the east-west and the north-south axes. The western coasts displayed average species richness and low diversity and evenness scores, while the eastern coasts showed high index scores all around. A similar pattern could be observed for the open Adriatic waters, where the N Adriatic showed overall higher index scores, compared to the S Adriatic. The shelf area along the strait of Sicily presented very high species richness, but relatively average diversity and low evenness, while the slope waters around the shelf had relatively low to average species richness, but high diversity and evenness. Cyprus showed high species richness only in the shallower waters around the island, but relatively moderate to low diversity and evenness scores, as opposed to Crete, whose shallower waters presented high values for all three indices.

Regarding the juvenile alpha diversity temporal trends, a significant large-scale trend was the drop of Shannon diversity and Pielou's evenness in the deeper waters of the Aegean, the Adriatic and, to a lesser degree, the strait of Sicily. The sharpest diversity and evenness drops were fairly localised along the coasts of Albania and CE Italy. The final notable drop in diversity and evenness was observed in the N Adriatic, across the W Istria. In regard to species richness, the area most affected by losses was the Ionian Sea. The Aegean and the Adriatic Seas also showed a loss of species sporadically. Nevertheless, some areas displayed notable positive trends in the juvenile alpha diversity. A fairly large area along the shelf waters from the SE Malta to the S of Sicily displayed a significant increase in Shannon diversity and Pielou's evenness. The waters all around the strait of Sicily showed an increase in species richness in general. The deeper waters of the S Adriatic also displayed sporadic gains in species richness. The Aegean Sea presented sporadic gains in all three indices across the area. Finally, positive trends for diversity and evenness were observed in the C Ionian Sea, in the southern and the northern Croatian archipelago, in the NC Adriatic Sea, around the Po river Delta and the mouth of the rivers Adige and Brenta (NW Adriatic), and in the Gulf of Manfredonia (W Adriatic).

According to the EHSA analysis, the most significant juvenile hot spots in the CE Mediterranean were located across the southern coasts of Cyprus and along the Morphou Bay, in the Dodecanese between the islands Samos and Kos (CE Aegean), and east of Limnos island (NE Aegean), along the Evros and Nestos river Deltas, the Gulf of Kavala and Thermaikos Gulf (N Aegean), in the Pagasetic Gulf and around the Attic peninsula (CW Aegean), in the central Cyclades (C Aegean), in the Gulf of Patras (C Ionian), along the strait of Corfu (N Ionian), along the coasts of Albania and in the southern Croatian archipelago (SE Adriatic), around the Marano and the Venetian lagoons, as well as south of the Po river Delta and the along the coasts of Ravenna (N Adriatic), in the Gulf of Manfredonia (CW Adriatic), in the south-eastern coasts of Sicily and in the shelf waters east of Malta (Figure 5.5). Finally, the deeper waters in the Aegean Sea, in the seas around Crete, in the NW Ionian Sea, in the S Adriatic and in the strait of Sicily were persistent juvenile cold spots. Several cold spots were also located in the CW Adriatic waters.

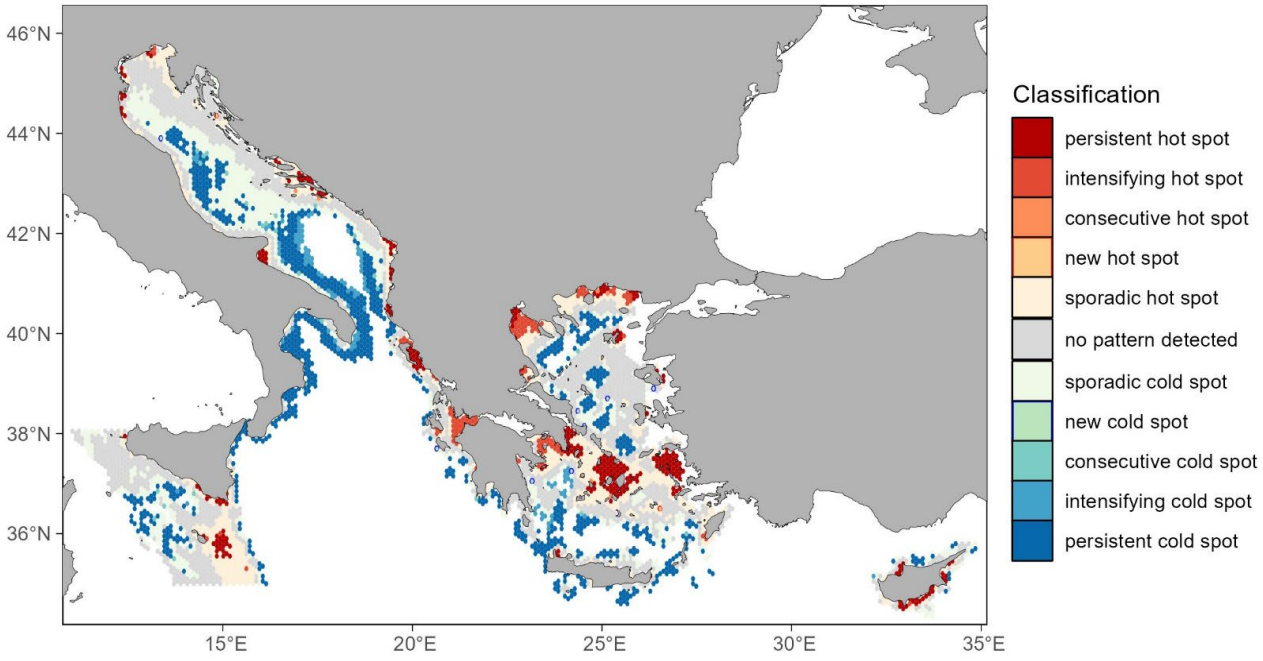

Figure 5.5. Significant (α = 0.01) juvenile fish hot and cold spots in the Central-Eastern Mediterranean. Areas were classified in accordance to the Emerging Hot Spot Analysis classification scheme.

5.4. Discussion

In the present study we used state-of-the-art joint species distribution modelling to reconstruct the state of biodiversity of juvenile fish in the CE Mediterranean, from 1999 to 2021. Through Hierarchical Modelling of Species Communities, we uncovered the environmental and anthropogenic drivers shaping their distributions, and by combining the modelling outputs with spatial statistical technics (EHSA) we identified areas of particular importance for conservation (juvenile fish hot spots) in the CE basin. According to our results the dominant environmental driver shaping the distributions of juvenile life-stages, and the demersal fish community as a whole, was depth (Figure 2). It is well known that demersal fish species inhabit inside specific depth niches and form distinct assemblages along the depth gradient (Fujita et al., 1995; Bergstad, 2009), and our model results corroborate this. Fish juvenile species richness peaked at shallow-most waters (0-50 m depth range) and formed a smaller secondary peak between 250-350 m, while juvenile abundance decreased almost linearly with depth (Figure 3). This was also reflected at the juvenile species richness map (Figure 4), where several of the shallow-most zones and areas over the shelf presented high richness scores.

Bottom temperature showed a positive correlation with juvenile species richness and abundance (Figure 3). Since fish species thrive under certain temperature ranges (Tzanatos et al., 2020), the interaction of temperature and depth forms a particular suitability range for species over the seafloor. But when sea warming is considered, some species may experience a range contraction, either northwards or towards deeper waters (Clark et al., 2020). Our results provide more evidence on this, since many deep areas, where generally vulnerable chondrichthyan juveniles reside (e.g. *Chimaera monstrosa, Centrophorus granulosus, Dalatias licha* and *Etmopterus spinax*) experienced a loss in two of the three alpha diversity indices (Shannon diversity and Pielou's evenness). Sea warming, though, might have favoured many other more thermophilic species, judging by the positive trends in species richness, most notably all around the strait of Sicily and in the North Aegean Sea (Figure 3).

Bottom salinity and chl*a* concentrations were the next most influential covariates (Figure 2), with salinity correlating negatively and chl*a* positively with juvenile species richness and abundance (Figure 3). This agrees with the EHSA results, which identified plenty significant juvenile hot spots near river mouths and deltas, and near lagoons (Figure 4). Productive fronts are generally important for successful recruitment and juvenile growth (Druon et al., 2015). Bar the above, this salinity-chl*a* gradient could also reflect a more general east-west gradient, which is prevalent in the Mediterranean.

Lastly, fishing pressure had a significant, albeit weak effect on the CE Mediterranean juvenile fish community (Figure 2). Interestingly, fishing pressure correlated positively with species richness and abundance (Figure 3). This find is possibly due to FPI correlating spatially with juvenile fish aggregations in shallower, more productive areas. In these areas, where trawling is frequently banned due to proximity with the coast or due to the presence of protected marine habitats, fishing is done by highly selective gears from artisanal fishers. Small scale fisheries might tend to gravitate towards these areas to catch the bigger adult fish that share these habitats, indirectly favouring the smaller juvenile life-stages by lowering their mortality from predation. Although here we *a priori* considered and modelled only fishing pressure as the dominant anthropogenic stressor on the juvenile fish community (other than sea warming), other stressors like the presence of extensive marine infrastructure might be very important locally (Mercader et al., 2017; Matic-Skoko et al., 2020).

As mentioned above, in the previous section, juvenile alpha diversity was highly heterogenous across the CE Mediterranean. Subarea patterns were significantly more pronounced than subbasin-wide patterns, with the only notable large-scale pattern being that along the depth gradient. The Aegean Sea arose as a very diverse area that presented high scores across all indices, with exceptionally high evenness. Additionally, species richness trended upwards in several locations around the area. Its northern part though, and especially Thermaikos Gulf, presented very low evenness, hinting that juvenile abundance was dominated by a few species. Nevertheless, several areas in the N Aegean, including Thermaikos, were identified to be significant (and intensifying) juvenile hot spots by the EHSA, suggesting that we shouldn't be pigeonholed into a single biodiversity index when prioritising conservation, but rather examine in a case-by-case basis which indices to consider. The Adriatic Sea displayed two very pronounced diversity patterns along the north-south and the east-west axis. The N Adriatic open waters presented a very diverse juvenile community, while the S Adriatic open waters showed the opposite pattern. Similarly, the E Adriatic coasts showed high biodiversity scores across the board, while the W Adriatic coasts had markedly low scores. Still, areas like the Gulf of Manfredonia and the Po river Delta are persistent juvenile hot spots according to the EHSA analysis. Worryingly, the Adriatic Sea was an area that recorded mostly losses in the juvenile alpha diversity. In the strait of Sicily, the alpha diversity followed the bottom's topographical features. The shelf area was characterised by very high species richness, but the more diverse and even juvenile communities were located on the slope along the shelf break. The strait of Sicily was the area that presented the most prominent gains in juvenile alpha diversity in the CE Mediterranean. Finally, the Ionian Sea showed very high scores in all indices. The CE Ionian presented an intensifying juvenile hot spot (Gulf of Patras) in an area where species richness trended significantly downwards. Perhaps the CE Ionian is an area where nursery habitat conservation measures should be prioritised. The N Ionian Sea also revealed a potential blind spot of our EHSA analysis. The south of the Salento peninsula that presented relatively high alpha diversity scores was classified as a cold spot, further corroborating against the use of single-index approaches for biodiversity conservation.

In conclusion, through the use of Hierarchical Modelling of Species Communities, we have shown that the most important environmental variables influencing juvenile fish distributions in the CE Mediterranean were (in order of significance) depth, bottom temperature, bottom salinity and chl*a* concentrations. Fishing pressure interacted significantly but had a weaker, positive, indirect effect on juvenile aggregations and richness. By utilising joint species distribution modelling and spatial statistical technics we were able to map for the first time the juvenile fish community alpha diversity patterns and hot spots in the area. Each subarea displayed distinct diversity and hot spot patterns, revealing that CE Mediterranean is a highly heterogenous area with substantial spatial complexity on its juvenile habitat structure.

5.5. References

Anonymous (2017). MEDITS-Handbook (Version 9). MEDITS Working Group. https://www.sibm.it/MEDITS%202011/docs/Medits_Handbook_2017_version_9_5-60417r.pdf

Baeza-González S, Kamakura N (2025) A methodological framework for tracing cluster life cycles: emerging hot spot analysis in evolutionary economic geography. Evolut Inst Econ Rev. https://doi.org/10.1007/s40844-025-00314-5

Bergstad, OA (2009) Fish: Demersal Fish (Life Histories, Behavior, Adaptations). In: Encyclopedia of Ocean Sciences (Second Edition), 458-466, Academic Press. https://doi.org/10.1016/B978-012374473-9.00673-1

Bianchi CN, Morri C, Chiantore M, Montefalcone M, Parravicini V, Rovere A (2012) Mediterranean Sea biodiversity between the legacy from the past and a future of change. In: Life Mediterr Sea 1: 55.

Bitetto I, Zupa W (2025). RoME - R Code to Perform Multiple Checks on MEDITS Survey Data. https://github.com/COISPA/RoME

Boudouresque CF, Blanfuné A, Harmelin-Vivien M, Personnic S, Ruitton S, Thibaut T, Verlaque M (2016). Where Seaweed Forests Meet Animal Forests: The Examples of Macroalgae in Coral Reefs and the Mediterranean Coralligenous Ecosystem. In: Marine Animal Forests. Springer, Cham. https://doi.org/10.1007/978-3-319-17001-5_48-1

Cheminée A, Sala E, Pastor J, Bodilis P, Thiriet P, Mangialajo L, Cottalorda J, Francour P (2013) Nursery value of Cystoseira forests for Mediterranean rocky reef fishes. Journal of Experimental Marine Biology and Ecology, 442, 70-79. https://doi.org/10.1016/j.jembe.2013.02.003

Cheminée A, Le Direach L, Rouanet E, Astruch P, Goujard A, Blanfuné A, Bonhomme D, Chassaing L, Jouvenel J, Ruitton S, Thibaut T, Harmelin-Vivien M (2021). All shallow coastal habitats matter as nurseries for Mediterranean juvenile fish. Sci Rep, 11, 14631. https://doi.org/10.1038/s41598-021-93557-2

Clark NJ, Kerry JT, Fraser CI (2020) Rapid winter warming could disrupt coastal marine fish community structure. Nat Clim Change 10: 862–867. https://doi.org/10.1038/s41558-020-0838-5

Coll M, Steenbeek J, Ben Rais Lasram F, Mouillot D, Cury P (2015) 'Low-hanging fruit' for conservation of marine vertebrate species at risk in the Mediterranean Sea. Glob Ecol Biogeogr 24: 226–239. https://doi.org/10.1111/geb.12250

Cuadros A, Cheminée A, Thiriet A, Moranta, Vidal E, Sintes J, Sagristá N, Cardona L (2017) The three-dimensional structure of Cymodocea nodosa meadows shapes juvenile fish assemblages at Fornells Bay (Minorca Island). Regional Studies in Marine Science, 14, 93-101. https://doi.org/10.1016/j.rsma.2017.05.011

D'Ortenzio F, D'Alcalà MR (2009) On the trophic regimes of the Mediterranean Sea: A satellite analysis. Biogeosciences 6: 139–148. https://doi.org/10.5194/bg-6-139-2009

Druon J, Fiorentino F, Murenu M, Knittweis L, Colloca F, Osio C, Mérigot B, Garofalo G, Mannini A, Jadaud A, Sbrana M, Scarcella G, Tserpes G, Peristeraki P, Carlucci R, Heikkonen J (2015). Modelling of European hake nurseries in the Mediterranean Sea: An ecological niche approach. Progress in Oceanography, 130, 188–204. https://doi.org/10.1016/j.pocean.2014.11.005

Escudier R, Clementi E, Cipollone A, Pistoia J, Drudi M, Grandi A, Lyubartsev V, Lecci R, Aydogdu A, Delrosso D (2021) A high-resolution reanalysis for the Mediterranean Sea. Front Earth Sci 9: 702285. https://doi.org/10.3389/feart.2021.702285 https://doi.org/10.3389/feart.2021.702285

Esri (2026) Emerging Hot Spot Analysis (Space Time Pattern Mining). ArcGIS Pro Documentation. https://pro.arcgis.com/en/pro-app/latest/tool-reference/space-time-pattern-mining/emerginghotspots.htm

Fujita T, Inada T, Ishito Y (1995) Depth-gradient structure of the demersal fish community on the continental shelf and upper slope off Sendai Bay, Japan. Mar Ecol Prog Ser 118:13-23 https://doi.org/10.3354/meps118013

Getis A, Ord JK (1992) The analysis of spatial association by use of distance statistics. Geogr Anal 24:189–206. https://doi.org/10.1111/j.1538-4632.1992.tb00261.x

Kavadas S, Maina I, Damalas D, Dokos I, Pantazi M, Vassilopoulou V (2015) Multi-Criteria Decision Analysis as a tool to extract fishing footprints and estimate fishing pressure: application to small scale coastal fisheries and implications for management in the context of the Maritime Spatial Planning Directive. Mediterranean Marine Science, 16(2), 294–304. https://doi.org/10.12681/mms.1087

Kavadas S., Chamodrakas I., Bitetto I., Zupa W., Maina I., Ligas A., Zilioli M., Accadia P., Dokos I., Kalkavouras K., Hattab T., Kapelonis A., Pantazi M., Touloumis K., Adamidou A., Adamowicz M.,

Angelini S., Arneri E., Carrara P., Casciaro L., Costantini I., Damalas D., Gancitano V., Garofalo G., Gibin M., Jelavic D., Kovsars M., Koutrakis M., Laiaki M., Mannini A., Maravelias C., Mifsud J., Moresis O., Musumeci C., Nicheva S., Perdichizzi A., Profeta A., Pyrounaki M., Raykov V., Sabatella E., Sartor P., Sbrana M., Tagliolato A., Thasitis I., Tiganov G., Tserpes G., Sgardeli V., Vukov I. (2025) Final Report of the RDBFIS "Hosting, maintenance and further development of the regional database for the Mediterranean and the Black Sea", Publications Office of the European Union, doi:10.2926/5619525

Lattanzi A, Bellisario B, Cimmaruta R (2024) A review of fish diversity in Mediterranean seagrass habitats, with a focus on functional traits. Rev Fish Biol Fisheries, 34, 1329–1349. https://doi.org/10.1007/s11160-024-09876-w

Legendre P, Anderson MJ (1999), Distance-based Redundancy Analysis: Testing multispecies responses in multifactorial ecological experiments. Ecological Monographs, 69: 1-24. https://doi.org/10.1890/0012-9615(1999)069[0001:DBRATM]2.0.CO;2

Mann HB (1945) Nonparametric tests against trend. Econometrica 13:245–259. https://doi.org/10.2307/1907187

Matić-Skoko S, Vrdoljak D, Uvanović H, Pavičić M, Tutman P, Varezić DB (2020) Early evidence of a shift in juvenile fish communities in response to conditions in nursery areas. Sci Rep, 10, 21078. https://doi.org/10.1038/s41598-020-78181-w

Mercader M, Mercière A, Saragoni G, Cheminée A, Crec'hriou R, Pastor J, Rider M, Dubas R, Lecaillon G, Boissery P, Lenfant P (2017) Small artificial habitats to enhance the nursery function for juvenile fish in a large commercial port of the Mediterranean. Ecological Engineering, 105, 78-86. https://doi.org/10.1016/j.ecoleng.2017.03.022

Ntouni MM, Lazaris A, Tzanatos E (2023) Patterns of fish occupancy of artificial habitats in the eastern Mediterranean shallow littoral. Mar Biol 170, 105. https://doi.org/10.1007/s00227-023-04253-w

Ord JK, Getis A (1995) Local spatial autocorrelation statistics: distributional issues and an application. Geogr Anal 27:286–306. https://doi.org/10.1111/j.1538-4632.1995.tb00912.x

Ovaskainen O, Abrego N (2020). Joint Species Distribution Modelling: With Applications in R. Cambridge University Press, Cambridge, UK. https://doi.org/10.1017/9781108591720

Rahman AU, Tikhonov G, Oksanen J, Rossi T, Ovaskainen O (2024) Accelerating joint species distribution modelling with Hmsc-HPC by GPU porting. PLoS Comput Biol 20(9): e1011914. https://doi.org/10.1371/journal.pcbi.1011914

Spedicato MT, Zupa W, Villamor A, Soni V, Puerta P, Fabien M, Fock H, Hidalgo M, Punzó A, López-López L, Mérigot B, Moura T, Henriques S, Oliveira P, Chaves C, Vasconcelos R, Rutterford L, Garcia C, Thompson M, Engelhard G, Beukhof E, Pecuchet L, Peristeraki P, Rozemeijer MJC, Jónsdóttir IG, Cronne L, Holdsworth N, Lindegren M (2024) - B-USEFUL. Report of available metadata and data gaps across case studies. Technical University of Denmark.

Teruzzi A, Di Biagio V, Feudale L, Bolzon G, Lazzari P, Salon S, Coidessa G, Cossarini G (2021) Mediterranean Sea Biogeochemical Reanalysis (CMEMS MED-Biogeochemistry, MedBFM3 system) (Version 1) [Data set]. Copernicus Monitoring Environment Marine Service (CMEMS). https://doi.org/10.25423/CMCC/MEDSEA_MULTIYEAR_BGC_006_008_MEDBFM3

Tzanatos E, Moukas C, Koutsidi M. 2020. Mediterranean nekton traits: distribution, relationships and significance for marine ecology monitoring and management. PeerJ 8:e8494 https://doi.org/10.7717/peerj.8494

Zurr AF (2012) A beginner's guide to generalized additive models with R. Highland Statistics Ltd., Newburgh, UK.

6 Interacting effects of anthropogenic and environmental pressures on biodiversity: a multi-scale approach

Authors: Alicia Gran, Manuel Hidalgo, Marion Billy, Silvia Blum, Walter Zupa, Stratos Batziakas, Bastien Merigot, Fabien Moullec, Panagiota Peristeraki, Maria Teresa Spedicato, Patricia Puerta

6.1. Introduction

The Mediterranean Sea, a well-known biodiversity hotspot (Coll et al., 2010), is one of the most exposed ecosystems to anthropogenic (e.g., pollution, direct habitat destruction) and environmental (e.g., warming, biological invasions) pressures, with fishing and climate change among its main threats (Colloca *et al.*, 2017; Pisano et al., 2020; O'Hara et al., 2024). Rather than acting in isolation, pressures can accumulate in space and time (Culhane et al., 2018; Halpern et al., 2019), enhancing the degradation of marine habitats, eroding their resilience, and deteriorating key ecosystem services – particularly, those dependent on marine biodiversity such as climate regulation or food provision (Balvanera et al., 2017).

Biodiversity is key in maintaining ecosystem stability and resilience under a context of intensifying pressures (Loreau, 2001; Isbell et al., 2015). Changes in biodiversity, especially when persistent, can weaken these properties, altering community composition and functioning and, in consequence, increasing vulnerability to further perturbations (Hooper et al., 2005; Oliver et al., 2015; Isbell et al., 2015; Hong et al., 2021). As predicting biodiversity responses is, therefore, a priority for effective management, it becomes challenging when multiple pressures act simultaneously. In such cases, pressures may act cumulatively, triggering additive effects, or interact in complex ways altering the expected biodiversity response through multiple pathways (Crain et al., 2008). These interactions are commonly described as synergistic, when combined effects trigger a stronger response than expected, or antagonistic, when one pressure reduces the effect of the other (Côte *et al*., 2016). However, the type, the magnitude, and even the direction of these effects cannot be generalised, but most likely vary with pressure intensity, biodiversity facet, and the ecological or biogeographic context in which they occur (Catford et al., 2022).

Within this dependency framework, both biodiversity and pressures are sensitive to the spatial scale (Gonzalez et al., 2020; Low et al., 2023). Most studies address cumulative effects at broad scales, capturing regional patterns, which may potentially mask local, ecologically relevant dynamics (Catford et al., 2022). Ignoring pressure's interactions and/or applying inappropriate spatial scales can lead to management actions that are ineffective, or even detrimental to marine ecosystems (i.e., mismanagement; Brown et al., 2013; Côté et al., 2016). Understanding which interactions are most critical, where they occur, at which scales, and which facets of biodiversity are most affected can therefore help prioritising management actions.

Despite their ecological and management relevance, interactions of cumulative effects still remain poorly addressed and understood, particularly, in heterogeneous and complex systems such as the Mediterranean Sea. Here, we assess how multiple pressures interact to shape the spatial patterns of three different taxonomic and functional biodiversity indicators in the demersal communities of the Western Mediterranean considering both local to regional scales. Specifically, (i) we identify the main interactions among pressures and characterise their direc-

tion, type and magnitude; and (ii) we spatially assess the role of interacting effects of temperature-productivity-fishing in the biodiversity responses.

6.2. Material and Methods

Study area and data availability

This study was conducted across the Western Mediterranean sub-basin, covering from the Strait of Gibraltar to the Strait of Sicily. Biodiversity was quantified using taxonomic and functional indicators that relied on fishery-independent abundance data of demersal communities collected during the Mediterranean International Bottom Trawl surveys (MEDITS). The MEDITS surveys are carried out annually during late spring-early summer following standardised protocols regarding sampling design, trawl gear characteristics, and biological data collection, thereby ensuring spatial and temporal comparability across the region (Spedicato et al., 2019; 2024). This study focuses on three regions (GSA06, GSA09 and GSA10) and on shelf community biodiversity (50–200 m) as a first case study (Fig. 1). A follow-up of Deliverable 3.2 will extend the same analytical approach to other Mediterranean areas and to slope communities (200–800 m).

Biological and trait data were compiled in the B-USEFUL project (Spedicato et al. 2024; Deliverable 2.2) and biodiversity indicators calculated within Deliverable 3.1, accounting for demersal species occurring in at least 1% of the sampling stations to ensure consistency across time series over the whole basin. The resulting dataset comprised 191 species, including 146 fishes, 24 cephalopods, and 21 decapod crustaceans. Functional diversity indicators were based on five categorical traits – body length, life span, vertical biological zone, diet, and temperature preference – selected according to their ecological relevance and data availability, and combined to define a total of 144 functional entities (see Deliverable 2.2 for details).

To cover different facets of biodiversity, we selected three biodiversity indicators, not strongly correlated, that exhibited contrasting responses during exploratory analyses, being: the *Shannon index* as a measure of taxonomic diversity (Shannon and Weaver, 1949), *Functional entities richness* to represent the diversity of functional roles (i.e. sum of functional entities number; Mouillot et al., 2014), and *Multidimensional functional evenness* to describe how regularly species abundances are distributed in the functional space (Villéger et al., 2008).

Environmental variables related to temperature, salinity and productivity were obtained from Copernicus Marine Service free-access repository (Nigam et al., 2021, Teruzzi et al., 2021), and were expressed as spring average (April-June), the concurrent MEDITS sampling season. Substrate type were characterised using the broad-scale European seabed habitat map (EUSeaMap; Vasquez et al., 2023), provided by the European Marine Observation Data Network (EMODnet), and subsequently simplified into five categories: *Posidonia*, hard substrate, sand, mud, and mixed sediment.

Anthropogenic pressure on demersal communities was quantified using fishing effort data derived from Automatic Identification System (AIS) records provided by Global Fishing Watch (Kroosma et al., 2018). A fishing effort index derived from AIS data as the average number of fishing days per year, accounting for overall demersal activity (dominated by trawling, with minor contributions from other demersal gears such as pots and traps, gillnets, and longlines). As AIS data are only considered reliable from 2012 onwards, biodiversity and environmental data were restricted to the same period, resulting in a final dataset comprising 656 sampling locations over a 10-year timeframe.

All biodiversity, environmental and anthropogenic variables were spatially and temporally aggregated using average values onto a hexagonal grid with a spatial resolution of 0.1° (Fig. 6.1), which constituted the basic spatial unit employed for all subsequent analyses. Both chlorophyll concentration and fishing effort were log-transformed prior to analysis to reduce skewness and improve model performance.

Biodiversity responses to interactions

Biodiversity responses to interactions between anthropogenic and environmental pressures were analysed following two main steps: (i) first, ranking importance of pairwise interactions through Random Forest at regional scales, and (ii) second, employing Generalised Linear Mixed Models (GLMM) to characterise the direction, type and magnitude of each interaction at both regional and local scales, which is the second objective of the study.

Multi-scale approach

Analyses were conducted at two different spatial scales to study cross-scale patterns in interactions between anthropogenic and environmental pressures. The regional scale was defined by Geographical Sub-Areas (GSAs) within the Western Mediterranean, corresponding to fisheries stock assessment and management units established by the General Fisheries Commission for the Mediterranean (GFCM) (Breuil, 1999); whereas the local scale was represented by 0.1° grid cells within each GSA (Figure 1).

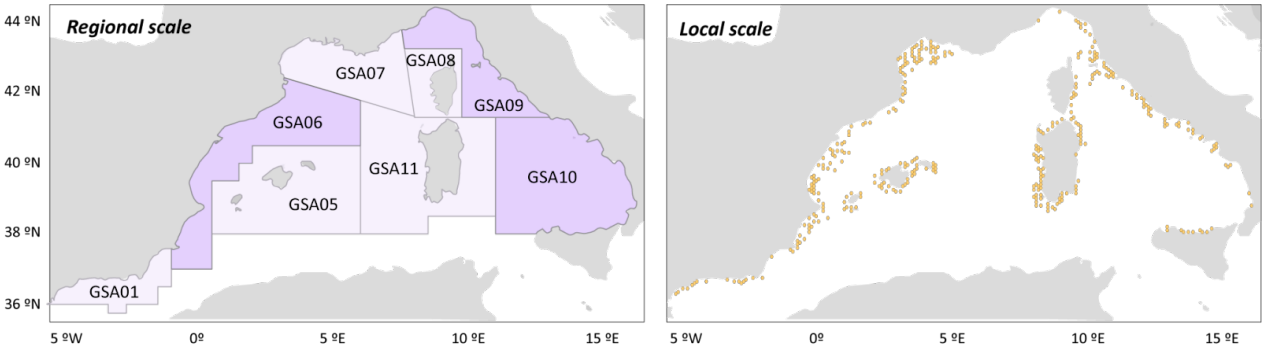

Figure 6.1. Regional (GSAs) and local (0.1° grid cells) scales used in the analysis of interactions in the Western Mediterranean. Dark purple highlights the study cases for this deliverable.

Variables and interactions selection

To identify the main drivers of biodiversity across the Western Mediterranean a Random Forest model ('randomForest' package; Liaw and Wiener, 2002) was conducted, including all environmental variables (including different measurements of temperature, salinity, productivity, and habitat structure) and anthropogenic pressures (fishing effort index). Based on variable and ecological relevance in the study area, chlorophyll concentration ($mg \cdot m^{-3}$), sea surface temperature (SST; °C), and demersal fishing effort index ($days \cdot yr^{-1}$) were selected as descriptors of productivity, temperature, and fishing pressure. Substrate type was also included in the model as a control variable to account for structural habitat difference. While substrate type contributed to improve model performance, it was not considered in the interaction analyses, as no meaningful or interpretable interaction patterns were detected in preliminary analyses.

Then pairwise interactions among these variables were ranked by hierarchical importance. Overall interaction strength (%) was quantified for each combination using Accumulated Local Effects (ALE)-based metrics ('iml' package; Molnar et al., 2018), representing the relative contribution of interactions to variability in model predictions, while also identifying directionality (i.e., which pressure modulates the effect of the other). Interactions were evaluated separately for each region.

Interaction characterisation

In a second step, interactions among pressures and their magnitudes were characterised, classifying them in three different types: additive, synergistic or antagonistic. For this purpose, we used Generalised Linear Mixed Models (GLMMs) fitted with the 'sdmTMB' package (Anderson et al., 2022), to account for the spatial autocorrelation of our data through spatial random fields to ensure more reliable estimates. All predictive variables were previously scaled from 0 to 1 to improve model convergence and comparability. For each pair of pressures, an additive model (Eq. 6.1) was compared to an interaction model (Eq. 6.2):

$$\text{Indicator} \sim A+B \qquad (1)$$

$$\text{Indicator} \sim A \times B \qquad (2)$$

The 'interaction effect' was calculated as the difference between predictions from the interaction and additive models, providing information on the nature of their combined effects (Côte *et al*., 2016). Thus, (i) a synergistic effect was indicated by positive values indicating amplifying effects, (ii) additive effects resulted when the difference was close to zero indicating independent effects that mainly sum up, (iii) and negative values indicated masking or antagonistic effects, where one pressure reduces the effect or the other (Fig. 2). The magnitude of the effect was quantified as the difference, either positive or negative, from the additive estimation. Only robust interactions were considered at each spatial scale, by applying thresholds based on the 10^{th} and 90^{th} percentiles of the interaction response distribution, separately to both the regional scale (calculated from mean interaction effects aggregated per GSA) and the local scale (mean interaction effects across cells). Interactions were then classified as (i) antagonistic (<10^{th} percentile), (ii) additive (10–90^{th} percentile), or (iii) synergistic (>90^{th} percentile); hereafter referred to as 'interaction type' (Figure 6.2).

Analyses were performed at both regional and local scales, with local interaction responses modelled independently for each region to account for context dependency. Interaction responses were finally mapped using yearly averages at both scales to visualise spatial variability and cross-scale patterns across the Western Mediterranean.

For the purpose of this deliverable, in this second step of the workflow we focused on two different case of study: (i) regional scale fishing-temperature characterisation for the Shannon index, with an example of the Italian coast (GSA09 and GSA10) for local scale, and (ii) fishing-productivity for Functional Entities Richness at regional scale, and the Northern Spanish coast (GSA06) at the local scale.

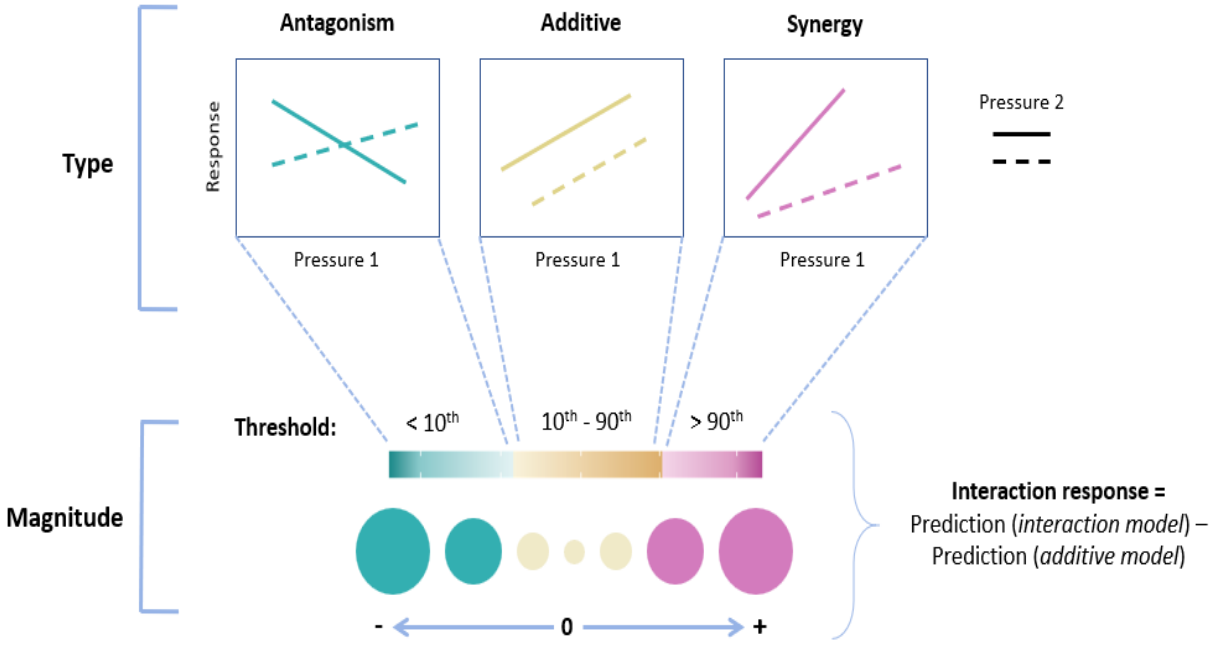

Figure 6.2. Conceptual framework to characterise additive and interaction responses between pressures.

6.3. Results

Random Forest models including the three main predictor variables (chlorophyll concentration, sea surface temperature, and demersal fishing effort) and substrate type applied on different indicators explained different fractions of biodiversity variance. The selected variables explained the highest proportion of variance (21.9%) on Functional Entities Richness, followed by Multidimensional Functional Evenness (14.2%), while the Shannon index showed the lowest one (6.3%). For the Shannon index, dominant interactions displayed a clear spatial structure across the Western Mediterranean, with temperature being involved in almost all interactions across regions. Along most of the Spanish, French, and Italian shelf, the Shannon index was mainly influenced by fishing-temperature interaction (Balearic Islands [GSA05], Northern Spain [GSA06], Gulf of Lion [GSA07], Southern Italy [GSA10]), while the north-eastern Italian coast was dominated by fishing-productivity interaction (GSA09). Conversely, in the central part of the sub-basin (Corsica [GSA08], Sardinia [GSA11]) and in the Northern Alboran Sea (GSA01), the interaction between productivity and temperature was the dominant (Figure 6.3). For functional diversity, patterns of dominant interactions changed across regions. In the case of Functional Entities Richness, fishing-productivity dominated in nearly all regions except the Gulf of Lion (GSA07), where the temperature-fishing interaction was again the main one. The Northern Alboran Sea (GSA01) and Corsica (GSA08) also maintained productivity-temperature as the main interaction compared to Shannon, whereas in other regions the dominant interaction shifted to combinations with fishing: in Sardinia (GSA11) interacting with temperature, and in the Balearic Islands (GSA05) and southern Italy (GSA10) replacing productivity as the pressure interacting with temperature (Figure 6.3). For Multidimensional Functional Evenness, the dominant interactions pattern differed from that observed for the other indicators. Fishing interacted with temperature in the Northern Alboran Sea (GSA01) and the Gulf of Lion (GSA07), while fishing-productivity was the main interaction in the Northern Spanish coast (GSA06) and in Southern Italy (GSA10). By contrast, the central part of the sub-basin (Balearic Islands [GSA05], Corsica [GSA08], Northern Italy [GSA09] and Sardinia [GSA11]) was mainly influenced by productivity-temperature interactions (Figure 6.3).

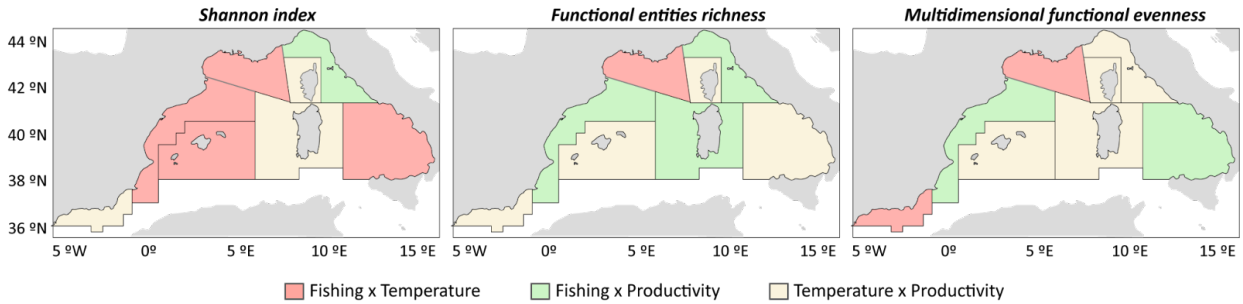

Figure 6.3. Principal interaction between variables across the Western Mediterranean for the Shannon (a), Functional Entities Richness (b) and Multidimensional Functional Evenness (c) indicators.

The direction, type and magnitude of interactions varied strongly depending on the region and biodiversity indicator. However, additive responses dominated most of the regions regardless of the biodiversity indicator and interacting variables (Figure 6.4). For instance, when considering the interaction between temperature and fishing for the Shannon index at the regional scale, westernmost regions showed additive interactions, but with a wide range of magnitudes. In some cases, the interaction value closely approached the threshold for a synergistic effect (e.g., Northern Alboran Sea – GSA01). At easternmost regions, however, the three interaction types were present, including a clear synergy of effects in Corsica (GSA08), an antagonism in northern Italy (GSA09), and additive responses with differing magnitudes in the south. Nevertheless contrasting patterns were observed at local scale which were masked at regional level. For example, strong local hotspots of both synergies, and antagonisms are detected in North Tyrrhenian Sea and Sicily and, Central Tyrrhenian Sea, respectively, although antagonistic, and additive interactions were detected at regional level (Figure 6.5).

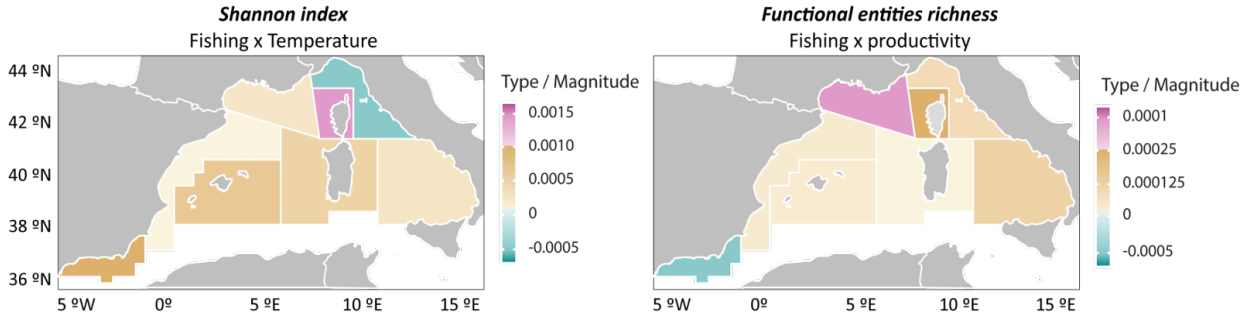

Figure 6.4. Type (additive, synergistic and antagonistic) and magnitude of interactions between fishing and temperature for the Shannon index (left) and between fishing-productivity for Functional entities richness (right) at regional scales across the Western Mediterranean. Additive effects are shown in light brown, synergies in pink and antagonisms in blue.

Additive interactions among fishing-productivity predominated across most of the subbasin for Functional Entities Richness, although cross-scale heterogeneity was also observed. Only the Northern Alboran Sea (GSA01), where fishing and productivity acted synergistically, and the Gulf of Lion (GSA07), where the interaction was antagonistic, differed from that pattern (Fig. 4). Local-scale analyses evidenced within-region variability in interaction type and magnitude. Along the Northern Spanish coast (GSA06), for instance, local hotspots of high-magnitude interactions were detected, with antagonistic interactions concentrating around the Ebro Delta and synergistic ones mainly occurring in the southern part of this region (Figure 6.5).

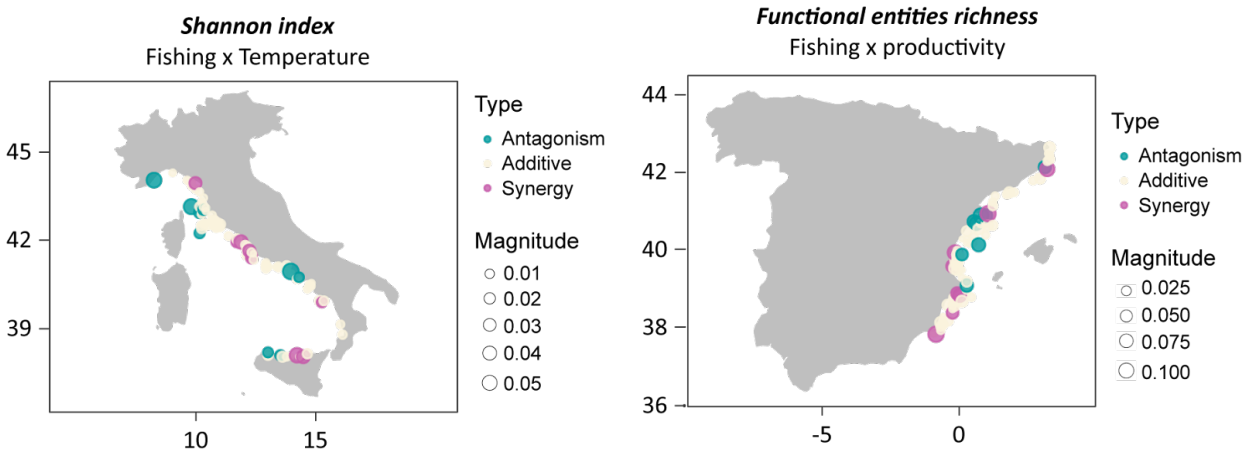

Figure 6.5. Type (additive, synergistic and antagonistic) and magnitude of interactions between fishing and temperature for the Shannon index (left) in the Italian coast (GSA09 and GSA10), and between fishing-productivity for Functional entities richness (right) in the Spanish coast (GSA06) at local scales. Additive effects are shown in light brown, synergies in pink and antagonisms in blue.

6.4. Discussion

Our study shows that cumulative effects of anthropogenic and environmental pressures on demersal biodiversity in the Western Mediterranean are widespread but strongly context-dependent, relying on the oceanographic and ecological context of the area, the spatial scale at which the biodiversity response is measured and also the biodiversity facet considered. The interactions across the sub-basin varied due to the gradients of temperature and productivity, and local fishing pressure, whose effects accumulate and interact in different ways. Hence, biodiversity responses cannot be interpreted through single- scale, pressure or indicator approaches, especially in environmentally heterogeneous and highly impacted systems such as the Mediterranean Sea (Coll et al. 2010, Nieblas et al., 2014; Colloca *et al.*, 2017).

Interactions among pressures were ecologically relevant across regions (large-scale), although their dominance relied on both the biodiversity indicator and ecological context. For the Shannon index, interaction patterns showed a clear spatial structure, with fishing being the main driver combined with environmental pressures in second place; particularly with temperature. This interaction dominates in several regions. Fishing-temperature interaction reflects the sensitivity of taxonomic diversity to both direct fishing mortality and thermal niches, as Shannon integrates species richness and relative abundances, which respond rapidly to changes in community size and composition already described in the Mediterranean (Bianchi et al., 2000; Gristina *et al*., 2006; Lindegren et al. 2025; Chapters 3-5), including directly some of our study regions, e.g., Veloy et al. (2022) for cephalopods and crustaceans.

Functional indicators, instead, displayed more complex patterns across the sub-basin. While fishing remained as a relevant driver, its interaction with productivity became more dominant for Functional Entities Richness, whereas both fishing-temperature and fishing-productivity shaped Multifunctional Evenness. Therefore, as the complexity of the biodiversity indicator increases, with increasing biodiversity facets accounted for by the indicator, more heterogeneous is the spatial pattern of the interactions among its drivers. This suggests that functional indicators are influenced by fishing pressure, but also by productivity. Similar dynamics have been reported for the Western Mediterranean, where community resilience and func-

tional reorganization were favoured by fluctuations in productivity, with additional long-term effects of fishing pressure making populations and communities more sensitive to natural fluctuations (Fu et al., 2018; Hidalgo et al., 2021). Trait mediated responses, such as those encompassed in the functional indicators, capture ecological processes (e.g., trophic relationships interplay, ecological preferences, niche availability) that are not recognisable from taxonomic diversity alone, highlighting their complementarity in assessing biodiversity responses to cumulative pressures. At the regional scale, both the type and magnitude of interactions were spatially structured with clear, region-specific patterns, reflecting the ecological and oceanographic complexity of the Western Mediterranean. For the Shannon index, interactions between fishing and temperature displayed contrasting responses between western and eastern regions, very likely due to the strong environmental gradients and regional differences in fishing intensity (Nieblas et al., 2014; Colloca *et al.*, 2017). In contrast, for Functional Entities Richness, highly productive regions such as the Alboran Sea and the Gulf of Lion (Bosc et al., 2004) presented more complex interactions, such as synergistic effects, whereas more oligotrophic areas were linked to weaker additive responses. Scale at which the biodiversity response is measured also influenced how cumulative pressures were interpreted (Gonzalez et al. 2020). While regional analyses captured broader ecological processes, local-scale assessments revealed hotspots of both synergistic and antagonistic interactions even if a different interaction is observed at the wider scale. Therefore, interactions among pressures are sensitive to spatial scale, being very likely modulated by the variability in habitat structure, community composition, and other environmental conditions. Caution should be posed in biodiversity status-pressure assessment considering spatial scale, since regional averages may overlook local processes potentially critical for ecosystem structure and functioning and result in misleading biodiversity status conclusions (Kenny et al. 2025).

By mapping where and how pressures interact, this study provides the first powerful approach for interpreting cumulative impacts on biodiversity status. Additive effects, while of great potential impact, are the easiest to target, as reducing any of the pressures will provide predictable improvements due to its cumulative nature (Darling and Cote, 2008). On the contrary, antagonistic and synergistic interaction effects are far more complex, where reducing one pressure may not translate into proportional recovery (Halpern et al. 2008; Brown et al. 2013), or in contrast, trigger disproportionate benefits (Crain et al. 2008). The strong spatial variability observed here suggests that understanding where and how pressures interact could help design more effective and context-aware conservation strategies in a system as environmentally complex and heavily impacted as the Western Mediterranean.

6.5. References

Anderson, S. C., Ward, E. J., English, P. A., & Barnett, L. A. (2022). sdmTMB: an R package for fast, flexible, and user-friendly generalized linear mixed effects models with spatial and spatiotemporal random fields. *BioRxiv*, 2022-03. https://doi.org/10.1101/2022.03.24.485545

Balvanera, P., Quijas, S., Karp, D. S., Ash, N., Bennett, E. M., Boumans, R., ..., & Walz, A. (2017). Ecosystem services. In The GEO handbook on biodiversity observation networks (pp. 39-78). Springer, Cham.https://doi.org/10.1007/978-3-319-27288-7_3

Bianchi, G., Gislason, H., Graham, K., Hill, L., Jin, X., Koranteng, K., ... & Zwanenburg, K. (2000). Impact of fishing on size composition and diversity of demersal fish communities. ICES Journal of marine Science, 57(3), 558-571. https://doi.org/10.1006/jmsc.2000.0727

Bosc, E., Bricaud, A., & Antoine, D. (2004). Seasonal and interannual variability in algal biomass and primary production in the Mediterranean Sea, as derived from 4 years of SeaWiFS observations. Global Biogeochemical Cycles, 18(1). https://doi.org/10.1029/2003GB002034

Breuil, C. (1999). The GFCM and the management of Mediterranean fisheries. In D. Symes (Ed.), Europe's Southern Waters: Management Issues and Practices (pp. 124-133). Fishing News Books.

Brown, C. J., Saunders, M. I., Possingham, H. P., & Richardson, A. J. (2013). Managing for interactions between local and global stressors of ecosystems. PloS one, 8(6), e65765. https://doi.org/10.1371/journal.pone.0065765

Catford, J. A., Wilson, J. R., Pyšek, P., Hulme, P. E., & Duncan, R. P. (2022). Addressing context dependence in ecology. *Trends in Ecology & Evolution*, *37*(2), 158-170. https://doi.org/10.3389/focsu.2023.1308125

Coll, M., Piroddi, C., Steenbeek, J., Kaschner, K., Ben Rais Lasram, F., Aguzzi, J., ... & Voultsiadou, E. (2010). The biodiversity of the Mediterranean Sea: estimates, patterns, and threats. *PloS one*, *5*(8), e11842. https://doi.org/10.1371/journal.pone.0011842

Colloca, F., Scarcella, G., & Libralato, S. (2017). Recent trends and impacts of fisheries exploitation on Mediterranean stocks and ecosystems. *Frontiers in Marine Science*, *4*, 244. https://doi.org/10.3389/fmars.2017.00244

Côté, I. M., Darling, E. S., & Brown, C. J. (2016). Interactions among ecosystem stressors and their importance in conservation. Proceedings of the Royal Society B: Biological Sciences, 283(1824), 20152592. https://doi.org/10.1098/rspb.2015.2592

Crain, C. M., Kroeker, K., & Halpern, B. S. (2008). Interactive and cumulative effects of multiple human stressors in marine systems. Ecology letters, 11(12), 1304-1315. https://doi.org/10.1111/j.1461-0248.2008.01253.x

Culhane, F. E., Frid, C. L., Royo Gelabert, E., White, L., & Robinson, L. A. (2018). Linking marine ecosystems with the services they supply: what are the relevant service providing units?. Ecological Applications, 28(7), 1740-1751. https://doi.org/10.1002/eap.1779

Darling, E. S., & Côté, I. M. (2008). Quantifying the evidence for ecological synergies. Ecology letters, 11(12), 1278-1286. https://doi.org/10.1111/j.1461-0248.2008.01243.x

Fu, Caihong, et al. "Risky business: the combined effects of fishing and changes in primary productivity on fish communities." Ecological Modelling 368 (2018): 265-276. https://doi.org/10.1016/j.ecolmodel.2017.12.003

Gonzalez, A., Germain, R. M., Srivastava, D. S., Filotas, E., Dee, L. E., Gravel, D., ... & Loreau, M. (2020). Scaling-up biodiversity-ecosystem functioning research. *Ecology Letters*, *23*(4), 757-776. https://doi.org/10.1111/ele.13456

Gristina, M., Bahri, T., Fiorentino, F., & Garofalo, G. (2006). Comparison of demersal fish assemblages in three areas of the Strait of Sicily under different trawling pressure. Fisheries Research, 81(1), 60-71. https://doi.org/10.1016/j.fishres.2006.05.010

Halpern, B. S., McLeod, K. L., Rosenberg, A. A., & Crowder, L. B. (2008). Managing for cumulative impacts in ecosystem-based management through ocean zoning. Ocean & Coastal Management, 51(3), 203-211. https://doi.org/10.1016/j.ocecoaman.2007.08.002

Halpern, B. S., Frazier, M., Afflerbach, J., Lowndes, J. S., Micheli, F., O'Hara, C., Scarborough, C., & Selkoe, K. A. (2019). Recent pace of change in human impact on the world's ocean. Scientific Reports, 9(1), 1-8. https://doi.org/10.1038/s41598-019-47201-9

Hidalgo, M., Vasilakopoulos, P., García-Ruiz, C., Esteban, A., López-López, L., & García-Gorriz, E. (2022). Resilience dynamics and productivity-driven shifts in the marine communities of the Western Mediterranean Sea. Journal of Animal Ecology, 91(2), 470-483. https://doi.org/10.1111/1365-2656.13648

Hong, P., Schmid, B., De Laender, F., Eisenhauer, N., Zhang, X., Chen, H., ... & Wang, S. (2022). Biodiversity promotes ecosystem functioning despite environmental change. *Ecology letters*, *25*(2), 555-569. https://doi.org/10.1111/ele.13936

Hooper, D. U., Chapin III, F. S., Ewel, J. J., Hector, A., Inchausti, P., Lavorel, S., ... & Wardle, D. A. (2005). Effects of biodiversity on ecosystem functioning: a consensus of current knowledge. *Ecological monographs*, *75*(1), 3-35. https://doi.org/10.1890/04-0922

Isbell, F., Craven, D., Connolly, J., Loreau, M., Schmid, B., Beierkuhnlein, C., ... & Eisenhauer, N. (2015). Biodiversity increases the resistance of ecosystem productivity to climate extremes. *Nature*, *526*(7574), 574-577. https://doi.org/10.1038/nature15374

Kroodsma, D. A., Mayorga, J., Hochberg, T., Miller, N. A., Boerder, K., Ferretti, F., ... & Worm, B. (2018). Tracking the global footprint of fisheries. *Science*, *359*(6378), 904-908. https://doi.org/10.1126/science.aao5646

Liaw A, & Wiener M (2002). Classification and Regression by randomForest. R News, 2(3):18–22. [http://CRAN.R-project.org/doc/Rnews/]

Lindegren, M., Hidalgo, M., Montanyes, M., Maioli, F., Weigel, B., van Denderen, D., Tikhnov, G., Ovaskainen, O., Degueurce, B., Jimenez, T., Golin, F., Jónsdóttir, I.G., Randhawa, H., Burgos, J., Zupa, W., Consiglio, A., Chiarini, M., Spedicato, M.T., Puerta, P., Gran, A., Moore, S., Pecuchet, L., Thompson, M., Greig, L., Cooper, K., Engelhard, G., Tiago, J., Rozemeijer, M., Henriques, S., Martins, A., Chaves, C., Vasconcelos, R., & Moura, T. (2025) – B-USEFUL. Report on temporal trends and spatial patterns of multiple biodiversity indicators. Technical University of Denmark. Available at: https://b-useful.eu/library/deliverables/

Low, J. M., Gladstone-Gallagher, R. V., Hewitt, J. E., Pilditch, C. A., Ellis, J. I., & Thrush, S. F. (2023). Using ecosystem response footprints to guide environmental management priorities. *Ecosystem Health and Sustainability*, *9*, 0115. https://doi.org/10.34133/ehs.0115

Loreau, M., Naeem, S., Inchausti, P., Bengtsson, J., Grime, J. P., Hector, A., ... & Wardle, D. A. (2001). Biodiversity and ecosystem functioning: current knowledge and future challenges. *science*, *294*(5543), 804-808. https://doi.org/10.1126/science.1064088

Molnar, C., Casalicchio, G., & Bischl, B. (2018). iml: An R package for interpretable machine learning. *Journal of Open Source Software*, *3*(26), 786.

Mouillot, D., Villéger, S., Parravicini, V., Kulbicki, M., Arias-González, J. E., Bender, M., ... & Bellwood, D. R. (2014). Functional over-redundancy and high functional vulnerability in global fish faunas on tropical reefs. *Proceedings of the National Academy of Sciences*, *111*(38), 13757-13762. https://doi.org/10.1073/pnas.1317625111

Nieblas, A. E., Drushka, K., Reygondeau, G., Rossi, V., Demarcq, H., Dubroca, L., & Bonhommeau, S. (2014). Defining Mediterranean and Black Sea biogeochemical subprovinces and synthetic ocean

indicators using mesoscale oceanographic features. PloS one, 9(10), e111251. https://doi.org/10.1371/journal.pone.0111251

Nigam, T., Escudier, R., Pistoia, J., Aydogdu, A., Omar, M., Clementi, E., Cipollone, A., Drudi, M., Grandi, A., Mariani, A., Lyubartsev, V., Lecci, R., Cretí, S., Masina, S., Coppini, G., & Pinardi, N. 2021. Mediterranean Sea Physical Reanalysis INTERIM (CMEMS MED-Currents, E3R1i system) (Version 1) [Data set]. Copernicus Monitoring Environment Marine Service (CMEMS). https://doi.org/10.25423/CMCC/MEDSEA_MULTIYEAR_PHY_006_004_E3R1I

O'Hara, C. C., Frazier, M., Valle, M., Butt, N., Kaschner, K., Klein, C., & Halpern, B. S. (2024). Cumulative human impacts on global marine fauna highlight risk to biological and functional diversity. *Plos one*, *19*(9), e0309788. https://doi.org/10.1371/journal.pone.0309788

Oliver, T. H., Isaac, N. J., August, T. A., Woodcock, B. A., Roy, D. B., & Bullock, J. M. (2015). Declining resilience of ecosystem functions under biodiversity loss. *Nature communications*, *6*(1), 10122. https://doi.org/10.1038/ncomms10122

Pisano, A., Marullo, S., Artale, V., Falcini, F., Yang, C., Leonelli, F. E., ... & Buongiorno Nardelli, B. (2020). New evidence of Mediterranean climate change and variability from sea surface temperature observations. *Remote Sensing*, *12*(1), 132. https://doi.org/10.3390/rs12010132

Shannon, C. E., & Weaver, W. (1949). The mathematical theory of communication. University of Illinois Press.

Spedicato, M.T., Massutí, E., Mérigot, B., Tserpes, G., Jadaud, A., & Relini, G.(2019). The MEDITS trawl survey specifications in an ecosystem approach to fishery management. Sciencia Marina, 83(S1), 9-20. https://doi.org/10.3989/scimar.04915.11X

Spedicato, M.T., Zupa, W., Villamor, A., Soni, V., Puerta, P., Moullec, F., Fock, H., Hidalgo, M., Punzón, A., López-López, L., Mérigot, B., Moura, T., Henriques, S., Oliveira, P., Chaves, C., Vasconcelos, R., Rutterford, L., Garcia, C., Thompson, M., Engelhard, G., Beukhof, E., Pecuchet, L., Peristeraki, P., Rozemeijer, M.J.C., Jónsdóttir, I.G., Cronne, L., Holdsworth, N., & Lindegren, M. (2024). B-USEFUL. Report of available metadata and data gaps across case studies. Technical University of Denmark. Available at: https://b-useful.eu/b-useful/uploads/D2.1-B-USEFUL_report.pdf

Teruzzi, A., Di Biagio, V., Feudale, L., Bolzon, G., Lazzari, P., Salon, S., Coidessa, G., & Cossarini, G. 2021. Mediterranean Sea Biogeochemical Reanalysis (CMEMS MED-Biogeochemistry, MedBFM3 system) (Version 1) [Data set]. Copernicus Monitoring Environment Marine Service (CMEMS). https://doi.org/10.25423/CMCC/MEDSEA_MULTIYEAR_BGC_006_008_MEDBFM3

Vasquez, M., Ségeat, B., Cordingley, A., Tilby, E., … (2023). EUSeaMap 2023, a European broad-scale seabed habitat map, Technical Report. Ref. EASME/EMFF/2020/3.1.11/Lot3/SI2.843624 – EMODnet Thematic Lot n° 3 – Seabed Habitats - D1.15. EMODnet. https://doi.org/10.13155/97116

Veloy, C., Hidalgo, M., Pennino, M. G., Garcia, E., Esteban, A., García-Ruiz, C., ... & Coll, M. (2022). Spatial-temporal variation of the Western Mediterranean Sea biodiversity along a latitudinal gradient. Ecological Indicators, 136, 108674. https://doi.org/10.1016/j.ecolind.2022.108674

Villéger, S., Mason, N. W., & Mouillot, D. (2008). New multidimensional functional diversity indices for a multifaceted framework in functional ecology. *Ecology*, *89*(8), 2290-2301. https://doi.org/10.1890/07-1206.1

7 State-Pressure relationships across contrasting ecosystems.

Authors: Alicia Gran, Patricia Puerta, Walter Zupa, Stratos Batziakas, Bastien Merigot, Fabien Moullec, Panagiota Peristeraki, Maria Teresa Spedicato, Daniel Van Denderen, Martin Lindegren, Manuel Hidalgo

7.1. Introduction

Biodiversity loss is a global environmental crisis (IPBES 2019; Keck et al., 2025), with marine ecosystems being increasingly affected by the intensification of anthropogenic and environmental pressures such as overfishing, direct habitat destruction, and climate change (Halpern et al., 2015; Simeoni et al., 2022; O'Hara et al., 2024). Together, these pressures are modifying the structure and functioning of marine ecosystems, with sound consequences for their stability, resilience, and the services they provide (Balvanera et al., 2017; Hong et al., 2022; O'Hara et al., 2024). The Western Mediterranean is particularly exposed to such changes, as it is simultaneously affected by high and long-lasting fishing pressure and, a rapid warming rate and increasing heatwaves frequency and strength (Vargas-Yáñez et al., 2008; Soto-Navarro et al., 2020; Ouled-Cheikh et al., 2022), among others, which altogether encompass strong environmental gradients and high spatial variation in communities composition and biodiversity over relatively short distances (Veloy et al., 2022; Flensborg et al., 2025). This situation creates a highly heterogeneous seascape in which environmental and anthropogenic pressures can accumulate, and possibly interact, in space and time, shaping biodiversity responses to pressures in complex ways (Culhane et al., 2018; Halpern et al., 2019; O'Hara et al., 2024, Chapter 6 in this deliverable).

Under these persistent cumulative pressures seascape, demersal biodiversity may experience critical changes in their structure and functioning, which could lead to shifting biodiversity baselines (Lilkendey et al., 2025). Therefore, for effective conservation and management measurements, it is essential to identify both baselines and thresholds of a given pressure in a given area where biodiversity can shift from relatively favourable states to increasingly degraded ones. Finding such shifts allows delineating areas with contrasting degrees of impact and prioritising context-dependent management strategies in order to increase the local and regional efficiency of measures and, ultimately, contain or reverse further global biodiversity loss. Therefore, since biodiversity state-pressure relationships are not uniform, they rely on the ecological or biogeographic context in which they occur, and may result in different sensitivities, resistant and resilience capacities of communities to increasing pressure levels may also differ (Tuomi et al., 2024; Flensborg et al., 2025; Keck et al., 2025).

Alongside this context dependency, biodiversity state-pressure relationships are also scale-dependent, as both pressures and biodiversity can impact or respond differently at different scales, e.g., the type and intensity of pressures vary across spatial scales (Gonzalez et al., 2020; Low et al., 2023). In consequence, ecologically relevant dynamics may be masked under broader spatial scales, potentially leading to misinterpretation of important biodiversity state-pressure relationships over local and regional scales (Chapter 6 of this deliverable). Understanding the impact of cumulative pressures on biodiversity across regions and spatial scales would help capture spatial heterogeneity in biodiversity state-pressure relationships and guide effective and context-aware conservation strategies to efficiently embrace national to international management measures.

In this study, we quantify how taxonomic and functional biodiversity state-pressure relationships of demersal communities of the Western Mediterranean vary across spatial scales under different scenarios of cumulative pressures, by (i) evaluating state-pressure relationships along a fishing gradient, under different environmental scenarios (productivity, temperature) and spatial scales (regional and subregional), (ii) identifying limiting thresholds of impact and (iii) spatially assessing the biodiversity state (low, increasingly or highly impacted) in the Western Mediterranean at a local scale.

7.2. Material and Methods

Study area and data availability

This study was conducted across the Western Mediterranean sub-basin, extending from the Strait of Gibraltar to the Strait of Sicily (Figure 7.1). This deliverable focuses on three different regions as first case studies, while a follow-up work of the Deliverable 3.2 will extend the same analytical approach to other Mediterranean and Atlantic areas.

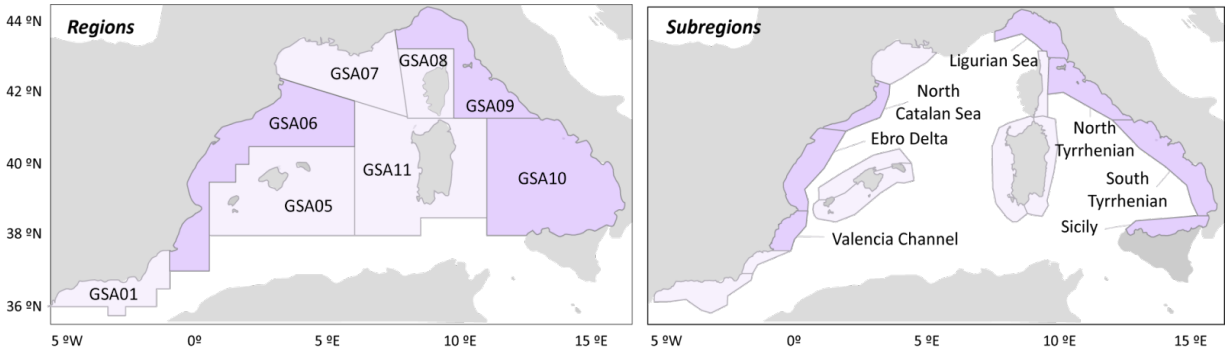

Figure 7.2. Regional (GSAs) and subregional (subregional ecoregions) scales used in the analysis of interactions in the Western Mediterranean. Dark purple highlights the study cases for this deliverable.

Biodiversity responses were quantified using species richness, an indicator obtained from previous work in the Task 3.1 of the project (Lindegren et al. 2025), known to be responsive to external natural and anthropogenic impacts, and also used to assess the Good Environmental Status (GES). However, subsequent analyses will compare these responses of taxonomic diversity with other functional indicators to assess complementarity of responses to cumulative pressures. Data originated from fishery-independent abundance data of demersal communities collected during the Mediterranean International Bottom Trawl (MEDITS) surveys (Spedicato et al., 2024), which benefit from spatially and temporally standardised and comparable dataset across the basin. These surveys are conducted annually in late spring-early summer following common protocols, with sampling carried out at depth-stratified stations using a bottom trawl gear with consistent characteristics across years and sampling locations (see Spedicato et al., 2019, 2024). To ensure robust statistical analyses, species richness was calculated considering only species occurring in at least 1% of the hauls across the full time series, resulting in a total of 146 fishes, 24 cephalopods, and 21 decapod crustaceans.

Environmental data, including spring (April – June; MEDITS sampling season) averages of chlorophyll concentration ($mg \cdot m^{-3}$) and sea surface temperature (SST; °C), were obtained from the Copernicus free-access repository (Nigam et al., 2021, Teruzzi et al., 2021). These variables were selected as effects of productivity and temperature on demersal communities, respective-

ly, due to their known influence and potential interactions with fishing activities in the region (Fu et al., 2018; O'Hara et al., 2024). . A fishing effort index was also used as a measure of fishing pressure, expressed as average fishing days per year through Automatic Identification System (AIS)-based data from Global Fishing Watch (Kroosma et al. 2018). The index mainly reflects bottom trawl activity. However, other demersal fishing gears (e.g., pots and traps, gillnets, longlines) are also included although they represent a very small contribution to total fishing effort within the study area. As AIS data are only reliable from 2012, biodiversity and environmental data were restricted to the same period, resulting in a final dataset comprising 656 sampling locations over a 10-year timeframe.

All biological, environmental and fishing effort data were aggregated to a common hexagonal grid of 0.1° resolution, which constituted the basic spatial unit for all analyses.

Biodiversity sensitivity and SAI assessment

Assessing the state of marine biodiversity under cumulative anthropogenic and environmental impacts requires identifying the levels of pressure at which biodiversity becomes adversely affected. Thus, significant adverse impacts (SAI), originally developed to assess vulnerability of deep-sea Vulnerable Marine Ecosystems (VMEs) (FAO, 2009, 2016), were adapted here to evaluate demersal communities by quantifying how biodiversity responds to increasing fishing pressure under different environmental scenarios, across scales and contrasting regions.

The relationship between biodiversity and fishing pressure was characterised using cumulative species richness curves (Kenny et al., 2025). All biodiversity observations across years were ranked along a gradient of increasing fishing effort. Species richness values were then cumulatively summed and expressed as a proportion of the total biodiversity observed in each spatial unit, resulting in normalised and directly comparable cumulative biodiversity curves ranging from 0 to 1 (Figure 7.2).

To determine the thresholds at which biodiversity responses to fishing effort shift between impact states, these empirical cumulative biodiversity curves were subsequently modelled using a logistic function. Following the approach proposed by Kenny et al. (2025), a four-parameter logistic function (1) was fitted to the relationship between proportional cumulative biodiversity and fishing effort:

$$y = y_0 + \frac{a}{1+\left(\frac{x}{x_0}\right)^b} \quad (1)$$

where 'y' represents the cumulative proportion of biodiversity (interpreted as progressive biodiversity loss since fishing activity will remove it), 'x' corresponds to fishing effort (log-transformed fishing days·yr^{-1}), and y_0, a, x_0 and b are model parameters (Fig. 1). Models were fitted using repeated non-linear least squares with multiple starting parameter combinations and conserving the best solution, implemented through the 'nls.multstart' package in R (Padfield et al., 2020), with a maximum of 500 iterations to ensure robust convergence (Figure 7.2).

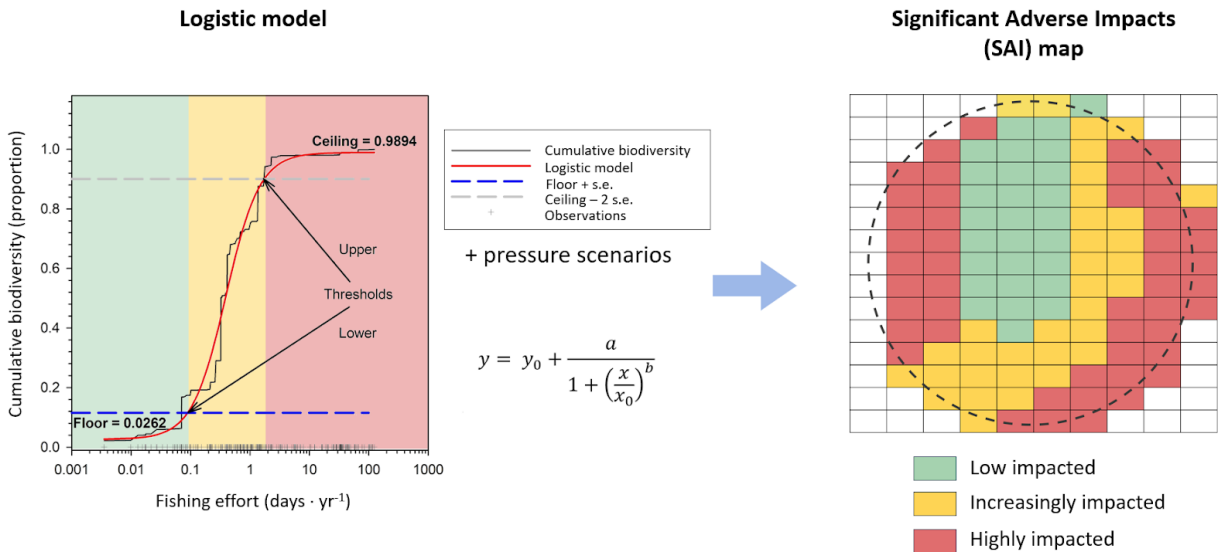

Figure 7.2. Methodological framework adapted from Kenny et al. (2025), in which a logistic model describing the cumulative biodiversity-fishing effort relationship is used to obtain impact thresholds of corresponding low, increasingly and highly impacted states.

From the fitted curves (1), lower and upper thresholds were obtained to define reference points for biodiversity-impact state (Figure 7.2). These thresholds were calculated by applying ±2 times the residual standard error (i.e., 95th confidence intervals) to the floor and ceiling of the fitted logistic cumulative biodiversity curve (limiting ceiling values at 1 when ceiling > 1; Kenny et al. 2025). The resulting thresholds delineate three state-pressure categories: (i) *low impacted* biodiversity, below the lower threshold, (ii) *increasingly impacted* biodiversity, between thresholds, and (iii) *highly impacted* biodiversity above the upper threshold. Fishing effort and cumulative biodiversity values associated with each threshold were obtained by solving the logistic equation (1) for 'x' and 'y' using the estimated parameters (Figure 7.2).

To account for environmental context, the cumulative biodiversity curves were modelled separately for two environmental scenarios or regimes (low and high) of either productivity and temperature. Environmental (low and high) scenarios were defined using the median values, chlorophyll concentration or SST, at each spatial unit. This approach ensured context dependency by allowing local gradients of fishing pressure and environmental conditions at each spatial unit, while maintaining comparability between scenarios and across units through the use of normalised cumulative biodiversity (see specific scenarios in Tables 1, 2 and 3 in results section). All models followed the same parameterisation and assumptions. Fishing effort and chlorophyll concentration were log-transformed prior to analysis.

Once thresholds were defined for each spatial unit (i.e., region and sub-region) and environmental scenario, observed biodiversity values in a given spatial unit were classified according to their position along the fitted curves, allowing each observation to be assigned to a low, increasingly, or highly impacted state.

Multi-scale approach

Analyses were conducted across three nested spatial scales to account for cross-scale patterns in biodiversity responses to cumulative anthropogenic and environmental impacts. Biodiversity state-pressure relationships were analysed at i) regional scale, considering the eight Geographical Sub-Areas (GSAs) located in the Western Mediterranean, which are delineated by the General Fisheries Commission for the Mediterranean (GFCM) for fisheries management (Breuil,

1999); ii) subregional scale, GSAs were subdivided into subregional ecoregions, defined according to existing biogeographic and ecological knowledge (e.g., Puerta et al., 2014; Billy, 2024) (Figure 7.1). In addition, biodiversity state was spatially assessed at iii) the local scale, performed at the level of 0.1° grid cells .

At the local scale, each 0.1° grid cell was assigned to one of the three impact categories based on its yearly-average species richness and fishing effort relative to the subregional thresholds, as interannual variability was low. Separate SAI spatial assessments were produced for low and high environmental scenarios, resulting in two maps per region illustrating the variability in biodiversity-impact states under the different scenarios (Figure 7.2).

7.3. Results

Four-parameter logistic models successfully captured the cumulative relationship between biodiversity loss along an increasing fishing pressure gradient across regions, environmental scenarios, and spatial scales (Figure 7.3 and 7.4). Overall, model performance was high, with RMSE values ranging from 0.013 to 0.047, indicating a close fit between observed and predicted cumulative biodiversity curves. In general, fitted curves provide a robust tool for identifying biodiversity sensitivity, resistance, and thresholds of cumulative fishing pressure under contrasting environmental scenarios. Increasing fishing pressure resulted in different cumulative biodiversity-state across regions, following similar yet displaced sigmoid-shaped response curves under contrasting environmental scenarios (Figure 7.3 and 7.4). In general, the environmental context modulated the initial state and rate of biodiversity loss rather than the overall shape of the response, affecting, therefore, the biodiversity baseline of increasing fishing impact. Thresholds from low to increasingly impacted states (lower) often show more variable values among regions, and environmental scenarios. At the subregional scale, cumulative curves differed from those observed at the regional scale; masking, in some cases, very different local dynamics.

Productivity strongly influenced the biodiversity response to fishing pressure across regions, also showing strong cross-scale variability (Figure 7.3; Tables 7.1, 7.2). Under low productivity scenarios, thresholds towards increasingly impacted states occurred at very low fishing pressure values and, in most regions, also collapsed to highly impacted states at lower fishing effort levels. Along the Spanish Mediterranean coast (GSA06), biodiversity showed marked high initial biodiversity values with no responses to small increases in fishing pressure. Biodiversity remains low impacted until 52 days·yr^{-1} and 65 days·yr^{-1} under low and high productivity scenarios (Table 7.1), respectively. This phase was followed by a steep slope, with biodiversity rapidly declining towards highly impacted states (> 0.95 biodiversity loss) at 556 and 579 days·yr^{-1} (Table 7.1), respectively. Subregions broadly reproduced the regional response, yet with notable differences in thresholds among subregions (Figure 7.3, Table 7.2). The biodiversity state of the North Catalan Sea required nearly twice the fishing effort to move from low to increasingly impacted state compared to other subregions. Conversely, the Ebro Delta and Valencia Channel reached highly impacted states at considerably lower fishing effort (478 and 412 days·yr^{-1}, respectively) than the surrounding subregions (Figure 7.3, Table 7.2).

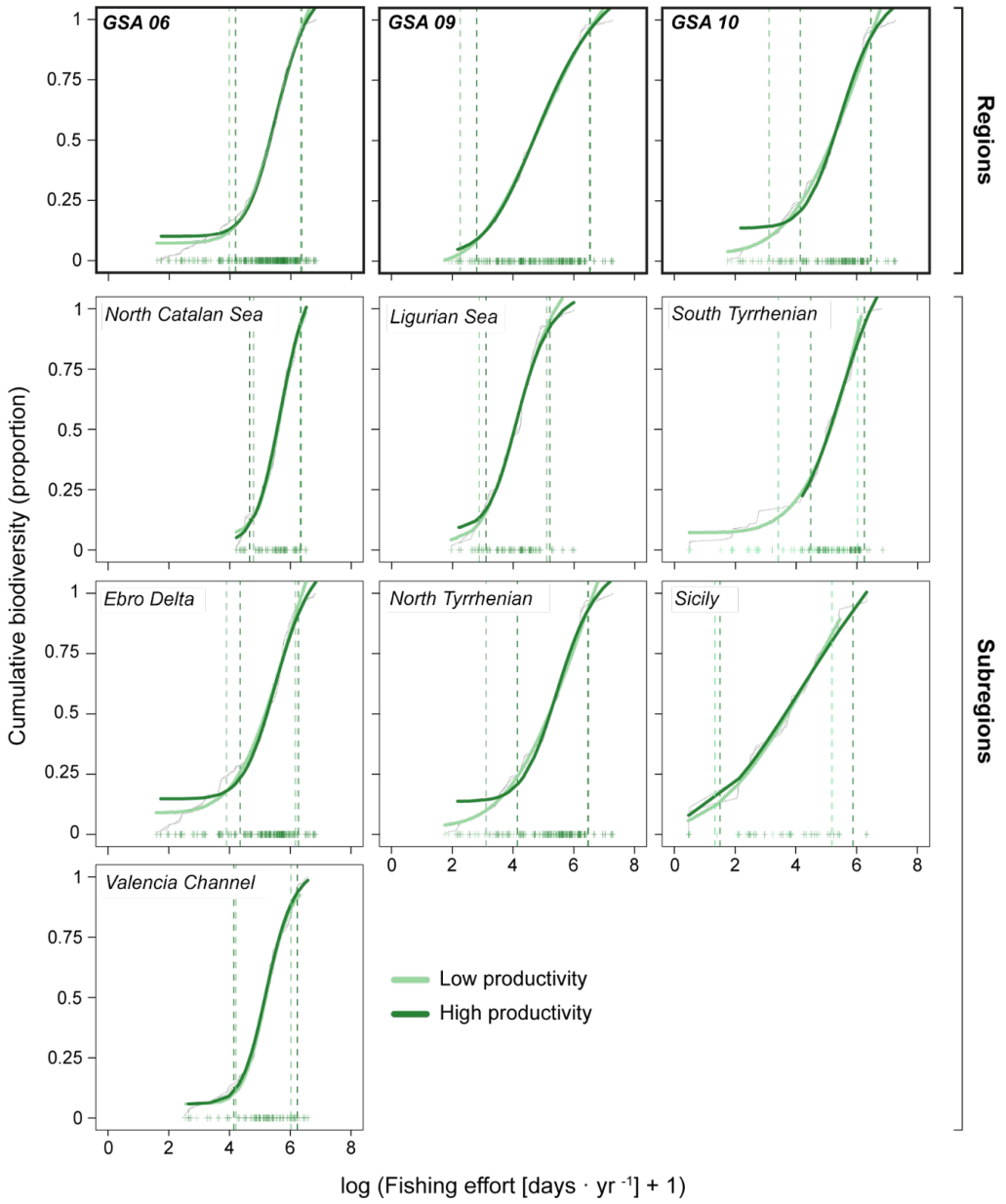

Figure 7.3. Relationship between proportional cumulative biodiversity and fishing effort. The grey line shows observed proportional cumulative biodiversity; whereas green lines represent the fitted four-parameter logistic model under low (light green) and high (dark green) productivity scenarios. Dashed vertical lines indicate the lower and upper impact thresholds for each scenario. The distribution of observations is shown at the bottom of each plot.

In contrast, the northern Italian coast (GSA09) displayed a transitioning to increasingly impacted at very low fishing effort values (9 and 16 days·yr^{-1} for low and high productivity), showing a smaller baseline of response to fishing (Figure 7.2, Table 7.1). However, the intermediate phase was prolongated until a much higher fishing effort values than in other regions (703 and 680 days·yr^{-1}, respectively) that marked the highly impacted state, probably related to the severe fishing impact of this area. At the subregional level, strong contrasted responses with higher subregional thresholds were found, especially under high productivity scenarios. Both the Ligurian Sea (21 days·yr^{-1}) and the North Tyrrhenian (61 days·yr^{-1}) may allow higher fishing effort without significant consequences for biodiversity than that suggested by the regional curve (7 days·yr^{-1}) (Figure 7.2, Table 7.2). Nevertheless, the Ligurian Sea reached an upper threshold at nearly four times lower fishing effort levels than those of the North Tyrrhenian

and the regional response, implying a likely long-lasting impact in this area (Figure 7.2, Table 7.3). The southern Italian coast (GSA10) showed the strongest environmental scenario-dependency. Under low productivity, biodiversity was lost rapidly, reaching the threshold of low impacted state at approximately 10 days·yr^{-1}, whereas under high productivity this shift occurs at 34 days·yr^{-1} (Figure 7.3, Table 7.1). Differences between productivity scenarios persisted across the fishing gradient, with biodiversity reaching highly impacted states at much higher values under high productivity despite similar response shapes. Subregions diverged strongly from the regional response. The South Tyrrhenian displayed marked differences between productivity scenarios, with remarkable lower values (29 days·yr^{-1}) in low productivity scenario than at high (88 days·yr^{-1}) one. While Sicily showed extreme lower threshold, shifting out of the low impacted state at only 3 – 4 days·yr^{-1}, its increasingly impacted state covers most of the response curve with a wide range of fishing pressure, particularly under high productivity (357 days·yr^{-1} vs. 179 days·yr^{-1} for low productivity), although reaching the impacted state at lower values than both the South Tyrrhenian and the overall regional response (Figure 7.2, Table 7.3).

Temperature-modified state-pressure relationships

Biodiversity responses under contrasting temperature regimes were more similar between thermal scenarios than those observed under productivity ones, even for cross-scale analyses (Figure 7.4, Table 7.1), meaning that biodiversity sensitivity to fishing impact was more independent of thermal conditions, with few exceptions. The Spanish coast (GSA06) showed again no changes as initial values of fishing pressure increase followed by rapid decline (Figure 7.4), with transitions to increasingly impacted states occurring at similar fishing effort under both temperature scenarios (58 days·yr^{-1}), while highly impacted states were reached between 559 (low temperature) and 581 (high temperature) days·yr^{-1}. Central subregions generally sharpened the regional decline, with the North Catalan Sea showing low diversity loss at initial values of fishing effort (102 and 119 days·yr^{-1} for low and high temperature), while upper thresholds remained very similar among subregions (Figure 7.4, Table 7.3). The northern Italian coast (GSA09) exhibited again the lowest impact values and fast response to small increase in fishing pressure, with biodiversity shifting to increasingly impacted at 11 – 12 days·yr^{-1}, and a strong resistance to further fishing pressure afterwards. Signals of collapse occur at a high impacted states of 674 – 719 days·yr^{-1} under low and high temperatures, respectively (Fig. 4, Table 3). Both subregions closely replicated the regional response. However, the Ligurian Sea reached highly impacted states at much lower fishing effort (176 days·yr^{-1} for both scenarios) than the North Tyrrhenian (632 and 672 days·yr^{-1}) and the overall regional curve (674 and 719 days·yr^{-1}) (Figure 7.4, Table 7.3). In the southern Italian coast (GSA10), thresholds from temperature scenarios were more similar between them compared to those observed under productivity. Biodiversity shifts occurred at nearly identical fishing effort levels under both temperature scenarios, with low impacted states occurring at 12 – 14 days·yr^{-1}, and highly impacted states reached at 502 – 506 days·yr^{-1}. Subregional temperature responses differed from the regional response. The South Tyrrhenian lower threshold increased by 11 and 33 days·yr^{-1} for low and high temperature compared to the regional curve, whereas in Sicily biodiversity loss remained highly sensitive to small fishing pressure (4 and 3 days·yr^{-1}). Notably, Sicily benefited greatly from low temperature scenario, reaching the highly impacted state threshold at 340 172 days·yr^{-1} compared to high temperature scenarios (168 days·yr^{-1}) (Figure 7.4, Table 7.3).

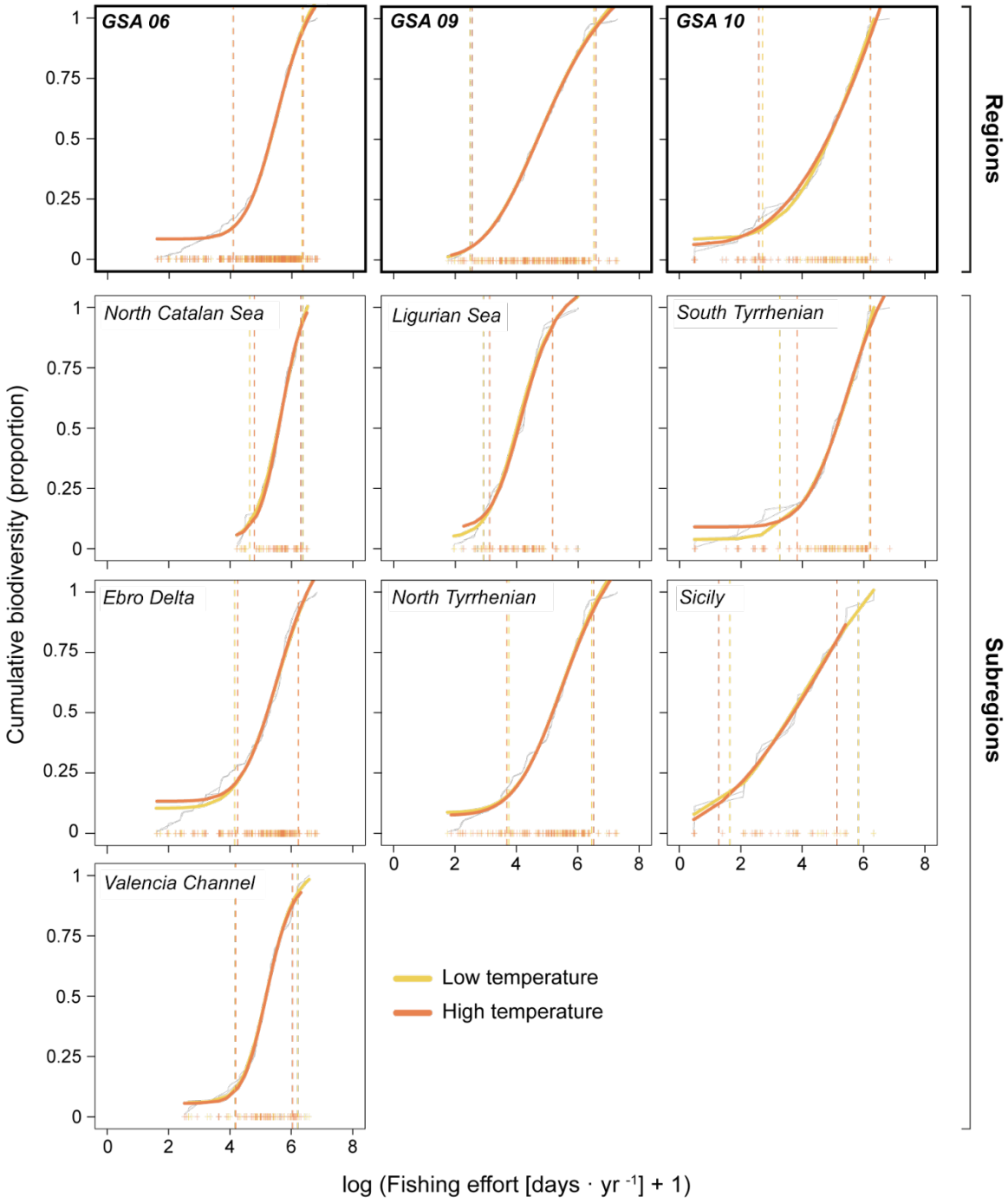

Figure 7.4. Relationship between proportional cumulative biodiversity and fishing effort. The grey line shows observed proportional cumulative biodiversity; whereas orange lines represent the fitted four-parameter logistic model under low (light orange) and high (dark orange) temperature scenarios. Dashed vertical lines indicate the lower and upper impact thresholds for each scenario. The distribution of observations is shown at the bottom of each plot.

Table 7.1. Impact thresholds of the proportional cumulative species richness in relation to fishing effort (days·yr^{-1}) under different environmental scenarios at region level. Values of productivity scenarios are indicated as chlorophyll concentration (mg·m^{-3}), while those for temperature are in ºC. n indicates the number of observations for each scenario.

				Fishing effort thresholds		Biodiversity thresholds	
Region	**Environmental scenario**	**Scenario**	**n**	**Lower**	**Upper**	**Lower**	**Upper**
GSA06	Productivity	Low [0.06 - 0.12]	258	52.27	555.80	0.12	0.95
		High (0.12 - 0.31]	258	64.59	578.90	0.15	0.95
	Temperature	Low [15.1 - 18.46]	258	57.90	559.19	0.13	0.95
		High (18.46 - 20.05]	258	58.05	580.53	0.13	0.95
GSA09	Productivity	Low [0.06 - 0.1]	167	8.60	702.96	0.03	0.97
		High (0.1 - 0.42]	166	15.51	679.60	0.09	0.96
	Temperature	Low [17.3 - 18.45]	167	10.87	673.81	0.05	0.96
		High (18.45 - 19.74]	166	11.66	718.89	0.06	0.96
GSA10	Productivity	Low [0.04 - 0.1]	100	10.23	482.99	0.12	0.94
		High (0.1 - 0.25]	100	33.91	554.66	0.22	0.96
	Temperature	Low [18.11 - 19.16]	100	14.02	502.17	0.13	0.96
		High (19.16 - 20.47]	100	12.31	505.84	0.13	0.93

Table 7.2. Impact thresholds of the proportional cumulative species richness in relation to fishing effort (days·yr^{-1}) under low and high productivity scenarios (chlorophyll concentration [mg·m^{-3}]). n indicates the number of observations for each scenario.

				Fishing effort thresholds		Biodiversity thresholds	
Region	**Subregion**	**Scenario**	**n**	**Lower**	**Upper**	**Lower**	**Upper**
GSA06	North Catalan Sea	Low [0.08 - 0.14]	54	118.33	556.95	0.13	0.92
		High (0.14 - 0.21]	53	104.83	571.89	0.11	0.95
	Ebro Delta	Low [0.06 - 0.11]	144	48.37	477.97	0.18	0.91
		High (0.11 - 0.31]	144	76.38	527.77	0.23	0.92
	Valencia Channel	Low [0.06 - 0.1]	61	66.51	412.35	0.11	0.87
		High (0.1 - 0.16]	60	61.99	505.84	0.11	0.93
GSA09	Ligurian Sea	Low [0.06 - 0.1]	56	16.98	165.89	0.11	0.93
		High (0.1 - 0.42]	55	21.41	183.06	0.17	0.93
	North Tyrrhenian	Low [0.06 - 0.1]	111	21.54	651.75	0.10	0.94
		High (0.1 - 0.19]	111	61.84	642.21	0.21	0.93
GSA10	South Tyrrhenian	Low [0.05 - 0.1]	75	29.39	414.90	0.13	0.90
		High (0.1 - 0.25]	75	87.88	519.19	0.29	0.93
	Sicilia	Low [0.04 - 0.1]	25	2.81	179.13	0.12	0.83
		High (0.1 - 0.08]	25	3.50	356.45	0.15	0.93

Table 7.3. Impact thresholds of the proportional cumulative species richness in relation to fishing effort (days·yr^{-1}) under low and high productivity scenarios (ºC). n indicates the number of observations for each scenario.

				Fishing effort thresholds		Biodiversity thresholds	
Region	**Subregion**	**Scenario**	**n**	**Lower**	**Upper**	**Lower**	**Upper**
GSA06	North Catalan Sea	Low [15.1 - 17.07]	54	102.15	582.24	0.11	0.95
		High (17.07 - 19.19]	53	119.38	545.73	0.12	0.92
	Ebro Delta	Low [16.64 - 18.51]	144	62.59	502.23	0.20	0.91
		High (18.51 - 20.05]	144	68.97	503.72	0.22	0.91
	Valencia Channel	Low [17.21 - 18.79]	61	63.78	497.17	0.11	0.93
		High (18.79 - 19.89]	60	64.85	418.67	0.11	0.88
GSA09	Ligurian Sea	Low [17.3 - 18.35]	56	17.76	176.37	0.12	0.93
		High (18.35 - 19.74]	55	21.86	175.72	0.17	0.92
	North Tyrrhenian	Low [17.51 - 18.47]	111	41.63	631.78	0.16	0.93
		High (18.47 - 19.62]	111	39.00	672.46	0.15	0.93
GSA10	South Tyrrhenian	Low [18.11 - 19.1]	75	25.27	495.63	0.09	0.94
		High (19.1 - 20.02]	75	45.27	507.70	0.16	0.93
	Sicilia	Low [18.41 - 19.42]	25	4.15	339.45	0.15	0.93
		High (19.42 - 20.47]	25	2.60	167.96	0.12	0.80

SAI assessment

The SAI assessment, based on subregion-specific impact thresholds (Tables 2 and 3), depicted nearly homogeneous spatial patterns of the biodiversity state across the Western Mediterranean. Along both, the Spanish (GSA06) and the Italian coasts (GSA09 and GSA10), increasingly impacted states predominated, with eventually localized hotspots of low and highly impacted biodiversity (Figure 7.5).

Overall, the spatial distribution of the biodiversity state varied with environmental scenarios. Under high productivity, several observations shifted from highly to increasingly impacted, or from increasingly impacted to low impacted states, suggesting that higher productivity increases resistance to fishing. Along the Italian coast, this shift occurred in most subregions except the Ligurian Sea, which remained largely stable across scenarios. Throughout the Spanish coast, biodiversity states were more spatially steady, with persistent hotspots of both low and highly impacted states. Nevertheless, the Valencia Channel and southern Ebro Delta

showed the greatest changes between productivity scenarios, with more observations shifting to increasingly or highly impacted states under low productivity.

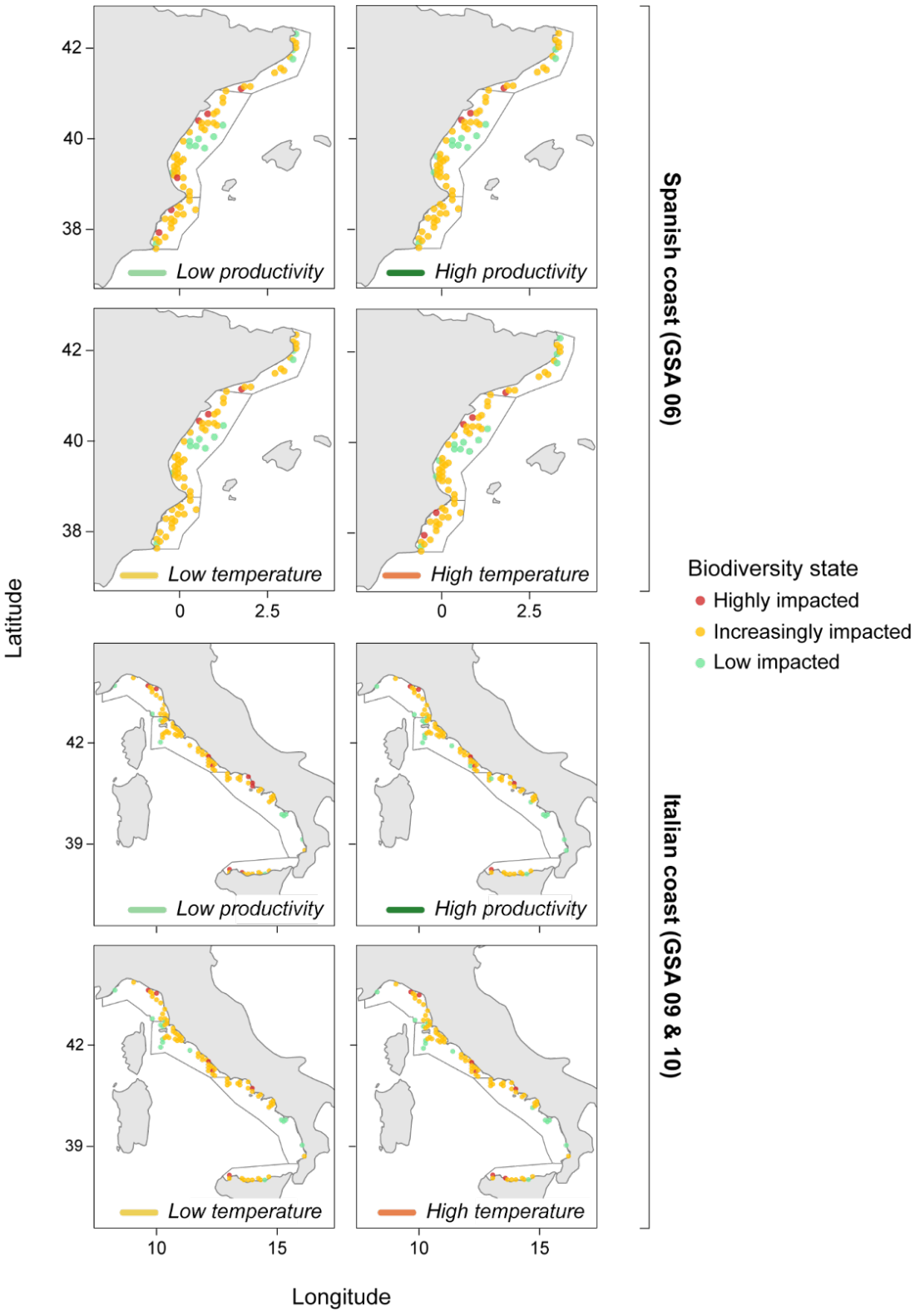

Figure 7.5. Biodiversity states in the Spanish and Italian shelf coasts using subregion-specific thresholds.

Temperature-modified shifts in biodiversity state were more localized and heterogeneous. Along the Spanish coast, high temperatures led to shifts from increasingly to highly impacted states in the Valencia Channel, while the Ebro Delta and the North Catalan Sea were more robust. In the Italian coast, biodiversity negatively shifted under high temperature in the North Tyrrhenian and Sicily, but improved in the South Tyrrhenian.

7.4. Discussion

Our results showed that the biodiversity state-pressure relationship (BPR) between richness and fishing pressure are region-specific, and, therefore, the pressure thresholds delimiting low/high impacted biodiversity are modulated by the environmental variability of the region. Our study shows that productivity is highly modulating how biodiversity responds to fishing, while the indirect effect of temperature on BPRs was negligible. While decay (i.e., slope) values of biodiversity-fishing relationship remained very similar across subregions, main differences between sub-regions and/or environmental scenarios occur at the floor (i.e. baseline) and ceiling of the logistic curves. Such differences, even when small, led to largely different fishing thresholds towards increasingly/highly impacted biodiversity states. Further research is needed to disentangle whether these different thresholds between environmental scenarios simply reflect two different biodiversity status or two contrasting responses to the fishing pressure. Long-lasting historical impact of fishing also may affect the biodiversity-fishing relationship (Farriols et al., 2017). For instance, the North Catalan Sea (GSA6), a heavily exploited area (Colloca et al., 2017), showed the highest minimum fishing intensities along the pressure gradient compared to neighbouring subregions. As a result, impacts on biodiversity are detected at higher fishing levels due to the lower baseline and the higher cumulative pressure needed for a meaningful biodiversity response. In contrast, biodiversity is increasingly impacted at much lower fishing pressure in the southern Italian subregions, particularly in northern Sicily, suggesting a higher sensitivity to fishing pressure in this ecosystem. However, once biodiversity began to decline, the shift to highly impacted state was more gradual, possibly related to its higher species richness and comparatively lower fishing pressure in this area (Farriols *et al*., 2019; Lindegren et al. 2025). These patterns highlight the east-west gradients of pressures observed across the Mediterranean and how regional averages may mask or mislead subregional variability in biodiversity sensitivity (e.g. Chapter 6 of this Deliverable report).

Productivity was the main environmental variable on modulating biodiversity responses to fishing. Under highly productive scenarios, biodiversity generally required higher fishing pressure to shift towards increasingly impacted states, suggesting that increased productivity enhances biodiversity resistance by sustaining more diverse, complex structural and trophic organisation (Fu et al., 2018). This was particularly evident in highly productive subregions such as the Ebro Delta and both North and South Tyrrhenian. Conversely, low-productivity scenarios were associated with greater sensitivity to fishing, in line with previous studies showing strong responses to relatively small environmental changes (Fu et al., 2018). Part of this response may be also linked to the differences in the baseline biodiversity, as high productivity scenarios often start from higher diversity levels (e.g., North and South Tyrrhenian subregions), as aforementioned. In contrast, biodiversity response to fishing impact measured by the BPRs was not clearly modulated by thermal conditions. While regional-scale patterns were similar under low and high temperature scenarios, subregional responses differed. In some subregions (e.g., Sicily, Valencia Channel, North Catalan Sea), lower temperatures were associated with greater sensitivity to fishing, whereas in some others (e.g., Ligurian Sea, Ebro Delta) temperature had neg-

ligible influence, or even an opposite effect (e.g., North and South Tyrrhenian), reducing the impact thresholds. Such variability may be linked to regional differences in species composition, as communities are adapted to local thermal conditions (Pecuchet et al., 2017), or high functional redundancy in terms of sensitive traits to climate change (Polo et al. 2025). Notably, SAI maps evidenced that most of the studied regions are already in an increasingly impacted state, with some localised hotspots of low or highly impacted biodiversity. The spatial distribution of the biodiversity state was also clearly context-dependent, with productivity largely modulating how fishing pressure translated into an ecological impact at local scale. However, the effect of temperature scenarios were minimal and more localised. High productivity scenarios generally improved the biodiversity status at local scale (Fu et al., 2018), and increased the baseline for a meaningful response to fishing impact. This was particularly evident along the Italian coast, with the exception of the Ligurian Sea, that remained relatively stable across scenarios. In regions with extensive continental shelves, such as the Ebro Delta and the North Tyrrhenian Sea, low-impact hotspots occurred at longer distances from the coastline, possibly associated with reduced fishing pressure of the bottom trawlers in deeper habitats.

In general, biodiversity sensitivity to fishing in the Western Mediterranean is strongly context dependent, but high productivity scenarios tended to improve biodiversity status and allowed for higher relative resistance of biodiversity to fishing pressure. However, our results highlight that large-scale fishing regulations are unlikely to achieve effective conservation outcomes everywhere. Instead, management strategies should adapt subregional environmental contexts in a dynamic and adaptive manner, particularly productivity, to better anticipate where fishing pressure is most likely to translate into biodiversity loss and benefit from more resilient areas that can tolerate larger effort without remarkable biodiversity loss.

7.5. References

Balvanera, P., Quijas, S., Karp, D. S., Ash, N., Bennett, E. M., Boumans, R., …, & Walz, A. (2017). Ecosystem services. In The GEO handbook on biodiversity observation networks (pp. 39-78). Springer, Cham.https://doi.org/10.1007/978-3-319-27288-7_3

Billy, M. (2024). Scale-dependent spatial patterns of biodiversity in the Western Mediterranean: an indicator-based approach. Master Thesis, 64 pp.

Breuil, C. (1999). The GFCM and the management of Mediterranean fisheries. In D. Symes (Ed.), Europe's Southern Waters: Management Issues and Practices (pp. 124-133). Fishing News Books.

Colloca, F., Scarcella, G., & Libralato, S. (2017). Recent trends and impacts of fisheries exploitation on Mediterranean stocks and ecosystems. *Frontiers in Marine Science*, *4*, 244. https://doi.org/10.3389/fmars.2017.00244

Culhane, F. E., Frid, C. L., Royo Gelabert, E., White, L., & Robinson, L. A. (2018). Linking marine ecosystems with the services they supply: what are the relevant service providing units?. Ecological Applications, 28(7), 1740-1751. https://doi.org/10.1002/eap.1779

FAO (2009). International Guidelines for the Management of Deep-Sea Fisheries in the High Seas Food and Agriculture Organization of the United Nations, Rome, p. 92.

FAO (2016). Vulnerable Marine Ecosystems: Processes and Practices in the High Seas. Anthony Thompson, Jessica Sanders, Merete Tandstad, Fabio Carocci and Jessica Fuller, eds. FAO Fisheries and Aquaculture Technical Paper No. 595. Rome, Italy.

Farriols, M. T., Ordines, F., Somerfield, P. J., Pasqual, C., Hidalgo, M., Guijarro, B., & Massutí, E. (2017). Bottom trawl impacts on Mediterranean demersal fish diversity: Not so obvious or are we too late?. Continental Shelf Research, 137, 84-102. https://doi.org/10.1016/j.csr.2016.11.011

Farriols, M., Ordines, F., Carbonara, P., Casciaro, L., Esteban, A., Follesa, C., ... & Massutí, E. (2019). Spatio-temporal trends in diversity of demersal fish assemblages in the Mediterranean. *Scientia Marina*, *83*(1), 189-206. https://hdl.handle.net/11584/283399

Flensborg, L. C., Montanyès, M., Vivó Pons, A., Carolina Da Silva, F., & Lindegren, M. (2025). Scale-dependent effects of biodiversity and stability on marine ecosystem dynamics. Ecography, e07539. https://doi.org/10.1002/ecog.07539

Fu, Caihong, et al. "Risky business: the combined effects of fishing and changes in primary productivity on fish communities." Ecological Modelling 368 (2018): 265-276. https://doi.org/10.1016/j.ecolmodel.2017.12.003

Gonzalez, A., Germain, R. M., Srivastava, D. S., Filotas, E., Dee, L. E., Gravel, D., ... & Loreau, M. (2020). Scaling-up biodiversity-ecosystem functioning research. *Ecology Letters*, *23*(4), 757-776. https://doi.org/10.1111/ele.13456

Halpern, B. S., Frazier, M., Potapenko, J., Casey, K. S., Koenig, K., Longo, C., ... & Walbridge, S. (2015). Spatial and temporal changes in cumulative human impacts on the world's ocean. Nature communications, 6(1), 7615. https://doi.org/10.1038/ncomms8615

Halpern, B. S., Frazier, M., Afflerbach, J., Lowndes, J. S., Micheli, F., O'Hara, C., Scarborough, C., & Selkoe, K. A. (2019). Recent pace of change in human impact on the world's ocean. Scientific Reports, 9(1), 1-8. https://doi.org/10.1038/s41598-019-47201-9

Hong, P., Schmid, B., De Laender, F., Eisenhauer, N., Zhang, X., Chen, H., ... & Wang, S. (2022). Biodiversity promotes ecosystem functioning despite environmental change. Ecology letters, 25(2), 555-569. https://doi.org/10.1111/ele.13936

IPBES (2019). In: Brondizio, E. S., Settele, J., Díaz, S. and Ngo, H. T. (eds), Global assessment report on biodiversity and ecosystem services of the intergovernmental science-policy platform on biodiversity and ecosystem services. – IPBES Secretariat, 1148.

Keck, F., Peller, T., Alther, R., Barouillet, C., Blackman, R., Capo, E., ... & Altermatt, F. (2025). The global human impact on biodiversity. Nature, 1-6. https://doi.org/10.1038/s41586-025-08752-2

Kenny, A. J., Pepin, P., Bell, J., Downie, A., Kenchington, E., Koen-Alonso, M., ... & Diz, D. (2025). Reference points for assessing significant adverse impacts on deep sea vulnerable marine ecosystems. *Ecological Indicators*, *172*, 113296. https://doi.org/10.1016/j.ecolind.2025.113296

Kroodsma, D. A., Mayorga, J., Hochberg, T., Miller, N. A., Boerder, K., Ferretti, F., ... & Worm, B. (2018). Tracking the global footprint of fisheries. *Science*, *359*(6378), 904-908. https://doi.org/10.1126/science.aao5646

Lilkendey, J., Hegg, J., Campbell, M., Zhang, J., Raby, H., Reid, M., ... & Sabetian, A. (2025). Overcoming Shifting Baselines: Paleo-Behaviour Reveals Industrial Revolution as Tipping Point. Global change biology, 31(1), e70038. https://doi.org/10.1111/gcb.70038

Lindegren, M., Hidalgo, M., Montanyes, M., Maioli, F., Weigel, B., van Denderen, D., Tikhnov, G., Ovaskainen, O., Degueurce, B., Jimenez, T., Golin, F., Jónsdóttir, I.G., Randhawa, H., Burgos, J., Zupa, W., Consiglio, A., Chiarini, M., Spedicato, M.T., Puerta, P., Gran, A., Moore, S., Pecuchet, L., Thompson, M., Greig, L., Cooper, K., Engelhard, G., Tiago, J., Rozemeijer, M., Henriques, S., Martins, A., Chaves,

C., Vasconcelos, R., & Moura, T. (2025) – B-USEFUL. Report on temporal trends and spatial patterns of multiple biodiversity indicators. Technical University of Denmark. Available at: https://b-useful.eu/library/deliverables/

Low, J. M., Gladstone-Gallagher, R. V., Hewitt, J. E., Pilditch, C. A., Ellis, J. I., & Thrush, S. F. (2023). Using ecosystem response footprints to guide environmental management priorities. *Ecosystem Health and Sustainability*, *9*, 0115. https://doi.org/10.34133/ehs.0115

Nigam, T., Escudier, R., Pistoia, J., Aydogdu, A., Omar, M., Clementi, E., Cipollone, A., Drudi, M., Grandi, A., Mariani, A., Lyubartsev, V., Lecci, R., Cretí, S., Masina, S., Coppini, G., & Pinardi, N. 2021. Mediterranean Sea Physical Reanalysis INTERIM (CMEMS MED-Currents, E3R1i system) (Version 1) [Data set]. Copernicus Monitoring Environment Marine Service (CMEMS). https://doi.org/10.25423/CMCC/MEDSEA_MULTIYEAR_PHY_006_004_E3R1I

O'Hara, C. C., Frazier, M., Valle, M., Butt, N., Kaschner, K., Klein, C., & Halpern, B. S. (2024). Cumulative human impacts on global marine fauna highlight risk to biological and functional diversity. *Plos one*, *19*(9), e0309788. https://doi.org/10.1371/journal.pone.0309788

Ouled-Cheikh, J., Coll, M., Cardona, L., Steenbeek, J., & Ramírez, F. (2022). Fisheries-enhanced pressure on Mediterranean regions and pelagic species already impacted by climate change. Elem Sci Anth, 10(1), 00028. https://doi.org/10.1525/elementa.2022.00028

Padfield, D., Matheson, G., & Windram, F. (2020). Package 'nls. multstart'. CRAN: Vienna, Austria, 1-5.

Pecuchet, L., Lindegren, M., Hidalgo, M., Delgado, M., Esteban, A., Fock, H. O., ... & Payne, M. R. (2017). From traits to life-history strategies: Deconstructing fish community composition across European seas. Global Ecology and Biogeography, 26(7), 812-822. https://doi.org/10.1111/geb.12587

Puerta, P., Hidalgo, M., González, M., Esteban, A., & Quetglas, A. (2014). Role of hydro-climatic and demographic processes on the spatio-temporal distribution of cephalopods in the western Mediterranean. Marine Ecology Progress Series, 514, 105–118. https://doi.org/10.3354/meps10972

Simeoni, C., Furlan, E., Pham, H. V., Critto, A., de Juan, S., Trégarot, E., ... & Marcomini, A. (2023). Evaluating the combined effect of climate and anthropogenic stressors on marine coastal ecosystems: Insights from a systematic review of cumulative impact assessment approaches. Science of the Total Environment, 861, 160687. https://doi.org/10.1016/j.scitotenv.2022.160687

Soto-Navarro, J., Jordá, G., Amores, Á., Cabos, W., Somot, S., Sevault, F., ... & Sein, D. (2020). Evolution of Mediterranean Sea water properties under climate change scenarios in the Med-CORDEX ensemble. Climate Dynamics, 54(3), 2135-2165. https://doi.org/10.1007/s00382-019-05105-4

Spedicato, M.T., Massutí, E., Mérigot, B., Tserpes, G., Jadaud, A., & Relini, G.(2019). The MEDITS trawl survey specifications in an ecosystem approach to fishery management. Sciencia Marina, 83(S1), 9-20. https://doi.org/10.3989/scimar.04915.11X

Spedicato, M.T., Zupa, W., Villamor, A., Soni, V., Puerta, P., Moullec, F., Fock, H., Hidalgo, M., Punzón, A., López-López, L., Mérigot, B., Moura, T., Henriques, S., Oliveira, P., Chaves, C., Vasconcelos, R., Rutterford, L., Garcia, C., Thompson, M., Engelhard, G., Beukhof, E., Pecuchet, L., Peristeraki, P., Rozemeijer, M.J.C., Jónsdóttir, I.G., Cronne, L., Holdsworth, N., & Lindegren, M. (2024). B-USEFUL. Report of available metadata and data gaps across case studies. Technical University of Denmark. Available at: https://b-useful.eu/b-useful/uploads/D2.1-B-USEFUL_report.pdf

Teruzzi, A., Di Biagio, V., Feudale, L., Bolzon, G., Lazzari, P., Salon, S., Coidessa, G., & Cossarini, G. 2021. Mediterranean Sea Biogeochemical Reanalysis (CMEMS MED-Biogeochemistry, MedBFM3 system)

(Version 1) [Data set]. Copernicus Monitoring Environment Marine Service (CMEMS). https://doi.org/10.25423/CMCC/MEDSEA_MULTIYEAR_BGC_006_008_MEDBFM3

Toumi, C., Gauthier, O., Grall, J., Thiébaut, É., & Boyé, A. (2024). Disentangling the effect of space, time, and environmental and anthropogenic drivers on coastal macrobenthic β diversity in contrasting habitats over 15 years. Science of the Total Environment, 946, 173919. https://doi.org/10.1016/j.scitotenv.2024.173919

Vargas-Yáñez, M., García, M. J., Salat, J., García-Martínez, M. D. C., Pascual, J., & Moya, F. (2008). Warming trends and decadal variability in the Western Mediterranean shelf. Global and Planetary Change, 63(2-3), 177-184. https://doi.org/10.1016/j.gloplacha.2007.09.001

Veloy, C., Hidalgo, M., Pennino, M. G., Garcia, E., Esteban, A., García-Ruiz, C., ... & Coll, M. (2022). Spatial-temporal variation of the Western Mediterranean Sea biodiversity along a latitudinal gradient. Ecological Indicators, 136, 108674. https://doi.org/10.1016/j.ecolind.2022.108674

8 Regime shifts and reorganization of fish and macro-invertebrate communities in warming and overexploited Mediterranean ecosystems

Authors: Alexandros Kaminas, Bastien Mérigot, Camilla Sguotti, Stratos Batziakas, Walter Zupa, Patricia Puerta, Manuel Hidalgo, Panagiota Peristeraki, Maria-Teresa Spedicato, Fabien Moullec.

8.1. Introduction

The biodiversity of freshwater, marine, and terrestrial ecosystems is significantly altered by global change, which induces abrupt or gradual alterations to biotic and abiotic components on a global scale (IPBES, 2019; Kroeker et al., 2020; Van Moorsel et al., 2023). Global change encompasses five anthropogenic drivers of biodiversity loss defined by the Intergovernmental Science-Policy Platform on Biodiversity and Ecosystem Services (IPBES), namely the overexploitation of marine resources, climate change, pollution, biological invasions and sea-use change (IPBES, 2019). Climate change, along with other drivers of global change such as increased nitrogen deposition and habitat disruption due to human activities, can influence species distribution and resource dynamics in both terrestrial and aquatic ecosystems (Sage, 2020). These direct drivers can, in turn, impact an ecosystem's resilience, a concept that has increasingly appeared in the scientific literature, often to indirectly describe ecosystem health and stability (Capdevila et al., 2021; Van Meerbeek et al., 2021). Resilience refers to a system's ability to "absorb change and to anticipate future perturbations through adaptive capacity" (Urruty et al., 2016). It includes the ability of a system to recover from disruptions such as anthropogenic activities, adjust to changes like climate variability, and absorb shocks like an extreme weather event. Unlike stability, resilience does not focus on equilibrium. It recognizes the dynamic nature of systems and their capacity for transition between different states (Liu et al., 2022). For example, ecosystems can be significantly impacted by the conversion of natural habitats for urbanization and agriculture, which can result in habitat loss and fragmentation (Theodorou, 2022). The ability of species to migrate or adapt to changing environmental conditions can be hindered by this fragmentation, which can also isolate populations and decrease genetic diversity (Delnevo et al., 2021). Because of this, ecosystems may become less resilient to disturbances such as climate change or invasive species introductions, increasing their vulnerability to collapse or degradation (Wang et al., 2022). Complimenting the notion of resilience, other concepts have been used to describe the response of an ecosystem to perturbation. The most widely known is the concept of regime shifts. Large-scale population and community reorganizations as well as nonlinear discontinuous dynamics in ecosystems (i.e., regime shifts) can result from anthropogenic pressures such as overfishing and climate change (Jungblut et al., 2018; Möllmann et al., 2021). Another concept refers to the "tipping point(s)" of a community against environmental or anthropogenic forcing. This term describes a "level of change in system properties beyond which a system reorganizes, often in a non-linear manner, and does not return to the initial state even if the drivers of the change are abated. For the climate system, the term refers to a critical threshold at which global or regional climate changes from one stable state to another stable state." (Ipcc, 2022). It has been used to signify the threshold after which a system under forcing shifts away from its current state into a different alternative state (Scheffer et al., 2001). Formally, tipping points in systems are described as a qualitative change in a system, known as a bifurcation in mathematical literature (Poincaré, 1885). Tipping points can be crossed, for instance, at specific warming levels, a particular decrease in marine dis-

solved O2, or a specific alteration in acid-base chemistry due to CO2 absorption from the atmosphere (Heinze et al., 2021). Reorganizations such as regime shifts are the result of exceeding a tipping point of an ecosystem (Heinze et al., 2021). In the late 1980s, the North Sea experienced a regime shift in its plankton composition due to rising temperatures (Beaugrand, 2004). This change, coupled with persistent overfishing, particularly of demersal fish like Atlantic cod, led to a collapse of the entire demersal ecosystem, with cod stocks plummeting from their previously abundant levels (Alheit et al., 2005; Lynam et al., 2017).

Understanding resilience and its potential for discerning regime shifts is of utmost importance for sustainable management and conservation. Identifying regime shifts can provide early warning signals of changes in systems such as fish and macro-invertebrate communities, enabling more adaptive and sustainable fisheries management practices (Dakos et al., 2015; Van Moorsel et al., 2023). Regime shifts may also be associated with climate-related changes and understanding them is essential for assessing the system's resilience to past, ongoing and future climate impacts. Indeed, sudden changes, such as a shift from a diverse and productive ecosystem to a less diverse and less productive one, can have severe consequences for marine resources and human activities dependent on these ecosystems (Sguotti et al., 2019, 2022b; Vasilakopoulos et al., 2017; Vasilakopoulos and Marshall, 2015).

The Mediterranean Sea ranks among the most overexploited and fastest-warming ocean regions (Beca-Carretero et al., 2020; Soto-Navarro et al., 2020). Large-scale changes in Mediterranean marine communities in response to sea warming have been previously documented (Azzurro et al., 2019; Piroddi et al., 2020).The Mediterranean Sea is exceptionally vulnerable to the diverse impacts of climate change, experiencing accelerated warming rates, increased extreme weather events, and shifts in productivity (Soto-Navarro et al., 2020). Additionally, it faces anthropogenic pressures such as overfishing and facilitated introduction of invasive species, contributing to a patchy structure in marine populations (Hidalgo et al., 2022). Consequently, the Mediterranean systems display heightened responsiveness to environmental fluctuations and are strongly influenced by climate-driven variables, including changes in primary production (Damalas et al., 2021). Environmentally-driven regime shifts in the Mediterranean basin were identified as the causes in change to several aspects of fisheries, such as the body condition of important small pelagic commercial species in areas such as the Gulf of Lion or Northern Spain (Bensebaini et al., 2022; Feuilloley et al., 2020; Saraux et al., 2019). Additionally, the influence of regime shifts in the quality of the stocks of commercially important demersal species has been noted in several works (Hidalgo et al., 2022; Vasilakopoulos and Marshall, 2015). The emergence of regime shifts may also impact the biodiversity of a community and permanently change species composition, as was the case with the coastal hard-bottom algal communities in Sardinia, which transformed into barrens upon perturbation by predators (Bianchelli et al., 2016; Melis et al., 2019). However, the studies that investigated the resilience of marine communities to anthropogenic and environmental pressures were carried out solely on a local scale (ca. 43.2% of the studies conducted in the Mediterranean Sea; see supp. materials Table 1) and the resilience of the studied systems is rarely quantified (only ca. 8% of the studies really quantified it; see supp. materials Table 1) (Peleg et al., 2020; Sguotti et al., 2023). Additionally, the different response types of the Mediterranean communities to sea warming and fishing pressure, potential shifts, shift mechanisms and resilience dynamics remain unknown at the entire Mediterranean scale. There is a general lack of a synthetic assessment on studies dedicated to resilience and possible regime shifts across the entirety of Mediterranean fish and macro-invertebrate communities, particularly considering the complex interplay of anthropogenic stressors and environmental variables. This gap in scientific understanding highlights the crucial need for studies that combine data from multiple areas to evaluate the resili-

ence and likelihood of regime shifts in Mediterranean marine ecosystems. To address these shortcomings, the present work takes a broader, multi-regional approach by assessing regime shifts and quantifying resilience across multiple Geographical Sub-Areas (GSAs) in the Mediterranean Sea using catastrophe theory.

The catastrophe theory can help identify the critical thresholds and abrupt transitions that occur in systems (Johnson and Dudgeon, 2024; Scheffer and Carpenter, 2003; Thom, 1974). It provides a framework for understanding how changes in external conditions brought on by modification of the control variables can lead to discontinuous shifts in the state of a system (Grasman et al., 2009). This theory also helps explain the existence of alternative stable states and the mechanisms that drive transitions between these states, as well as hysteresis in a system (i.e the inability of the system to recover even after the causal forcing has subsided) (Scheffer and Carpenter, 2003). Catastrophe theory can be roughly understood as a "bifurcation theory from a topological perspective". In the context of ecosystems, catastrophe theory can be used to model and analyze the dynamics of critical transitions, such as sudden changes in species composition, vegetation cover, or water clarity in lakes (Scheffer and Carpenter, 2003). By applying catastrophe theory in modeling approaches, researchers can identify the conditions under which regime shifts are likely to occur, as well as the factors that contribute to the resilience or vulnerability of ecosystems to such shifts (Scheffer et al., 2001; Scheffer and Carpenter, 2003). The cusp catastrophe accounts for a three-dimensional system, in which an additional external variable acts as a splitting factor, changing the response of the system from linear and continuous to nonlinear and discontinuous in reaction to varying types of external drivers (Grasman et al., 2009). It also takes into account the concept of multiple states, showing how systems can exist in various configurations or regimes (Thom, 2018). Moreover, it outlines scenarios in which certain system states become inaccessible under specific conditions. For example, an ecosystem state might become unattainable after certain environmental parameters permanently fall within a predetermined range. Finally, the cusp model provides a geometric interface to understand and visualize "sudden jumps" in systems, which quickly lead to a change of state. These observed patterns and behaviors are common across many different types of natural phenomena and systems, whether they occur independently or in combination (Stewart, 1983). These observed behaviors are common to many different types of natural phenomena and systems, either separately or in combination (Stewart, 1983).

The main research questions of our study are how key stressors, including temperature change and fishing pressure, influence fish and macro-invertebrate (cephalopod and crustacean) communities in Mediterranean ecosystems, if regime shifts occurred, and are these communities resilient to these stressors. To address this question, the following objectives are outlined. First, this work aims to assess nonlinear discontinuous dynamics, specifically regime shifts, within the studied western mediterranean communities using the stochastic CUSP model, rooted in catastrophe theory. Second, it aims to discern the influence of temperature change and fishing pressure on the dynamics of these communities. Third, it focused on evaluating the resilience of western Mediterranean ecosystems to anthropogenic and environmental stressors. It is hypothesized that Mediterranean communities experiencing the combined effects of temperature change and fishing pressure will show nonlinear discontinuous shifts in community structure (Damalas et al., 2021). Additionally, it is supposed that changes in the abundance of fish and macro-invertebrate communities in Mediterranean ecosystems are influenced by temperature variability and fishing pressure to some degree (Piroddi et al., 2020). Finally, it is anticipated that Mediterranean communities exhibiting lower resilience, due to intense environmental and anthropogenic stressors, are more likely to undergo regime shifts than systems that receive lower levels of forcing (Heinze et al., 2021).

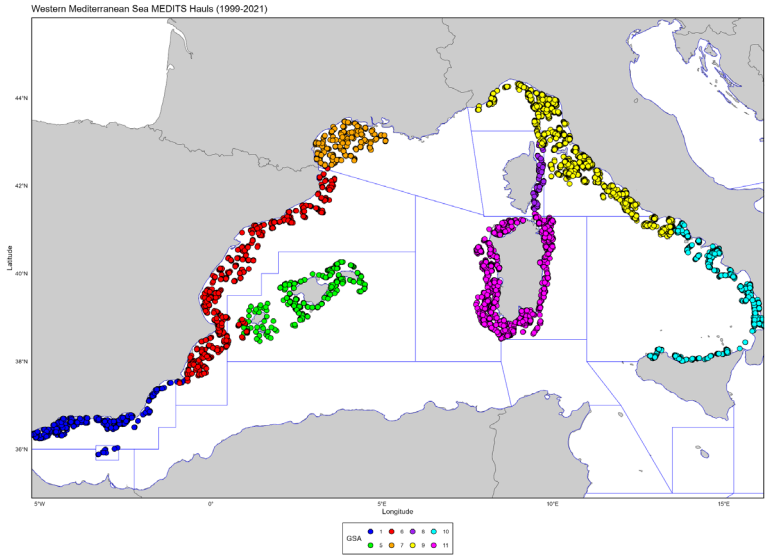

Figure 8.1. Map of the study area in the western Mediterranean Sea. Each circle corresponds to a sampling station for the MEDITS survey from 1999 to 2021. The color code corresponds to the different GSAs.

8.2. Material and Methods

Survey method and data collection

Data on marine communities were collected from the annual MEDITS scientific bottom trawl surveys conducted between May and July from 1999 to 2021 (Bertrand et al., 2002; Spedicato et al., 2020). These surveys took place over the continental shelf (10 to 200 m depth) and the continental slope (200 to 800 m depth) of the northern Mediterranean Sea (Fig 1). The study area ranged from 35.88°N to 44.33°N and 5.21°W to 16.18°E and was divided into Geographical Sub-Areas (GSAs) with boundaries set by the General Fisheries Commission for the Mediterranean Sea (as per resolution GFCM/33/2009/2, http://www.gfcm.org). The zones analyzed in this work focused on the western basin, and included GSA 1 (Alboran Sea), GSA 5 (Balearic Islands), GSA 6 (Northern Spain), GSA 7 (Gulf of Lion), GSA 8 (Corsica), GSA 9 (Ligurian and Northern Tyrrhenian Sea), GSA 10 (Southern and Central Tyrrhenian Sea), and GSA 11 (Sardinia) (Fig. 8.1). Sampling methods were standardized across all GSAs and years using a bottom trawl GOC-73 with a 20-mm cod-end mesh size. All tows were performed during daylight hours at a speed of 3 knots. The duration of each tow was standardized to 30 minutes for shelf stations and 60 minutes for slope stations to accommodate potential challenges of deep hauls (Bertrand et al., 2002). For each species the mean abundance per year and GSA (N.km²) was calculated as:

$$Abundance_{s,j,y} = \sum_{i=1}^{n} (TN_{s,j,y,i} / swept\ area_{j,y,i}) / n \quad (Eq\ 1)$$

Where s is a species, j a GSA and y a given year. TN is the total number of individuals in the haul, calculated for each species, and n is the total number of hauls conducted in GSA j during year y with the swept area calculated as follows:

$$Swept\ area_{i} = (Wing\ opening_{i} / 10000) \times (Distance_{i} / 1000) \quad (Eq\ 2)$$

Where swept area is the area spanned by the scientific trawler vessel, transformed from meters² to km², the wing opening, transformed from decameters² to km² is the area spanned by

the trawl net's entrance while in full motion. For each haul i, we computed the corresponding density. Hauls conducted in certain years were not available in the dataset for select GSAs. Specifically, hauls for the year 2000 in GSA 1, hauls conducted in 2000 and 2003 in GSA 5 as well as hauls for the years 2002 and 2020 in GSA 8 could not be considered in this work.

The MEDITS surveys identified a total of 361 marine species between 1999 and 2021 in 12571 hauls. Rare species, i.e species occurring in less than 1% of the hauls were excluded from further analysis. According to the histograms of species percentage of occurrence, most species are concentrated at the lower end of the x-axis, suggesting they are rare and appear in a small fraction of the hauls. Conversely, a smaller number of species appear frequently, as indicated by bars toward the higher end of the x-axis. The majority of rare species were small crustaceans, while fish and cephalopod species were generally not as rare. After filtering, hauls were aggregated per year and the mean abundance of species was calculated.

Anthropogenic and Environmental data

We used the overall fishing capacity per GSA and year to depict the influence of fishing pressure on the marine communities. The total fishing capacity can be seen as a proxy of the fishing effort and is the only fishing pressure information (considering both small fishing vessels and industrial fishing fleets) available between 1999 and 2021 and at the western Mediterranean scale. The fishing capacity data, expressed as Gross Tonnage (GT, in m^3) were extracted from the EU Fleet Register database [https://webgate.ec.europa.eu/] from 1999-2021. This dataset encompasses vessels ranging from 3.36 to 45.24 m. Regarding environmental data, sea bottom temperature (SBT, in °C) was retrieved from the Copernicus open-access database. SBT is closely linked to marine system productivity, influencing metabolic rates, and water stratification (Pennino et al., 2013). Specifically, the dataset Mediterranean Sea Physics Reanalysis by Escudier et al. (2020) was accessed and yearly mean potential temperature was extracted with a high horizontal resolution of 1/24°.

Analysis of Marine Community Dynamics

Principal Component Analysis

To understand the overall trends in the marine community of each GSA, we used principal component analysis (PCA), a statistical method for dimensionality reduction in datasets, to simplify our large dataset into just a few key components summarizing the main variations of the data. As a result, the historical trend of the marine community could be reduced to several axes, each of which explaining a portion of the variability found in the species community. Only the two first axes, encompassing the main variability, were kept (Sguotti et al., 2022a). The coordinates of years on axes 1 and 2 were extracted and used to analyze the overall community trends over time in the cusp models ran for each GSA. Euclidean distances among years on the first two axes of the PCA were used in hierarchical clustering to analyze changes in the marine community over the course of the selected time period (Legendre and Gallagher, 2001). The average linkage method, which yields more "faithful" results than other hierarchical clustering algorithms, was used to cluster the studied years (Mérigot et al., 2010). The optimal number of clusters was determined using the NbClust R package, which evaluates 30 indices to identify the best clustering scheme. It then proposes the most suitable number of clusters based on the majority rule from these evaluations (Charrad et al., 2014).

Bayesian Change Point Analysis

We performed Bayesian Change Point Analysis (BCP) to detect sudden shifts in Mediterranean marine communities' dynamics. The method calculates the posterior probability of an abrupt change occurring at any given point in the time series (Barry and Hartigan, 1993). It uses a Markov chain Monte Carlo approach to assess the probability that there is a significant difference in the posterior means before and after a potential change point (Erdman and Emerson, 2007). With a posterior probability ranging from 0 to 1, the threshold for identifying significant change points was set at a posterior probability greater than 0.7, considering the substantial yearly fluctuations observed in species abundance within the time series. All BCP analyses were conducted with the 'bcp' R package (Erdman and Emerson, 2007).

Stochastic cusp modeling

To detect whether the marine communities of the Western Mediterranean exhibited discontinuous behavior, this study utilized the stochastic cusp model, which allows for the identification of discontinuous dynamics, such as regime shifts, within a system influenced by two interrelated external factors (Diks and Wang, 2016; Sguotti et al., 2019; Thom, 1977). This model describes abrupt transitions in the equilibrium state of a state variable Y using two control variables, α and β. The potential function takes the following canonical form:

$$-V(y;\alpha;\beta) = \alpha y + 1/2\,\beta y^2 - 1/4 y^4 \quad (Eq\ 3)$$

This equation creates a cusp equilibrium surface, which acts as a response surface in regression, and predicts the dependent variable y based on canonical coordinates (α, β). Notably, for certain combinations of these variables, it can predict two possible values for y and "antipredict" an intermediate value, indicating non-occurrence of specific states (Cobb, 1981). The slope of the potential function represents the rate of change of the system, depending on the forcing of the two control variables. To be appropriate for empirical data, which frequently exhibit random variations (stochasticity), a Wiener process with variance σ^2 was added to the equation to transform it as a stochastic differential equation (SDE) (Cobb and Watson, 1980):

$$-dV(y;\alpha;\beta)/\,dz = (-y^3 + \beta y + \alpha)dt + \sigma dWt = 0 \quad (Eq\ 4)$$

In this equation, the initial segment signifies the drift term, which accounts for the deterministic trend in the process. The segment σ denotes the diffusion parameter, it determines the volatility or the degree of randomness in the process. W_t represents the Wiener process. The variable α, known as the asymmetry variable, directly impacts the size of the state variable and is linked to fishing capacity in this work, reflecting how fishing effort affects the community's state. Meanwhile, β, the bifurcation variable, can transform the relationship between α and the state variable from a smooth, linear one to a nonlinear, discontinuous one, potentially leading to regime shifts. This study utilized a linear model of β in relation to Sea Surface Temperature (SBT), indicating that variations in SBT may impact the way fishing pressure influences community composition, potentially resulting in regime shifts and events such as hysteresis. Changes in temperature have been known to impact an ecosystem's productivity (Brierley and Kingsford,

2009), which means that even minor adjustments to fishing pressure could significantly influence the ecosystem under varying environmental regimes. The canonical state variable y and the parameters α and β are estimated as linear functions of observable (Eqs 5a) or independent (Eqs. 5b and 5c) variables using a likelihood approach (Diks and Wang, 2016; Grasman et al., 2009):

$$y = w0 + w1Abundance \quad (Eq\ 5a)$$

$$\alpha = \alpha 0 + \alpha 1 Fishing\ Pressure \quad (Eq\ 5b)$$

$$\beta = \beta 0 + \beta 1 SBT \quad (Eq\ 5c)$$

where w0, α0 and β0 are the intercepts and w1, α1 and β1 are the slopes of the models. These variables were substituted into Eq. (4).

If the system follows a discontinuous path, it will exhibit two stable and one unstable equilibria; if it follows a continuous path, it will only exhibit one. The solution of (Eqs 4), which is used to derive the Cardan's discriminant (δ), determines the number of equilibria in the system:

$$\delta = 27\alpha - 4\beta^{3} \quad (Eq\ 6)$$

Which produces one solution when δ > 0 and three solutions when δ < 0. The bifurcation set, where δ = 0, is a cusp-shaped area on the plane (Fig. 8.2). By default, the summary of the basic cusp model function compares the cusp model's results to that of a linear regression model by computing a pseudo-R2 statistic measure, AIC and BIC. The pseudo-R^2 measure is preferred and used for cusp catastrophe model applications because it provides a measure of explained variance similar to the traditional R2 in ordinary regression models. However, in the context of cusp catastrophe models, defining error variance is not straightforward due to the model's irregular nature. In ordinary regression, the predicted value generally represents the expected outcome of the dependent variable based on the independent variables. In contrast, the cusp catastrophe model may predict multiple values for the dependent variable with a given set of independent variables (Grasman et al., 2009). In the pseudo-R2 measure for cusp catastrophe models, error variance is defined as the variance of the differences between the observed (or estimated) states and the mode of the distribution that most closely aligns with these values. This statistic assesses the goodness of fit of the model by quantifying the proportion of variance in the dependent variable that is explained by the independent variables. (Cobb and Watson, 1980; Grasman et al., 2009). Additionally, since the cusp density function doesn't involve nested models, evaluating its fit isn't based on differences in likelihood. Instead, alternative indicators such as Akaike information criterion (AIC) and Bayesian Information criterion (BIC) are employed. These fit indices, along with an AIC corrected for small sample sizes (AICc; Burnham et al., 2011), are computed by the summary function.

The Cusp Resilience Assessment (CUSPRA) approach, developed by Sguotti et al. (2023) was used to evaluate the findings of the cusp model and to allow for a meaningful commentary of the resilience in the studied areas. CUSPRA estimates how close a system is to a tipping point, which could lead to a shift into a new state or regime. CUSPRA provides a quantitative indicator of resilience (RA) that is directly applicable in ecosystem-based management settings. In CUSPRA, the resilience indicator (RA) is derived from two main components: the vertical distance (V) and the horizontal distance (H) within the 2D cusp model representation. The vertical distance (V) gauges the separation between the state variable and the region representing linear dynamics, driven by changes in the bifurcation variable (b). Meanwhile, the horizontal distance (H) measures the system's distance from the instability/cusp area, where three states are

possible, reflecting its proximity to a potential tipping point. These distances (V and H) are combined in an equation and then transformed using a hyperbolic tangent function to yield the overall resilience estimate (RA), which is scaled between 0 and 1. Resilience is low and the system is nearing a tipping point if RA is near zero, indicating that it is in a highly transient state. Alternatively, resilience is strong and the system is in a stable state far from a tipping point if RA is close to 1. Finally, CUSPRA also provides guidelines to determine when a cusp result is meaningful. These guidelines, based on the works of (Cobb, 1998) stipulate that: i) The pseudo-R^2 of the cusp model must be no less than 0,3, ii) the Delta AICc, which is the difference in the AICc values between the linear and the cusp models, must be positive. This means the cusp model should have a lower AICc than the linear model, iii) the percentage of points inside the bifurcation set must be no less than 10% and iv) the p-value of the state variable Y must not exceed 0.05.

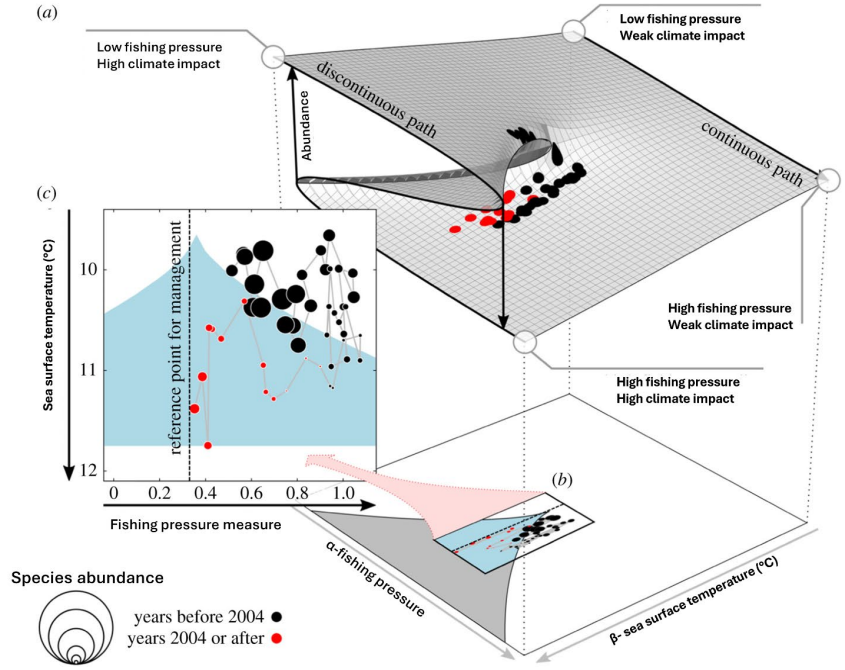

Figure 8.2. The stochastic cusp model provides a way to visualize species abundance dynamics influenced by two variables: fishing pressure (α) and sea surface temperature (β). In the typical three-dimensional representation (a), species abundance can follow either a continuous or discontinuous path depending on these variables. This can be simplified into a two-dimensional projection (b & c), where the bifurcation area, indicating where the marine community data resides, is shaded in gray and light blue. Here, species abundance is represented by filled dots, with the radius proportional to the values on the principal component (PC) axis used as input. Red dots specifically highlight the last 10 years of the time series. The vertical dotted line marks the current management target, and note that the y-axis is reversed, with temperature increasing downward. Adapted from Sguotti et al. (2019).

8.3. Results

Spatio-temporal changes in species abundances

The GSAs exhibited various trends in their community structures over time. GSA 1, 6, and 10 initially had diverse communities with various fish and cephalopod species, later shifting to simpler structures dominated by crustaceans and a few generalist fish. GSA 5 showed a replacement of smaller species by larger-bodied predators. GSA 7, and 8 also started with a mix of species but transitioned to crustacean-dominated communities after key years such as 2006, 2012, and 2015. GSA 9 showed fish-dominated communities initially, and significant shifts around the years 2002 and 2005. GSA 11 initially experienced high diversity with medium to large-sized

predators, moving towards a smaller set of species after 2009. The number of species considered varied according to the GSA analyzed.

In GSA 1, PCA with 174 species revealed that the first two PCs explained ~23.12% of total variance. PC1 is driven by cephalopods like *Sepia orbignyana*, *Loligo forbesii*, and small generalist predators such as *Serranus hepatus*. PC2 is driven by active predatory crustaceans like *Processa nouveli*, *Geryon longipes*, and *Squilla mantis*. Initially, the community was associated with a diverse array of species spanning all considered taxa. However, a noticeable change occurred after 2007, when the community was primarily influenced by a different set of species, predominantly crustaceans. In 2013-2014, the community was driven by a limited number of species, notably *Dardanus arrosor* and *Squilla mantis*. Subsequently, the community composition underwent another change, associated with a different diverse set of species (Fig. 8.3).

For GSA 5, the PCA was conducted with 190 species, and the first two PCs together had 35.2% explained variance. PC1 is mainly driven by bony fish, specifically ambush predators such as *Scorpaena notata* and *Scorpaena scrofa*. PC2's values are driven by the abundance of benthopelagic species such as the crustaceans *Plesionika edwardsii* and *Parapenaeus longirostris* as well as bony fish and elasmobranchs. Initially, the community is associated with a few species, such as the crustaceans *Solenocera membranacea* and *Calocaris macandreae*. After 2006, a more diverse set of mostly larger-bodied species, comprising all taxa, became prominent. The year 2017 stands out as only being driven by a few species such as *Hymenocephalus italicus* and *P. longirostris*.

In GSA 6, the PCA was conducted with 170 species, and the two axes had 29.9% explained variance. PC1 is driven by bathydemersal bony fish species such as *Symphurus nigrescens* as well as more shallow-living species such as *Lesuerigobius friesii*. PC2 is associated with the abundance of small crab species such as *Ethusa mascarone* and *D. arrosor*. At the start of the time series, the community was driven by the abundance of a few species like *Ophisurus serpens*. However, the years 2000-2002 and 2005 were more related with the abundance of fish like *Cepola macrophtalma* and crustaceans such as *Bathynectes maravigna* in PC2.The year 2006 was related to the abundance of the generalist fish *S. hepatus* and crustacean *Munida intermedia*. After 2006, the community is mostly associated with the abundance of a few generalist fish species like *Pagrus sp.*, *Capros aper* and *Glossanodon leioglossus*.

For GSA 7, the PCA was performed with 141 species,and the first two PCs explained ~29.9% of the variance. PC1 is mainly associated with crab species such as *Pagurus excavatus* and *Macropodia tenuirostris*. Contrarily, PC2 is driven by active predator and generalist fish species such as the small spotted catshark (*Scyliorhinus canicula*), Thor's scaldfish *Arnoglossus thori* and *S. hepatus*. In the start of the time series and until 2006, the community is mostly related to changes in the abundance of species like *Dicentrarchus labrax* and *M. merluccius* until 2011. After 2012, the community is solely driven by the fluctuations in abundance of invertebrates, mostly crustaceans like *P. longirostris* and *Liocarcinus depurator*. The year 2013 also seems to be associated with different invertebrate species such as *Inachus dorsettensis*.

In GSA 8, the PCA was conducted with 146 species, and the first two axes captured ~26.2% of the variance. PC1 is driven by deep-water crustaceans such as *Polycheles typhlops* as well as demersal fish predators like *Spondyliosoma cantharus* and *M. merluccius*. PC2 is solely driven by small bony fish like *Blennius ocellaris* and *S. hepatus*. At the start of the time series and until 2011, the community is mostly driven by changes in fish and cephalopod species like *Chelidonicthys cuculus*, and *S. orbignyana*. After 2012, the community is solely driven by the abundance of crustaceans like *Pagurus alatus* and *P. longirostris*, with the exception of 2015, driven by fish species like *Carapus acus*.

For GSA 9, the PCA was conducted with 145 species, and the two PCs captured ~26.2% of the variance. PC1 is driven by an assortment of species, such as the commercially important benthopelagic crustacean *P. longirostris*, the minute cephalopod *Rondeletia minor* and bony fish predators such as *Capros aper*. PC2 is instead only driven by larger predatory fish species, such as the elasmobranchs *Scyliorhinus.canicula*, *Etmopterus spinax* and the bony fish *S. notata*. The community seems to be driven by the fluctuations in abundance of fish species for all years. In 2002, the community was driven only by species in the Scorpaena genus. A change to another set of fish species driving the community was recorded for 2005.

In GSA 10, the PCA was performed with 141 species and the first two axes explained ~27.3% of the variance. Changes in abundance of the cephalopod *Sepia elegans* seem to drive PC1, while an assortment of fish and crustacean species like *Arnoglossus laterna* and *Plesionika acanthonotus* (respectively) also contributed to the axis. PC2 is principally driven by the crustacean predators *G.longipes* and *Spinolambrus macrochelos*, and to a smaller degree by the cephalopod *Sepietta neglecta* and small to medium sized bony fish and elasmobranch predators. At the start of the time series and for the years 2001-2003, the community is related to the abundance of fish and cephalopods like *A. laterna* and *S. neglecta* respectively. The rest of the years until 2017 are associated with an assortment of mostly crustacean species. After 2017, the community is only associated with the abundance of a handful of fish and cephalopod species like *Lepidopus caudatus* and *Todarodes sagittatus*, respectively. In 2021, the dominant species changes to the cephalopod *Todaropsis eblanae*.

Lastly, in GSA 11, the PCA was performed with 136 species and the first two PCs explained 33.2% of the variance. PC1 is driven by medium to large-sized bony fish and elasmobranch predators like the blackmouth catshark (*Galeus melastomus*), the speckled ray (*Raja polystigma*) and the Greater weever (*Trachinus draco*). PC2 again driven by medium to large-sized predators, this time bony fish like *S. cantharu*s and *Epigonus telescopus*. The community seems to be associated with the abundance of a diverse set of fish species like *M. merluccius* and *T. draco* until the year 2009. An exception is 2007, which is related with different fish species like *Chelidonichthys lucerna*. After 2009, the community is only associated with fluctuations in abundance of a few fish and cephalopod species like *Macroramphosus scolopax* and *L. forbesii* respectively.

Detection of abrupt changes in species abundance

The Bayesian change point analysis revealed significant changes in species abundances for 7 of the 8 studied GSAs (except GSA 9). Several GSAs shared common significant change points: GSAs 1 and 11 both experienced notable changes in 2006 and 2007, while GSA 9 saw significant shifts in 2003. Additionally, 2006 was a year of change in community abundance for GSAs 1, 6, and 10. The years around 2015 were also significant for GSAs 5 and 8.

Specifically, in GSA 1, the years 2006 and 2007 were identified as significant change points for the marine community. In GSA 5, 2006 and then 2015-2017 showed a significantly different species composition. For GSA 7, notable changes seem to have taken place in 2010. In GSA 8, the method detected that significant changes shaped the community abundances in the years 2011, 2014-2015. The BCP approach identified that in GSA 9, 2005 was a year of significant change in community abundances. In GSA 10, 2003 and 2019 seemed to harbor a change in the abundances of the marine community. Lastly, in GSA 11, 2006-2007 were detected as years of significant change in the species composition of the area (Fig 8.3).

For the average linkage clustering method, the years 2003 in GSAs 1 and 9, 2006 in GSAs 1, 6, and 10, and 2012, 2015, and 2017 in GSAs 7, 8, and 5 respectively, were associated with unique clusters. For the rest of the GSAs, a more uniform cluster arrangement was observed, with cluster groups displaying a linear progression over time. For the communities that had more than 2 Cluster groups, in GSA 5, the community seems to shift in terms of abundance after 2005 and until 2021, with 2017 having a unique composition. For GSA 7, the marine community changes significantly after 2010, with cluster 2 including the years 2010-2021 (except 2012). A similar pattern is depicted in GSA 8, where the years become associated with Cluster 2 after 2010 (except 2015). In GSA 10, the community significantly changed in 2003, after which all years until 2019 are associated with Cluster 2, followed by Cluster 3. Lastly, in GSA 11, with the exception of 2007, the community changes in terms of species abundance after 2012, belonging to Cluster 3 (Fig. 8.3).

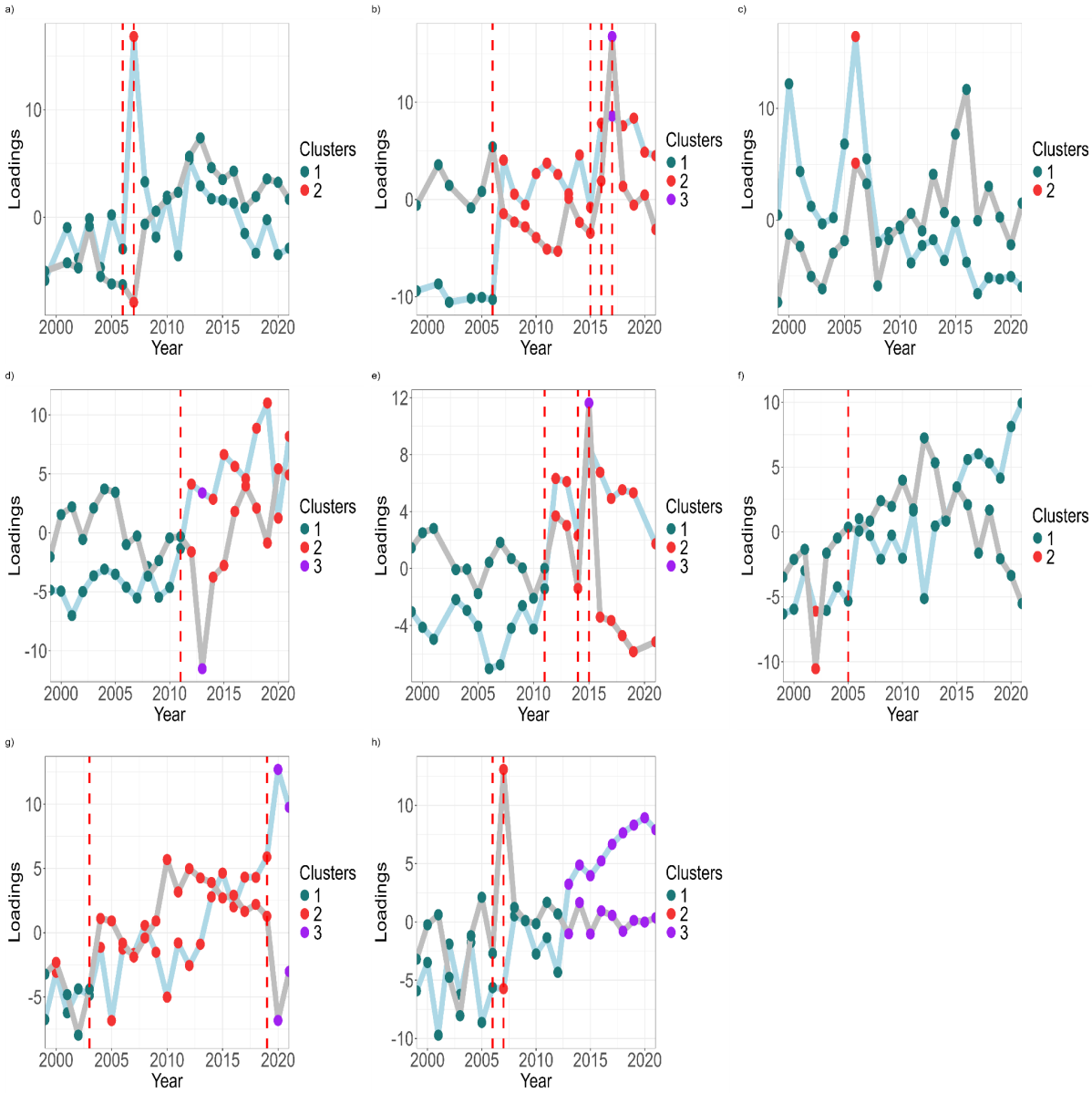

Figure 8.3. Changes in the loadings of PC1 and PC2 of a Principal Components Analysis based on species abundance over time in the areas under study. For every GSA, the loadings of PC1 and PC2 are shown, with colors denoting the various phases detected through cluster analysis. Axis 1 values are colored light-blue and axis 2 values are colored gray. The red-dotted lines represent the years where a significant change in the communities was detected by Bayesian Change Point (BCP) analysis.

Stochastic cusp modeling

For each GSA, all fitted stochastic cusp models had pseudo-R^2, AIC, BIC and AICc criteria superior to the ones reported by the linear models. The application of the cusp model found significant discontinuous behavior in 6 of the 8 GSAs, specifically in GSAs 1, 5, 6, 7, 8 and 10 (Fig. 8.4). The CUSP model describes diverse community dynamics across GSAs. GSA 1, 6 and 7 exhibit transitions between stable and unstable states, while GSA 5 and GSA 8 show prolonged instability. Additionally, GSA 10 shows potential for a reorganization event in recent years. Fishing pressure and SBT influence community dynamics differently across GSAs, with varying significance levels. The presence of potential hysteresis was also evident in GSA 7 and GSA 8.

In GSA 1, the entirety of the community, except for the years 2013-2014, resided inside the instability area for PC1, where multiple states are possible for the system. The results of the PCA depicted a constant turnover of the most important species per year, with the years 2013-2014 being associated with only a few species. This new state in PC1 was characterized by the prevalence of species like the crustaceans *D. arrosor* and *S. mantis*. However, the state collapsed after the year 2014 and the community again showed discontinuous behavior until the end of the time series. SBT and fishing pressure do not seem to be a significant predictor for the model ($p>0.05$). In GSA 5, where PC2 is kept, the community seems to exhibit discontinuous behavior for the entire time series. Specifically, a change from smaller-sized species to larger predators was noted starting from 2007, but the community did not seem to reach a new resilient state for the time series. SBT and fishing pressure were not significant predictors of community abundance in the model. In GSA 6, where PC1 was kept, the community entered the instability area for the first time in 2001, exiting in 2003 and once again inhabiting the bifurcation set for the years 2006-2008, until 2014, the rest of the years rest outside the instability. Initially, the community started from a resilient state where species like Ophisurus serpens were prevalent in the community, but from 2000-2002 and 2005, species such as *C. macrophtalma* and *B. maravigna* became dominant. In 2006, *S. hepatus* and *M. intermedia*, and in 2016, *E. mascarone* became prominent. However, after 2016, the community saw a decline in diversity, with only a few generalist fish species remaining, like *P. pagrus*, *C. aper*, and *G. leioglossus*. This is a potentially new resilient state, characterized by a few dominant species. The chosen drivers, especially fishing pressure, were significant predictors of species abundance in the model. For the PC1 in GSA 7, the community started in a highly resilient state in 1999. However, the community entered an instability phase in 2007. Except for 2010, all subsequent years fall within the bifurcation set. The community seems to exhibit a rotation of important fish species between the year groups 1999-2006 and 2006-2011. However, from 2012, crustacean species seem to replace fish as the most dominant taxonomic group. In 2010, the community briefly attained a resilient phase before again showing discontinuous behavior. Only fishing pressure was a significant predictor of species abundance for this model. Here, a return for the system to pre-shift conditions is likely not possible due to hysteresis, as briefly shown in the year 2017 when the driver forcing was lower than surrounding years and the community did not exit the instability area. The decrease needed to dislodge the community from the bifurcation set would also likely not be feasible, and even if SBT was significant to the model, it is unlikely to show a declining trend in the future. The PC2 did not pass the CUSPRA evaluation for this GSA. In GSA 8, the portion of the community captured in PC1 seems to be entirely within the instability area, except in 2021. Fishing pressure was a more significant predictor for the model but none of the two drivers were significant. For the PC2, the community starts in a resilient state, but after 2013 all the years reside in the instability area until the end of the time series. According to the PCA results, initially and until 2011, the community dynamics were primarily influenced by

changes in fish and cephalopod species. However, after 2012, there was a notable shift, and the community became predominantly driven by the abundance of crustaceans, particularly *P. alatus* and *P. longirostris*, with the exception of 2015, where fish species like *C. acus* were more dominant. SBT in PC2 was the sole significant predictor of species abundance for this model. Similarly to GSA 7, the future recovery of the pre-shift conditions after the regime shift is unlikely for the community depicted in the PC2 axis. Briefly experienced in 2018, where the SBT for the system subsided and the community remained in the bifurcation set. As a long term decline in SBT is not likely, and any reduction in fishing pressure, even if it was significant in the model, would not dislodge the system from the bifurcation set, the system will likely not recover its previous state. Lastly, in GSA 10, where only PC2 was kept, the community is in a resilient state for the majority of the time series, only entering the instability area after the year 2017. After 2017, the community is dominated by few fish and cephalopod species, potentially indicating the start of a reorganization event. The two chosen drivers were not significant predictors for this model.

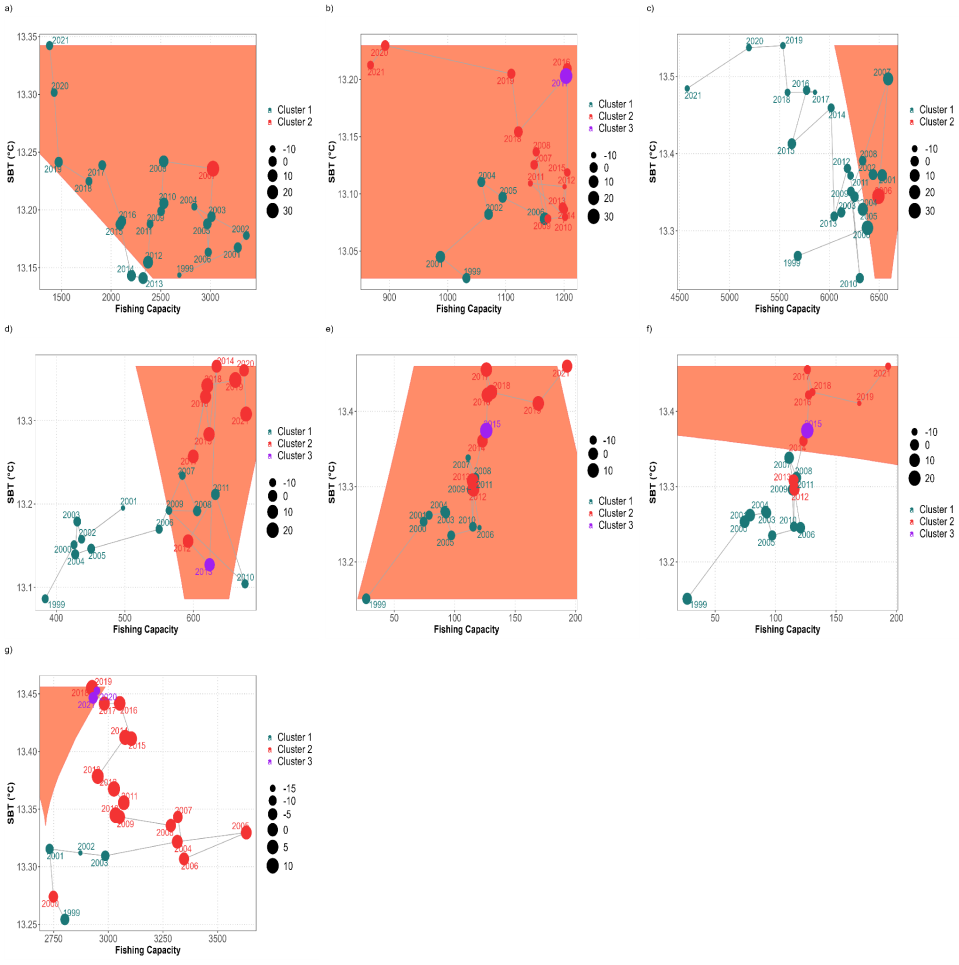

Figure 8.4. Results of the stochastic cusp models in the western Mediterranean Sea, obtained using PC axis scores as the state variable, modeled against Fishing Capacity (x-axis) and Sea Bottom Temperature (y-axis). Plots a and b show the first principal component (PC1) of GSA 1 and the second principal component (PC2) of GSA 5, respectively. Plots c and d represent the first principal components (PC1) of GSA 6 and GSA 7. Plots e and f display both the first and second principal components (PC1/PC2) of GSA 8. Lastly, plot g represents the second principal component (PC2) of GSA 10. The points for years in the plots are coloured after their respective cluster group, and their size depends on the values of the input axis. The orange-shaded region represents the instability area, situated between the tipping points where multiple equilibria exist. Geometrically, this area corresponds to the region beneath the cusp fold. Systems transitioning in and out of this area have either undergone or are on the brink of a regime shift. The x-y axes are not uniform between GSAs, as they fluctuate with the value ranges of the drivers in each area.

The resilience of the studied communities that showed discontinuous behavior was quantified with the resilience estimate (RA) and confirmed the qualitative finding of the cusp model (Fig. 8.5). The analysis showed varying levels of resilience across GSAs and years. GSA 1 and GSA 5 generally exhibited very low resilience, probably due to being close to crossing a tipping point. In contrast, GSA 7 and GSA 10 show a decrease in resilience, with fluctuations observed over time. GSA 6 shows situational resilience and is the only area where resilience increased over time. GSA 8 experiences consistently low resilience in PC1, while the part of the community explained in PC2 showed periods of lower resilience towards the end of the time series. The PC1 axis in GSA 1 did not exceed 0.16, indicating extremely low resilience for the generalist cephalopod and fish predators captured by the PCA component. For the PC2 axis, the invertebrate community, ~ 54% of years had RA values around 0.5 and higher, indicating a more resilient portion of the community. In GSA 5, the benthopelagic crustacean community captured in PC2 showed extremely low resilience, with most years having RA values <0.1. For GSA 6, the community described in the values of PC1, composed of bathydemersal and demersal bony fish, was only situationally unstable. Specifically, ~56% of years had RA values of around 0.5 and higher. In GSA 7, the community of mainly crab species, as shown by the cusp plot (Fig. 8.4), starts from extremely high resilience (RA > 0.75) and enters a low resilience phase after 2005, especially in the last years of the time series. The PC1 axis of GSA 8, mostly driven by deep-water crustaceans and demersal fish, has extremely low RA values for the entire time series (RA < 0.25). Contrarily, the PC2 axis, mostly driven by small bony fish, briefly shows lower resilience in 2007, while entering a very low resilience phase after 2014. Lastly, in GSA 10, the PC2 axis, primarily influenced by predatory crustaceans, small cephalopods, and both bony and elasmobranch fish, exhibited high resilience for most of the time series, particularly between 2004 and 2008. However, it declined to low resilience during the last four years of the time series.

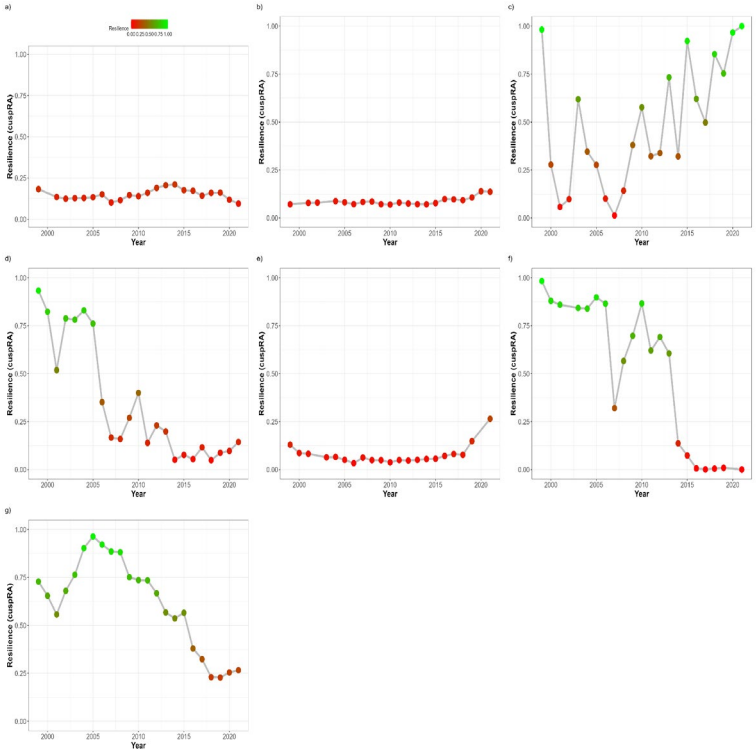

Figure 8.5. Resilience assessment values per year for each geographical sub-areas from the CUSPRA analysis. The color gradient ranges from red (closer to 0, indicating lower resilience) to green (closer to 1, indicating higher resilience), with intermediate colors representing varying levels of resilience.

8.4. Discussion

This work investigates for the first time whether abrupt, non-linear, and discontinuous shifts have impacted demersal marine communities in the Western Mediterranean Sea across multiple (2+) Geographical Sub-Areas (GSAs). By analyzing 361 species, it examines the influence of fishing pressure and environmental change as drivers of marine community dynamics. Additionally, the resilience of these areas is quantified using catastrophe-theory analysis, making a novel contribution to the current literature.

Limitations of the study

Certain limitations that were inherent to the dataset and methods were still present in this study. Temperature and fishing pressure were considered as the most important drivers of marine communities in our study, as they have been noted to have profound impacts on community dynamics (Brind'Amour et al., 2016; Sguotti et al., 2019). However, other combinations of drivers such as primary productivity, salinity and SST could have major influences on marine communities. For instance, Hidalgo et al (2022) showed productivity driven shifts in Northern Spain (GSA 6) and the Alboran Sea (GSA 1) areas. Future studies involving the cusp model should investigate other drivers or a combination of several drivers in order to best explain community dynamics (Blöcker et al., 2023). Climatic indices for phenomena such as the Atlantic Multidecadal Oscillation (AMO) or the North Atlantic Oscillation (NAO) should also be considered as drivers in areas with adequate forcing (Hidalgo et al., 2022; Sguotti et al., 2022b). The synergistic effect of multiple drivers is another limitation inherent to the cusp approach, as it can only consider the effect of two drivers for a system at a time. This limitation could be addressed by a study comparing different combinations of drivers and α-β variables for the cusp model for a marine community. Additionally, the study could not account for the fishing activities conducted in the studied areas from vessels who do not dock at any of the available 254 Mediterranean ports of the dataset. However, the effect of these vessels on the demersal communities is expected to be low, as French, Italian and Spanish vessels, which are the main commercial vessels conducting fishing activities in the area, were fully considered in this work (Bănaru et al., 2013). Moreover, while fishing capacity measures such as Gross tonnage are competent proxies of fishing pressure (Sguotti et al., 2022a), a study would greatly benefit from directly utilizing a fishing effort time series if available. Furthermore, in order to best capture community trends, a study should consider both pelagic and demersal species. This was not possible in this study, as MEDITS surveys are only conducted with bottom trawls and do not accurately capture pelagic species. Ideally, a study aiming to describe macro-scale trends in the studied marine communities would also benefit from a more expansive time series.

Detected and potential regime shifts in the Western Mediterranean Sea

The study revealed low resilience and discontinuous behavior in marine communities across multiple GSAs. For the Northern Alboran Sea (GSA 1), results partly matched previous reports of regime shifts due to environmental factors. In Northern Spain (GSA 6), findings aligned with extant research on a regime shift favoring short-lived species. In the Gulf of Lion (GSA 7), the observed patterns were consistent with past studies noting significant shifts. For the Balearic Islands (GSA 5), a regime shift is noted for the last 20 years for the first time. Similarly, in Corsica (GSA 8), new evidence of discontinuous behavior is also noted for the first time. In the Ligurian

Sea (GSA 9), no regime shift was detected for the demersal communities in this work and in available literature. The Tyrrhenian Sea (GSA 10) showed potential signs of an emerging regime shift. In the marine communities around Sardinia (GSA 11), no significant shifts were detected. In general, the differences in results compared to previous studies could generally be attributed to variations in study area scale, drivers considered, and time periods analyzed.

For the Northern Alboran Sea (GSA 1), Hidalgo et al. (2022) identified a regime shift in the year 2001 which forced the community into a new state. The regime shift favored species of short life span, such as benthic cephalopods and crustaceans. These species being favored suggested an increased efficiency of energy transfer to the benthic ecosystems. However, opportunistic fish species were not equally favored, likely due to their specialized behavior and trophic interactions, making them more sensitive to changes in productivity regimes. The current study similarly highlights discontinuous behavior in the marine community, and notes the dominance of benthic cephalopods. The CUSPRA analysis also showed that the community had extremely low resilience for all years (RA<0.2) (Fig 5), hinting at the reorganization taking place due to some species being favored over others. In the start of the time series, the community is already exhibiting discontinuous behavior and thus 2001 could not be determined as the start of the regime shift. However, this could be explained by the unavailability of year 2000 in the dataset, potentially obscuring a conclusion based on the association for the years 1999:2001. The new state of the community is also not visible in this work. Rather, the community remained inside the instability area until the end of the time series (2021). This discrepancy could be explained by the difference in the selected drivers and system descriptors, as Hidalgo et al (2022) used SST, chlorophyll-a concentration and biomass data to explain the community dynamics with a fold bifurcation approach.

For the Balearic Islands (GSA 5), a phase transition akin to a regime shift was identified by Hidalgo et al. (2009) in the population dynamics of the European Hake (M. merluccius) in two distinct instances, the first in 1980 and the second in 1995. The reason for these shifts is hypothesized to be a fluctuation in atmospheric conditions. In this work, the part of the community which was mainly driven by bony fish did not show significant discontinuous behavior. However, PC2, which was mostly driven by benthopelagic crustaceans and sharks, as well as macrourid fish species, showed discontinuous behavior and extremely low resilience for the entire time series, hinting at a potential future crossing of a tipping point. The change from smaller-sized species to larger predators noted from 2007 seems to not depend on any of the chosen drivers, and more scientific attention is required to explain the community's response.

In Northern Spain (GSA 6), a new state following a regime shift was detected in 2009 (Hidalgo et al., 2022). In this shift, caused by fluctuations in SST and primary productivity, commercial and non-commercial fish species exhibited synchronous patterns, with certain species declining sharply, especially opportunistic non-commercial and some periodic species. In contrast, commercial fish species were favored during this transition. The years 2007 and 2008 were noted to exhibit very low resilience but were unable to be definitively categorized as a regime year due to methodological limitations. Specifically, 2008 was considered the attractor year, forming the fold bifurcations, and the resilience of the system state was quantified based on the distance of each state from the attractor. In this work, the new stable state following the year 2009 is clearly detected in the cusp model. Discontinuous behavior is noted for the community starting from the years 2001-2002 as well as 2006-2008, confirming that the low resilience detected in the previous study for 2007 and 2008 was due to discontinuous dynamics.

In the Gulf of Lion (GSA 7), some studies report regime shifts in analyzed subsets of the pelagic and demersal communities in perhaps the most eminent example of a regime

shift occurring in the Western Mediterranean Sea (Bensebaini et al., 2022; Brosset et al., 2016; Feuilloley et al., 2020). Bensebaini et al (2022) noted that environmentally driven changes in the body condition of small pelagic fish (22 species) have been observed in the Gulf of Lion since 2008, leading to a significant fishery crisis. Demersal fish species were also noted to exhibit a common shift between 2006 and 2009. Feuilloley et al (2020) reported that over the past 30 years, the Gulf of Lion has experienced a rapid decline in chlorophyll-a concentration in the mid-2000s, a continuous rise in sea surface temperature, and a diminished nutrient output from the Rhone River. These environmental changes were hypothesized to have likely impacted the lower trophic levels, particularly plankton, thereby affecting the small pelagic fish community. In this work, based on 141 species in GSA 7, the community exhibits a similar pattern and enters the instability area after 2006, mostly driven by changes in fishing pressure instead of environmental conditions. From the PCA, a replacement of fish species by crustaceans was noted in this study. This replacement seems consistent with the impacted density and body condition of demersal fish observed by Bensebaini et al. (2022). The cusp model also detected the possible effects of hysteresis, hinting at a potentially irreversible change in the part of the community captured in PC1.

For the Island of Corsica (GSA 8), no regime shift has been reported in the local marine communities in the literature. In contrast, in the present study, both axes showed discontinuous behavior. Similarly to GSA 7, a replacement of fish and cephalopod species by crustaceans seemed to be taking place in GSA 8. First, PC1, mainly driven by deep-water crustaceans and demersal fish predators, almost always showed low resilience and discontinuous patterns. The dynamics of PC1 were not related to SBT or fishing pressure, thus more research is needed to understand the dynamics for this part of the community. The community trends explained in PC2, driven by smaller-sized bony fish, are initially resilient but showed discontinuous behavior and low resilience after 2013, mostly contingent on changes in temperature. The community captured in PC2 also exhibits signs of hysteresis, as a long-term decline in SBT is not likely, and the community will probably be unable to restore pre-shift conditions (Vargas-Yáñez et al., 2017).

In the Ligurian Sea (GSA 9), two local studies, conducted in the Mesco and Portofino reefs, found evidence of regime shifts occurring in the sessile invertebrate communities (Gatti et al., 2017, 2015). The regime shift in the Mesco reef at the end of the 1980s was primarily driven by a strong warming trend of surface water temperatures. The regime shift in the Portofino reef during the 1980s-1990s was also driven by the rapid warming of marine waters. In this study, no discontinuous behavior or regime shift was detected for the demersal communities of GSA 9.

For the Southern and central Tyrrhenian Sea (GSA 10) a shift event was reported for zooplanktonic communities in the Gulf of Naples (Mazzocchi et al., 2023). Two main temporal shifts were identified: one in 1985-87, and another after 2011, likely related to local atmospheric forcing. The shift significantly impacted various zooplankton species. However, the study did not address the direct impact on larger species like fish or crustaceans. In this study, the community was generally resilient but showed discontinuous behavior and low resilience for the last years of the time series (2018-2021), potentially marking the start of a regime shift. In 2011, the community seemed to be in a very resilient state. The differences in results between the aforementioned study and this research might be explained by various factors. First, the species and community considered were different, with the study by Mazzocchi et al (2023) considering zooplankton communities instead of demersal ones. Secondly, the spatial scale of the previous study (Gulf of Naples), did not permit the analysis of community behavior across

GSA 10. In the event of a very localized regime shift impacting the demersal fish and macro-invertebrate communities, its identification in this work would probably not be possible.

For the waters around Sardinia (GSA 11), a study by Bianchelli et al (2016) reports community behavior consistent with the after-effects of regime shift in 2014, such as loss of biodiversity and density transitions. The shift concerned the hard-bottom macroalgal meadows in the Mediterranean Sea, including Sardinia. The overgrazing by sea urchins, favored by the removal of their predators, played a significant role in the transition from productive macroalgal ecosystems to less diverse and less productive barren grounds dominated by encrusting coralline algae. However, these studies did not address whether this shift also impacted the demersal communities. Additionally, they did not consider an extensive time period or sampling range around Sardinian waters, making it difficult to conclude that a regime shift significantly affected the demersal communities of GSA 11. In the current study, no regime shifts or similar behaviors were detected for GSA 11. Specifically, the cusp model, which had an adequate R2 only in PC1, depicted a very resilient demersal community with no discontinuous behavior.

Lastly, the entirety of the Western Mediterranean Sea was shown to exhibit discontinuous dynamics at a basin scale. A study by Vasilakopoulos et al (2017) applied the Integrated Resilience Assessment (IRA) framework to analyze the response of Mediterranean marine communities to sea warming from 1985 to 2013. The study revealed multiple regime shifts and alternate basins of attraction in both the eastern and western Mediterranean systems, indicating discontinuous dynamics in response to environmental changes. Particularly, in the western Mediterranean Sea, the years 1999-2004 were noted to display behavior akin to a regime shift with hysteresis. In the current work, the years in the period 1999-2004 inhabited the bifurcation set for only 3 of the cusp models, and as such it cannot be said that the dynamics detected by Vasilakopoulos et al (2017) were also noted by our research. The differences between the results of the two studies are likely due to several factors: the scale of the study area, the drivers considered, and the time scale. The study by Vasilakopoulos et al (2017) covered the entire western basin, included SST as a driver, and spanned 35 years, whereas the current study focused on GSAs, did not include SST, and covered 23 years.

Implications for management and future outlook

We demonstrated that discontinuous, state-dependent dynamics are affecting at least half 6 out of the 8 GSAs considered in this study. The results of this work illustrate the utility of catastrophe model approaches in detecting both acknowledged and previously unnoticed shifts in warming and overexploited Mediterranean ecosystems. Over the few decades, several marine communities have undergone significant changes, often resulting in new structures that could be simpler than the previous state, potentially dominated by only a few species or a certain taxonomic group. For instance, some communities have become dominated by crustaceans, which replaced the old fish regime (Pauly et al., 1998; Steneck et al., 2013). In this work, similar replacement was noted for certain areas, such as GSA 7 and GSA 8, informing on the trends in community structuring. This does not only help in understanding the current ecosystem behavior in the studied areas, but also provides insights for fisheries management and conservation purposes. For example, in the case of the GSA 6, the results of the cusp model indicate that a slight reduction in fishing pressure in the years 2000, 2005 or 2008 could have pulled the system away from demonstrating discontinuous dynamics and into a more resilient state. In a contrasted example, the cusp model applied to the Balearic islands (GSA 5) describes that no feasible reduction in the fishing of commercially-important species like *P. edwardsii* and *P. longirostris* could have prevented the community from entering the instability area. Moreover, in areas

such as GSA 8, where the changes are temperature-dependent, restoring pre-reorganization conditions by managing fishing pressure is likely impossible, because short-term mitigation of ocean warming is not feasible (Steffen et al., 2011). Given the ever-increasing impacts of climate change and associated challenges like invasive species (IAS), information on community dynamics and vulnerability to regime shifts will be crucial for developing effective management strategies for marine resources and biodiversity in the Mediterranean Sea (Kourantidou et al., 2021).

8.5. References

Alheit, J., Möllmann, C., Dutz, J., Kornilovs, G., Loewe, P., Mohrholz, V., Wasmund, N., 2005. Synchronous ecological regime shifts in the central Baltic and the North Sea in the late 1980s. ICES J. Mar. Sci. 62, 1205–1215. https://doi.org/10.1016/j.icesjms.2005.04.024

Azzurro, E., Sbragaglia, V., Cerri, J., Bariche, M., Bolognini, L., Ben Souissi, J., Busoni, G., Coco, S., Chryssanthi, A., Fanelli, E., Ghanem, R., Garrabou, J., Gianni, F., Grati, F., Kolitari, J., Letterio, G., Lipej, L., Mazzoldi, C., Milone, N., Pannacciulli, F., Pešić, A., Samuel-Rhoads, Y., Saponari, L., Tomanic, J., Eda Topçu, N., Vargiu, G., Moschella, P., 2019. Climate change, biological invasions, and the shifting distribution of Mediterranean fishes: A large-scale survey based on local ecological knowledge. Glob. Change Biol. 25, 2779–2792. https://doi.org/10.1111/gcb.14670

Bănaru, D., Mellon-Duval, C., Roos, D., Bigot, J.-L., Souplet, A., Jadaud, A., Beaubrun, P., Fromentin, J.-M., 2013. Trophic structure in the Gulf of Lions marine ecosystem (north-western Mediterranean Sea) and fishing impacts. J. Mar. Syst. 111–112, 45–68. https://doi.org/10.1016/j.jmarsys.2012.09.010

Barry, D., Hartigan, J.A., 1993. A Bayesian Analysis for Change Point Problems. J. Am. Stat. Assoc. 88, 309–319. https://doi.org/10.1080/01621459.1993.10594323

Beaugrand, G., 2004. The North Sea regime shift: Evidence, causes, mechanisms and consequences. Prog. Oceanogr. 60, 245–262. https://doi.org/10.1016/j.pocean.2004.02.018

Beca-Carretero, P., Teichberg, M., Winters, G., Procaccini, G., Reuter, H., 2020. Projected Rapid Habitat Expansion of Tropical Seagrass Species in the Mediterranean Sea as Climate Change Progresses. Front. Plant Sci. 11, 555376. https://doi.org/10.3389/fpls.2020.555376

Bensebaini, C.M., Certain, G., Billet, N., Jadaud, A., Gourguet, S., Hattab, T., Fromentin, J.M., 2022. Interactions between demersal fish body condition and density during the regime shift of the Gulf of Lions. ICES J. Mar. Sci. 79, 1765–1776. https://doi.org/10.1093/icesjms/fsac106

Bertrand, J.A., Gil De Sola, L., Papaconstantinou, C., Relini, G., Souplet, A., 2002. The general specifications of the MEDITS surveys. Sci. Mar. 66, 9. https://doi.org/10.3989/scimar.2002.66s29

Bianchelli, S., Buschi, E., Danovaro, R., Pusceddu, A., 2016. Biodiversity loss and turnover in alternative states in the Mediterranean Sea: a case study on meiofauna. Sci. Rep. 6, 34544. https://doi.org/10.1038/srep34544

Blöcker, A., Sguotti, C., Möllmann, C., 2023. Discontinuous dynamics in North Sea cod Gadus morhua caused by ecosystem change. Mar. Ecol. Prog. Ser. 713, 133–149. https://doi.org/10.3354/meps14342

Brierley, A.S., Kingsford, M.J., 2009. Impacts of Climate Change on Marine Organisms and Ecosystems. Curr. Biol. 19, R602–R614. https://doi.org/10.1016/j.cub.2009.05.046

Brind'Amour, A., Rochet, M., Ordines, F., Hosack, G., Berthelé, O., Mérigot, B., Carbonara, P., Follesa, M., Jadaud, A., Lefkaditou, E., Maiorano, P., Peristeraki, P., Mannini, A., Rabiller, M., Spedicato, M., Tserpes, G., Trenkel, V., 2016. Environmental drivers explain regional variation of changes in fish and invertebrate functional groups across the Mediterranean Sea from 1994 to 2012. Mar. Ecol. Prog. Ser. 562, 19–35. https://doi.org/10.3354/meps11912

Brosset, P., Le Bourg, B., Costalago, D., Bănaru, D., Van Beveren, E., Bourdeix, J., Fromentin, J., Ménard, F., Saraux, C., 2016. Linking small pelagic dietary shifts with ecosystem changes in the Gulf of Lions. Mar. Ecol. Prog. Ser. 554, 157–171. https://doi.org/10.3354/meps11796

Burnham, K.P., Anderson, D.R., Huyvaert, K.P., 2011. AIC model selection and multimodel inference in behavioral ecology: some background, observations, and comparisons. Behav. Ecol. Sociobiol. 65, 23–35. https://doi.org/10.1007/s00265-010-1029-6

Capdevila, P., Stott, I., Oliveras Menor, I., Stouffer, D.B., Raimundo, R.L.G., White, H., Barbour, M., Salguero-Gómez, R., 2021. Reconciling resilience across ecological systems, species and subdisciplines. J. Ecol. 109, 3102–3113. https://doi.org/10.1111/1365-2745.13775

Charrad, M., Ghazzali, N., Boiteau, V., Niknafs, A., 2014. NbClust : An R Package for Determining the Relevant Number of Clusters in a Data Set. J. Stat. Softw. 61. https://doi.org/10.18637/jss.v061.i06

Cobb, L., 1998. An Introduction to Cusp Surface Analysis. (Technical report). Aetheling Consultants, Louisville, CO, USA.

Cobb, L., 1981. Parameter estimation for the cusp catastrophe model. Behav. Sci. 26, 75–78. https://doi.org/10.1002/bs.3830260107

Cobb, L., Watson, B., 1980. Statistical catastrophe theory: An overview. Math. Model. 1, 311–317. https://doi.org/10.1016/0270-0255(80)90041-X

Dakos, V., Carpenter, S.R., Van Nes, E.H., Scheffer, M., 2015. Resilience indicators: prospects and limitations for early warnings of regime shifts. Philos. Trans. R. Soc. B Biol. Sci. 370, 20130263. https://doi.org/10.1098/rstb.2013.0263

Damalas, D., Sgardeli, V., Vasilakopoulos, P., Tserpes, G., Maravelias, C., 2021. Evidence of climate-driven regime shifts in the Aegean Sea's demersal resources: A study spanning six decades. Ecol. Evol. 11, 16951–16971. https://doi.org/10.1002/ece3.8330

Delnevo, N., Piotti, A., Carbognani, M., Van Etten, E.J., Stock, W.D., Field, D.L., Byrne, M., 2021. Genetic and ecological consequences of recent habitat fragmentation in a narrow endemic plant species within an urban context. Biodivers. Conserv. 30, 3457–3478. https://doi.org/10.1007/s10531-021-02256-x

Diks, C., Wang, J., 2016. Can a stochastic cusp catastrophe model explain housing market crashes? J. Econ. Dyn. Control 69, 68–88. https://doi.org/10.1016/j.jedc.2016.05.008

Erdman, C., Emerson, J.W., 2007. bcp : An R Package for Performing a Bayesian Analysis of Change Point Problems. J. Stat. Softw. 23. https://doi.org/10.18637/jss.v023.i03

Escudier, R., Clementi, E., Omar, M., Cipollone, A., Pistoia, J., Aydogdu, A., Drudi, M., Grandi, A., Lyubartsev, V., Lecci, R., Cretí, S., Masina, S., Coppini, G., Pinardi, N., 2020. Mediterranean Sea Physical Reanalysis (CMEMS MED-Currents, E3R1 system): MEDSEA_MULTIYEAR_PHY_006_004. https://doi.org/10.25423/CMCC/MEDSEA_MULTIYEAR_PHY_006_004_E3R1

Feuilloley, G., Fromentin, J.-M., Stemmann, L., Demarcq, H., Estournel, C., Saraux, C., 2020. Concomitant changes in the environment and small pelagic fish community of the Gulf of Lions. Prog. Oceanogr. 186, 102375. https://doi.org/10.1016/j.pocean.2020.102375

Gatti, G., Bianchi, C.N., Montefalcone, M., Venturini, S., Diviacco, G., Morri, C., 2017. Observational information on a temperate reef community helps understanding the marine climate and ecosystem shift of the 1980–90s. Mar. Pollut. Bull. 114, 528–538. https://doi.org/10.1016/j.marpolbul.2016.10.022

Gatti, G., Bianchi, C.N., Parravicini, V., Rovere, A., Peirano, A., Montefalcone, M., Massa, F., Morri, C., 2015. Ecological Change, Sliding Baselines and the Importance of Historical Data: Lessons from Combing Observational and Quantitative Data on a Temperate Reef Over 70 Years. PLOS ONE 10, e0118581. https://doi.org/10.1371/journal.pone.0118581

Grasman, R.P.P.P., Maas, H.L.J.V.D., Wagenmakers, E.-J., 2009. Fitting the Cusp Catastrophe in R : A cusp Package Primer. J. Stat. Softw. 32. https://doi.org/10.18637/jss.v032.i08

Heinze, C., Blenckner, T., Martins, H., Rusiecka, D., Döscher, R., Gehlen, M., Gruber, N., Holland, E., Hov, Ø., Joos, F., Matthews, J.B.R., Rødven, R., Wilson, S., 2021. The quiet crossing of ocean tipping points. Proc. Natl. Acad. Sci. 118, e2008478118. https://doi.org/10.1073/pnas.2008478118

Hidalgo, M., Massutí, E., Guijarro, B., Moranta, J., Ciannelli, L., Lloret, J., Oliver, P., Stenseth, N.C., 2009. Population effects and changes in life history traits in relation to phase transitions induced by long-term fishery harvesting: European hake (Merluccius merluccius) off the Balearic Islands. Can. J. Fish. Aquat. Sci. 66, 1355–1370. https://doi.org/10.1139/F09-081

Hidalgo, M., Vasilakopoulos, P., García-Ruiz, C., Esteban, A., López-López, L., García-Gorriz, E., 2022. Resilience dynamics and productivity-driven shifts in the marine communities of the Western Mediterranean Sea. J. Anim. Ecol. 91, 470–483. https://doi.org/10.1111/1365-2656.13648

IPBES, 2019. Summary for policymakers of the global assessment report on biodiversity and ecosystem services. Zenodo. https://doi.org/10.5281/ZENODO.3553458

Ipcc, 2022. The Ocean and Cryosphere in a Changing Climate: Special Report of the Intergovernmental Panel on Climate Change, 1st ed. Cambridge University Press. https://doi.org/10.1017/9781009157964

Johnson, C.R., Dudgeon, S., 2024. Understanding change in benthic marine systems. Ann. Bot. 133, 131–144. https://doi.org/10.1093/aob/mcad187

Jungblut, S., Liebich, V., Bode, M. (Eds.), 2018. YOUMARES 8 – Oceans Across Boundaries: Learning from each other: Proceedings of the 2017 conference for YOUng MARine RESearchers in Kiel, Germany. Springer International Publishing, Cham. https://doi.org/10.1007/978-3-319-93284-2

Kourantidou, M., Cuthbert, R.N., Haubrock, P.J., Novoa, A., Taylor, N.G., Leroy, B., Capinha, C., Renault, D., Angulo, E., Diagne, C., Courchamp, F., 2021. Economic costs of invasive alien species in the Mediterranean basin. NeoBiota 67, 427–458. https://doi.org/10.3897/neobiota.67.58926

Kroeker, K.J., Bell, L.E., Donham, E.M., Hoshijima, U., Lummis, S., Toy, J.A., Willis-Norton, E., 2020. Ecological change in dynamic environments: Accounting for temporal environmental variability in studies of ocean change biology. Glob. Change Biol. 26, 54–67. https://doi.org/10.1111/gcb.14868

Legendre, P., Gallagher, E.D., 2001. Ecologically meaningful transformations for ordination of species data. Oecologia 129, 271–280. https://doi.org/10.1007/s004420100716

Liu, X., Li, D., Ma, M., Szymanski, B.K., Stanley, H.E., Gao, J., 2022. Network resilience. Phys. Rep. 971, 1–108. https://doi.org/10.1016/j.physrep.2022.04.002

Lynam, C.P., Llope, M., Möllmann, C., Helaouët, P., Bayliss-Brown, G.A., Stenseth, N.C., 2017. Interaction between top-down and bottom-up control in marine food webs. Proc. Natl. Acad. Sci. 114, 1952–1957. https://doi.org/10.1073/pnas.1621037114

Mazzocchi, M.G., Di Capua, I., Kokoszka, F., Margiotta, F., d'Alcalà, M.R., Sarno, D., Zingone, A., Licandro, P., 2023. Coastal mesozooplankton respond to decadal environmental changes via community restructuring. Mar. Ecol. 44, e12746. https://doi.org/10.1111/maec.12746

Melis, R., Ceccherelli, G., Piazzi, L., Rustici, M., 2019. Macroalgal forests and sea urchin barrens: Structural complexity loss, fisheries exploitation and catastrophic regime shifts. Ecol. Complex. 37, 32–37. https://doi.org/10.1016/j.ecocom.2018.12.005

Mérigot, B., Durbec, J.-P., Gaertner, J.-C., 2010. On goodness-of-fit measure for dendrogram-based analyses. Ecology 91, 1850–1859. https://doi.org/10.1890/09-1387.1

Möllmann, C., Cormon, X., Funk, S., Otto, S.A., Schmidt, J.O., Schwermer, H., Sguotti, C., Voss, R., Quaas, M., 2021. Tipping point realized in cod fishery. Sci. Rep. 11, 14259. https://doi.org/10.1038/s41598-021-93843-z

Pauly, D., Christensen, V., Dalsgaard, J., Froese, R., Torres, F., 1998. Fishing Down Marine Food Webs. Science 279, 860–863. https://doi.org/10.1126/science.279.5352.860

Peleg, O., Guy-Haim, T., Yeruham, E., Silverman, J., Rilov, G., 2020. Tropicalization may invert trophic state and carbon budget of shallow temperate rocky reefs. J. Ecol. 108, 844–854. https://doi.org/10.1111/1365-2745.13329

Pennino, M.G., Muñoz, F., Conesa, D., López-Quílez, A., Bellido, J.M., 2013. Modeling sensitive elasmobranch habitats. J. Sea Res. 83, 209–218. https://doi.org/10.1016/j.seares.2013.03.005

Piroddi, C., Colloca, F., Tsikliras, A.C., 2020. The living marine resources in the Mediterranean Sea Large Marine Ecosystem. Environ. Dev. 36, 100555. https://doi.org/10.1016/j.envdev.2020.100555

Poincaré, H., 1885. Sur l'équilibre d'une masse fluide animée d'un mouvement de rotation. Bull. Astron. 2, 109–118. https://doi.org/10.3406/bastr.1885.2592

Sage, R.F., 2020. Global change biology: A primer. Glob. Change Biol. 26, 3–30. https://doi.org/10.1111/gcb.14893

Saraux, C., Van Beveren, E., Brosset, P., Queiros, Q., Bourdeix, J.-H., Dutto, G., Gasset, E., Jac, C., Bonhommeau, S., Fromentin, J.-M., 2019. Small pelagic fish dynamics: A review of mechanisms in the Gulf of Lions. Deep Sea Res. Part II Top. Stud. Oceanogr. 159, 52–61. https://doi.org/10.1016/j.dsr2.2018.02.010

Scheffer, M., Carpenter, S., Foley, J.A., Folke, C., Walker, B., 2001. Catastrophic shifts in ecosystems. Nature 413, 591–596. https://doi.org/10.1038/35098000

Scheffer, M., Carpenter, S.R., 2003. Catastrophic regime shifts in ecosystems: linking theory to observation. Trends Ecol. Evol. 18, 648–656. https://doi.org/10.1016/j.tree.2003.09.002

Sguotti, C., Bischoff, A., Conversi, A., Mazzoldi, C., Möllmann, C., Barausse, A., 2022a. Stable landings mask irreversible community reorganizations in an overexploited Mediterranean ecosystem. J. Anim. Ecol. 91, 2465–2479. https://doi.org/10.1111/1365-2656.13831

Sguotti, C., Blöcker, A.M., Färber, L., Blanz, B., Cormier, R., Diekmann, R., Letschert, J., Rambo, H., Stollberg, N., Stelzenmüller, V., Stier, A.C., Möllmann, C., 2022b. Irreversibility of regime shifts in the North Sea. Front. Mar. Sci. 9, 945204. https://doi.org/10.3389/fmars.2022.945204

Sguotti, C., Otto, S.A., Frelat, R., Langbehn, T.J., Ryberg, M.P., Lindegren, M., Durant, J.M., Chr. Stenseth, N., Möllmann, C., 2019. Catastrophic dynamics limit Atlantic cod recovery. Proc. R. Soc. B Biol. Sci. 286, 20182877. https://doi.org/10.1098/rspb.2018.2877

Sguotti, C., Vasilakopoulos, P., Tzanatos, E., Frelat, R., 2023. Resilience assessment in complex natural systems. https://doi.org/10.1101/2023.09.12.557305

Soto-Navarro, J., Jordá, G., Amores, A., Cabos, W., Somot, S., Sevault, F., Macías, D., Djurdjevic, V., Sannino, G., Li, L., Sein, D., 2020. Evolution of Mediterranean Sea water properties under climate change scenarios in the Med-CORDEX ensemble. Clim. Dyn. 54, 2135–2165. https://doi.org/10.1007/s00382-019-05105-4

Spedicato, M.T., Massutí, E., Mérigot, B., Tserpes, G., Jadaud, A., Relini, G., 2020. The MEDITS trawl survey specifications in an ecosystem approach to fishery management. Sci. Mar. 83, 9. https://doi.org/10.3989/scimar.04915.11X

Steffen, W., Grinevald, J., Crutzen, P., McNeill, J., 2011. The Anthropocene: conceptual and historical perspectives. Philos. Trans. R. Soc. Math. Phys. Eng. Sci. 369, 842–867. https://doi.org/10.1098/rsta.2010.0327

Steneck, R.S., Leland, A., McNaught, D.C., Vavrinec, J., 2013. Ecosystem Flips, Locks, and Feedbacks: the Lasting Effects of Fisheries on Maine's Kelp Forest Ecosystem. Bull. Mar. Sci. 89, 31–55. https://doi.org/10.5343/bms.2011.1148

Stewart, I., 1983. Elementary catastrophe theory. IEEE Trans. Circuits Syst. 30, 578–586. https://doi.org/10.1109/TCS.1983.1085392

Theodorou, P., 2022. The effects of urbanisation on ecological interactions. Curr. Opin. Insect Sci. 52, 100922. https://doi.org/10.1016/j.cois.2022.100922

Thom, R., 2018. Structural Stability And Morphogenesis. CRC Press.

Thom, R., 1977. Structural Stability, Catastrophe Theory, and Applied Mathematics. SIAM Rev. 19, 189–201. https://doi.org/10.1137/1019036

Thom, R., 1974. Stabilité structurelle et morphogenèse. Poetics 3, 7–19. https://doi.org/10.1016/0304-422X(74)90010-2

Urruty, N., Tailliez-Lefebvre, D., Huyghe, C., 2016. Stability, robustness, vulnerability and resilience of agricultural systems. A review. Agron. Sustain. Dev. 36, 15. https://doi.org/10.1007/s13593-015-0347-5

Van Meerbeek, K., Jucker, T., Svenning, J., 2021. Unifying the concepts of stability and resilience in ecology. J. Ecol. 109, 3114–3132. https://doi.org/10.1111/1365-2745.13651

Van Moorsel, S.J., Thébault, E., Radchuk, V., Narwani, A., Montoya, J.M., Dakos, V., Holmes, M., De Laender, F., Pennekamp, F., 2023. Predicting effects of multiple interacting global change drivers across trophic levels. Glob. Change Biol. 29, 1223–1238. https://doi.org/10.1111/gcb.16548

Vargas-Yáñez, M., García-Martínez, M.C., Moya, F., Balbín, R., López-Jurado, J.L., Serra, M., Zunino, P., Pascual, J., Salat, J., 2017. Updating temperature and salinity mean values and trends in the Western Mediterranean: The RADMED project. Prog. Oceanogr. 157, 27–46. https://doi.org/10.1016/j.pocean.2017.09.004

Vasilakopoulos, P., Marshall, C.T., 2015. Resilience and tipping points of an exploited fish population over six decades. Glob. Change Biol. 21, 1834–1847. https://doi.org/10.1111/gcb.12845

Vasilakopoulos, P., Raitsos, D.E., Tzanatos, E., Maravelias, C.D., 2017. Resilience and regime shifts in a marine biodiversity hotspot. Sci. Rep. 7, 13647. https://doi.org/10.1038/s41598-017-13852-9

Wang, S., Cui, Z., Lin, J., Xie, J., Su, K., 2022. The coupling relationship between urbanization and ecological resilience in the Pearl River Delta. J. Geogr. Sci. 32, 44–64. https://doi.org/10.1007/s11442-022-1935-3.

9 Developing a roadmap for marine biodiversity: past, present and near future change in plankton, benthos and fish assemblages

Authors: Elena Couce, Lily Greig, Georg H. Engelhard, John K. Pinnegar, Keith M. Cooper, Pierre Hélaouët, Laurene Pecuchet, Myron A. Peck, Martin Lindegren, Murray S.A. Thompson

9.1. Introduction

The study Global biodiversity is undergoing rapid transformation under intensifying human pressures and climate change (Brondízio et al. 2019) with marine ecosystems facing particularly acute risks (Chust et al. 2024; Poloczanska et al. 2013). These biodiversity changes have undermined essential ecosystem functions and services for human wellbeing (Brondízio et al. 2019; Cardinale et al. 2012; Halpern et al. 2015; Jouffray et al. 2020) with projected trends that could jeopardize global food security (du Pontavice et al. 2020; Pecl et al. 2017). Despite this wealth of evidence of climate-driven changes in marine biodiversity, little is known about how responses differ across co-occurring assemblages, e.g., phytoplankton, zooplankton, benthos and fish. This is partly due to the scarcity of high-quality biodiversity data (Cardinale et al. 2018) and biases caused by substantial differences in the spatial and temporal distribution of survey data across different assemblages (Dornales et al. 2019). Large-scale assessments, therefore, typically either combine biodiversity trends from multiple assemblages into a single overall estimate (Poloczanska et al. 2013; Chust et al. 2024; Molinos et al. 2016) or focus on change within an assemblage (Benedetti et al. 2021; Fernandes et al. 2013; Kléparski et al. 2023), often relying on indicator species, such as taxa of commercial interest or conservation concern (Couce, Pinnegar, & Townhill 2025; Jones & Cheung 2015; Townhill et al. 2023). Biodiversity assessments need to go beyond indicator species to gauge a more complete picture of change which can be multidimensional and scale-dependent (Chao et al. 2012; Chase et al. 2018; Whittaker, 1960). Thus, significant knowledge gaps remain in understanding past, present and future climate change effects on biodiversity within and between assemblages because the contribution of many species has not been quantified.

Among the species whose contributions remain poorly quantified, rare species are particularly overlooked because their distributions are poorly understood (Jones & Cheung 2015; Townhill et al. 2023; but see Couce, Pinnegar, & Townhill 2025 for distribution models of rarer taxa), yet they contribute disproportionately to species richness (Fisher, Corbet & Williams 1943; McGill et al. 2007; Preston, 1948) and play crucial roles in ecosystems. For example, they can enhance ecosystem stability and resilience by contributing unique combinations of traits (Kunze et al. 2025; Mouillot et al. 2013) and by providing weak links in food webs (Gellner & McCann, 2016; McCann, Hastings & Huxel, 1998; Säterberg et al. 2019). Determining how biodiversity is changing within and between assemblages in a systematic way, including the contributions of rare species, is critical because shifts in the distribution of diversity in food webs, from resources to consumers, constrain nutrient uptake and the efficiency of biomass production (Cardinale et al. 2012; Wang & Brose, 2018).

Rarefaction and extrapolation based on Hill numbers provide a unified framework to quantify biodiversity across multiple dimensions and spatial scales (Chao et al. 2014; Chao et al. 2023). This includes α-diversity (sample-level species richness), β-diversity (regional differences in species composition among samples), and γ-diversity (regional species richness). Comparing

Hill numbers of order 0 and 2, which estimate total species richness and the number of dominant species, respectively, allows us to quantify the relative contribution of rare species. Here we conduct the first systematic, multidimensional assessment of biodiversity change across four co-occurring marine assemblages in the Northeast Atlantic: phytoplankton, zooplankton, benthos (i.e. seafloor-inhabiting macroinvertebrates), and fish. Using extensive long-term survey data, we reconstruct past and present biodiversity patterns for each assemblage and train Bayesian additive regression trees (BART) models to project changes from 1993 to 2030. We expected climate change to (i) drive consistent increases in γ-diversity across assemblages, because warming generally increases species richness in temperate ecosystems through poleward migration. We further anticipated (ii) differences in the rate and magnitude of change among assemblages, reflecting contrasts in mobility, life-history traits, and dispersal capacity. Finally, we expected (iii) these shifts to be driven by increases in rare species and declines in common species, as climate migrants prosper. By developing predictive biodiversity indicators that capture climate-driven change across multiple dimensions and spatial scales, we provide an integrated framework to inform conservation strategies and guide progress towards international biodiversity targets under shifting baselines.

9.2. Material and Methods

The study Survey data

Phytoplankton and zooplankton data were obtained from the Continuous Plankton Recorder survey (**https://doi.org/10.17031/668cf6b093d22**; accessed 9 July 2024). Samples were collected using a Continuous Plankton Recorder that is towed behind ships and continuously filters plankton from the water column using a moving band of silk gauze (270 µm mesh) at a depth of around 7 m (see Batten et al. 2003). Observations with unique spatial and temporal information correspond to a tow length of approximately 10 nautical miles and a volume of 3 m3 of seawater (henceforth, plankton samples). Because it is unfeasible to count all phytoplankton in each sample, sample counts per taxa were derived by statistically resampling to estimate mean sample-level abundance. Phytoplankton counts were then rescaled to approximate the initial subsample counts (i.e. with many singletons which are typical of community samples and are required to estimate the effective number of species, see below) by dividing each taxa count by the lowest taxa count for that sample and rounded to the nearest whole number. Zooplankton counts were estimated at the sample-level using organisms ≥ 2 mm meaning no statistical resampling nor rescaling was required. We make use of phytoplankton (n taxa = 173) and zooplankton (n taxa = 119) data available from 1980-2021 for the northeast Atlantic downloaded on 09/07/2024, including information from 114925 samples (Figure S9.10). Benthic macroinvertebrate data were sourced from the OneBenthic database (https://rconnect.cefas.co.uk/onebenthic_portal/; accessed 7 November 2024), with all publicly available data downloaded on 7 November 2024, including information on 3,700 taxa from 29,403 comparable grab and core samples (henceforth benthos samples, i.e., sampled using a 0.1 m² grab or core and processed using a 1 mm sieve) collected between 1985-2023 from shelf waters of the northeast Atlantic (Figure S10). Fish observations from otter trawl surveys from across the northeast Atlantic spanning years 1983-2020 and including 513 taxa were obtained from Lynam & Ribeiro (2022) who collated multiple surveys stored on the ICES database of trawl surveys (DATRAS). Hauls (henceforth, fish samples) had a mean swept area of 0.7 km2 (sd = 0.02; with a mean duration of 31.7 minutes).

All data on biota incorporate taxonomic information from the World Register of Marine Species (WoRMS Editorial Board, 2024), with each taxon uniquely identified by its 'aphiaID', allowing data to be outputted using standardized nomenclature. Taxonomic resolution varied considerably among assemblages. Phytoplankton were identified with the lowest precision (15% to species, 46% to genus, none to family, and 39% only to class or higher). Most zooplankton records were resolved to species (69% to species, 6% to genus, 6% to family, and 19% to class or above), this precision was higher for benthic invertebrates (79% to species, 14% to genus, 3% to family, and 4% to class or higher). Fish achieved the highest resolution, with nearly all records (99%) identified to species and only 1% to genus or higher. Given this variability, we used the highest available taxonomic resolution for phytoplankton, zooplankton, and benthos, retaining records identified to species, genus, and family, while restricting fish to species-level data. This approach maximizes the retention of both taxonomic detail and abundance information across assemblages, while acknowledging that diversity indices, particularly for phytoplankton, capture broader taxonomic richness rather than species richness alone.

Biodiversity estimation

Rarefaction and extrapolation based on Hill numbers provide a unified framework for estimating α-, β-, and γ-diversity that corrects for biases arising from variable sample sizes and sampling effort, and is applicable across different assemblages (Chao et al. 2014; Chao et al. 2023; Schindler, Armstrong & Reed, 2015). Diversity estimates were all generated per assemblage. To estimate α-diversity, we calculated species richness for each sample at twice the mean sample count for that assemblage (20 for phytoplankton, 42 for zooplankton, 365 for benthos, and 15933 for fish) using individual-based rarefaction and extrapolation. γ-diversity was estimated for the time and location of each sample by incorporating nine surrounding samples (selected at random where more than 9 were available) collected within 6 months and within 75 km of that sample and applying sample-based rarefaction and extrapolation to 20 samples. Where <9 surrounding samples were available, γ-diversity estimates were dropped because variation in the number of samples can incorporate more or less ß-diversity, biasing estimates (Thompson et al. 2021). ß-diversity is an estimate of the effective number of communities in a given area and was calculated as:

$$ß = \gamma / \bar{\alpha} \qquad (1)$$

where $\bar{\alpha}$ represents mean α-diversity (Jost, 2007; Tuomisto, 2010).

α-, ß-, and γ-diversity estimates were made for Hill number 0 (the effective number of species; i.e. species richness). These were supplemented with γ-diversity estimates made for Hill number 2 (the effective number of dominant species; i.e. inverse Simpson index). Moving from Hill number 0 to 2 down weights the importance of rare species, hence the contribution of rare species can be assessed by comparing across them. We assess the proportion p of rare species as follows:

$$p = 1 - (\gamma_2 / \gamma_0) \qquad (2)$$

where γ_2 represents γ-diversity of dominant species and γ_0 represents γ-diversity of all species. Because the BART models for γ_0and γ_2were fitted separately, they do not enforce the math-

ematical constraint $\gamma_0 \geq \gamma_2$ everywhere, which can occasionally yield implausible rare-species fractions slightly outside the admissible interval [0,1]. These artefacts were extremely uncommon and very small in magnitude: clipped values were almost exclusively minor negative deviations close to zero (median –0.02 to –0.11), and on average only 0.00 – 0.08% of grid cells per assemblage and scenario showed any out-of-range values (maximum 0.07 – 0.70%). All values were clipped to [0,1]prior to computing temporal averages and rates of change. Given their rarity and minimal size, these corrections have no influence on the results. All analyses for the study were performed using the R Statistical Software (R Core Team, 2024), specifically here, all rarefaction and extrapolation analyses were conducted using the R package iNEXT (Hsieh et al. 2016). We provide a worked example of how we estimated diversity here: **https://github.com/MurraySAThompson/biodiversity-estimation-across-spatial-scales-and-Hill-numbers**.

Environmental predictors

Statistically downscaled CMIP6 monthly projections of temperature, salinity, and oxygen for the time period 1993-2100 (Kristiansen, Butenschön, & Peck, 2024) provided temporally varying environmental data. This 1/12 degree downscaled dataset was re-gridded onto a 5 x 5 km grid, and annual averages were calculated. For each grid cell and each year, the standard deviations of all monthly values of temperature, oxygen and salinity within a 75-km spatial radius were also calculated, to include intra-annual environmental heterogeneity of the physical variables within the model known to be important in marine ecosystem diversity assessments (Thompson et al. 2021; Thompson et al. 2023). The static variables used were bathymetry (from the General Bathymetric Chart of the Oceans GEBCO; www.gebco.net, at 15s resolution), substrate composition (Wilson et al. 2018), shear stress (Bricheno, Wolf & Aldridge, 2015; Burchard & Bolding, 2002; mean of the annual averages in the 7 year period 1975-1981; and the standard deviation of the annual averages within this period), and finally, distance to coast.

For the phytoplankton and zooplankton assemblages, sea surface environmental variables were used (and other variables associated with the seafloor were not used, i.e. shear stress and its standard deviation and sand, mud and gravel percentage), whilst for the benthos and fish, seabed estimates of the variables were selected. Samples were then linked to the environmental data using their date and spatial information. Where there were multiple samples for an assemblage per grid cell per year, mean estimates were calculated for each of the biodiversity indices. The final number of grid cells with diversity estimates were 23345, 25321, 8505 and 23320 for phytoplankton, zooplankton, benthos and fish assemblages, respectively.

Selection of environmental predictors and biodiversity indices

If an environmental variable was highly correlated with another (R^2>0.7) the less ecologically relevant one was excluded. Because sample locations differed among assemblages, correlations between environmental predictors also varied, resulting in assemblage-specific sets of explanatory variables (Fig. S9.8-S9.9). After removing highly correlated predictors, the variables included in the BART models for phytoplankton and zooplankton were sea surface temperature and salinity, bathymetry and distance to coast; for benthos, sea bottom oxygen and its standard deviation, sea bottom salinity and temperature, shear stress and its standard deviation, mud and sand percentage, bathymetry, and distance to coast; and for fish, all static and dynamic environmental variables were retained.

Statistical modelling

We used Bayesian Additive Regression Trees (BART; Chipman, George & McCulloch, 2010) to project the biodiversity indices in time and space for each of the four assemblages, based on their relationships with the environmental predictors. BART is a machine-learning approach that combines an ensemble of regression trees, with each tree estimating a small and different part of the response variable. Predictions are made through sequential splitting of explanatory variables. Unlike other ensemble tree methods, such as Random Forest and Boosted Trees, BART constructs its ensemble within a Bayesian framework, where both tree structure and terminal node predictions are governed by prior distributions. Like other tree-based approaches, it can represent non-linear relationships and interactions among variables and handle missing data, but it also provides formal uncertainty estimates—a feature often missing from other spatial distribution models—while performing as well as or better than comparable methods (Chipman, George & McCulloch, 2010; Fuster-Alonso et al. 2025). We used the 'bartMachine' R package (Kapelner, & Bleich, 2016) for our modelling.

The BART models were trained in the periods 1993-2021 (phytoplankton and zooplankton), 1993-2023 (benthos), 1993-2020 (fish), and then projected over the study region for the period 1993-2030. We projected biodiversity change under three climate change scenarios representing low, medium, and high greenhouse gas emissions (SSP1–2.6, SSP2–4.5, and SSP5–8.5). Here, we primarily focus on SSP2–4.5 to explore spatial patterns of change. The prediction region used for plankton is larger than for benthos and fish because the substrate composition data used for the latter models is spatially limited, and additionally because the benthic and fish sample data is limited to the coastal shelf, so we avoid projecting far from the model training region. To assess model performance, BART models were evaluated using 10-fold cross-validation. The training data was randomly partitioned into 10 subsets. For each fold, the model was trained on 9 subsets and tested on the remaining one. Performance was assessed by calculating the pseudo-R2 between predicted and observed values. The validity of model predictions were also assessed using MESS maps (Elith, Kearney, & Phillips, 2010). MESS maps identify regions and time periods where (any) environmental explanatory variables are out of range of that used to train the model and thus where predictions are considered less reliable. For the MESS maps, hashed out regions indicate regions where any environmental variable is outside the training range. A summary of the modelling steps used in this study is given Fig. 9.1.

Sen's slope is a non-parametric method that can quantitatively estimate the magnitude of change where assumptions for linear regression are not met (Sen, 1968) and we use this to capture temporal change in our biodiversity indices. For each grid cell, we compute Sen's slope for the linear rate of change between each biodiversity index and year between 1993 to 2030, based on SSP2-4.5, and report whether temporal trends were significant using the trend R package (Pohlert, 2020). We integrate the diversity across the four assemblages by calculating the value of total relative γ-diversity to investigate overall biodiversity patterns. To do so, we normalised the γ-diversity for each assemblage to a scale of 0-1, and then summed across them. The final values range between 0-4 and represents the total relative γ-diversity. Change from the total relative γ-diversity was then estimated using the reference period (1993-1999) as the baseline and the changes calculated are under SSP2-4.5.

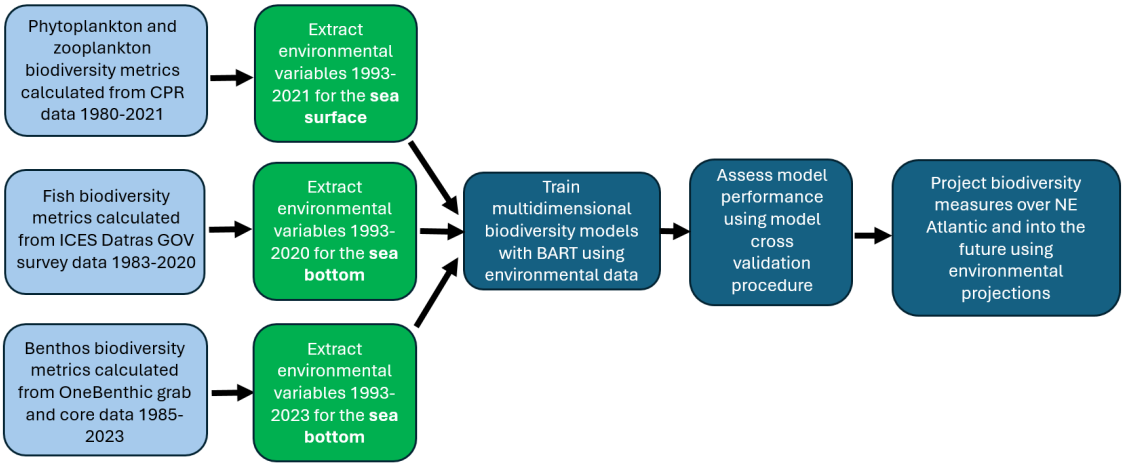

Figure 9.1. Summary of our modelling methods

In Fig. 9.2, we illustrate the processes driving temporal change in spatial biodiversity patterns. Regional species richness increases when the arrival of new species outpaces extirpations (Jones, Dornelas, & Magurran, 2020). If newcomers are rare (i.e. with low spatial occupancy), both species richness and the percentage of rarity will increase. In contrast, if arrivals are mainly abundant species (i.e. rapidly becoming widespread), species richness will increase but the percentage of rarity will decrease. Changes can also occur through shifts in the occupancy of existing species with no change in species richness: range contraction of abundant species increases rarity, while range expansion of rare species decreases rarity. Where regional extirpation exceeds regional species increases: if losses are skewed towards rare species, both species richness and rarity decline; whereas, if abundant species are mostly lost, richness decreases but the proportion of rarity increases. These processes are not mutually exclusive meaning when temporal change is observed, multiple mechanisms may be acting simultaneously to shape patterns of biodiversity. We aimed to reveal the dominant processes determining temporal change in spatial biodiversity patterns and how changing environmental conditions could affect these.

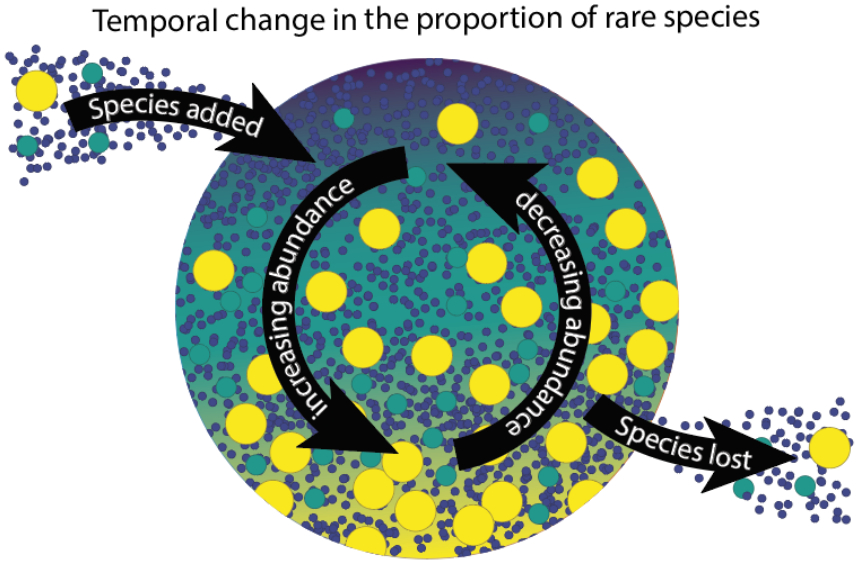

Figure 9.2. Changes in the proportion of rare species (small dark blue points) vs more common (middle-sized green points) and dominant species (large yellow points) within a region can result from three processes: the arrival of new species, the disappearance of existing species, and shifts in the abundance or range of species already present.

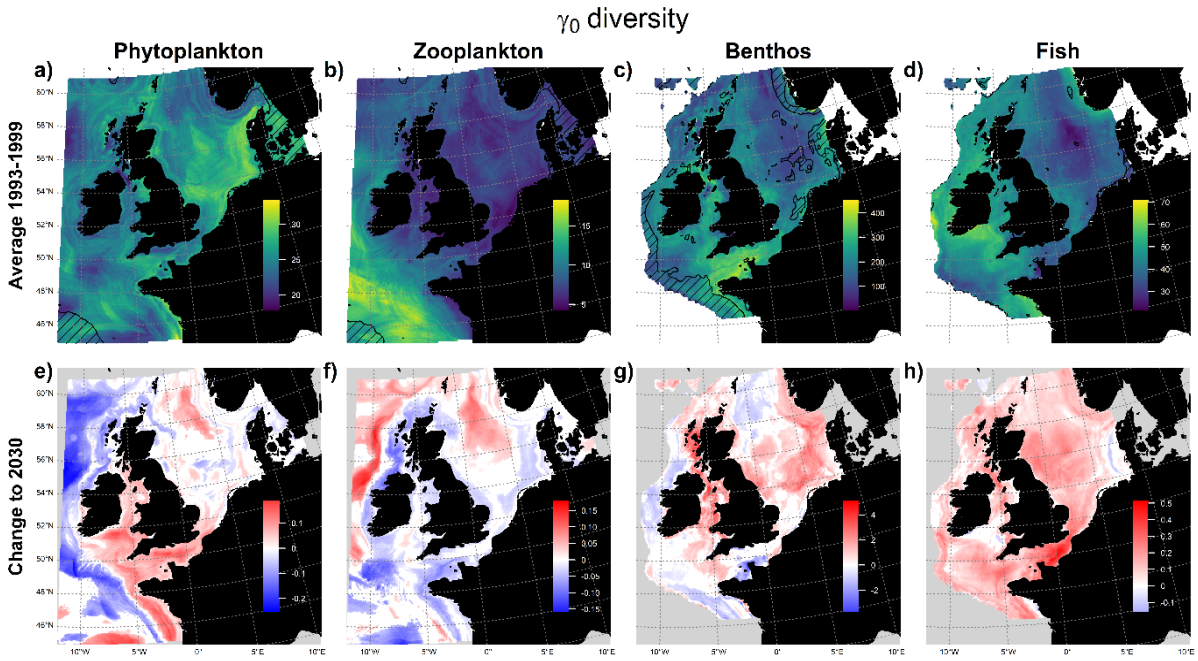

Figure 9.3. Spatial patterns in γ-diversity Hill number 0 (a-d) and its temporal change (e-h) for phytoplankton (a, e), zooplankton (b, f), benthos (c, g) and fish (d, h). Spatial patterns were calculated as means for the reference period of 1993-1999, with hashed regions indicating where environmental variables were outside the models' training range. Annual change (Sen's slopes) was estimated for the period 1993-2030 under SSP2-4.5. Red and blue cells are areas having significant increasing and decreasing trends, respectively, while white cells are areas with non-significant change. Projections for benthos and fish cover a smaller area compared to those for plankton because the former were constrained to regions with data on seabed substrate (i.e. a predictor in their models).

9.3. Results

Climate-driven biodiversity change across assemblages (Hill number 0)

Our model projections reveal pronounced differences in γ-diversity trends among assemblages, contradicting our first hypothesis. Specifically, γ-diversity is projected to increase widely for fish and benthos, decrease for zooplankton, and show contrasting regional patterns of change for phytoplankton (Fig. 9.3; Figs. S9.1-S9.2; Table 9.1). For fish and benthos, increases were consistent across scales and scenarios, with widespread gains in γ- and β-diversity and largely positive changes in α-diversity, though benthic α-diversity showed localized declines (Figs. S9.1–S9.4). Zooplankton exhibited widespread and consistent decreases in α-diversity in the continental shelf, and contrasting regional patters of change in β-diversity (Figs. S9.3-S9.4). Phytoplankton α-diversity declined across most of the region but increased along the southern UK, Ireland, and French coastline, with the area of increase expanding under stronger warming until nearly ubiquitous under SSP5-8.5 (Fig. S9.3). β-diversity for phytoplankton was predominantly decreasing, with scattered increases, indicating a tendency toward homogenization of species composition (Fig. S9.4). For both phytoplankton and zooplankton α- and β-diversity, model fits were low (Table 9.1). For models of γ-diversity and Hill number 0, climate-related variables (temperature, salinity, oxygen, and their variability) consistently explained more variation than static habitat predictors such as substrate composition (Fig. S9.6). Summed across the four assemblages, widespread increases in γ-diversity are projected (Fig. 4). While differences in sampling, analytical methods and taxonomic resolution among assemblages mean absolute species numbers are not directly comparable, normalizing each assemblage's γ-diversity and weighting them equally allows us to derive a composite indicator of broad ecosystem-level change, while

avoiding dominance by highly speciose assemblages such as benthos. This integrative view highlights where overall biodiversity is projected to increase or decline, and complements the assemblage-specific results by indicating regions where changes are consistent or divergent across trophic levels—information that can help identify potential conservation priority areas.

Table 9.1. R^2 values for BART models showing the proportion of variance in each response (i.e. diversity type and Hill number) explained by the predictors (see Fig. S8), averaged over the posterior draws.

Diversity type	Hill number	Phytoplankton	Zooplankton	Benthos	Fish
γ	0	0.14	0.41	0.68	0.63
γ	2	0.16	0.45	0.69	0.85
α	0	0.02	0.07	0.47	0.39
β	0	0.01	0.23	0.56	0.44

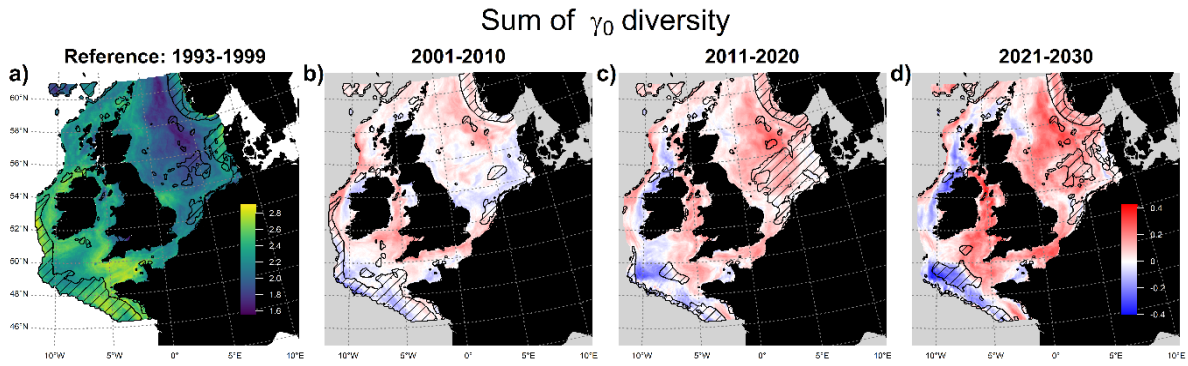

Figure 9.4. Total relative γ-diversity across assemblages. Relative γ-diversity (Hill number 0) summed across phytoplankton, zooplankton, benthos and fish (equal weighting after normalizing assemblage-specific estimates) for (a) the reference period 1993-1999. Change in total relative γ-diversity compared to the reference period for b) 2001-2010, c) 2011-2020, and d) 2021-2030 based on SSP2-4.5. Hashed areas show regions where projected environmental variables were outside any of the models' training ranges. This composite indicator highlights areas where biodiversity increases or declines consistently across assemblages.

Differences in rates of change among assemblages (Hill number 0)

Our projections confirm our second hypothesis, showing clear differences in the rates and even direction of temporal change among assemblages. Under SSP2-4.5 and between 1993-2030, fish and benthos γ-diversity increased by 0.3% and 0.4% per year on average, respectively (Fig. 9.1g-h; Fig. S9.1k-l), whereas phytoplankton and zooplankton γ-diversity declined by ~0.1% per year on average (Fig. 9.1e-f; Fig. S9.1i-j).

Rare species contribution to biodiversity (Hill numbers 0, 2)

Projected patterns of change in the proportion of rare species to γ-diversity provide partial support for our third hypothesis, highlighting the role of rare species in driving climate-related biodiversity change while revealing more complex patterns than a simple climate-driven arrival of new species. The magnitude and direction of the changes varied markedly across assemblages and regions (Fig. 9.5; Figs. S9.1m-p, S9.5).

For benthos and fish, widespread declines in the proportion of rare species were projected across the North Sea coincided with widespread increasing species richness, reflected range expansion, but in the western region the proportion of rare species increased, driven instead by the arrival of new rare species (Fig. 9.5c-d; Fig. S9.5 c,g,k and d,h,l for benthos and fish, respec-

tively). For zooplankton, concurrent declines in the proportion of rare species and γ-diversity in the Celtic Sea suggest biodiversity loss primarily through extirpation of rare species (Fig. 9.5b; Fig. S9.5b,f,j). By contrast, simultaneous increases in the proportion of rare zooplankton species and γ-diversity across much of the higher latitude areas of the study region highlight biodiversity change driven by the addition of new rare species. For phytoplankton, declines in both the proportion of rare species and γ-diversity coincided in the northwest of the study region, signaling the loss of rarer taxa, while in the coastal regions of the Bay of Biscay, Celtic Sea southeast of Ireland, western Channel and north-central North Sea, increases in both metrics indicated biodiversity change driven by the arrival of rare phytoplankton species (Fig. 9.5a; Fig. S9.5a,e,i). Similar to the models of Hill number 0, climate-related variables generally explained more variation than static habitat predictors for models of Hill number 2 (Fig. S9.7).

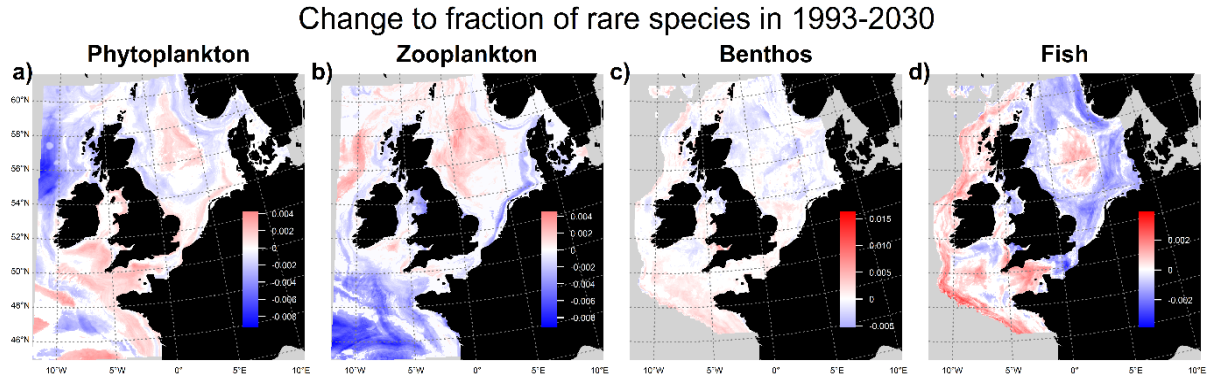

Figure 9.5. Annual change (Sen's slopes) in the proportions of rare species for γ-diversity in a) phytoplankton, b) zooplankton, c) benthos, and d) fish for the period 1993-2030 under SSP2-4.5. Red and blue cells show significant (p <0.05) increasing and decreasing annual change, respectively, with white cells showing areas with non-significant change.

9.4. Discussion

Our multidimensional assessment of biodiversity projections across co-occurring marine assemblages revealed divergent temporal trajectories under climate change. Notably, widespread increases in species richness projected particularly for fish but also benthos to a lesser extent, were not matched by similar changes for zooplankton and phytoplankton. Changes in the proportion of rare species were central to climate-driven marine biodiversity change but was more complex than a simple poleward influx of species from the south. Crucially, assessing changes in the proportion of rare species can reveal biodiversity shifts not evident from species richness or composition alone, offering early warning of change before extirpations and supporting the development of indicators that enable preventive rather than reactive policy interventions (Leadley et al. 2022; Stevenson et al. 2021). By projecting emergent biodiversity patterns directly, explicitly incorporating rare species, and quantifying uncertainty, our framework extends and complements results from conventional and emerging species-distribution models that focus only on subsets of taxa (Cheung et al. 2009; Gordó-Vilaseca et al. 2023; Gordó-Vilaseca et al. 2024). The projections reveal divergent responses to climate change across the marine food web. Such imbalances could alter ecosystem structure and energy flow (du Pontavice et al. 2020; Pecl et al. 2017). In particular, declines in prey diversity (e.g., zooplankton) may weaken the 'portfolio effect', whereby a diverse prey base stabilizes energy transfer to higher trophic levels (Doak et al. 2008; Schindler, Armstrong & Reed, 2015; Wang & Loreau, 2014). If biodiversity gains occur primarily among predators, such as piscivorous fish in the Northeast Atlantic (Thompson yet al. 2023), this decoupling between trophic levels could destabilize food webs

and ultimately threaten food security in fisheries that depend on primary and secondary production in plankton (Lynam et al. 2017). Conservation strategies that integrate predictive indicators capable of detecting contrasting food-web responses will be essential to sustaining ecosystem functions, ensuring food security, and achieving international biodiversity targets under climate change. Future work could refine our approach by integrating additional ecosystem components and improving climate and human-pressure projections, further strengthening its capacity to inform adaptive management. Our findings offer a framework to assess progress towards biodiversity targets under shifting baselines, supporting global and regional policy frameworks for biodiversity protection and conservation. More specifically, we provide leading indicators that can inform preventive action, rather than those that simply document change once it has occurred (Stevenson et al. 2021). Embedding such indicators within the policy cycle and explicitly linking them to decision-making that accounts for climate-driven shifting baselines has been widely called for (Elliot et al. 2015; Leadley et al. 2022; Stevenson et al. 2021), yet no such framework currently exists for the Northeast Atlantic. Here, we advance this goal by developing a suite of complementary biodiversity indicators capable of assessing current status and projecting future trends across assemblages in response to climate change.

9.5. References

Batten, S.D. et al. CPR sampling: the technical background, materials and methods, consistency and comparability. Prog. Oceanogr. 58, 193–215 (2003). https://doi.org/10.1016/j.pocean.2003.08.004

Benedetti, F., Vogt, M., Elizondo, U.H. et al. Major restructuring of marine plankton assemblages under global warming. Nature Communications, 12, 5226. https://doi.org/10.1038/s41467-021-25385-x

Bricheno, L. M. & Wolf, J. & Aldridge, J. Distribution of natural disturbance due to wave and tidal bed currents around the UK. Continental Shelf Research 109, 67–77 (2015). https://doi.org/10.1016/j.csr.2015.09.013

Brondízio, E. S., Settele, J., Díaz, S., & Ngo, H. T. (eds.) Global assessment report on biodiversity and ecosystem services of the Intergovernmental Science-Policy Platform on Biodiversity and Ecosystem Services. IPBES secretariat, Bonn, Germany (2019). https://doi.org/10.5281/zenodo.3831673

Burchard, H. & Bolding, K. GETM, a general estuarine transport model. Scientific documentation. In Technical report EUR 20253 en. European Commission, Ispra (2002).

Cardinale, B. J., Duffy, J. E., Gonzalez, A., Hooper, D. U., Perrings, C., Venail, P. et al. Biodiversity loss and its impact on humanity. Nature 486, 59–67 (2012). https://doi.org/10.1038/nature11148

Cardinale, B. J., Gonzalez, A., Duffy, J. E., Hooper, D. U., Perrings, C., Venail, P. et al. Is local biodiversity declining or not? A summary of the debate over analysis of species richness time trends. Biological Conservation 219, 175–183 (2018). https://doi.org/10.1016/j.biocon.2017.12.021

Centre for Environment, Fisheries and Aquaculture Science (Cefas). ONEBenthic database. https://rconnect.cefas.co.uk/onebenthic_portal/ (accessed 7 November 2024).

Chao, A. et al. Rarefaction and extrapolation with beta diversity under a framework of Hill numbers: the iNEXT.beta3D standardization. Ecological Monographs 93, e1588 (2023) . Ecological Monographs, 93, e1588. https://doi.org/10.1002/ecm.1588

Chao, A., Chiu, C.H., Hsieh, T.C. & Inouye, B.D. Proposing a resolution to debates on diversity partitioning. Ecology 93, 2037–2051 (2012). https://doi.org/10.1890/11-1817.1

Chao, A., Gotelli, N.J., Hsieh, T.C., Sander, E.L., Ma, K.H., Colwell, R.K. & Ellison, A.M. Rarefaction and extrapolation with Hill numbers: a framework for sampling and estimation in species diversity studies. Ecological Monographs 84, 45–67 (2014). https://doi.org/10.1890/13-0133.1

Chase, J.M., McGill, B.J., McGlinn, D.J., May, F., Blowes, S.A., Xiao, X., Knight, T.M., Purschke, O. & Gotelli, N.J. Embracing scale-dependence to achieve a deeper understanding of biodiversity and its change across communities. Ecology Letters 21, 1737–1751 (2018). https://doi.org/10.1111/ele.13151

Cheung, W.W.L. et al. Projecting global marine biodiversity impacts under climate change scenarios. Fish and Fisheries 10, 235–251 (2009). https://doi.org/10.1111/j.1467-2979.2008.00315.x

Chipman, H. A., George, E. I. & McCulloch, R. E. BART: Bayesian additive regression trees. Ann. Appl. Stat. 4, 266–298 (2010). https://doi.org/10.1214/09-aoas285

Chust, G., Villarino, E., McLean, M., Mieszkowska, N., Benedetti-Cecchi, L., Bulleri, F. et al. Cross-basin and cross-taxa patterns of marine community tropicalization and deborealization in warming European seas. Nature Communications. Nature Communications, 15, 2126 (2024). https://doi.org/10.1038/s41467-024-46526-y

Couce, E., Pinnegar, J.K. & Townhill, B.L. Climate change resilience of vulnerable marine species in northwest Europe. Marine Biology 172, 116 (2025) . L. Climate change resilience of vulnerable marine species in northwest Europe. Marine Biology, 172, 116. https://doi.org/10.1007/s00227-025-04672-x

Doak, D.F. et al. The statistical inevitability of stability–diversity relationships in community ecology. The American Naturalist 151, 264–276 (1998). https://doi.org/10.1086/286117

Dornelas, M. et al. BioTIME: A database of biodiversity time series for the Anthropocene. Global Ecology and Biogeography 27, 760–786 (2018). https://doi.org/10.1111/geb.12729

du Pontavice, H., Gascuel, D., Reygondeau, G., Maureaud, A. & Cheung, W. W. L. Climate change undermines the global functioning of marine food webs. Global Change Biology 26, 1306–1318 (2020). https://doi.org/10.1111/gcb.14944

Elith, J., Kearney, M. & Phillips, S. The art of modelling range-shifting species. Methods in Ecology and Evolution 1, 330–342 (2010). https://doi.org/10.1111/j.2041-210x.2010.00036.x

Elliott, M. Borja, A., McQuatters-Gollop, A., Mazik, K., Birchenough, S., Painting, S., Peck, M.A. Force majeure: will climate change affect our ability to attain Good Environmental Status for marine biodiversity? Marine Pollution Bulletin 95, 7–27 (2015). https://doi.org/10.1016/j.marpolbul.2015.03.015

Fernandes, J.A., Cheung, W.W.L., Jennings, S., Butenschön, M., de Mora, L., Frölicher, T.L., Barange, M. & Grant, A. Modelling the effects of climate change on the distribution and production of marine fishes: accounting for trophic interactions in a dynamic bioclimate envelope model. Global Change Biology 19, 2596–2607 (2013). https://doi.org/10.1111/gcb.12231

Fisher, R.A., Corbet, A.S. & Williams, C.B. The relation between the number of species and the number of individuals in a random sample of an animal population. Journal of Animal Ecology 12, 42–58 (1943). https://doi.org/10.2307/1411

Fuster-Alonso, A., Mestre-Tomás, J., Baez, J. et al. Machine learning applied to global-scale species distribution models. Scientific Reports, 15, 37534. https://doi.org/10.1038/s41598-025-20797-x

García Molinos, J., Halpern, B. S., Schoeman, D. S., Brown, C. J., Kiessling, W., Moore, P. J. et al. Climate velocity and the future global redistribution of marine biodiversity. Nature Climate Change 6, 83–88 (2016). https://doi.org/10.1038/nclimate2769

Gellner, G. & McCann, K.S. Consistent role of weak and strong interactions in high- and low-diversity trophic food webs. Nature Communications, 7, 11180 (2016). https://doi.org/10.1038/ncomms11180

Gordo-Vilaseca, C., Costello, M.J., Coll, M. et al. Future trends of marine fish biomass distributions from the North Sea to the Barents Sea. Nature Communications, 15, 5637 (2024). https://doi.org/10.1038/s41467-024-49911-9

Gordó-Vilaseca, C. et al. Three decades of increasing fish biodiversity across the northeast Atlantic and the Arctic Ocean. Proceedings of the National Academy of Sciences, 120, e2120869120 (2023). https://doi.org/10.1073/pnas.2303163120

Halpern, B. S., Frazier, M., Potapenko, J., Casey, K. S., Koenig, K., Longo, C. et al. Spatial and temporal changes in cumulative human impacts on the world's ocean. Nature Communications 6, 7615 (2015). https://doi.org/10.1038/ncomms8615

Hsieh, T. C., Ma, K. H. & Chao, A. iNEXT: An R package for rarefaction and extrapolation of species diversity (Hill numbers). Methods in Ecology and Evolution 7, 1451–1456 (2016). https://doi.org/10.1111/2041-210x.12613

Jones, F. A. M., Dornelas, M. & Magurran, A. E. Recent increases in assemblage rarity are linked to increasing local immigration. R. Soc. Open Sci., 7, 192045 (2020). https://doi.org/10.1098/rsos.192045

Jones, M.C. & Cheung, W.W.L. Multi-model ensemble projections of climate change effects on global marine biodiversity. ICES Journal of Marine Science 72, 741–752 (2015). https://doi.org/10.1093/icesjms/fsu172

Jost, L. Partitioning diversity into independent alpha and beta components. Ecology 88, 2427–2439 (2007). https://doi.org/10.1890/06-1736.1

Jouffray, J.-B., Blasiak, R., Norström, A. V., Österblom, H. & Nyström, M. The Blue Acceleration: The Trajectory of Human Expansion into the Ocean. One Earth 2, 43–54 (2020). https://doi.org/10.1016/j.oneear.2019.12.016

Kapelner, A. & Bleich, J. bartMachine: Machine learning with Bayesian additive regression trees. J. Stat. Softw. 70, 1–40 (2016). https://doi.org/10.18637/jss.v070.i04

Kléparski, L., Beaugrand, G., Edwards, M. & Ostle, C. Phytoplankton life strategies, phenological shifts and climate change in the North Atlantic Ocean from 1850 to 2100. Global Change Biology 29, 3833–3849 (2023). https://doi.org/10.1111/gcb.16709

Kristiansen, T., Butenschön, M. & Peck, M.A. Statistically downscaled CMIP6 ocean variables for European waters. Scientific Reports 14, 1–20 (2024). https://doi.org/10.1038/s41598-024-51160-1

Kunze, C. et al. Partitioning species contributions to ecological stability in disturbed communities. Ecological Monographs 95, e1636 (2025). https://doi.org/10.1002/ecm.1636

Leadley, P. et al. Achieving global biodiversity goals by 2050 requires urgent and integrated actions. One Earth 5, 597–603 (2022). https://doi.org/10.32942/osf.io/hy7a2

Lynam, C. P., Llope, M., Möllmann, C., Helaouët, P., Bayliss-Brown, G. A. & Stenseth, N. C. Interaction between top-down and bottom-up control in marine food webs. Proceedings of the National Academy of Sciences 114, 1952–1957 (2017). https://doi.org/10.1073/pnas.1621037114

Lynam, C.P. & Ribeiro, J. A data product derived from Northeast Atlantic groundfish data from scientific trawl surveys 1983–2020. Cefas Data Hub https://doi.org/10.14466/CefasDataHub.126 (2022).

Marine Biological Association. Continuous Plankton Recorder (CPR) Survey dataset. https://doi.org/10.17031/668cf6b093d22 (accessed 9 July 2024).

McCann, K., Hastings, A. & Huxel, G. Weak trophic interactions and the balance of nature. Nature 395, 794–798 (1998). https://doi.org/10.1038/27427

McGill, B.J. et al. Species abundance distributions: moving beyond single prediction theories to integration within an ecological framework. Ecology Letters 10, 995–1015 (2007). https://doi.org/10.1111/j.1461-0248.2007.01094.x

Mouillot, D. et al. Rare species support vulnerable functions in high-diversity ecosystems. PLOS Biology 11, e1001569 (2013). https://doi.org/10.1371/journal.pbio.1001569

Pecl, G. T. et al. Biodiversity redistribution under climate change: Impacts on ecosystems and human well-being. Science 355, eaai9214 (2017). https://doi.org/10.1126/science.aai9214

Pohlert, T. Trend: non-parametric trend tests and change-point detection. R package version 1, 4 (2020). https://doi.org/10.32614/cran.package.trend

Poloczanska, E. S., Brown, C. J., Sydeman, W. J., Kiessling, W., Schoeman, D. S., Moore, P. J. et al. Global imprint of climate change on marine life. Nature Climate Change 3, 919–925 (2013). https://doi.org/10.1038/nclimate1958

Preston, F.W. The commonness, and rarity, of species. Ecology 29, 254–283 (1948). https://doi.org/10.2307/1930989

R Core Team. R: A language and environment for statistical computing. Version 4.4.1. R Foundation for Statistical Computing, Vienna, Austria (2024). https://doi.org/10.32614/r.manuals

Schindler, D.E., Armstrong, J.B. & Reed, T.E. The portfolio concept in ecology and evolution. Frontiers in Ecology and the Environment 13, 257–263 (2015). https://doi.org/10.1890/140275

Sen, P. K. Estimates of the regression coefficient based on Kendall's tau. J. Am. Stat. Assoc. 63, 1379–1389 (1968). https://doi.org/10.1080/01621459.1968.10480934

Stevenson, S.L. et al. Matching biodiversity indicators to policy needs. Conserv. Biol. 35, 522–532 (2021). https://doi.org/10.1111/cobi.13575

Säterberg, T. et al. A potential role for rare species in ecosystem dynamics. Scientific Reports 9, 11107 (2019). https://doi.org/10.1038/s41598-019-47541-6

Thompson, M. S. A. et al. What's hot and what's not: Making sense of biodiversity 'hotspots'. Global Change Biology 27, 521–535 (2021). https://doi.org/10.1111/gcb.15443

Thompson, M.S.A., Couce, E., Schratzberger, M. & Lynam, C.P. Climate change affects the distribution of diversity across marine food webs. Global Change Biology 29, 6606–6619 (2023). https://doi.org/10.1111/gcb.16881

Townhill, B.L., Couce, E., Tinker, J., Kay, S. & Pinnegar, J.K. Climate change projections of commercial fish distribution and suitable habitat around north western Europe. Fish and Fisheries 24, 848–862 (2023). https://doi.org/10.1111/faf.12773

Tuomisto, H. A diversity of beta diversities: Straightening up a concept gone awry. Part 1. Defining beta diversity as a function of alpha and gamma diversity. Ecography 33, 2–22 (2010). https://doi.org/10.1111/j.1600-0587.2009.05880.x

Wang, S. & Brose, U. Biodiversity and ecosystem functioning in food webs: the vertical diversity hypothesis. Ecology Letters 21, 9–20 (2018). https://doi.org/10.1111/ele.12865

Wang, S. & Loreau, M. Ecosystem stability in space: α, β and γ variability. Ecology Letters 17, 891–901 (2014). https://doi.org/10.1111/ele.12292

Whittaker, R.H. Vegetation of the Siskiyou Mountains, Oregon and California. Ecological Monographs 30, 279–338 (1960). https://doi.org/10.2307/1943563

Wilson, R. J., Speirs, D. C., Sabatino, A. & Heath, M. R. A synthetic map of the north-west European shelf sedimentary environment for applications in marine science. Earth System Science Data 10, 109–130 (2018). https://doi.org/10.5194/essd-10-109-2018

WoRMS Editorial Board. World Register of Marine Species. https://www.marinespecies.org (2024). https://doi.org/10.32614/cran.package.worrms

10 Spatiotemporal biodiversity patterns and hotspots of fish communities on the Portuguese continental shelf and upper slope

Authors: Rita Vasconcelos, André Martins, Sofia Henriques, Corina Chaves, Teresa Moura

10.1. Introduction

The demersal fish community available to bottom trawling of the Portuguese continental shelf and upper slope, located in the west and south Atlantic coast of the Iberian Peninsula (Portuguese waters of ICES Subdivision 27.9.a) has been monitored annually by IPMA since 1979 with dedicated research surveys. Community spatio-temporal patterns, namely alpha diversity indices and species composition, have been characterized previously by Gomes et al. (2001), Sousa et al. (2005, 2006) and Moura et al. (2020). Patterns of individual species, based on this monitoring data, also have been analysed, focusing on commercially important species, notably in the context of fisheries stock assessment and marine strategy framework directive but also in other scientific and management contexts. Response of functional traits of these communities to fishing levels within different main spatial areas have also been explored (Henriques et al. 2014).

The present study aimed at analysing and characterizing the biodiversity of demersal fish communities in the Portuguese continental shelf and slope, more specifically the spatial and temporal patterns of biodiversity and to identify areas with persistently high and low taxonomic alpha diversity (respectively hotspots and coldspots). Two biodiversity facets were considered, namely taxonomic (based on species taxonomic identities) and functional (based on species functional traits), and, in both cases, both alpha and beta diversity indices were considered for the characterization of biodiversity. Moreover, patterns of functional traits were explored with Community Weighed Means (and Proportions).

10.2. Material and Methods

The analysis was based on data from the Portuguese International Bottom Trawl Survey in Quarter 4 (PT-PGFS-Q4), implemented by IPMA in the scope of the EU Fisheries Data Collection Framework. This survey takes place in the Portuguese continental platform and upper slope, since 1979, and the data used in the present study corresponds to the period between 2005 and 2023, with some missing years (2012, 2018-2020) and with a discontinuity due to change of vessel and fishing net between 2005-2017 versus 2021-2023. The design of the survey includes the combination of 12 latitudinal sectors, with three depth strata (20-100m, 101-200m, 201-500m), resulting in a total of 36 sampled strata, which are the basic design-based unit for this survey. For the purpose of analysis in the present study, the 12 sectors were combined into three latitudinal areas (northwest, southwest and south), considering results from previous studies (Sousa et al., 2005; Moura et al., 2020). The northwest area includes the five northern most latitudinal sectors of the western coast (until Cape Carvoeiro), the southwest area the four southernmost latitudinal sectors of the western coast (until Cape São Vicente), and the south area the remaining three coastal sectors which in this case are longitudinal and not latitudinal.

Only fish data was selected for the analysis, which initially consisted of 203 species, but due to missing functional traits data only 194 species were considered. The fish biomass data was log10 transformed for all analysis, considered as the weight caught by one hour of trawling (kg.h-1). For each fish species, a series of functional traits were characterized (Table 10.1), based on several publicly available databases (including the Rfishbase package from Boettiger et al., 2012, the MEDITS project, Polo et al., 2024, Butt et al., 2022, Koutsidi et al., 2020, Beukhof et al., 2019 and Henriques 2007 and 2013) and complemented with expert knowledge when needed. The set of traits selected aimed at characterizing different aspects of the species life history (body length, age at maturity, fecundity), habitat use (mobility, depth, vertical biological zone, thermal tolerance) and trophic ecology (diet, trophic level). Much of the information on these traits was compiled from different datasets, however, thermal tolerance information was entirely based on Butt et al. (2022), where species range data from AquaMaps was considered (Table 10.1). Correlation of the functional traits in the data set was below 0.95.

A series of alpha diversity indices (Table 10.2) were computed at the level of each sample (i.e. haul). A series of beta diversity indices (Table 10.3) were also computed. For both alpha and beta diversity indices, log10 transformed biomass was used for weighing. After the alpha and beta diversity indices computation, both a time series and a spatial analysis was performed.

The time series analysis of alpha and beta diversity indices was performed at the level of 9 strata originated from the division of the latitudinal areas (northwest, southwest and south) by the depth strata (20-100m, 101-200m, 201-500m) and considering two time periods (2005-2017 and 2021-2023). For the time series of beta diversity indices, in each latitudinal area*depth strata, pairwise values were computed between each sample of each year versus each sample of the reference years, which were: for the 2005-2007 time period, the years between 2005 and 2010 and, for the 2021-2023 time period, all the three years; in all cases pairwise values from the same year were excluded. The aim is to explore, within a latitudinal area*depth strata, how much the samples in a year are dissimilar to the samples from the beginning of the time period.

For the spatial analysis of indices (i.e. maps presented), three different time periods were considered (2005-2010; 2011-2017; 2021-2023). Due to uneven numbers of samples in the 36 sampled strata in a time period, the original observed samples were used to create bootstrapped replicates (at the level of the sampled strata and for each time period) through resampling with replacement, with each of these replicates containing the same amount of samples in the sampled strata. The objective was not to standardize the number of samples between strata within a time period, but to generate variability in the samples that mirrors the randomness of samples in each strata obtained per time period. This procedure was repeated 1000 times, and a final bootstrapped average was obtained for each of the 36 sampled strata by time period. For both the alpha and beta diversity indices, this procedure was done with the diversity index values already previously calculated before bootstrapping; and in the case of beta diversity indices an additional step was done before bootstrapping which consisted of obtaining one single index value per sample per year, by averaging all the pairwise index values of that sample with all other samples of the same year.

To identify persistent hotspots and coldspots of each diversity index, annual maps by strata were produced. Once again, bootstrapping was used, as described above, but the data was considered by year instead of time period. In each annual map, the sampled areas with index values above the 90th percentile (hotspots) were reclassified into 1, the sampled areas with

index values below the 10th percentile were classified into -1 and the remaining sampled areas (i.e. with index values between the 90th and the 10th percentile) were classified to 0. For each index, an average of the annual reclassified values of each of the 36 strata was determined for the period 2005-2017.

The Community weighted mean (CWM) of each numeric functional trait in each haul was determined as the mean value of that trait across all species, weighted by the species biomass. In the case of categorical functional traits, the Community weight proportion of each trait category in each haul was determined as the relative proportion of biomass of each trait category.

Table 10.1. Functional traits used in the study. Group of traits, type and metrics (or levels when the variable is categorical) are also presented for each functional trait.

Group of traits	Functional trait	Type	Metric (for Numeric Traits) / Categories (for Categorical Traits)
Life-history	Body length	Numeric	Centimetres
	Age at maturity	Numeric	Years
	Fecundity	Numeric	Number of eggs or offspring
Habitat use	Mobility	Ordered Categorical	sedentary; territorial; medium mobility; high mobility
	Depth (max)	Numeric	Meters
	Vertical biological zone	Categorical	bathydemersal; bathypelagic; benthopelagic; demersal; pelagic-neritic; pelagic-oceanic; reef-associated
	Thermal tolerance	Ordered Categorical	0-2,5°C; 2,5-5°C; 5-7,5°C; 7,5-10°C; 10-15°C; >15°C
Trophic ecology	Diet	Categorical	herbivorous; planktivorous; piscivorous; benthivorous; generalist
	Trophic level	Continuous	Estimated from mean trophic level of preys + 1

Table 10.2. Indices of taxonomic and functional alpha diversity used in the study. Biodiversity facet, definition, ecological context and details are also presented for each index.

Biodiversity facet	Index	Definition	Ecological Context	Details
Taxonomic	Species Richness	The total number of distinct species present in a community	The simplest measure of biodiversity, capturing how many species coexist in a community. Does not account for dominance, rarity, or relative abundances.	Calculated as a simple count of species. Highly sensitive to sampling effort and spatial scale. Often used as a baseline component of biodiversity and in combination with evenness or functional indices.
	Pielou's Evenness	The ratio between Shannon diversity and species richness, indicating how evenly individuals are distributed among species.	Measures the uniformity of species abundances. High values (close to 1) mean species have similar abundances; low values indicate dominance by few species.	Ranges from 0 (complete dominance) to 1 (perfect evenness). Sensitive to both species richness and abundance distribution.
	Simpson's Dominance	The probability that two randomly selected individuals belong to the same species. Reflects the dominance of common species.	Indicates dominance structure: high values mean few dominant species; low values reflect higher diversity and more equitable communities.	Ranges from 0 (high diversity) to 1 (one species dominates. Sensitive to abundant species.
Functional	Functional Richness	The volume of the convex hull enclosing all species in multidimensional trait space.	Captures the range of functional strategies within a community. High FRic = wide ecological roles; low FRic = functional redundancy or environmental filtering.	Only meaningful if species > number of trait axes (to create a convex hull).
	Functional Evenness	Regularity in the distribution of species abundances and distances along the minimum spanning tree in trait space.	Measures how evenly functional space is filled by species or biomass. High FEve = balanced occupation of functional space; low FEve = aggregation in trait space.	Requires ≥3 species (to create a minimum of two branches). Ranges from 0 (irregular) to 1 (regular).
	Functional Divergence	The degree to which abundant species lie toward the edges of the functional trait space compared to its centre.	Indicates whether dominant species exploit extreme trait values (high FDiv) or cluster near the mean (low FDiv). Reflects niche differentiation and competition.	Valid only if number of species > number of trait axes (convex hull required).
	Functional Dispersion	The mean distance of each species to the community centroid in trait space, weighted by abundance.	Describes functional heterogeneity within communities. High FDis = species are functionally dissimilar; low FDis = trait clustering.	Does not require a minimum number of species.

Table 10.3. Indices of taxonomic and functional beta diversity used in the study. Biodiversity facet, definition, ecological context and details are also presented for each index.

Biodiversity facet	Index	Definition	Ecological Context	Details / Components
Taxonomic	Taxonomic Jaccard	Compositional similarity between two communities based on species presence/absence	Values near 1 → communities share most species; near 0 → communities share few or no species	Turnover: species replacements; Nestedness: difference due to species loss/gain.
Taxonomic	Taxonomic Simpson dissimilarity	Measures turnover in species composition between communities, focusing only on the replacement of species and ignoring differences in richness.	High values indicate that assemblages share few species and differ mainly by species replacement; low values mean strong overlap in species identities.	Derived from the Simpson dissimilarity coefficient, which isolates the turnover component of the Sørensen or Jaccard dissimilarities. Represents the pure turnover component of beta diversity; nestedness is not included.
Taxonomic	Taxonomic Bray–Curtis	Compositional dissimilarity considering species abundances	Sensitive to both presence/absence and dominance; high values → very different communities	Balanced variation: abundance replacement among shared species, analogous to turnover; Abundance gradients: differences in total abundance or dominance due to losses or gains in abundance, analogous to nestedness. Together, these components describe whether dissimilarity is driven mainly by reciprocal changes in species abundances or by unidirectional abundance differences between assemblages.
Taxonomic	Taxonomic Rao Quadratic Entropy	Dissimilarity weighted by species abundances	Integrates presence/absence and abundance differences; high values → very distinct communities	Overall dissimilarity; no explicit turnover/nestedness decomposition
Functional	Functional Jaccard	Functional dissimilarity between two assemblages based on the overlap (or not) of species in functional trait space (presence/absence of trait-combinations)	Values close to 1 → large functional dissimilarity (few shared functional strategies); values near 0 → assemblages share similar trait combinations	It computes convex hulls and overlaps in trait space. Turnover component: functional replacement (non-shared trait combinations) between assemblages (if no overlap); Nestedness-resultant component: dissimilarity due to one assemblage being functionally a subset of the other's strategies (trait space nestedness)
Functional	Functional Rao Quadratic Entropy	Dissimilarity weighted by species abundances and functional trait differences	High values → communities differ in both trait composition and abundances	Overall dissimilarity; no explicit turnover/nestedness decomposition

10.3. Results and Discussion

The study Taxonomic and Functional alpha diversity indices

The fish communities of the Portuguese continental shelf and upper slope in 2005-2023, as evidenced by the data from the PT-PGFS-Q4, have major spatial contrasts in alpha diversity as a function of latitude and depth. These contrasts are generally in line with previous studies for this community and data set (Gomes et al. 2001, Sousa et al 2005, 2006, Moura et al. 2020). Namely, in the shallower depth strata, species richness increased from north to south (Figure 10.1.a), which is a known macroecological pattern previously described across many groups

(e.g. Gaston 2000), whereas this latitudinal pattern was not seen in the other depth strata; in the south area, species richness decreased from the shallower to the deeper strata, an ecological pattern which has been described in many regions such as the Northeast Atlantic (e.g. Gislason et al. 2020). Moreover, functional richness (Figure 10.1.b), divergence and dispersion (Supplementary Figure S10.2.b, c.) had a similar pattern to species richness, though less marked. This indicates a degree of functional redundancy due to species with similar traits in the studied continental shelf and slope sampled with bottom trawl, as was shown to occur in other marine fish communities (e.g. Mouillot et al. 2014). In contrast, Simpson dominance had an approximately opposite pattern to this pattern (Supplementary Figure S10.1.b). No spatial patterns were evident in Pielou evenness and Functional evenness (Supplementary Figure S10.1.a and Supplementary Figure S10.2.a).

These results are aligned with the general spatial pattern of those indices across the 36 strata in the three time periods (Taxonomic - Supplementary Figure S10.3.a, b; Functional - Supplementary Figure S10.4-d), as well as the hotspots and coldspots of biodiversity identified (Taxonomic - Figures 10.2.a, Supplementary Figure S10.5.a, b; Functional - Figures 10.2.b, Supplementary Figure S10.6.a-c). Persistent hotspots of species richness, functional richness, divergence and dispersion were especially in the south and also southwest areas while the opposite was seen in Simpson dominance, whereas coldspots are in the north area where nonetheless the little importance of hot spots is in intermediate depths.

In what concerns temporal patterns of change, it should be highlighted that the two time series (2005-2017 versus 2021-2023) should not be directly compared, as justified in the methods section. No marked patterns or trends of change through time (2005-2017) in the alpha diversity taxonomic and functional indices are evident (Figures 10.1a, b, Supplementary Figure S10.1.a, b, Figure S10.2.a, b, c.).

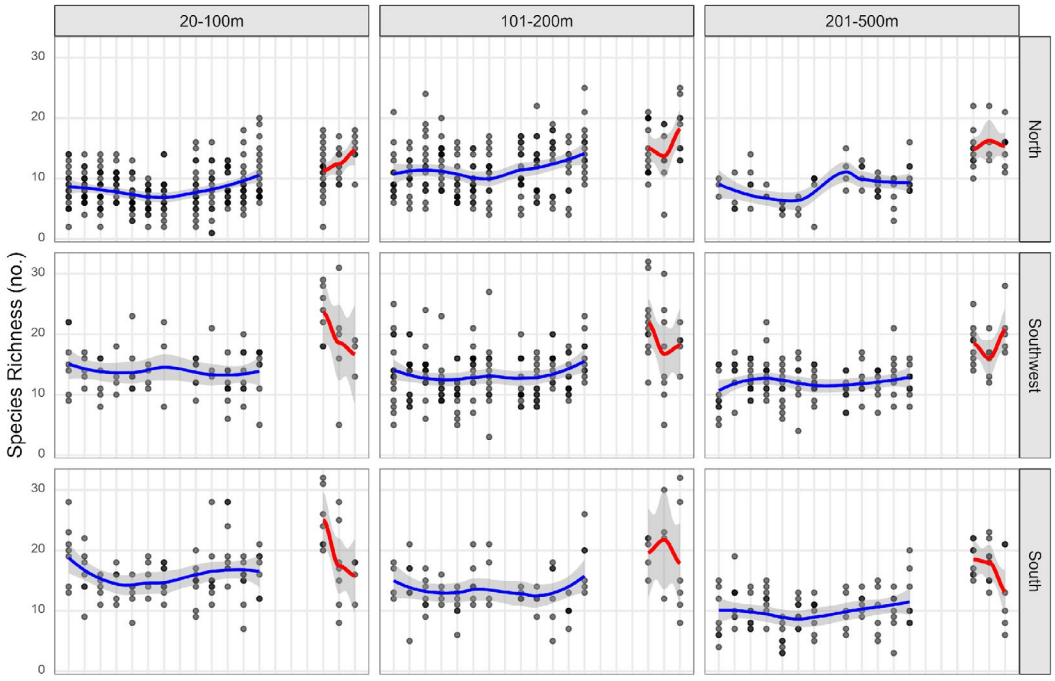

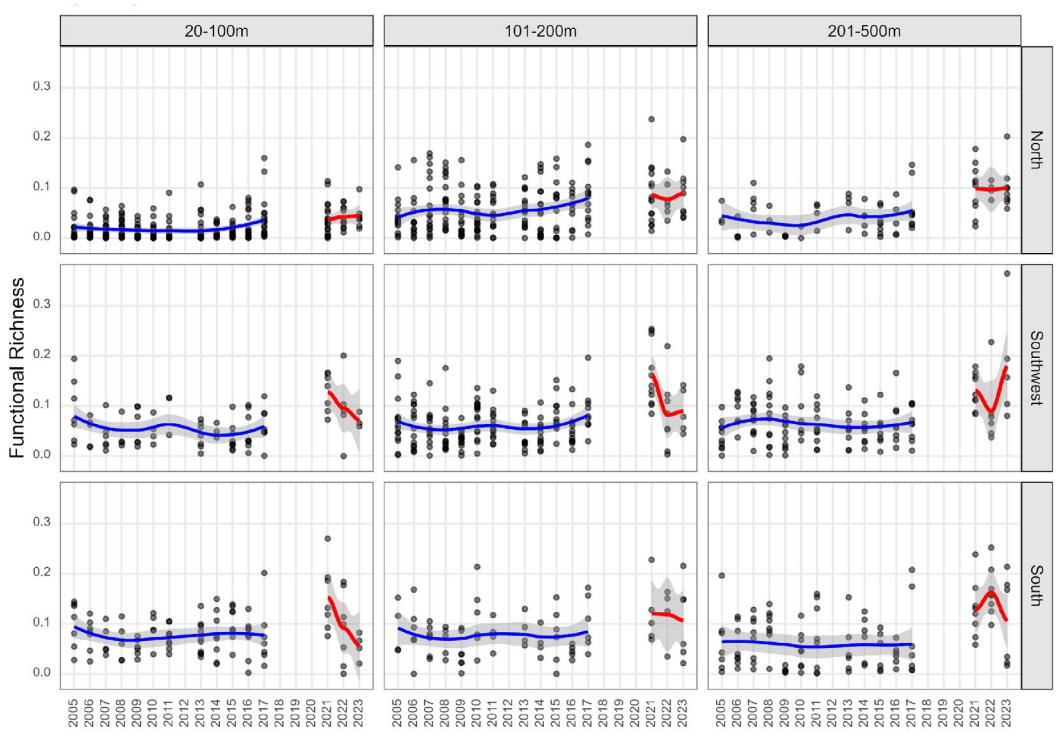

Figure 10.1. a, b. Alpha diversity indices Species Richness (top 3 panels) and Functional Richness (bottom 3 panels) per year, between 2005-2017 and 2021-2023, in each of the nine latitudinal area*depth strata of the fish communities of the continental shelf and upper slope of the Portuguese coast as sampled in PT-PGFS-Q4 (International Bottom Trawl Survey Quarter 4 in Portuguese waters of ICES 27.9.a). In each plot each point is a haul, and the line is the "smoothed trend line with the method "loess" with a 95% confidence interval band.

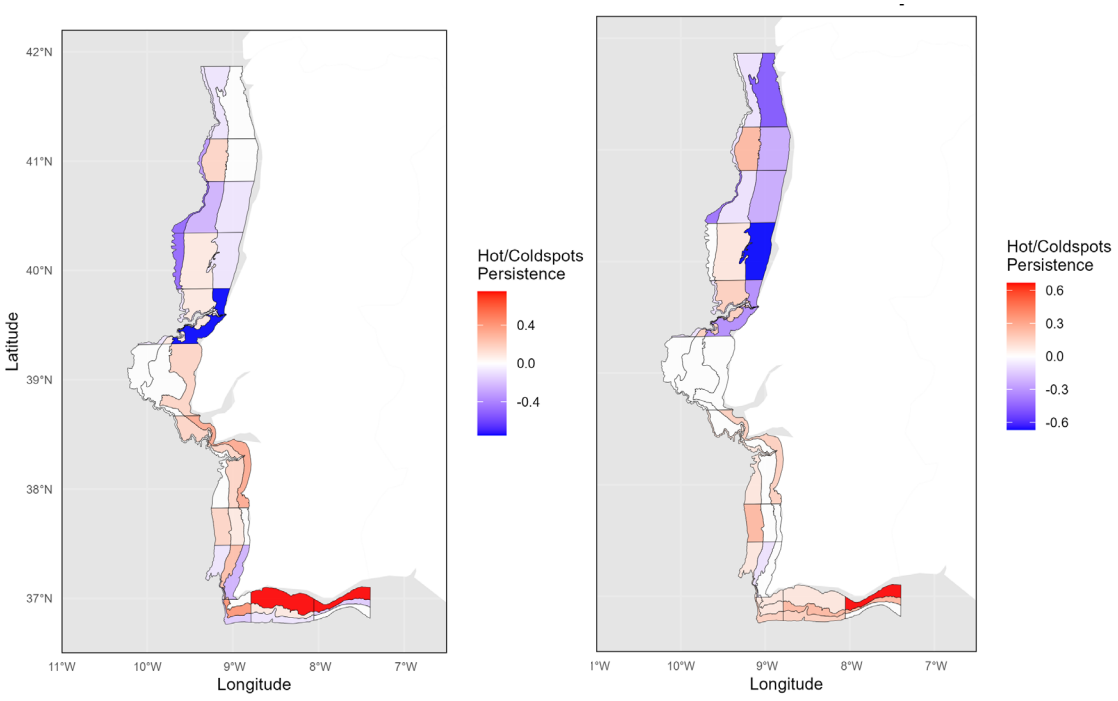

Figure 10.2. a, b. Persistence of hotspots and coldspots of the alpha diversity indices Species Richness and Functional Richness in the time period 2005-2017 in each of the 36 sampled strata of the fish communities of the continental shelf and upper slope of the Portuguese coast as sampled in PT-PGFS-IBTS Q4 (International Bottom Trawl Survey Quarter 4 in Portuguese waters of ICES 27.9.a).

Community weighed means (and proportions) of functional traits

In the fish communities of the Portuguese continental shelf and upper slope in 2005-2023, as evidenced by the data from the PT-PGFS-Q4, community weighted means of functional traits have major spatial contrasts from the northern to the southern area and also from the shallower to the deeper strata. Namely, in the shallower depth strata, body length decreased from north to south, a latitudinal macroecological pattern that has been previously described and is known as the Bergmann's rule (e.g. Ashton et al., 2000) (Figure 10.3.a). However, this pattern is not clear in the other two depth strata (since the known macroecological latitudinal pattern referred does not necessarily apply in deep water; e.g. Fisher et al., 2010, Lin and Costello 2023); whereas in the south area, body length increased from the shallower to the deeper strata, an ecological pattern "bigger deeper" that has been previously described in several cases but with context-dependent patterns (e.g. Mindel et al., 2017). Age at maturity, trophic level and maximum depth of distribution increased from the shallower to the deeper strata in each latitudinal area, an ecological pattern described for age at maturity in bony fishes (Drazen and Haedrich, 2012) and elasmobranchs (Rigby and Simpfendorfer, 2015), and in the case of age at maturity especially with a more pronounced manner from the southern to the northern area (Figures 10.3.b, i and e). High mobility was the most abundant mobility trait in 7 of the 9 latitudinal area*depth strata, followed by moderately mobile except in the recent years of north*medium depth and north*deep strata where this was inverted (Figure 10.3.d). In the north and southwest areas, the relative proportion of highly mobile species decreased from the shallower to the deeper strata, while the moderately mobile species and the (much less abundant) sedentary species increased. This importance of highly mobile species in demersal habitats and their decrease with depth has been previously described (e.g. Gordon and Bergstad 1992). The sedentary and especially the territorial mobility were the least important, which is expected since the samples are in soft substrate, and such species are more relevant in rocky substrate, which are more complex in structure and provide shelter (e.g. Buchheim and Hixon, 2017). No spatial patterns were evident in fecundity (Figure 10.3.c).

From the six ordered categories of thermal tolerance (from wide, i.e. >15ºC, to narrow, i.e. 0-2.5ºC, thermal tolerance), the highest relative proportion was represented by the 3rd most tolerant category (7.5-10ºC), followed by the 2nd most tolerant (10-15ºC) in all 9 latitudinal area*depth strata (Figure 10.3.g). In the north area, the relative proportion of the most important category (i.e. the 2nd most tolerant: 7.5-10ºC) was much higher than the others in the shallower stratum and decreased in importance towards the deeper strata contrarily to the second most important category (i.e. the 2nd most tolerant: 10-15ºC) which increased in importance. In contrast, in the southwest and south areas, the relative proportion of these two categories of the trait increased from the shallower to the deeper strata. Next, in terms of relative proportion were, in the north area, the 4th most tolerant category (i.e. 5-7.5ºC) and the 1st most tolerant (i.e. >15ºC) and finally the 5th most tolerant (i.e. 2.5-5ºC). Meanwhile, in the southwest and south area the following categories were: in the shallowest depths, the 5th (2.5-5ºC) or the 4th most tolerant (i.e. 5-7.5ºC); in the mid depths, the 4th most tolerant (i.e. 5-7.5ºC) and finally the 5th most tolerant (i.e. 2.5-5ºC); in the deeper depths, the 1st most tolerant (i.e. >15ºC), followed by the 5th most tolerant (i.e. 2.5-5ºC) or the 4th most tolerant (i.e. 5-7.5ºC) class.

From another perspective, in the all three latitude areas, the 5th and 4th most tolerant categories (i.e. 2.5-5 and 5-7.5ºC, respectively) decreased in importance from the shallowest to the deeper depths, while the 3rd most tolerant (i.e. 7.5-10ºC) had mixed variation

depending on the latitude (also decreasing in the north, and increasing in the south), and while the 2nd and the wider tolerance categories increased (i.e. 10-15 and >15ºC, with one exception). The least tolerant category (i.e. 0-2.5º) was not represented. These patterns are aligned with previous descriptions that marine species at higher latitudes experience greater seasonal temperature variation and are consequently predicted to withstand greater temperature extremes (e.g. Sunday et al. 2010).

From the seven classes of vertical distribution, the most important classes in terms of relative proportion differed with the latitudinal area*depth strata (Figure 10.3.f). In terms of relative proportion, demersal species were the most important in 7 of 9 area*depth strata, which is expected considering that the sampling device used was a bottom trawl and that the range of depths sampled was between 20 and 500m on the continental shelf and upper slope. In the shallower and intermediate depth strata, demersal species were followed by benthopelagic (or equaled in the case of southwest) and by pelagic-neritic species whereas in the deeper strata, they were followed by bathypelagic species and then by bathydemersal species (or by benthopelagic species in the south*deep stratum). This pattern is fully expected considering the increase of depth. Following in importance were, in most shallow and intermediate depths, bathydemersal and bathypelagic species while, in deeper depths, benthopelagic and pelagic-neritic species were the most relevant. Last in importance were, in most shallow and intermediate depths, reef-associated species followed by pelagic-oceanic species, while in deeper depths, mostly these same species but in inverse order. From another perspective, from the shallower to the deeper depths, benthopelagic and pelagic-neritic species decreased in importance whilst, inversely, bathydemersal and bathypelagic species increased in importance; demersal, pelagic-oceanic and reef-associated species had mixed variations with depth.

Generalist diet was the most abundant in all 9 latitudinal area*depth strata. In 8 of these 9 strata it was mostly followed by benthivorous and then by planktivorous In the south*deep stratum it was followed by planktivorous and only then by benthivorous (Figure 10.3.h). In the southwest and south areas, the relative proportion of generalist species increased from the shallower to deeper strata (reaching approximately the same proportion as in the three depth strata in the north) whereas the relative proportion of benthivorous species decreased. Piscivorous diets had a lower importance (except in the north*intermediate depth stratum), while herbivorous diets occurred only in the southwest*shallow stratum and were the least important.

As for change in the community weighted means (and proportions) of functional traits through time (2005-2017), some particular functional traits seem to decrease or increase through time in particular latitudinal area*depth strata, such as: a decrease of body length through time in the deeper strata, especially in the south area, an increase in age at maturity in the intermediate and deeper depths of the north area; a decrease in the relative proportion of highly mobile species in all depths of the north and southwest accompanied by an increase in the relative proportion of moderately mobile species (Figure 10.3.a-i).

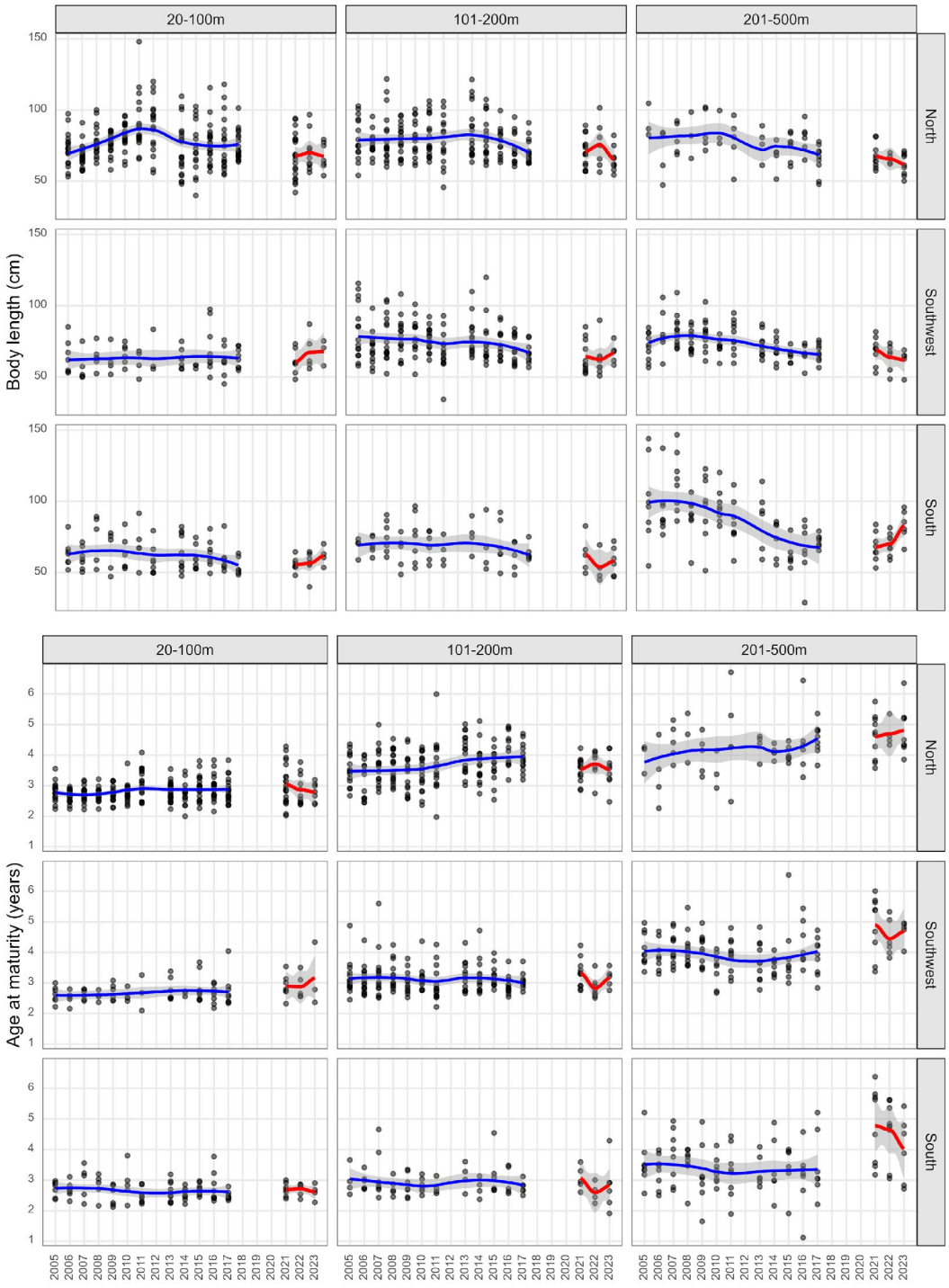

Figure 10.3. a, b. Community weighed mean of the functional traits Body length (top 3 panels) and Age at maturity (bottom 3 panels), per year between 2005-2017 and 2021-2023, in each of the nine latitudinal area*depth strata of the fish communities of the continental shelf and upper slope of the Portuguese coast as sampled in PT-PGFS-IBTS Q4 (International Bottom Trawl Survey Quarter 4 in Portuguese waters of ICES 27.9.a). In each plot each point is a haul, and the line is the "smoothed trend line with the method "loess" with a 95% confidence interval band.

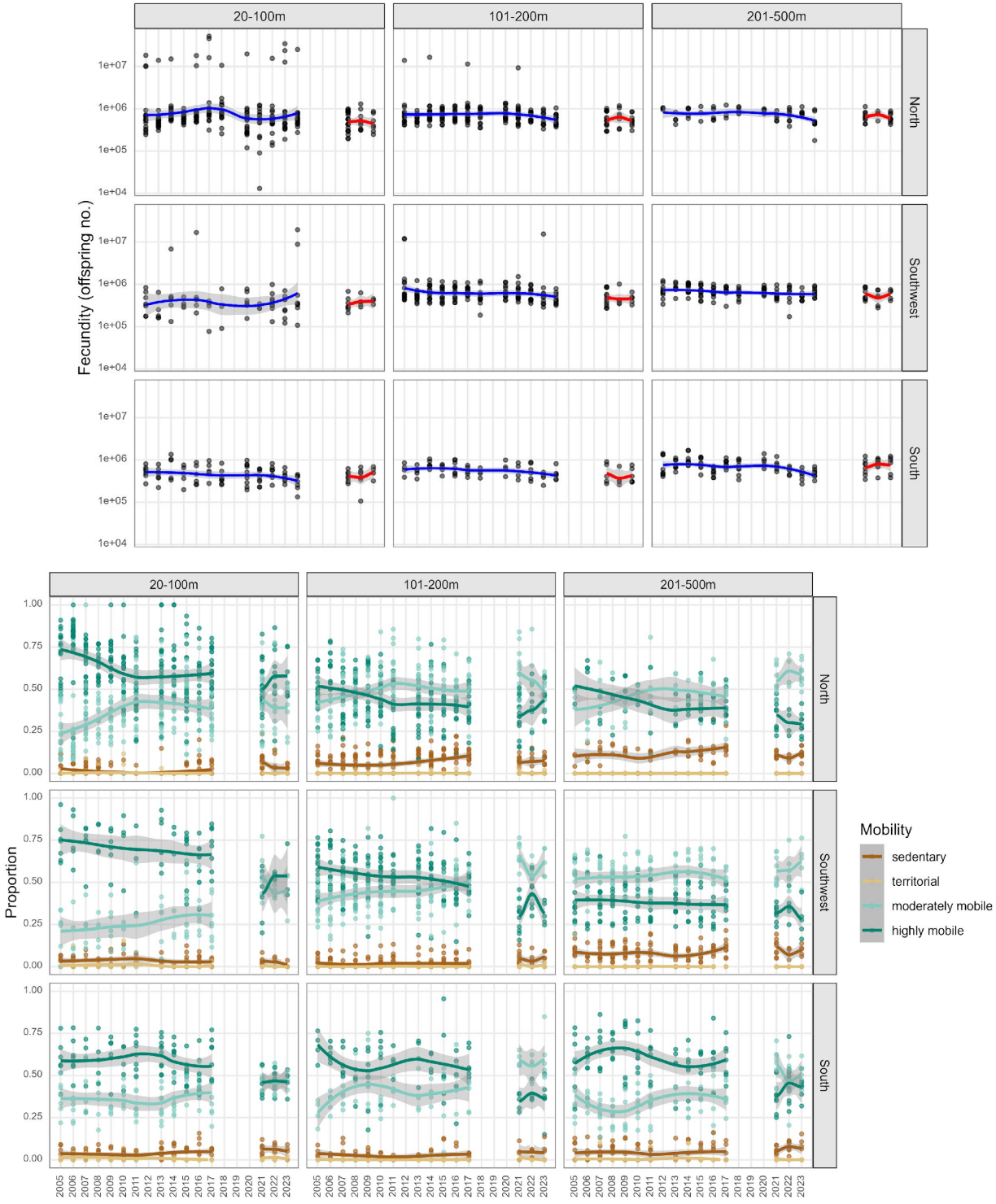

Figure 10.3.c, d. Community weighed mean of the functional traits Fecundity (top 3 panels) and Mobility (bottom 3 panels), per year between 2005-2017 and 2021-2023, in each of the nine latitudinal area*depth strata of the fish communities of the continental shelf and upper slope of the Portuguese coast as sampled in PT-PGFS-IBTS Q4 (International Bottom Trawl Survey Quarter 4 in Portuguese waters of ICES 27.9.a). In each plot each point is a haul, and the line is the "smoothed trend line with the method "loess" with a 95% confidence interval band.

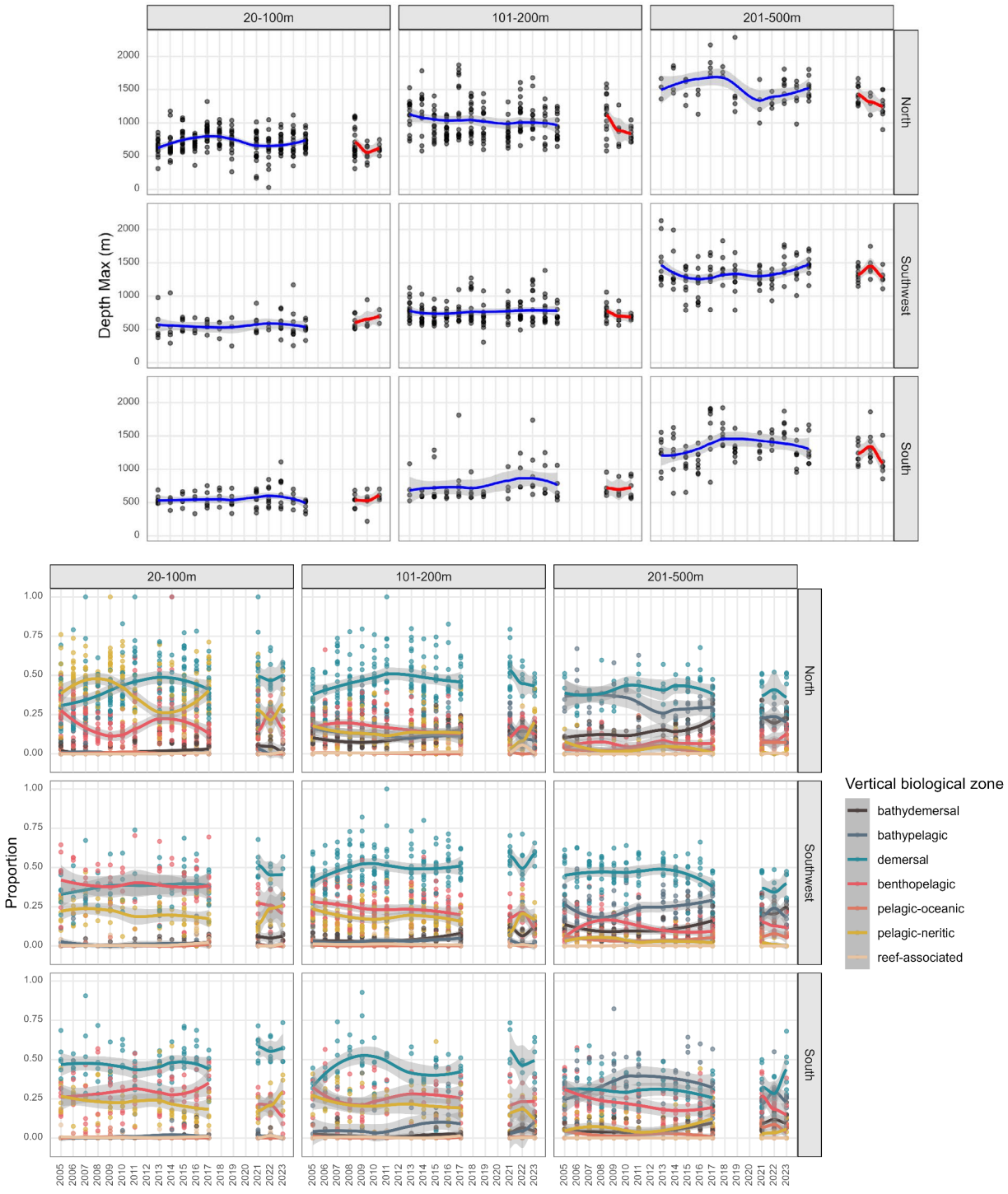

Figure 10.3.e, f. Community weighed mean of the functional traits Maximum Depth (top 3 panels) and Vertical biological zone (bottom 3 panels), per year between 2005-2017 and 2021-2023, in each of the nine latitudinal area*depth strata of the fish communities of the continental shelf and upper slope of the Portuguese coast as sampled in PT-PGFS-IBTS Q4 (International Bottom Trawl Survey Quarter 4 in Portuguese waters of ICES 27.9.a). In each plot each point is a haul, and the line is the "smoothed trend line with the method "loess" with a 95% confidence interval band.

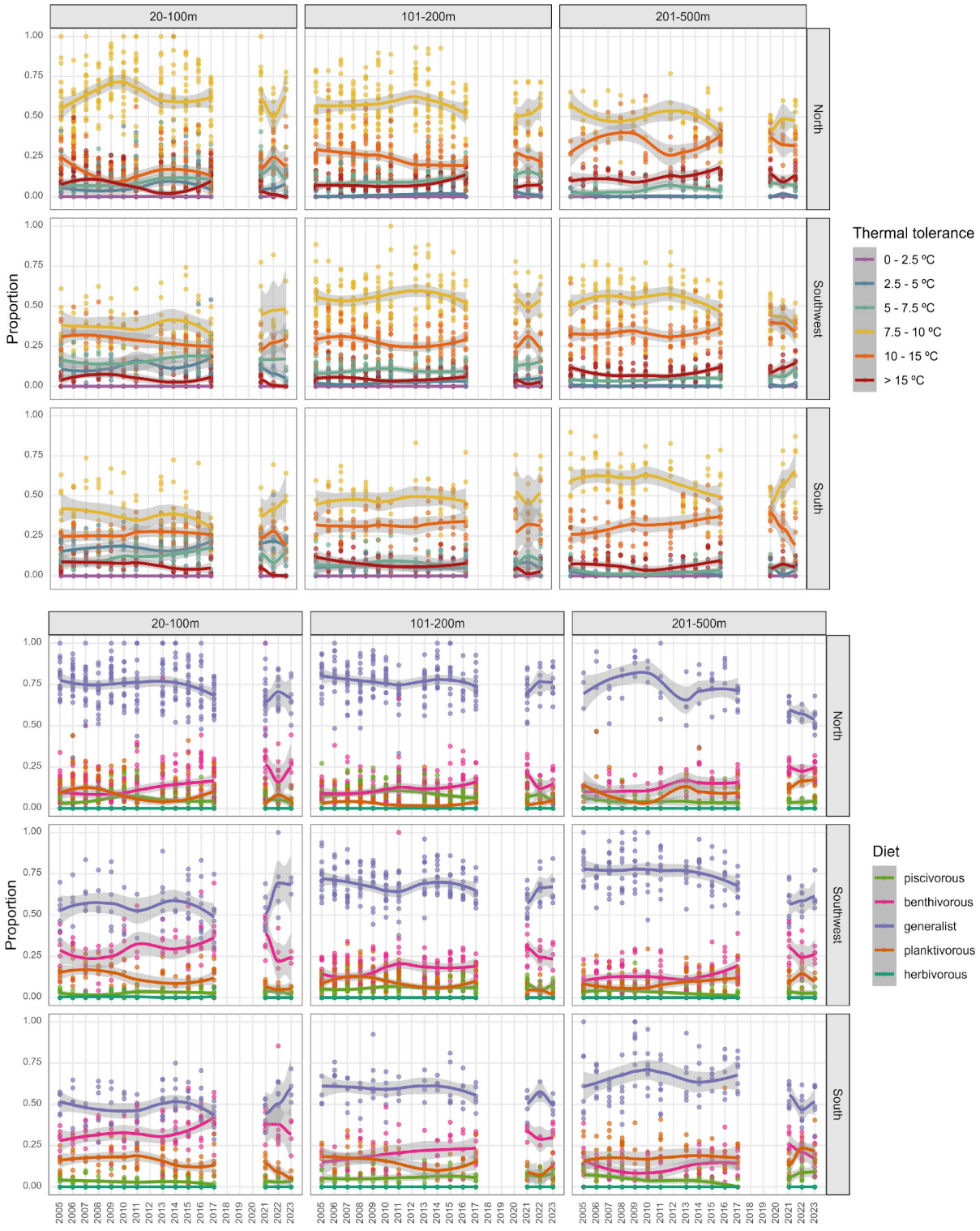

Figure 3.2.3.g, h. Community weighed mean of the functional traits Thermal tolerance (top 3 panels) and Diet (bottom 3 panels), per year between 2005-2017 and 2021-2023, in each of the nine latitudinal area*depth strata of the fish communities of the continental shelf and upper slope of the Portuguese coast as sampled in PT-PGFS-IBTS Q4 (International Bottom Trawl Survey Quarter 4 in Portuguese waters of ICES 27.9.a). In each plot each point is a haul, and the line is the "smoothed trend line with the method "loess" with a 95% confidence interval band.

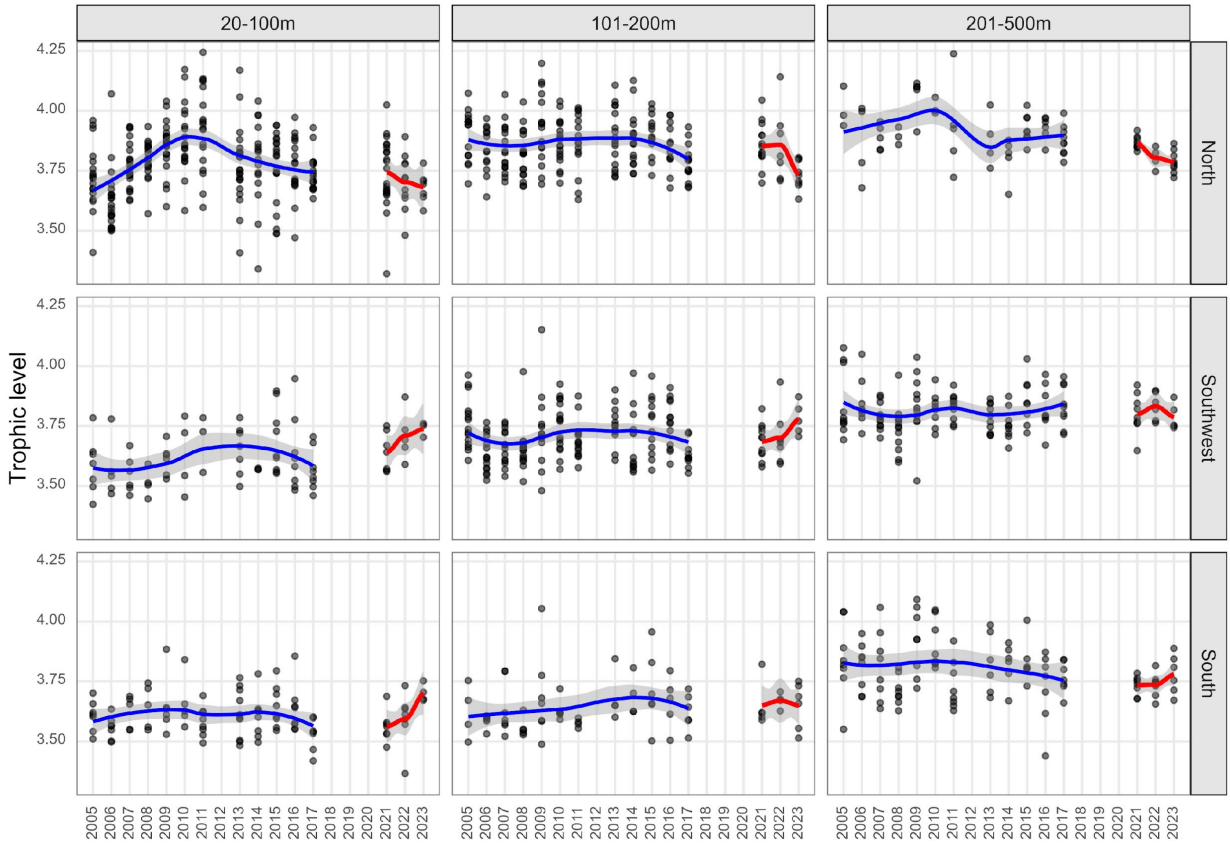

Figure 10.3.i. Community weighed mean of the functional trait Trophic level, per year between 2005-2017 and 2021-2023, in each of the nine latitudinal area*depth strata of the fish communities of the continental shelf and upper slope of the Portuguese coast as sampled in PT-PGFS-IBTS Q4 (International Bottom Trawl Survey Quarter 4 in Portuguese waters of ICES 27.9.a). In each plot each point is a haul, and the line is the "smoothed trend line with the method "loess" with a 95% confidence interval band.

Taxonomic and functional beta diversity indices

Beta diversity of the fish communities of the continental shelf and upper slope of Portugal in 2005-2023, as evidenced by the data from the PT-PGFS-Q4 research survey at sea, also show spatial patterns. In all 9 latitudinal area*depth strata, for both taxonomic (Supplementary Figure S10.7.a-h) and functional (Supplementary Figure S10.8.a-d) facets of biodiversity, Jaccard dissimilarity in each latitudinal area*depth strata (between samples of a year and samples of the reference years in the beginning of the respective time period) was higher than Bray-Curtis dissimilarity. This could indicate dissimilarity between years being driven more by species presence/absence than relative biomass among shared species, which suggests an importance of environmental filtering processes driving community composition and/or variability in catches. These patterns may be better understood, for example, by determining the species driving the dissimilarity among years. In addition, the decomposition of each of these taxonomic and functional beta diversity indices revealed that turnover processes (Jaccard turnover and the analogous Bray-Curtis Balanced variation for abundance data) were much more important compared to nestedness processes (Jaccard nestedness and analogous Bray-Curtis abundance gradients). This could indicate that dissimilarity between years is dominated by species replacement and balanced abundance shifts, indicating distinct community compositions rather than nested subsets.This may also support the importance of environmental filtering processes, with different taxa and functional traits favoured under different conditions (in that strata in different years),

and/or of variability in catches, as referred above. In some latitudinal area*depth strata (especially the north*deep stratum), taxonomic Jaccard turnover and nestedness (between samples of a year and samples of the reference years in the beginning of the time period) varied more noticeably than in the other latitudinal area*depth strata, which may be due to a lower number of samples in this stratum. In the north area, functional Jaccard dissimilarity (between samples of a year and samples of the reference years in the beginning of the respective time period) was slightly higher than in the other latitudinal areas, possibly suggesting a larger interannual variation in functional traits in this area. This variation may possibly be related to the high environmental variability typical of these latitudes, which leads to differing environmental conditions (and consequent traits that better adapt to those conditions) driven, for example, by freshwater runoff from several estuaries and the strong influence of north–northwest winds and currents. Taxonomic Simpson turnover results were close to the Jaccard component of turnover. Rao's Q (between samples of a year and samples of the reference years in the beginning of the respective time period) was higher in taxonomic than in the functional facet in all 9 latitudinal area*depth strata, suggesting that differences in species identity tend to be functionally similar, which indicates the existence of functional redundancy and of environmental filtering processes. Taxonomic Rao's Q was higher and less variable (between samples of a year and samples of the reference years in the beginning of the time period) in the two shallower depth strata , possibly suggesting consistently higher interannual variation than in the deep strata which is less exposed to atmospheric forcing (from winds and currents) and to variations in environmental conditions (e.g. from temperature and runoff); this contrast was not observed in Functional Rao's Q.

Maps of those indices across the 36 strata in the three time periods (Taxonomic – Supplementary Figures S10.9.a-h; Functional – Supplementary Figures S10.11.a-d), as well as the hotspots and coldspots of biodiversity identified (Taxonomic - Figure 10.4.a, b, c, Supplementary Figure S10.10.a-e; Functional - Figure 10.5.a, b, c, S10.11.a-d), revealed marked spatial patterns. These patterns are more evident in the hotspots and coldspots maps, which highlighted that species richness, in several cases, contrasts with Taxonomic Jaccard dissimilarity and turnover component, Simpson turnover, Bray-Curtis dissimilarity and balanced variation (turnover component). The nestedness component (of taxonomic and functional Jaccard and of Bray-Curtis dissimilarity) is highly marked when comparing the north area (mostly with hotspots) with the southwest and the south areas (mostly with coldspots) where turnover becomes more important. It is important to note that the north area is delimited to the south by Cape Carvoeiro, which is located just south of the Nazaré canyon, which can possibly act as a biogeographical barrier to dispersal in this marine ecosystem. The latitudinal increase in nestedness and decrease in turnover, in parallel with a decrease in species richness, have been previously described as a macroecological pattern for several biological groups (Soininen et al., 2018; Chaudhary and Costello, 2023; Baselga, 2010). The differential importance of turnover and nestedness to the north and south of this area may be the result of effects such as the contrast in species richness to the north (poorer) and south (richer), colonization from richer and poorer species pools north and south of the barrier, as well as stronger environmental filtering north of the barrier.

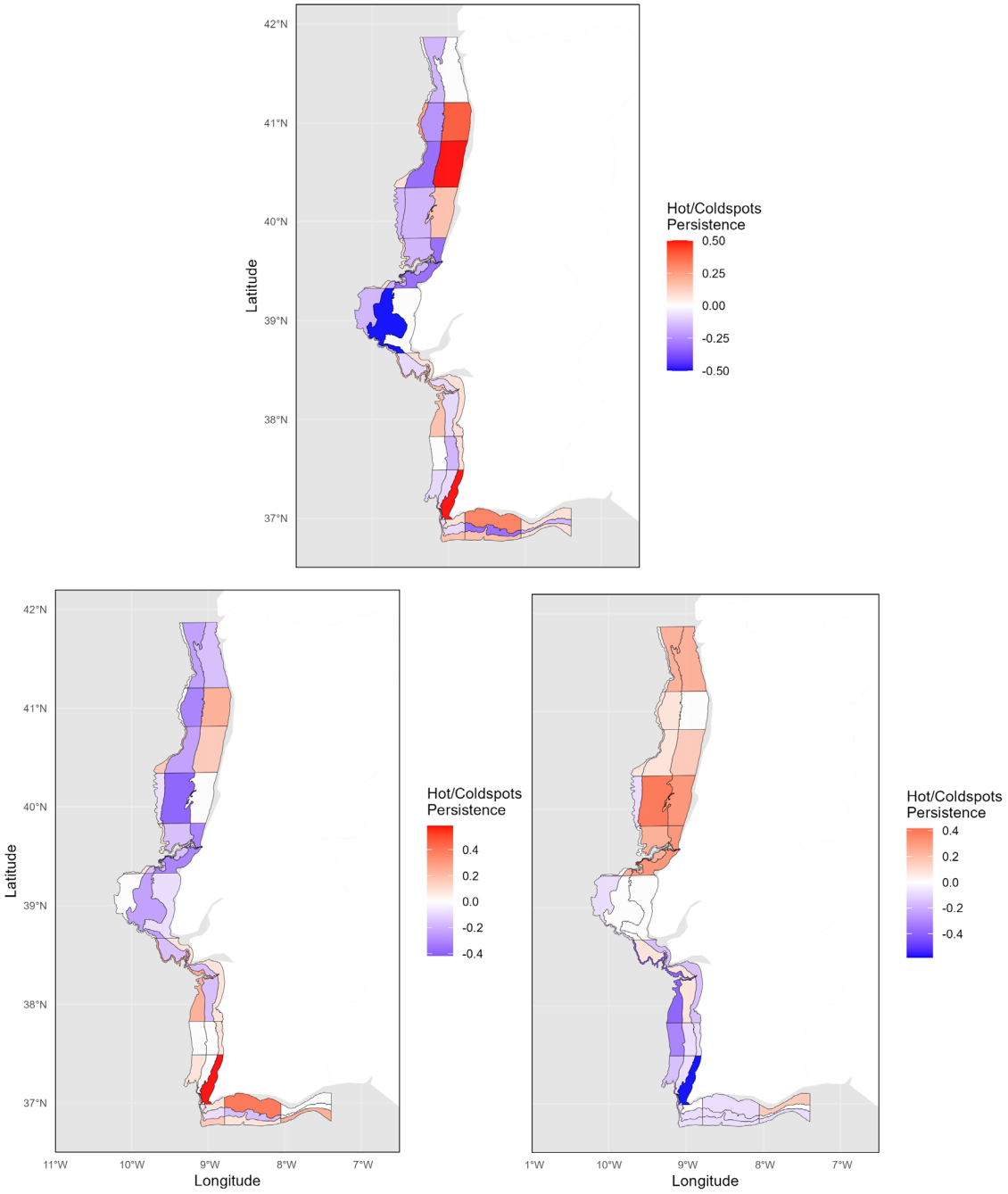

Figure 10.4. a, b, c. Persistence of hotspots and coldspots of taxonomic beta diversity index Jaccard Dissimilarity and components of Turnover and Nestedness in the time period 2005-2017 in each of the 36 sampled strata of the fish communities of the continental shelf and upper slope of the Portuguese coast as sampled in PT-PGFS-IBTS Q4 (International Bottom Trawl Survey Quarter 4 in Portuguese waters of ICES 27.9.a).

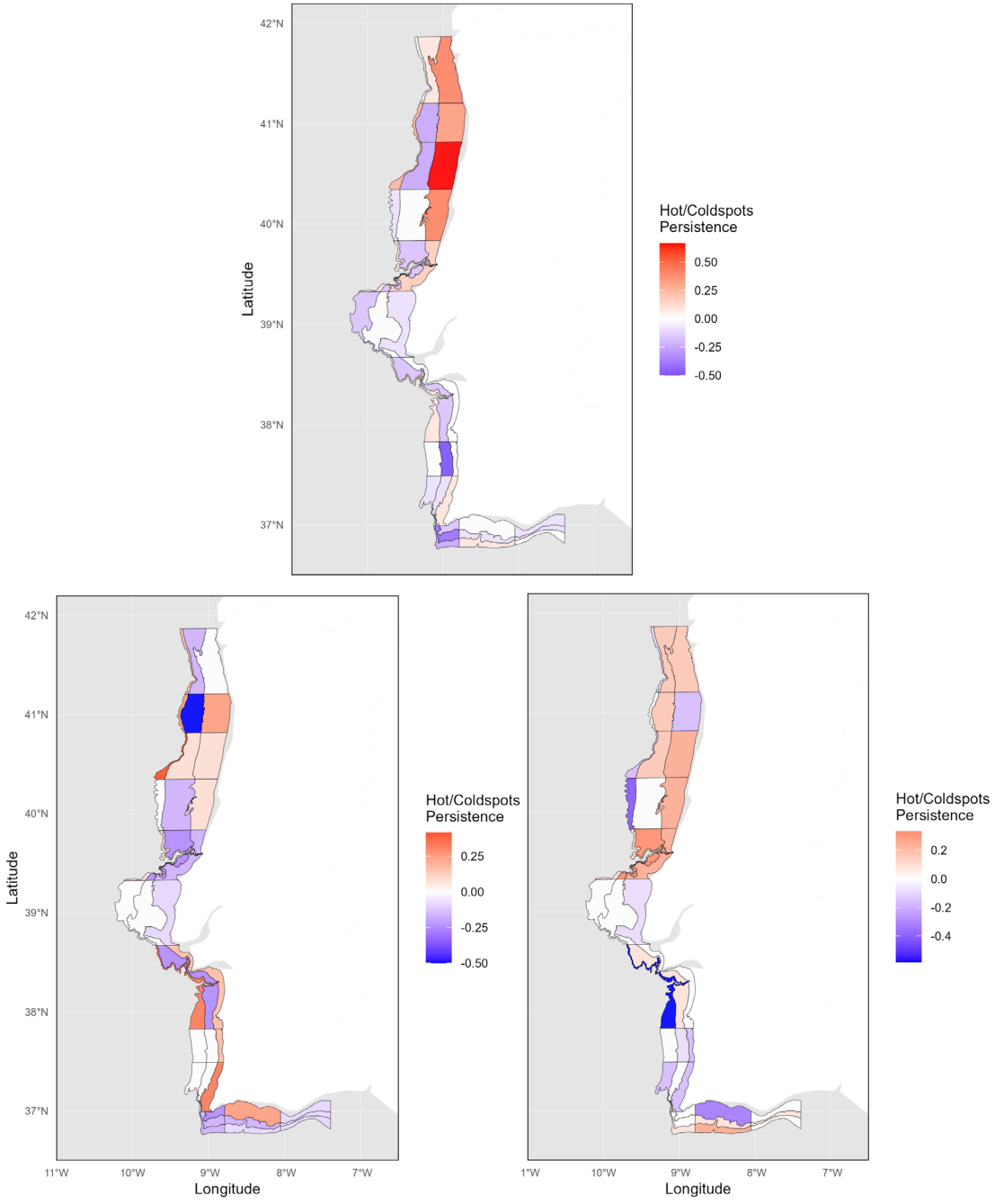

Figure 3.2.5. a, b, c. Persistence of hotspots and coldspots of functional beta diversity index Functional Jaccard Dissimilarity and components of Turnover and Nestedness in the time period 2005-2017 in each of the 36 sampled strata of the fish communities of the continental shelf and upper slope of the Portuguese coast as sampled in PT-PGFS-IBTS Q4 (International Bottom Trawl Survey Quarter 4 in Portuguese waters of ICES 27.9.a).

Final remarks

Along the Portuguese coast there is spatial variation in environmental variables and in fishing effort, and there have also been changes in these variables through time. Further analysis will be implemented to explore and quantify the relationship of alpha and beta diversity indices and of community weighted means and proportions of functional traits with environmental variables (e.g. temperature, salinity, oxygen) and with fishing effort.

10.4. References

Ashton, K. G., Tracy, M. C., de Queiroz, A., 2000. Is Bergmann's rule valid for mammals? The American Naturalist, 156(4), 390–415. doi: 10.1086/303400.

Baselga, A., 2010. Partitioning the turnover and nestedness components of beta diversity. Global Ecology and Biogeography, 19(1), 134–143. doi: 10.1111/j.1466-8238.2009.00490.x.

Beukhof, E., Dencker, T.S., Palomares, M., Maureaud, A., 2019. A trait collection of marine fish species from north atlantic and northeast pacific continental shelf seas. doi:10.1594/PANGAEA.900866.

Boettiger, C., Lang, D.T., Wainwright, P.C., 2012. rfishbase: exploring, manipulating and visualizing fishbase data from r. Journal of Fish Biology 81, 2030–2039. doi:10.1111/j.1095-8649.2012.03464.x.

Buchheim, J., Clynick, B., Hixon, M.A., 2017. Links between fish community structure and habitat complexity of a rocky reef in the Gulf of California threatened by development: Implications for mitigation measures. Ocean & Coastal Management, 137, 96–106. doi: 10.1016/j.ocecoaman.2016.12.013.

Butt, N., Halpern, B.S., O'Hara, C.C., Allcock, A.L., Polidoro, B., Sherman, S., Byrne, M., Birkeland, C., Dwyer, R.G., Frazier, M., Woodworth, B.K., Arango, C.P., Kingsford, M.J., Udyawer, V., Hutchings, P., Scanes, E., McClaren, E.J., Maxwell, S.M., Diaz-Pulido, G., Dugan, E., Simmons, B.A., Wenger, A.S., Linardich, C., Klein, C.J., 2022. A trait-based framework for assessing the vulnerability of marine species to human impacts. Ecosphere 13. doi:10.1002/ecs2.3919.

Chaudhary, C., Costello, M.J., 2023. Marine species turnover but not richness, peaks at the Equator. Progress in Oceanography, 210, 102941. doi: 10.1016/j.pocean.2022.102941.

Drazen, J.C., Haedrich, R.L., 2012. A continuum of life histories in deep-sea demersal fishes. Deep-Sea Research Part I: Oceanographic Research Papers, 61, 34–42. Doi: 10.1016/j.dsr.2011.11.002.

Fisher, J.A.D., Frank, K.T., Leggett, W.C., 2010. Global variation in marine fish body size and its role in biodiversity–ecosystem functioning. Marine Ecology Progress Series, 405, 1–13. doi: 10.3354/meps08601.

Gaston, K.J., 2000, Global patterns in biodiversity. Nature, 405, 220–227. doi: 10.1038/35012228.

Gislason, H., Collie, J., MacKenzie, B. R., Nielsen, A., Borges, M. de F., Bottari, T., Chaves, C., Dolgov, A. V., Dulčić, J., Duplisea, D., Fock, H. O., Gascuel, D., Gil de Sola, L., Hiddink, J. G., ter Hofstede, R., Isajlović, I., Jónas P. Jonasson, O. Jørgensen, K. Kristinsson, G. Marteinsdottir, H. Masski, S. Matić-Skoko, M. R. Payne, M. Peharda, J. Reinert, J. Sólmundsson, C. Silva, L. Stefansdottir, F. Velasco & N. Vrgoč (2020) Species richness in North Atlantic fish: Process concealed by pattern. Global Ecology and Biogeography, 29(5), 842–856. doi: 10.1111/geb.13068.

Gomes, M.C., Serrão, E., Borges, M.F., 2001. Spatial patterns of groundfish assemblages on the continental shelf of Portugal. ICES Journal of Marine Science 58(3), 633–647. doi: 10.1006/jmsc.2001.1052.

Gordon, J. D. M., Bergstad, O. A., 1992. Species composition of demersal fish in the Rockall Trough, north-eastern Atlantic, as determined by different trawls. Journal of the Marine Biological Association of the United Kingdom, 72(1), 213–230. Doi: 10.1017/S002531540004889X.

Henriques, S., 2007. Comparative analysis of the efficacy of multimetric indices based on fish communities in order to assess the ecological quality of coastal waters. mathesis. Faculdade de Ciências da Universidade de Lisboa.

Henriques, S., 2013. Marine fish assemblages as indicators of anthropogenic pressures: identifying sensitive metrics. Faculdade de Ciências da Universidade de Lisboa.

Henriques, S., Pais, M.P., Vasconcelos, R.P., Murta, A., Azevedo, M., Costa, M.J., Cabral, H.N., 2014. Structural and functional trends indicate fishing pressure on marine fish assemblages. Journal of Applied Ecology 51, 623–631. doi: 10.1111/1365-2664.12235.

Koutsidi, M., Moukas, C., Tzanatos, E., 2020. Trait-based life strategies, ecological niches, and niche overlap in the nekton of the data-poor mediterranean sea. Ecology and Evolution 10, 7129–7144. doi:10.1002/ece3.6414.

Lin, H.-Y., Costello, M.J., 2023. Body size and trophic level increase with latitude, and decrease in the deep-sea and Antarctica, for marine fish species. PeerJ Life & Environment, 11, e15880. doi: 10.7717/peerj.15880.

Marques, J.F., Santos, M.J., Cabral H.N. 2009. Zoogeographical patterns of flatfish (Pleuronectiformes) parasites in the Northeast Atlantic and the importance of the Portuguese coast as a transitional area. Scientia Marina, 73(3): 461-471. Doi: 10.3989/scimar.2009.73n3461.

Mindel, B. L., Neat, F. C., Webb, T. J., Blanchard, J. L., 2017. Size-based indicators show depth-dependent change over time in the deep sea. ICES Journal of Marine Science, 75(1), 113–121. doi: 10.1093/icesjms/fsx110.

Mouillot, D., Villéger, S., Parravicini, V., Kulbicki, M., Arias-González, J. E., Bender, M., Chabanet, P., Floeter, S.R., Friedlander, A., Vigliola, L., Bellwood, D. R., 2014. Functional over-redundancy and high functional vulnerability in global fish faunas on tropical reefs. Proceedings of the National Academy of Sciences, 111(38), 13757–13762. doi: 10.1073/pnas.

Moura, T., Chaves, C., Figueiredo, I., Mendes, H., Moreno, A., Silva, C., Vasconcelos, R.P., Azevedo, M., 2020. Assessing spatio-temporal changes in marine communities along the Portuguese continental shelf and upper slope based on 25 years of bottom trawl surveys. Marine Environmental Research, 160, 105044. doi: 10.1016/j.marenvres.2020.105044.

Polo, J., Punzón, A., Hidalgo, M., Pecuchet, L., Sainz-Bariáin, M., González-Irusta, J.M., Esteban, A., García, E., Vivas, M., Gil de Sola, L., López-López, L., 2024. Community's ecological traits reflect spatio- temporal variability of climate change impacts. Environmental and Sustainability Indicators 23, 100421. doi:10.1016/j.indic.2024.100421.

Rigby, C.L., Simpfendorfer, C.A., 2015. Patterns in life history traits of deep-water chondrichthyans. Deep-Sea Research Part II: Topical Studies in Oceanography, 115, 30–40. doi: 10.1016/j.dsr2.2013.09.004.

Soininen, J., Heino, J., Wang, J., 2018. A meta-analysis of nestedness and turnover components of beta diversity across organisms and ecosystems. Global Ecology and Biogeography, 27(1), 96–109. doi: 10.1111/geb.12660.

Sousa, P., Azevedo, M., Gomes, M.C., 2005. Demersal assemblages off Portugal: mapping, seasonal, and temporal patterns. Fisheries Research. 75(1–3), 120–137. doi: 0.1016/j.fishres.2005.03.012.

Sousa, P., Azevedo, M., Gomes, M.C., 2006. Species-richness patterns in space, depth, and time (1989-1999) of the Portuguese fauna sampled by bottom trawl. Aquatic Living Resources 19(2), 93–103. doi: 10.1051/alr:2006009.

Sunday, J.M., Bates, A.E., Dulvy, N.K., 2011. Global analysis of thermal tolerance and latitude in ectotherms. Proceedings of the Royal Society B: Biological Sciences, 278(1713), 1823–1830. doi: 10.1098/rspb.2010.1295.

11 Spatial variability in State-Pressure Relationships and Cumulative Impacts on North Sea Benthic Biodiversity

Authors: Justin Tiano, Georg Engelhard, Marcel Rozemeijer

11.1. Introduction

The North Sea supports a diverse benthic invertebrate community, that influence ecosystem functions such as nutrient cycling, sediment mixing, and habitat provisioning. These communities are influenced by a combination of natural and human-induced pressures, including bottom trawling, nutrient enrichment, and climate-driven changes in sea temperature. Understanding how these pressures interact to shape biodiversity is essential for meeting policy objectives such as the MSFD's (Marine Strategy Framework Directive) "Good Environmental Status" (GES) for Descriptor 1 on biodiversity (and Descriptor 6 on Seabed integrity).

State-pressure relationships refer to the links between the "state" of the ecosystem and the intensity or presence of specific pressures, such as trawling effort, nutrient concentrations, and sea surface temperature. By quantifying these relationships, we can assess how each pressure influences biodiversity, whether positively, negatively, or nonlinearly, and how these effects vary across space.

Cumulative impacts describe the combined effect of multiple pressures acting simultaneously on biodiversity. Even if individual pressures have modest consequences, their additive impacts can lead to greater overall change, potentially pushing systems toward unfavorable states (Knight et al., 2013, Piet et al., 2021). Cumulative impact indices, derived from fitted statistical models, allow us to integrate the magnitude and direction of multiple stressors into spatially explicit assessments, identifying areas where biodiversity is most at risk.

This chapter uses North Sea invertebrate data collected from the annual ICES Beam Trawl Survey (BTS) to investigate state-pressure relationships and cumulative impacts on species richness (mostly epibenthos). Analyses were conducted across four broad regional quadrants of the North Sea, allowing comparison of relationships in different environmental and fishing contexts. We specifically examine how sea surface temperature (SST), trawling effort, phosphorus, and nitrogen relate to species richness, and how these relationships vary geographically. We also map cumulative impact indices to highlight areas of the North Sea where the combined negative effects of these pressures are greatest, as well as regions where pressures appear to have less influence on biodiversity.

11.2. Material and Methods

Survey data

This analysis focused on spatial patterns in species richness of North Sea benthic invertebrates (mostly epibenthic), using data from the annual ICES Beam Trawl Survey (BTS) collected between 2000 and 2024. Survey coverage extended from 51°N to 58°N and 3°W to 9°E, encompassing the central and southern North Sea. All invertebrate records were extracted from the ICES DATRAS database for Quarter 3 hauls conducted by the Netherlands, Germany, the United Kingdom, and Belgium. Belgian BTS data for 2000–2009, 2010, and 2016 were excluded due to

closed species lists limiting detection of rare taxa. Only epibenthic invertebrates and cephalopods were retained, with species richness calculated as the total number of taxa per haul.

Environmental covariates associated with each haul included depth, median sediment grain size, orbital current velocity (Wilson et al., 2018), annual mean sea surface temperature (SST; Copernicus Marine Service, 1993–2020), and reconstructed swept-area trawling effort (Couce et al., 2020). Mean concentrations of dissolved inorganic nitrogen and phosphorus were derived from Copernicus Marine Service (1993–2020).

Study area

We first mapped the spatial distributions of all environmental covariates across the North Sea to visualise gradients and potential hotspots (Figure 11.1.). The analysis was constrained to the areas sampled by the North Sea BTS, which range from a depth from approximately 20m in the southern and eastern North Sea to over 140 m off the eastern coast of Scotland. Spatial gradients were evident for all numeric environmental co-variates with the southern North Sea exhibiting higher chlorophyll-a, SST, and trawling effort. Phosphorus hotspots were concentrated off the northern and southern coasts of East Anglia in England the while nitrogen concentrations were highest off the Netherlands coast (Figure 11.1). Table 11.1 summarizes the mean, min and max values of these environmental variables per sub-regional quadrant.

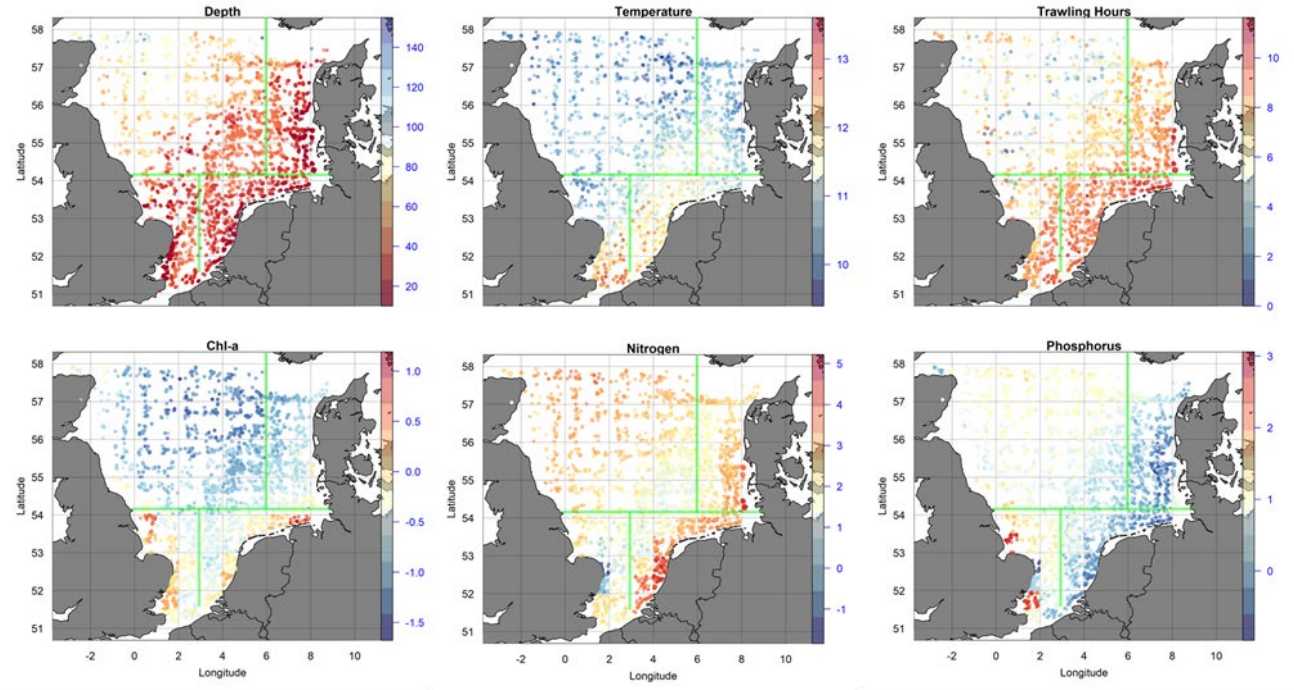

Figure 11.1. Maps of abiotic North Sea variables. Trawling hours (effort per ICES rectangle), and Chl-a, and nitrogen, and phosphorus concentrations (mmol m^{-3}) are log-transformed. Green lines delineate northwest (NW), northeast (NE), southwest (SW), and southeast (SE) spatial quadrants specified for analysis.

Table 11.1. Averages and ranges of environmental variables associated with each spatial quadrant of the North Sea. Values are reported as mean, with minimum and maximum in parentheses.

Variable	Unit	NW	NE	SW	SE
Chl-a concentration	mmol m^{-3}	0.49 (0.19–1.6)	0.76 (0.25–2.2)	1.26 (0.5–3.1)	1.10 (0.5–3.3)
Depth	m	58 (19–155)	34 (12–71)	32 (10–88)	28 (12–54)
Trawling effort	Hours per ICES rectangle	4,152 (1–34,150)	16,271 (116–124,046)	12,065 (10–43,424)	27,060 (123–71,251)
Nitrogen concentration	mmol m^{-3}	5.6 (0.73–30)	9.0 (1.3–60)	2.7 (0.05–12)	15.0 (0.45–38.99)
Phosphorus concentration	mmol m^{-3}	0.30 (0.07–0.77)	0.16 (0.03–0.42)	0.58 (0.04–2.5)	0.16 (0.05–0.46)
N:P ratio	–	17 (2.8–113)	73 (5.3–484)	7.5 (0.80–90)	141 (1.6–477.81)
Sea surface temperature	°C	11.0 (8.9–12.0)	11.0 (8.9–12.0)	12.0 (9.5–13.6)	11.7 (9.6–13.29)

Raw covariate-richness relationships

Relationships between species richness and each covariate were then explored in raw form using scatterplots and smooth fits to identify non-linear patterns. Species richness was also compared with the abundance of selected fish species to provide broader biological context. Only covariates with statistically significant relationships to richness were retained for further statistical modelling. Variance inflation factor (VIF) analysis indicated no problematic multicollinearity among the selected covariates. However, log(chl-a) was excluded from the final spatial models because its apparent relationship with richness was likely driven by its correlation with depth.

Quadrant delineation

To assess regional differences in state–pressure relationships, the North Sea was divided into four quadrants representing the northwest (NW), northeast (NE), southwest (SW), and southeast (SE) based on ecological and environmental gradients. The northern quadrants were separated from the southern ones at 54°N, corresponding to a marked decline in chlorophyll-a concentrations above this latitude. The NW quadrant was further defined west of 6°E, reflecting historical patterns where species richness was highest above 54°N and westward before shifting east and southwards over time. The SW quadrant contains pronounced phosphorus hotspots, while the SE quadrant contains the most prominent nitrogen hotspots as well as the highest trawl effort. This stratification allowed the effects of environmental pressures to be assessed in the context of distinct regional conditions.

Modelling state–pressure relationships

We modelled state-pressure relationships, defined as the statistical links between the state of biodiversity (species richness) and key environmental pressures (trawling effort, nitrogen, phosphorus, and SST), using the *sdmTMB* package in R (Anderson et al., 2022). Models were fitted separately for each quadrant, with the following general structure:

$$\textbf{Richness} = \beta 0 + f1(\text{Depth}) + \beta 1 \cdot \text{Gear} + \beta 2 \cdot \text{Sediment type} + f2(\text{Nitrogen}) + f3(\text{Phosphorus}) + f4(\text{Trawling effort}) + f5(\text{SST}) + f6(\text{Ship}) + \varepsilon$$

where:

- **Richness** is the number of invertebrate taxa per haul.
- f1 (*Depth*) is a smooth effect of depth, modelled using thin-plate regression splines with $k = 3$.
- *Gear* and *Sediment_type* are categorical fixed effects with coefficients β1 and β2.
- f2 (*Nitrogen*) and f3 (*Phosphorus*) and are smooth effects of log-transformed nitrogen and phosphorus concentrations, each modelled with $k = 4$.
- f4 (*Trawling effort*) is a smooth effect of log-transformed annual trawling effort hours per ICES rectangle ($k = 3$).
- f5(*SST*) is a smooth effect of annual mean sea surface temperature ($k = 3$).
- f6(*Ship*) is a random intercept for survey vessel.
- Spatial correlation was modelled with a Gaussian Markov random field via the SPDE approach on a triangulated mesh, and temporal correlation with an AR(1) spatiotemporal structure across years.
- ε is the model error term, assuming a Gaussian distribution with a log link.

Cumulative impact index

To assess combined pressure effects, we also fitted the above *sdmTMB* model to the full North Sea dataset. From this model, we extracted the partial effects of SST, trawling effort, nitrogen, and phosphorus at each haul location. Two cumulative impact indices were then calculated:

1. **Negative-effect index** – summing only the negative partial effects, representing where pressures were associated with decreases in species richness in the fitted model.
2. **Absolute-effect index** – summing the absolute value of all partial effects, representing overall sensitivity to pressures regardless of direction (positive or negative).
3. **Positive-effect index** – summing only the positive partial effects, representing areas where pressures were associated with increases in species richness in the fitted model.

The indices were interpolated across the study area to produce spatially explicit cumulative impact maps.

Multivariate community-environment relationships

Co-inertia analysis was used to explore how environmental variables covaried with species composition, both for the full North Sea (results in appendix) and within each quadrant (Dolédec and Chessel, 1994). Species abundance data were Hellinger-transformed and ordinated using a scaled principal component analysis (PCA), while environmental variables were standardized. Co-inertia analysis was then applied, using the ade4 package, to quantify the shared co-structure between the species and environmental ordinations, and results were visualised as biplots (Dray and Dufour, 2007).

All plotting and statistical analyses were performed in R (R Core Team 2025).

11.3. Results

Nutrient–chlorophyll relationships varied considerably between North Sea quadrants (Figure 11.2 and S11.1-S11.4). In the NW quadrant, phosphorus and nitrogen concentrations were strongly positively correlated, while Chl-a declined with increasing nitrogen (Figures S11.1 and S11.2). NE exhibited a U-shaped relationship between phosophorus and nitrogen and a non-linear positive relationship of Chl-a to nitrogen and N:P ratio (Figures S11.1 and S11.2). The SW quadrant showed non-linear patterns, with U-shaped relationships of Chl-a with both nitrogen and phosphorus concentrations, and variable responses to the N:P ratio (Figures S11.2-S11.4). In the SE quadrant, nitrogen and phosphorus were negatively correlated, Chl-a increased with nitrogen but declined with phosphorus, with higher values at elevated N:P ratios (Figures S11.1-S11.4). Across the entire North Sea, raw relationships were more scattered, with weak but non-linear trends between Chl-a and nutrient concentrations and a broadly positive relationship between N:P ratio and Chl-a (Figure 11.2).

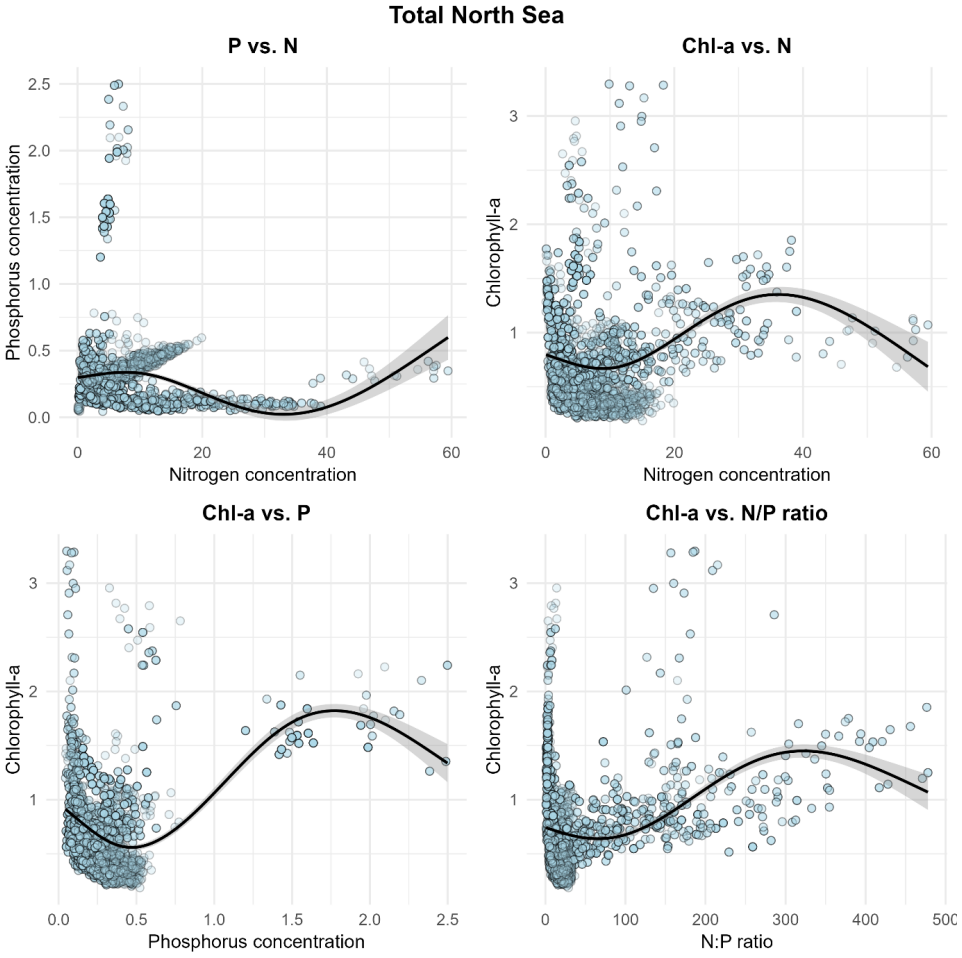

Figure 11.2. Scatterplots of nutrient relationships across the North Sea and within individual quadrants. Panels show pairwise relationships between nitrogen, phosphorus, chlorophyll-a, and the N:P ratio, with points representing individual hauls and black lines indicating smoothed fits (GAMs with 95% confidence intervals).

Raw richness-covariate relationships across the entire North Sea basin showed that log-transformed phosphorus concentrations and trawling effort each explained approximately 19% of invertebrate species richness, with depth and log-transformed chlorophyll a concentrations explaining 18% and 10% respectively (Figure 11.3). Nitrogen concentrations and SST explained only 6% and 5% of species richness though all relationships were statistically significant ($p < 0.001$). Spatially aggregated depth data was positively correlated overall to species richness while trawling effort, chl-a, and temperature, were negatively correlated. Raw relationships for log-transformed phosphorus and nitrogen concentrations showed clear non-linear relationships with species richness showing local maxima at intermediate concentrations(~10 mmol m^{-3} Nitrogen; ~0.3 mmol m^{-3} Phosphorus).

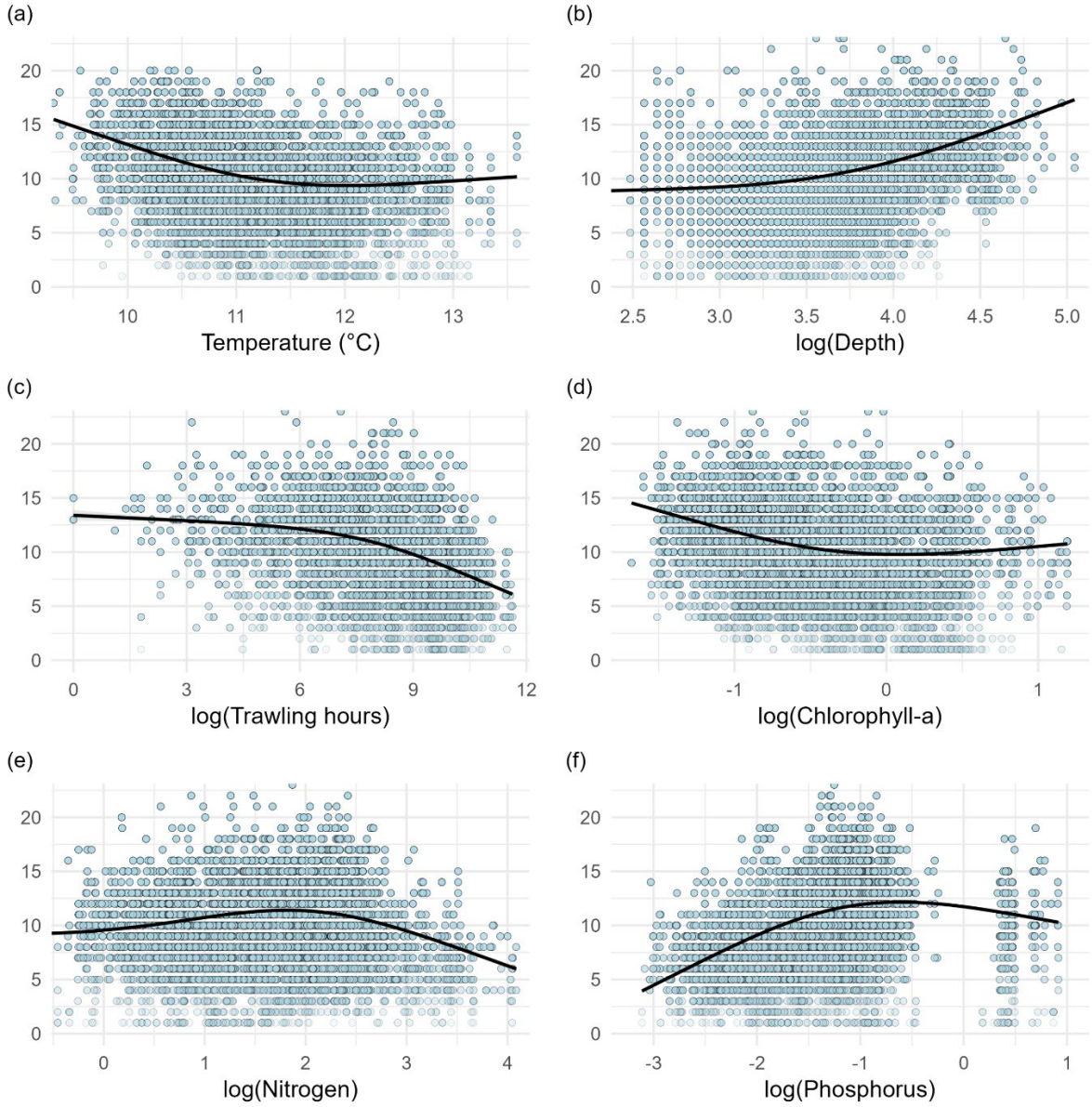

Figure 11.3. Raw relationships between species richness and selected abiotic (temperature, depth, trawling effort, nitrogen, phosphorus, chlorophyll-a) variables across the North Sea. Points show individual hauls; lines represent smooth fits from separate GAMs.

Functional forms of state–pressure relationships by quadrant

Modelled relationships between species richness and environmental pressures varied markedly across the four North Sea quadrants. In the northern areas (NW and NE), sea surface temperature (SST) exhibited a clear negative relationship with species richness, whereas in both southern quadrants (SW and SE) the relationship was positive, with species richness increasing at higher temperatures (Figure 11.4). Trawling effort showed a hump-shaped pattern in the NW, with species richness peaking at intermediate effort before declining, while in the NE and SE the effect was negative and approximately linear. In contrast, the SW quadrant showed a positive relationship between trawling effort and species richness. Nitrogen concentration was generally associated with reduced species richness in the NW, NE, and SE, although the pattern in the SW was non-linear, with declines at both low and high concentrations. Phosphorus effects differed strongly by region: relationships were negative in both northern quadrants, strongly positive in the SW, and U-shaped in the SE, with species richness lowest at intermediate concentrations (Figure 11.4).

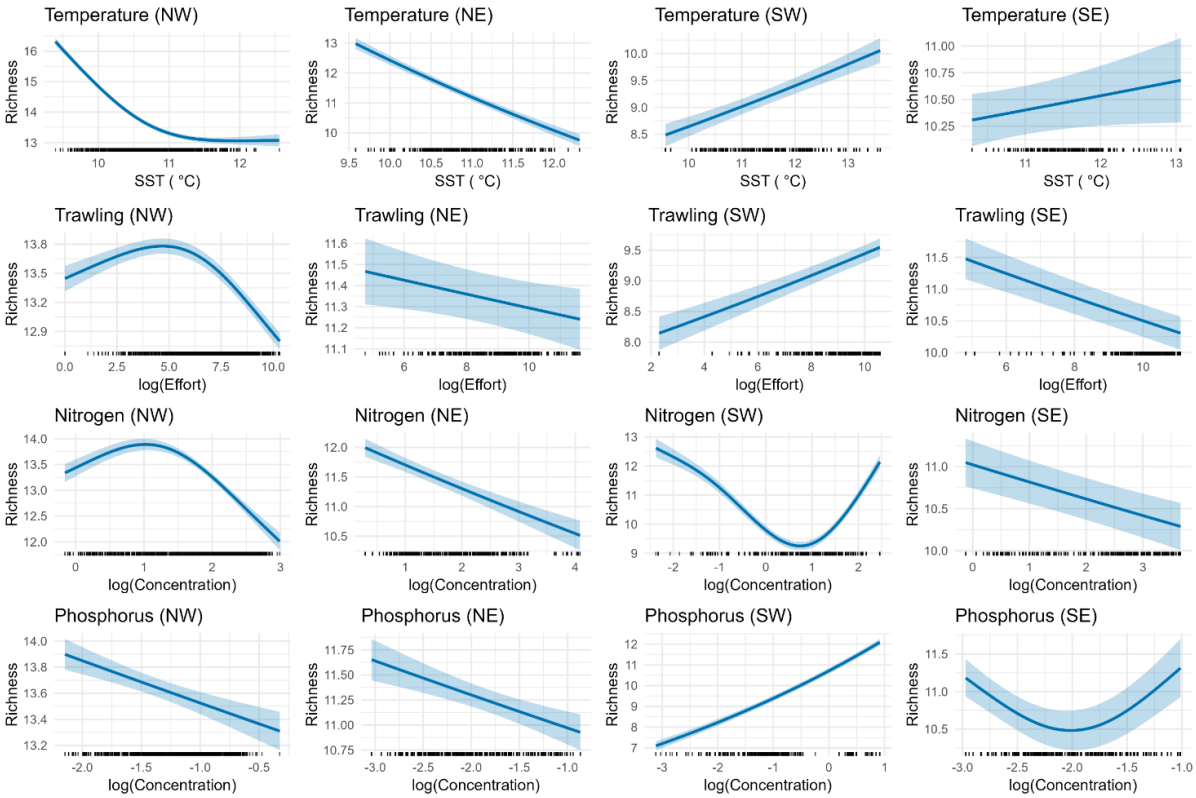

Figure 11.4. Functional forms of state–pressure relationships for species richness in four North Sea quadrants (NW, NE, SW, SE) derived from sdmTMB models. Shaded areas show 95% confidence intervals.

Co-inertia biplots by sub-region

Co-inertia biplots were used to visualize the joint co-structure between species composition and environmental variables within each North Sea quadrant (Figure 11.5). In all cases, Monte Carlo tests using 999 iterations, showed highly significant associations between the two datasets ($p = 0.001$), indicating that variation in community structure is strongly related to environmental gradients.

NW (quadrant 1) exhibited the highest proportion of variance explained by Axis 1 (horizontal; 75%), suggesting that depth and current velocity and longitude (West to East) as the strongest environmental gradients driving species composition in the area (Figure 11.5). There, SST and trawling effort and current speed cluster on the left side of Axis 1 with the majority of taxa projecting the opposite direction along the right side of the ordination. The horizontal Axis 1 also exerted the strongest influence on the NE co-structure (quadrant 2, 70%) forming an opposing gradient between chl-a on the left side and depth on the opposite end. Here, nitrogen and trawling form strong pressures with many taxa clustering on the opposite direction. SW (quadrant 3) features a more balanced co-structure with 48% of the variance explained by Axis 1 and 29% on Axis 2 (vertical axis). Here, SST and current speed form the strongest environmental gradients with several taxa aligning with the latter which also opposes trawling effort. SE (quadrant 4) features the main gradient as Axis 1 (64% variance explained) with 25% of the variance explained in Axis 2. This area shows the strongest effects coming from nitrogen and phosphorus concentrations which are located on opposite ends of Axis 1 with many taxa (other than Crangon crangon) more closely aligned with phosphorus and opposed to nitrogen (Figure 11.5).

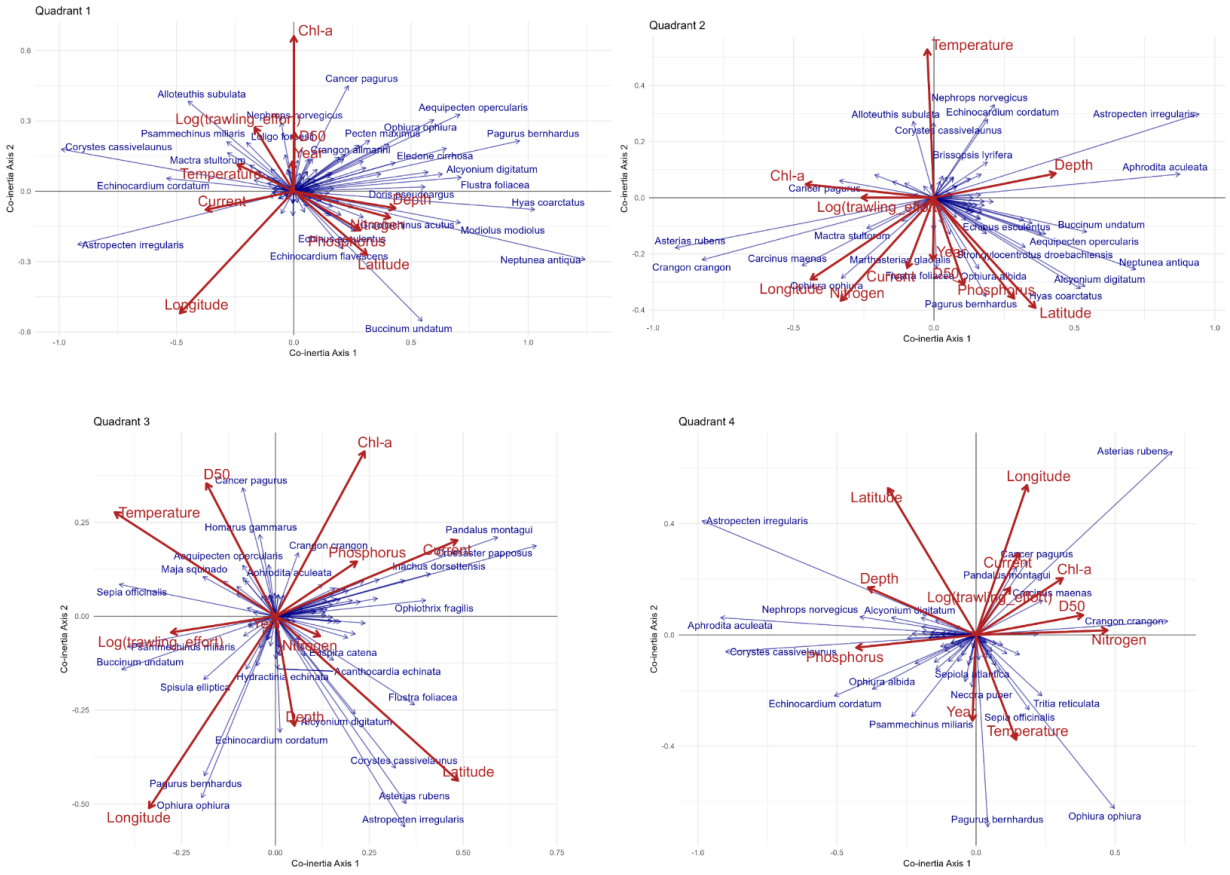

Figure 11.5. Co-inertia analysis of relationships between environmental variables (red arrows) and species composition (blue arrows) in four North Sea quadrants (Quadrant 1 = NW, Quadrant 2 = NE, Quadrant 3 = SW, Quadrant 4 = SE).

Cumulative impacts

Cumulative impacts (based on the pressures SST, trawling effort, nitrogen, and phosphorus) were divided into either cumulative negative, positive, or absolute impacts on species richness taken by extracting their partial effects from the full North Sea spatio-temporal model. Figure 11.6 shows categorical (low/medium/high) impact classes derived by dividing the data range into tertiles with each class representing one-third of the distribution values. The negative index shows the highest values clustering along the southern and eastern margins of the North Sea, forming a belt from the Belgian to Danish coasts. From there, medium values extend towards the eastern central shelf, while the lowest values occur over the central offshore area towards the northwest. The positive index highlights areas where the partial effects of pressures were associated with increases in species richness. These higher values are more scattered across the North Sea, but are particularly visible in some offshore regions of the northern and western North Sea. The absolute index, which combines both positive and negative effects, shows a similar pattern of high impact areas in the same coastal zones but the footprint extends to the coastal areas of east Anglia where phosphorus concentrations are high and also towards the north of the North Sea where there are intermediate nitrogen concentrations. The absolute impacts index also exhibits a low-impact area within the central offshore North Sea (Figure 11.6). Each index was rescaled across its own data range.

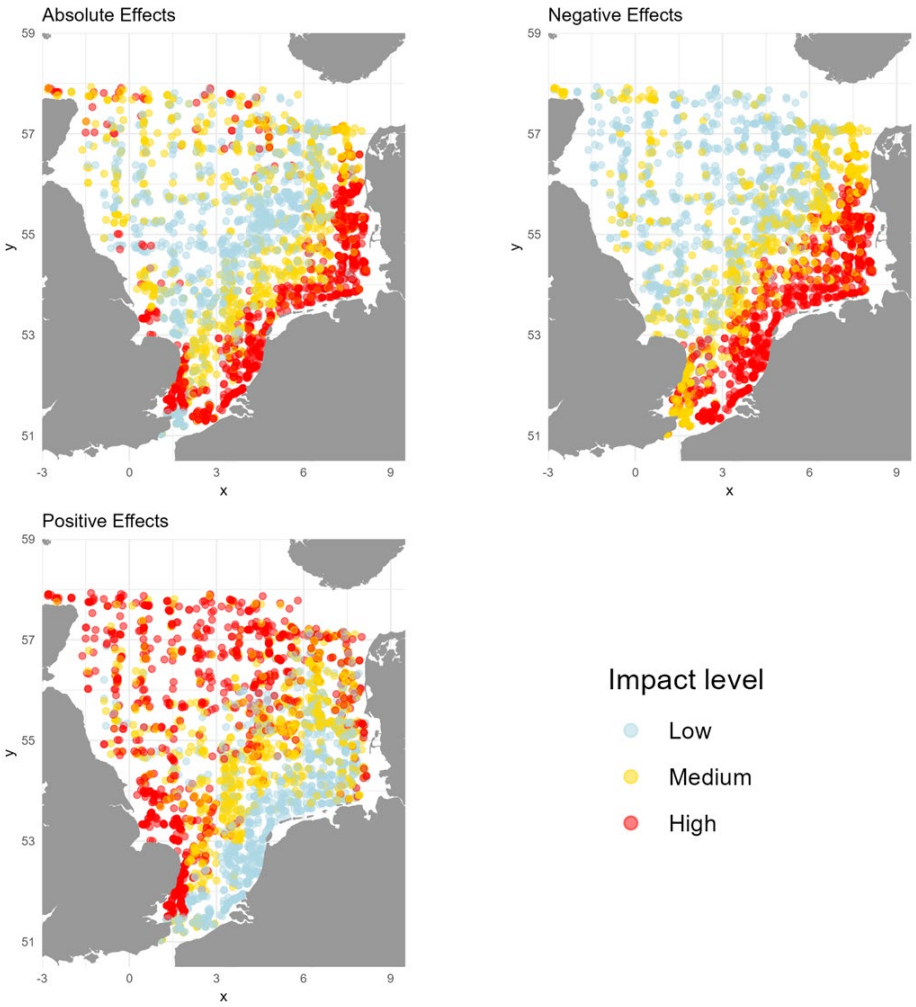

Figure 11.6. Spatial distribution of cumulative impact indices for species richness in the North Sea, calculated from rescaled partial effects of SST, trawling effort, nitrogen, and phosphorus. Panels show absolute, negative, and positive indices partitioned by categorical impact classes (Low/Medium/High).

11.4. Discussion

General implications

This research applied fisheries-independent trawl survey data to quantify spatial variation in state-pressure relationships and cumulative impacts on benthic invertebrate biodiversity in the North Sea. By focusing on species richness as an indicator, we identified key pressures in trawling effort, nutrient enrichment (nitrogen, phosphorus), and SST, that exhibit markedly different effects depending on the subregion. The observed spatial gradients are broadly consistent with earlier North Sea benthic studies that documented higher richness and community stability in more northerly areas of the North Sea (Callaway et al., 2002; Reiss et al., 2010). Our findings extend the prior knowledge to include the functional response forms and cumulative impacts from anthropogenic pressures and detailed multi-variate ordinations, to be able to show variability in area-based pressures in how they influence local biodiversity. These results reinforce the need for region-specific management approaches under the Marine Strategy Framework Directive's Good Environmental Status (GES) objectives.

Raw co-variate relationships with species richness

Chlorophyll-a showed a marginally negative trend with species richness as concentrations increased from approximately 0.20 to 0.74 mmol m^{-3} (Figure 11.3). However, interpretation is complicated by strong correlations with depth and with nutrient concentrations, which differ regionally (e.g. chl-a correlating more with phosphorus in the southwest and with nitrogen in the southeast, (***Figure 1***). This makes its independent contribution difficult to isolate from co-varying drivers. For this reason, chlorophyll-a was excluded from the spatial models and cumulative impact indices, though it remains ecologically important and contributes to the multivariate ordination analyses.

Quadrant delineation

The areas were chosen based on patterns in pressures. They are in broad agreement with different ecohydrodynamic regions described by van Leeuwen et al. (2015), which in turn are reflected in different phytoplankton (Capuzzo et al. 2018) and zooplankton dynamics by region (Pitois & Fox 2006). The SE is relatively shallow and dominated by inflow from the English Channel and the rivers Rhine and Meuse (associated with high nutrient inputs, particularly of nitrates; van Leeuwen et al. 2015) featuring relatively high phytoplankton productivity (Capuzzo et al. 2018). SW includes permanently mixed areas and is influenced by inflow from the north. This area has locally high phosphate input from the English rivers and features relatively high turbidity (Capuzzo et al. 2018). The NW is a relatively deep region characterized by seasonal stratification and lower phytoplankton productivity compared to other more coastal zones. Finally the NE quadrant, more shallow than NW, is bordered by the very deep Norwegian Trench to the north (though outside our study area) and is influenced by both continental riverine inputs and inflow from the North Atlantic Current, and features some areas with high productivity though lower than the southern regions (van Leeuwen et al. 2015). The southern (and south-eastern) North Sea is warmer in summer but generally also colder in winter than the northern (north-western) North Sea (Dye et al. 2013), and subject to greater beam trawl pressure (Couce et al. 2020) – noting the warming temperature trend and reduction in beam trawl pressure.

Fishing pressure

Trawling effort was generally negatively linked with species richness, although the positive relationship in the SW quadrant highlights the complexity of interpreting state-pressure patterns. In the SW, it may be possible that fishing activity overlaps with naturally richer habitats rather than trawling being the cause for higher species richness. The trawl-reduced reduction of benthic biodiversity has been well documented, although there can be situations where low or intermediate trawling can be beneficial for certain species. Certain opportunistic or disturbance tolerant taxa may benefit from low to moderate levels of disturbances such as trawling which may increase food availability in bottom-up controlled systems (van Denderen et al., 2013).

Nutrients

Nutrient effects on chlorophyll-a, a proxy for primary productivity, were similarly region-specific. In the eastern quadrants (NE and SE), higher nitrogen (N) to phosphorus (P) ratios were positively correlated with chl-a while phosphorus showed negative correlations. This suggests P limitation as excess N inputs dominate (Figure 11, S11.3 and S4). In contrast, western quadrants (NW and SW) appears to show stronger indications of N limitation most evidenced by overall declining relationships between chl-a and N:P ratios (despite some outliers; Figure S11.4). However, non-linear responses in these areas suggest more complex responses. In the SW, where P concentrations are the highest in the basin, U-shaped chl-a–nutrient relationships indicate that enrichment only translates into elevated biomass under certain conditions, potentially limited by turbidity, light, or grazing (Figures S11.3 and S11.4). In the NW, nitrogen and phosphorus correlated strongly reflecting the Atlantic inflow, but higher nutrient concentrations were not associated with higher chl-a potentially suggesting a decoupling between nutrient supply and primary production in this deeper, stratified region (Figure S11.1).

Increases in nutrients can lead to fast-growing phytoplankton (i.e. Phaeocystis blooms), often at the expense of diversity. Decomposition and increased deposition of algae can lead to oxygen depletion in bottom waters which can kill sensitive benthic invertebrates (e.g. echinoderms, crustaceans, mollusks). Opportunistic polychaetas often dominate after hypoxic events (Diaz & Rosenberg, 2008). While direct, spatially explicit studies between eutrophication and epibenthic responses are not common in the North Sea, for which, strong tidal currents and mixing may mitigate negative eutrophication in many areas, certain locations are more prone to eutrophication risk. Rachor & Nehmer (2003) showed how benthic communities in the German Bight were affected by eutrophication, with declines in sensitive bivalves and increases in opportunistic polychaetes. Also areas with stratification might be subject to oxygen depletion in bottom waters (Topcu & Brockmann, 2015).

Nutrient effects on invertebrate species richness in the North Sea also varied by region. While N typically showed negative responses across the basin, P exhibited more heterogenous effects with increased species richness correlating with higher P concentrations in southern quadrants compared with clear negative relationships in more northern quadrants (Figure 11.4). This is consistent with prior evidence that benthic communities in the North Sea to not act uniformly across the basin but respond to environmental gradients in ways that reflect both local environmental conditions and historical disturbance regimes (Kenny et al. 2018).

Co-inertia analyses

The co-inertia analyses provided complementary evidence that species composition and environmental variables are tightly coupled and that species richness can be broken down into more complex sub-units. A cloud of species were often aligned opposite to pressures such bottom trawling or temperature, however, certain species were also correlated with the pressures themselves. Northern areas showed positive correlations between temperature and the squid species, *Alloteuthis subulata* while eastern areas showed strong positive correlations between trawling and the benthic scavenger, Cancer pagurus (Figure 11.4). The strength and direction of nutrient effects different by subregion. For instance, SE area exhibited inverse correlations between nitrogen and phosphorus concentrations while nutrient concentrations were positively correlated in SW and NW.

Cumulative impacts

The cumulative impact maps synthesize these findings into spatially explicit indices of pressure influence. The negative-effect index identified a continuous band of high cumulative pressure along the southern and eastern coasts, from the Belgian to the Danish areas. These areas are consistent with high trawling and nitrogen enrichment (Figure 11.6). In contrast, the positive-effect index revealed regions where pressures were associated with increases in species richness, such as areas in the SW areas where phosphorus input is high, specific locations along the Danish coastline in NE, and more offshore regions. These patterns may reflect conditions where intermediate levels of certain pressures, such as nutrients or temperature, create opportunities for greater niche diversity or support taxa adapted to these environments. The absolute-effect index which combines positive and negative responses, revealed a broader footprint of strong pressure effects, including areas of high phosphorus and nitrogen in the southern and eastern North Sea and is likely influenced strongly by temperature in the south as evidenced in the functional form analysis (Figure 11.4). The absolute index reveals a central offshore region with relatively low cumulative influence, which may represent a potential refuge for biodiversity under current conditions.

Implications and Conclusions

From a management perspective, these patterns demonstrate the limitations of uniform, basin-wide measures for biodiversity protection. The spatial heterogeneity in pressure–richness relationships suggests that mitigation strategies, whether aimed at reducing trawling impacts, nutrient inputs, or responding to climate-driven changes, should be tailored to the environmental and ecological context of each region. This highlights the importance of combining statistical approaches with spatially resolved anthropogenic impacts datasets to identify where pressures may act synergistically, where they may be less influential, and where conservation interventions are likely to be the most effective.

While the BTS data provide extensive spatial coverage, several limitations should be noted. Beam trawl surveys target epifaunal communities and may under-sample small-bodied infauna, potentially biasing richness estimates toward more mobile or conspicuous taxa. Identification expertise has improved over time, which may influence long-term trends, though the focus on spatial variation in recent years reduces this concern. Finally, the observational nature of the data limits the ability to infer causality; experimental or mechanistic modelling approaches could help disentangle the direct and indirect effects of pressures on benthic biodiversity.

In summary, this analysis demonstrates how fisheries-independent survey data, coupled with spatial modelling approaches, can reveal the complexity and spatial variability of biodiversity-pressure relationships in a heavily used marine system. The results provide a spatially explicit baseline for assessing risks to benthic biodiversity and support the development of targeted, region-specific management actions in the North Sea.

11.5. References

Anderson, S. C., Ward, E. J., English, P. A., Barnett, L. A. K., & Thorson, J. T. (2022). sdmTMB: An R package for fast, flexible, and user-friendly generalized linear mixed effects models with spatial and spatiotemporal random fields. bioRxiv. https://doi.org/10.1101/2022.03.24.485545

Callaway, R., Alsvåg, J., de Boois, I., Cotter, J., Ford, A., Hinz, H., Jennings, S., Kröncke, I., Lancaster, J., Piet, G., Prince, P., & Ehrich, S. (2002). Diversity and community structure of epibenthic invertebrates and fish in the North Sea. ICES Journal of Marine Science, 59(6), 1199–1214. https://doi.org/10.1006/jmsc.2002.1288

Capuzzo, E., Lynam, C. P., Barry, J., Stephens, D., Forster, R. M., Greenwood, N., McQuatters-Gollop, A., Silva, T., van Leeuwen, S. M., & Engelhard, G. H. (2017). A decline in primary production in the North Sea over 25 years, associated with reductions in zooplankton abundance and fish stock recruitment. Global Change Biology, 24(1), e352–e364. https://doi.org/10.1111/gcb.13916

Diaz, R. J., & Rosenberg, R. (2008). Spreading dead zones and consequences for marine ecosystems. Science, 321(5891), 926–929. https://doi.org/10.1126/science.1156401

Dolédec, S., & Chessel, D. (1994). Co-inertia analysis: An alternative method for studying species–environment relationships. Freshwater Biology, 31(3), 277–294. https://doi.org/10.1111/j.1365-2427.1994.tb01741.x

Dray, S., & Dufour, A.-B. (2007). The ade4 package: Implementing the duality diagram for ecologists. Journal of Statistical Software, 22(4), 1–20. https://doi.org/10.18637/jss.v022.i04

Dye, S. R., Hughes, S. L., Tinker, J., Berry, D. I., Holliday, N. P., Kent, E. C., Kennington, K., Inall, M., Smyth, T., Nolan, G., Lyons, K., Andres, O., & Beszczynska-Möller, A. (2013). Impacts of climate change on temperature (air and sea). MCCIP Science Review 2013, 1–12. https://doi.org/10.14465/2013.arc01.001

Kenny, A. J., Jenkins, C., Wood, D., Bolam, S. G., Mitchell, P., Scougal, C., & Judd, A. (2018). Assessing cumulative human activities, pressures, and impacts on North Sea benthic habitats using a biological traits approach. ICES Journal of Marine Science, 75(3), 1080–1092. https://doi.org/10.1093/icesjms/fsx205

Knights, A. M., Koss, R. S., & Robinson, L. A. (2013). Identifying common pressure pathways from a complex network of human activities to support ecosystem-based management. Ecological Applications, 23(4), 755–765. https://doi.org/10.1890/12-1137.1

Piet, G. J., Tamis, J. E., Volwater, J., de Vries, P., van der Wal, J. T., & Jongbloed, R. H. (2021). A roadmap towards quantitative cumulative impact assessments: Every step of the way. Science of the Total Environment, 784, 146847. https://doi.org/10.1016/j.scitotenv.2021.146847

Pitois, S. G., & Fox, C. J. (2006). Long-term changes in zooplankton biomass concentration and mean size over the Northwest European shelf inferred from Continuous Plankton Recorder data. ICES Journal of Marine Science, 63(5), 785–798. https://doi.org/10.1016/j.icesjms.2006.03.008

R Core Team. (2025). R: A language and environment for statistical computing (Version 4.4.1). R Foundation for Statistical Computing. https://www.R-project.org/

Rachor, E., & Nehmer, P. (2003). Ergebnisse der Bodenfaunauntersuchungen in der Deutschen Bucht während der Jahre 1989–1999. Berichte zur Polar- und Meeresforschung, 442, 1–66. https://doi.org/10.2312/BzPM_0442_2003

Reiss, H., Degraer, S., Duineveld, G. C. A., Kröncke, I., Aldridge, J., Craeymeersch, J., Eggleton, J. D., Hillewaert, H., Lavaleye, M. S. S., Moll, A., Pohlmann, T., Rachor, E., Robertson, M., vanden Berghe, E., van Hoey, G., & Rees, H. L. (2010). Spatial patterns of infauna, epifauna, and demersal fish communities in the North Sea. ICES Journal of Marine Science, 67(2), 278–293. https://doi.org/10.1093/icesjms/fsp253

Topcu H.D., U.H. Brockmann (2015). Seasonal oxygen depletion in the North Sea, a review. Marine Pollution Bulletin 99: 5-27 https://doi.org/10.1016/j.marpolbul.2015.06.021.

van Denderen, P. D., van Kooten, T., & Rijnsdorp, A. D. (2013). When does fishing lead to more fish? Community consequences of bottom trawl fisheries in demersal food webs. Proceedings of the Royal Society B: Biological Sciences, 280(1769), 20131883. https://doi.org/10.1098/rspb.2013.1883

van Leeuwen, S., Tett, P., Mills, D., & van der Molen, J. (2015). Stratified and non-stratified areas in the North Sea: Long-term variability and biological and policy implications. Journal of Geophysical Research: Oceans, 120(7), 4670–4686. https://doi.org/10.1002/2014JC010485.

12 Spatial Variability Seafloor risk assessment framework and state of seabed habitats in relation to bottom trawling

Authors: Daniel van Denderen & Martin Lindegren

12.1. Introduction

Seafloor ecosystems in the Northeast Atlantic and the Baltic Sea account for more than 14 million km^2, an area 1.4 times larger than continental Europe. The seafloor ecosystem is home to >2500 benthic invertebrate species that represent virtually all known phyla. They form a wide variety of communities across distinct habitat types and support a range of ecological processes, from nutrient cycling and organic matter degradation to providing essential habitats and food to fish. Human activities, such as bottom fishing, aggregate dredging, sediment disposal and renewable energy devices, exert pressures on these benthic habitats (Foden et al., 2011; Kenny et al., 2018). Managing those pressures is a central component of modern ecosystem-based marine management. Within European waters, this responsibility is anchored in the Marine Strategy Framework Directive (MSFD), which aims to achieve Good Environmental Status (GES) across regional seas. Descriptor 6 (D6), Seafloor Integrity, specifically requires that the structure and functions of benthic ecosystems are maintained and that human activities do not compromise their long-term resilience. Implementing D6 is data-intensive, because benthic habitats are diverse and influenced by both natural dynamics and anthropogenic pressures making it a (financially) demanding task to monitor benthic state, especially in offshore areas. Direct monitoring typically relies on sediment grabs, cores and bottom trawl samples. These approaches are costly, labour-intensive, and limited in spatial and temporal coverage (Painting et al., 2020). Consequently, no existing monitoring programme can match the scale of human activities or the natural variability of benthic communities across European seas. This mismatch between monitoring capacity and assessment requirements has resulted in insufficient direct evidence of benthic status to evaluate GES or to inform spatially resolved management. This stands in contrast to coastal ecological assessments under the Water Framework Directive, which are monitored through continuous programmes (Van Hoey et al., 2019).

Risk-based assessment methods have been developed to evaluate the likely consequences of human activities on the seafloor in offshore areas (Korpinen et al., 2012; Pitcher et al., 2017). Most approaches rely on expert-judgement frameworks, which currently provide the only practical means to assess the multitude of human pressures (e.g. fishing, pollution, climate change) acting simultaneously on benthic habitats. In addition, quantitative and mechanistic methods have been developed to focus on specific human activities. Among these, the approach of Pitcher et al. (2017) has become a key framework for assessing the risk from bottom-trawl fishing abrasion, the dominant pressure on seafloor habitats across much of the European Seas (ICES, 2019). Bottom-trawl abrasion of the seafloor is caused by gears such as beam trawls, otter trawls, and scallop dredges. These gears physically disturb and mobilize the sediment and cause damage and mortality to the benthic fauna (Sciberras et al., 2018; van der Reijden et al., 2025). These physical impacts may reduce habitat complexity and influence the ability of seafloor habitats to sustain biodiversity, provide nursery and feeding grounds for fish, and maintain ecosystem functions such as nutrient cycling and carbon storage (Epstein et al., 2022; Sci-

berras et al., 2016; van Denderen et al., 2013). Over time, intensive bottom-trawl activity can lead to shifts in community composition, favoring opportunistic species over long-lived, slow-growing organisms (Hiddink et al., 2018; Kaiser et al., 2000; van Denderen et al., 2015). This chapter applies the risk assessment methodology as currently implemented in ICES advice and developed by the ICES Working Group on Fisheries Benthic Impact and Trade-offs (ICES, 2022). Following Pitcher et al. (2017), it uses the logistic growth equation to estimate relative benthic state, representing changes in benthic community biomass relative to carrying capacity, based on depletion mortality from trawl gears (Hiddink et al., 2017) and the recoverability of the benthic community under equilibrium conditions. Unlike Pitcher et al. (2017), recoverability here is estimated using local, empirical information on benthic longevity, reflecting findings by Hiddink et al. (2019) that recovery rates are inversely related to species lifespan.The chapter starts with a summary of two recent manuscripts. The first manuscript describes the most recent assessment of bottom trawl impacts on the status of seabed communities in European Seas (Box 12.1). The second manuscript evaluates the effectiveness of the current Nature 2000 network to protect benthic communities from these bottom trawl impacts (Box 12.2). Both papers were partially supported by the B-Useful project. Afterwards, we explore ways to integrate the risk assessment framework with Hierarchical Modelling of Species Communities (HMSC), as applied to benthic communities within the B-Useful project.

Box 12.1. Summary of the paper: *Hiddink et al. (accepted) Assessment of bottom trawl impacts on the status of seabed communities in European Seas*

This paper presents a Europe-wide quantitative assessment of bottom-trawling impacts, incorporating regional drivers of seabed-community sensitivity across the Baltic, Atlantic, Mediterranean, and Black Sea continental shelves. Regional sensitivity was estimated using sampling data from box cores, grabs, and trawl surveys (Figure B12.1.1). Benthic impact was assessed by combining the spatial distribution of bottom-fishing activity (Figure B12.1.2) with estimates of benthic community longevity. Results are presented for two risk-based indicators of seabed status (Figure B1.3). The findings indicate low trawling intensity and high seabed status in the Black, Baltic, and Aegean–Levantine Seas, whereas the Western Mediterranean, Ionian and Central Mediterranean, and Adriatic Seas are the most heavily impacted.

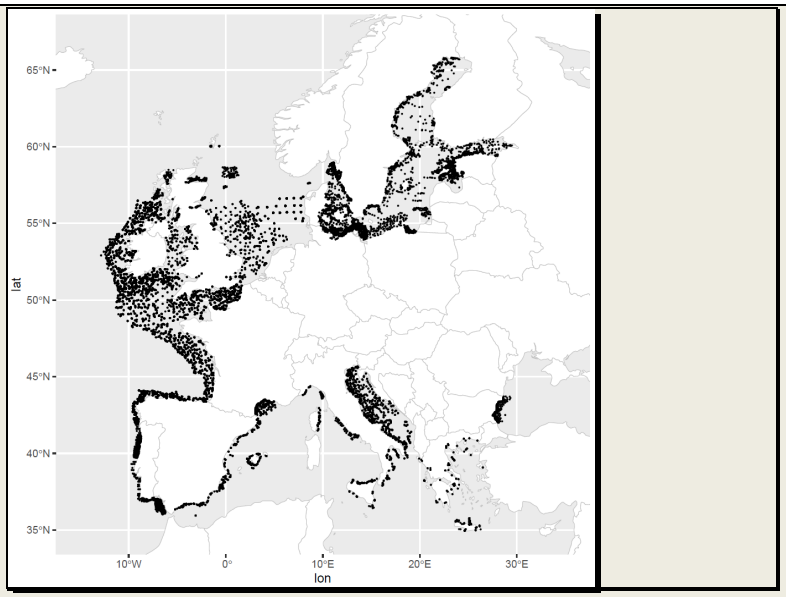

Figure B12.1.1. Map of the sampling stations used to predict benthic community sensitivity. Despite the broad coverage, the sampled area still represents a small fraction of the total assessed area. Sampling biomass by longevity is available for most areas via van Denderen et al. (2025).

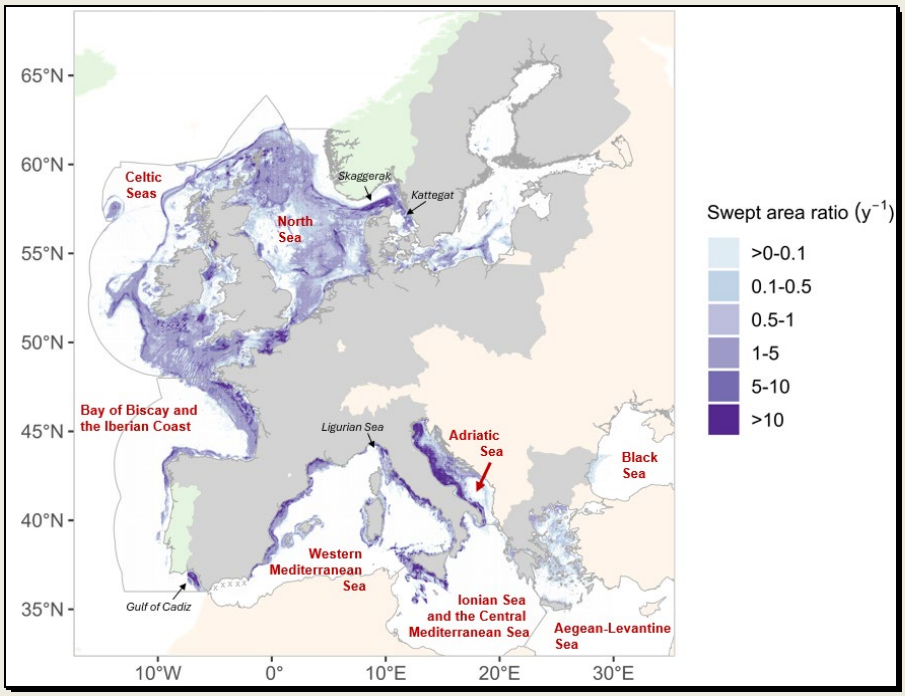

Figure B12.1.2. Annual average fishing intensity expressed as swept area ratio per year (2016 to 2022 for most areas). Data is included from countries marked dark grey, supplemented with incomplete data from countries in light green. Figure taken from Hiddink et al. (accepted). Fishing intensity data is available for most areas via van Denderen et al. (2025).

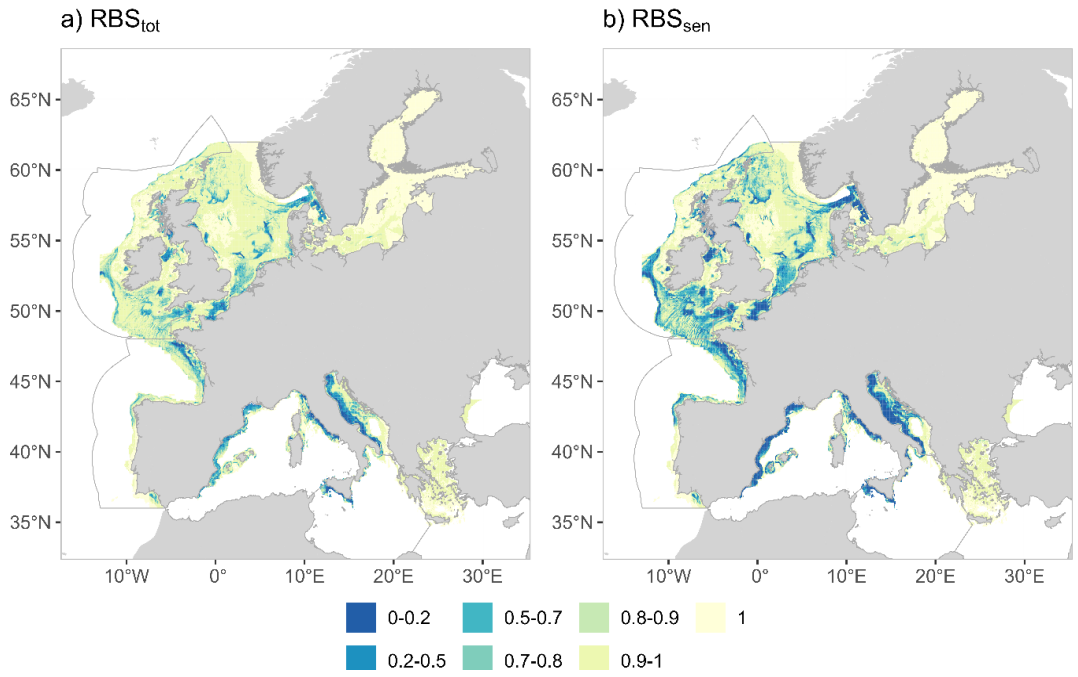

Figure B12.3. Maps of benthic state for (a) RBS_{tot} (biomass of the benthic community relative to its carrying capacity) and (b) RBS_{sen} (biomass of the 10% most sensitive fauna in the benthic community relative to its carrying capacity) averaging the estimates for both infauna and epifauna where they are overlapping. Figure taken from Hiddink et al. (accepted). Benthic state data is available for most areas via van Denderen et al. (2025).

Box 12.2. Summary of the paper: *van der Reijden (in prep.) Evaluating the efficacy of the current European network of marine protected areas for seafloor protection from mobile bottom-contacting fishing gears*

The benthic impact risk assessment framework for bottom-trawling (Box 12.1) provides a tool for evaluating different management scenarios (ICES, 2021). One such scenario is the '30×30' target, which aims to protect 30% of marine ecosystems by 2030 while contributing to GES. To achieve the '30×30' target, the European Commission urges Member States to prioritize the elimination of mobile bottom fishing in Natura 2000 sites designated under the Habitats Directive. This paper assesses how closing the Natura 2000 network to all bottom-trawling activities could influence the condition of seabed habitats across the Greater North Sea, Celtic Seas, Baltic Sea, and the Iberian Coast and Bay of Biscay (Figure B12.2.1). It includes different closure and fisheries displacement scenarios.

The study finds that Natura 2000 site coverage varies widely between habitat types with most overlap in shallow waters (Figure B12.2.1). All examined types of bottom fishing occur within the network, accounting for 10% (Baltic Sea) to 40% (Bay of Biscay and Iberian

Coast) of regional bottom fishing effort. Closing sites to bottom trawling would disproportionately impact fisheries concentrated in them, such as beam trawls targeting shrimp and mollusks, which derive nearly all landings from Natura 2000 areas. Benthic impact assessments indicate that closures generally increase areas with high benthic state, but displaced fishing can intensify pressure on unprotected, sensitive habitats, sometimes leading to a net decline in benthic condition for certain habitat types.

The paper concludes that the closing of Natura 2000 sites from bottom trawling could improve the overall benthic state and contribute to EU conservation goals. However, uneven habitat representation and unmanaged displacement risks may undermine ecological gains while causing high socioeconomic costs.

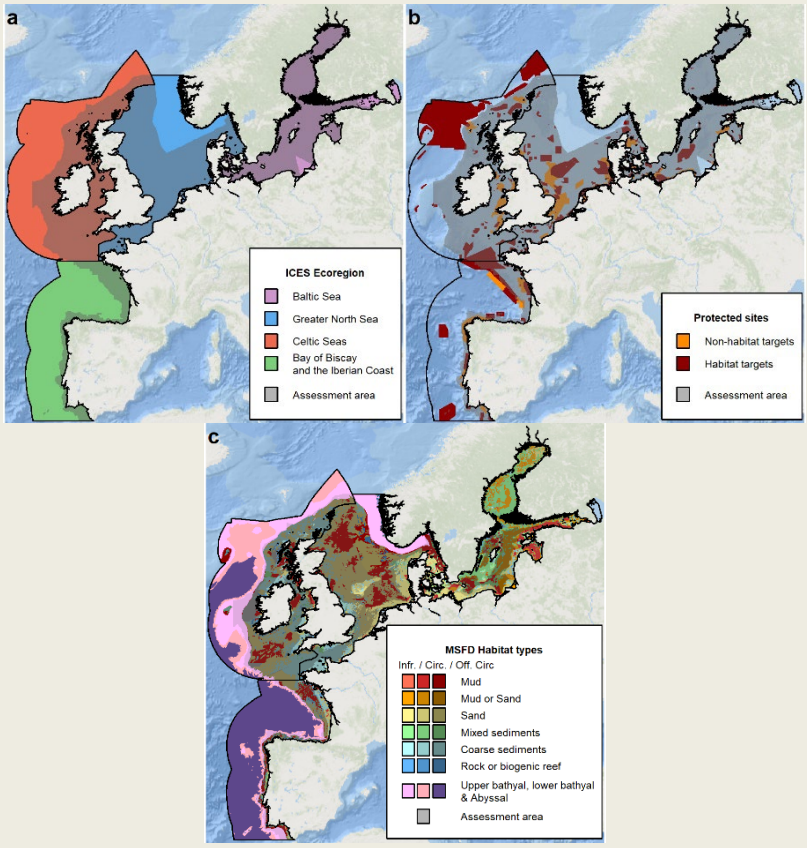

Figure B12.2.1. Maps of the a) assessed ecoregions, b) Natura 2000 sites with/without benthic habitat targets and c) MSFD habitat types. Figure taken from van der Reijden et al. (in prep.).

Combining species distribution models with the risk assessment framework

The current risk-assessment framework depends on predicting the reference, or undisturbed longevity–biomass distribution of benthic communities. This prediction is generated using a statistical model in which cumulative biomass is the response variable and species longevity together with environmental conditions serve as predictors (Rijnsdorp et al., 2018). Because longevity–biomass relationships vary with environmental settings, benthic sensitivity also differs

among regions. For example, the low-salinity conditions of the Baltic Sea do not support long-lived fauna, creating a clear gradient in species longevity from predominantly short-lived fauna (<5 years) in the northern Baltic to a dominance of long-lived fauna (> 10 years) in the more saline Kattegat (van Denderen et al., 2019). These differences in biomass distribution translate into varying impacts to bottom-trawling disturbance since recovery rates are inversely related to species lifespan (Hiddink et al., 2018) (Figure 12.1).

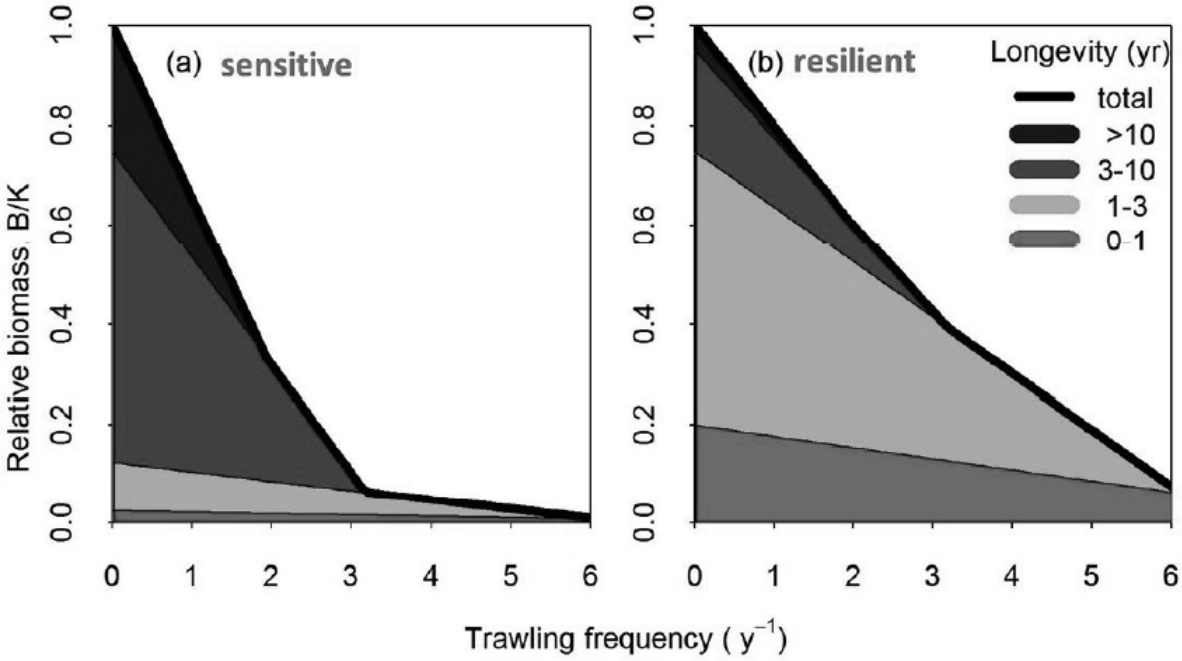

Figure 12.1. An example of how the longevity distribution of a benthic community at no trawling affects the response of total community biomass to bottom trawling (ICES, 2022).

The longevity–biomass distribution is currently estimated by assigning each benthic species to a longevity class and calculating how much of the community's biomass falls into each class at each sampling site. These classes are then translated into a smooth, continuous curve that describes how the proportion of biomass increases with species' longevity, rising from near zero for short-lived species to near one for long-lived species (Figure 12.2).

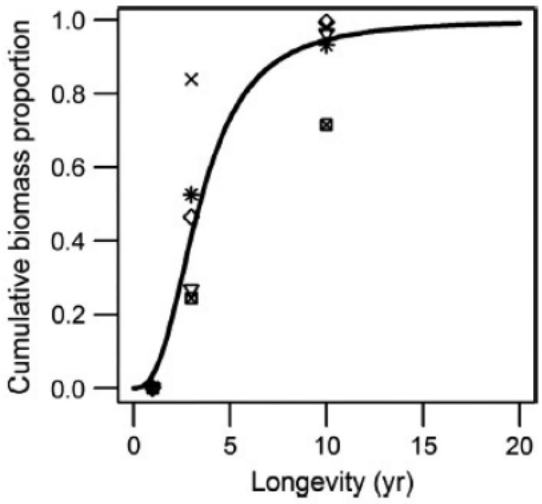

Figure 12.2. An example of the cumulative biomass–longevity relationship estimated from the observed cumulative biomass by longevity class (1, 1–3, 3–10 yr) in five sampling stations. Different symbols indicate the five different locations. Figure taken from Rijnsdorp et al. (2018).

The longevity-biomass approach allows estimating changes in total community biomass and the biomass of a specific group of species with a certain longevity, e.g. the biomass of the 10% most sensitive fauna in the benthic community (ICES, 2022). The approach does not allow for predictions of changes in biodiversity metrics such as evenness, Simpson's index, or species richness. This is because the FBIT approach solely relies on a prediction of the cumulative biomass-longevity relation and does not specify how this relation links back to specific species.

Within the B-Useful project, several studies have estimated the biomass distribution of benthic species using HMSC. HMSC is a statistical framework used to model the distribution of multiple species at the same time, allowing it to account for shared environmental responses, species interactions, and spatial or temporal structure. Once the outputs of HMSC models become available, they can be used to replace the biomass-longevity distribution with predicted species-by-biomass information within the risk assessment approach, where the recovery rate of each species is now determined by longevity. A risk assessment using HMSC can still estimate changes in total community biomass and the biomass of sensitive species. It can also predict how biodiversity metrics respond to trawling. However, it is uncertain how well the approach can capture declines in biodiversity indicators. This uncertainty is reinforced by the fact that most biodiversity indicators are less responsive to trawling disturbance than either total biomass or trait-based biomass metrics that reflect benthic sensitivity (van Denderen et al. 2025). Here we use 10 empirical bottom-trawl gradient studies to predict declines in total biomass and four biodiversity indicators. As a baseline, we use species-level biomass data at the undisturbed conditions of the trawling gradient. We then evaluate how well the model reproduces observed declines across the different indicators. Demonstrating skill in this context would support applying the same approach to HMSC outputs and estimate declines in biodiversity metrics.

12.2. Material and Methods

We selected seven trawling gradients from van Denderen et al. (2024) in which benthic indicators had previously been shown to respond to trawling disturbance (Figure 12.1; Table 12.1). For each gradient, we quantified species richness, total biomass, the Shannon diversity index, and the Simpson diversity index; the two diversity indices were calculated using biomass rather than abundance.

Sampling stations within the lowest tercile of fishing intensity were classified as representing undisturbed reference conditions. All species recorded in these reference stations were matched to a longevity trait database. We then predicted the biomass decline of each species over the gradient. Here we used the logistic growth model following Pitcher et al. (2017) and ICES (2022). The model equation is:

$$B_i = (1 - F \times d/r_i) * K_i$$

where B_i is biomass of species i, F is trawling intensity expressed as the swept area ratio, d is the depletion rate which is a parameter that varies with the type of the gear (Table 1), r_i is the intrinsic growth rate that is approximated from the longevity value of each species and K_i is the biomass (i.e. carrying capacity) of species i in the undisturbed stations.

The parameters d and r were obtained from a global meta-analysis. To account for parameter uncertainty and variability in species composition, the predicted decline of each species was resampled 500 times. In each iteration, values of d and r were sampled according to their uncertainty, and one reference station was randomly selected to determine species presence and corresponding biomass. We obtained biomass trajectories across the full range of trawling intensities by running the model for each species. These trajectories were then used to derive total biomass, species richness, evenness, and the Simpson diversity index along the gradient. Predicted responses were directly compared with observed changes in these indicators. To estimate declines in species richness, we defined a biomass detectability threshold for each gradient. This detectability threshold was set at half the lowest biomass recorded for a single-species observation within that gradient study. The threshold differed across gradient datasets because sampling protocols varied among studies (e.g., differences in sampling gear or sieve size).

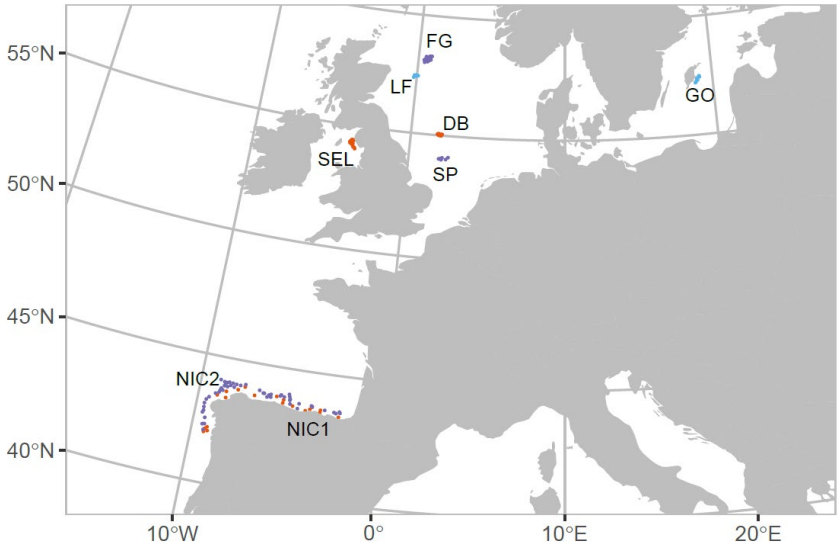

Figure 12.3. Map of sampling locations for the seven bottom trawl gradient studies. Benthic state data is available for most areas via van Denderen et al. (2024).

Table 12.1. Overview of the seven gradient studies, including the baseline fishing intensity (note that a SAR of 0.1 indicates that a benthic community is trawled, on average, once every 10 years), the dominant commercial fishing type, the depletion rate used to predict impacts, and the abbreviated study name.

Gradient	Mean baseline fishing intensity (SAR)	Dominant fishing type	Depletion rate (median value)	Abbreviated name
Sellafield	0.5	Otter trawl for Nephrops	0.10	SEL
Doggerbank	0.21	Otter and beam trawl	(0.06 + 0.14)/2	DB
Long Forties	0.21	Scallop dredge	0.20	LF
Fladen ground	0.24	Otter trawl for Nephrops	0.10	FG
Silver Pit	0.16	Otter and beam trawl	(0.06 + 0.14)/2	SP
North Iberian Coast sand	0.02	Otter trawl for demersal fish	0.06	NIC1
North Iberian Coast bathyal mud	0.08	Otter trawl for demersal fish	0.06	NIC2
Gotland	0	Otter trawl for demersal fish	0.06	GO

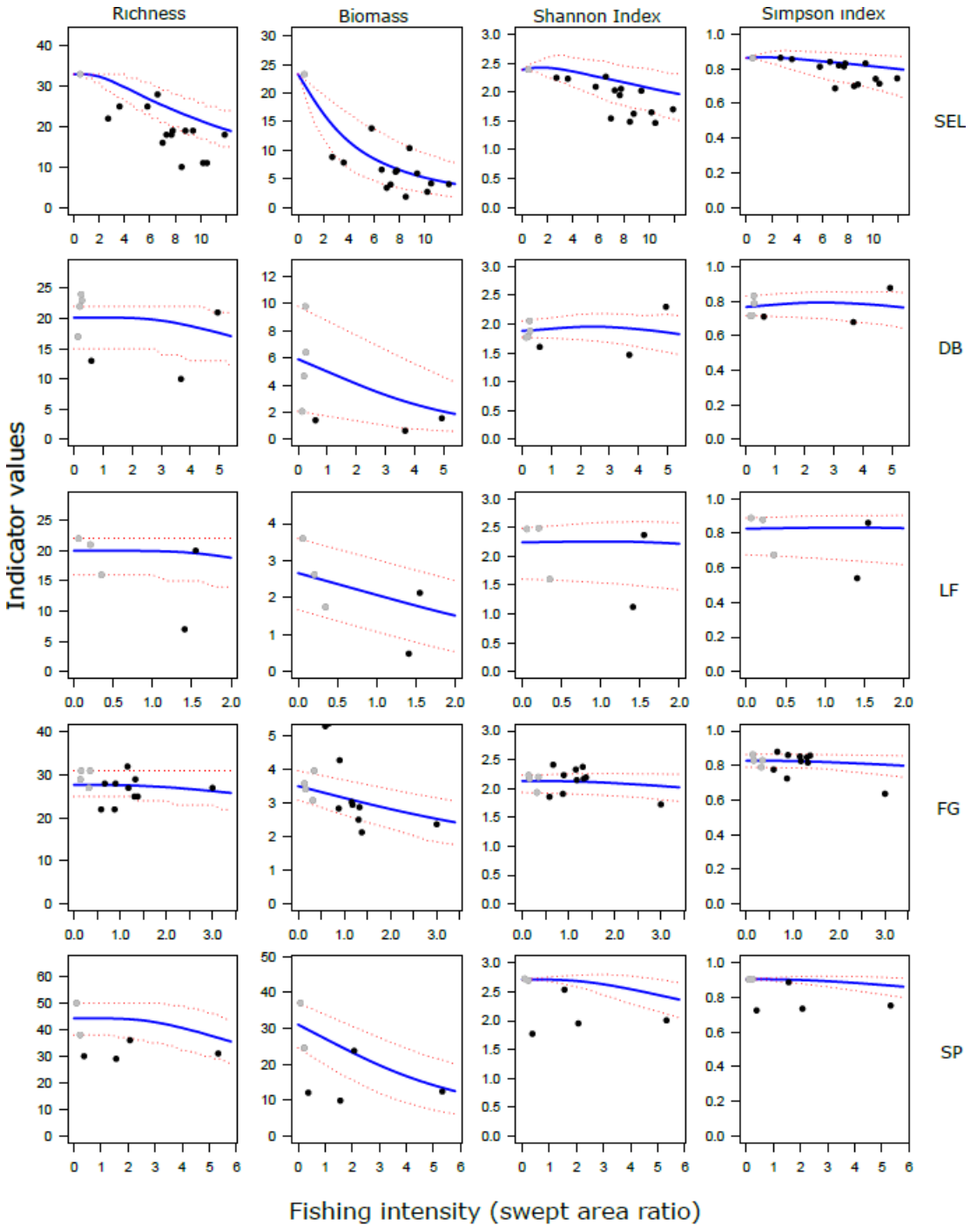
Richness
Biomass
Shannon Index
Simpson index
SEL
DB
LF
FG
SP
Indicator values
Fishing intensity (swept area ratio)

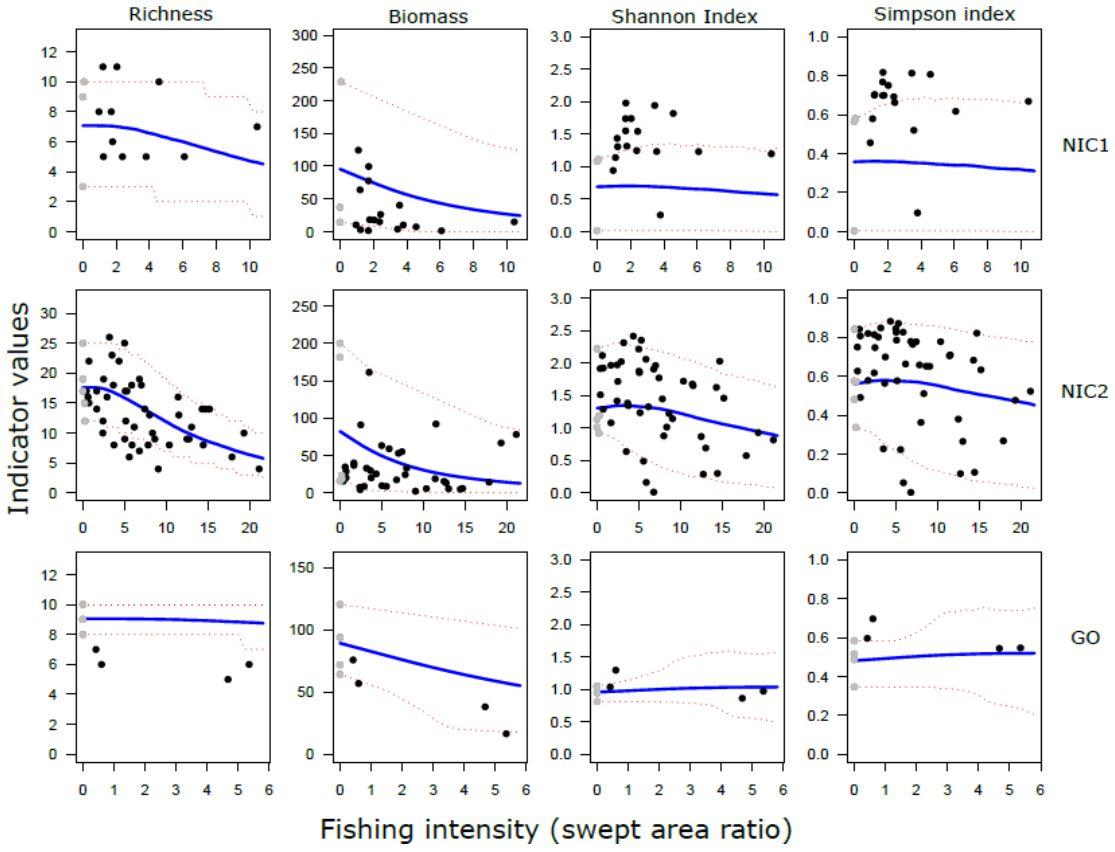

Figure 12.4. Changes in modeled (blue lines) and empirically estimated richness, biomass, Shannon index and Simpson index for each sampling location. The red lines show the 95% confidence interval by 500x resampling of the reference stations (grey dots) and depletion and recovery parameters. Names are equal to Table 1. Richness and biomass values vary in units between locations due to differences in sampling design (van Denderen et al., 2024). Fishing intensity is the annual average swept area ratio.

12.3. Material and Methods

Changes in species richness, biomass, Shannon index, and Simpson index are shown in Figure 4. Richness and biomass generally decline with increasing trawling intensity, whereas both the Shannon and Simpson indices exhibit a weak hump-shaped pattern. This hump-shaped response is driven by shifts in benthic community composition, the decline in biomass of previously dominant species and the exclusion of rare species. In both the empirical observations and the model-based predictions, biomass shows the strongest response to trawling (Figure 12.4 and 12.5). At some locations, biomass in the most heavily trawled third of stations is around 40% lower than in the least trawled third. Richness also declines, with particularly pronounced reductions at certain stations. In contrast, neither the Shannon nor Simpson index exhibits a clear decline with increasing trawling intensity, and both decrease by no more than 20%. Both the Sellafield sampling location and the North Iberian Coast bathyal mud exhibit the clearest declines across all indicators. These sites are also among the most heavily fished, with SAR values exceeding 10 per year; meaning the benthic community is, on average, disturbed by trawling more than ten times annually (Figure 12.4). While the indicators describe community-level responses, the underlying dynamics can also be examined at the species level. Species-level changes in benthic community composition are most readily visualized for the Sellafield dataset, which includes only a single reference station; as a result, species composition is fixed and not resampled. Figure 6 shows the differences between observed and predicted changes,

with the model-based predictions displaying the expected smoother trajectories. Three species, *Notomastus* sp., *Jaxea* sp. and *Bolocera* sp., are absent from the reference station and therefore not included in the model. These results suggest that, despite the relatively close match at the community level (Figure 12.4), agreement at the species level is weaker. This is expected, as the model relies on simplified assumptions and there is no ability to have biomass increases with trawling intensity.

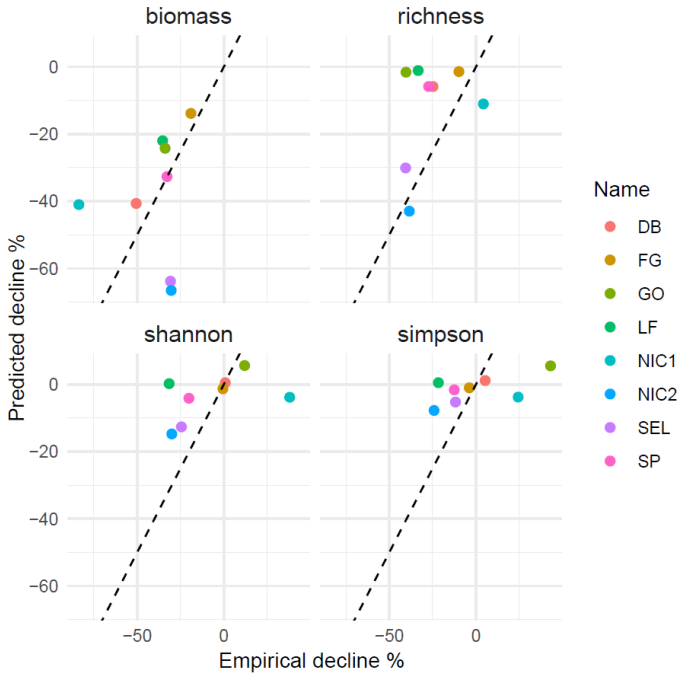

Figure 12.5. Predicted versus observed decline for the one-third of stations with the lowest fishing intensity compared to the one-third with the highest fishing intensity. Station names correspond to those used in Table 1.

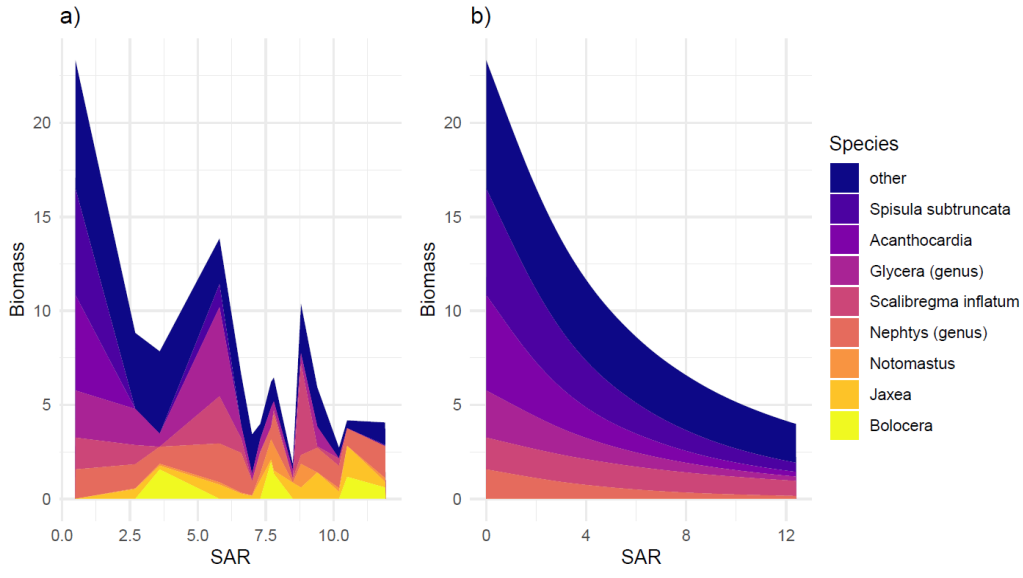

Figure 12.6. Observed (a) and predicted (b) changes for the most common species in the Sellafield gradient. Predicted changes represent the average decline calculated over 500 resampled parameters of d and r. Notomastus sp., Jaxea sp., and Bolocera sp. are not found in the reference station and are therefore not modeled.

12.4. Discussion

The assessment tool is designed to identify areas most at risk from bottom fishing disturbance by accounting for gear-specific depletion mortality and the varying sensitivities of benthic fauna. It operates across multiple regions and enables comparison of bottom fishing impacts within specific habitats, across ecoregions, and at the basin-wide scale (Box 12.1). In addition, the tool can be used to run scenario analyses, including the implementation of marine protected areas and fishing-effort displacement scenarios (Box 12.2). The indicators currently estimated by the tool include total biomass and the biomass of the most sensitive organisms, each reflecting different properties of the benthic community. Total biomass is primarily linked to benthic structure and ecosystem functioning, whereas the most sensitive organisms may have higher conservation value. The final indicator to be applied under MSFD Descriptor 6 has not yet been determined and will likely consist of a combination of indicators to capture different components of the benthic ecosystem (van Denderen et al. 2024). Here, we demonstrate that the tool can be used to estimate changes in multiple biodiversity parameters, with most success for species richness. In our analysis, we use empirical gradient data in which species occurrence and biomass are known under undisturbed and low fishing conditions. To apply the tool at larger spatial scales, where data availability becomes limiting, it is necessary to predict species' occurrence and biomass. Such predictions are currently generated within the B-Useful project using a range of species distribution models, including hierarchical community models (e.g. HMSC) and single-species models. The assessment of benthic fauna will be further enhanced once we can assess changes in species richness, together with total biomass and the biomass of the most sensitive organisms, as this will allow for a more comprehensive representation of the benthic community. However, the accuracy of the assessment is likely to remain constrained by the challenges associated with predicting the spatial and temporal biomass distribution of benthic species given current data limitations. It is expected that improvements in data coverage, spatial-temporal model development, and integration of multiple data sources will progressively reduce these uncertainties and strengthen the reliability of future assessments.

12.5. References

Epstein, G., Middelburg, J. J., Hawkins, J. P., Norris, C. R., & Roberts, C. M. (2022). The impact of mobile demersal fishing on carbon storage in seabed sediments. Global Change Biology, 28(9), 2875–2894.

Foden, J., Rogers, S. I., & Jones, A. P. (2011). Human pressures on UK seabed habitats: a cumulative impact assessment. Marine Ecology Progress Series, 428, 33–47.

Hiddink, J. G., Jennings, S., Sciberras, M., Bolam, S. G., Cambiè, G., McConnaughey, R. A., Mazor, T., Hilborn, R., Collie, J. S., Pitcher, R., Parma, A. M., Suuronen, P., Kaiser, M. J., & Rijnsdorp, A. D. (2018). Assessing bottom-trawling impacts based on the longevity of benthic invertebrates. Journal of Applied Ecology, 56, 1075–1084. https://doi.org/10.1111/1365-2664.13278

Hiddink, J. G., Jennings, S., Sciberras, M., Szostek, C. L., Hughes, K. M., Ellis, N.,.....Kaiser, M. J. (2017). Global analysis of depletion and recovery of seabed biota after bottom trawling disturbance. Proceedings of the National Academy of Sciences, 114(31), 8301–8306.

ICES. (2022). Technical guideline document for assessing fishing impact from mobile bottom-contacting fishing gears (version 2, 27 February 2022). within: Report from the working group on Fisheries Benthic Impact and Trade-Offs.

Kaiser, M. J., Ramsay, K., Richardson, C. A., Spence, F. E., & Brand, A. R. (2000). Chronic fishing disturbance has changed shelf sea benthic community structure. Journal of Animal Ecology, 69(3), 494–503. https://doi.org/10.1046/j.1365-2656.2000.00412.x

Kenny, A. J., Jenkins, C., Wood, D., Bolam, S. G., Mitchell, P., Scougal, C., & Judd, A. (2018). Assessing cumulative human activities, pressures, and impacts on North Sea benthic habitats using a biological traits approach. ICES Journal of Marine Science, 75(3), 1080–1092. https://doi.org/10.1093/icesjms/fsx205

Korpinen, S., Meski, L., Andersen, J. H., & Laamanen, M. (2012). Human pressures and their potential impact on the Baltic Sea ecosystem. Ecological Indicators, 15(1), 105–114. https://doi.org/10.1016/j.ecolind.2011.09.023

Painting, S. J., Collingridge, K. A., Durand, D., Grémare, A., Créach, V., Arvanitidis, C., & Bernard, G. (2020). Marine monitoring in Europe: is it adequate to address environmental threats and pressures? Ocean Sci., 16(1), 235–252. https://doi.org/10.5194/os-16-235-2020

Pitcher, C. R., Ellis, N., Jennings, S., Hiddink, J. G., Mazor, T., Kaiser, M. J., Kangas, M. I., McConnaughey, R. A., Parma, A. M., Rijnsdorp, A. D., Suuronen, P., Collie, J. S., Amoroso, R., Hughes, K. M., & Hilborn, R. (2017). Estimating the sustainability of towed fishing-gear impacts on seabed habitats: a simple quantitative risk assessment method applicable to data-limited fisheries. Methods in Ecology and Evolution, 8(4), 472–480. https://doi.org/10.1111/2041-210X.12705

Rijnsdorp, A. D., Bolam, S. G., Garcia, C., Hiddink, J. G., Hintzen, N. T., van Denderen, D. P., & Van Kooten, T. (2018). Estimating sensitivity of seabed habitats to disturbance by bottom trawling based on the longevity of benthic fauna. Ecological Applications, 28(5), 1302–1312. https://doi.org/10.1002/eap.1731

Sciberras, M., Hiddink, J. G., Jennings, S., Szostek, C. L., Hughes, K. M., Kneafsey, B., Clarke, L. J., Ellis, N., Rijnsdorp, A. D., McConnaughey, R. A., Hilborn, R., Collie, J. S., Pitcher, C. R., Amoroso, R. O., Parma, A. M., Suuronen, P., & Kaiser, M. J. (2018). Response of benthic fauna to experimental bottom fishing: A global meta-analysis. Fish and Fisheries, 19(4), 698–715. https://doi.org/10.1111/faf.12283

Sciberras, M., Parker, R., Powell, C., Robertson, C., Kröger, S., Bolam, S., & Hiddink, J. G. (2016). Impacts of bottom fishing on the sediment infaunal community and biogeochemistry of cohesive and non-cohesive sediments. Limnology and Oceanography, 61(6), 2076–2089.

van der Reijden, K. J., Eigaard, O. R., Bastardie, F., van Denderen, P. D., & O'Neill, F. G. (2025). A gear component approach to trawling impact and sediment mobilization assessments. ICES Journal of Marine Science, 82(7), fsaf106. https://doi.org/10.1093/icesjms/fsaf106

van Denderen, P. D., Bolam, S. G., Friedland, R., Hiddink, J. G., Norén, K., Rijnsdorp, A. D., Sköld, M., Törnroos, A., Virtanen, E. A., & Valanko, S. (2019). Evaluating impacts of bottom trawling and hypoxia on benthic communities at the local, habitat, and regional scale using a modelling approach. ICES Journal of Marine Science, 77(1), 278–289. https://doi.org/10.1093/icesjms/fsz219

van Denderen, P. D., Bolam, S., Hiddink, J., Jennings, S., Kenny, A., Rijnsdorp, A., & van Kooten, T. (2015). Similar effects of bottom trawling and natural disturbance on composition and function of benthic communities across habitats. Marine Ecology Progress Series, 541, 31–43.

van Denderen, P. D., Plaza-Morlote, M., Vaz, S., Wijnhoven, S., Borja, A., Fernandez-Arcaya, U., González-Irusta, J. M., Hansen, J. L. S., Katsiaras, N.,… Valanko, S. (2024). Complementarity and sensitivity of benthic state indicators to bottom-trawl fishing disturbance. Ecological Applications, 34(8), e3050. https://doi.org/https://doi.org/10.1002/eap.3050

van Denderen, P. D., van Kooten, T., & Rijnsdorp, A. D. (2013). When does fishing lead to more fish? Community consequences of bottom trawl fisheries in demersal food webs. Proceedings of the Royal Society B: Biological Sciences, 280(1769), 20131883. https://doi.org/10.1098/rspb.2013.1883

Van Hoey, G., Bonne, W., Muxica, I., Josefson, A., Borgersen, G., Rygg, B., Borja, A., Philips, G., Miles, A. I., & Dubois, S. (2019). Coastal waters North East Atlantic Geographic Intercalibration Group. Benthic invertebrate fauna ecological assessment methods. https://doi.org/10.2760/16318

13 Wadden Sea endofauna sensitivity to fisheries and natural disturbance

Authors: Heino Fock

13.1. Introduction, Methods and Results

The responses to a given intensity of fishing disturbance can be influenced by the extent to which these species and communities are preconditioned to disturbance by natural processes, in particular waves and currents. Diesing et al. (2013) developed an additive model of probabilities to assess the portion of North Sea seafloor more affected by either natural or trawling disturbance. In this chapter, we measured the sensitivities towards trawling and natural disturbance at species level in a highly dynamic habitat. The effects of beam trawl fisheries for brown shrimp (*Crangon crangon*) on 2 predominant fishery-relevant habitat types in the sublittoral of the Wadden Sea of northern Germany and Denmark were investigated. The large-scale and chronic effects of fishing were determined along gradients of fishing intensity in the Wadden Sea of Lower Saxony, Schleswig-Holstein and Denmark. For this purpose, methods were developed to represent small-scale differences in fishing effort using satellite data in Wadden Sea tidal creek systems. Gradient analysis (GA) was carried out on fine and medium sands with ripple structure as well as on fields with colonization of the tree tube worm *Lanice conchilega.* All surveys were conducted in the sublittoral. A total of 427 endofauna samples (Fock et al. 2023) were examined from 2019, 2020, and 2021. This new method to evaluate sensitivity is based on an ordination-based approach instead of applying trait-based scoring. In direct gradient analysis, a species-by-sites matrix (Y) is simultaneously analyzed by an environmental factors-by-sites matrix (X), so that all the variance of Y that is related to X is displayed, but not the entire variance of Y (Legendre and Legendre 1998), i.e. the analysis of Y is constrained by the analysis of X. In such constrained ordination plots, variables are represented by arrows, which point in the direction of maximum change in the value of the associated variable, and the arrow length is proportional to this maximum rate of change. In the perpendicular direction, the variable does not change in value (Ter Braak and Verdonschot 1995). The interpretation of contributions of variables as arrows opens the opportunity to describe the relationships between two variables in terms of vector algebra as scalar product (Figure 13.1). Of the species vector $\vec{a}$ the part of it related to the environmental vector $\vec{e}$, that is, $\vec{a}_{\vec{e}}$ (Eq.13.1) equivalent to the sensitivity $I_{a,e}$ of the species towards this variable, normalized to the absolute value of the environmental variable to make the sensitivities comparable between environmental variables:

$$I_{a,e} = \frac{\vec{a} \circ \vec{e}}{|\vec{e}|}$$

(Eq. 13.1)

The species-environment canonical correspondence model contained three variables: fishing effort and mud content as significant variables and natural disturbance as the variable of interest. The plot of sensitivities of these three variables shows a significant relationship to mud content along the vertical axis (Figure 13.2). Removing this effect of sediment composition leaves a significant relationship between sensitivity towards trawling and sensitivity towards natural disturbance ($p<0.001$) in this high dynamic environment. At species level, positive sensi-

tivities of fishing and natural disturbance were linked to lower mud content, that is, presence in genuine sand habitats.

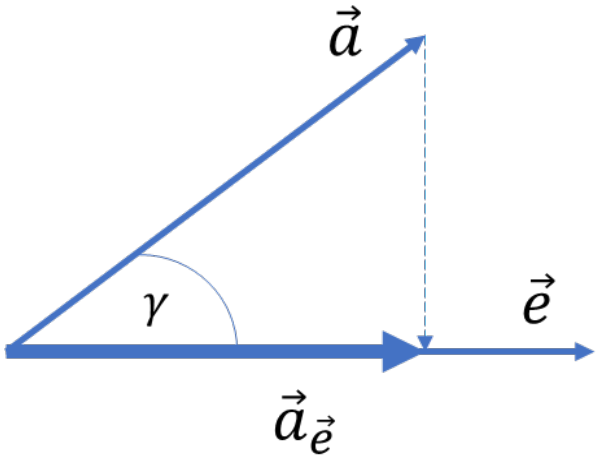

Figure 13.1 Vector-based model to estimate sensitivity, that is, $\vec{a}_{\vec{e}}$, of species with vector $\vec{a}$ in relation to the environmental vector $\vec{e}$.

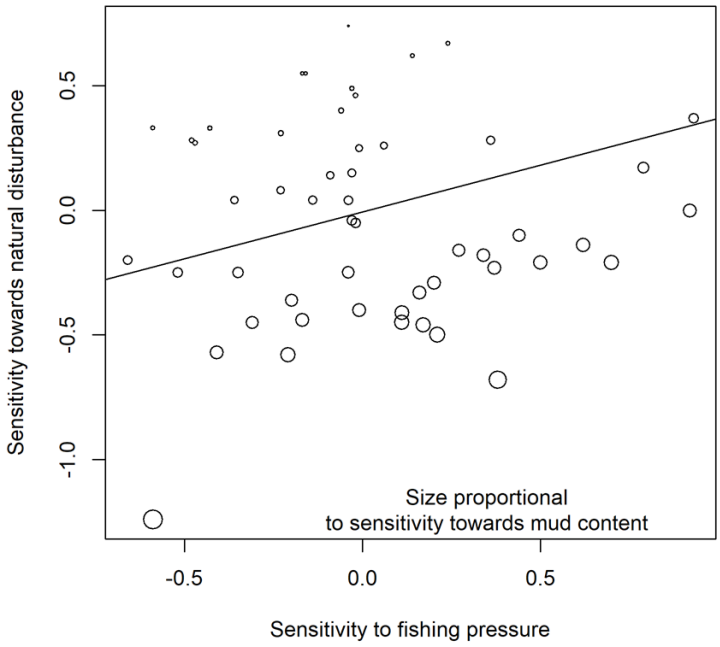

Figure 13.2. Sensitivities of 52 species of the subtidal Wadden Sea in relation to mud content (sediment composition), fishing pressure (trawling swept-area-ratio) and natural disturbance (bottom shear stress) and the significant relationship between sensitivities of fishing pressure and natural disturbance after removing the effect of sediment composition (regression line).

13.2. References

Diesing, M., Stephens, D., and Aldridge, J. 2013. A proposed method for assessing the extent of the seabed significantly affected by demersal fishing in the Greater North Sea. ICES Journal of Marine Science, 70: 1085–1096.

Fock, H., Dammann, R., Kraus, G., Rebecca, A. M., González, A. L., Nielsen, P., Nowicki, M., *et al.* 2023. Auswirkungen der Garnelenfischerei auf Habitate und Lebensgemeinschaften im Küstenmeer der Norddeutschen Bundesländer Schleswig- Holstein, Hamburg und Niedersachsen (CRANIMPACT). Thünen Report 107. Thünen Inst. 227 pp.

Legendre, P., and Legendre, L. 1998. Numerical ecology. Elsevier B.V., Amsterdam. 870 pp.

Ter Braak, C. J. F., and Verdonschot, P. F. M. 1995. Canonical correspondence analysis and related multivariate methods in aquatic ecology. Aquatic Sciences, 57: 255–289.

14 Sensitivity of North Atlantic and Northeastern Pacific fish communities to multiple environmental stressors

Authors: Fernanda Silva, Antoni Vivó-Pons , Daniel van Denderen, Federico Maioli, Marcel Solé, Martin Lindegren

14.1. Introduction

Climate change imposes widespread impacts on biodiversity across time and space (McGill et al., 2015). One of the most extensively studied effects is the influence of increasing temperature on species distribution patterns (Munday et al., 2013; Pinsky et al., 2020). This is particularly pronounced for marine ectotherms lacking the ability to physiologically regulate their body temperature (Van Der Walt et al., 2021). Hence, as the temperature changes, species must either tolerate, move or adapt to new conditions to avoid physiological stress or even local extinction (Pecl et al, 2017). However, in the era of the Anthropocene, the increasing importance of temperature as a general stress factor opens the question as to what extent this variable will combine with other potential stressors shaping marine communities through cumulative impacts (Andrello et al., 2014). In the ocean, higher temperatures can lead to sustained changes in salinity due to variations in the hydrological patterns and in the rates of precipitation and evaporation (Skliris et al., 2014). Warmer waters also decrease oxygen levels while driving up metabolic rates, leading to a mismatch between oxygen demand and availability (Doney et al., 2012). Additionally, global warming affects wind patterns and ocean currents, creating a cascade of events altering stratification, nutrient fluxes and primary production (Behrenfeld et al., 2006; Boyce et al., 2010; Doney et al., 2012). To better understand and anticipate future responses and impacts of climate change on marine life, a more holistic approach accounting for the joint sensitivity of a changing ocean environment beyond temperature is therefore needed (Pörtner et al., 2005). Here we develop a comprehensive, multi-factor approach to evaluate and compare the overall community sensitivity of marine fish along multiple climate-related stressors. Because proximity to environmental limits often correlates with population-level responses (Hamblin et al., 2017), the difference between upper and lower limits and the *in-situ* conditions experienced can provide an index of a species' tolerance to current and future climate change (Pinsky et al., 2019; Van Der Walt et al., 2021). Here we quantify the single and joint Environmental Safety Margins (ESM) between species tolerance ranges relative to the actual set of environmental conditions experienced by communities sampled in both time and space.

14.2. Material and Methods

Species and biomass data for marine fish communities were obtained from long-term scientific bottom-trawl surveys across the continental shelves of the Northeast Pacific, Northwest Atlantic, and Northeast Atlantic (Maureaud et al., 2021). A total of 1,553 demersal fish species from 227,740 unique hauls covering the time period from 1993 to 2021 were included in the analysis. To evaluate species' tolerance ranges, survey data were standardized across space and time, assigned to hexagonal grid cells, and grouped into three decadal periods (1993–2002,

2003–2012, and 2013–2021). Since sampling effort was not uniform across areas, we constructed species accumulation curves (SACs) to assess the completeness of sampling for each cell and decade combination. Subsequently, we fitted a Michaelis-Menten function to each SAC and estimated the asymptotic species richness using the R package *vegan* (Oksanen et al., 2016). For each cell, we then calculated the number of hauls required to reach 75% completeness of the estimated asymptotic species richness. To further standardize the dataset, we randomly resampled the estimated number of hauls 99 times (with replacement) and calculated the safety margin metrics for each iteration.

To estimate the ESM we extracted the environmental tolerance limits of each species based on the fitted environmental envelopes from AquaMaps (Hodapp et al., 2023; Ready et al., 2010). AquaMaps predictions have been validated using independent and effort-corrected survey data (Ready et al., 2010) and the model performance has been found to be similar to other presence-only species distribution models (Hodapp et al., 2023). Furthermore, we extracted environmental conditions for bottom temperature, salinity and oxygen values by averaging the four highest and lowest monthly values within each unique sampling event (cell and decade). The data were sourced from the ice-ocean model NEMO-Nordic (https://doi.org/10.48670/moi-00013), available through the Copernicus Marine Service (https://marine.copernicus.eu/). Upper (USM) and lower (LSM) safety margins were calculated for each species (i) per cell per decade and weighted by biomass, following an adjusted version of the method described by Van Der Walt et al. (2021):

$$\mathbf{USM}_i = X_{\text{max},i} - X_{\text{max, env}}$$

$$\mathbf{LSM}_i = X_{\text{min, env}} - X'_{\text{min},i}$$

where X denotes the maximum (max) and minimum (min) values of the environment (env) vs the reported species tolerance limits (i). LSM was calculated for all environmental variables, whereas USM was computed only for temperature, as higher concentrations of salinity and oxygen are not expected to limit or increase marine fish species vulnerability. Average USM and LSM values for all variables were then aggregated per grid cell and decade across iterations, resulting in an overall ESM for each community. To enhance visual comparisons of overall ESMs, radar charts were employed to illustrate variations over time and across biogeographic provinces defined by Spalding et al. (2007). The individual ESMs (i.e., USM Temperature, LSM Temperature, LSM Salinity, and LSM Oxygen) were scaled using Min-Max Normalization, ensuring they ranged between 0 and 1. The sum of the four normalized values was then used as a cumulative metric of overall safety margin. In addition, the proportion of species with positive ("safe") values for at least one ESM metric was estimated, where values near 1 indicate that most species are within their safe environmental conditions.

To test whether the calculated ESMs differed from the expected distribution given the species tolerances observed across all the marine provinces, we used a null model based on the randomization of species environmental envelopes. To build the null model, we generated 99 randomized environment tolerance limits for assemblages. Tolerances were drawn from the entire species pool, while holding the species richness estimated in each grid cell and decade constant. We then shuffled the environmental tolerances to obtain random estimates of ESMs. We quantified the Standardized Effect Size (SES) as the difference between observed and random ESM using the following equation: SES = (mean ESM – mean ESM_{null}) / standard deviation ESM_{null}. The SES indicates the number of SDs by which the observed ESMs deviate from the

mean expected ESMs derived from the null models. Positive SES values indicate that ESM is higher than would be expected by chance (communities safer and far from their environmental limits), whereas negative values indicate that ESM is lower than expected by chance (communities closer to their environmental limits). Observed ESM values outside the 95% confidence interval can thus be considered different from the null model (Gotelli, 2000).

To assess the relationship between the estimated joint ESMs to human pressures, we utilized the most up-to-date marine pressure data available at ~1 × 1 km resolution from Halpern et al. (2019). Cumulative impact was calculated by summing raster layers representing 11 stressors, grouped into three categories: (1) Fishing: commercial demersal (destructive, non-destructive high bycatch, non-destructive low bycatch), pelagic (high and low bycatch), and artisanal; (2) Ocean-based: shipping; and (3) Land-based: nutrient pollution, organic chemical pollution, direct human impact, and light pollution. To account for temporal variability, we computed the average value of each group per grid cell over the period 2003–2013. The cumulative safety margins used in the models were aligned with the temporal span of anthropogenic pressures (2003–2013).

Finally, data on MPAs, marine reserves, and other effective area-based conservation measures were obtained from the publicly available Protected Planet database. This database provides the World Database on Protected Areas, a key global resource for area-based conservation efforts. We created a map of protected areas overlaid with hexagonal grid cells containing fish data and calculated the percentage of each cell covered by any type of MPA. The relationship between cumulative safety margins and MPA coverage was then modeled using Generalized Additive Models, which allow for nonlinear relationships.

14.3. Results

We find pronounced large-scale patterns in the joint ESMs with higher-latitude communities, particularly in the North-east Atlantic exhibiting larger margins and relatively fewer species at risk (Fig. 14.1a-b). In contrast, a greater proportion of species are experiencing “unsafe” conditions (closer to their tolerance limits) in lower-latitude communities (e.g., the Gulf of Mexico) and semi-enclosed estuarine systems (e.g., the Baltic Sea and Gulf of St Lawrence). The underlying environmental stressors determining the overall degree of safety differ markedly between marine provinces (Fig. 14.1c). Notably, the higher safety in the Arctic and Northern European Seas is manifested by large margins across all environmental stressors, except for LSM Temp (i.e., low temperatures), while the Warm temperate Northwest Atlantic demonstrates small margins for all. These differences in the overall ESM and their underlying stressors are fairly consistent over time. However, in some regions a slight decline in overall safety is evident, especially with regards to decreasing USM Temp in more recent decades, likely resulting from warming.

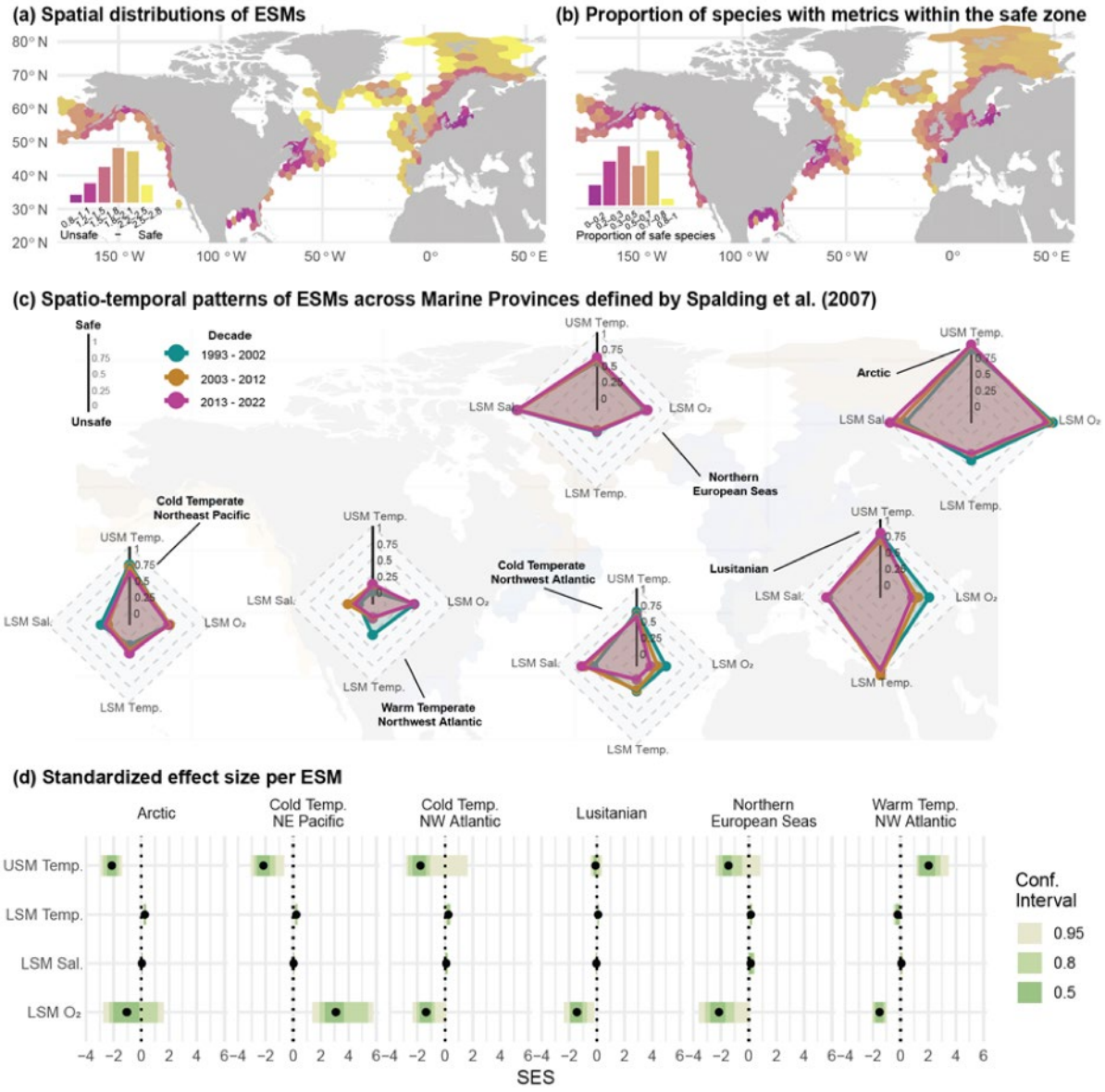

Figure 14.1. ESMs and their underlying stressors across areas and decades. (a) Spatial distributions of overall ESMs, reflecting the sum of standardized ESM for each environmental stressors (z-transformed and averaged across species and decades by grid cells). (b) The proportion of species within each grid cell displaying ESMs values above zero (i.e., safe conditions). (c) Spatio-temporal patterns of standardized ESMs by marine provinces and decades (colored polygons) ranging from 0 (completely unsafe) to 1 (completely safe). (d) Standardized Effect Size (SES) per ESM and province aiming to distinguish between patterns in ESM arising from environmental filtering from and those expected by chance where points represent mean values with corresponding confidence intervals (colors).

The null model shows different patterns for the provinces studied (Fig. 14.1d). For instance, USM Temp was found to be significantly lower in the Arctic and Cold temperate Northwest Atlantic, indicating that communities are closer to their upper thermal limits and thus less safe than expected by chance. Similarly, greater SES for LSM O_2 was found for the Cold Temperate Northeast Pacific. Regarding the anthropogenic pressures, our results reveal a strong negative association between the joint ESM and multiple human activities (Fig. 14.2a-c). Finally, we show no relationship between the current coverage of MPAs and the overall degree of safety throughout the area (Fig. 14.2d).

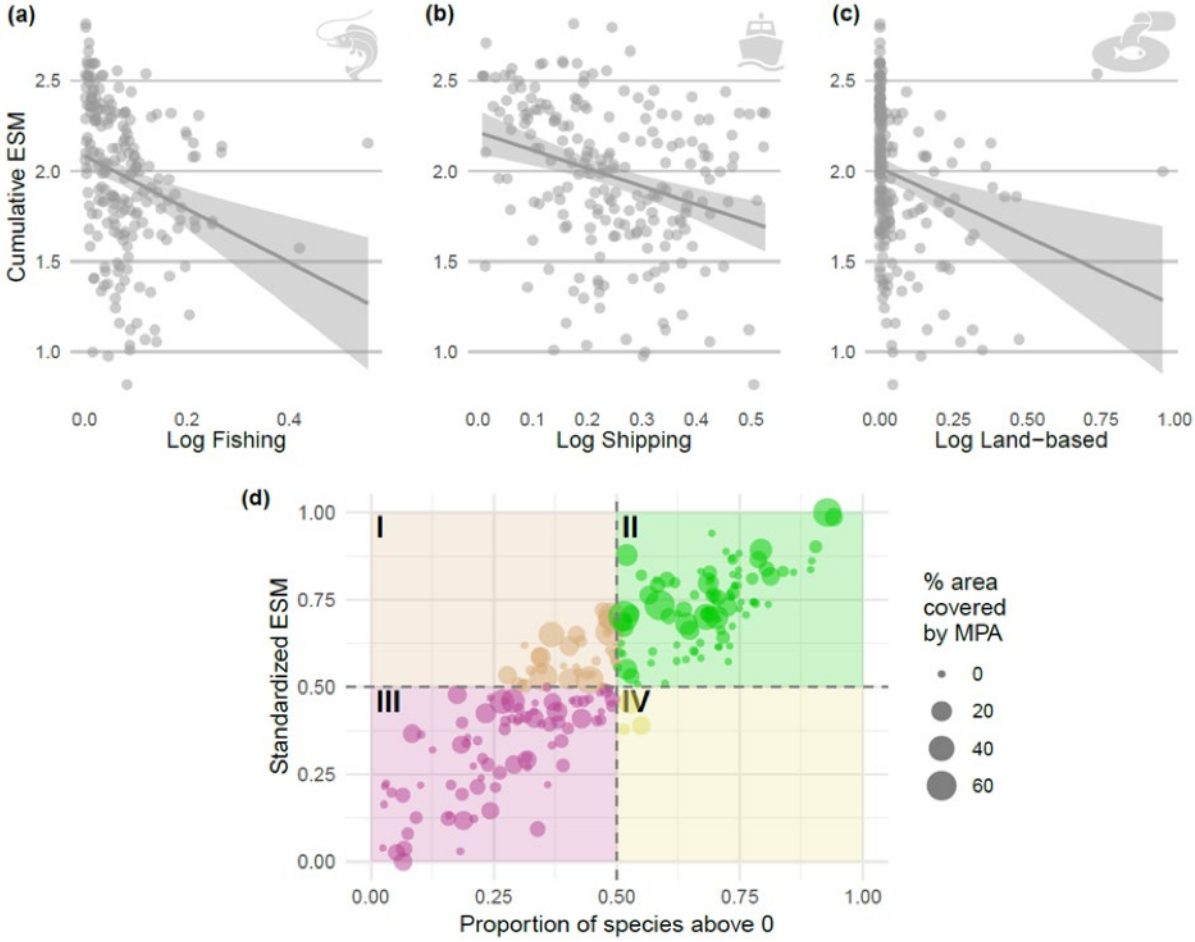

Figure 14.2. Effects of human pressures and protection on community safety margins. (a–c) Linear regression models showing consistent negative relationships between cumulative ESM (sum across all ESMs) and human pressures from fishing (industrial tonnes of catch/year), shipping (traffic index/year), and land-based activities (index/km^2). (d) Relationship between standardized ESMs and the proportion of "safe" species (ESM>0. Values near 0 indicate that most species are living at or beyond their environmental limits, whereas values near 1 indicate that they remain within safe conditions). The colored quadrants represent: (I) high safety maintained by only a few species above zero; (II) high safety with most species above zero; (III) low safety with only a few species above zero; and (IV) low safety with most species still above zero. The size of the points reflects the percentage of each grid cell covered by MPAs.

14.4. Discussion

Taken together, our results reveal different spatial patterns for joint ESM, reflecting the severity of environmental stressors and the community composition of each location. The safest communities are particularly those in the Arctic and the northeast Atlantic, as shown by the highest ESM values. Based on the SES, the USM Temp was significantly lower in these regions, which is a reflection of the dominance of cold-adapted species with relatively narrow upper thermal tolerance ranges compared to the entire species pool (Bongaarts, 2019). In contrast, the Warm Temperate province exhibited values of USM Temp larger than expected from the null model, likely reflecting the presence and prevalence of more warm-affinity species adapted to higher temperatures. Similarly, greater SES for LSM O_2 was found for the Cold Temperate Northeast Pacific, indicating communities better adapted to low oxygen concentrations, likely resulting from exposure to past and current hypoxia caused by the widespread oxygen minimum zones in this region (Busecke et al., 2022; Moffitt et al., 2015; Ross et al., 2020).

Overall, our findings indicate the important role of environmental filtering structuring marine fish communities (Beukhof et al., 2019; Cadotte and Tucker, 2017) by selecting species with particular traits capable of tolerating the range of environmental conditions in a given area. Such environmental filtering is consistent with physiological and behavioral adaptations that enhance tolerance to environmental stressors (Fusi et al., 2024). For example, ectotherms exposed to extreme high or low temperatures may produce heat shock or antifreeze proteins to mitigate cellular damage and physiological disruption (Fusi et al., 2024; Kim et al., 2017). Similarly, mobile species may simply avoid exposure to such extremes by seeking habitats with more favorable conditions, such as migrating toward higher latitudes or into deep waters (Pinsky et al., 2020). This phenotypic and behavioral plasticity may likely contribute to the persistence of communities even under extreme or generally unsafe conditions, reflected by low ESMs in for instance the Gulf of Mexico and the Baltic Sea. However, the degree to which these, or other communities will continue to persist will be profoundly altered by the rapid rate of climate change globally, both in terms of means and variability. Hence, species and communities showing generally safe margins over the past 30 years may rapidly approach or exceed their physiological tolerance limits with continued warming. This is particularly urgent for more cold-adapted species where any magnitude of change in terms of absolute values will have a disproportionate effect due to their generally narrower niche widths, at least compared to species adapted to more seasonal environments. Hence, provinces currently displaying “safe” conditions, such as the Arctic, will likely be more vulnerable to future environmental changes. While ESMs provide valuable insights into community-level vulnerability, their interpretation should be approached with caution. Especially, since sub-lethal stress can cause mortality or local extinctions well before safety margins reach zero, while some species may display physiological acclimatization or behavioral flexibility that confers greater resilience than currently estimated (Pinsky et al., 2019). Moreover, safety at the community level does not guarantee protection for individual species, since environmental shifts may disproportionately affect specific taxa, leading to cascading community reorganization if colonizers respond differently to change. Finally, some aspects of species’ ecological niches remain poorly characterized, introducing uncertainty that may either over- or underestimate ESMs. For instance, climate change may expose parts of the fundamental niche that are currently inaccessible (Chevalier et al., 2024) and incorporating these facets could improve predictions of community vulnerability.

While climate change is recognized as one of the major threats to biodiversity with impacts likely to accelerate during the coming decades (Bongaarts, 2019), other human stressors can strongly limit species’ capacity to tolerate and adapt to shifting climatic conditions. Our results show that communities that are currently most vulnerable to multiple environmental conditions are also those potentially most impacted by other human activities and pressures. Together, these interacting pressures may significantly amplify risks and accelerate ecological decline in marine ecosystems by jointly affecting multiple ecological processes of species related to feeding, growth, reproduction, and survival. Finally, the lack of relationship between MPA coverage and the overall degree of safety throughout the area suggests that MPAs may not be fully effective in safeguarding communities. Although MPAs are not specifically designed for climate change mitigation, they can enhance fish community resistance and resilience by acting as a refugia and steppingstones for dispersal, and safe zones for climate vulnerable species (Roberts et al., 2017).

14.5. Conclusion

The ESM approach, which accounts for the joint sensitivity of species and communities to multiple environmental stressors beyond warming, represents a more robust, precautionary, and broadly applicable framework for climate risk assessment. This framework can inform the designation of MPAs towards a better prioritization of global conservation efforts for biodiversity and overall sustainability. Integrating our approach into conservation planning could further enhance protection outcomes and help align management actions with global policy targets, such as the Kunming–Montreal Global Biodiversity Framework's goal to protect 30% of the ocean by 2030.

14.6. References

Andrello, M., Mouillot, D., Somot, S., Thuiller, W., Manel, S., 2014. Additive effects of climate change on connectivity between marine protected areas and larval supply to fished areas. Diversity and Distributions n/a-n/a. https://doi.org/10.1111/ddi.12250

Behrenfeld, M.J., O'Malley, R.T., Siegel, D.A., McClain, C.R., Sarmiento, J.L., Feldman, G.C., Milligan, A.J., Falkowski, P.G., Letelier, R.M., Boss, E.S., 2006. Climate-driven trends in contemporary ocean productivity. Nature 444, 752–755. https://doi.org/10.1038/nature05317

Beukhof, E., Frelat, R., Pecuchet, L., Maureaud, A., Dencker, T.S., Sólmundsson, J., Punzón, A., Primicerio, R., Hidalgo, M., Möllmann, C., Lindegren, M., 2019. Marine fish traits follow fast-slow continuum across oceans. Scientific reports 9, 17878–17878. https://doi.org/10.1038/s41598-019-53998-2

Bongaarts, J., 2019. IPBES, 2019. Summary for policymakers of the global assessment report on biodiversity and ecosystem services of the Intergovernmental Science-Policy Platform on Biodiversity and Ecosystem Services, Population and Development Review. https://doi.org/10.1111/padr.12283

Boyce, D.G., Lewis, M.R., Worm, B., 2010. Global phytoplankton decline over the past century. Nature 466, 591–596. https://doi.org/10.1038/nature09268

Busecke, J.J.M., Resplandy, L., Ditkovsky, S.J., John, J.G., 2022. Diverging Fates of the Pacific Ocean Oxygen Minimum Zone and Its Core in a Warming World. AGU Advances 3, e2021AV000470. https://doi.org/10.1029/2021AV000470

Cadotte, M.W., Tucker, C.M., 2017. Should Environmental Filtering be Abandoned? Trends in Ecology & Evolution 32, 429–437. https://doi.org/10.1016/j.tree.2017.03.004

Chevalier, M., Broennimann, O., Guisan, A., 2024. Climate change may reveal currently unavailable parts of species' ecological niches. Nat Ecol Evol 8, 1298–1310. https://doi.org/10.1038/s41559-024-02426-4

Doney, S.C., Ruckelshaus, M., Emmett Duffy, J., Barry, J.P., Chan, F., English, C.A., Galindo, H.M., Grebmeier, J.M., Hollowed, A.B., Knowlton, N., Polovina, J., Rabalais, N.N., Sydeman, W.J., Talley, L.D., 2012. Climate Change Impacts on Marine Ecosystems. Annual Review of Marine Science 4, 11–37. https://doi.org/10.1146/annurev-marine-041911-111611

Fusi, M., Barausse, A., Booth, J.M., Chapman, E., Daffonchio, D., Sanderson, W., Diele, K., Giomi, F., 2024. The predictability of fluctuating environments shapes the thermal tolerance of marine ectotherms and compensates narrow safety margins. Sci Rep 14, 26174. https://doi.org/10.1038/s41598-024-77621-1

Gotelli, N.J., 2000. Null Model Analysis of Species Co-Occurrence Patterns. Ecology 81, 2606–2606. https://doi.org/10.2307/177478

Halpern, B.S., Frazier, M., Afflerbach, J., Lowndes, J.S., Micheli, F., O'Hara, C., Scarborough, C., Selkoe, K.A., 2019. Recent pace of change in human impact on the world's ocean. Sci Rep 9, 11609. https://doi.org/10.1038/s41598-019-47201-9

Hamblin, A.L., Youngsteadt, E., López-Uribe, M.M., Frank, S.D., 2017. Physiological thermal limits predict differential responses of bees to urban heat-island effects. Biol. Lett. 13, 20170125. https://doi.org/10.1098/rsbl.2017.0125

Hodapp, D., Roca, I.T., Fiorentino, D., Garilao, C., Kaschner, K., Kesner-Reyes, K., Schneider, B., Segschneider, J., Kocsis, Á.T., Kiessling, W., Brey, T., Froese, R., 2023. Climate change disrupts core habitats of marine species. Global Change Biology 29, 3304–3317. https://doi.org/10.1111/gcb.16612

Kim, H., Lee, J., Hur, Y., Lee, C., Park, S.-H., Koo, B.-W., 2017. Marine Antifreeze Proteins: Structure, Function, and Application to Cryopreservation as a Potential Cryoprotectant. Marine Drugs 15, 27. https://doi.org/10.3390/md15020027

Maureaud, A., Frelat, R., Pécuchet, L., Shackell, N., Mérigot, B., Pinsky, M.L.,….T. Thorson, J., 2021. Are we ready to track climate-driven shifts in marine species across international boundaries? - A global survey of scientific bottom trawl data. Global Change Biology 27, 220–236. https://doi.org/10.1111/gcb.15404

McGill, B.J., Dornelas, M., Gotelli, N.J., Magurran, A.E., 2015. Fifteen forms of biodiversity trend in the anthropocene. Trends in Ecology and Evolution 30, 104–113. https://doi.org/10.1016/j.tree.2014.11.006

Moffitt, S.E., Moffitt, R.A., Sauthoff, W., Davis, C.V., Hewett, K., Hill, T.M., 2015. Paleoceanographic Insights on Recent Oxygen Minimum Zone Expansion: Lessons for Modern Oceanography. PLoS ONE 10, e0115246. https://doi.org/10.1371/journal.pone.0115246

Munday, P.L., Warner, R.R., Monro, K., Pandolfi, J.M., Marshall, D.J., 2013. Predicting evolutionary responses to climate change in the sea. Ecology Letters 16, 1488–1500. https://doi.org/10.1111/ele.12185

Oksanen, J., Blanchet, F.G., Kindt, R., Legendre, P., Minchin, P.R., O'Hara, R.B., Simpson, G.L., Solymos, P., Stevens, H.H., Wagner, H., 2016. vegan: Community Ecology Package. R package version 2.3-4. https://CRAN.R-project.org/package=vegan.

Pecl, G.T., et al, 2017. Biodiversity redistribution under climate change: impacts on ecosystems and human well-being. Science 355, 6332–6332. https://doi.org/10.1126/science.aai9214

Pinsky, M.L., Eikeset, A.M., McCauley, D.J., Payne, J.L., Sunday, J.M., 2019. Greater vulnerability to warming of marine versus terrestrial ectotherms. Nature 569, 108–111. https://doi.org/10.1038/s41586-019-1132-4

Pinsky, M.L., Selden, R.L., Kitchel, Z.J., 2020. Climate-Driven Shifts in Marine Species Ranges: Scaling from Organisms to Communities. Annual Review of Marine Science 12, 153–179. https://doi.org/10.1146/annurev-marine-010419-010916

Pörtner, H.O., Langenbuch, M., Michaelidis, B., 2005. Synergistic effects of temperature extremes, hypoxia, and increases in CO2 on marine animals: From Earth history to global change. Journal of Geophysical Research C: Oceans 110, 1–15. https://doi.org/10.1029/2004JC002561

Ready, J., Kaschner, K., South, A.B., Eastwood, P.D., Rees, T., Rius, J., Agbayani, E., Kullander, S., Froese, R., 2010. Predicting the distributions of marine organisms at the global scale. Ecological Modelling 221, 467–478. https://doi.org/10.1016/j.ecolmodel.2009.10.025

Roberts, C.M., O'Leary, B.C., McCauley, D.J., Cury, P.M., Duarte, C.M., Lubchenco, J., Pauly, D., Sáenz-Arroyo, A., Sumaila, U.R., Wilson, R.W., Worm, B., Castilla, J.C., 2017. Marine reserves can mitigate and promote adaptation to climate change. Proc. Natl. Acad. Sci. U.S.A. 114, 6167–6175. https://doi.org/10.1073/pnas.1701262114

Ross, T., Du Preez, C., Ianson, D., 2020. Rapid deep ocean deoxygenation and acidification threaten life on Northeast Pacific seamounts. Global Change Biology 26, 6424–6444. https://doi.org/10.1111/gcb.15307

Skliris, N., Marsh, R., Josey, S.A., Good, S.A., Liu, C., Allan, R.P., 2014. Salinity changes in the World Ocean since 1950 in relation to changing surface freshwater fluxes. Clim Dyn 43, 709–736. https://doi.org/10.1007/s00382-014-2131-7

Spalding, M.D., Fox, H.E., Allen, G.R., Davidson, N., Ferdaña, Z.A., Finlayson, M., Halpern, B.S., Jorge, M.A., Lombana, J.AL., Lourie, S.A., Martin, K.D., Manus, E.C., Molnar, J., Recchia, C.A., Robertson, J., 2007. Marine ecoregions of the world: A bioregionalization of coastal and shelf areas. BioScience 57, 573–583.

Van Der Walt, K.-A., Porri, F., Potts, W.M., Duncan, M.I., James, N.C., 2021. Thermal tolerance, safety margins and vulnerability of coastal species: Projected impact of climate change induced cold water variability in a temperate African region. Marine Environmental Research 169, 105346. https://doi.org/10.1016/j.marenvres.2021.105346

15 Multidimensional tracking of marine species redistribution under climate change

Authors: Federico Maioli, Daniel van Denderen, Marcel Montanyès, Martin Lindegren

15.1. Introduction

The world's oceans are warming rapidly, driving a major reorganization of marine biodiversity (IPCC, 2022). Marine species are widely expected to respond to ocean warming by tracking their thermal niches—the temperature ranges suitable for survival and reproduction (Grinnell, 1917). Such tracking often involves shifts in geographic distribution (Tingley et al., 2009). Consistent with this expectation, studies across marine taxa and regions have documented widespread poleward and deepward movements, making range shifts one of the most frequently reported biological responses to climate change (Parmesan et al., 2003; Parmesan, 2006; Poloczanska et al., 2013; Poloczanska et al., 2016). These redistributions reshape marine ecosystems and influence resource management and conservation planning worldwide (Pinsky et al., 2018; Pecl et al., 2017; Palacios-Abrantes et al., 2025).

At the same time, observed responses often depart from this general pattern. Many marine populations remain stationary or shift in directions that deviate from poleward or deepward trends, even under sustained warming (Fuchs et al., 2020; Rubenstein et al., 2023; Lawlor et al., 2024). This variability reflects, in part, the complex spatial structure of ocean warming, including heterogeneous climate velocities and physical constraints imposed by coastlines, bathymetry, and ocean circulation (Burrows et al., 2011; Pinsky et al., 2013). As a result, it remains unclear whether heterogeneous species responses combine into a coherent, cross-regional redistribution pattern during ocean warming, or whether opposing movements cancel out at broader spatial scales.

Determining whether species responses combine into coherent redistribution patterns requires evaluating movement across multiple spatial dimensions simultaneously. Most studies, however, examine redistribution along a single gradient at a time—most commonly latitude, and less often depth (Lenoir et al., 2015). While these approaches have revealed important climate-related patterns, they provide limited insight into how species combine movements along different spatial dimensions and what this means for net redistribution across regions. In marine systems, species may shift horizontally, move vertically into cooler waters, remain in place while tolerating greater thermal exposure, or combine these strategies (Nye et al., 2009). Without integrating these responses, we lack a complete picture of climate-driven redistribution under ocean warming (Lawlor et al., 2024; Fredston et al., 2025).

To address this gap, we develop and apply a multidimensional framework that evaluates climate-driven redistribution across three complementary dimensions: horizontal range shifts (changes in range centroids), vertical redistributions (realized depth niches), and changes in realized thermal niches. This framework allows us to assess not only the direction and magnitude of spatial movements, but also whether such movements effectively track shifting thermal environments. If populations fully follow changing isotherms, their realized thermal niches should remain stable through time; systematic warming of realized niches instead indicates incomplete tracking and increasing thermal exposure. We apply this framework to decades of standardized scientific bottom-trawl surveys encompassing more than 200 well-sampled demersal fish popu-

lations across 11 regions of the North Atlantic and Northeast Pacific. These regions span broad latitudinal and climatic gradients, include some of the fastest-warming continental shelf seas (Pershing et al., 2015; Song et al., 2023), and contain some of the most comprehensive long-term records of marine biodiversity change (Maureaud et al., 2021; Maureaud et al., 2024). Using spatiotemporal and Bayesian mixed-effects models, we estimate long-term trends in species' horizontal distributions, depth niches, and realized thermal niches. By examining these responses both within and across regions, we assess whether species-level movements combine into coherent redistribution patterns and evaluate the extent to which such movements reduce thermal exposure under ocean warming.

15.2. Material and Methods

Data sources

Fish observations. We compiled fish biomass density data (kg km^{-2}) from a large collection of standardized, fishery-independent bottom-trawl surveys (Maureaud et al., 2024). Each trawl deployment (haul) recorded species-specific catch biomass standardized by the sampled ("swept") area, together with haul location, depth, and timing. We selected surveys with consistent sampling protocols and at least 15 years of coverage, yielding 17 surveys across 11 regions in the North Atlantic and Northeast Pacific (Figure 15.1).

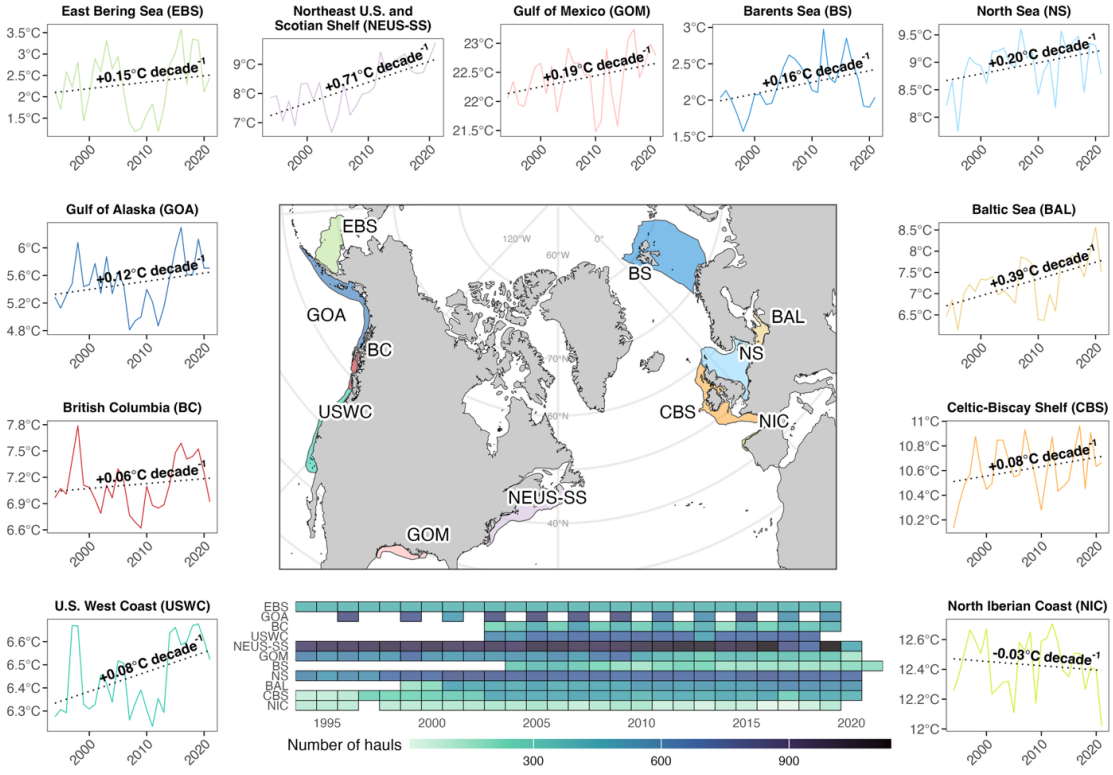

Figure 15.1. Overview of survey coverage and bottom temperature trends. The central map shows the regions included in the analysis, with colored polygons indicating region extents. The tile plot summarizes the number of hauls per region by year. Surrounding panels display regional trends in mean bottom temperature over time; bold values indicate the estimated decadal rate of temperature change.

To ensure robust estimation of species' spatial and temporal dynamics, we retained only taxa that (i) together accounted for 99% of cumulative regional biomass, (ii) occurred in at least 15% of hauls within a region, and (iii) were sampled in at least two hauls per year. These criteria re-

sulted in 226 fish populations (species–region combinations) across all regions (Supplementary Figure S15.1).

Environmental data. We obtained bottom-temperature data from the Copernicus Global Ocean Physics Reanalysis (European Union–Copernicus Marine Service, 2018), which provides monthly estimates at 1/12° (~7 km) resolution. Although in situ temperature measurements were available for some surveys in certain years, we used this reanalysis product to obtain temporally averaged and spatially consistent temperature time series across all regions. Bathymetric data were derived from the GEBCO 2023 dataset (GEBCO Bathymetric Compilation Group, 2023), which provides global seafloor depth at approximately 400-m resolution.

Spatiotemporal modeling

Model structure. We modeled species distributions and their temporal dynamics using spatiotemporal generalized linear mixed-effects models (GLMMs), an approach widely applied in fisheries science (Thorson et al., 2015; Thorson et al., 2016). For each species, biomass density was modeled with a Tweedie distribution, using year (treated as a factor) and log-transformed depth (modeled as a second-order polynomial) as predictors. Survey identity and quarter were included as fixed effects where appropriate to account for differences in sampling design and seasonal variation. Spatial and spatiotemporal variation were captured using random fields approximated via the stochastic partial differential equation (SPDE) approach with Gaussian Markov random fields (Lindgren et al., 2011). Models were implemented in R using the sdmTMB package (Anderson et al., 2024), which integrates finite-element meshes constructed with fmesher (Lindgren et al., 2025) into Template Model Builder (Kristensen et al., 2016).

Prediction grid and environmental matching. After model fitting and validation, we predicted species-specific biomass densities on a 4 × 4 km spatial grid (in local UTM coordinates) covering each region for all available years. For each grid cell, we assigned bathymetry and the average bottom temperature over the 12 months preceding the earliest survey month in that region. This procedure produced a consistent spatiotemporal dataset of predicted biomass, depth, and temperature for downstream analyses.

Derivation of multidimensional spatial and thermal-niche metrics. To quantify species responses to ocean warming, we derived annual metrics describing both spatial redistribution and thermal exposure. These metrics included horizontal range centroids (UTM northing and easting), realized depth niches, and realized thermal niches. Horizontal redistribution was quantified using biomass-weighted range centroids rather than range edges, as centroids are less sensitive to noise and provide a more stable measure of overall distributional change (Shoo et al., 2006). Range centroids were calculated as the biomass-weighted mean UTM northing and easting across grid cells. Realized depth and thermal niches were computed as biomass-weighted averages of depth and bottom temperature, respectively, summarizing the environmental conditions most intensively occupied by each species (Table 15.1). All metrics were derived from predicted biomass densities generated by the fitted spatiotemporal models.

Table 15.1 Summary of annual spatial and thermal metrics used to quantify species' distributional and thermal responses to ocean warming.

Name	Metric	Definition / Formula	Interpretation
Range centroid (UTM northing)	Density-weighted northing	$\bar{y} = \Sigma(y_i \times D_i) / \Sigma D_i$, where y_i is the UTM northing of grid cell *i* and D_i is predicted biomass density.	Tracks north–south shifts in the centre of the species' distribution.
Range centroid (UTM easting)	Density-weighted easting	$\bar{x} = \Sigma(x_i \times D_i) / \Sigma D_i$, where x_i is the UTM easting of grid cell *i*.	Tracks east–west shifts in the centre of the species' distribution.
Depth niche	Density-weighted depth	$\bar{z} = \Sigma(z_i \times D_i) / \Sigma D_i$, where z_i is depth in grid cell *i*.	Captures changes in vertical habitat use.
Thermal niche	Density-weighted temperature	$\bar{T} = \Sigma(T_i \times D_i) / \Sigma D_i$, where T_i is bottom temperature in grid cell *i*.	Reflects thermal conditions in occupied habitat.

The Bayesian trend analysis

We estimated temporal trends in spatial and thermal metrics using Bayesian mixed-effects models that jointly model multiple, potentially correlated responses. Each response was modeled using a Student-t likelihood to provide robustness to extreme values (e.g. Anderson et al., 2017), with uncertainty from the spatiotemporal modeling propagated via observation-specific standard errors. Correlations among responses were captured using a region-specific multivariate normal covariance structure, allowing shared variation among spatial and thermal metrics to be estimated explicitly. Temporal trends were modeled hierarchically as varying slopes, including a global effect of time, region-level deviations, and species-specific deviations nested within regions. To improve interpretability and facilitate model fitting, both the response variables and the time predictor were mean-centered within each species–region combination, such that their means equal zero. Under this parameterization, intercepts were omitted and all coefficients represent deviations from the species–region mean. Time was rescaled to decades, allowing slope parameters to be interpreted directly as rates of change per decade. Thus the model can be written as:

$$y_i^{(j)} \sim \text{Student-t}\left(\nu^{(j)}, \mu_i^{(j)}, \sqrt{(\sigma^{(j)})^2 + (s_i^{(j)})^2}\right), \qquad j = 1, \ldots, 4, \tag{1}$$

$$\mu_i^{(j)} = \beta^{(j)} \cdot \text{decade}_i + \beta^{(j)}_{\text{reg}[r[i]]} \cdot \text{decade}_i + \beta^{(j)}_{\text{reg:sp}[r[i],s[i]]} \cdot \text{decade}_i, \tag{2}$$

$$\beta^{(j)}_{\text{reg}[r]} \sim \text{N}\left(0, \sigma^{(j)}_{\text{reg}}\right), \tag{3}$$

$$\begin{bmatrix} \beta^{(1)}_{\text{reg:sp}[r,s]} \\ \beta^{(2)}_{\text{reg:sp}[r,s]} \\ \beta^{(3)}_{\text{reg:sp}[r,s]} \\ \beta^{(4)}_{\text{reg:sp}[r,s]} \end{bmatrix} \sim \text{MVN}(\mathbf{0},\, \mathbf{S}_r\, \mathbf{R}_r\, \mathbf{S}_r), \qquad \text{for each species } s \text{ in region } r \tag{4}$$

$$\mathbf{S}_r = \begin{bmatrix} \sigma^{(1)}_{\text{reg:sp},r} & 0 & 0 & 0 \\ 0 & \sigma^{(2)}_{\text{reg:sp},r} & 0 & 0 \\ 0 & 0 & \sigma^{(3)}_{\text{reg:sp},r} & 0 \\ 0 & 0 & 0 & \sigma^{(4)}_{\text{reg:sp},r} \end{bmatrix}, \tag{5}$$

$$\mathbf{R}_r = \begin{bmatrix} 1 & \rho_{12} & \rho_{13} & \rho_{14} \\ \rho_{12} & 1 & \rho_{23} & \rho_{24} \\ \rho_{13} & \rho_{23} & 1 & \rho_{34} \\ \rho_{14} & \rho_{24} & \rho_{34} & 1 \end{bmatrix}. \tag{6}$$

Here, y_i^j denotes the response variable j for observation i, where j corresponds to the latitudinal centroid, longitudinal centroid, depth niche, or thermal niche (Table 1). The term s_i^j represents the known standard error associated with observation i, σ^j is a response-specific residual scale parameter, and v^j denotes the degrees of freedom. The linear predictor μ_i^j (Eq. 1) models temporal trends as varying slopes, including a global effect of time, region-specific deviations, and species-specific deviations nested within regions. Species-level slope deviations were modeled jointly across responses using a multivariate normal distribution with region-specific covariance matrices $\Sigma_r = S_r R_r S_r$. This structure allows temporal trends in different response variables to be correlated among species within the same region, as determined by the correlation matrix R_r, while allowing both the magnitude and structure of these correlations to vary among regions. Priors were weakly informative and guided by published rates of range shifts, depth changes, and ocean warming (Appendix A). Models were fitted in R using the *brms* package (Bürkner, 2017), which interfaces with Stan via *rstan*. Each model was run with four Markov chain Monte Carlo (MCMC) chains of 4,000 iterations, with the first 2,000 iterations discarded as warm-up. The remaining 2,000 samples per chain (8,000 total post-warm-up draws) were used to characterize the posterior distribution. Convergence was assessed using a potential scale reduction factor (R-hat) less than 1.01, absence of divergent transitions, and effective sample sizes greater than 400 for all key parameters (Vehtari et al., 2021).

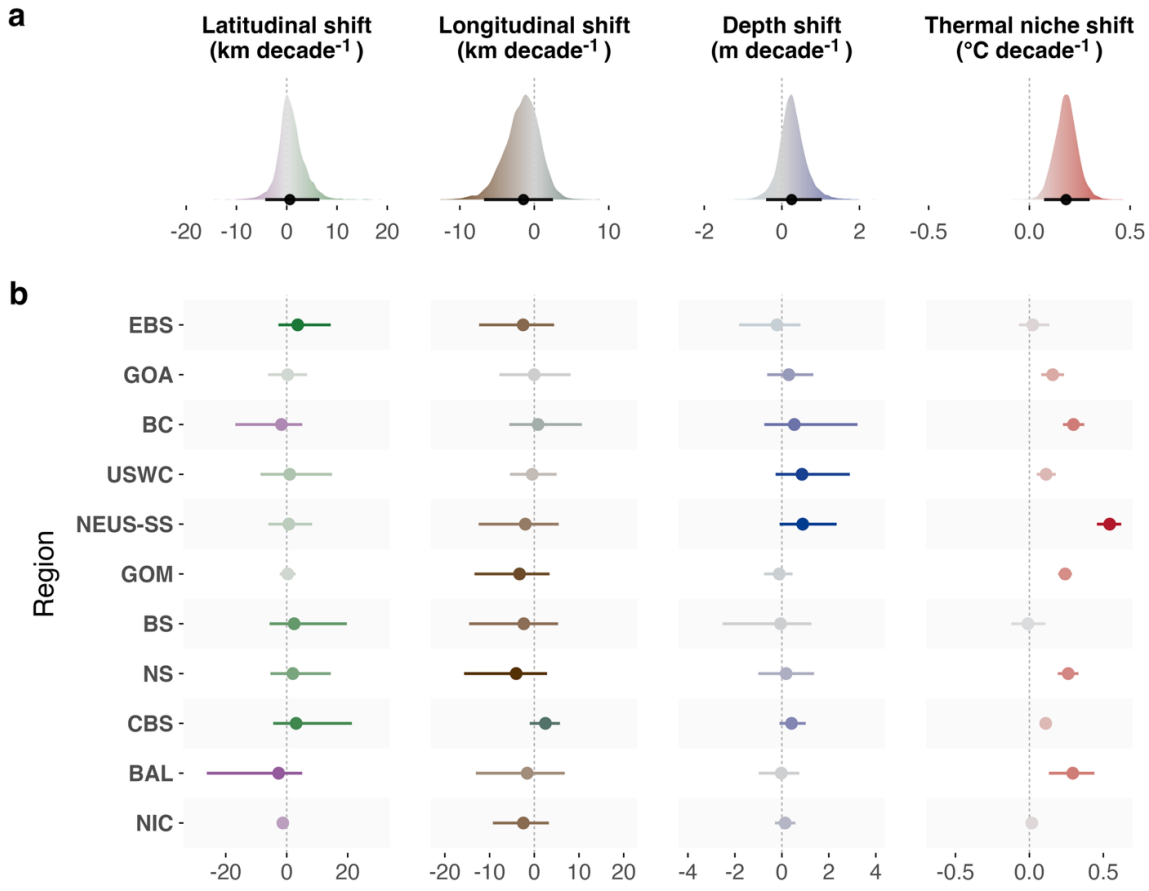

Figure 15.2. Trends in distributional shifts of demersal fish species, shown from left to right for latitudinal, longitudinal, depth, and thermal niche dimensions. Points and horizontal lines indicate posterior medians and 95% Bayesian credible intervals of decadal trends. (a) Global posterior slopes across all regions. (b) Region-specific posterior slopes. In (a), interval shading reflects the posterior distribution along a continuous gradient; in (b), color indicates median effect size, with more intense colors representing larger deviations from zero. Marine regions: EBS = Eastern Bering Sea, GOA= Gulf of Alaska, BC = British Columbia, USWC = U.S. West Coast, NEUS-SS =Northeast U.S. and Scotian Shelf, GOM = Gulf of Mexico, BS = Barents Sea, NS =North Sea, CBS = Celtic–Biscay Shelf, BAL = Baltic Sea, NIC = Northern Iberian Coast.

15.3. Results

No net spatial shifts, but consistent warming of realized thermal niches

Across species and regions, we found little evidence for consistent directional shifts in latitude or longitude. Global posterior estimates for latitudinal change were centered near zero (median 0.63 km per decade; 95% credible interval: −4.27 to 6.51 km), as were longitudinal shifts (median −1.45 km per decade; 95% credible interval: −6.76 to 2.51 km; Figure 15.2a). Depth exhibited a slightly stronger, though still uncertain, tendency toward deepening (median 0.25 m per decade; 95% credible interval: −0.40 to 1.03 m). In contrast, realized thermal niches warmed consistently across species and regions, with a global median increase of 0.18 °C per decade (95% credible interval: 0.07 to 0.30 °C).

Limited average spatial shifts, but coordinated species responses within some regions

At the regional scale, posterior slopes for spatial redistribution varied in direction but were generally small and uncertain, offering limited evidence for consistent changes in mean latitude, longitude, or depth across species (Figure 15.2b). Depth showed the clearest—though still modest and variable—signals, with weak deepening trends along the U.S. West Coast (median 0.86 m per decade; 95% credible interval: −0.27 to 2.89 m) and the Northeast U.S. and Scotian Shelf (median 0.89 m per decade; 95% credible interval: −0.10 to 2.33 m). Despite weak regional averages, many species within some regions shifted in the same direction (Figure 15.3). In the Eastern Bering Sea, 64% of species moved northward, with a similar proportion shifting northward in the North Sea (60%), whereas six of eight species in the Baltic Sea shifted southward. Depth shifts were also directionally consistent in some regions, with many species deepening in the Northeast U.S. and Scotian Shelf (39%) and British Columbia (34%), while relatively few species moved shallower. In contrast, several regions showed no detectable spatial shifts: for example, no species in the Gulf of Alaska shifted in latitude, longitude, or depth, and depth distributions did not change in the Northern Iberian Coast. Realized thermal niches warmed in nearly all regions and closely tracked regional ocean warming rates (Spearman's $\rho = 0.79$, $n = 11$, $p = 0.0036$; Figure 15.1). The Eastern Bering Sea, Barents Sea, and Northern Iberian Coast were the only regions without widespread thermal-niche warming.

Although thermal-niche warming was widespread, in some regions species that shifted poleward or deeper experienced smaller increases in their thermal-niche temperatures. Negative correlations between latitudinal shifts and thermal-niche warming were strongest in the Northeast U.S. and Scotian Shelf ($\rho = -0.88$, 95% CI: −0.99 to −0.66), the Celtic–Biscay Shelf ($\rho = -0.85$, 95% CI: −0.98 to −0.52), the North Sea ($\rho = -0.81$, 95% CI: −0.98 to −0.43), and the Eastern Bering Sea ($\rho = -0.63$, 95% CI: −0.94 to −0.01). Depth shifts showed similar negative associations with thermal-niche warming in the Gulf of Mexico ($\rho = -0.79$, 95% CI: −0.98 to −0.38), British Columbia ($\rho = -0.72$, 95% CI: −0.97 to −0.23), and the North Sea ($\rho = -0.69$, 95% CI: −0.95 to −0.23). Longitudinal shifts generally showed weak or no relationship with thermal-niche change, except in the Northeast U.S. and Scotian Shelf, where longitudinal movements co-varied strongly with latitude ($\rho = 0.86$, 95% CI: 0.68 to 0.96). Spatial shifts along different axes also co-varied in several regions. In British Columbia, the U.S. West Coast, the Northeast U.S. and Scotian Shelf, and the Gulf of Mexico, latitudinal and longitudinal shifts were associated, reflecting coast-parallel movement. In contrast, in the North Sea, latitudinal shifts were correlated with depth shifts, such that northward movements tended to coincide with deepening ($\rho = 0.86$, 95% CI: 0.62 to 0.97).

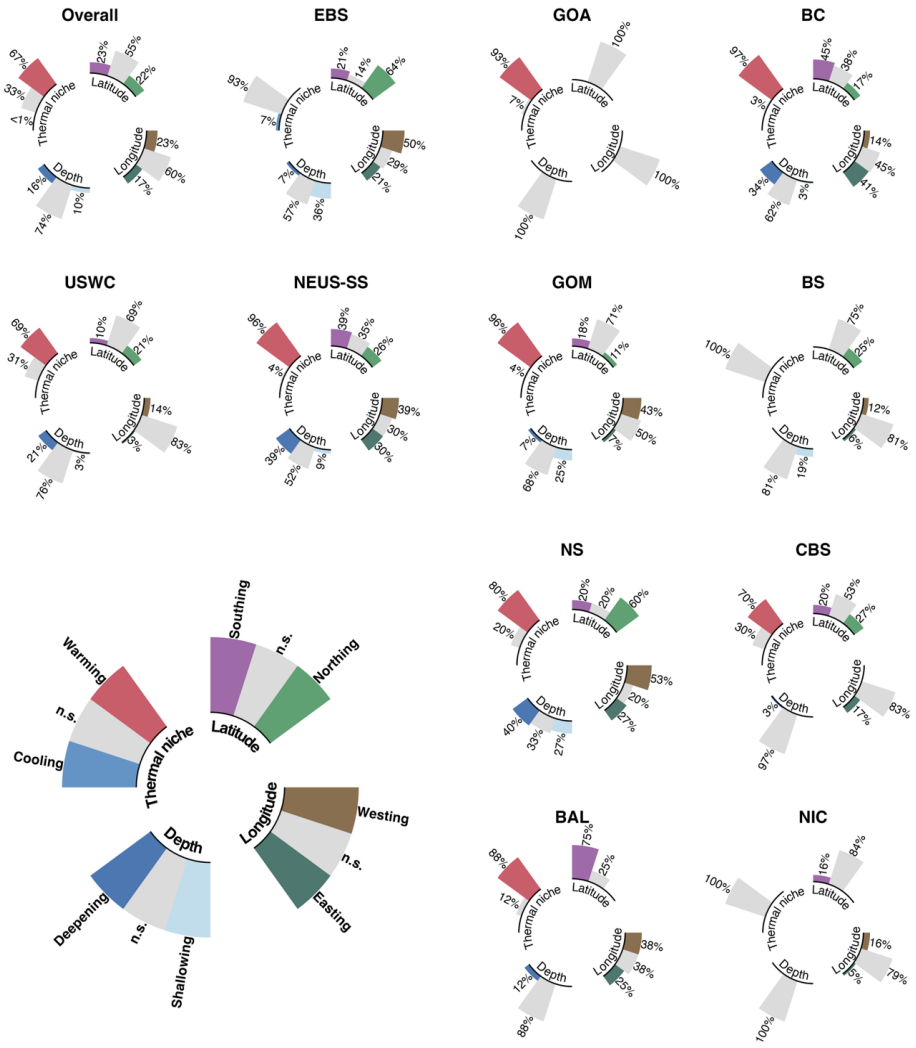

Figure 15.3. Proportion of species with supported distributional shifts over time. Trends are shown for latitudinal, longitudinal, depth, and thermal niche shifts. Bar plots indicate the proportion of species per region showing a particular response, with shifts considered supported if at least 95% of the posterior distribution excludes zero; otherwise, shifts are marked as non-significant (n.s.). Marine regions: EBS = Eastern Bering Sea, GOA = Gulf of Alaska, BC = British Columbia, USWC = U.S. West Coast, NEUS-SS = Northeast U.S. and Scotian Shelf, GOM = Gulf of Mexico, BS = Barents Sea, NS = North Sea, CBS = Celtic–Biscay Shelf, BAL = Baltic Sea, NIC = Northern Iberian Coast.

Species show heterogeneous spatial shifts, while thermal-niche warming is widespread

At the species level, spatial redistribution was highly heterogeneous in both direction and magnitude (Figure 15.3; Supplementary Fig. S15.1). Approximately 45% of the 226 populations exhibited significant latitudinal shifts, with northward and southward movements occurring in similar proportions. The most extreme northward shift occurred in *Molva molva* in the Celtic–Biscay Shelf (197.2 km per decade; 95% credible interval: 142.3 to 242.6 km), while the largest southward shift occurred in *Atheresthes stomias* on the U.S. West Coast (−106.4 km per decade; 95% credible interval: −136.1 to −77.9 km). Longitudinal shifts were detected in 40% of species, with 23% moving westward and 17% eastward. The strongest eastward shift was observed in *Harengula jaguana* in the Gulf of Mexico (116.2 km per decade; 95% credible interval: 89.1 to 142.9 km), while the strongest westward shift occurred in *Squalus acanthias* in the Northeast U.S. and Scotian Shelf (−109.3 km per decade; 95% credible interval: −139.8 to −78.3 km). Depth shifts were less frequent, with 16% of species moving deeper and 10% moving shal-

lower. The strongest deepening occurred in *Squalus suckleyi* in British Columbia (32.4 m per decade; 95% credible interval: 25.2 to 39.5 m), while the greatest shallowing occurred in *Anoplopoma fimbria* in British Columbia (−15.8 m per decade; 95% credible interval: −37.2 to 1.0 m). In contrast to the heterogeneity of spatial responses, warming of realized thermal niches was widespread. 67% of species experienced significant increases in thermal-niche temperature, with the strongest warming observed in *Squalus acanthias* in the Northeast U.S. and Scotian Shelf (1.10 °C per decade; 95% credible interval: 0.91 to 1.31 °C). Only three species exhibited evidence of cooling.

15.4. Discussion

Marine biodiversity is reorganizing under ocean warming, and numerous studies have documented poleward and deepward shifts across taxa and regions (Poloczanska et al., 2013; Dulvy et al., 2008; Poloczanska et al., 2016; Perry et al., 2005). These patterns have often been interpreted as evidence for a pervasive, directional redistribution of marine life in response to climate change. Our results complicate this narrative. Analyzing more than 200 demersal fish populations across 11 continental shelf regions, we found little evidence for consistent, net spatial redistribution along latitude, longitude, or depth when responses were aggregated across regions. Instead, species-level movements were highly variable and often balanced out across species and regions, yielding weak average trends at cross-regional scales, with coherence emerging only in some regions. At the same time, realized thermal niches warmed across most species and regions.

The lack of strong net spatial redistribution contrasts with several cross-regional syntheses reporting substantial, directional range shifts. For example, Poloczanska et al. (2013) estimated mean poleward movements of approximately 30–70 km per decade at species' centroids and leading edges, with comparable rates reported in the BioShifts database (Lenoir et al., 2020). By comparison, the cross-regional trends we estimate were one to two orders of magnitude smaller and showed no consistent direction. Importantly, weak net spatial redistribution does not imply an absence of biological response to ocean warming. Rather, it reflects the diversity of redistribution pathways available to marine species and the constraints that shape them. Although temperature gradients broadly align with latitude and depth, local bathymetry, coastlines, ocean circulation, and habitat structure create region-specific pathways for movement (Pinsky et al., 2013; García Molinos et al., 2016). Species traits, habitat associations, and non-thermal drivers such as fishing pressure, oxygen availability, and prey distributions further modulate these responses (Sunday et al., 2015; Deutsch et al., 2015; Wisz et al., 2013; Bandara et al., 2024). Together, these factors generate heterogeneous—and sometimes opposing—species-level movements within and among regions under similar warming trends, producing weak aggregate signals at broader spatial scales.

Across regions, one signal was nonetheless consistent: widespread warming of realized thermal niches. Most species experienced increasing temperatures in the habitats they occupied, even where spatial redistribution occurred, suggesting that redistribution rarely provided full thermal compensation under ocean warming. Rather than maintaining stable thermal conditions through uniform isotherm tracking, these patterns align with growing evidence that realized thermal niches can be dynamic under climate change (Fredston et al., 2021; Ward et al., 2024). Thermal compensation nonetheless emerged in some regions, where species that shifted poleward or deeper tended to experience smaller increases in thermal-niche temperature. In systems with strong latitudinal temperature gradients, such as the Eastern Bering Sea and the North Sea, poleward movements were associated with reduced niche warming. In regions

with weaker latitudinal gradients or steep depth gradients—such as the Gulf of Mexico and British Columbia—depth provided the primary pathway for partial mitigation. The North Sea represents a particularly coherent case, with many species shifting in concert poleward and deepward, reflecting tightly coupled horizontal and vertical thermal gradients. There, well-documented examples such as North Sea cod illustrate that effective thermal tracking can occur under specific geographic and environmental configurations (Perry et al., 2005; Engelhard et al., 2014), but such cases remain the exception rather than the rule.

Our analysis focuses on well-sampled species from standardized surveys, enabling consistent estimation of spatial and thermal metrics and explicit propagation of uncertainty across multiple dimensions of redistribution. This design results in narrower taxonomic and geographic coverage than global syntheses, but it allows redistribution pathways to be evaluated within a unified statistical framework. Many cross-regional analyses pool heterogeneous datasets and rely on summary metrics such as range edges, often without explicitly accounting for uncertainty in underlying shifts (Brown et al., 2016; Lenoir et al., 2020; Dahms et al., 2023). By contrast, our two-step framework estimates spatial and thermal metrics directly from standardized survey data and models temporal trends jointly across multiple dimensions. This approach propagates uncertainty from observations to species-, region-, and cross-regional summaries and allows correlations among redistribution pathways to vary among regions. These methodological differences likely explain why we detect weaker net redistribution signals at cross-regional scales than earlier syntheses.

Taken together, our results show that climate-driven redistribution of marine species does not manifest as a simple, cross-regional shift toward cooler habitats along predictable axes. Instead, redistribution reflects multidimensional, context-dependent responses shaped by local environmental gradients, physical constraints, and species-specific ecological pathways. When responses are aggregated across regions, these heterogeneous trajectories often offset one another, yielding weak net redistribution despite sustained ocean warming. This complexity challenges assumptions of uniform poleward or deepward tracking and underscores the need for multidimensional approaches to anticipate biodiversity responses under continued climate change.

15.5. References

Anderson, S. C., & Ward, E. J. (2019). Black-swan events in animal populations. Proceedings of the National Academy of Sciences, 116, 7902–7907.

Bandara, K., et al. (2024). The importance of non-thermal drivers in shaping marine species distributions under climate change. Global Change Biology, 30, e17012.

Brown, C. J., et al. (2016). Ecological and methodological drivers of species' distributional shifts. Ecology Letters, 19, 96–104.

Burkner, P.-C. (2017). brms: An R package for Bayesian multilevel models using Stan. Journal of Statistical Software, 80, 1–28.

Burrows, M. T., et al. (2011). The pace of shifting climate in marine and terrestrial ecosystems. Science, 334, 652–655.

Copernicus Marine Service. (2018). Global Ocean Physics Reanalysis. European Union.

Dahms, S., et al. (2023). Temperature-driven range shifts in marine species: A synthesis. Nature Climate Change, 13, 123–130.

Deutsch, C., et al. (2015). Climate change tightens a metabolic constraint on marine habitats. Science, 348, 1132–1135.

Dulvy, N. K., et al. (2008). Climate change and deepening of the North Sea fish assemblage. Proceedings of the Royal Society B, 275, 1965–1973.

Engelhard, G. H., et al. (2014). Climate change and fishing drive North Sea cod distribution. Global Change Biology, 20, 1209–1219.

Fredston, A., et al. (2021). Range shifts and the dynamics of thermal niches. Nature Climate Change, 11, 933–939.

Fredston, A., et al. (2025). Reimagining species redistribution under climate change. Trends in Ecology & Evolution, 40, 1–14.

Fuchs, H. L., et al. (2020). Wrong-way range shifts in a warming ocean. Global Change Biology, 26, 2564–2579.

Garcia Molinos, J., et al. (2016). Climate velocity and the future of biodiversity. Science, 354, 657–660.

Grinnell, J. (1917). The niche-relationships of the California thrasher. The Auk, 34, 427–433.

IPCC. (2022). IPCC Special Report on the Ocean and Cryosphere in a Changing Climate. Cambridge University Press.

Lawlor, D. A., et al. (2024). Mechanisms underlying variable species range shifts. Ecology Letters, 27, 412–425.

Lenoir, J., et al. (2015). Climate-related shifts in species distributions. Ecology Letters, 18, 1072–1083.

Lenoir, J., et al. (2020). Species range shifts in a changing world: The BioShifts database. Global Ecology and Biogeography, 29, 1462–1473.

Maureaud, A., et al. (2021). Are we ready to track climate-driven changes in marine biodiversity? Global Change Biology, 27, 235–249.

Maureaud, A., et al. (2024). FishGlob: A global database of standardized bottom-trawl surveys. Scientific Data, 11, 101.

Nye, J. A., et al. (2009). Climate-related shifts in the spatial distribution of marine fishes. Marine Ecology Progress Series, 393, 111–129.

Palacios-Abrantes, J., et al. (2025). Climate impacts on fisheries and food security. Nature Climate Change, 15, 45–53.

Parmesan, C., & Yohe, G. (2003). A globally coherent fingerprint of climate change impacts. Nature, 421, 37–42.

Parmesan, C. (2006). Ecological and evolutionary responses to recent climate change. Annual Review of Ecology, Evolution, and Systematics, 37, 637–669.

Perry, A. L., et al. (2005). Climate change and distribution shifts in marine fishes. Science, 308, 1912–1915.

Pinsky, M. L., et al. (2013). Marine taxa track local climate velocities. Science, 341, 1239–1242.

Pinsky, M. L., et al. (2018). Preparing ocean governance for species redistribution. Science, 360, 1189–1191.

Poloczanska, E. S., et al. (2013). Global imprint of climate change on marine life. Nature Climate Change, 3, 919–925.

Poloczanska, E. S., et al. (2016). Responses of marine organisms to climate change across oceans. Global Change Biology, 22, 1540–1562.

Rubenstein, D. R., et al. (2023). Climate change and the limits of adaptive redistribution. Ecology, 104, e3912.

Shoo, L. P., et al. (2006). Detecting shifts in species distributions. Global Ecology and Biogeography, 15, 472–486.

Sunday, J. M., et al. (2015). Species traits and thermal tolerance shape responses to warming. Nature Climate Change, 5, 695–700.

Tingley, M. W., et al. (2009). Birds track their climatic niche. Proceedings of the National Academy of Sciences, 106, 19637–19643.

Vehtari, A., et al. (2021). Rank-normalization, folding, and localization. Bayesian Analysis, 16, 667–718.

Ward, E. J., et al. (2024). Winners and losers under ocean warming. Nature Ecology & Evolution, 8, 112–121.

Wisz, M. S., et al. (2013). The role of biotic interactions in shaping species distributions. Biology Letters, 9, 20130245.

16 Summary, implications and perspectives

16.1. General discussion

The key outcomes presented in this deliverable report highlights the role of environmental drivers and anthropogenic pressures in shaping marine biodiversity through broad range of marine ecosystems and organisms sampled along European shelf seas from the Eastern Mediterranean Sea to Greenland and Barents Sea, and non-European waters (Northeaster Atlantic and Northwestern Pacific). All these ecosystems are exposed to very different regional and local environmental conditions, both in terms of climate and hydrography, but also with regards to the type and level of human activities and their associated pressures. To assess their role, the B-USEFUL team has applied a diversity of analytical methods and statistical modeling including joint species distribution models, univariate and multivariate regressions, and multivariate analyses, over a range of spatial resolutions including both the scale of observations (i.e. resolution) and the scale of the biodiversity responses. Despite of all these differences, the general results consistently show that: *i)* the combination of environmental gradients with local drivers shape the baselines for biodiversity spatial variation, *ii)* context dependence and cross-scale approaches are needed to explain global and regional biodiversity patters, and *iii)* the interactions of cumulative pressures and the context dependence explain the spatial heterogeneity of biodiversity-pressure relationships. All these results together evidence the need to develop region-specific management approaches under the Marine Strategy Framework Directive's Good Environmental Status (GES) objectives, and urge for careful assessments of where and under what conditions conservation interventions are likely to be the most effective.

I) Role of environmental gradients and local drivers – Depth and sea-bottom level variables (mainly bottom temperature and salinity) are the primary drivers of community composition and biodiversity facets (e.g. Essential Biodiversity Variables, EBV). This indicates the important role of environmental filtering structuring marine fish communities by selecting species with particular traits capable of thriving over a particular range of environmental conditions in a given area. Those drivers mainly represent environmental gradients (e.g. Chapters 1, 2, 4, 9, 10 and 13), while other local processes associated to natural environmental variability can also influence biodiversity, such as hydrography, water column stratification and primary production dynamics. Local pressures, however, are mainly represented by anthropogenic impacts, which in the context of nektobenthic and epibenthic communities are mainly associated to a secondary but meaningful effect of fishing pressure (e.g. Chapters 1, 3, 4, 5 11 and 12).

Functional and life history traits explained a substantial fraction of among-species variation in responses, particularly to temperature and anthropogenic drivers, highlighting the mechanistic role of functional traits in mediating species-environment relationships (Lindegren et al. 2025, Puerta et al. in review, Chapters 2, 3, 4 12, 14 and 15). Also, in many regions, fish communities are strongly structured by ontogenetic variation in responses to gradients and pressures. Chapters 2 and 3, focused in the Mediterranean Sea, demonstrates that life stages should be treated as distinct ecological entities with potentially divergent niches, sensitivities, and vulnerabilities to global change. These studies show that depth and temperature emerged as dominant drivers of both juvenile and adult distributions, reflecting the high vertical geographic structuring in the rapid warming of Mediterranean ecosystems. Phylogeny also captures latent ecological dimensions not fully described by the available trait data, contributing to explain the mechanisms of species–life stage niches and community assembly, and to strengthen trait-based links between environmental gradients and fish diversity (Chapters 1, 2, 4, 9).

Some studies were are able to contrast responses across food web components by applying the same modeling platform (Northeast Atlantic, Chapter 9) and reveal divergent responses to climate change across the different trophic levels, which are amplified under future projected scenarios. For instance, if biodiversity gains occur primarily among predators, such as piscivorous fish, this decoupling between trophic levels could destabilize food webs and ultimately threaten food security in fisheries that depend on primary and secondary production in plankton. Such imbalances could alter ecosystem structure and energy flow shifting the baselines supporting biodiversity protection and conservation (see section 16.2).

Cumulative effects and complex interactions in the biodiversity responses has been approached in all areas of the B-USEFUL project evidencing that fishing, local environment and climate do not act independently in modifying biodiversity. Beyond cumulative, they are interacting drivers of community change. In the Mediterranean, trawling effects amplified in shallow, thermally stressed areas where communities are near physiological limits or dominated by long-living, slow-recovering species (Chapters 4-5), while region- and context-dependent interactions were identified. More specifically, the three general types of cumulative effects (additive, synergistic and antagonistic) have been identified and quantified in contrasting regions of the Mediterranean Sea (Chapter 6), with dominant interactions displaying a clear spatial structure in terms of temperature, primary production and fishing impacts. Al local scale, dominant interactions were downscaled to local hotspots of high-magnitude synergistic or antagonistic interactions (Chapter 6). The impact of the combined influence of fishing pressure and environmental change also explains discontinuous dynamics and abrupt transitions (i.e., regime shifts) in marine Mediterranean communities (Chapter 8), which in many cases have turned to be dominated by less species and/or a reduced number of traits (Chapters 3, 8, Puerta et al. in review).

Studies focused exclusively on epibenthic ecosystems in the Northeast Atlantic, applied functional response forms and cumulative impacts from a series of anthropogenic pressures (Chapter 11), and a trait-based risk assessment methodology to assess the impact of bottom-trawl activity (Chapter 12). Chapter 11 illustrates how the combined effect of trawling effort, nutrient enrichment (nitrogen, phosphorus), and SST, that exhibit markedly different effects depending on the subregion over the North Sea (see below), showed a clear variability in area-based pressures and how they influence local biodiversity. This study applies an integrative absolute-effect index to combine positive and negative responses and map the intensity of the footprint of cumulative pressure effects. In the Chapter 12, a longevity-biomass approach allows estimating changes in total community biomass and the biomass of a specific group of species with a certain longevity of the benthos community. The assessment tool will contribute to identify areas most at risk from bottom fishing disturbance by accounting for gear-specific depletion mortality and the varying sensitivities of benthic fauna. This tool has been demonstrated useful to estimate changes in multiple biodiversity facets, with the greatest success for species richness.

II) Context dependence and cross-scale biodiversity responses – Combining alfa (α-), beta(ß-) and gamma(γ)-biodiversity analyses including a set of potential environmental and anthropogenic drivers keeps a robust way to describe integratively the mechanisms of biodiversity variation from local to regional scales. For the Mediterranean Sea, cumulative human impacts associated to coastal development and fishing pressure remain concentrated along productive shelves and coastal areas, so the observed erosion of α-diversity in these areas is consistent with the co-occurrence of strong climatic and anthropogenic stressors (Chapters 1-3). Decreas-

ing ß-diversity is generally reported due to the declining of dissimilarity at local and wider scale, or due to biotic homogenization driven by the preferential loss of sensitive species and expansion of more tolerant taxa. However, some areas report increasing distance-structured turnover associated to the spatially heterogeneous climatic forcing, fishing-induced erosion and decreasing ecological similarity. Communities are rapidly reorganizing, particularly in high latitudes of both Mediterranean basins, with stronger turnover likely driven by medialization processes, shallow hydrography, eutrophication and long-term exploitation, known to produce strong assemblage dynamics (Chapter 3). In the Northeast Atlantic, the combination of α-, ß- and γ-diversity calculated across Hill numbers and Bayesian Additive Regression Trees analyses contribute to assess biodiversity reporting cycles, i.e. past, present and near future (Chapter 9). This chapter shows that climate change is modifying biodiversity both within assemblages, altering the contribution of rare species, and across the food web. Species richness is increasing for fish and benthos, reflecting poleward migration, but decreasing for phytoplankton and zooplankton, potentially disrupting energy transfer from lower to higher trophic levels with marked spatial heterogeneity. Geographic and bathymetric gradients also shape α-, ß- and γ-biodiversity over the Portuguese coast (Chapter 10). Given the known spatial variation in environmental variables and in fishing effort in this area, further analysis will be implemented to explore and quantify the relationship of α-, ß- and γ-biodiversity, and of community weighted means and proportions of functional traits, with environmental variables (e.g. temperature, salinity, oxygen) and with fishing effort across the Portuguese coast.

Many of the chapters of this Deliverable report have applied a cross-scale approach, replicating the same analytical framework across different resolution of data aggregation. The Chapter 6 evidence how multiple pressures interact to shape the spatial patterns of three different taxonomic and functional biodiversity indicators considering both local to regional scales. This study identifies, at regional scale, the main interactions among pressures and characterize their direction, type and magnitude; in addition, it also spatially assesses the role of dominant interacting effects of temperature-productivity-fishing in the biodiversity responses over local scales. Chapter 7 and 11 applied different methods to assess biodiversity-pressure relationships (see below) across different scales: (i) to successfully quantify limiting thresholds of impact to spatially assess the biodiversity state (Chapter 7, currently applied over the Mediterranean Sea but being expanded to Atlantic regions as well); and (ii) to differentiate and contrast the functional form of anthropogenic impacts on benthic biodiversity across contrasting scales (Chapter 11).

The importance of considering as much as possible the context dependence in understanding the biodiversity responses to environmental and anthropogenic impacts is highlighted in many studies. Chapters 3-7 and 11 stress the limitations of uniform, basin-wide measures for biodiversity protection and thus, the variety of cumulative impacts should be tailored to the environmental and ecological context of each region. Additionally, Chapters 15 shows robust evidence across Atlantic and Pacific groundfish communities that climate-driven redistribution of marine species does not occur as a simple, cross-regional shift toward cooler habitats along predictable axes. Instead, redistribution reflects multidimensional, context-dependent responses shaped by local environmental gradients, physical constraints, and species-specific ecological pathways. All Mediterranean focused Chapters (3-8) also pay careful attention to the context-dependent interpretation of the results, between and within sub-basins and regions.

III) Spatial heterogeneity of biodiversity-pressure relationships (BPRs) – Several chapters investigate in detail the spatial heterogeneity in biodiversity–pressure relationships. Baselines of

biodiversity state, functional forms of the impacts, rates of biodiversity response, among others, are critical information emerging from BPRs needed to scientifically inform region-specific management approaches. Chapter 7 specifically focuses in identifying the limiting thresholds of impact calculated from regional and sub-regional BPRs with bottom fishing impact under different environmental regimes (productivity, temperature). This study demonstrates that primarily productivity strongly influenced the biodiversity response to fishing pressure. Under low productivity regimes, biodiversity loss was generally higher, with thresholds towards increasingly impacted states occurring at much lower fishing pressure values than in the opposite regime. Biodiversity responses under contrasting temperature scenarios were more similar between thermal regimes than those observed (at least for the Mediterranean Sea), meaning that biodiversity sensitivity to fishing impact was generally more independent of thermal conditions.

In Chapter 11, functional response forms and cumulative impacts from anthropogenic pressures show variability in area-based pressures and how they influence local benthic biodiversity, highlighting the complexity of interpreting state-pressure patterns. As an illustrative example, trawling effort was generally negatively linked with species richness in the North Sea, although the positive relationship in the southwest region suggests that fishing activity could overlap with naturally richer habitats rather than trawling being the cause, or alternatively, due to situations where low or intermediate trawling can be beneficial for certain species.

16.2. Management implications

The ultimate objective of B-USEFUL is to contribute to achieve policy goals of EU Green Deal and the Biodiversity Strategy 2030 by developing user-oriented tools and solutions to conserve and protect marine biodiversity. It also responds to the current Marine Strategy Framework Directive's Good Environmental Status (GES) challenges and those of other regional and national strategies. All Chapters in the present report provide substantial advances in **three main directions**: reporting **MPA mismatch** with areas that should be designed to maximize biodiversity conservation and, the need of **shifting baselines** and **context dependence** in the measures to apply.

I) Numerous chapters evidence the **strong mismatch** between the current European and International **MPA network** and the areas that should be designed achieve the policy goals according to the B-USUFUL results. Chapter 14 reports an evident lack of relationship between MPA coverage and the overall degree of safety margins (Environmental Safety Margins, ESM) throughout the area, which suggests that MPAs may not be fully effective in safeguarding communities. At the Mediterranean level, Chapter 4 identified emerging dynamic hotspots and coldspots of abundance and biodiversity across multiple species and life stages (juveniles and adults). This community-based Essential Fish Habitats (EFHs) remain outside the current Mediterranean MPA network, with Approximately 76% of their surface falling outside MPAs, and with the majority of designated EFHs subject only to minimal or light protection.

While more specific work in relation to MPA network and the biodiversity risks will be presented in the coming Deliverable 4.3 report, Chapter 12 (focused in benthic biodiversity) already reports how **closing the Natura 2000 network to all bottom-trawling activities** could influence the condition of seabed habitats across the Greater North Sea, Celtic Seas, Baltic Sea, and the Iberian Coast and Bay of Biscay, including potential different closure and fisheries displacement scenarios. The Chapter also highlights that closing sites to bottom trawling would disproportionately impact fisheries concentrated on them, such as beam trawls, which derive nearly all landings from Natura 2000 areas. Benthic impact assessments indicate that closures

generally increase in? areas with high benthic state, but displaced fishing can intensify pressure on unprotected, sensitive habitats, sometimes leading to a net decline in benthic condition for certain habitat types.

II) Numerous chapters also provide the scientific basis to design **shifting state baselines** supporting global and regional policy frameworks for biodiversity protection and conservation. This information leads to developing indicators that can inform preventive action, rather than those that simply document change once it has occurred. Such indicators need to be embedded within the policy cycle and clearly linked to the decision-making. Chapter 9 has explicitly faced that and developed a suite of complementary biodiversity indicators for the Northeast Atlantic regions accounting for climate-driven shifting baselines and, capable of assessing current status and projected future trends across assemblages in response to climate change. Chapter 7 also identifies spatially- and environmental regime-dependent baselines as reported by the spatial heterogeneity in the BPRs. BPRs are able to capture cumulative relationship between biodiversity loss along an increasing fishing pressure gradient across regions, environmental conditions, and spatial scales, and thus, identifying shifting baselines considered to quantify the different limiting thresholds of impact.

III) Finally, most chapters report the limitations of uniform, basin-wide measures for biodiversity protection. **Spatial heterogeneity in biodiversity responses** observed over the report suggests that management and mitigation strategies aimed at reducing climatic and anthropogenic impacts should be tailored to the environmental and ecological or climatic circumstances in each region, and sustained in **context-dependent measures and indicators**. This information will instrumental in critically interpreting biodiversity projections based on the SSP-RCP scenarios (WP 5 and see Section 16.3 below).

Taking all this together, results and tools provided by the B-USEFUL team will contribute to revise the European policies in relation to the biodiversity conservation.

16.3. Perspectives

The direct application of the knowledge and tools presented in this Deliverable are the ongoing work in Biodiversity Risk Assessment (WP 4) and the forecasting and scenario simulations (WP 5) under development. As an example, match/mismatch analyses between biodiversity hot- and coldspots (Chapters 3-5, 9, 14) and protected areas is being currently performed transversally over all the European Seas under research. Also, taking advantage of the Joint Species Distribution Models applied transversally over all regions (Lindegren et al. 2025; Deliverable 3.1) and many of the results included in the present Deliverable based on other statistical and modeling approaches, projections will be developed by using spatially explicit seasonal-to-decadal forecasts of environmental variables and long-term SSPs-RCP scenarios. As jan illustrative example, Chapter 9 shows how the development of a suite of complementary biodiversity indicators capable of assessing current status has been extended and projected into the future to provide trends across assemblages and regions in response to climate change. A similar approach is being extended to all B-USEFUL areas. Finally, some of the work here presented and focused in some areas (e.g. Chapter 7 on biodiversity-pressure relationships currently focused in the Mediterranean) will extended to other Atlantic areas.

17. Appendices

The *Appendices* linked to this report comprise auxiliary material regarding data, modelling approaches and additional results for each of the sections, associated to different areas and organism groups.

A. Appendix: Alpha and Beta diversity and cumulative impacts in the Mediterranean Sea

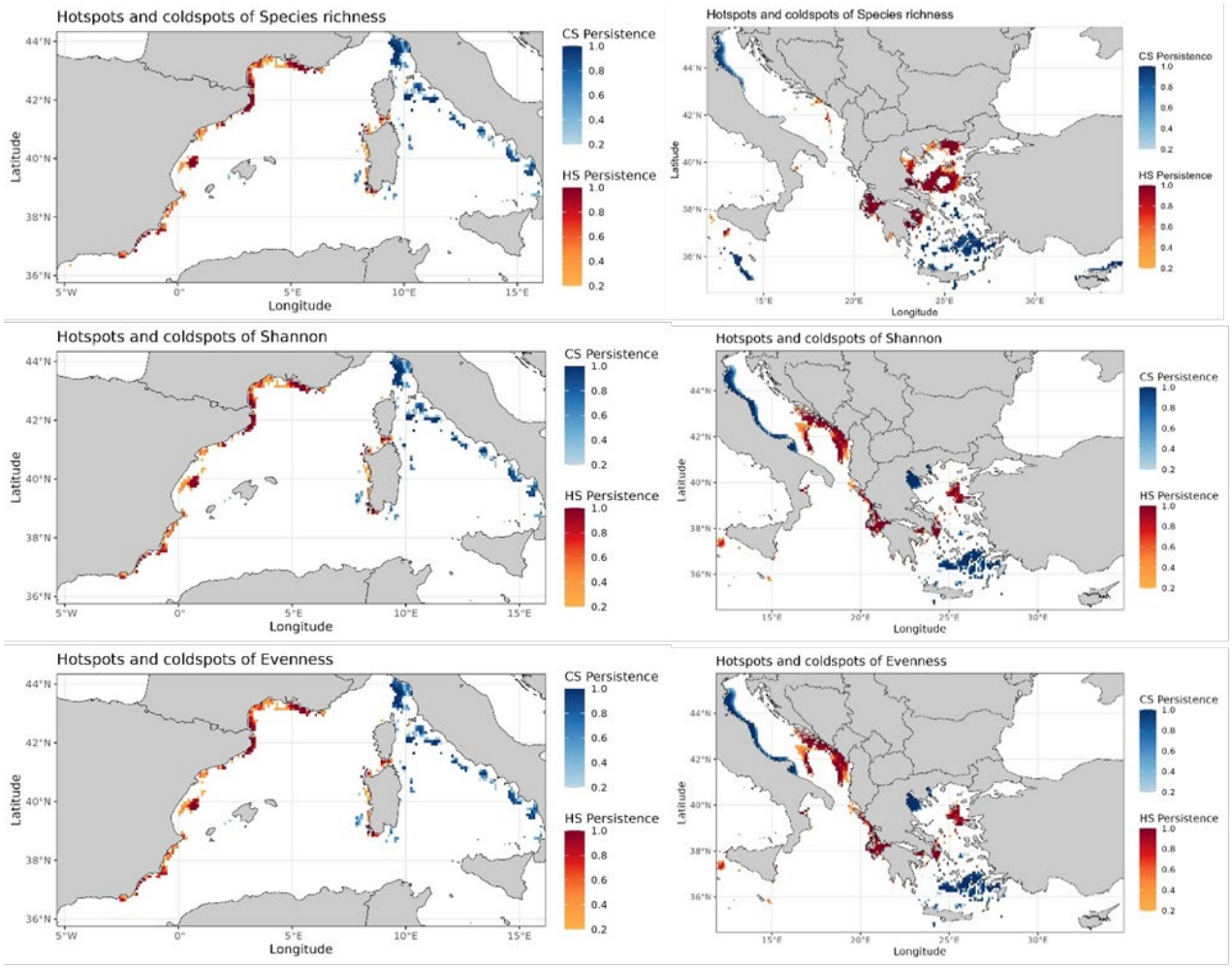

Figure S3.1. Estimated hotspots (red color scale) and coldspots (blue color scale) for α-diversity indices covering the Western Mediterranean Sea (on the left column) and the Central-Eastern Mediterranean Sea (on the right column). The first row reports the species richness maps, the second row reports the maps for the Shannon index and the third reports the maps of evenness index.

Table S3.1. summary of the Spearman temporal trends estimated for the α-diversity metrics (species richness, Shannon and evenness indices) at different spatial scale (sub-area and GSA). Significance codes: "***" p < 0.001; "**" 0.001 ≤ p < 0.01; "*" 0.01 ≤ p < 0.05; "ns" corresponds to non-significant trends with p ≥ 0.05. The table also reports the percentage variation in the α-diversity indices estimated in the time series (1999-2021).

		SPECIES RICHNESS			SHANNON			EVENNESS		
sub-area	**GSA**	**Spearman (rho)**	**p-value**	**difference (%)**	**Spearman (rho)**	**p-value**	**difference (%)**	**Spearman (rho)**	**p-value**	**difference (%)**
WMS		**-0.095**	***	**-6.5**	**-0.100**	***	**-2.1**	**-0.072**	***	**-1.5**
	GSA 1	-0.108	***	-4.9	-0.106	***	-1.6	-0.069	**	-1.0
	GSA 5	-0.101	***	-3.0	-0.110	***	-1.4	-0.058	***	-0.8
	GSA 6	-0.032	**	-7.4	-0.042	***	-1.0	0.003	n.s.	-
	GSA 7	-0.153	***	-10.8	-0.164	***	-2.0	-0.117	***	-1.4
	GSA 8	-0.144	***	-13.4	-0.150	***	-3.0	-0.125	***	-2.4
	GSA 9	-0.180	***	-5.3	-0.185	***	-3.9	-0.160	***	-3.3
	GSA 10	-0.075	***	-9.8	-0.087	***	-1.4	-0.049	***	-0.8
	GSA 11	-0.124	***	-7.2	-0.131	***	-2.8	-0.105	***	-2.3
CMS		**-0.026**	***	**-2.0**	**-0.023**	**	**-0.7**	**-0.014**	*	**-0.4**
	GSA 15	-0.062	***	-4.2	-0.032	*	-0.8	-0.017	n.s.	-
	GSA 16	-0.022	n.s.	-	-0.030	*	-1.0	-0.020	n.s.	-
	GSA 19	-0.012	n.s.	-	-0.012	n.s.	-	-0.003	n.s.	-
	GSA 20	-0.008	n.s.	-	-0.016	n.s.	-	-0.006	n.s.	-
AS		**-0.052**	***	**-3.6**	**-0.033**	***	**-1.3**	**-0.025**	***	**-1.0**
	GSA 17	-0.082	***	-4.9	-0.050	***	-1.8	-0.040	***	-1.4
	GSA 18	0.004	n.s.	-	-0.006	n.s.	-	0.002	n.s.	-
EMS		**-0.027**	***	**-3.3**	**-0.026**	***	**-1.3**	**-0.020**	***	**-1.0**
	GSA 22	-0.030	***	-3.6	-0.030	***	-1.5	-0.024	***	-1.1
	GSA 23	-0.014	n.s.	-	-0.004	n.s.	-	0.004	n.s.	-
	GSA 25	-0.003	n.s.	-	0.003	n.s.	-	0.017	n.s.	-

Table S3.2. Summary of the Spearman temporal trends estimated for the a and b parameters of the power functions used to estimate the annual relationships between the Jaccard index and the distance between grid cells covering the study areas. Significance codes: "***" p < 0.001; "**" 0.001 ≤ p < 0.01; "*" 0.01 ≤ p < 0.05; "ns" corresponds to non-significant trends with p ≥ 0.05.

		a		b	
sub-area	**GSA**	**Spearman (rho)**	**p-value**	**Spearman (rho)**	**p-value**
WMS		0.444	n.s.	0.393	n.s.
	GSA 1	0.079	n.s.	0.156	n.s.
	GSA 5	-0.314	n.s.	-0.389	n.s.
	GSA 6	-0.067	n.s.	-0.092	n.s.
	GSA 7	0.299	n.s.	0.305	n.s.
	GSA 8	0.250	n.s.	0.278	n.s.
	GSA 9	-0.600	**	-0.488	*
	GSA 10	-0.565	**	-0.437	*
	GSA 11	-0.310	n.s.	-0.260	n.s.
CMS		0.153	n.s.	0.265	n.s.
	GSA 15	0.701	***	0.731	***
	GSA 16	0.250	n.s.	0.281	n.s.
	GSA 19	-0.048	n.s.	-0.077	n.s.
	GSA 20	0.662	***	0.728	***
AS		0.051	n.s.	-0.002	n.s.
	GSA 17	-0.111	n.s.	-0.155	n.s.
	GSA 18	-0.349	n.s.	-0.393	n.s.
EMS		0.307	n.s.	0.425	*
	GSA 22	0.064	n.s.	0.300	n.s.
	GSA 23	0.631	**	0.665	***
	GSA 25	0.099	n.s.	0.191	n.s.

Table S3.3. Summary of the Spearman spatial trends estimated for the temporal diversity along the longitudinal and the latitudinal gradients estimated along the Mediterranean sub-regions and GSAs. The total temporal beta diversity was decomposed in the turnover and nestedness components. Significance codes: "***" $p < 0.001$; "**" $0.001 \leq p < 0.01$; "*" $0.01 \leq p < 0.05$; "ns" corresponds to non-significant trends with $p \geq 0.05$.

		Longitude						Latitude					
		total		turnover		nestedness		total		turnover		nestedness	
sub-area	GSA	Spearman (rho)	p-value	Spearman (rho)	p-value	Spearman (rho)	p-value	Spearman (rho)	p-value	Spearman (rho)	p-value	Spearman (rho)	p-value
WMS		0.354	***	0.118	***	0.291	***	0.157	***	0.027	N.S.	0.196	***
	GSA 1	-0.098	N.S.	0.048	N.S.	-0.198	*	-0.322	**	-0.229	*	-0.144	N.S.
	GSA 5	0.334	***	0.357	***	-0.014	N.S.	0.390	***	0.440	***	-0.017	N.S.
	GSA 6	0.307	***	0.188	***	0.209	***	0.235	***	0.113	*	0.224	***
	GSA 7	-0.426	***	-0.419	***	-0.123	N.S.	-0.377	***	-0.442	***	0.019	N.S.
	GSA 8	0.196	N.S.	0.157	N.S.	0.027	N.S.	0.142	N.S.	0.187	N.S.	-0.039	N.S.
	GSA 9	-0.010	N.S.	-0.155	*	0.202	***	-0.169	**	-0.039	N.S.	-0.191	**
	GSA 10	-0.037	N.S.	-0.085	N.S.	0.101	N.S.	0.102	N.S.	-0.013	N.S.	0.136	*
	GSA 11	-0.247	***	0.013	N.S.	-0.229	***	-0.104	N.S.	-0.108	N.S.	0.037	N.S.
CMS		0.084	*	0.047	N.S.	0.036	N.S.	0.155	***	0.139	***	0.036	N.S.
	GSA 15	0.434	***	0.329	***	0.251	***	0.467	***	0.271	***	0.312	***
	GSA 16	0.044	N.S.	0.051	N.S.	-0.024	N.S.	0.108	N.S.	0.100	N.S.	0.028	N.S.
	GSA 19	0.201	**	-0.132	N.S.	0.370	***	0.232	***	-0.059	N.S.	0.308	***
	GSA 20	-0.046	N.S.	-0.251	**	0.177	*	0.148	N.S.	0.335	***	-0.165	*
AS		-0.179	***	-0.168	***	-0.014	N.S.	0.079	**	0.178	***	-0.123	***
	GSA 17	-0.170	***	-0.200	***	0.014	N.S.	0.012	N.S.	0.181	***	-0.209	***
	GSA 18	-0.102	N.S.	0.125	*	-0.200	***	0.023	N.S.	0.055	N.S.	-0.048	N.S.
EMS		-0.277	***	-0.274	***	-0.102	***	0.284	***	0.307	***	0.112	***
	GSA 22	-0.221	***	-0.251	***	-0.043	N.S.	0.280	***	0.287	***	0.117	***
	GSA 23	-0.325	***	-0.262	**	-0.188	*	0.148	N.S.	0.084	N.S.	0.098	N.S.
	GSA 25	-0.151	N.S.	0.009	N.S.	-0.238	*	-0.223	*	-0.156	N.S.	-0.155	N.S.

Table **S3.4.** Summary of the significant contributions of environmental and anthropogenic drivers in each GDM model fitted along the Mediterranean sub-basins and GSAs. Significant effect of the drivers is reported with the "X" symbol ($p < 0.05$).

sub-area	GSA	depth	sst	btemp	so	bso	chl	fe
WMS		X		X	X	X		
	GSA 1	X		X	X	X		X
	GSA 5	X		X		X		
	GSA 6	X		X	X	X		
	GSA 7	X		X		X	X	X
	GSA 8	X		X		X		
	GSA 9	X	X	X		X		X
	GSA 10	X		X	X	X		
	GSA 11	X		X	X	X		
CMS		X		X	X	X	X	X
	GSA 15	X		X	X	X	X	
	GSA 16	X		X	X	X	X	
	GSA 19	X		X	X		X	
	GSA 20	X		X			X	X
AS		X	X	X	X	X	X	X
	GSA 17	X	X	X	X	X	X	X
	GSA 18	X		X	X	X	X	X
EMS		X	X	X	X		X	X
	GSA 22	X	X	X	X		X	X
	GSA 23	X	X	X				
	GSA 25	X	X	X				

B. Appendix: Biodiversity status and drivers of fish juvenile life-stages in the Central-Eastern Mediterranean Sea

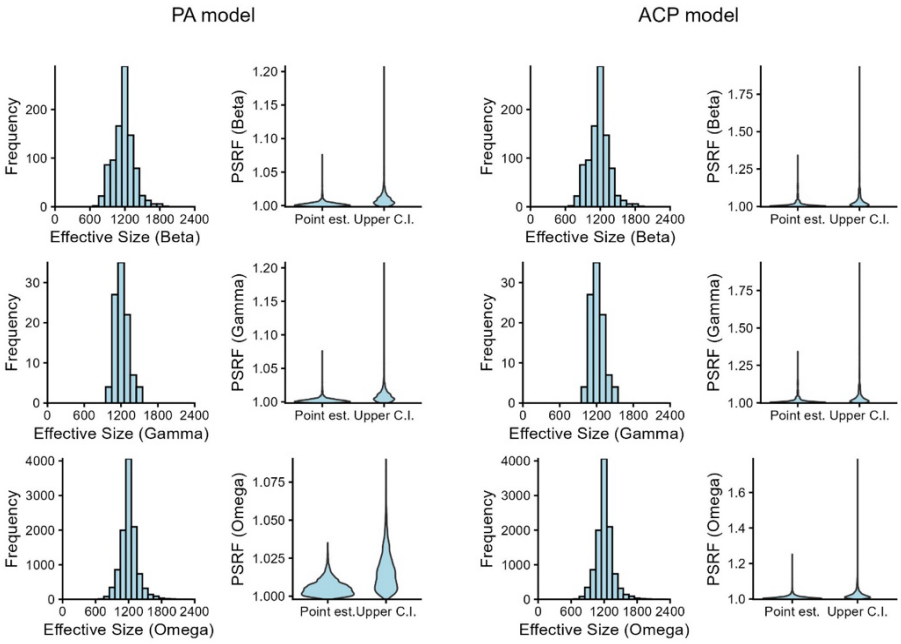

Figure S5.1. Markov Chain Monte Carlo convergence diagnostics for the Beta, Gamma and Omega HMSC model parameters. PA model: Presence/Absence model, ACP model: Abundance Conditional on Presence model, PSRF: potential scale reduction factor.

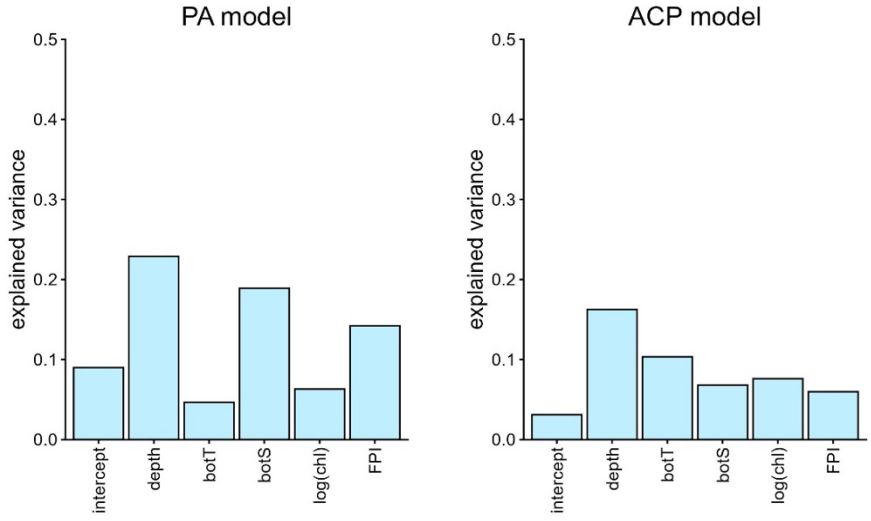

Figure S5.2. Species responses to the covariates attributable to traits for the Presence/Absence (PA) and the Abundance Conditional on Presence (ACP) model. botT: bottom temperature, botS: bottom salinity, log(chl): log-transformed surface chl*a* concentrations, FPI: fishing pressure index.

C. Appendix: Spatiotemporal biodiversity patterns and hotspots of fish communities on the Portuguese continental shelf and upper slope

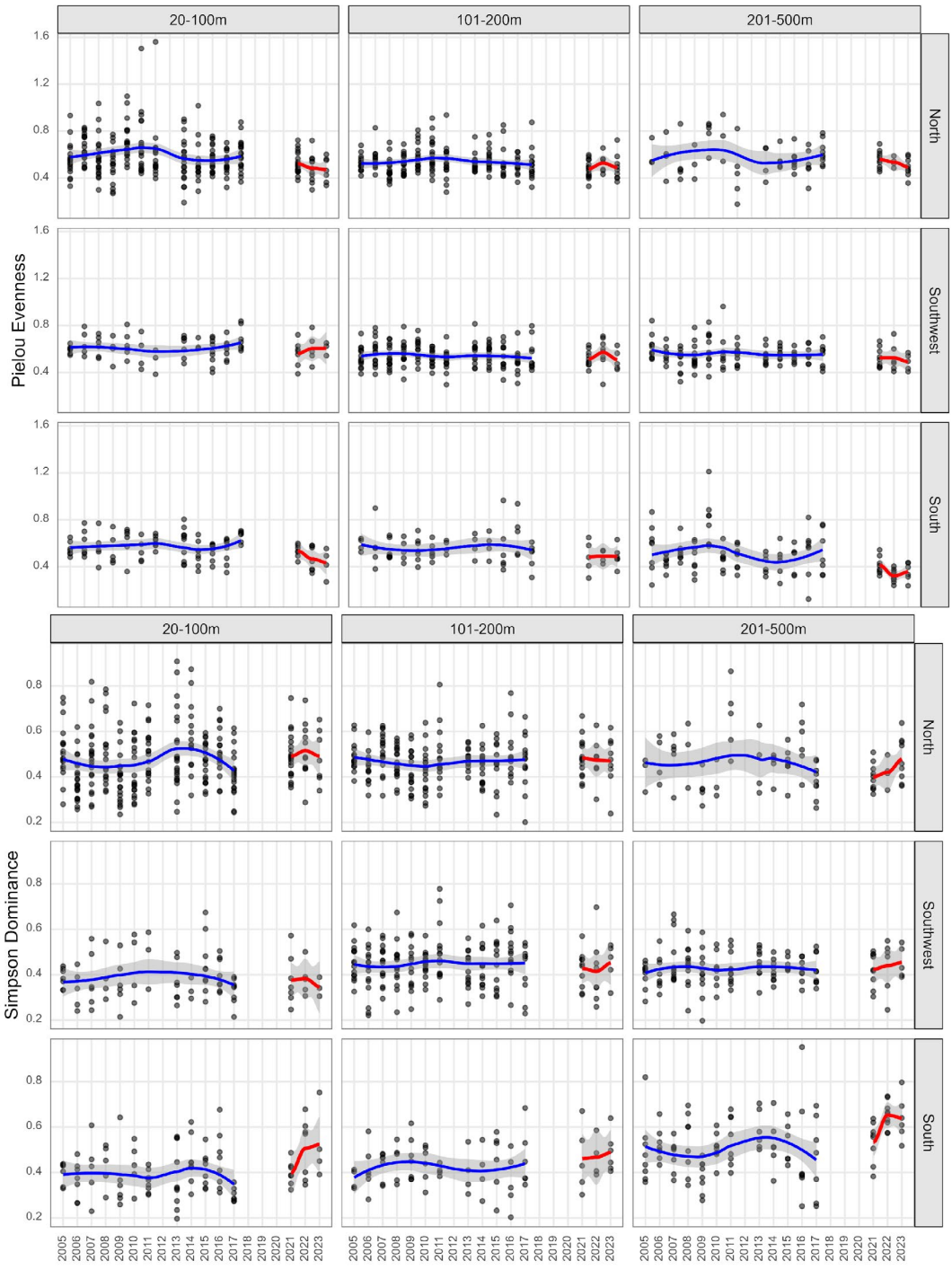

Figure S10.1.a, b. Taxonomic alpha diversity indices Pielou Evenness (top 3 panels) and Simpson Dominance (bottom 3 panels) per year, between 2005-2017 and 2021-2023, in each of the nine latitudinal area*depth strata of the fish communities of the continental shelf and upper slope of the Portuguese coast as sampled in PT-PGFS-IBTS Q4 (International Bottom Trawl Survey Quarter 4 in Portuguese waters of ICES 27.9.a). In each plot each point is a haul, and the line is the "smoothed trend line with the method "loess" with a 95% confidence interval band.

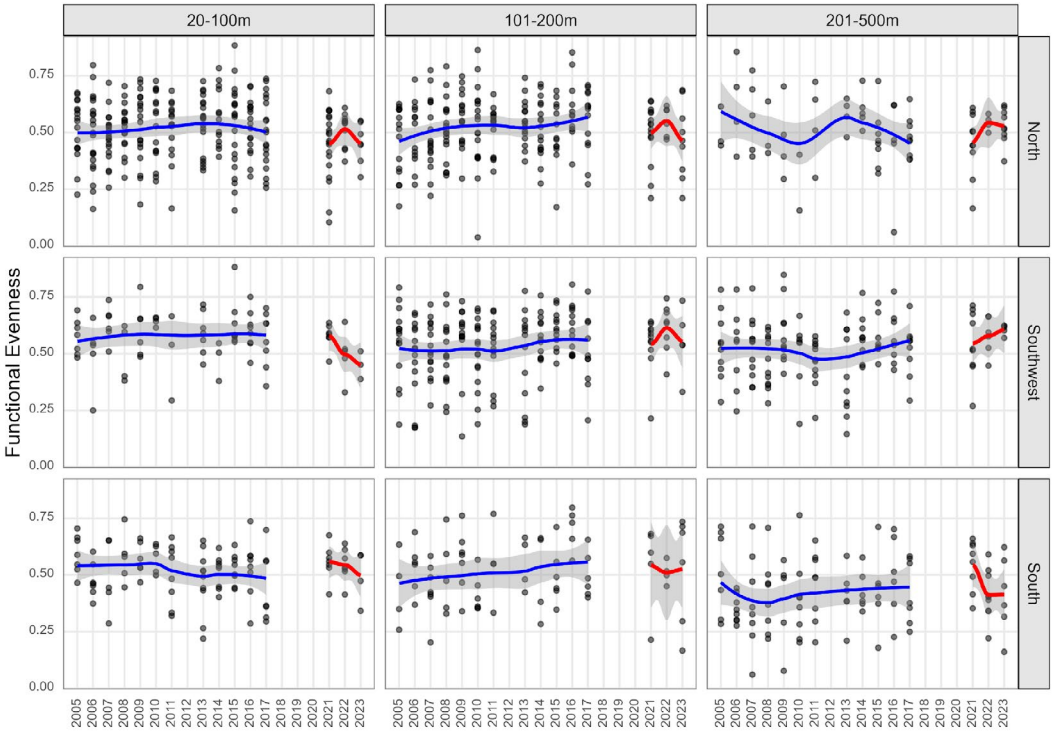

Figure S10.2.a. Functional alpha diversity index Functional Evenness per year, between 2005-2017 and 2021-2023, in each of the nine latitude*depth strata of the fish communities of the continental shelf and upper slope of the Portuguese coast as sampled in PT-PGFS-IBTS Q4 (International Bottom Trawl Survey Quarter 4 in Portuguese waters of ICES 27.9.a). In each plot each point is a haul, and the line is the "smoothed trend line with the method "loess" with a 95% confidence interval band.

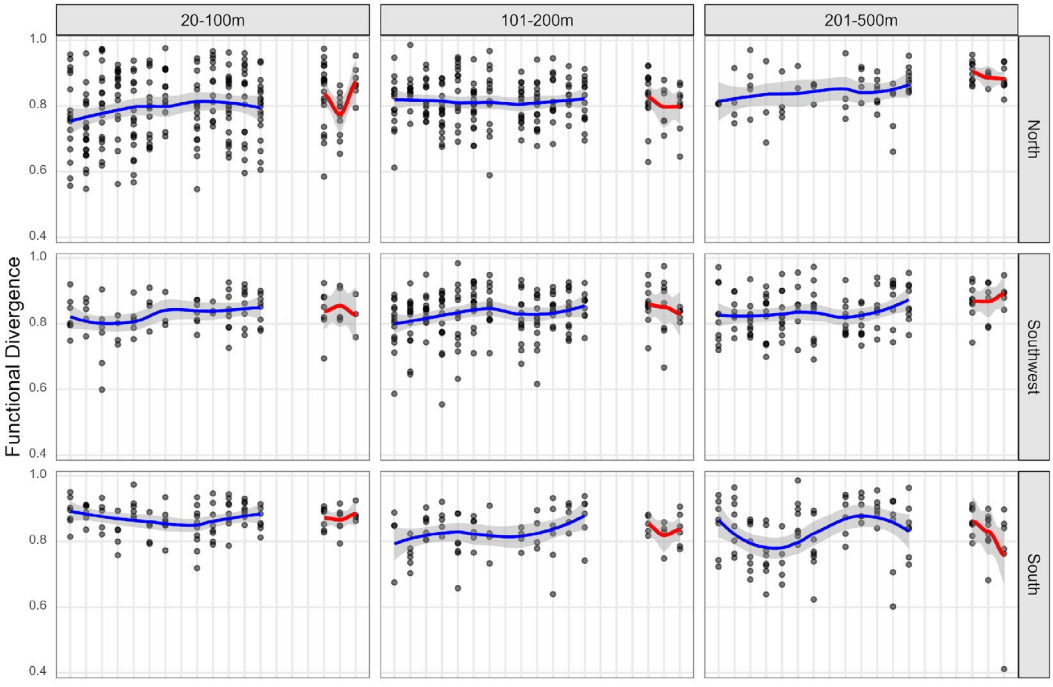

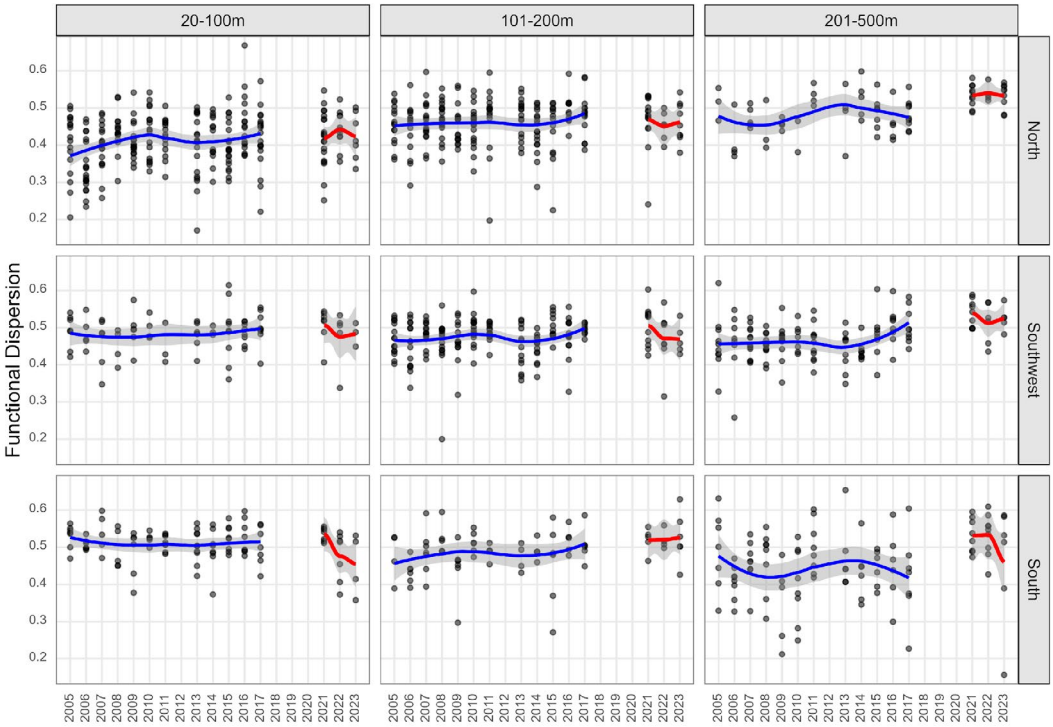

Figure S10.2.b, c. Functional alpha diversity indices Functional Divergence (top 3 panels) and Functional Dispersion (bottom 3 panels) per year, between 2005-2017 and 2021-2023, in each of the nine latitude*depth strata of the fish communities of the continental shelf and upper slope of the Portuguese coast as sampled in PT-PGFS-IBTS Q4 (International Bottom Trawl Survey Quarter 4 in Portuguese waters of ICES 27.9.a). In each plot each point is a haul, and the line is the "smoothed trend line with the method "loess" with a 95% confidence interval band.

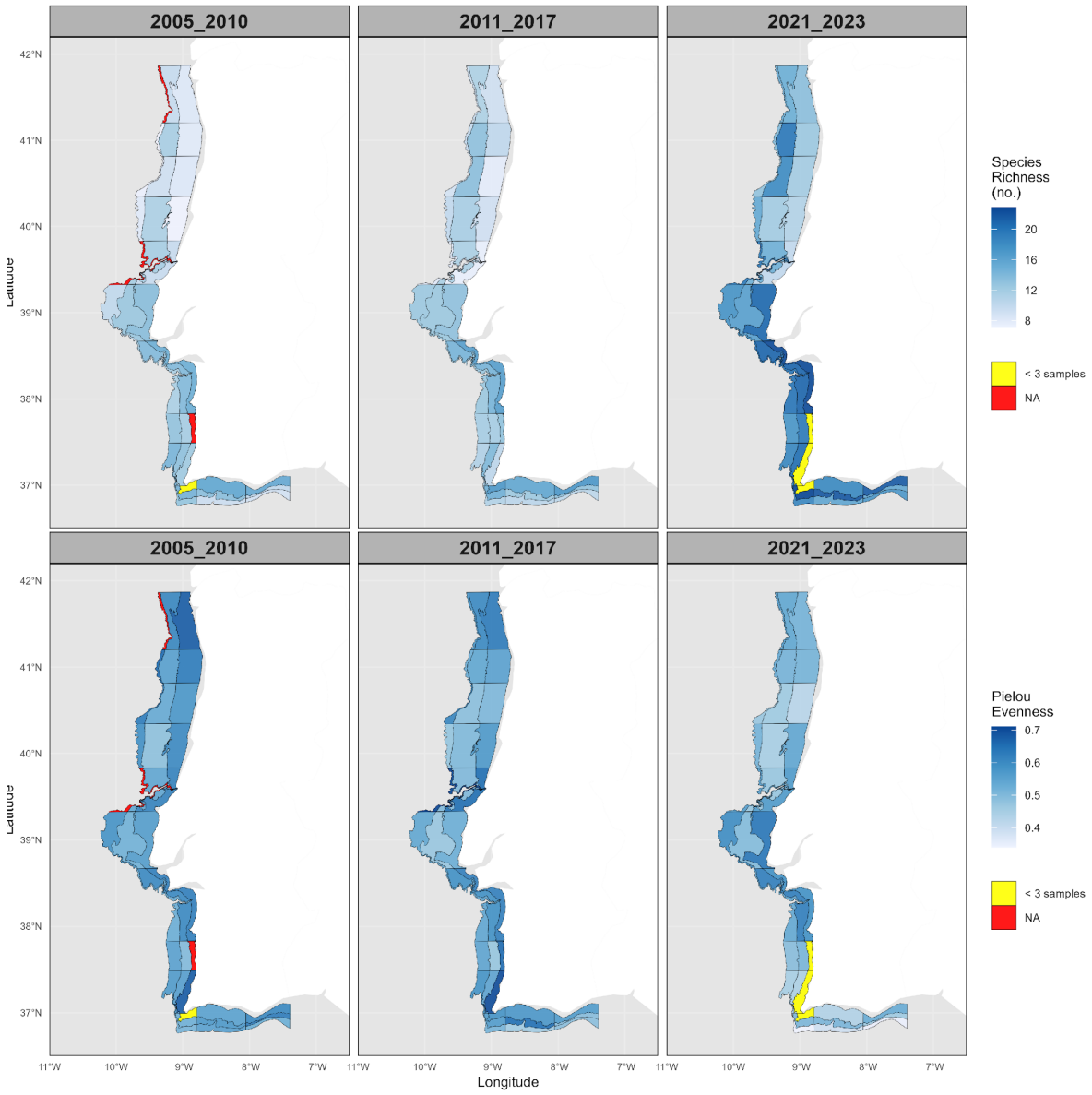

Figure S10.3.a, b. Taxonomic alpha diversity indices Species Richness (top panel) and Pielou Evenness (bottom panel) in three time periods (2005-2010, 2011-2017, 2021-2023) in each of the 36 sampled strata of the fish communities of the continental shelf and upper slope of the Portuguese coast as sampled in PT-PGFS-IBTS Q4 (International Bottom Trawl Survey Quarter 4 in Portuguese waters of IC-ES 27.9.a).

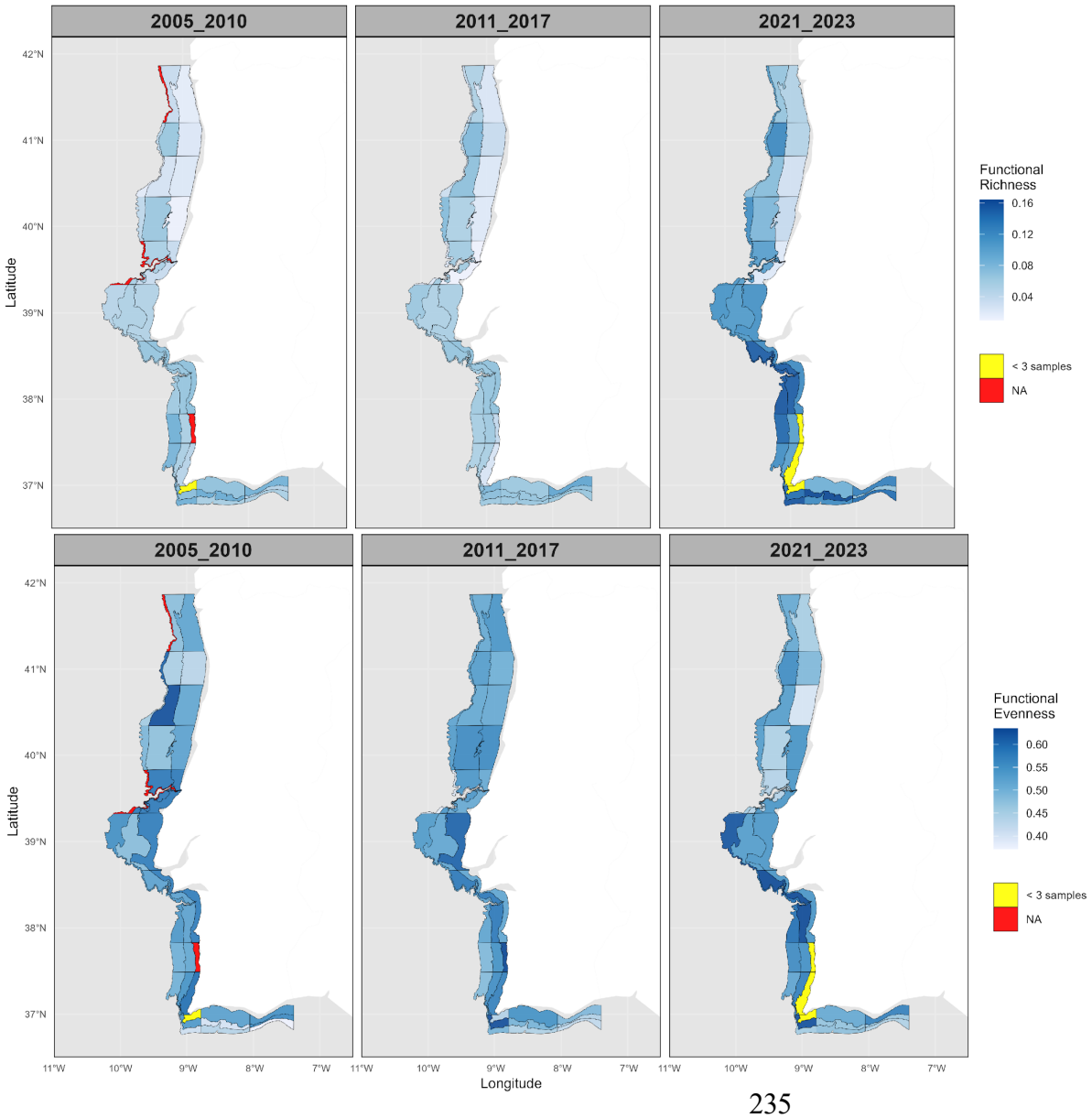

Figure S10.4.a, b. Functional alpha diversity indices Functional Richness (top panel) and Functional Evenness (bottom panel) in three time periods (2005-2010, 2011-2017, 2021-2023) in each of the 36 sampled strata of the fish communities of the continental shelf and upper slope of the Portuguese coast as sampled in PT-PGFS-IBTS Q4 (International Bottom Trawl Survey Quarter 4 in Portuguese waters of ICES 27.9.a).

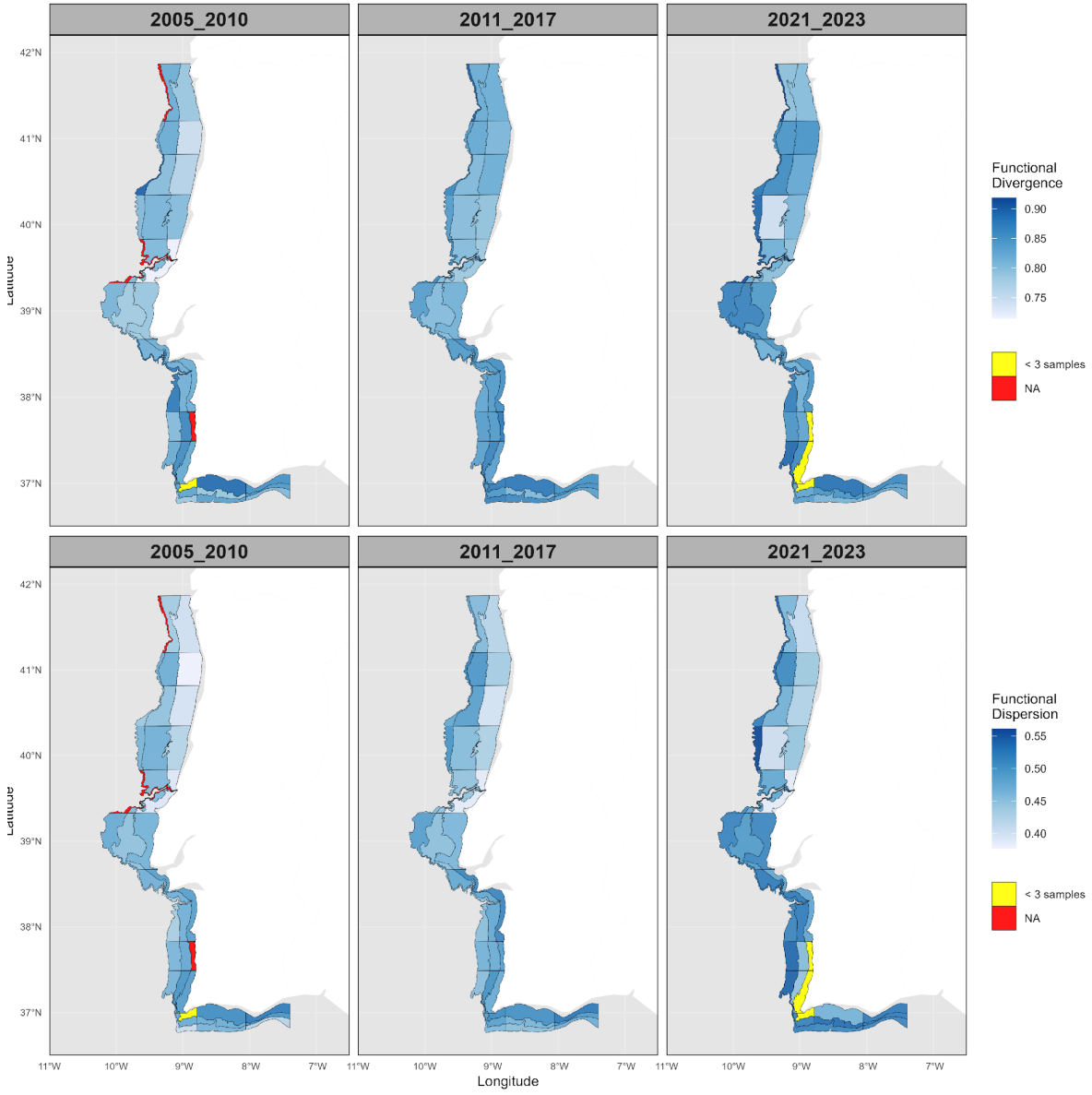

Figure S10.4.c, d. Functional alpha diversity index Functional Divergence (top panel) and Functional Dispersion (bottom panel) in three time periods (2005-2010, 2011-2017, 2021-2023) in each of the 36 sampled strata of the fish communities of the continental shelf and slope of the Portuguese coast as sampled in PT-PGFS-IBTS Q4 (International Bottom Trawl Survey Quarter 4 in Portuguese waters of ICES 27.9.a).

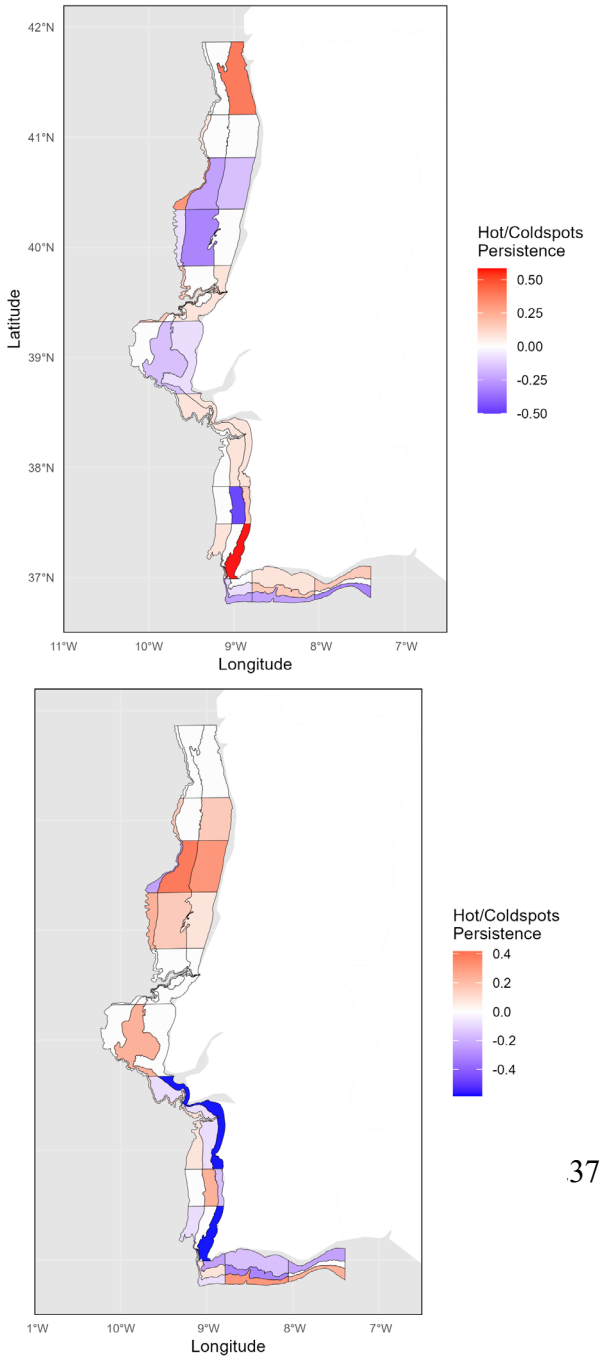

Figure S10.5.a, b. Persistence of hotspots and coldspots of the taxonomic alpha diversity indices Pielou Evenness and Simpson Dominance in the time period 2005-2017 in each of the 36 sampled strata of the fish communities of the continental shelf and upper slope of the Portuguese coast as sampled in PT-PGFS-IBTS Q4 (International Bottom Trawl Survey Quarter 4 in Portuguese waters of ICES 27.9.a).

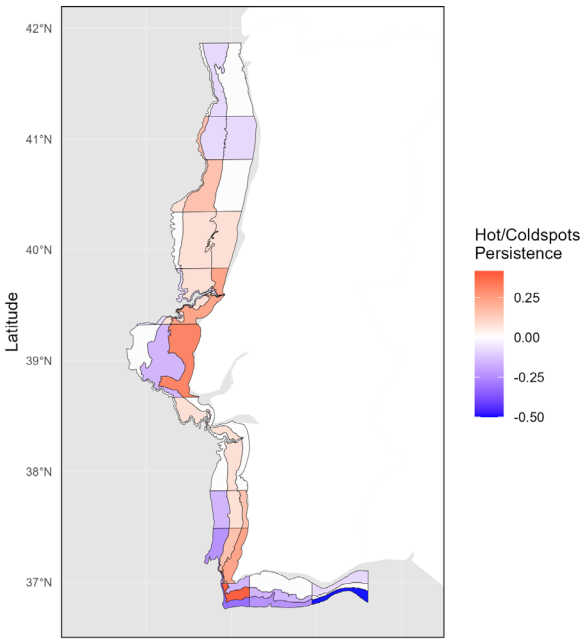
42°N
41°N
40°N
39°N
38°N
37°N
Latitude
Hot/Coldspots
Persistence
0.25
0.00
-0.25
-0.50

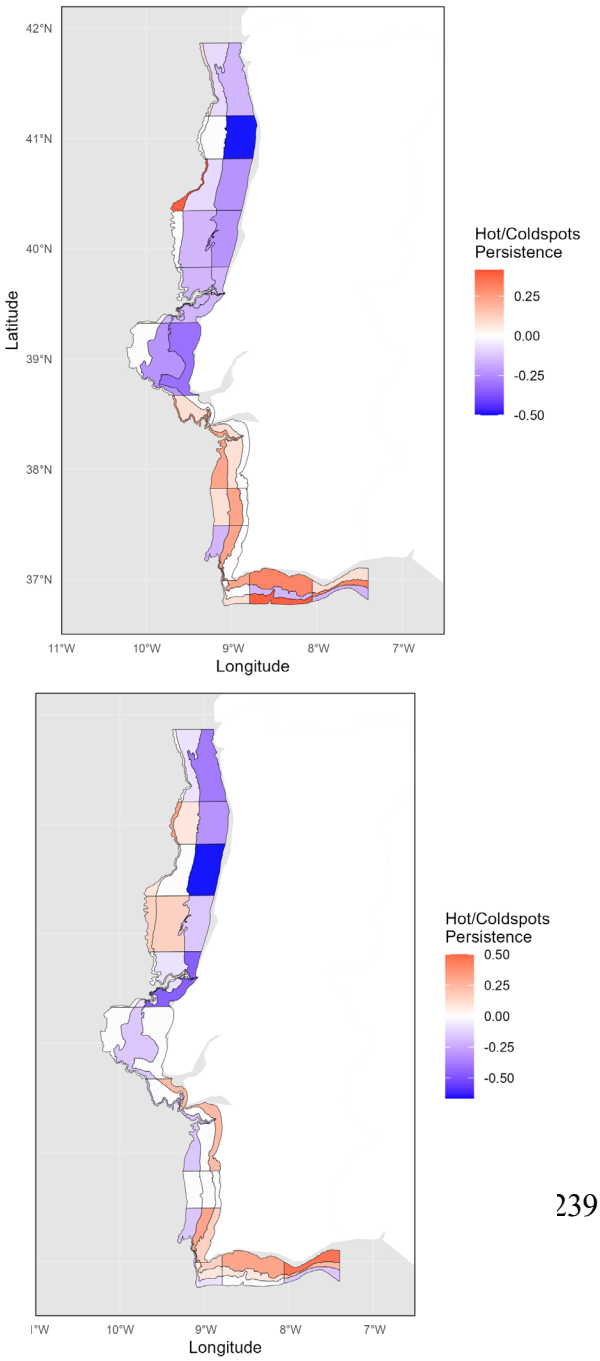

239

Figure S10.6.a, b, c. Persistence of hotspots and coldspots of the functional alpha diversity indices Functional Evenness, Functional Divergence and Functional Dispersion in three time periods (2005-2010, 2011-2017, 2021-2023) in each of the 36 sampled strata of the fish communities of the continental shelf and upper slope of the Portuguese coast as sampled in PT-PGFS-IBTS Q4 (International Bottom Trawl Survey Quarter 4 in Portuguese waters of ICES 27.9.a).

D. **Appendix:** Developing a roadmap for marine biodiversity: past, present and near future change in plankton, benthos and fish assemblages

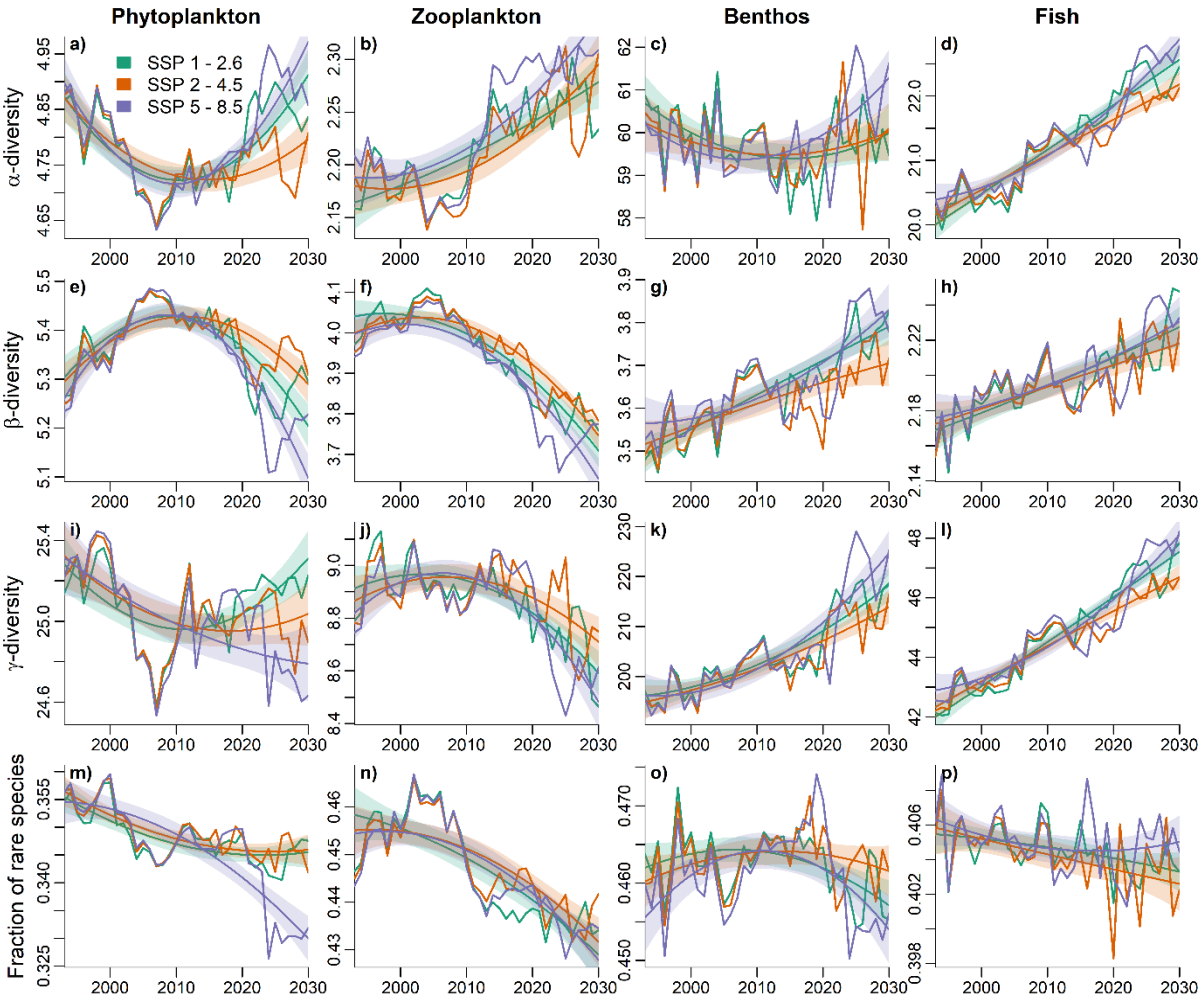

Figure S9.1. the projected mean temporal trend across the study region in α- (a-d), ß- (e-h), γ-diversity (i-l), and the proportion of rarer species (m-p) for phytoplankton (a,e,i,m), zooplankton (b,f,j,n), benthos (c,g,k,o) and fish (d,h,l,p) for the three emission scenarios SSP1-2.6, SSP2-4.5 and SSP5-8.5.

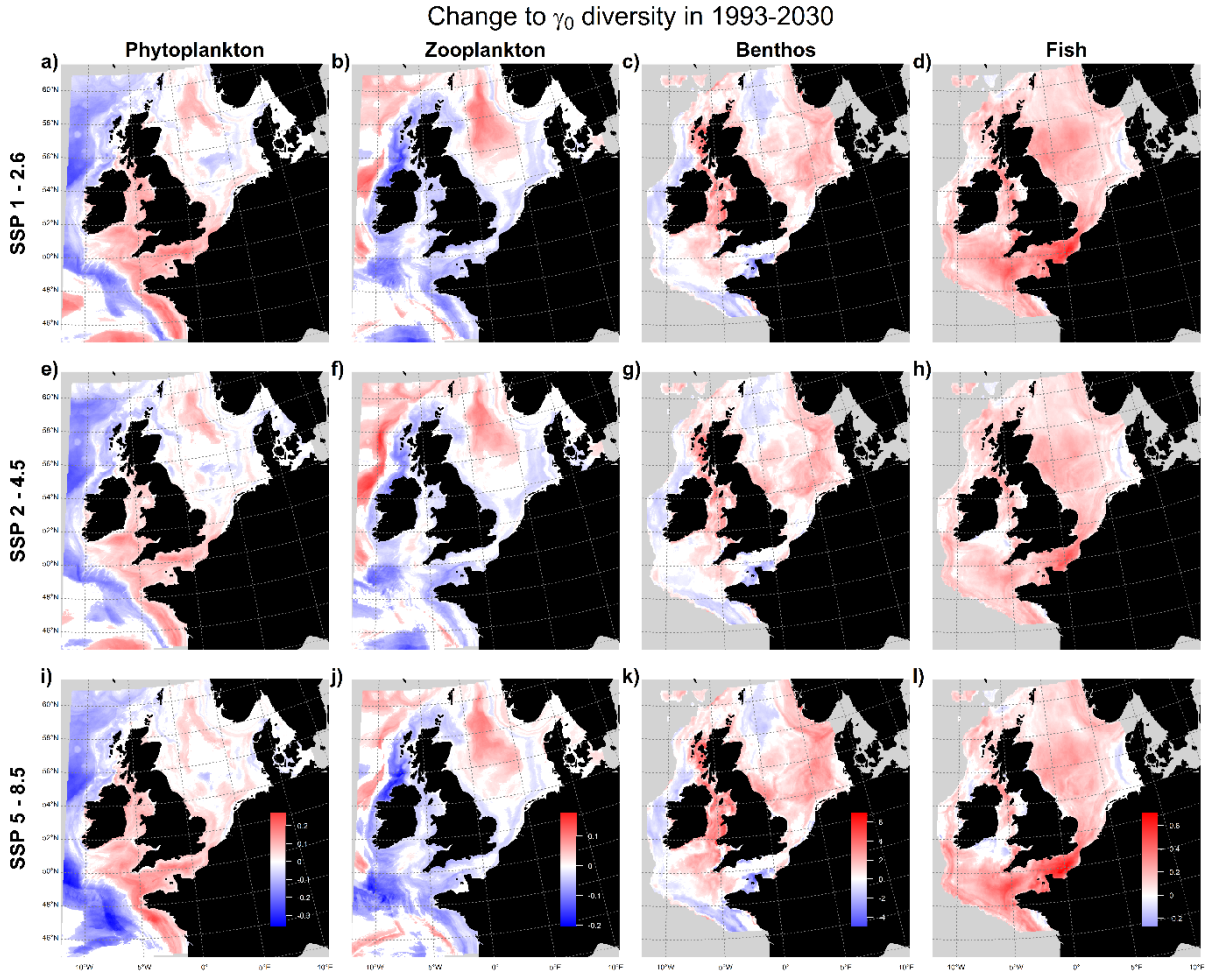

Figure S9.2. The projected annual change (Sen's slope) in γ-diversity (Hill number 0) for phytoplankton (a,e,i), zooplankton (b,f,j), benthos (c,g,k), and fish from 1993 – 2030 based on SSP1-2.6 (a-c), SSP2-4.5 (e-h) and SSP5-8.5 (i-l). The colourbars shown in the bottom row (plots i-l) apply to each column. Red and blue cells show significant (p <0.05) increasing and decreasing annual change, respectively, with white cells showing areas with non-significant change.

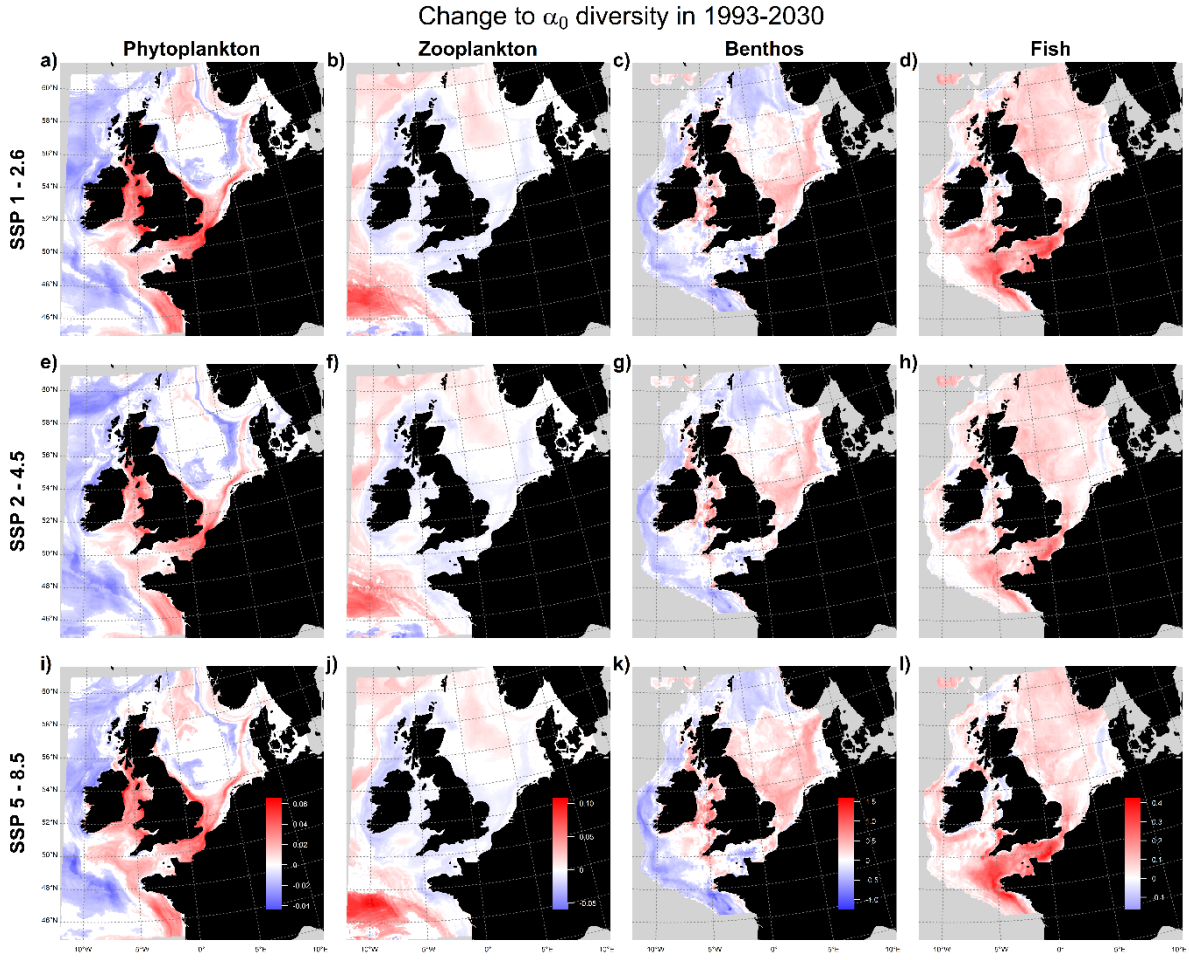

Figure S9.3. The projected annual change (Sen's slope) in α-diversity (Hill number 0) for phytoplankton (a,e,i), zooplankton (b,f,j), benthos (c,g,k), and fish from 1993 – 2100 based on SSP1-2.6 (a-c), SSP2-4.5 (e-h) and SSP5-8.5 (i-l). The colourbars shown in the bottom row (plots i-l) apply to each column. Red and blue cells show significant (p <0.05) increasing and decreasing annual change, respectively, with white cells showing areas with non-significant change.

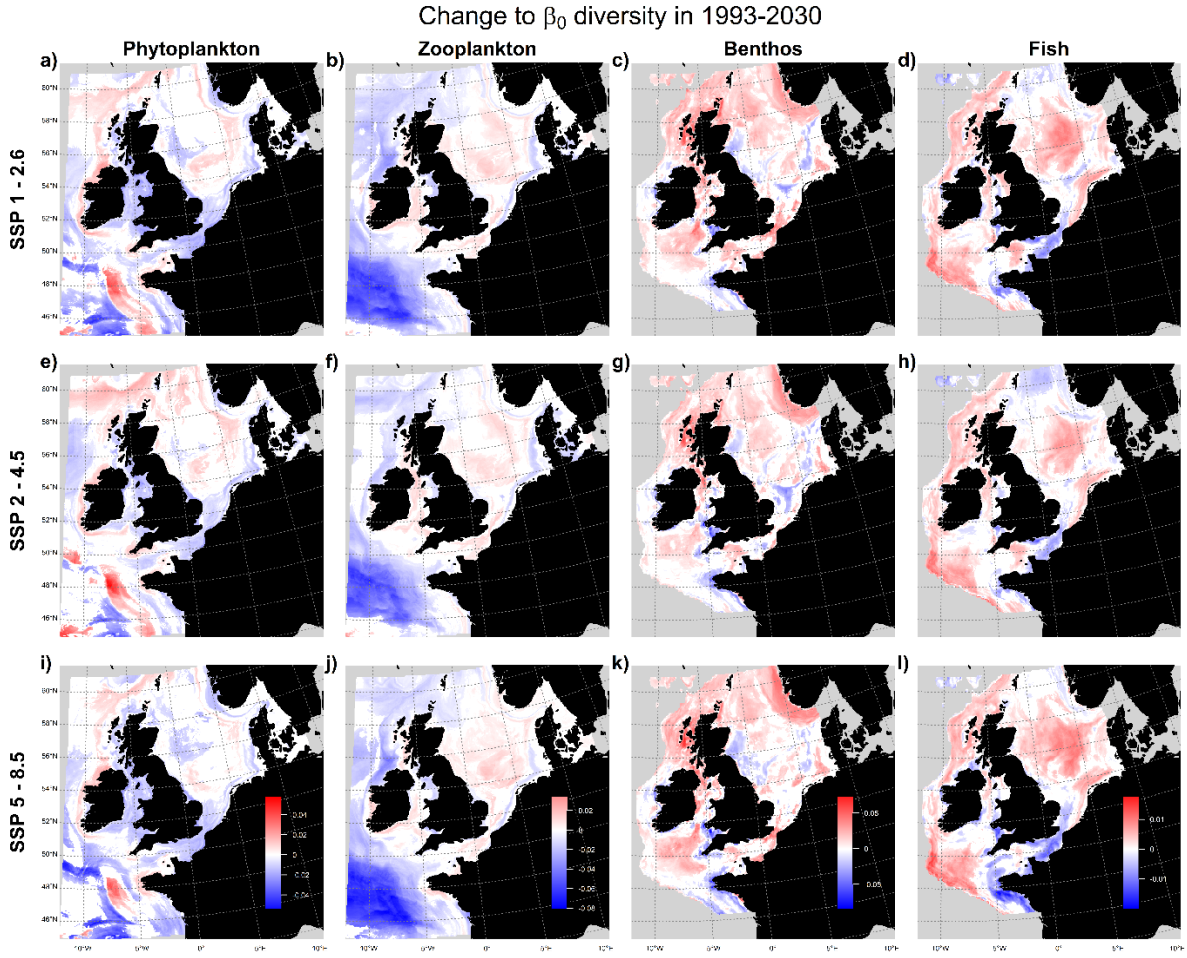

Figure S9.4. The projected annual change (Sen's slope) in ß-diversity (Hill number 0) for phytoplankton (a,e,i), zooplankton (b,f,j), benthos (c,g,k), and fish from 1993 – 2030 based on SSP1-2.6 (a-c), SSP2-4.5 (e-h) and SSP5-8.5 (i-l). The colourbars shown in the bottom row (plots i-l) apply to each column. Red and blue cells show significant (p <0.05) increasing and decreasing annual change, respectively, with white cells showing areas with non-significant change.

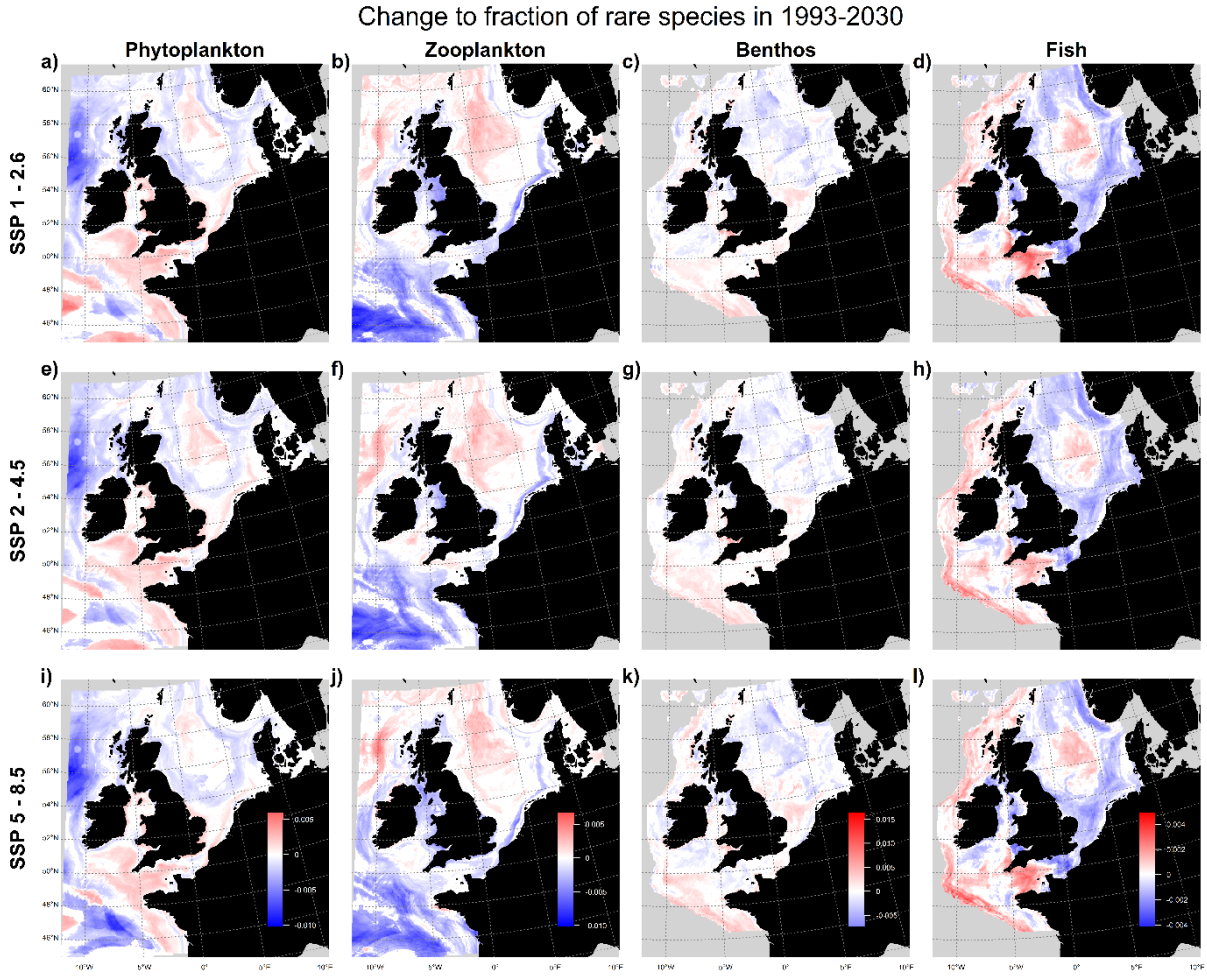

Figure S9.5. The projected annual change (Sen's slope) in the fraction of rare species for phytoplankton (a,e,i), zooplankton (b,f,j), benthos (c,g,k), and fish from 1993 – 2030 based on SSP1-2.6 (a-c), SSP2-4.5 (e-h) and SSP5-8.5 (i-l). The colourbars shown in the bottom row (plots i-l) apply to each column. Red and blue cells show significant (p <0.05) increasing and decreasing annual change, respectively, with white cells showing areas with non-significant change.

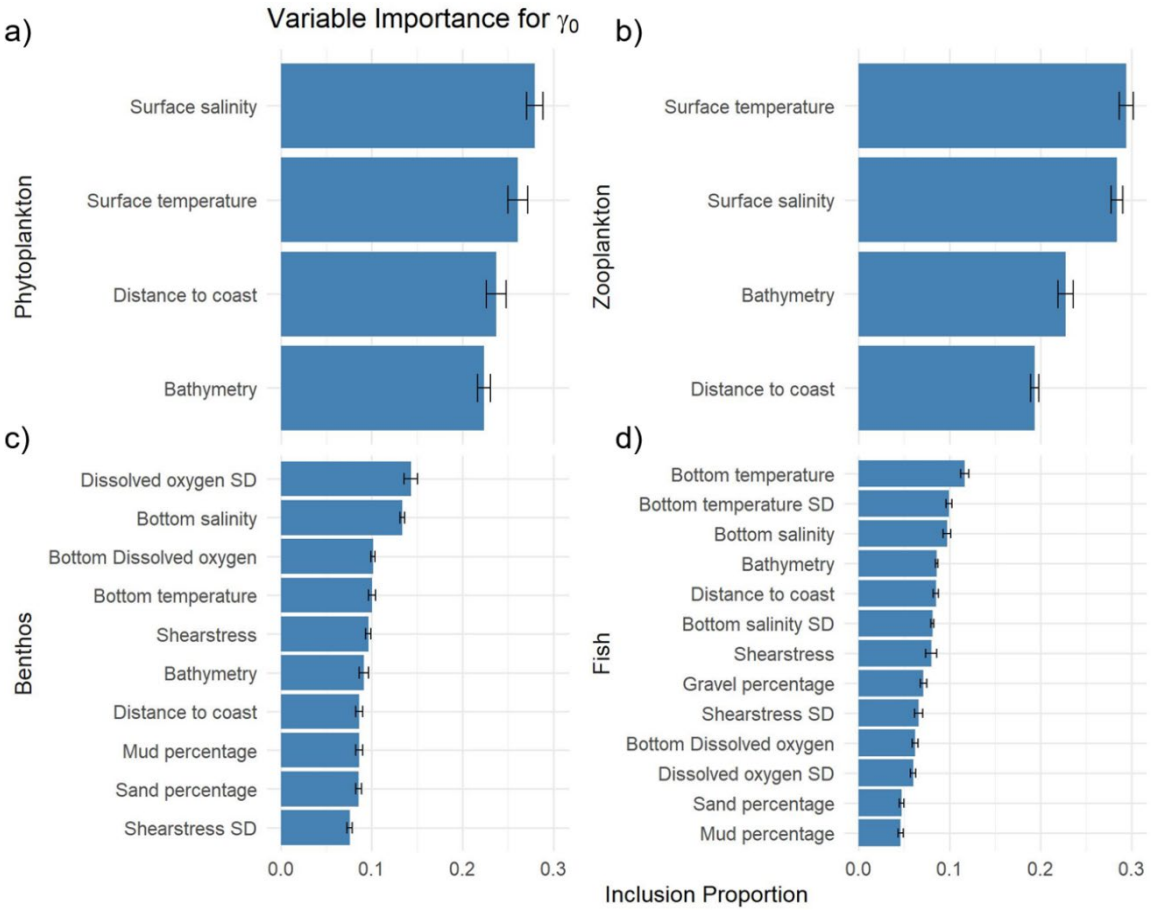

Figure S9.6. Variable importance for the models of γ-diversity based on Hill number 0 for (a) phytoplankton, (b) zooplankton, (c) benthos, and (d) fish.

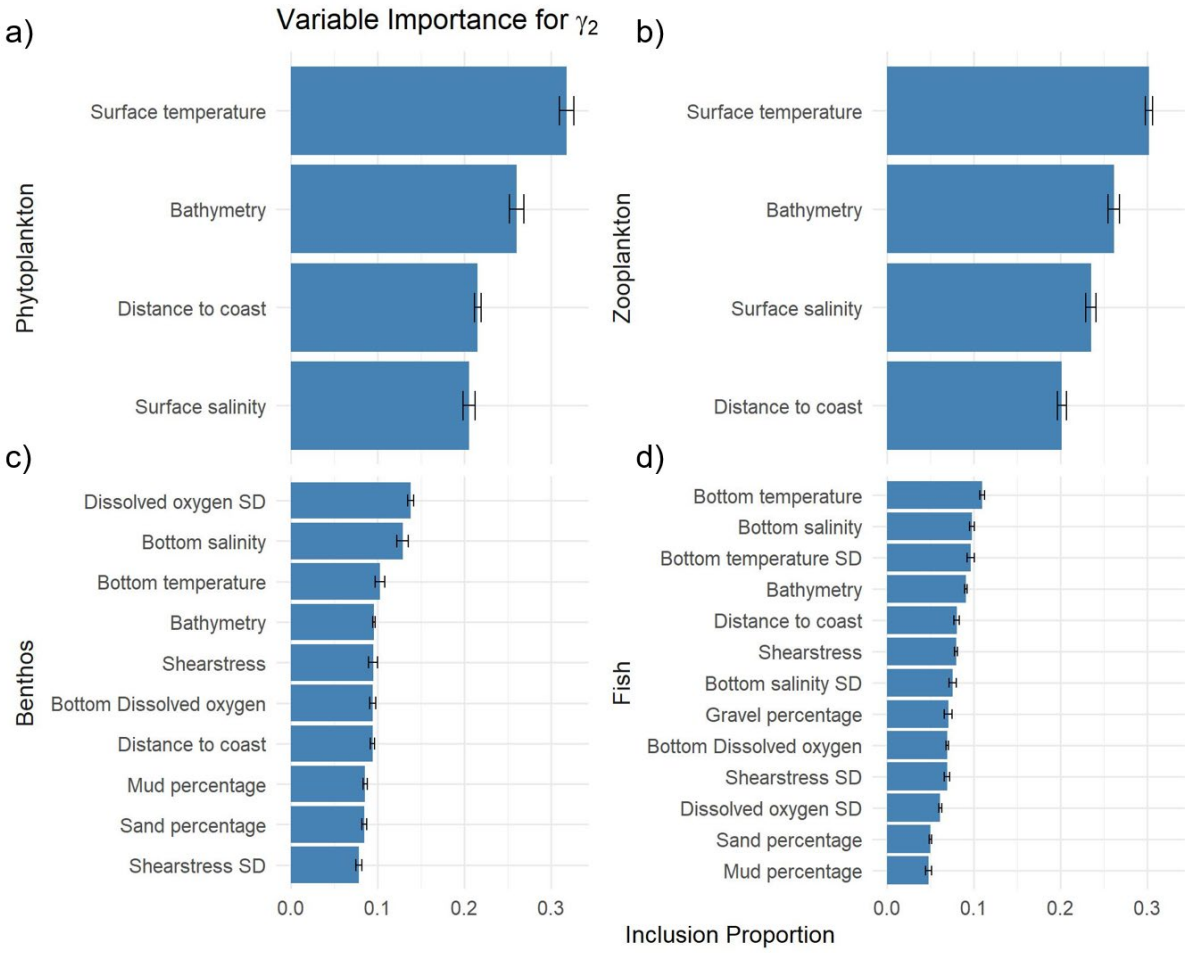

Figure S9.7. Variable importance for the models of γ-diversity based on Hill number 2 for (a) phytoplankton, (b) zooplankton, (c) benthos, and (d) fish.

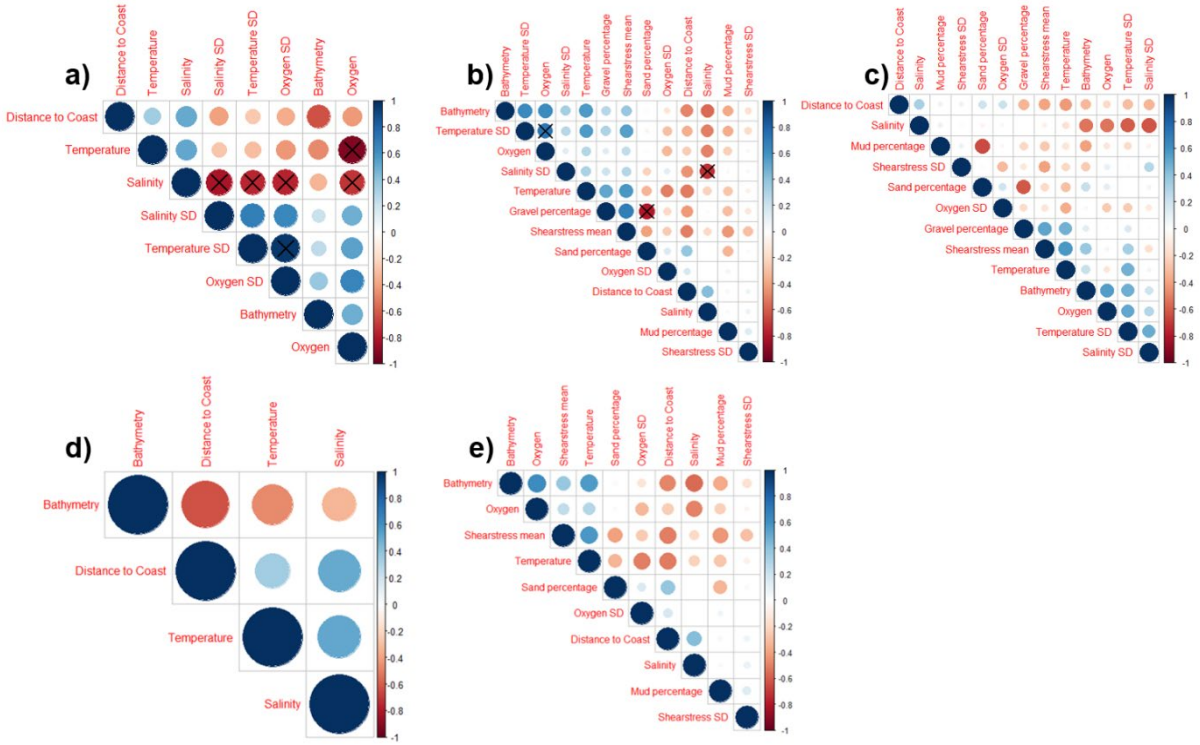

Figure S10.8. Pairwise Pearson correlation coefficients among all environmental covariates, evaluated based on available observations. Black crosses indicate correlations exceeding 0.7 across the full set of environmental variables used for (a) phytoplankton and zooplankton, (b) benthos, and (c) fish. The final set of variables included in our models for (d) phytoplankton and zooplankton and (e) benthos, respectively. All variables were retained for fish. The suffix "SD" denotes the standard deviation of the 12 monthly means per year across all locations within a 75 km radius of each grid cell, as a measure of environmental spatio-temporal heterogeneity. For shear stress, "SD" refers instead to the standard deviation across 7 annual means, because data were not available at the same spatio-temporal resolution as the other variables.

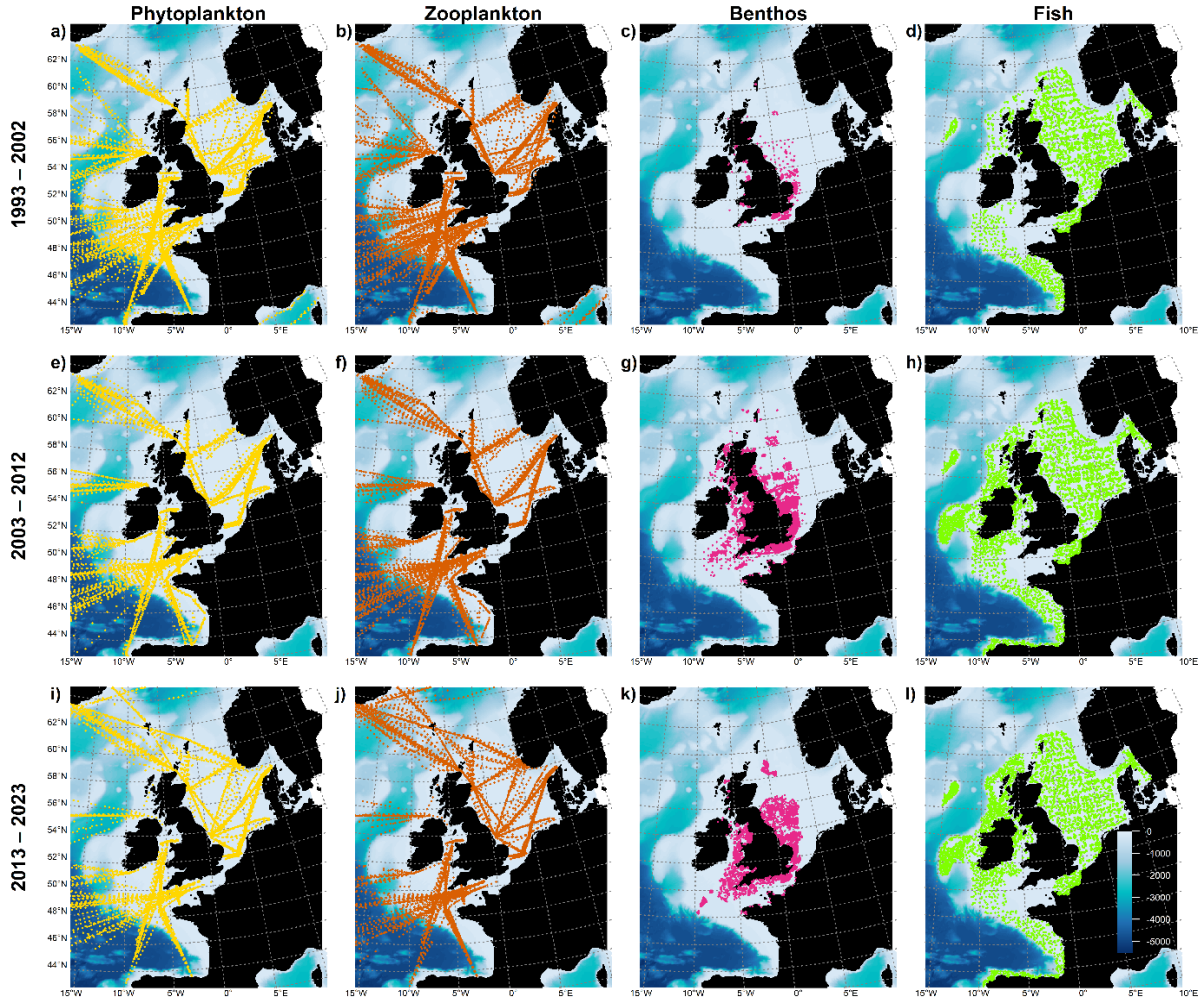

Figure S9.9. Decadal survey coverage across assemblages. Spatial distribution of sampling points for 1993–2002 (a–d), 2003–2012 (e–h), and 2013–2023 (i–l), shown over a bathymetric colour map (blue). Phytoplankton (a,e,i) and zooplankton (b,f,j) samples exhibit broadly similar spatial coverage, benthic samples (c,g,k) are concentrated along the coast, and fish samples (d, h, l) are largely restricted to the continental shelf.

E. Appendix: Spatial Variability in State–Pressure Relationships and Cumulative Impacts on North Sea Benthic Biodiversity

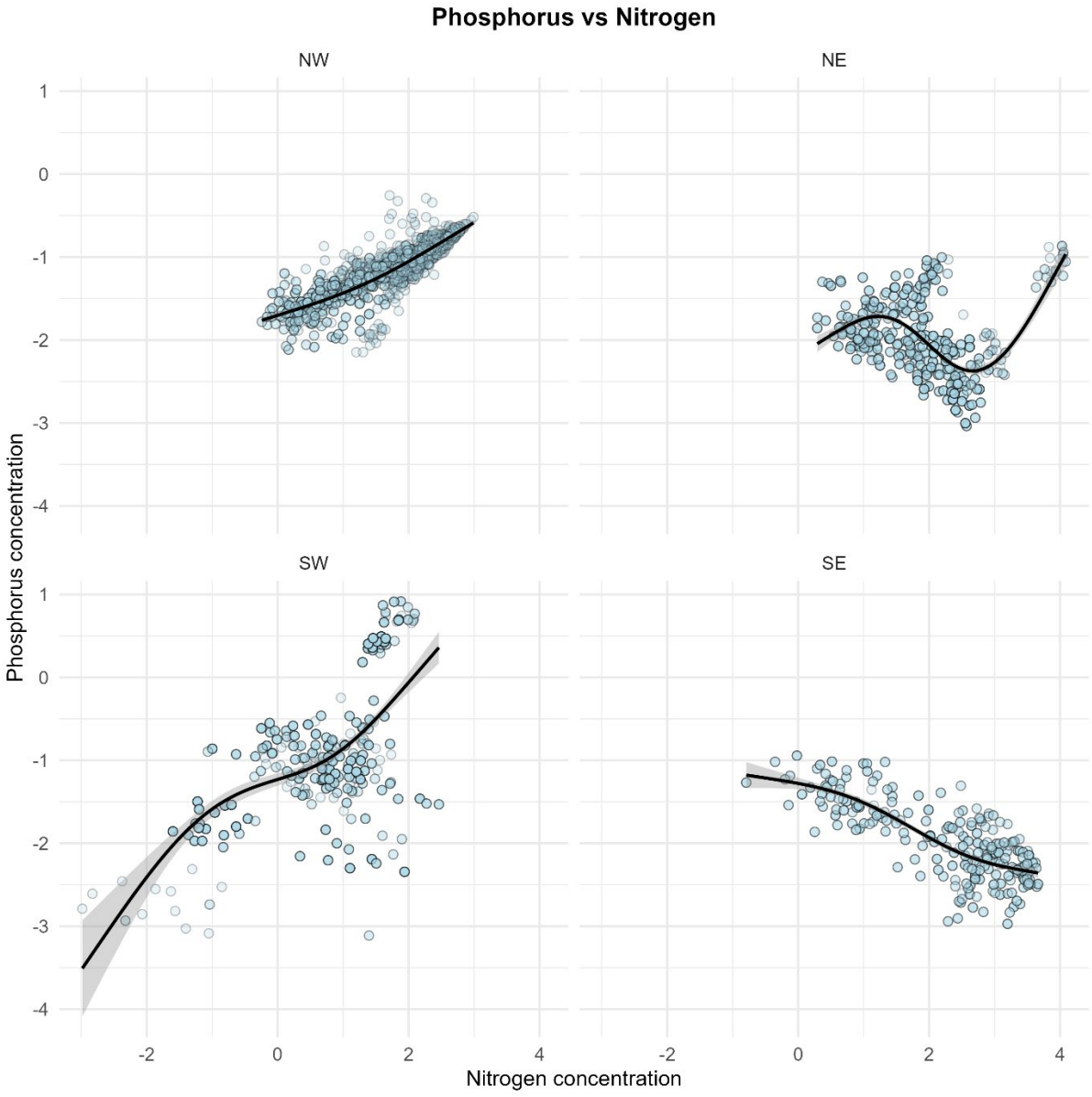

Figure S11.1. Scatterplots of log-transformed phosphorus vs. nitrogen concentrations within the 4 quadrants (NW, NE, SW, and SE). Panels show pairwise relationships between with points representing individual hauls and black lines indicating smoothed fits (GAMs with 95% confidence intervals).

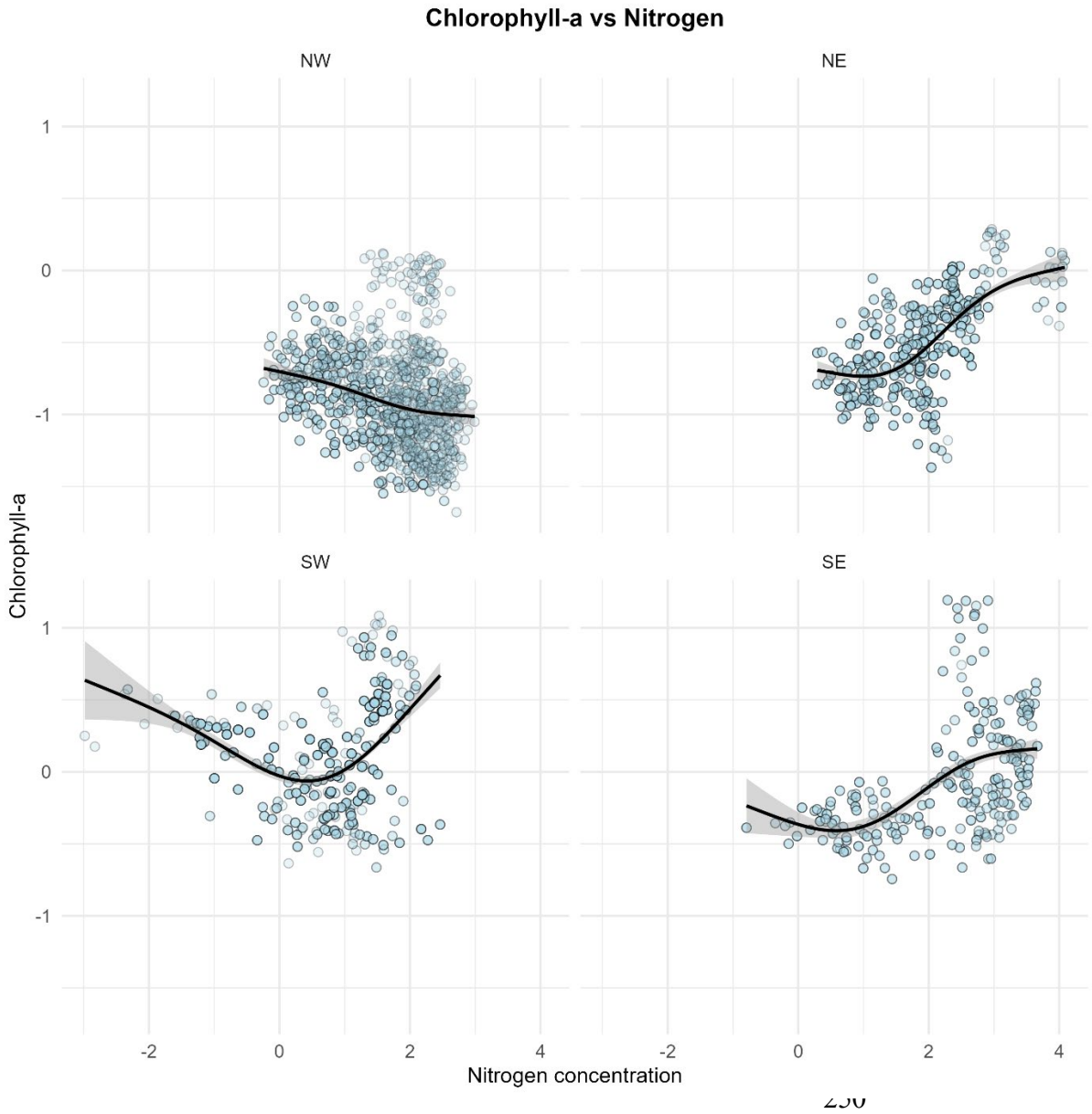

Figure S11.2. Scatterplots of log-transformed chlorophyll-a vs. nitrogen concentrations within the 4 quadrants (NW, NE, SW, and SE). Panels show pairwise relationships between with points representing individual hauls and black lines indicating smoothed fits (GAMs with 95% confidence intervals).

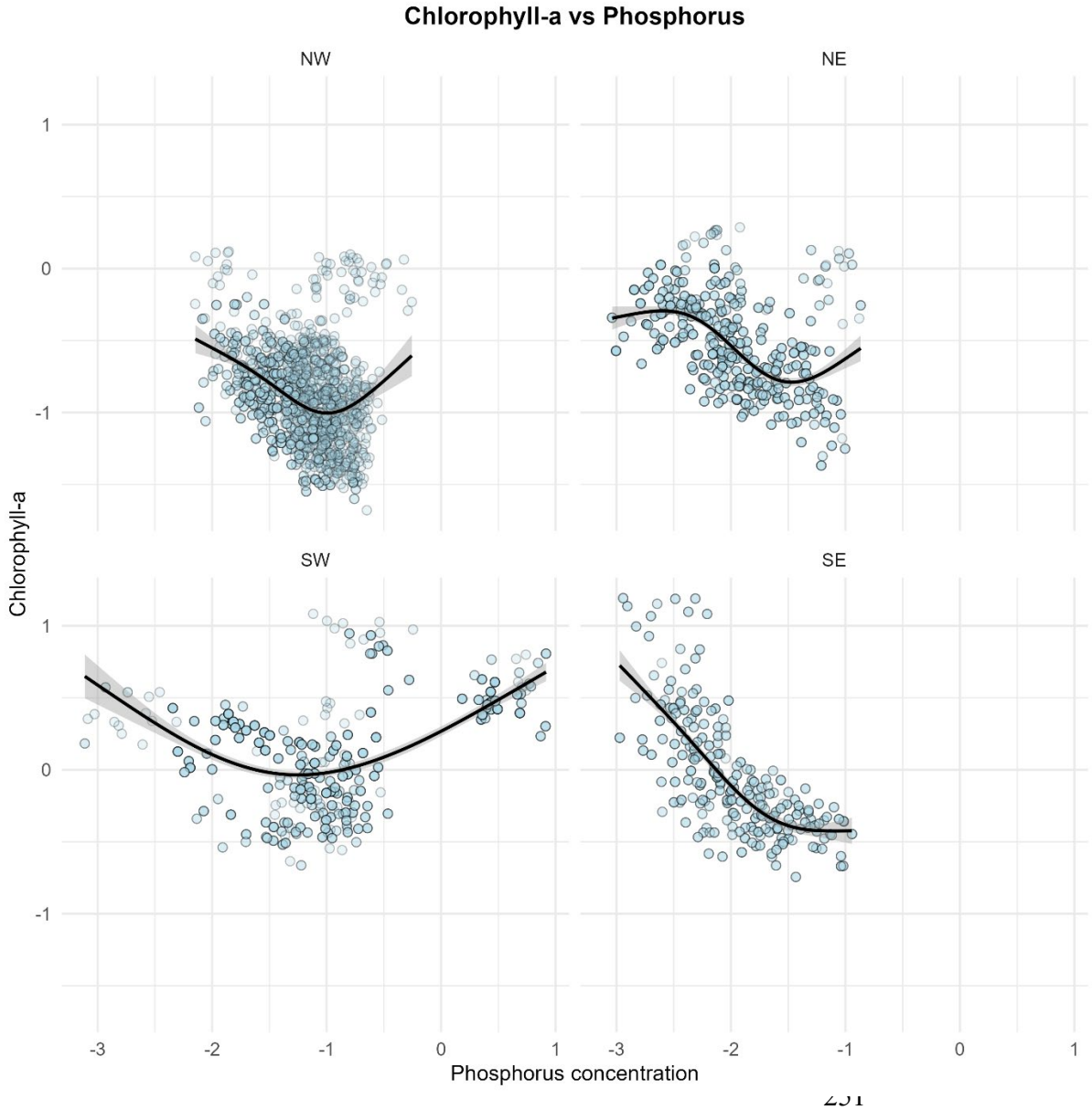

Figure S11.3. Scatterplots of log-transformed chlorophyll-a vs. phosphorus concentrations within the 4 quadrants (NW, NE, SW, and SE). Panels show pairwise relationships between with points representing individual hauls and black lines indicating smoothed fits (GAMs with 95% confidence intervals).

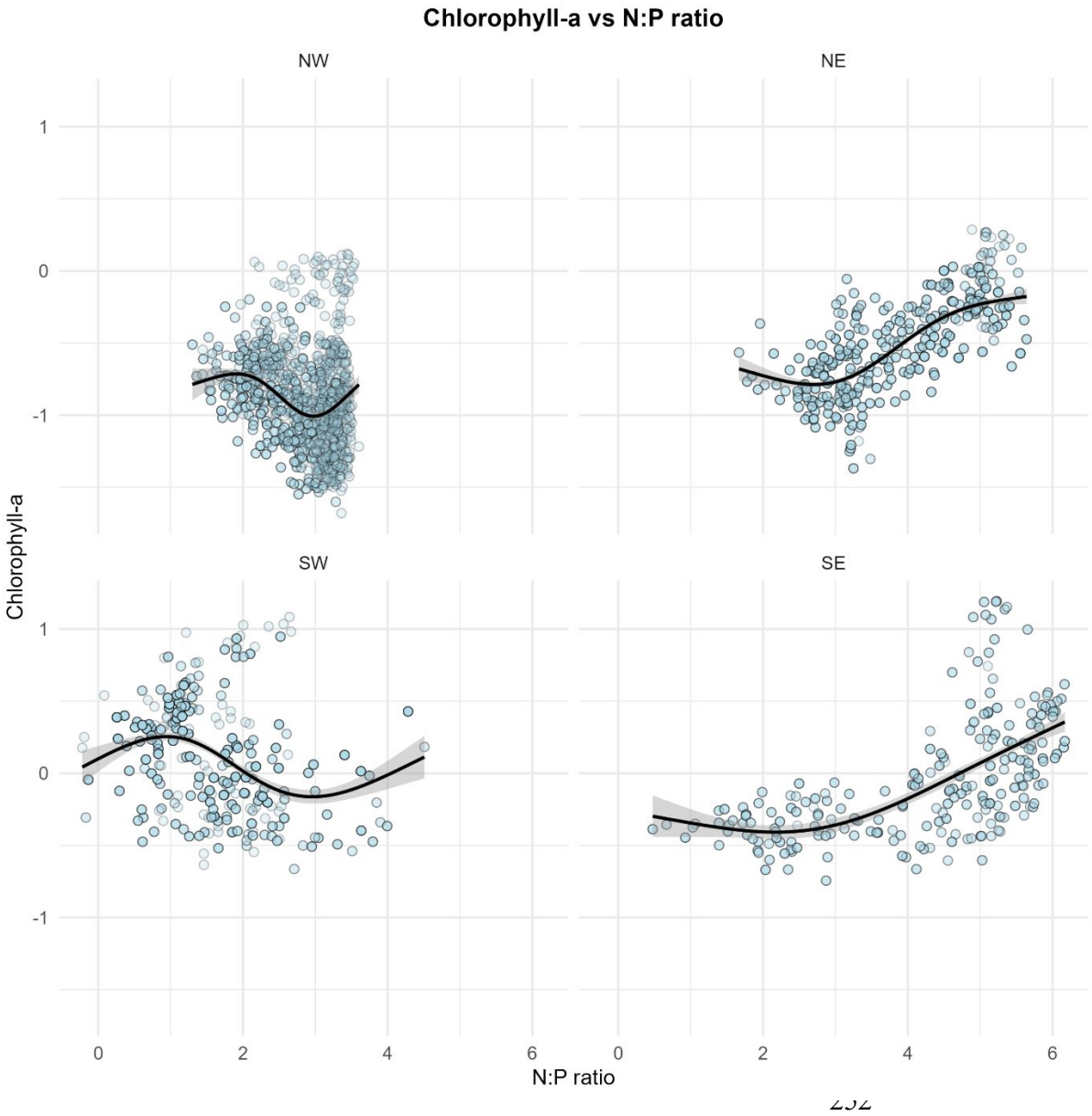

Figure S11.4. Scatterplots of log-transformed chlorophyll-a vs. nitrogen-to-phosphorus concentrations within the 4 quadrants (NW, NE, SW, and SE). Panels show pairwise relationships between with points representing individual hauls and black lines indicating smoothed fits (GAMs with 95% confidence intervals).

F. **Appendix:** Multidimensional tracking of marine species redistribution under climate change

Figure S15.1. Species-specific trend shifts. Color shows median effect size; more intense colors indicate larger deviations from zero. Points and lines show median and 95% CI. Marine regions: EBS = Eastern Bering Sea, GOA= Gulf of Alaska, BC = British Columbia, USWC = U.S. West Coast, NEUS-SS = Northeast U.S. and Scotian Shelf, GOM = Gulf of Mexico, BS = Barents Sea, NS = North Sea, CBS = Celtic–Biscay Shelf, BAL = Baltic Sea, NIC = Northern Iberian Coast.

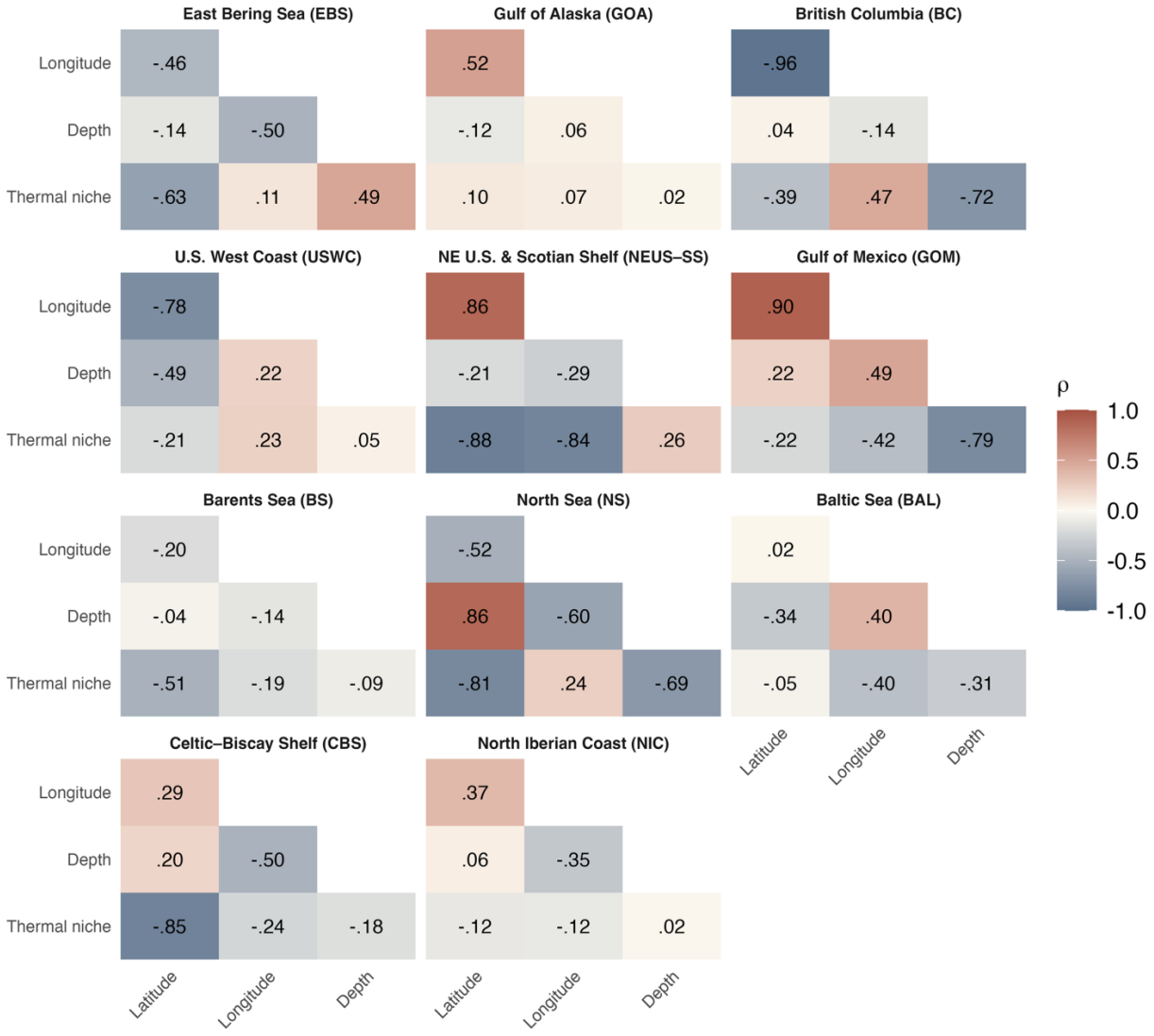

Figure S15.2. Heatmap of posterior mean correlations (ρ) between trends in latitude, longitude, depth, and realized thermal niche across regions. Colors indicate the strength and direction of associations.

Text S15

All prior distributions are summarized in Table S15.1. Throughout, Normal(μ, σ) and Student-t(ν, μ, σ) denote distributions with location parameter μ and dispersion parameter σ, where σ corresponds to the standard deviation for the Normal distribution and the scale parameter for the Student-t distribution, and ν denotes the degrees of freedom.

Table S15.1. Prior distributions for model parameters. Fixed effects (β), group-level and standard deviations (σ), degrees of freedom (ν) for the Student-t distribution, and the correlation matrix of region-level effects (Rr). The source column indicates whether the prior was changed from the default.

Prior distribution	Parameter	Effect / Coefficient	Response	Source
LKJ(1)	R_r	Correlation matrix	All responses	Default
Normal(0, 50)	β	Decade effect	Latitudinal centroid	User
Normal(0, 50)	β	Decade effect	Longitudinal centroid	User
Normal(0, 5)	β	Decade effect	Depth niche	User
Normal(0, 0.5)	β	Decade effect	Thermal niche	User
Gamma(2, 0.1)	ν	Degrees of freedom	Latitudinal centroid	Default
Gamma(2, 0.1)	ν	Degrees of freedom	Longitudinal centroid	Default
Gamma(2, 0.1)	ν	Degrees of freedom	Depth niche	Default
Gamma(2, 0.1)	ν	Degrees of freedom	Thermal niche	Default
Student-t(3, 0, 30.8)	σ	Residual SD	Latitudinal centroid	Default
Student-t(3, 0, 28.3)	σ	Residual SD	Longitudinal centroid	Default
Student-t(3, 0, 3.9)	σ	Residual SD	Depth niche	Default
Student-t(3, 0, 2.5)	σ	Residual SD	Thermal niche	Default
Student-t(3, 0, 30)	σ	Decade SD (region)	Latitudinal centroid	User
Student-t(3, 0, 30)	σ	Decade SD (region)	Longitudinal centroid	User
Student-t(3, 0, 10)	σ	Decade SD (region)	Depth niche	User
Student-t(3, 0, 0.2)	σ	Decade SD (region)	Thermal niche	User
Student-t(3, 0, 40)	σ	Decade SD (region × species)	Latitudinal centroid	User
Student-t(3, 0, 40)	σ	Decade SD (region × species)	Longitudinal centroid	User
Student-t(3, 0, 20)	σ	Decade SD (region × species)	Depth niche	User
Student-t(3, 0, 0.4)	σ	Decade SD (region × species)	Thermal niche	User

We specified weakly informative priors for global temporal slopes (decadal effects) based on published rates of range shifts, depth changes, and ocean warming (Fig. B1a). For latitudinal and longitudinal centroids, we used Normal(0, 50) km per decade priors, accommodating reported shifts of up to approximately 30 km per decade in marine taxa. For depth trends, we applied a Normal(0, 5) m per decade prior, consistent with reported deepening rates of approximately 3.6 m per decade in North Sea demersal fish. For thermal niches, we used a Normal(0, 0.5) °C per decade prior, encompassing rates observed in rapidly warming continental shelf seas.

To model variation in temporal slopes among groups, we assigned Student-t distributions with three degrees of freedom, truncated to positive values, allowing substantial but biologically plausible variation. Region-level slope standard deviations followed Student-t(3, 0, 30) km per decade priors for spatial centroids, Student-t(3, 0, 10) m per decade for depth, and Student-t(3, 0, 0.2) °C per decade for thermal niches. For species nested within regions, we specified broader priors—Student-t(3, 0, 40) km per decade, Student-t(3, 0, 20) m per decade, and Student-t(3, 0, 0.4) °C per decade, respectively.

These priors were consistent with the empirical variability observed in the data and provided appropriate regularization while remaining flexible enough to capture biologically plausible trends (Fig. S15.3b–c). All remaining model parameters used the default priors implemented in the *brms* package (Table S15.1).

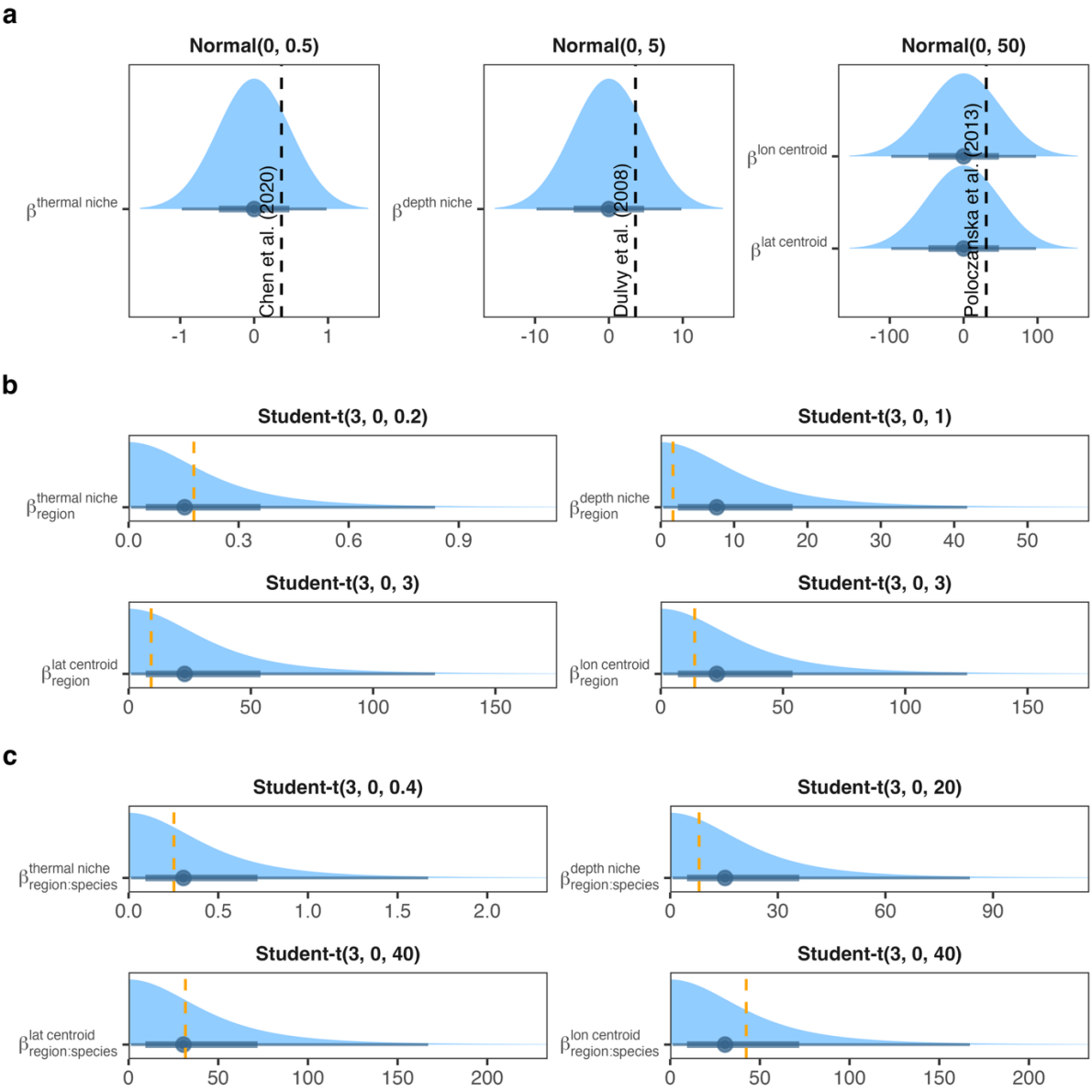

Figure S15.3. Prior specification and validation for temporal trend parameters. (a) Priors for global temporal slopes (decade effects) shown relative to literature-reported values (black dashed lines). (b) Priors for region-level slope variation compared with empirical distributions from the data (orange dashed lines). (c) Priors for species-level slope variation nested within regions compared with empirical distributions (orange dashed lines). Priors are weakly informative and consistent with observed variability, providing regularization without constraining plausible trends.